ACS SYMPOSIUM SERIES 711

Vanadium Compounds

Chemistry, Biochemistry, and Therapeutic Applications

EDITED BY
Alan S. Tracey and Debbie C. Crans

Vanadium Compounds

Downloaded by 89.163.35.42 on October 31, 2012 | http://pubs.acs.org
Publication Date: December 10, 1998 | doi: 10.1021/bk-1998-0711.fw001

In Vanadium Compounds; Tracey, A., et al.;
ACS Symposium Series; American Chemical Society: Washington, DC, 1998.

Downloaded by 89.163.35.42 on October 31, 2012 | http://pubs.acs.org
Publication Date: December 10, 1998 | doi: 10.1021/bk-1998-0711.fw001

ACS SYMPOSIUM SERIES 711

Vanadium Compounds

Chemistry, Biochemistry, and Therapeutic Applications

Alan S. Tracey, EDITOR
Simon Fraser University

Debbie C. Crans, EDITOR
Colorado State University

American Chemical Society, Washington, DC

Downloaded by 89.163.35.42 on October 31, 2012 | http://pubs.acs.org
Publication Date: December 10, 1998 | doi: 10.1021/bk-1998-0711.fw001

QP 535 .V2V353 1998 c.1

Vanadium compounds :
chemistry, biochemistry,

Library of Congress Cataloging-in-Publication Data

Vanadium compounds : biochemistry; chemistry, and therapeutic applications /
Alan S. Tracey, Debbie C. Crans, editors.

p. cm.—(ACS symposium series ; ISSN 0097-6156 ; 711)

Includes bibliographical references and index.

ISBN 0-8412-3589-9

1. Vanadium—Physiological effect—Congresses. 2. Vanadium—Therapeutic use—Congresses. 3. Vanadium—Congresses.

I. Tracey, Alan S., II. Crans, Debbie Catharina. III. Series.

QP535.V2V353 1998
572′.52522—dc21 98-25963
CIP

The paper used in this publication meets the minimum requirements of American National Standard for Information Sciences—Permanence of Paper for Printed Library Materials, ANSI Z39.48-1984.

Copyright © 1998 American Chemical Society

Distributed by Oxford University Press

All Rights Reserved. Reprographic copying beyond that permitted by Sections 107 or 108 of the U.S. Copyright Act is allowed for internal use only, provided that a per-chapter fee of $20.00 plus $0.25 per page is paid to the Copyright Clearance Center, Inc., 222 Rosewood Drive, Danvers, MA 01923, USA. Republication or reproduction for sale of pages in this book is permitted only under license from ACS. Direct these and other permissions requests to ACS Copyright Office, Publications Division, 1155 16th Street, N.W., Washington, DC 20036.

The citation of trade names and/or names of manufacturers in this publication is not to be construed as an endorsement or as approval by ACS of the commercial products or services referenced herein; nor should the mere reference herein to any drawing, specification, chemical process, or other data be regarded as a license or as a conveyance of any right or permission to the holder, reader, or any other person or corporation, to manufacture, reproduce, use, or sell any patented invention or copyrighted work that may in any way be related thereto. Registered names, trademarks, etc., used in this publication, even without specific indication thereof, are not to be considered unprotected by law.

PRINTED IN THE UNITED STATES OF AMERICA

Downloaded by 89.163.35.42 on October 31, 2012 | http://pubs.acs.org
Publication Date: December 10, 1998 | doi: 10.1021/bk-1998-0711.fw001

American Chemical Society
Library
1155 16th St. N. W.
Washington, D. C. 20036

Advisory Board

ACS Symposium Series

Mary E. Castellion
ChemEdit Company

Arthur B. Ellis
University of Wisconsin at Madison

Jeffrey S. Gaffney
Argonne National Laboratory

Gunda I. Georg
University of Kansas

Lawrence P. Klemann
Nabisco Foods Group

Richard N. Loeppky
University of Missouri

Cynthia A. Maryanoff
R. W. Johnson Pharmaceutical
Research Institute

Roger A. Minear
University of Illinois
at Urbana–Champaign

Omkaram Nalamasu
AT&T Bell Laboratories

Kinam Park
Purdue University

Katherine R. Porter
Duke University

Douglas A. Smith
The DAS Group, Inc.

Martin R. Tant
Eastman Chemical Co.

Michael D. Taylor
Parke-Davis Pharmaceutical
Research

Leroy B. Townsend
University of Michigan

William C. Walker
DuPont Company

Downloaded by 89.163.35.42 on October 31, 2012 | http://pubs.acs.org
Publication Date: December 10, 1998 | doi: 10.1021/bk-1998-0711.fw001

Downloaded by 89.163.35.42 on October 31, 2012 | http://pubs.acs.org
Publication Date: December 10, 1998 | doi: 10.1021/bk-1998-0711.fw001

Foreword

THE ACS SYMPOSIUM SERIES was first published in 1974 to provide a mechanism for publishing symposia quickly in book form. The purpose of the series is to publish timely, comprehensive books developed from ACS sponsored symposia based on current scientific research. Occasionally, books are developed from symposia sponsored by other organizations when the topic is of keen interest to the chemistry audience.

Before agreeing to publish a book, the proposed table of contents is reviewed for appropriate and comprehensive coverage and for interest to the audience. Some papers may be excluded in order to better focus the book; others may be added to provide comprehensiveness. When appropriate, overview or introductory chapters are added. Drafts of chapters are peer-reviewed prior to final acceptance or rejection, and manuscripts are prepared in camera-ready format.

As a rule, only original research papers and original review papers are included in the volumes. Verbatim reproductions of previously published papers are not accepted.

ACS BOOKS DEPARTMENT

Preface

During the past 15 years an explosive growth has occurred in the chemistry and biochemistry of vanadium compounds. Much of this interest had been fueled by the various roles that vanadium plays as a phosphate mimic in biochemical systems, either activating or inhibiting a large number of phosphate-metabolizing enzymes according to the role that phosphate plays in those systems. However, equally important in promoting this interest was the discovery of vanadium-dependent enzymes, the vanadium-dependent haloperoxidases and nitrogenases. As will be seen from these Proceedings, the uses and applications of vanadium-containing compounds now outstrips the aims and aspirations of much of the earlier work.

Progress in several areas of the applications and properties of vanadium compounds has greatly stimulated the exploration of vanadium chemistry in aqueous and organic media. The papers described in this volume were developed from the Symposium entitled "Chemistry, Biochemistry, and Therapeutic Applications of Vanadium Compounds" held at the 5th North American Chemical Congress that took place in Cancun, November 10–14, 1997. Although the participants in this symposium represented many worldwide groups, not all active areas of vanadium chemistry or vanadium life science were present. A few additional contributions were solicited to provide the proceedings with a slightly broader scope. Prior to this symposium, other symposia on various aspects of vanadium science had been held and some of those meetings resulted in symposium proceedings (*1–2*). In addition, three monologues have recently been published (*3–5*). For those readers interested in the growth of this general field, we have provided a summary of those meetings below. To our knowledge the first meeting in Vanadium science was entitled "Role of Vanadium in Biology" and was held in 1986 at the Federation of American Societies for Experimental Biology meeting. A synopsis from this Symposium was reported in the Federation Proceedings (*1*). A second symposium with a chemical emphasis entitled "Biochemistry of Vanadium" was held at the 45th American Chemical Society Southeast Regional Meeting in Johnson City, Tennessee, in 1993. A third symposium with a pharmacological emphasis was held in 1994 in Montreal entitled "Vanadium: Biochemistry, Physiology, and Potential Use in Diabetes Therapy" and the symposium proceeding from this meeting resulted in a special volume of *Molecular and Cellular Biochemistry* (2). Recently, vanadium chemistry for the

In Vanadium Compounds; Tracey, A., et al.;
ACS Symposium Series; American Chemical Society: Washington, DC, 1998.

Downloaded by 89.163.35.42 on October 31, 2012 | http://pubs.acs.org
Publication Date: December 10, 1998 | doi: 10.1021/bk-1998-0711.pr001

first time was given a session at the 8th International Conference for Bioinorganic Chemistry in Yokohama, Japan, in 1997. That meeting was followed by the Symposium from which this Proceedings was developed. In this symposium, vanadium chemistry and biochemistry were closely coupled with therapeutic applications of vanadium compounds. Its timeliness and success is not only reflected in the quality of the contributions in this volume, but also in the fact that sequels for the symposium are in the planning stages.

This Symposium Proceedings is divided into three sections, each of which is proceeded by an introduction and a brief general review of the area. The first section consists of 12 chapters that describe research in aqueous and non-aqueous vanadium chemistry. The introductory chapter for the chemistry section of the proceedings reviews the simple aqueous vanadium chemistry of direct relevance to biological studies. In addition, it provides some information on model chemistry and other non-aqeuous chemistry not described in detail in the following chapters and serves to point the reader toward detailed descriptions of various areas (including the biochemistry and therapeutic sections) in the Symposium Proceedings. The second section, consisting of nine chapters describing contributions in areas of vanadium biochemistry, commences with Chapter 13 which provides a general review that is not limited to biochemical topics presented at the symposium. The introduction to the final seven chapters section provides a brief review of the current state of the art in the pharmacology and therapeutic applications of vanadium compounds. The final contribution in this section, Chapter 28, describes the effects of vanadium administered as oral tablets to diabetic humans.

As was obvious at the Symposium and from chapters in this volume, the current level of understanding of the vanadium chemistry and the mechanisms of action in biology has increased vastly in the past decade. The recent advances in understanding the aqueous chemistry of vanadium, in some sense corresponds to a shift from a purely inorganic focus to a emphasis on the biological and medicinal aspects of today. Although not all current studies may lead to successful applications, the increased interest in not only the simple vanadium salts but also organic vanadium derivatives, suggests that at some future time, vanadium compounds with reduced toxicity and increased therapeutic value will be identified. The symposium giving rise to these proceedings focused attention on the importance of understanding the interrelationships between the aqueous chemistry, the biochemistry, and therapeutic utilization of vanadium compounds. The details available in many of the following chapters will directly or indirectly emphasize those relationships.

Downloaded by 89.163.35.42 on October 31, 2012 | http://pubs.acs.org
Publication Date: December 10, 1998 | doi: 10.1021/bk-1998-0711.pr001

References

1. Nechay, B. R.; Nanninga, L. B.; Nechay, P. S. E.; Post, R. L.; Grantham, J. J.; Macara, I. G.; Kubena, L. Fl.; Philips, T. D.; Nielsen, F. H. *FASEB Fed. Proc.* **1986,** *45,* 123–132.
2. Vanadium Compounds: Biochemical and Therapeutic Applications; Srivastava, A. K.; Chiasson, J.-L., Eds; Focused issue in *Mol. Cell. Biochem.* **1995,** 153.
3. "Vanadium in the Environment." In *Adv. Environ. Science Technol.*Nriagu, J. O., Ed.; John Wiley & Sons, Inc: New York, 1998; Vol. 23, Parts 1 and 2.
4. *Vanadium and Its Role for Life; Metal Ions in Biological Systems,* Sigel, H.; Sigel, A., Eds.; Marcel Dekker, Inc.: New York, 1995; Vol. 31.
5. *Vanadium in Biological Systems*; Chasteen, N. D., Ed.; Kluwer Academic Publishers: Dordrecht, Netherlands, 1990.

ALAN S. TRACEY
DEPARTMENT OF CHEMISTRY AND
INSTITUTE OF MOLECULAR BIOLOGY AND BIOCHEMISTRY
SIMON FRASER UNIVERSITY
BURNABY, BRITISH COLUMBIA V5A 1S6
CANADA

DEBBIE C. CRANS
DEPARTMENT OF CHEMISTRY
COLORADO STATE UNIVERSITY
FT. COLLINS, CO 80523–1872

Downloaded by 89.163.35.42 on October 31, 2012 | http://pubs.acs.org
Publication Date: December 10, 1998 | doi: 10.1021/bk-1998-0711.pr001

Chapter 1

The Chemistry of Vanadium in Aqueous and Nonaqueous Solution

Debbie C. Crans[1] and Alan S. Tracey[2]

[1]Department of Chemistry and Cell and Molecular Biology Program, Colorado State University, Fort Collins, CO 80523–1872
[2]Department of Chemistry and Institute of Molecular Biology and Biochemistry, Simon Fraser University, Burnaby, British Columbia V5A 1S6, Canada

Downloaded by 89.163.35.42 on October 31, 2012 | http://pubs.acs.org
Publication Date: December 10, 1998 | doi: 10.1021/bk-1998-0711.ch001

This chapter summarizes the aqueous chemistry of vanadium in oxidation states III, IV and V and briefly describes chemistry in nonaqueous solutions. Although this chapter focuses on vanadium chemistry, it serves as an introduction for this Symposium Proceedings. An emphasis has been placed on the description of bioinorganic aspects of vanadium chemistry including speciation in aqueous solutions, hydrolytic and redox reactions with small biogenic molecules, and interactions with amino acids, peptides and proteins. In addition, compounds are described of particular interest for modeling various aspects of enzyme activities exhibited by haloperoxidases, nitrogenases, and phosphatases. Finally, compounds exhibiting insulin-mimetic properties are described and some of their chemistry is summarized. Given the recent increased interest in vanadium chemistry, it is impossible to describe all aspects of current and exciting areas that are under exploration. Thus for some areas of vanadium chemistry, referral to the appropriate literature is made. Furthermore, references also will be made to the biochemical, and pharmacological aspects of vanadium science described elsewhere in these Symposium Proceedings.

Vanadium is a trace metal that is found naturally both in soil and water (1). Vanadium compounds have been prepared in many oxidation states three of which, vanadium(III), (IV) and (V), exist in biological systems and in the environment. The chemistry of the two latter oxidation states, in the forms of vanadyl (vanadium(IV)) and vanadate (vanadium(V)), is particularly relevant to the action and effects of vanadium compounds in mammals. In this introductory chapter, an overview of various aspects of aqueous and nonaqueous chemistry of vanadyl and vanadate chemistry that are of direct biochemical relevance is given although other important recent advances are briefly mentioned. In the 27 accompanying chapters of the Symposium Proceedings various aspects of a variety of research areas will be described in depth. Four extensive compendia on vanadium chemistry and biochemistry have recently become available (1-3) and in addition to the many contributions in these compendia, a series of additional reviews focusing on various aspects of vanadium science have been reported (4-30).

In aqueous solution, both vanadate and vanadyl oxoions undergo a number of hydrolytic and self-condensation reactions which distinguish the aqueous chemistry (Fig. 1) from the chemistry in nonaqueous medium. These reactions are very sensitive to the pH of the solution and the presence of potential ligands which can coordinate to the vanadium and form a number of complexes with different coordination geometries. Furthermore complications arise because of the facile interconversion between oxidation states. Vanadate, under some conditions, is an oxidizing agent and can be readily reduced to either vanadium(IV) or (III) with production of an oxidized product. In the neutral and basic pH ranges, air oxidation will quickly regenerate vanadate unless the vanadium(IV) is tightly complexed to good stabilizing ligands. For instance, free aqueous vanadium(IV) in the form of vanadyl is stable to air oxidation only under acidic conditions. The appropriate use of reducing compounds can maintain the vanadium(IV) oxidation state and extend the stability of such systems to include physiological conditions.

Downloaded by 89.163.35.42 on October 31, 2012 | http://pubs.acs.org
Publication Date: December 10, 1998 | doi: 10.1021/bk-1998-0711.ch001

Natural Occurrences of Vanadium.

Vanadium is a ubiquitous element dispersed throughout the earth's crust, rivers, lakes, and oceans (1). In the earthÕs crust it exists naturally in a number of minerals in oxidation states III, IV and V. In most of the minerals the vanadium is found as an oxide but occasionally it assumes the role of a metal cation. Because of the extensive use of vanadyl sulfate ($VOSO_4$) and sodium metavanadate ($NaVO_3$) as insulin mimetic agents and in research, it is of interest to mention that they both occur naturally (31). In fossil fuels, vanadium is strongly complexed by various organic ligands and, because of this, can be concentrated to rather high concentrations - up to a few percent (32). Interestingly, the vanadium(IV) porphyrin is the most stable metal porphyrin complex known (33). In rivers, lakes and oceans, vanadium exists as the monomeric vanadium(V) oxoanion, vanadate, and given the pH of most natural waters, the most common form is $H_2VO_4^-$. The levels of vanadium are variable with an average concentration of about 10^{-5} g/L (7); the fresh water concentrations being quite variable and significantly higher than those of the oceans (1).

The burning or processing of vanadium-rich oils (such as the Boscan or Cerro Negro crudes from Venezuela) in the absence of proper precautions can lead to the release of significant amounts of airborne vanadium into the environment (1). Such releases are frequently in the form of the vanadium(V) oxide, V_2O_5, and other oxides. These compounds will disperse once they are released and upon reaction with water the

Downloaded by 89.163.35.42 on October 31, 2012 | http://pubs.acs.org
Publication Date: December 10, 1998 | doi: 10.1021/bk-1998-0711.ch001

soluble forms will generate vanadium(V) oxoanions which will be leached into the rivers, lakes and oceans where subsequent incorporation into sediments can occur (1).

There are several mechanisms by which vanadium can enter the food chain (1). The vanadium in soil and water is transported into plants such as beans, beets, barley, wheat and other foods. Vanadium often is accumulated in the roots and seeds of plants, and some foods such as cereal can contain significant vanadium concentrations. Although the function of vanadium in mammals is not yet known (Chapter 13) there is considerable evidence that suggest vanadium is an essential element (Chapter 23). The toxicity of vanadium has been documented in animals and humans; it appears that orally administered vanadium is the least toxic, and intravenously administered vanadium is the most toxic (Chapter 22). $VOSO_4$ for some time has been commercially available to the public as a nutritional supplement (Chapter 22 and 28). In addition, many dietary mineral supplements contain vanadium, a fact that has allowed continued human studies with vanadium salts despite and unfavorable therapeutic index in rodents (Chapter 28).

Aqueous Oxovanadium Chemistry.

Upon dissolution, vanadium in oxidation states III, IV and V can undergo hydrolytic, acid/base, condensation and redox reactions (Fig. 1). The implications of this are that

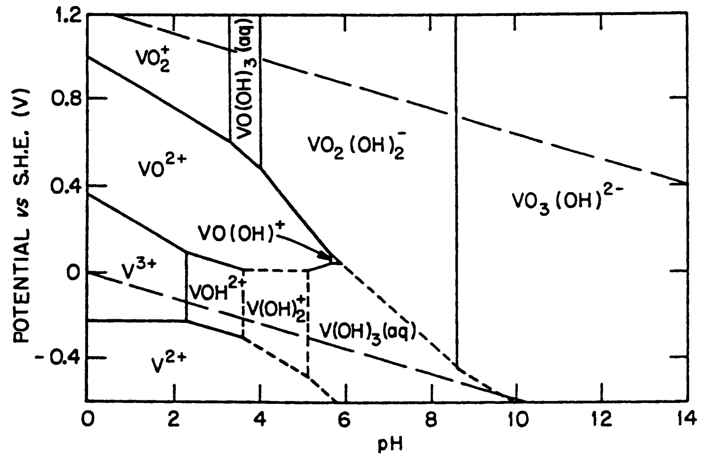

Fig. 1 Speciation diagram showing the oxidation state of vanadium species as a function of pH and reduction potential (versus standard hydrogen electrode). At boundary lines species in adjacent regions are present in equal concentrations. Boundaries indicated by short dashed lines are less certain than those indicated by bold lines. The upper and lower longer dashed lines indicate the upper and lower limits of the stability of water. Reproduced with permission from Ref. 4.

Copyright 1976 John Wiley & Sons.

these species are unlikely to remain in their solid-state form upon dissolution or ingestion. The situation is further complicated by the fact that the chemistry differs widely between the three oxidation states. This is readily illustrated by the fact that, in aqueous solution, both vanadium(III) and (IV) species are cationic while vanadium(V) species are anionic.

Much of the driving force for studies of vanadium compounds can be attributed to the recognition of the potential biochemical and therapeutic importance of this element. However, many of the recent advances in vanadium chemistry derive from the increased recognition that modern spectroscopic tools are exceptionally informative when applied to the study of vanadium compounds. Vanadium(V) is a diamagnetic d^0 metal and is conveniently studied using ^{51}V NMR spectroscopy, other NMR spectroscopies (ligand nuclei) and electronic and vibrational spectroscopies (2-3). Vanadium(IV) is a paramagnetic d^1 metal and is conveniently studied using EPR spectroscopy (2-3), electronic and vibrational spectroscopies and recent techniques such as ESEEM and ENDOR (3, 35) have expanded the structural information that can be obtained for these systems. In contrast to vanadium(IV) and (V), the techniques available for the study of paramagnetic d^2 vanadium(III) species are more restricted for use in structural characterization (2-3). A major problem with the study of the V(III) oxidation state is that EPR and associated techniques often do not provide useful structural probes. This, undoubtedly, is partially responsible for the slower pace of reports of new compounds and their characterization. In the following sections the three oxidation states will be described separately.

Vanadium(III). A fundamental problem encountered during the study of the aqueous chemistry of vanadium(III) is the limited potential and pH range over which this oxidation state is stable (2-3). The hydrolytic reactions and number of species formed in aqueous solution of this oxidation state appear to be as rich as the two higher oxidation states and include both monomeric and higher oligomeric cationic species. The deprotonation of the monomeric species $[V(H_2O)_6]^{3+}$ and $[V(OH)(H_2O)_5]^{2+}$ (Fig. 2) occurs readily since the pK_a values are about 2.6 and 4.2, respectively. The major monomeric species that is stable in the neutral pH range is thus $[V(OH)_2(H_2O)_4]^+$. Dimeric and trimeric species are also stable and form in solutions with millimolar vanadium concentrations. Characterization of the speciation of solvated vanadium(III)

Downloaded by 89.163.35.42 on October 31, 2012 | http://pubs.acs.org
Publication Date: December 10, 1998 | doi: 10.1021/bk-1998-0711.ch001

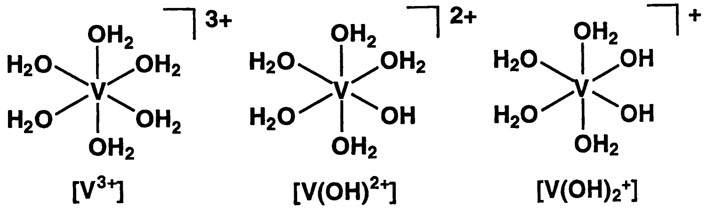

Fig. 2 Hydrated structures for V(III): $[V(H_2O)_6^{3+}]$, $[V(OH)(H_2O)_5^{2+}]$ and $[V(OH)_2(H_2O)_4^+]$ (see ref. 2).

often requires a combination of potentiometry and electrochemistry, the interpretation of which is often problematic (2). Complexes of vanadium(III) with sufficiently reducing ligands can exist in aqueous solution. Indeed, a large fraction of the vanadium in ascidians and other similar organisms is in oxidation state III (Chapter 19) indicating that the chemistry of this oxidation state is important in specific biological niches. Whether or not oxidation state III in the future will be implicated in redox chemistry of relevance to the insulin mimetic action of vanadium compounds remains to be determined.

Downloaded by 89.163.35.42 on October 31, 2012 | http://pubs.acs.org
Publication Date: December 10, 1998 | doi: 10.1021/bk-1998-0711.ch001

Vanadium(IV). Dissolution of $VOSO_4$ in acidic aqueous solutions yields the hydrated vanadyl cation ($VO(H_2O)_5^{2+}$ (Fig. 3)) commonly abbreviated as VO^{2+} (See Ref. 5a). This species is air stable in acidic solutions (6, 35, 36). Raising the pH into the physiological range generates several oligomeric and polymeric spin-paired species that are EPR silent. This complicates studies of "simple" vanadyl solutions in the physiological pH range. The speciation and aqueous equilibria have been described in detail elsewhere (5a, Chapter 7). Some of the polymeric forms are highly insoluble and result in precipitates (5a). In the neutral pH range, the aqueous equilibria limit the concentration of hydrated monomeric VO^{2+} to between 10^{-6} to 10^{-9} M (depending on specific pH) regardless of the amounts of $VOSO_4$ added to the solution (5a). However, because of vanadium(IV)'s high affinity for most oxygen-, nitrogen- and sulfur-containing ligands (9) complexation can prevent the formation of the polymeric precipitates. For example 100 mM hepes (N-2-hydroxyethylpiperazine-NÕ-2-ethanesulfonic acid) buffer will prevent precipitation in solutions prepared from a pH 2, 50 mM $VOSO_4$ (5a). Furthermore, the monomer-oligomer equilibria can be used advantageously since observation of EPR visible complexes in this pH range demonstrate the formation of a vanadium(IV)-protein (or vanadium(IV)-ligand complex).

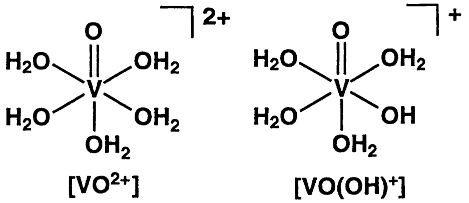

Fig. 3 Hydrated Structure for VO^{2+}: [$VO(H_2O)_5^{2+}$] and [$VO(OH)(H_2O)_4^{+}$] (see refs. 5a).

Vanadium(V). In the physiological pH range at concentrations below about 1 mM, vanadate exists predominantly in monomeric form as the $H_2VO_4^-$ anion (5b, 37, Chapters 2 and 3). This is true even when solids such as $NaVO_3$, NH_4VO_3, Na_3VO_4 and V_2O_5 have been used to prepare the stock solutions (38). The stoichiometries, charges, formation constants, pK_a values and ^{51}V NMR chemical shifts for the major vanadium(V) species in aqueous solution is summarized in Table 1. In addition, the proposed structures are shown in Fig. 4. All the protonation states can be described by the general formula $H_nVO_4^{(3-n)-}$ where n can take on integer values from 0 to 3. Thermodynamic measurements are consistent with four-coordinate vanadium atoms in both VO_4^{3-} and HVO_4^{2-} ions (39-40), supporting the analogy between vanadate monomer and inorganic phosphate (see below the discussion of biochemical relevance of phosphate analogy). However, observation of the neutral fully protonated species, H_3VO_4 (its pK_a value is estimated around 3.6), is limited at best to a narrow pH range around pH 3 (41). Further protonation of this species is favorable since structural rearrangements combined with hydrations give an octahedral complex, $VO_2(H_2O)_4^+$ frequently referred to as the cationic form of vanadium(V), VO_2^+ (41-42, see also Chapters 2 and 3).

The vanadate-phosphate analogy is apparent when examining the pK_a values for the vanadate monomer (see below for biologically relevant aspects). The pK_a values

Table 1 Stoichiometry, Formation Constants, pK_a values and ^{51}V NMR chemical shifts for the major Vanadium(V) Species in Aqueous Solution.[a]

Species	p,q	log b_{pq}[b]	pK_a	d(^{51}V) (ppm)[c]
VO_4^{3-}	-2,1	-21.31		-541.2
HVO_4^{2-}	-1,1	-7.91	13.4	-538.8
$H_2VO_4^-$	0,1		7.91	-560.4
VO_2^+	2,1	6.97		-545
$V_2O_7^{4-}$	-2,2	-15.13		-561.0
$HV_2O_7^{3-}$	1,2	-5.39	9.74	-563.5
$H_2V_2O_7^{2-}$	0,2	2.90	8.29	-572.7
$V_4O_{13}^{6-}$	-2.4	-8.5		-566 to -585[d]
$HV_4O_{13}^{5-}$	-1,4	0.4	8.9	-566 to -585[d]
$V_4O_{12}^{4-}$	0,4	10.04		-577.6
$V_5O_{15}^{5-}$	0,5	12.43		-586.0
$V_{10}O_{28}^{6-}$	4,10	51.98		-422, -496, -513
$HV_{10}O_{28}^{5-}$	5,10	58.12	6.14	-424, -500, -516
$H_2V_{10}O_{28}^{4-}$	6,10	61.80	3.68	-425, -506, -524
$H_3V_{10}O_{28}^{3-}$	7,10	63.37	1.57	-427, -515, -534

[a] Ionic strength = 0.6 M Na(Cl). Data taken from Ref. 2.

[b] log b for the equilibria $pH^+ + 1(H_2VO_4^-) = (H^+)_p(H_2H_2VO_4^-)_q$.

[c] d ^{51}V relative to $VOCl_3$.

[d] A value in the indicated range has been reported.

for the $H_2VO_4^-$ and HVO_4^{2-} ions are dependent on the nature and concentrations of the counter ions. At low ionic strength, the values are 8.7 (pK_{a2}) (39-40) and 12 (pK_{a3}) (5, 37), respectively. With the addition of an electrolyte, pK_{a2} is substantially decreased, to 8.3 in 1.0 M KCl (39) and to 8.0 in 3.0 M $NaClO_4$ (43)). Large

Downloaded by 89.163.35.42 on October 31, 2012 | http://pubs.acs.org
Publication Date: December 10, 1998 | doi: 10.1021/bk-1998-0711.ch001

changes in the pK_{a2} values have also been reported for aqueous-alcoholic mixtures (44).

Monomeric vanadate readily undergoes condensation reactions with many nucleophilic ligands, including other vanadate derivatives. In solutions containing millimolar and higher vanadium(V) concentrations, the major species in solution are the various oligomers shown in Fig. 4 (2-3, Chapter 2). Under acidic conditions, with pH values ranging from 3 to 6, the predominant oligomer is decavanadate, $V_{10}O_{28}^{6-}$ abbreviated V_{10}. This complex anion is the only major vanadium(V) oxoanion that is colored; it forms beautiful yellow-orange solutions. From pH 6 to 10, the major oligomeric species include a dimer (V_2), cyclic tetramer (V_4) and cyclic pentamer (V_5) which are all colorless (38-39, 42). Above pH 10, the anionic monomer is the favored species, whereas below pH 3 the cationic monomer is the major species. Additional oligomers, such as linear V_3, V_4, V_5 and V_6, are also formed in limited concentrations throughout various pH ranges (38, 42). Colorless oxovanadium(V) ions interconvert in aqueous solution, and stock solutions may contain a variety of oxoanions that quickly generate $H_2VO_4^-$ upon dilution into an *in vitro* or *in vivo* system at neutral pH. However, when obtaining colored (yellow-orange) stock solutions heating is often necessary to convert the hydrolytically more resistant V_{10} to the colorless oxoanions.

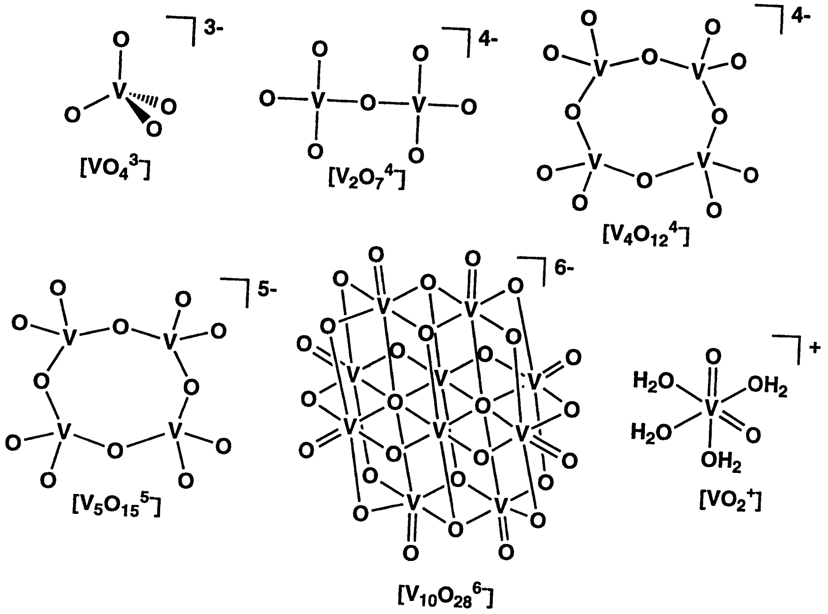

Fig. 4 Aqueous Structures for the deprotonated major oxovanadium(V) ions.

Often in the past, the condensation reactions generating the V_2, V_4 and V_5 species were not considered in biochemical studies, even when studies were carried out using

Downloaded by 89.163.35.42 on October 31, 2012 | http://pubs.acs.org
Publication Date: December 10, 1998 | doi: 10.1021/bk-1998-0711.ch001

millimolar or higher concentrations of vanadate. Perhaps surprisingly, the effect of each oxoanion is different since enzymes can distinguish between the different species (the lifetimes of the oxoanions are sufficiently long). This presents a major problem when interpreting the results of vanadate mixtures (2). For example, V_2 is a potent inhibitor of phosphoglycerate mutase (25, 45) while V_4 inhibits a series of enzymes involved in the pentose phosphate shunt (25, 46) and glucose metabolism (25, 47), of which some enzymes also are inhibited by V_2 (25, 46). Correct interpretation of the biochemical data from mixtures requires that each oxoanion species be considered separately (presumably these solutions are at equilibrium since only a few milliseconds is required to reach equilibrium in solutions of colorless oxovanadates). The nature of the interaction of these enzymes with oxometalates has not yet been structurally characterized although preliminary studies in this area have been reported (25, 29, 48-49). Although there is no doubt oxovanadium anions interact with enzymes binding phosphates and polyphosphates, affinity for these anions are also observed for other enzymes (devoid of such interactions). This suggests it would be a premature simplification to expect the interactions between vanadium(V) ions and proteins to be dictated by interactions observed for the corresponding phosphates (25, 29).

Downloaded by 89.163.35.42 on October 31, 2012 | http://pubs.acs.org
Publication Date: December 10, 1998 | doi: 10.1021/bk-1998-0711.ch001

Aqueous Interactions of Vanadium(IV) and (V) in Aqueous Solutions with Ligands

Both vanadium(IV) and (V) undergo a wide range of chemistry with a variety of ligands (1-3, 9). The biochemical importance of the reactions of vanadium with various functionalities is significant because enzymes and other biological molecules commonly contain hydroxylate, carboxylate, phenolate, imidazole, thiolate and other coordinating functionalities. When a residue is appropriately placed spatially, a reaction can occur between such a residue and vanadium, whether it be in the active site of an enzyme, deeply buried in a transport protein or freely dissolved in the cytoplasm of a cell. Given the analogy between vanadate and phosphate and the abundance of phosphate-binding environments in proteins and other biomolecules, it is reasonable to expect that many favorable binding environments for vanadate exist.

In the last decade, the growth in physiologically relevant aqueous vanadium chemistry has focused extensively on vanadium(V) systems (1-3). This focus, to a large extent, is based on the analogy between vanadate and phosphate but also has been driven by the versatility of NMR spectroscopy and its ability to quickly provide structural and equilibrium information on a complex reaction systems. One decade ago there was significantly more information available on vanadium(IV) systems (see for example 5a, 9) than for vanadium(V). However, as will be evident from the contributions in this Symposium Proceedings, at this time the aqueous reactions of vanadium(V) with biologically relevant ligands is now understood in greater detail than corresponding reactions of vanadium(IV). However, significant advances are also being made in this area (11 and Chapters 4, 6-7, 12, 19, 26-27). Recognizing the facility with which the vanadium(IV) and (V) oxidation state convert, it should be noted that often a detailed understanding of the reaction chemistry is lacking, particularly where redox reactions readily occur. As a consequence many aspects of aqueous vanadium chemistry remains unclear. The consequences of this lack of knowledge are particularly evident when interpreting the results of *in vivo* studies. In such cases it is often difficult to even specify the oxidation state of the active vanadium species.

Reactions of Vanadium(IV) with Inorganic Ligands. Hydrated vanadyl (commonly abbreviated VO^{2+}) reacts readily oxygen-, nitrogen- and sulfur-containing ligands (5a, 9). For example, vanadyl cation is known to form complexes with carbonate (2), phosphonates (51) and phosphates (51-52) and other inorganic ligands (1-3, 9). In addition, ligands such as pyridine, imidazole and other amine bases (53-54) and deprotonated sulfides (54) form complexes with vanadyl cation. Important ligands in this group include the nucleotides and nucleic acids where the phosphate group is involved in the coordination to the vanadium. Many of the structural details pertaining to the nucleotide complexation mode (and with other ligands) to vanadyl cation have been elucidated by ENDOR spectroscopy (2, 55, Chapter 7). Vanadyl cation also readily forms complexes with halides in aqueous solutions (50). Whether the adduct remains stable or undergoes redox or hydrolytic reactions determines the nature of the resulting complex. Accordingly, some of the ligands that successfully form complexes with vanadium(V) in aqueous solutions do not form stable vanadium(IV) complexes. Hydrogen peroxide is a particular interesting example of a ligand that does not form an isolatable vanadium(IV) complex.

Reactions of Vanadium(IV) with Organic Ligands. In Fig. 5 a selected number of coordination geometries observed in vanadium(IV) complexes with O and N donor functionalities are illustrated. Vanadyl cation forms strong complexes with carboxylate functionalities, and these complexes are typically more stable than corresponding complexes with aryloxide and alkoxide functionalities. However,

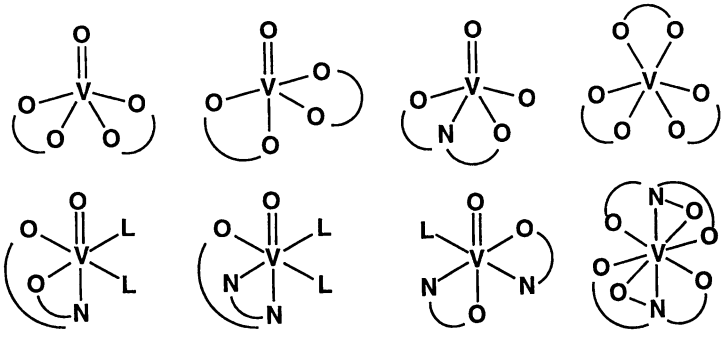

Fig. 5 Selected examples of coordination environments for vanadium(IV) with ligands containing O and N donor functionalities.

Downloaded by 89.163.35.42 on October 31, 2012 | http://pubs.acs.org
Publication Date: December 10, 1998 | doi: 10.1021/bk-1998-0711.ch001

neutral functionalities, such as the carbonyl group, also can be good ligands for vanadyl cation (53). Ligands such as aromatic amines, including pyridine and imidazole, form stronger complexes with vanadyl cation than alkyl amine bases (51). Since most biogenic ligands contain more than one functionality that has a significant affinity for reaction with the vanadyl cation, there is no shortage of potential reactions of vanadyl cation with biogenic ligands (51-55).

Many ligands of physiological interest contain more than one oxygen functionality and form strong complexes with vanadyl cation (2). Of particular interest are hydroxycarboxylic acids, phosphocarboxylates, nucleosides, nucleotides (see above) and catechols (51-55, Chapters 4, 6-7, 12). As an example, a-hydroxycarboxylates form particularly strong complexes with the vanadyl cation (52b-52c). Citric acid and tartaric acid and other hydroxycarboxylates such as glyceric and lactic acid are important metabolites, some of which are directly related to glucose metabolism. Nucleosides form complexes with vanadyl cation (2) although these complexes are not as strong as the corresponding complexes with nucleotides (52, Chapter 7). The high affinity that the vanadyl cation has for catechols (55) has been documented, but the colorful chemistry is not limited to this oxidation state (Chapter 19). Vanadyl cation reacts readily with peptides and forms mixtures of complexes that, in many cases, have only been characterized with respect to stoichiometry and stability (5a, 9). Recent work has included spectroscopic characterizations and they have shown that complexation is predominantly governed by strong coordination to the carboxylate moiety with only weak interactions with the amine nitrogen (56). Sulfur-containing ligands, particularly in conjunction with carboxylate moieties, such as cysteine and glutathione form strong complexes, at pH values near the pK_a value for the thiol (52, 56). Given the affinity of simple peptides for vanadyl cation it is not surprising that strong complexes are observed for proteins such as serum albumin (57).

A number of vanadium(IV) complexes have been examined for their insulin-mimetic activities (58-60). It has been shown that ligands such as bis(pyrrolidine-*N*-carbodithioate (58), cysteine and cystine (60), picolinic acid and other N,O-containing ligands (59) and recently N,N-ethylenediamine diacetic acid (58) form complexes that have promising insulin-mimetic activities. A vanadium-hydroxypyridone complex (of which the maltolato ligand is the most well-studied derivative) also had improved insulin-mimetic properties relative to simple vanadate and vanadyl salts (61-62, Chapter 26 and 27). In addition, *in vitro* studies with $VO(acac)_2$ demonstrated that this simple 1,3-diketonate vanadium(IV) complex induced a significantly greater insulin-mimetic response on lipogenesis than vanadyl sulfate (63, Chapters 6 and 24). Since most of these are known compounds, these newly-discovered biological effects have significantly increased the interest in the chemistry of these and related compounds. Chapter 6 describes the isomers that form in aqueous solutions of $VO(acac)_2$, Chapter 26 corresponding chemistry and pharmacology of the maltolato complex, and Chapter 27 details some of the structure-reactivity principles of known and novel vanadium(IV) complexes with N,O donor ligands.

Reactions of Vanadium(IV) with Ligands Of Particular Biological Interest. The strong complexation of vanadyl cation to a large number of inorganic and organic

Downloaded by 89.163.35.42 on October 31, 2012 | http://pubs.acs.org
Publication Date: December 10, 1998 | doi: 10.1021/bk-1998-0711.ch001

ligands (5a, 9) complicates biological studies with $VOSO_4$. In almost no biological study will vanadyl cation remain uncomplexed and thus the interpretation of what species is inducing the biological response is difficult. Even relatively innocuous buffers such as carbonate form complexes with vanadyl cation. Thus, in many studies the choice of buffer may be essential to the biological response that is to be studied. This may be advantageous since in some cases, the buffer can be chosen to facilitate the study and prevent precipitation of unwanted polymeric vanadium(IV) oxometalate (6). Equally beneficial is to use the vanadyl-buffer EPR signature to report on the presence free vanadyl cation (2, 5a, 35). Although the chemistry of VO^{2+} is significantly different from the chemistry of Mg^{2+} and Zn^{2+}, VO^{2+} has been reported to be able to substitute for these cations in enzymes (1-2, 5a, 64-66, Chapter 7). Perhaps the complex formation is responsible for the ability of vanadyl to catalyze the dephosphorylation of 2,3-bisphosphoglycerate (67).

An extensively studied vanadium(IV) complex is the natural product, amavadin (11, 68-72). This complex occurs in the mushroom genus *Amanita* and its biological role is still a topic of considerable interest (Chapter 18). Structurally this complex is of interest since amavadin is a rare example of a ÒbareÓ (non-oxo-containing (19)) vanadium(IV) complex with an uncommon eight-coordinate geometry. Since the first discoveries of these "bare" vanadium(IV) complexes, a series of these complexes have been reported (73-74). In addition to structure, this complex is unusually stable and only surpassed in stability by the vanadyl porphyrins.

Reactions of Vanadium(V) with Inorganic Ligands. Vanadate readily forms complexes with ligands containing oxygen, nitrogen and sulfur donor functionalities (1-3). Weak complexes form between vanadate and carbonate, phosphate, arsenate, chromate and similar ligands (2-3). The formation constant for the simple phosphovanadate is about 20 M^{-1} (75). This formation constant is sufficiently high that the care must be taken when using phosphate buffers in studies with vanadate since the speciation under such conditions is very different from that in other aqueous solutions. The biochemical and insulin-mimetic communities are particularly interested in the use of hydrogen peroxide as an inorganic ligand (O_2^{2-}) to vanadium(V). Numerous studies have been carried out on the simplest system, both on the complexation of vanadate by hydrogen peroxide (15, 19, 23, 76-80) and on the oxidative mechanisms available to the peroxo complexes formed (15, 19, 81). A number of peroxovanadium(V) complexes are produced, including mono, bis, tris and tetra peroxo complexes. An almost quantitative complexation of hydrogen peroxide by vanadate occurs under a range of conditions. The light or metal ion initiated disproportionation of peroxovanadium(V) complexes leads to the release of oxygen and water. The peroxovanadates tend to be excellent oxidants. However, in the absence of reducing substrates diperoxovanadium(V) compounds are generally quite stable hydrolytically in the neutral and slightly alkaline pH range.

Aqueous peroxovanadates coordinate a large number of ancillary ligands, including substituted carboxylic acids (82-84), amino acids (85), peptides (86, 87) and nucleosides (88) to form both mono and diperoxovanadium-ligand complexes. These types of complexes have been studied even more extensively than the parent systems because of their favorable catalytic properties and their potent insulin-mimetic

Downloaded by 89.163.35.42 on October 31, 2012 | http://pubs.acs.org
Publication Date: December 10, 1998 | doi: 10.1021/bk-1998-0711.ch001

properties. Numerous chapters in these proceedings are dedicated to various aspects of peroxovanadium chemistry, biochemistry and insulin-mimetic action. Chapters 6, 8-10, 12 and 25 describe structural aspects of peroxo complexes and Chapters 10 and 12 describe the relationship between structure and activity. It has been possible to modify the reactivity and properties of the oxidation system by changes in solvents and substrates. Chapters 10, 12 and 14-16 describe studies related to chemical and/or biochemical aspects of haloperoxidases and Chapters 6, 20-21, and 24-25 describe insulin-mimetic studies with peroxovanadium complexes and analogs.

The isoelectronic analog of the peroxo ligand, the hydroxylamido (NH_2O^-) group, and its vanadium complexes, has recently been of interest to the insulin-mimetic community (see Chapters 6 and 20). Several complexes were studied by the Wieghardt group more than two decades ago, where a range of different hydroxylamido vanadium complexes were characterized (89-92). Recently, the reaction of vanadate with hydroxylamine was examined in aqueous solution (93-94), and in combination with the structural characterization of related systems, it is clear that this hydrogen peroxide analog offers additional handles on investigation of chemical reactivity of peroxo-type metal complexes (93-95, Chapters 6 and 20). It appears the hydroxylamido complexes are kinetically more inert than peroxovanadium complexes. Some intriguing differences in reactivity also exist between the hydroxylamido and peroxo complexes (95, Chapter 20). For example, the reaction of the bis(N,N-dimethylhydroxamido)vanadate with sulfur-containing ligands such as cysteine results in generation of stable products (Chapter 20). Alkylated hydroxylamido vanadium(IV) complexes have been a long-standing interest due to the occurrence of the natural product amavadin (12, 68-72). Recently the corresponding vanadium(V) complexes have been reported (2, 68-69).

Reactions of Vanadium(V) with Monodentate Organic. The singly and doubly protonated vanadate ions, the species that exist under physiological conditions, react readily with hydroxylic compounds, alcohols or acids, to generate complexes often referred to as esters and acid anhydrides in line with the vanadate-phosphate analogy (1-3, 14). It is generally believed that these aqueous complexes will be four-coordinate. The formation constants for aliphatic and aromatic alcohols are very small, typically in the range of 0.2 M^{-1} for the formation of alkyl esters (44, 51) and about 1.0 M^{-1} for phenyl and tyrosyl vanadate esters (101). Carboxylic acids react with vanadate to form complexes in which the coordination number increases to five or six. Vanadium-carboxylates are sometimes referred to as vanadate anhydrides (102) due to their structural similarity to organic acid anhydrides.

Somewhat surprisingly, few studies providing evidence for formation of vanadium complexes of monodentate amide-containing ligands have been reported. Characterization of such products could be complicated by low formation constants and may explain the lack of observation of complexes with any aliphatic amines. Aromatic amines, such as pyridine and imidazole, have been found to form weak complexes with vanadate (102-103). However, in the presence of ancillary ligands, both aliphatic and aromatic amines form stable ternary complexes as has been reported in the cases of Tris buffer and imidazole (104).

Downloaded by 89.163.35.42 on October 31, 2012 | http://pubs.acs.org
Publication Date: December 10, 1998 | doi: 10.1021/bk-1998-0711.ch001

Although vanadate may form monodentate complexes with thiols, these have not been observed by ^{51}V NMR spectroscopy. However, it is generally believed that thiols reduce vanadate to give vanadyl cation and disulfides (1-3). Information concerning complexation and oxidation of thiol groups is not yet available and will be an area of future importance (see below).

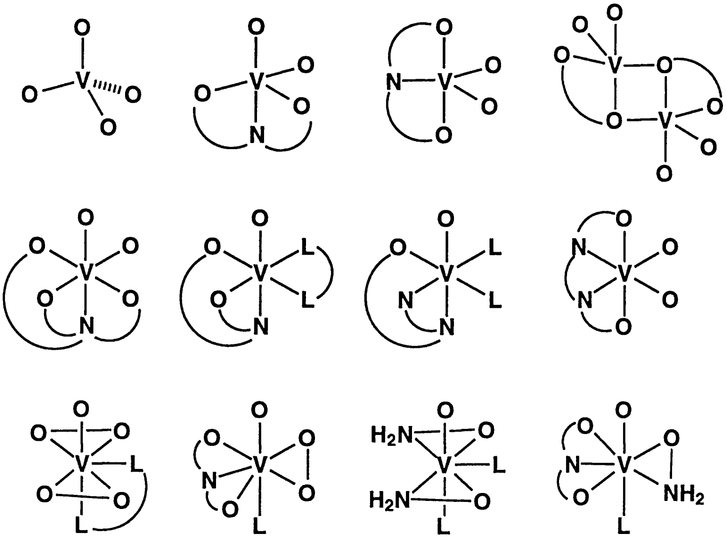

Fig. 6 Selected examples of coordination environments for vanadium(V) with ligands containing O and N donor functionalities.

Reactions of Vanadium(V) with Bidentate and Multidentate Organic Ligands. Ligands In some cases complexes of a multidentate ligand with vanadium(IV) and (V) are structurally quite similar (58, 68, 96-98) and in other cases they are very different (99-100). Although some structural patterns may be emerging, to little data is still available to establish firm guidelines. The many detailed studies of vanadium(V) systems, often including structural information, have resulted in a much better understanding of the vanadium(V) complexes in aqueous solution and most of this work will be summarized below (see also Fig. 6).

Vanadate readily reacts with 1,2-diols to form several products of which the major is a 2:2 complex (105-106). The initial interest in these types of complexes was generated in the 1970's when it was found that a nucleoside-vanadate complex was a potent inhibitor for ribonuclease A (107, Chapter 13). The structure of the 2:2 vanadium-nucleoside complex has been the source of many studies, presumably making this type of vanadium complex one of the best characterized species in solution (see the $[VO]_2$ core Fig. 6 and Chapter 2). Although the simple vanadate-nucleoside esters do form, their stability is much lower than the major 2:2 species. The 2:2 complex is significantly stabilized when the 1,2 diol is sterically locked in

Downloaded by 89.163.35.42 on October 31, 2012 | http://pubs.acs.org
Publication Date: December 10, 1998 | doi: 10.1021/bk-1998-0711.ch001

a ring system, as in for instance cyclohexane diols (108), pyranose forms of various monosaccharides (108) and in nucleosides (104, 109-111). So far the configuration generating the most stable complex is the cis coplanar arrangement of the 2Õ,3Õ-hydroxyls of the ribose ring in nucleosides.

Similar complexes with 1,3-diols have not been reported for aqueous solution despite various attempts to observe them (105, 108). The sensitivity of complex stability with respect to regio and conformational geometry of ligand geometry is apparent in this system. The recent successful structural characterization of a 2:2 vanadate-adenosine complex (110) and existing model systems (112-115) now allow examination of structural models of related complexes. These complexes (110, 112, 114-115) are built around a four-membered $[VO]_2$ core and the number of species observed in the NMR spectra for the cases of chiral 1,2-diols is now simply explained as structural isomers. The monomeric 1:1 form of this complex, which is particularly interesting from biochemical points of view, has only been indirectly observed. Spectroscopic evidence suggests that the dimerization constant is on the order of 10^6 or 10^7 M^{-1} and accordingly the 1:1 species will exist in comparably low concentrations regardless of its formation constant (116). Despite the favorable formation of these 2:2 complexes, tris(hydroxymethyl)aminomethane (117) and imidazole (104) have been shown to effectively compete and generate a vanadate-nucleoside-ligand ternary complex. The origin of the high stability for these ternary complexes is not yet known.

Several studies of the reaction of multidentate thiols and vanadate have been described (Chapters 4-5 and 20). Perhaps important is the recognition that vanadium(V) does form stable complexes with thiol-containing ligands, some of which have been structurally characterized (118-122). In addition, a recent solution study of vanadate with DTT showed the study of these complexes is quite tractable even in aqueous solution (118). Thus the general belief that thiols oxidize vanadate must be modified to recognize that many factors influence the rate of reduction (123) including the concentration of the components (123), the accessibility of the thiol (47), and the thermodynamic stability of all the possible vanadium-thiol and vanadium-disulfide complexes. That accessibility of the thiol can be important has been illustrated by the addition of vanadate to glycerol-3-phosphate dehydrogenase (47). Despite the presence of the thiol in the active site, the inhibition by vanadate is reversible and thus does not involve redox chemistry (47). Various recent reports of various complexes formed by a variety of sulfur-containing multidentate ligands is discussed in Chapter 4 while complexes formed between vanadate and thiolate and h^2-sulfenate ligands (120) are described in Chapter 5.

Numerous studies of the interactions of amino acids, peptides and peptide-like ligands with vanadate have been reported (124-129). Amino acids only form weak complexes with vanadate. The only well-characterized systems of this type are stabilized by the presence of an additional ligand, such ligands include SchiffÕs bases (130-131), a peroxo (86, 132, Chapter 6, 8-9) or a hydroxylamido (Chapter 6 and 20) groups. Dipeptides form complexes with vanadate coordinated through the carboxylate, the amine functionalities and the deprotonated nitrogen of the peptide bond (93-95, 128-129). Replacement of the carboxylate by a hydroxymethyl leads to the corresponding, albeit less stable, product involving the coordination of the

Downloaded by 89.163.35.42 on October 31, 2012 | http://pubs.acs.org
Publication Date: December 10, 1998 | doi: 10.1021/bk-1998-0711.ch001

hydroxymethyl group. These studies suggest that oligopeptides will form stable vanadate complexes involving the amide backbone, and side chains such as serine, lysine or glutamate should coordinate to vanadate as demonstrated in simple model peptides.

Reactivity of Aqueous Vanadium Complexes of Particular Biological Interest. The high affinity of vanadate for almost all functionalities makes it difficult (as in the case of vanadyl cation) to design experiments in which only free vanadate is present in solution (25). Since most reactions are reversible, an equilibrium solution will be formed that contains both free and complexed vanadate. The choice of buffer is also important since it will determine what types of additional species will be present in the solution and such species might compromise the observed results. Thiols and other reducing molecules (such as a-hydroxy ketones and aldehydes) may reduce vanadate to vanadyl cation and this may preclude the interpretations of the experimental observations. An example of how complications can arise is provided by the two redox buffers dithiothreitol (DTT) and 2-mercaptoethanol (63, 133). At high concentrations, both of these two closely related buffers convert vanadate to the vanadyl cation. This reduction of vanadate by DTT is sufficiently slow that a detailed study of complex formation with the latter has been reported (63, 133a). A characterization of the 2-mercaptoethanol system currently underway required studies by both NMR and EPR spectroscopy to define both the vanadium(IV) and (V) complexes (133b). Studies with gluthathione recently have suggested that this ligand, like DTT, only slowly reduces vanadate at pH 7.5 (63) even though other reports in the past documented the reduction of vanadate by various thiols (133a). If DTT or gluthathione do not significantly reduce vanadate during the course of a study but only complexes vanadate, then the presence of these redox buffers in the biological systems may not be as problematic as previously believed. A detailed characterization of the redox chemistry of such solutions and the dependence of redox chemistry on pH are of key interest to the biological community.

Vanadate has been found to cleave the myosin subfragment 1 upon irradiation (2-3, 134). This photocleaved S1 will form a new vanadate complex which, upon a second irradiation, will result in two fragments. The fact that the cleavage occurs at Ser-180 suggested a high degree of binding- and cleavage-specificity. Subsequently a series of similar studies with other enzymes was carried out (3). Recently a reaction mechanism was proposed in which oxygen adds to a free radical on the a-carbon of Ser-180 and is followed by a Criegee-type rearrangement (135). The effects of vanadium compounds on cleavage of DNA recently have been examined by several groups. The effects of vanadium compounds in different oxidation states also have been examined and cleavage of DNA has been reported in the presence (136-138) and absence (139) of hydrogen peroxide. The active species of the latter type of complex has been suggested to be a dinuclear vanadium(III) complex and appears to act through a combination of electrostatic and intercalative effects (139). Structural motifs from the extended solid of this compound and the possible interactions with DNA furthermore have also been modeled (140).

The chemistry of peroxovanadium ligand complexes has been of interest from the point of preparing both structural and functional analogs for the vanadium-dependent

Downloaded by 89.163.35.42 on October 31, 2012 | http://pubs.acs.org
Publication Date: December 10, 1998 | doi: 10.1021/bk-1998-0711.ch001

bromo- and haloperoxidases. The chemistry and biochemistry of these enzymes are the subjects of several chapters in these symposium proceedings, including Chapters 10 and 12 describing model chemistry of the haloperoxidases, Chapter 15 describing the substrate specificity of bromoperoxidase, and Chapters 14 and 16 describing the X-ray structure and analogy with the conserved active site in these enzymes with that of acid phosphatases.

Vanadate itself is a potent inhibitor of many enzymes, including protein tyrosine phosphatases (11, 140). It is generally believed this inhibition is mainly due to the ability of vanadate to act as a transition state analog and form a five-coordinate-vanadate-enzyme complex that mimic the transition states (or high energy intermediates) of enzyme catalyzed phosphate ester hydrolysis (9, 11, 24). The oxidative chemistry that peroxovanadium compounds undergo in the presence of protein tyrosine kinases is not observed with vanadate (see below), nor is it expected to be observed with other less redox-active vanadium compounds. One study has focused on testing the potency of vanadium complexes in different coordination geometries. Since compounds designed to structurally resemble the transition state are likely to have strong affinities for the protein, it is probable that the vanadium geometry of the transition state complex will be most inhibitory. If a five-coordinate-phosphate-enzyme complex is the transition state (or a high energy maximum), five-coordinate vanadium complexes should be the most potent inhibitors. Indeed, it was found that five-coordinate vanadium species is a more potent inhibitor than six- and seven-coordinate vanadium complexes (142, Chapters 13 and 24). However, all the vanadium compounds examined had a significant affinity as phosphatase inhibitors. This result suggest that other stabilizing factors are equally or more important than the structural analogy with the transition state.

A crucial aspect of the chemistry of peroxovanadium complexes is their reactions with sulfur groups. This type of reaction is important because thiol groups in compounds such as cysteine, glutathione and dithiothreitol are rapidly oxidized by peroxovanadate. Many enzymes contain essential thiol groups that are subject to oxidation. For example, it has been shown that the active site cysteine in protein tyrosine phosphatases 1B and Lar are rapidly oxidized by peroxovanadate but not by vanadate (141, and Chapters 20 and 24-25). These results document the importance of redox properties of vanadium compounds in inhibition of protein tyrosine phosphatases. Enzyme inactivation in a kinetic assay will manifest itself as enzyme inhibition. Thus a key question in kinetic studies with vanadium compounds is to determine whether the inhibition is of a reversible type or an irreversible (inactivation) type. In cells, processes that lead to inhibition of enzymes by vanadium derivatives may include both reversible and irreversible inactivation of the enzymes and the question should be considered whether the natural cellular generation of hydrogen peroxide, given its high affinity for vanadate, may be a mode of action.

Studies with the isoelectronic analogs of peroxovanadium derivatives may very well induce some of the same desirable insulin-mimetic responses as the peroxo complex. Indeed, the studies with bis(N,N-dimethylhydroxylamido)vanadate reveal this compound is a good micromolar inhibitor of at least two protein tyrosine phosphatases (Chapters 13 and 20). Interestingly, however, this compound is a reversible inhibitor (Chapter 20).

Downloaded by 89.163.35.42 on October 31, 2012 | http://pubs.acs.org
Publication Date: December 10, 1998 | doi: 10.1021/bk-1998-0711.ch001

The inhibition of phosphorylases (other than phosphatases) by vanadate has generally been explained by the phosphate-vanadate analogy in the phosphoester hydrolysis transition state (10, 13, 25). Thus, the five-coordinate near-trigonal bipyramidal geometry of the vanadate-enzyme complex will provide several stabilizing interactions not possible for phosphate, resulting in conversion of such a transition state to a stable vanadate-enzyme intermediate. In particularly favorable situations, the K_i for vanadate may be five or six orders of magnitude less than the K_m for the phosphorylated substrate (see below for detailed discussion of the related case of an organic vanadate transition state analog). One of the well-studied phosphorylases is ribonuclease (107, 143). In addition to kinetic and detailed chemical studies to examine the nature of the inhibiting complex, two early reports of an X-ray structure of the vanadate-uridine-ribonuclease complex were published (See Chapter 13). Despite the potency of the inhibition, recent evidence suggests that the inhibitor is only partially (about 40 or 50 %) capitalizing on all the possible stabilization enjoyed by a perfect mimic of the phosphate transfer step (143). Similar observations have been reported for phosphoglucomutase (144). This observation is consistent with the expectation that a number of factors would be involved in complexing the vanadium in the active site when compared to phosphate binding. Such factors included influences of the slightly longer V-O bonds when compared to P-O bonds, the difference in hydrogen-bond acceptor properties and other factors of the tight binding of a hydrophilic molecule to a protein. This group of enzymes includes ATPases, phosphatases, ribonucleases, mutases and other enzymes (2-3,10) and some of these enzymes may be linked to the insulin-mimetic properties of vanadate and other vanadium compounds (Chapter 13, 21-22).

Despite the small formation constants of aromatic and aliphatic vanadate esters, such complexes can undergo enzymatic catalysis by enzymes normally acting on the corresponding phosphate ester (4, 146-148). This effect is also related to the phosphate-vanadate analogy and the fact that vanadate esters are good structural mimics of tetrahedral phosphate esters (ground state structural analog). Glucose-6-phosphate dehydrogenase and its conversion of glucose-6-vanadate to gluconic acid is the most well-studied example (146-147). Another intriguing example of this type of chemistry and enzymology is the formation of the vanadate analog of NADP, NADV (147-148). The NADV forms readily from NAD and vanadate and, to date, NADV appears to be the NADP-analog with one of the best reported K_{at}/K_m ratios for alcohol dehydrogenase (148). Although this phenomena is quite general the complex analysis of the chemistry and the enzymology is presumable responsible for the few reports in this area (146-148).

A mechanism which is related to both mechanisms described above, is one in which vanadate might modify enzyme activity by forming a covalent intermediate in the active site (3, 10). For instance, if an enzyme must be phosphorylated on a tyrosine residue to become active, formation of a covalent vanadate-tyrosine ester could activate the enzyme. This attractive proposal was originally presented for the insulin receptor (10, 149, Chapter 22), and although speculative and difficult to prove, it presents an intriguing mechanistic possibility. The basis for this proposal, as opposed to a similar activation of an enzyme containing a serine or threonine phosphate functionality, lies in the relative thermodynamic stabilities of the two types

Downloaded by 89.163.35.42 on October 31, 2012 | http://pubs.acs.org
Publication Date: December 10, 1998 | doi: 10.1021/bk-1998-0711.ch001

of phosphoesters (149)). Threonine or serine phosphates thermodynamically are significantly more stable than tyrosine phosphates, there being about 4 orders of magnitude difference in the corresponding phosphate ester formation constants. On the other hand, the thermodynamic stability of serine and threonine vanadates are similar to tyrosine vanadates. In the inactive state, the equilibrium levels of phosphorylated enzyme is maintained by the catalytic activity of the appropriate phosphatase so that serine/threonine enzyme phosphate levels will be greater than enzyme tyrosine phosphate levels. Under similar conditions, but in the presence of vanadate rather than phosphate, the levels of serine, threonine and tyrosine vanadate esters will be similar. It is therefore possible, under biological conditions, to have vanadate levels such that serine/threonine vanadate ester concentrations are lower than or comparable to serine/threonine phosphate levels but simultaneously have tyrosine vanadate ester concentrations that are orders of magnitude higher than the corresponding tyrosine phosphate levels. A consequence of this is that it is possible that enzymes requiring a phosphotyrosine for their function could be activated while the serine/threonine type of enzyme remain inactive.

For tyrosine kinases that have an autophosphorylation function, formation of tyrosine vanadate could initiate a cascade effect that leads to a rapid buildup of the phosphorylated enzyme and a subsequent physiological response (10, 149).

Downloaded by 89.163.35.42 on October 31, 2012 | http://pubs.acs.org
Publication Date: December 10, 1998 | doi: 10.1021/bk-1998-0711.ch001

Nonaqueous Vanadium(IV) and Vanadium(V) Chemistry.

Most organic vanadium complexes have been prepared and characterized in nonaqueous solvents (2-3, 19-21). This can be attributed to 1) the lack of solubility of many desirable ligands, 2) the greater lability of many complexes in an aqueous environment, and 3) the applications of vanadium complexes as synthetic intermediates in organic synthesis (16, 21, 24, 31, Chapter 10). A great deal of interesting work has been reported in this area, but most of it is beyond the scope of this review. We have, however, chosen to highlight some areas which may be or become particularly relevant to those working in various areas related to bioinorganic vanadium chemistry.

Model Studies; Enzymes, Substrates, Inhibitors and Natural Products. Studies of synthetic models of bromo- and haloperoxidases have been exceedingly successful, and the research efforts have provided interesting and diverse approaches to this field (150-155, Chapters 9, 10, 11 and 12). Although many studies have attempted to structurally characterize the simple vanadate-amino acid complexes, for the more successful studies an additional ligand was included in the complex (153-155). Studies of this type often include comparisons of vanadium complexes in more than one oxidation state (96-97, 151, Chapter 12). The structural analogy between model systems and the enzyme active site has been demonstrated and studies are now focusing on the functional aspects of the haloperoxidase reaction (Chapter 10 and 12). Indeed one aspect of such considerations is the focus on substrate specificity of the haloperoxidases (Chapter 15).

The vanadium-dependent nitrogenase has also attracted a great deal of interest (Chapter 17) fueled by the X-ray structure of the vanadium cofactor complex (156).

Downloaded by 89.163.35.42 on October 31, 2012 | http://pubs.acs.org
Publication Date: December 10, 1998 | doi: 10.1021/bk-1998-0711.ch001

Much of this vanadium-sulfur chemistry involves lower oxidation states of vanadium and will not be further described here (156-159). Recently, a vanadium(V) homocitrate complex was characterized (156). This complex accurately mimics the coordination of homocitrate to the cofactor in the nitrogenase and facilitated a hypothesis concerning the function of homocitrate in the biosynthesis of FeMoCo. Such information and that from other model studies (158-159) provide guidance for future studies with a functional focus.

Significant effort has been placed on structurally documenting the structural analogy between vanadate and phosphate esters (14, 110, 112-115, 155, 160-163). In these studies, the goal was to isolate and crystallize vanadium(V) compounds in order to investigate the structural similarity between the ground state of phosphate esters and an associative transition state geometry of phosphate ester hydrolysis with the corresponding four- and five-coordinate vanadium(V) complexes. This goal has, only partially, been achieved. Indeed, four-coordinate vanadium(V) complexes have been prepared in organic solvents and structurally characterized (113, 155, 160). However, in none of these complexes is the vanadium center surrounded by exclusively oxo, alkoxy or sulfoxo ligands. A number of five-coordinate vanadium complexes document the structural analogy between the associative five-coordinate transition states of phosphate ester (or anhydride) hydrolysis and that of five-coordinate vanadium compounds. These complexes include both mono- and dinuclear complexes, most with distorted (110, 112, 115, 161-162) and others with more ideal (155, 163) trigonal bipyramidal geometries.

Significant progress has been made in structural characterization of vanadium(V) 1,2-diol complexes. Importantly, the five-coordinate geometry for the aqueous complex was substantiated by the characterization of the 2:2 adenosine complex (110), lending credibility to earlier model systems (112, 114). However, not all 1,2-diol systems are five-coordinate, as shown in several systems containing six-coordinate vanadium (164-165). Such complexes distinguish themselves from others in that they remain neutral by protonating one of the hydroxyl groups in the 1,2-diol. Solid-state and solution spectroscopic studies on a series of 1:2 vanadium(V)-1,2-diol complexes which resist characterization by X-ray crystallography also suggested coordination of a protonated hydroxyl group (114). Interestingly, in aqueous solutions the major species are not of the latter type, regardless of available functionalities on the ligand.

Vanadium carbohydrate chemistry has been plagued by the lack of readily available crystalline compounds for structural characterization and by the fact that too many complexes are formed for detailed structural solution characterization (28). Advances in this area has been made particularly in the more tractable systems involving vanadate-methyl glucoside complexes (108). Furthermore, a breakthrough in this area was achieved by the isolation and characterization by X-ray crystallography of a vanadium(V) complex with methyl 4,6-*O*-benzylidene-α-**D**-mannopyranoside (166), and a related structure of the vanadium(V) complex with quinic acid (1(R),3(R),4(R),5(R)-tetrahydroxycyclohexanecarboxylic acid) (167). These structural characterizations lend further credibility to the earlier work on related vanadium(IV) complexes (168) which were characterized to a more limited degree. In light of the potential applications of carbohydrates as chiral synthons (169), its seems likely that their utilization as vanadium complexes will develop in the future.

Downloaded by 89.163.35.42 on October 31, 2012 | http://pubs.acs.org
Publication Date: December 10, 1998 | doi: 10.1021/bk-1998-0711.ch001

Amavadin and the unique chemical properties of this natural product continue to intrigue scientists. Electrochemical studies of the redox chemistry have been explored and the reaction of thiols with amavadin analogs was examined (170). In addition, the fact that model vanadium(IV) complexes are easily oxidized to the corresponding vanadium(V) complex has allowed detailed structural solution studies to be carried out (68). Indeed, the vanadium(V) complex has virtually an identical ligand coordination geometry to the vanadium(IV) derivative. The preparation and study of new ligands systems continues to expand our knowledge of these fascinating compounds.

Catalytic Applications. As is described in detail in Chapters 10-12, the development of the vanadium chemistry of relevance to catalytic reactions remains an important area. The utilization of vanadium and other metal ions as catalysts in organic synthesis has recently been reviewed (16, 21, 31). Studies with the peroxovanadium picolinic acid system continue to generate novel and surprising results both with respect to mechanistic insights and potential applications (171-173). Other complexes such as the vanadium(V) salicylaldoximes show remarkable reactivity in the presence of several nitriles (174). In addition, novel systems are being developed (Chapter 11) that may form a bridge between the studies of heterogeneous catalysts with dispersed vanadium oxide (175). Some aspects of vanadium(V) nitrido chemistry has recently been examined (176-177), and an organometallic vanadium(V) dinitrogen complex has been structurally characterized (178).

Additional Vanadium Chemistry. The characterization of mixed-valence vanadium(IV,V) complexes has been of general worldwide interest. Indeed, using the definitions by Day (179) Type I, II and III complexes have now been structurally and magnetically characterized (131b, 180-185). These complexes are interesting not only from the perspective of their magnetic properties (180-181), but also because some of the catalytic reactions appear to go through dinuclear intermediate(s) (171) and thus mixed-valence species may be essential for some catalytic reactions. However, the biological properties of dinuclear vanadium compounds other than the simple oxoanion is an area needing exploration. The information available suggests that this group of compounds has unique potential (95, 139, Chapter 20).

Solid state studies of vanadium compounds, particularly those in which thermochemical synthesis was employed, have demonstrated the wealth of coordination geometries and possible interconnectivities available to many vanadium compounds. Structures of interesting complexes with phosphono ligands have been reported (186-188) while a variety of interesting oxometalate structures have also been described (186-193). In some of the latter complexes it was possible to correlate structure with sequential substitution of vanadium(V) by vanadium(IV) (193).

Summary.

It is evident from this material described in this brief review that the aqueous chemistry of vanadium is being developed at an explosive rate. Although to a great extend, this interest has been fueled by potential biochemical and therapeutic applications, it is clear that the applications go far beyond this. The catalytic applications of vanadium in chemistry and industry has been an important area of research for many years. As apparent from the chemistry covered in this review and the chapters in this Symposium Proceedings, the recent advances in aqueous chemistry is beginning to augment the catalytic applications of vanadium.

Acknowledgment.

We thank Dr. Kirk Cryer for assistance in preparation of this manuscript. DCC thanks the Institutes for General Medical Sciences at the National Institutes of Health and AST thanks NSERC Canada for financial support.

References.

1. Nriagu, J. O. Ed. *Vanadium in the Environment.* in *Adv. Environ. Science Technol.* John Wiley & Sons, Inc: New York, **1998**; Vols. 30 and 31.
2. A. Sigel, H.Sigel, A. Eds. *Vanadium and Its Role for Life; Metal Ions In Biological Systems*, Marcel Dekker, Inc.: New York. **1995**; Vol. 31. b. Srivastava, A. K.; Chiasson, J.-L. (Eds.) *Vanadium Compounds: Biochemical and Therapeutic Applications*: Focused issue in *Mol. Cell. Biochemistry*, **1995**; Vol. 153.
3. Chasteen, N. D. Ed. *Vanadium in Biological Systems*; Kluwer Academic Publishers: Dordrecht, The Nederlands, **1990**.
4. Baes, C. F.; Mesmer, R. E. *The Hydrolysis of Cations*; Wiley Interscience: New York, **1976**; pp 197-210.
5. a. Chasteen, N. D. in *Biological Magnetic Resonance*, Berliner, L.; Reuben, J.Eds. Plenum Press: New York, **1981**; Vol. 53, pp 53-119. b. Chasteen, N. D. in *Structure and Bonding*, Clarke, M. J.; Goodenough, J. B.; Ibers, J. A.; J¿rgensen, C. K.; Mingos, D. M. P.; Neilands, J. B.; Palmer, G. A.; Reinen, D.; Sadler, P. J.; Weiss, R.; Williams, R. J. P. Eds. Springer-Verlag: New York, **1983**; pp. 105-138.
6. Boyd, D. W.; Kustin, K. *Adv. Inorg. Biochem.* **1984**, *6*, 311-365.
7. Holloway, C. E.; Melnik, M. *Rev. Inorg. Chem.* **1985**, *7*, 75-159.
8. Nechay, B. R.; Nanninga, L. B.; Nechay, P. S. E.; Post, R. L.; Grantham, J. J.; Macara, I. G.; Kubena, L. Fl.; Philips, T. D.; Nielsen, F. H. *Fed, Proc.* **1986**, *45*, 123-132.
9. Vilas Boas, L. V.; Costa Pessoa, J. in *Comprehensive Coordination Chemistry. The Synthesis, Reactions, Properties and Application of Coordination Compounds*; vol. 3 Wilkinson, G.; Gillard, R. D.; McCleverty, J. A. Eds.; Pergamon Press: New York, 1987; pp. 453-583.
10. Gresser, M. J.; Tracey, A. S.; Stankiewicz, P. J. *Adv. Prot.Phosphatases* **1987**, *4*, 35-57.
11. Frausto da Silva, J. J. R. *Chem. Spec. Bioaval.* **1989**, *1*, 139-150.
12. Saito, K.; Sasaki, Y. *Pure Appl. Chem.* **1988**, *60*, 1123-1132.
13. Posner, B. I.; Shaver, A.; Fantus, I. G. in *New Antidiabetic Drugs*, Bailey, C. J.; Flatt, P. R. Eds.; Smith, Gordon; London, **1990**: Chapter 8, pp 107-118.
14. Howarth, O. W. *Prog. Nucl. Magn. Reson. Spec.* **1990**, *22*, 453-485.

Downloaded by 89.163.35.42 on October 31, 2012 | http://pubs.acs.org
Publication Date: December 10, 1998 | doi: 10.1021/bk-1998-0711.ch001

15. Wever, R.; Kustin, K. *Adv. Inorg. Biochem.* **1990**, *35*, 81-115.
16. Bonchio, M.; Conte, V.; Coppa, F.; Di Furia, F.; Modena, G. *in Dioxygen Activation and Homogeneous Catalytic Oxidation*; Sim^ndi, L. I. Ed.; Elsevier Science Publichers: Amsterdam, **1991**; pp 497-504.
17. Chen, Q.; Zubieta, J. *Coord. Chem. Rev.* **1992**, *114*, 107-167.
18. Shechter, Y. *Diabetes*, **1990**, *39*, 1-5.
19. Butler, A.; Carrano, C. J., *Coord. Chem. Rev.* **1991**, *109*, 61-105.
20. Rehder, D. *Angew. Chem., Int. Ed. Engl.* **1991**, *30*, 148-167.
21. Conte, V.; Di. Furia, F. in *Catalytic Oxidations with Hydrogen Peroxide as Oxidants*; Strukul, G. Ed.; Kluwer Academic Publishers: Dordrecht, **1992**; pp 223-252.
22. Muller, A.; Pope, M. T. Eds. *Polyoxometalates: From Platonic Solids to AntiRetroviral Activity*, Kluwer Academic: Dordrecht, **1993**; Several contributions in this compendium involve vanadium chemistry.
23. Stern, A.; Yin, X.; Tsang, S.-S.; Davison, A.; Moon, J. *Biochem. Cell Biol.* **1993**, *71*, 103-112.
24. a. Butler, A.; Walker, J. V. *Chem. Rev.* **1993**, *93*, 1937-1944. b. 49. b. Butler, A.; Clague, M. J.; Meister, G. *Chem. Rev.* **1994**, *94*, 625-638.
25. a. Crans, D. C. *Comm. Inorg. Chem.* **1994**, *16*, 1-33. b. Crans, D. C. *Comm. Inorg. Chem.* **1994**, *16*, 35-76.
26. Brichard, S. M.; Henquin, J. C. *Trends Pharmacol. Sci.* **1995**, 16, 265-270.
27. Domingo, J. L. 1996. *Reprod. Toxicol.* **1996**, *10*, 175-182.
28. Verchere, J.-F.; Chapelle, S.; Xin, F.; Crans, D. C. *Prog. Inorg. Chem.* **1997**, *47*, 837-945.
29. Hill, C. *Chem. Rev.* **1997**, *98*, 327-357.
30. Gouzerh, P.; Proust, A. *Chem. Rev.* **1998**, *98*, 77-170.
31. Hirao, T. *Chem. Rev.* **1997**, *97*, 2707-2724.
32. Roberts, W. L.; Campbell, T. J.; Rapp, G. R. *Encyclopedia of Minerals*, 2nd ed. Van Nostrand Reinhold Company; New York, **1990**.
33. Biggs, W. R.; Fetzer, J. C.; Brown, R. J.; Reynolds, J. G. *Liquid Fuels Technol.* **1985**, *3*, 397-421.
34. Walker, F. A.; Hui, E.; Walker, J. M. *J. Am. Chem. Soc.* **1975**, *97*, 2390-2397.
35. Mustafi, D.; Makinen, M. W. *Inorg. Chem.* **1988**, *27*, 3360-3368.
36. Francavilla, J.; Chasteen, N. D. *Inorg. Chem.* **1975**, *14*, 2860-2862.
37. Heath, E.; Howarth, O. W. *J. Chem. Soc., Dalton Trans.* **1981**, 1105-1110.
38. Crans, D. C.; Mahroof-Tahir, M.; Keramidas, A. D. *Mol. Cell. Biochem.* **1995**, *153*, 17-24.
39. Tracey, A. S.; Jaswal, J. S.; Angus-Dunne, S. J. *Inorg. Chem.* **1995**, *34*, 5680-5685.
40. Larson, J. W. *J. Chem. Eng. Data* **1995**, *40*, 1276-1280.
41. Cruywagen, J. J.; Heyns, J. B. B.; Westra, A. N. *Inorg. Chem.* **1996**, *35*, 1556-1559.
42. Pettersson, L.; Hedman, B.; Nenner, A.-M.; Andersson, I. *Acta Chem.Scand.* **1985**, *A 39*, 499-506.
43. Pettersson, L.; Andersson, I.; Hedman, B. *Chem. Scr.* **1985**, *25*, 309-317.
44. Tracey, A. S.; Galeffi, B.; Mahjour, S. *Can. J. Chem.* **1988**, *66*, 2294-2298.

Downloaded by 89.163.35.42 on October 31, 2012 | http://pubs.acs.org
Publication Date: December 10, 1998 | doi: 10.1021/bk-1998-0711.ch001

Downloaded by 89.163.35.42 on October 31, 2012 | http://pubs.acs.org
Publication Date: December 10, 1998 | doi: 10.1021/bk-1998-0711.ch001

45. Stankiewicz, P. J.; Gresser, M. J.; Tracey, A. S.; Hass, L. F. *Biochemistry* **1987**, *26*, 1264-1269.
46. Crans, D. C.; Schelble, S. M. *Biochemistry* **1990**, *29*, 6698-6706.
47. Crans, D. C.; Simone, C. M. *Biochemistry* **1991**, *30*, 6734-6741.
48. Crans, D. C. In *Polyoxometalates: From Platonic Solids to Anti-Retroviral Activity*; Müller, A. and Pope, M. T., Eds.; Kluwer Academic Publishers: The Netherlands, **1993**, pp. 399-406.
49. a. Crans, D. C.; Mahroof-Tahir, M.; Anderson, O. P.; Miller, M. M. *Inorg. Chem.* **1994**, *33*, 5586-5590. b. Farabakhsh, M.; Schmidt, H.; Rehder, D., *Chem. Ber./Recueil* **1997**, *130*, 1123-1127.
50. Selbin, J. *Chem. Rev.* **1965**, *65*, 153-175.
51. a. Sanna, D.; Micera, G.; Buglyó, P.; Kiss, T. *J. Chem. Soc., Dalton Trans.* **1996**, 87-92. b. Kiss, T.; Buglyó, P.; Sanna, D.; Micera, G.; Decock, P.; Dewaele, D., *Inorg. Chim. Acta* **1995**, *239*, 145-153. c. Micera, G.; Sanna, D.; Dessi, A.; Kiss, T.; Buglyó, P. *Gazz. Chim. Ital.* **1993**, *123*, 573-577. d. Branca, M.; Micera, G.; Dessi, A.; Sanna, D.; Raymond, K. N. *Inorg. Chem.* **1990**, *29*, 1586-1589.
52. a. Etcheverry, S. B.; Ferrer, E. G.; Baran, E. J. *Z. Naturforsch.* **1989**, *44b*, 1355-1358. b. Williams, P. A. M.; Baran, E. J. *J. Inorg. Biochem.* **1993**, *50*, 101-106. c. Alberico, E.; Dewaele, D.; Kiss, T.; Micera, G. *J. Chem. Soc., Dalton Trans.* **1995**, 425-430.
53. a. Tasiopoulos, A. J.; Vlahos, A. T.; Keramidas, A. D.; Kabanos, T. A.; Deligiannakis, Y. G.; Raptopoulou, C. P.; Terzis, A. *Angew. Chem. Int. Ed. Engl.* **1996**, *35*, 2531-2533. b. Keramidas, A. D.; Papaioannou, A. B.; Vlahos, A.; Kabanos, T. A.; Bonas, G.; Makriyannis, A.; Rapropoulou, C. P.; Terzis, A. *Inorg. Chem.* **1996**, *35*.
54. Cornman, C. R.; Zovinka, E. P.; Meixner, M. H. *Inorg. Chem.* **1995**, *34*, 5099-5100.
55. Mustafi, D.; Telser, J.; Makinen, M. W. *J. Am. Chem. Soc.* **1992**, *114*, 6219-6226.
56. Dessi, A.; Micera, G.; Sanna, D. *J. Inorg. Biochem.* **1993**, *52*, 275-286.
57. Chasteen, N. D.; Francavilla, J. *J. Phys. Chem.* **1976**, *80*, 867-871.
58. Kawabe, K.; Tadokoro, M.; Kojima, Y.; Fujisawa, Y.; Sakurai, H. *Chem. Lett.* **1998**, 9-10.
59. Sakurai, H.; Fujii, K.; Watanabe, H.; Tamura, H. *Biochem. Biophys. Res. Commun.* **1995** 214,1095-1101.
60. Watanabe, H.; Nakai, M.; Komazawa, K.; Sakurai, H. *J. Med. Chem.* **1994**, *37*, 876-877.
61. McNeill, J. H.; Yuen, V. G.; Hoveyda, H. R.; Orvig, C. *J. Med. Chem.* **1992**, *35*, 1489-1491.
62. Caravan, P.; Gelmini, L.; Glover, N.; Herring, F. G.; Li, H.; McNeill, J. H.; Rettig, S. J.; Setyawati, I. A.; Shuter, E.; Sun, Y.; Tracey, A. S.; Yuen, V. G.; Orvig, C. *J. Am. Chem. Soc.* **1995**, *117*, 12759-12770.
63. Li, J.; Elberg, G.; Crans, D. C.; Shechter, Y. *Biochemistry* **1996**, *35*, 8314-8318.
64. Zhang, C.; Markham, G. D.; LoBrutto, R. *Biochemistry*, **1993**, *32*, 9866-9873.
65. Lord, K. A.; Reed, G. H. *Arch. Biochem. Biophys.* **1990**, *281*, 124-131.

66. Watanabe, H.; Nakai, M.; Komazawa, K.; Sakurai, H. *J. Med. Chem.* **1994**, *37*, 876-877.
67. Stankiewicz, P. J. *Arch. Biochem. Biophys.* **1989**, *270*, 489-494.
68. Smith, P. D.; Berry, R. E.; Harben, S. M.; Beddoes, R. L.; Helliwell, M.; Collison, D.; Garner, C. D. *J. Chem. Soc., Dalton Trans.* **1997**, 4509-4516.
69. Armstrong, E. M.; Beddoes, R. L.; Calviou, L. J.; Charnock, J. M.; Collison, D.; Ertok, N.; Naismith, J. H.; Garner, C. D. *J. Am. Chem. Soc.* **1993**, *115*, 807-808.
70. Carrondo, M. A. A. F. d. C. T.; Duarte, M. T. L. S.; Pessoa, J. C.; Silva, J. A.; Frausto da Silva, J. J. R.; Vaz, M. C. T. A.; Vilas-Boas, L. F. *J. Chem. Soc., Chem. Commun.* **1988**, 1158-1159.
71. Kneifel, H.; Bayer, E. *J. Am. Chem. Soc.* **1986**, *108*, 3075-3077.
72. Bayer, E.; Koch, E.; Anderegg, G. *Angew. Chem. Int. Ed. Engl.* **1987**, *26*, 545-546.
73. Kabanos, T. A.; Slawin, A. M. Z.; Williams, D. J.; Woollins, J. D. *J. Chem. Soc. Dalton Trans.* **1992**, 1423-1427.
74. Kabanos, T. A.; Woollins, J. D. *J. Chem. Soc., Dalton Trans.* **1991**, 1347-1350.
75. Gresser, M. J.; Tracey, A. S.; Parkinson, K. M. *J. Am. Chem. Soc.* **1986**, *108*, 6229-6234.
76. Conte, V.; Di Furia, F.; Moro, S. *J. Molec. Catal.* **1994**, *94*, 323-333.
77. Harrison, A. T.; Howarth, O. W. *J. Chem. Soc., Dalton Trans.* **1985**, 1173-1177.
78. Jaswal, J. S.; Tracey, A. S. *Inorg. Chem.* **1991**, *30*, 3718-3722.
79. Djordjevic, C.; Vuletic, N.; Renslo, M. L.; Puryear, B. C.; Alimard, R. *Mol. Cell. Biochem.* **1995**, *153*, 25-29.
80. Shaver, A.; Ng, J. B.; Hall, D. A. *Mol. Cell. Biochem.* **1995**, *153*, 5-15.
81. Conte, V.; Di Furia, F.; Moro, S. *J. Molec. Catal.* **1995**, *104*, 159-169.
82. Siv^k, M.; Schwendt, P. *Trans. Met. Chem.* **1989**, *14*, 273-276.
83. Wieghardt, K. *Inorg. Chem.* **1978**, *17*, 57-64.
84. Shaver, A.; Ng, J. B.; Hall, D. A.; Soo Lum, B.; Posner, B. I. *Inorg. Chem.* **1993**, *32*, 3109-3113.
85. Tracey, A. S.; Jaswal, J. S. *Inorg. Chem.* **1993**, *32*, 4235-4243.
86. Einstein, F. W. B.; Batchelor, R. J.; Angus-Dunne, S. J.; Tracey, A. S. *Inorg. Chem.* **1996**, *35*, 1680-1684.
87. Jaswal, J. S.; Tracey, A. S. *J. Am. Chem. Soc.* **1993**, *115*, 5600-5607.
88. Djordjevic, C.; Wilkins, P. L.; Sinn, E.; Butcher, R. J. *Inorg. Chim. Acta* **1995**, *230*, 241-244.
89. Wieghardt, K.; Quilitzsch, U.; Nuber, B.; Weiss, J. *Angew. Chem. Int. Ed. Engl.* **1978**, *17*, 351-352.
90. Quilizsch, U.; Wieghardt, K. *Z. Naturforsch.* **1979**, *34b*, 640-641.
91. Quilizsch, U.; Wieghardt, K. *Z. Naturforsch.* **1981**, *36b*, 683-686.
92. Nuber, B.; Weiss, J. *Acta Cryst.*, **1981**, *B37*, 947-948.
93. Paul, P. C.; Angus-Dunne, S. J.; Batchelor, R. J.; Einstein, F. W. B.; Tracey, A. S. *Can. J. Chem.* **1997**, *75*, 183-191.
94. Paul, P. C.; Angus-Dunne, S. J.; Batchelor, R. J.; Einstein, F. W. B.; Tracey, A. S. *Can. J. Chem.* **1997**, *75*, 429-440.
95. Keramidas, A. D.; Miller, S. M.; Anderson, O. P.; Crans, D. C. *J. Am. Chem. Soc.* **1997**, *119*, 5447-5448.

Downloaded by 89.163.35.42 on October 31, 2012 | http://pubs.acs.org
Publication Date: December 10, 1998 | doi: 10.1021/bk-1998-0711.ch001

96. Kojima, A.; Okazaki, K.; Ooi, S. I.; Saito, K. *Inorg. Chem.* **1983**, *22*, 1168-1174.
97. Mahroof-Tahir, M.; Keramidas, A. D.; Goldfarb, R. B.; Anderson, O. P.; Miller, S. M.; Crans, D. C. *Inorg. Chem.* **1997**, *36*, 1657-1668.
98. Crans, D. C.; Keramidas, A. D.; Mahroof-Tahir, M.; Anderson, O. P.; Miller, S. M. *Inorg. Chem.* **1996**, *35*, 3599-3606.
99. Scheidt, W. R.; Countryman, R.; Hoard, J. L. *J. Am. Chem. Soc.* **1971**, *93*, 3878-3882.
100. Kangjing, Z.; Xiaoping, L. *J. Struct. Chem.* **1987**, *6*, 14-16.
101. Galeffi, B.; Tracey, A. S. *Can. J. Chem.* **1988**, *66,* 2565-2569.
102. Tracey, A. S.; Li, H.; Gresser, M. J. *Inorg. Chem.* **1990**, *29*, 2267-2271.
103. a. Tracey, A. S.; Gresser, M. J. *Inorg. Chem.* **1988**, *27*, 1269-1275. b. Elvingson, K.; Crans, D. C.; Pettersson, L. *J. Am. Chem. Soc.* **1997**, *119*, 7005-7012.
104. Crans, D. C.; Schelble, S. M.; Theisen, L. A. *J. Org. Chem.* **1991**, *56*, 1266-1274.
105. Gresser, M. J.; Tracey, A. S. *J. Am. Chem. Soc.* **1986**, *108*, 1935-1939.
106. Ray, W. J.,Jr.; Crans, D. C.; Zheng, J.; Burgner, J. W.,II; Deng, H.; Mahroof-Tahir, M. *J. Am. Chem. Soc.* **1995**, *117*, 6015-6026.
107. Lindquist, R. N.; Lynn, J. L.,Jr.; Lienhard, G. E. *J. Am. Chem. Soc.* **1973**, *95*, 8762-8768.
108. Tracey, A. S.; Gresser, M. J. *Inorg. Chem.* **1988**, *27*, 2695-2702.
109. Richter, J.; Rehder, D. *Z. Naturforsch.* **1991**, *46b*, 1613-1620.
110. Angus-Dunne, S. J.; Batchelor, R. J.; Tracey, A. S.; Einstein, F. W. B. *J. Am. Chem. Soc.* **1995**, *117*, 5292-5296.
111. Geraldes, F. G. C.; Castro, M. M. C. A. J. *Inorg. Biochem.* **1989**, *35*, 79-93.
112. Crans, D. C.; Felty, R. A.; Miller, M. M. *J. Am. Chem. Soc.* **1991**, *113*, 265-269.
113. Crans, D. C.; Felty, R. A.; Anderson, O. P.; Miller, M. M. *Inorg. Chem.* **1993**, *32*, 247-248.
114. Hambley, T. W.; Judd, R. J.; Lay, P. A. *Inorg. Chem.* **1992**, 31, 343-345.
115. Crans, D. C.; Felty, R. A.; Eckert, H.; Das, N. *Inorg. Chem.* **1994**, *33*, 2427-2438.
116. Tracey, A. S.; Leon-Lai, C. H. *Inorg. Chem.* **1991**, 30, 3200-3204.
117. Tracey, A. S.; Jaswal, J. S.; Gresser, M. J.; Rehder, D. *Inorg. Chem.* **1990**, 29, 4283-4288.
118. Paul, P. C.; Tracey, A. S. *J. Biol. Inorg. Chem.* **1997**, *2*, 644-651.
119. a. Tsagkalidis, W.; Rodewald, D.; Rehder, D., *Inorg. Chem.* **1995**, *34*, 1943-1945. b. Farabakhsh, M.; Nekola, H.; Schmidt, H.; Rehder, D., *Chem. Ber./Recueil* **1997**, *130*, 1129-1133.
120. Cornman, C. R.; Stauffer, T. C.; Boyle, P. D. *J. Am. Chem. Soc.* **1997**, *119*, 5986-5987.
121. Sakurai, H.; Taira, Z.-E.; Sakai, N. *Inorg. Chim. Acta.* **1988**, *151*, 85-86.
122. Zhang, Y.-P.; Holm, R. H. *Inorg. Chem.* **1988**, *27*, 3875-3876.
123. Garner, M.; Reglinski, J.; Smith, W. E.; McMurray, J.; Abdullah, I.; Wilson, R., *J. Biol. Inorg. Chem.* **1997**, *2*, 235-241.

Downloaded by 89.163.35.42 on October 31, 2012 | http://pubs.acs.org
Publication Date: December 10, 1998 | doi: 10.1021/bk-1998-0711.ch001

124. Rehder, D. *Inorg. Chem.* **1988**, *27*, 4312-4316.

125. Crans, D. C.; Bunch, R. L.; Theisen, L. A. *J. Am. Chem. Soc.* **1989**, *111*, 7597-7607.

126. Jaswal, J. S.; Tracey, A. S. *Can. J. Chem.* **1991**, *69*, 1600-1607.

127. Elvingson, K.; Fritzsche, M.; Rehder, D.; Pettersson, L. *Angew. Chem., Int. Ed. Engl.* **1994**, *48*, 878-885.

128. Tracey, A. S.; Jaswal, J. S.; Nxumalo, F.; Angus-Dunne, S. J. *Can. J. Chem.* **1995**, *73*, 489-498.

129. Crans, D. C.; Holst, H.; Keramidas, A. D.; Rehder, D. *Inorg. Chem.* **1995**, *34*, 2524-2534.

130. Vergopoulos, V.; Priebsch, W.; Fritzsche, M.; Rehder, D. *Inorg. Chem.* **1993**, *32*, 1844-1849.

131. a. Dutta, S. K.; Tiekink, E.R.T.; Chaudhury, M., *Polyhedron* **1997**, *16*, 1863-1871. b. Dutta, S.K.; Kumar, S. B.; Bhattacharyya, S.; Tiekink, E. R.; Chakravorty, A., *Inorg. Chem.* **1997**, *36*, 4954-4960.

132. Crans, D. C.; Keramidas, A. D.; Hoover-Litty, H.; Anderson, O. P.; Miller, S. M.; Lemoine, L. M.; Pleasic-Williams, S.; Vandenberg, M.; Rossomando, A. J.; Sweet, L. J., *J. Am. Chem. Soc.* **1997**, *119*, 5447-5448.

133. a. Macara, I. G.; Kustin, K.; Cantley, L. C. Jr. *Biochim. Biophys.. Acta.* **1980**, *629,* 95-106. b. Crans, D. C.; Zhang, B.; Keramidas, A. D.; Roberts, C. R. Manuscript in preparation.

134. Cremo, C. R.; Grammer, J. C.; Yount, R. G. *J. Biol. Chem.* **1989**, *264*, 6608-6611.

135. Grammer, J. C.; Loo, J. A.; Edmonds, C. G.; Cremo, C. R.; Yount, R. G. *Biochemistry* **1996**, *35*, 15582-15592.

136. Sreedhara, A.; Susa, N.; Patwardhan, A.; Rao, C. P. *Biochem. Biophys. Res. Comm.* **1996**, *224*, 115-120.

137. Hiort, C.; Goodisman, J.; Dabrowiak, J. C. *Mol. Cell. Biochem.* **1995**, *153*, 31-36.

138. Barr-David, G.; Hambley, T. W.; Irwin, J. A.; Judd, R. J.; Lay, P. A.; Martin, B. D.; Bramley, R.; Dixon, N. E.; Hendry, P.; Ji, J.-Y.; Baker, R. S. U.; Bonin, A. M. *Inorg. Chem.* **1992**, *31*, 4906-4908.

139. Otieno, T.; Bond, M. R.; Mokry, L. M.; Walter, R. B.; Carrano, C. J. *J. Chem. Soc., Chem. Commun.* **1996**, 37-38.

140. Dean, N. S.; Mokry, L. M.; Bond, M. R.; O'Connor, C. J.; Carrano, C. J. *Inorg. Chem.* **1996**, *35*, 2818-2825.

141. Huyer, G.; Liu, S.; Kelly, J.; Moffat, J.; Payette, P.; Kennedy, B.; Tsaprailis, G.; Gresser, M. J.; Ramachandran, C. *J. Biol. Chem.* **1997**, *272*, 843-851.

142. Crans, D. C.; Keramidas, A. D.; Drouza, C. *Phosphorus, Sulfur, and Silicon* **1996**, *109-110*, 245-248.

143. Leon-Lai, C. H.; Gresser, M. J.; Tracey, A. S. *Can J. Chem.* **1996**, 74, 38-48.

144. Ray, W. J.,Jr.; Puvathingal, J. M. *Biochemistry* **1990**, *29*, 2790-2801.

145. Drueckhammer, D. G.; Durrwachter, J. R.; Pederson, D. C.; Crans, D. C.; Daniels, L.; Wong, C.-H. *J. Org. Chem.* **1989**, *54*, 70-77.

146. Nour-Eldeen, A. F.; Craig, M. M.; Gresser, M. J. *J. Biol. Chem.* **1985**, *260*, 6836-6842.

Downloaded by 89.163.35.42 on October 31, 2012 | http://pubs.acs.org
Publication Date: December 10, 1998 | doi: 10.1021/bk-1998-0711.ch001

147. Crans, D., C.; Simone, C. M.; Blanchard, J. S. *J. Am. Chem. Soc.* **1992**, *114*, 4926-4928.

148. Crans, D. C.; Marshman, R. W.; Nielsen, R.; Felty, I. *J. Org. Chem.* **1993**, *58*, 2244-2252.

149. Tracey, A. S.; Gresser, M. J. *Proc. Natl. Acac. Sci. USA*, **1986**, *83*, 609-613.

150. a. Clague, M. J.; Keder, N. L.; Butler, A. *Inorg. Chem.* **1993**, *32*, 4754-4761. b. de la Rosa, R. I.; Clague, M. J.; Butler, A. *J. Am. Chem. Soc.* **1992**, *114*, 760-761.

151. a. Hamstra, B. J.; Houseman, A. L. P.; Colpas, G. J.; Kampf, J. W.; LeBrutto, R.; Frasch, W. D.; Pecoraro, V. L., *Inorg. Chem.* **1997**, *36*, 4866-4874. b. Colpas, G. J.; Hamstra, B. J.; Kampf, J. W.; Pecoraro, V. L. *J. Am. Chem. Soc.* **1996**, *118*, 3469-3478.

152. Bashirpoor, M.; Schmidt, H.; Schulzke, C.; Rehder, D. *Chem. Ber./Recueil* **1997**, *130*, 651-657.

153. Rath, S. P.; Mondal, S.; Ghosh, T. *Trans. Met. Chem.* **1996**, *21*, 309-311.

154. Mondal, S.; Dutta, S.; Chakravorty, A. *J. Chem. Soc., Dalton Trans.* **1995**, 1115-1120.

155. a. Asgedom, G.; Sreedhara, A.; Kivikoski, J.; Rao, C. P. *Polyhedron* **1997**, *16*, 643-651. b. Feher, F. J.; Waltzer, J. F. *Inorg. Chem.* **1991**, *30*, 1689-1694.

156. Wright, D. W.; Chang, R. T.; Mandal, S. K.; Armstrong, W. H.; Orme-Johnson, W. H., *J. Biol. Inorg. Chem.* **1996**, *1*, 143-151.

157. a. Reynolds, J. G.; Sendlinger, S. C.; Murray, A. M.; Huffman, J. C.; Christou, G. *Inorg. Chem.* 1995, 34, 5745-5752. b. Schmidt, H.; Bashirpoor, M.; Rehder, D., *J. Chem. Soc., Dalton Trans.* **1996**, 3865-3870.

158. Money, J. K.; Folting, K.; Huffman, J. C.; Christou, G. *Inorg. Chem.* **1987**, *26*, 944-948.

159. Kovacs, J. A.; Holm, R. H. *Inorg. Chem.* **1987**, *26*, 702-711.

160. Toscano, P. J.; Schermerhorn, E. J.; Dettelbacher, C.; Macherone, D.; Zubieta, J. *J. Chem. Soc., Chem. Commun.* **1991**, 933-934.

161. Priebsch, W.; Rehder, D. *Inorg. Chem.* **1990**, *29*, 3013-3019.

162. Hillerns, F.; Olbrich, F.; Behrens, U.; Rehder, D. *Angew. Chem. Int. Ed. Engl.* **1992**, *4*, 447-448.

163. a. Mokry, L.; Carrano, C. J. *Inorg. Chem.* **1993**, *32*, 6119-6121. b. Cornman, C. R.; Geiser-Bush, K. M.; Rowley, S. P.; Boyle, P. D. *Inorg. Chem.* **1997**, *36*, 6401-6408.

164. Rath, S. P.; Mondal, S.; Chakravorty, A. *Inorg. Chim. Acta* **1997**, *263*, 247-253.

165. Mondal, S.; Prasad Rath, S.; Dutta, S.; Chakravorty, A. *J. Chem. Soc., Dalton Trans.* **1996**, 99-103.

166. Zhang, B.; Zhang, S.; Wang, K. *J. Chem. Soc. Dalton Trans.* **1996**, 3257-6263.

167. Codd, R.; Hambley, T. W.; Lay, P. A. *Inorg. Chem.* **1995**, *34*, 877-882.

168 Sreedhara, A.; Rao, C. P.; Rao, B. J., *Carbo. Res.* **1996**, *289*, 39-53.

169. Piarulli, U.; Floriani, C. *Prog. Inorg. Chem.* **1996**, *45*, 393-391

170. Fátima, M.; da Silva, G. C.; da Silva, J. A. L.; Fraústo da Silva, J. J. R.; Pombeiro, A. J. L.; Amatore, C.; Verpeaux, J.-N. *J. Am. Chem. Soc.* **1996**, *118*, 7568-7573.

Downloaded by 89.163.35.42 on October 31, 2012 | http://pubs.acs.org
Publication Date: December 10, 1998 | doi: 10.1021/bk-1998-0711.ch001

171. Conte, V.; Di Furia, F.; Moro, S. *J. Phys. Org. Chem.* **1996**, *9*, 329-336.
172. Bonchio, M.; Conte, V.; Di Furia, F.; Modena, G.; Moro, S. *J. Org. Chem.* **1994**, *59*, 6262-6267.
173. Nugent, W. A.; RajanBabu, T. V.; Burk, M. J. *Science* **1993**, *259*, 479-483.
174. Grigg, J.; Collison, D.; Garner, C. D.; Helliwell, M.; Tasker, P. A.; Thorpe, J. M. *J. Chem. Soc., Chem. Commun.* **1993**, 1807-1809.
175. Tran, K.; Stiegman, A. E.; Scott, G. W. *Inorg. Chim. Acta* **1996**, *243*, 185-191.
176. Niemann, A.; Bossek, U.; Haselhorst, G.; Wieghardt, K.; Nuber, B. *Inorg. Chem.* **1996**, *35*, 906-915.
177. a. Sable, D. B.; Armstrong, W. H. *Inorg. Chem.* **1992**, *31*, 161-163. b. Murray, H. H.; Novick, S. G.; Armstorng, W. H., *J. Clus. Sci.* **1993**, *4*, 439-451.
178. Rehder, D.; Woitha, C.; Priebsch, W.; Gailus, H. *J. Chem. Commun., Chem. Commun.* **1992**, *4*, 364-365.
179. Robin, M. B.; Day, P. Adv. *Inorg. Chem. Radiochem.* Academic Press; New York, **1976**; pp. 247-422.
180. Schulz, D.; Weyhermüller, T.; Wieghardt, K.; Nuber, B. *Inorg. Chim. Acta* **1995**, *240*, 217-229.
181. Neves, A.; Wieghardt, K.; Nuber, B.; Weiss, J. *Inorg. Chim. Acta* **1988**, *150*, 183-187.
182. Holwerda, R. A.; Whittlesey, B. R.; Nilges, M. J. *Inorg. Chem.* **1998**, *37*, 64-68.
183. Mondal, S.; Ghosh, P.; Chakravorty, A. *Inorg. Chem.* **1997**, *36*, 59-63.
184. Kumagai, H.; Kawata, S.; Kitagawa, S.; Kanamori, K.; Okamoto, K.-I. *Chem. Lett.* **1997**, 249-250.
185. Nishizawa, M.; Hirotsu, K.; Ooi, S.; Saito, K. *J. Chem. Soc., Chem. Commun.* **1979**, 707-708.
186. Otieno, T.; Mokry, L. M.; Bond, M. R.; Carrano, C. J.; Dean, N. S. *Inorg. Chem.* **1996**, *35*, 850-856.
187. Soghomonian, V.; Chen, Q.; Haushalter, R. C.; Zubieta, J.; O'Connor, C. J. *Science* **1993**, *259*, 1596-1599.
188. Soghomonian, V.; Chen, Q.; Zhang, Y.; Haushalter, R. C.; O'Connor, C. J.; Tao, C.; Zubieta J., *Inorg. Chem.* **1995**, *34*, 3509-3519.
189. Soghomonian, V.; Haushalter, R. C.; Zubieta, J.; O'Connor, C. J., *Inorg. Chem.* **1996**, *35*, 2826-2830.
190.. Muller, A.; Hovemeier, K.; Rohlfing, R. *Angew. Chem. Int. Ed. Engl.* **1992**, *31*, 1192.
191. Chen, Q.; Zubieta, J. *Angew. Chem. Int. Ed. Engl.* **1993**, *32*, 261-263.
192. Chang, Y.-D.; Salta, J. Zubieta, J., *Angew. Chem. Int. Ed. Engl* **1994**, *33*, 325-327.
193. Kahn, M. I.; Chen, Q.; Goshorn, D. P.; Zubieta, J.; *Inorg. Chem.* **1993**, *32*, 672-680.

Downloaded by 89.163.35.42 on October 31, 2012 | http://pubs.acs.org
Publication Date: December 10, 1998 | doi: 10.1021/bk-1998-0711.ch001

Downloaded by MONASH UNIV on October 31, 2012 | http://pubs.acs.org
Publication Date: December 10, 1998 | doi: 10.1021/bk-1998-0711.ch002

Chapter 2

Studies of Vanadate-Organic Ligand Systems Using Potentiometry and NMR Spectroscopy

Lage Pettersson and Katarina Elvingson

Department of Inorganic Chemistry, Umeå University, SE-901 87 Umeå, Sweden

The aqueous speciation in some vanadium-organic ligand systems of biochemical interest has been determined by combined potentiometric (glass electrode) and quantitative ^{51}V NMR data. Data (25 °C, 0.600/0.150 M Na(Cl) medium) have been collected over wide pH, [V], [ligand]/[V] ranges and evaluated using the least squares computer program LAKE, which is capable of simultaneously treating multimethod data. The results from the following systems will be reported: i) vanadate-dipeptides (alanylhistidine / alanylglycine / prolylalanine) ii) vanadate-nucleosides (adenosine / uridine with and without imidazole present) and iii) vanadate-maltol. Formation constants are tabulated for both the inorganic vanadate and the vanadate-organic ligand species. Distribution diagrams are used to illustrate equilibrium conditions. Some structural remarks are given.

The present paper is a summary and extended discussion of earlier work by the authors (*1-6*) on the aqueous equilibria of some biologically important vanadium(V)-organic ligand systems. The ligands studied (Figure 1) were chosen because of their proposed biogenic or therapeutic action when complexed to vanadium. As knowledge of the complete speciation and accurate pH-independent formation constants in the systems studied was limited prior to our work, the contribution is significant. Combination of potentiometry and ^{51}V NMR spectroscopy is a powerful method for determining the complete speciation and has therefore been used. However, special precautions must be adopted. These will be discussed and commented upon in the Experimental section. To obtain accurate pH-independent formation constants of the vanadate - organic ligand species, the subsystems must be well known for the specific experimental conditions. A firm knowledge of the hydrolysis of V(V) is of special importance since the inorganic vanadate speciation is strongly dependent on the ionic medium.

In Vanadium Compounds; Tracey, A., et al.;
ACS Symposium Series; American Chemical Society: Washington, DC, 1998.

Downloaded by MONASH UNIV on October 31, 2012 | http://pubs.acs.org
Publication Date: December 10, 1998 | doi: 10.1021/bk-1998-0711.ch002

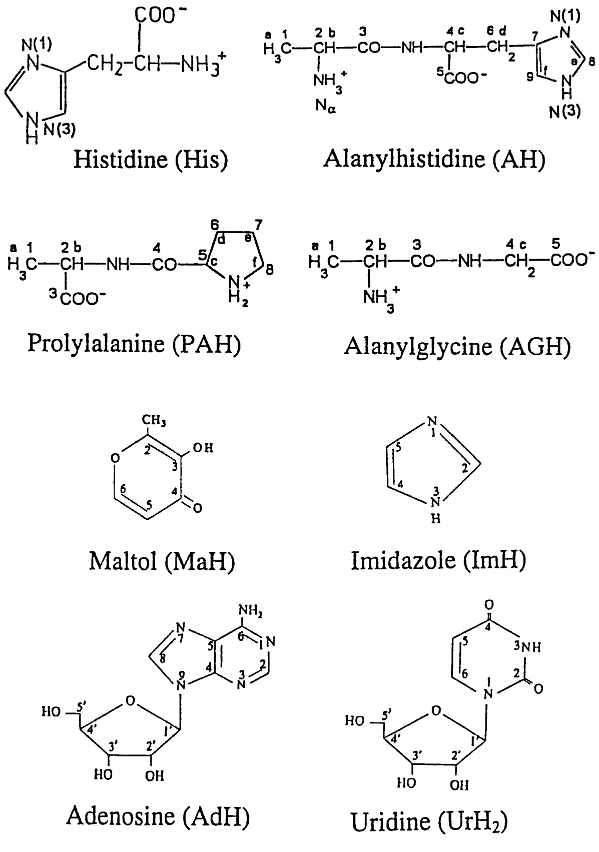

Histidine (His)

Alanylhistidine (AH)

Prolylalanine (PAH)

Alanylglycine (AGH)

Maltol (MaH)

Imidazole (ImH)

Adenosine (AdH)

Uridine (UrH_2)

Figure 1. Ligands studied.

For a more complete description of the systems, including references to the literature, and for experimental details, the reader is referred to References 1-6 and citations therein.

Experimental

In equilibrium analysis, the combination of potentiometric titrations and quantitative ^{51}V NMR measurements on solutions with accurately known pH values is a powerful method for determining the speciation. However, an ionic medium should always be used. When anion equilibria are being studied, the concentration of the cation in the medium should be kept constant. The present studies were performed in 0.600 or 0.150 M Na(Cl) at constant temperature (25 °C) and over a wide pH range. Buffers were not used by two reasons. They impose restrictions upon pH and some buffers can even interact with the system under study. Instead, pH was adjusted with HCl or NaOH. Interactions with undesirable carbonate species were avoided by protecting neutral and alkaline solutions from air. To avoid interference from vanadium(IV), all systems were checked for paramagnetism by ESR spectroscopy. For a relevant computational treatment of the experimental data, the total concentration of each component has to be exactly known. Moreover, when quantitative multimethod data are collected, access to a computer program capable to treat such data is of vital importance. In the present work, the LAKE program has been used.

Downloaded by MONASH UNIV on October 31, 2012 | http://pubs.acs.org
Publication Date: December 10, 1998 | doi: 10.1021/bk-1998-0711.ch002

Potentiometric Measurements. Potentiometric data were obtained from titrations and from separate pH measurements on individual samples.

All titrations were carried out with an automated, computer controlled potentiometric titrator. The free hydrogen ion concentration was determined by measuring the emf of the cell:

- Ag,AgCl / 0.600 M/0.150 M Na(Cl) // equilibrium solution / glass electrode +

The measured emf (in mV) is expressed according to:

$$E = E_0 + 59.157\cdot\log [H^+] + E_j$$

E_j is the liquid junction potential at the 0.600 M/0.150 M Na(Cl) // equilibrium solution interface and is, for the experimental setup used, given by

$$E_j/\text{mV} = -76/-331\cdot[H^+] + 42.5/143\cdot K_W\cdot [H^+]^{-1}$$

for 0.600 M/0.150 M Na(Cl).

$K_W = 1.875 \cdot 10^{-14}/1.746 \cdot 10^{-14}$ is the ionic product of water in 0.600 M/0.150 M Na(Cl) at 25 °C (*7,5*). E_0 is a constant determined separately in a solution with known $[H^+]$ immediately before and after each titration.

When titrations were unsuitable (slow equilibria, spontaneous reduction) and for ^{51}V NMR solutions, individual samples were prepared and pH measured with a combination electrode, which had been calibrated against buffer solutions of known $[H^+]$ in 0.600 M or 0.150 M Na(Cl).

^{51}V NMR Measurements. Spectra were recorded at 131.5 MHz (11.7 T) and 25 ± 1 °C, using a Bruker AM-500 spectrometer. The chemical shifts are reported relative to the external reference $VOCl_3$ (0 ppm). The field frequency stabilisation was locked to deuterium by placing the 8 mm sample tubes into 10 mm tubes containing D_2O. A 90° pulse angle was employed. Due to short relaxation times a relaxation delay of 10 ms was sufficient. By careful phasing and baseline correction of the spectra, resonances could generally be accurately evaluated.

Equilibria and Mass Balances. The equilibria studied are all written with the components H^+, $H_2VO_4^-$, LH(1) and LH(2). LH(1) refers to the zero charged ligand of interest: alanylhistidine (AH), histidine (HIS), prolylalanine (PAH), alanylglycine (AGH), maltol (MaH), adenosine (AdH) or uridine (UrH2). LH(2) refers to zero charged imidazole (ImH). Thus, the complexes are formed according to:

$$pH^+ + qH_2VO_4^- + rLH(1) + sLH(2) \rightleftharpoons (H^+)_p(H_2VO_4^-)_q\,(LH(1))_r\,(LH(2))_s{}^{p-q} \quad (1)$$

Overall formation constants are denoted $\beta_{p,q,r,s}$ and complexes are often given the notation (p,q,r,s) or $V_xL(1)_yL(2)_z{}^{n-}$. The total concentrations of vanadium, LH(1) and LH(2) are denoted $[V]_{tot}$, $[L(1)]_{tot}$ and $[L(2)]_{tot}$, respectively.

By combining the law of mass action with the conservation equation, the total concentrations of each component are given by equations (2) to (5):

$$H = h - K_wh^{-1} + \Sigma\Sigma p\beta_{p,q}h^pb^q + \Sigma\Sigma p\beta_{p,r}h^pc^r + \Sigma\Sigma p\beta_{p,s}h^pd^s + \Sigma\Sigma\Sigma p\beta_{p,q,r}h^pb^qc^r + \Sigma\Sigma\Sigma p\beta_{p,q,s}h^pb^qd^s + \Sigma\Sigma\Sigma p\beta_{p,r,s}h^pc^rd^s + \Sigma\Sigma\Sigma\Sigma p\beta_{p,q,r,s}h^pb^qc^rd^s \quad (2)$$

$$B = b + \Sigma\Sigma q\beta_{p,q}h^pb^q + \Sigma\Sigma\Sigma q\beta_{p,q,r}h^pb^qc^r + \Sigma\Sigma\Sigma q\beta_{p,q,s}h^pb^qd^s + \Sigma\Sigma\Sigma\Sigma q\beta_{p,q,r,s}h^pb^qc^rd^s \quad (3)$$

$$C = c + \Sigma\Sigma r\beta_{p,r}h^pc^r + \Sigma\Sigma\Sigma r\beta_{p,q,r}h^pb^qc^r + \Sigma\Sigma\Sigma r\beta_{p,r,s}h^pc^rd^s + \Sigma\Sigma\Sigma\Sigma r\beta_{p,q,r,s}h^pb^qc^rd^s \quad (4)$$

$$D = d + \Sigma\Sigma s\beta_{p,s}h^pd^s + \Sigma\Sigma\Sigma s\beta_{p,q,s}h^pb^qd^s + \Sigma\Sigma\Sigma s\beta_{p,r,s}h^pc^rd^s + \Sigma\Sigma\Sigma\Sigma s\beta_{p,q,r,s}h^pb^qc^rd^s \quad (5)$$

H is the total concentration of H^+ over the zero level of H_2O and chosen components. B, C and D are the total concentrations of vanadium and ligands, while h, b, c and d are the corresponding free concentrations.

Computer Programs. To obtain reliable deconvoluted integral data UXNMR/P version 1.1 and WIN-NMR version 950901.0 were utilized.

To determine the stoichiometry (p,q,r,s) and corresponding formation constants $(\beta_{p,q,r,s})$ of the complexes formed the least squares program LAKE was used (*8*). LAKE is able to calculate formation constants with standard deviations (3σ) from, for instance, potentiometric data obtained in titrations or from separate pH measurements, quantitative integral NMR data, NMR shift data or combined potentiometric-NMR data. Formation constants for systematically chosen complexes $(H^+)_p(H_2VO_4^-)_q$ $LH(1))_r\,(LH(2))_s{}^{p-q}$ are varied so that the error squares sum, $U = \Sigma\,(W_i \cdot \Delta A_i)^2$, is minimized. For NMR data, several complexes with the same or different nuclearities

Downloaded by MONASH UNIV on October 31, 2012 | http://pubs.acs.org
Publication Date: December 10, 1998 | doi: 10.1021/bk-1998-0711.ch002

can be included in the same peak integral. Thus, it is possible to test whether a resonance originates from more than one species. The complex, or set of complexes, giving the lowest *U*-value represents the model, which best explains the experimental data. A_i can be either the total concentration of components, free species concentrations, NMR peak integrals, chemical shifts or combinations of these. W_i is a weighting factor that must be chosen to give the different types of data their proper contributions to the sum of residuals. In this work a weighting factor was used which gives the NMR peak integrals a larger contribution to the sum of residuals than the potentiometric data. In addition, a weighting factor, which gives different vanadium concentrations similar contributions to the error squares sum, was often employed.

The program SOLGASWATER (*9*) was used for modeling, and for calculation and plotting of distribution diagrams.

Downloaded by MONASH UNIV on October 31, 2012 | http://pubs.acs.org
Publication Date: December 10, 1998 | doi: 10.1021/bk-1998-0711.ch002

Evaluation of Equilibria. To obtain precise pH-independent formation constants of the vanadate - organic ligand species, the hydrolysis constants of V(V) and the acidity constants of the ligand must be well known for the specific ionic medium. Thus, the equilibria of the systems can be summarized by three main reactions: the hydrolysis of vanadium, the protonation of the ligands and the formation of three and four component complexes.

The two component H^+-vanadate system in 0.600 and 0.150 M Na(Cl) media was known from earlier work (*10,5*). The acid-base properties of the ligands were evaluated using potentiometric titration data. The three and four component equilibria were evaluated using a combination of potentiometric and ^{51}V NMR data. In the LAKE calculations potentiometric data consisted of both titration data and separately measured pH values. For NMR data only integral data were used, since no decisive ^{51}V chemical shift differences occurred for the complexes formed.

Results and Discussion

The H^+-vanadate System. The hydrolysis of pentavalent vanadium, V(V), is very complex. It was not until the powerful combination of potentiometry and ^{51}V NMR spectroscopy was used, that the speciation was determined in the whole pH region and for a single ionic medium [0.600 M Na(Cl)] (*10*).

In highly alkaline solutions a mononuclear tetrahedral anion, VO_4^{3-}, is the only existing species. In less alkaline solutions (pH ca. 11) the monoprotonated monomer HVO_4^{2-} and its dimer, $V_2O_7^{4-}$, are the main species. When lowering the pH further, linear trimeric, tetrameric and probably pentameric species are formed as well, all having tetrahedrally coordinated vanadium chain structures. At neutral pH, in the so-called metavanadate range, $H_2VO_4^-$, $H_2V_2O_7^{2-}$, and cyclic oligovanadate species ($V_4O_{12}^{4-}$, $V_5O_{15}^{5-}$ and $V_6O_{18}^{6-}$) with a charge of -1 per vanadium are formed. In these colourless species vanadium is believed to be tetrahedrally coordinated to oxygen.

In the slightly acidic pH region yellow/orange decavanadate complexes are formed, $H_nV_{10}O_{28}^{(6-n)-}$, n = 0-3. In these species vanadium is octahedrally coordinated to oxygen. Upon further acidification the decamers decompose to the pale yellow monomeric cation, VO_2^+. Protonation of $H_2VO_4^-$ to form VO_2^+ occurs virtually in a single step, and the existence of an uncharged monomer has been questioned (*11,12*).

Subsequent redetermined formation constants in the 0.600 M Na(Cl) medium and constants obtained in 0.150 M (*5*) and 0.010 M Na(CI) medium (Andersson, I.; Pettersson, L., unpublished data) are given in Table I.

Owing to the great variety of nuclearity (1 to 10) and charge (-6 to +1) of the species formed, the relative abundance of the mono-, di-, tri-, tetra-, penta-, hexa-, and deca-species is dependent not only on pH and the total vanadium concentration, but also on the ionic strength of the medium (*13,14*). The medium dependence is illustrated in distribution diagrams (Figure 2) for three different Na(Cl) media. At physiological pH, in the so-called metavanadate range, the relative abundance of the mono-, di-, tetra-, and penta-species differ considerably. In the strongest medium (artificial seawater medium) the tetramer is the predominating species but on a fourfold dilution of the medium (physiological medium), the monomer starts to predominate and markedly so in the most diluted medium studied. Evidently, the ionic medium (especially the cation concentration) must be kept constant when studying vanadate equilibria.

Downloaded by MONASH UNIV on October 31, 2012 | http://pubs.acs.org
Publication Date: December 10, 1998 | doi: 10.1021/bk-1998-0711.ch002

The H^+-Vanadate-Histidine and H^+-Vanadate-Dipeptide Systems. In order to model vanadium binding to proteins, the complexation between vanadate (V) and the amino acid histidine (His) and with the dipeptides alanylhistidine (AH), alanylglycine (AGH) and prolylalanine (PAH) was studied. The structures of the ligands are shown in Figure 1.

Histidine was shown to form complexes with vanadate in a wide pH range. ^{51}V NMR spectra show two sharp resonances originating from V-His complexes; at –544 ppm and -571 ppm. Complexation occurs at pH 3, reaches a maximum at around pH 5.4 and ends at pH approximately 8. However, owing to spontaneous reduction of V(V) to V(IV), the speciation could not be determined (*1*).

In all the *dipeptide* systems studied, V-AH, V-AGH and V-PAH (0.600 M Na(Cl)), a single V-ligand ^{51}V resonance is obtained at -518, -512, and -495 ppm, respectively. The shift values are all independent of pH and for all three dipeptides, complexation occurs in a wide pH range from around 3 to 10. Equilibrium was shown to be reached after 5 h in the V-AH and V-AGH systems, and after 60 h in the V-PAH system. The V-AH and V-PAH complexes are remarkably stronger than the V-AGH complex. The reason for this could be that hydrogen bonding between the N-heterocycles in solution provides an additional stabilization. Evaluation of the combined potentiometric and quantitative ^{51}V NMR data shows that for all systems a -1 charged 1:1 vanadate-to-dipeptide complex is formed. For the V-PAH and V-AGH systems, data are completely explained by this single species. For the V-AH system, an additional non-charged complex is formed. Formation constants for the complexes, as well as acidity constants for the uncomplexed dipeptides are summarized in Table II. The pK_a value of the uncharged VAH species (6.89) is very similar to one of the pK_a values of the ligand itself (6.85), which strongly indicates that the imino nitrogen of the imidazole ring provides the protonation site. Thus, if the protonation/deprotonation site is at a distance from the vanadium atom and no NMR shift changes occur, potentiometric data are necessary to obtain the complete speciation.

The difference in complexation strength is illustrated in Figure 3. The distribution diagram is calculated using the constants in Table II and the vanadate constants from Table I (0.600 M Na(Cl) medium). This is a model calculation since the five-component equilibria has not been studied. However, as mixed ligand complexes are not likely to be formed, the distribution diagram should reflect a true equilibrium

Downloaded by MONASH UNIV on October 31, 2012 | http://pubs.acs.org
Publication Date: December 10, 1998 | doi: 10.1021/bk-1998-0711.ch002

Table I. Formation Constants of the H^+ - HVO_4^- System Obtained in Different Na(Cl) Media

(p,q)	Formula	NMR Assign.	logβ			pK_a		
			0.600M	0.150M	0.010M	0.600M	0.150M	0.010M
-2,1	VO_4^{3-}	V_1^{3-}	-21.31	-	-	-	-	-
-1,1	HVO_4^{2-}	V_1^{2-}	-7.946	-8.17	-8.467	13.36	-	-
0,1	$H_2VO_4^-$	V_1^-	0	0	0	7.946	8.17	8.467
2,1	VO_2^+	V_1^+	6.919	7.00	7.139	-	-	-
-2,2	$V_2O_7^{4-}$	V_2^{4-}	-15.23	-16.19	-	-	-	-
-1,2	$HV_2O_7^{3-}$	V_2^{3-}	-5.44	-5.85	-6.45	9.79	10.34	-
0,2	$H_2V_2O_7^{2-}$	V_2^{2-}	2.79	2.65	2.47	8.23	8.50	8.92
-2,4	$V_4O_{13}^{6-}$	$l\text{-}V_4^{6-}$	-8.60	-9.98	-	-	-	-
-1,4	$HV_4O_{13}^{5-}$	$l\text{-}V_4^{5-}$	0.13	-0.63	-	8.73	9.35	-
0,4	$V_4O_{12}^{4-}$	V_4^{4-}	9.89	9.24	8.38	-	-	-
0,5	$V_5O_{15}^{5-}$	V_5^{5-}	12.16	11.17	-	-	-	-
0,6	$V_6O_{18}^{6-}$	V_6^{6-}	13.9	-	-	-	-	-
4,10	$V_{10}O_{28}^{6-}$	V_{10}^{6-}	51.76	50.28	-	-	-	-
5,10	$HV_{10}O_{28}^{5-}$	V_{10}^{5-}	57.83	56.90	56.32	6.07	6.62	-
6,10	$H_2V_{10}O_{28}^{4-}$	V_{10}^{4-}	61.43	61.07	61.14	3.61	4.17	4.82
7,10	$H_3V_{10}O_{28}^{3-}$	V_{10}^{3-}	62.64	62.93	63.63	1.21	1.86	2.49

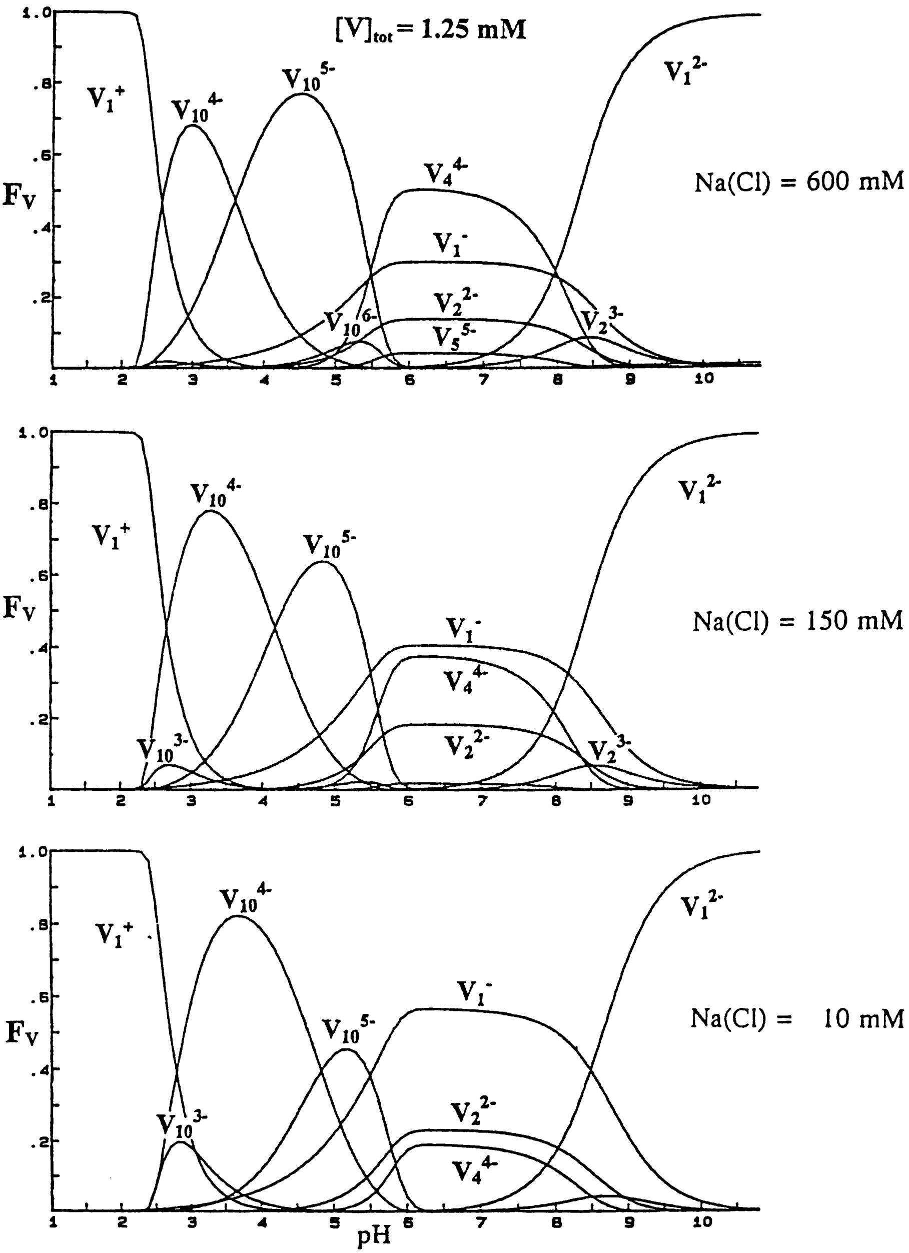

Figure 2. Distribution diagrams for $[V]_{tot} = 1.25$ mM at three different Na(Cl) media. F_v is defined as the ratio between $[V]$ in a given species and $[V]_{tot}$ in the solution. Formation constants used for the calculations are from Table I.

Downloaded by MONASH UNIV on October 31, 2012 | http://pubs.acs.org
Publication Date: December 10, 1998 | doi: 10.1021/bk-1998-0711.ch002

Downloaded by MONASH UNIV on October 31, 2012 | http://pubs.acs.org
Publication Date: December 10, 1998 | doi: 10.1021/bk-1998-0711.ch002

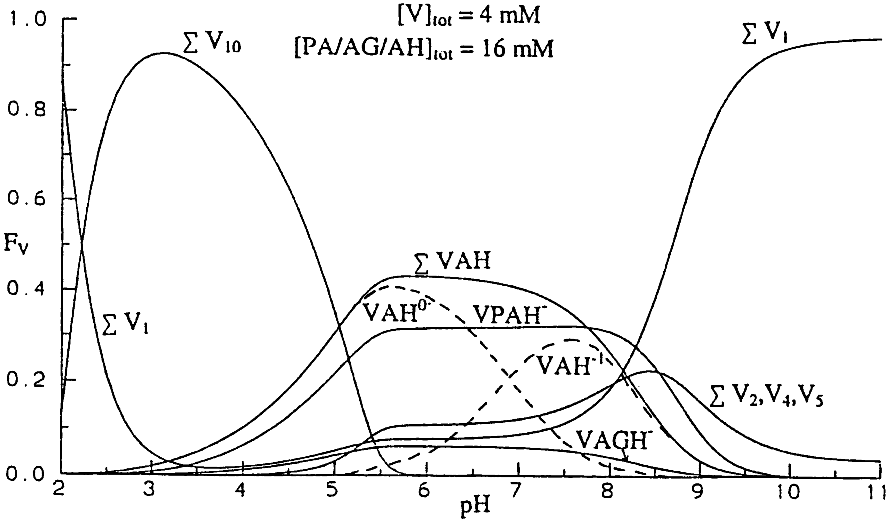

Figure 3. Distribution of vanadium at $[V]_{tot} = 4$ mM and $[\text{peptide}]_{tot} = 16$ mM.

(Reproduced with permission from reference 2. Copyright 1997 Acta Chemie Scandinavica.)

condition. It is evident that the amount of vanadium bound to AGH is much lower than that bound to PAH or AH, regardless of pH.

Table II. Formation Constants (β) in the Dipeptide Systems

(p,q,r,s)	Notation	$\log \beta$ (3σ)	pK_a
2,0,1,0	AH^{2+}	9.609 (20)	2.76
1,0,1,0	AH^{+}	6.845 (11)	6.85
0,0,1,0	AH	0	8.08
-1,0,1,0	AH^{-}	-8.076 (19)	-
1,0,1,0	PAH_2^{+}	3.27 (1)	3.27
0,0,1,0	PAH	0	8.79
-1,0,1,0	PA^{-}	-8.79 (1)	-
1,0,1,0	AGH_2^{+}	3.15 (2)	3.15
0,0,1,0	AGH	0	8.11
-1,0,1,0	AG^{-}	-8.11 (2)	-
1,1,1,0	VAH	9.44 (5)	6.89
0,1,1,0	VAH^{-}	2.55 (4)	-
0,1,1,0	$VPAH^{-}$	2.44 (2)	-
0,1,1,0	$VAGH^{-}$	1.715 (9)	-

The H^+-Vanadate-Nucleoside-Imidazole systems. The coordination of both vanadium(V) and vanadium(IV) to nucleotides and their constituents *(e.g.* nucleosides) are known to be potent inhibitors of several enzymes such as ATPases and ribonucleases (*15*).

We have in the pH range 2 – 11 studied the coordination of vanadate(V) to one purine (adenosine, AdH) and one pyrimidine (uridine, UrH_2) nucleoside. In addition, imidazole (ImH) was added to these systems in order to examine its effects on vanadate-nucleoside complexation. ImH is a residue often found in enzymes, many of which interact strongly with vanadate. ImH has also been a commonly used buffer in bioinorganic studies. Equilibration is fast at neutral and alkaline pH. Complexes form within a few minutes. In acid solutions, however, equilibration requires approximately 24 h due to the slow decomposition of initially formed decavanadates.

The acidity constants for adenosine, uridine and imidazole in 0.600 M Na(Cl) and at 25 °C, are compiled in Table III. The molecular structures of the ligands are shown in Figure 1 and the full results, including structural and kinetic aspects, are reported in References 3 and 4.

Downloaded by MONASH UNIV on October 31, 2012 | http://pubs.acs.org
Publication Date: December 10, 1998 | doi: 10.1021/bk-1998-0711.ch002

The H^+-$H_2VO_4^-$-Adenosine/Uridine Systems. The complexation in the two vanadate-nucleoside systems is essentially the same. The complexes formed give rise to a broad asymmetrical ^{51}V NMR resonance at -523 ppm. Varying pH, vanadate or ligand concentrations or concentration ratios affected neither the chemical shift nor the shape of the resonance. Resolution enhancement of both -523 ppm ^{51}V NMR resonances reveals three peaks. The higher Δ_{shift} between the outer peaks of adenosine (6.3 compared to 5.2 ppm for uridine) is in accordance with earlier results, where a more bulky ligand is seen to resolve more (*16*). Complexation occurs in a wide pH range from around 3 to 10. In addition to the –523 resonance, a minor (<2% of $[V]_{tot}$) symmetrical resonance at -507 ppm is present in alkaline solutions (pH > 8) in both systems. A series of representative spectra at $[Ur]_{tot}$ / $[V]_{tot}$ = 8 is shown in Figure 4. As can be seen, the –523 resonance overlaps with a decavanadate resonance between pH 3.6 and 5.6 and in order to obtain accurate integral values a reliable deconvolution program must be employed.

The final results from all LAKE calculations (pK_a values of the ligands and formation constants of the vanadate - nucleoside complexes) are summarized in Table III.

Table III. Formation Constants (β) in the Nucleoside/Imidazole Systems [0.600 M Na(Cl)]

(p,q,r,s)	Notation	log β (3σ)	pK_a
1,0,1,0	AdH_2^+	3.668 (8)	3.668
0,0,1,0	AdH	0 -	12.00
-1,0,1,0	Ad^-	-12.00 (6)	-
0,0,1,0	UrH_2	0	9.02
-1,0,1,0	UrH^-	-9.02 (1)	12.59
-2,0,1,0	Ur^{2-}	-21.61 (13)	-
1,0,0,1	ImH_2^+	7.124 (2)	7.124
0,0,0,1	ImH	0 -	-
1,2,2,0	$V_2Ad_2^-$	11.89 (8)	4.21
0,2,2,0	$V_2Ad_2^{2-}$	7.68 (1)	-
0,1,1,1	$VAdIm^-$	3.04 (2)	-
0,2,2,0	$V_2Ur_2^{2-}$	7.66 (2)	8.75
-1,2,2,0	$V_2Ur_2^{3-}$	-1.09 (4)	-
*-1,1,1,0	VUr^{2-}	-7.43 (33)	-
0,1,1,1	$VUrIm^-$	3.12 (4)	9.38
-1,1,1,1	$VUrIm^{2-}$	-6.26 (20)	- -

* the minor -507 ppm ^{51}V NMR resonance

Downloaded by MONASH UNIV on October 31, 2012 | http://pubs.acs.org
Publication Date: December 10, 1998 | doi: 10.1021/bk-1998-0711.ch002

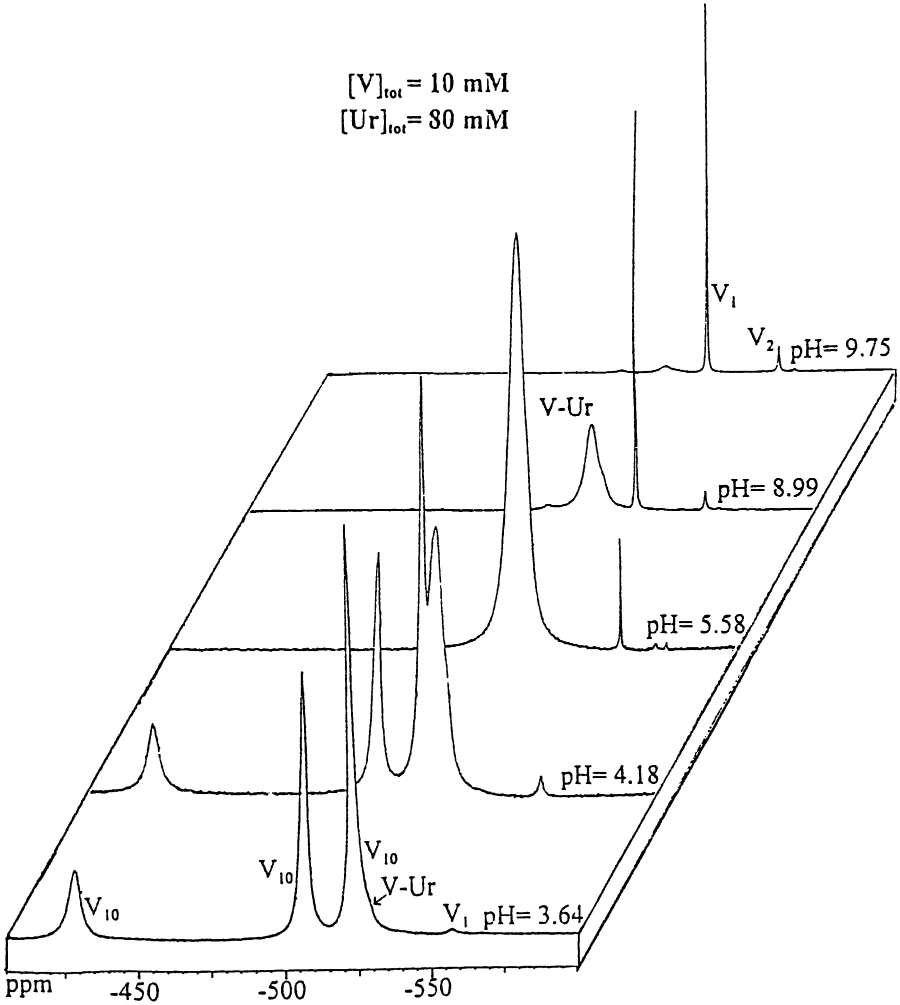

Figure 4. ^{51}V NMR spectra of vanadate-uridine solutions at different pH values.

Downloaded by MONASH UNIV on October 31, 2012 | http://pubs.acs.org
Publication Date: December 10, 1998 | doi: 10.1021/bk-1998-0711.ch002

Both nucleosides form strong -2 charged 2:2 complexes with vanadate (the -523 ppm resonance). However, whereas uridine forms a deprotonated -3 charged species, adenosine forms an additional protonated -1 charged species. The reason for this difference is to be found in the acid-base properties of the uncomplexed nucleosides. Lack of change of the chemical shift for the ^{51}V NMR resonance with pH suggests that the protonation of the 2:2 complexes in the V-AdH system and the deprotonation in the V-UrH_2 system is likely to occur at some distance from the vanadium atom. Since the pK_a value of the protonated -1 charged V_2Ad_2 species (4.21) differs by only 0.54 units from adenosine itself and the difference between the pK_a values of the -2 charged V_2Ur_2 species and uridine is only 0.27 units, the protonation site is presumably located on the base part of the nucleosides As mentioned above, resolution enhancement of the -523 ppm resonances gives three signals. Since the calculations unambiguously showed that complexes of 2:2 composition completely explained the potentiometric and ^{51}V NMR integral data, the three signals must represent isomers.

The complex giving rise to the -507 ppm resonance could in the uridine system be proposed to have a 1: 1 stoichiometry and a charge of -2. The composition is most probably the same for the V-AdH system.

A distribution diagram for 10 mM vanadium and an eight-fold excess of uridine is shown in Figure 5. The curves have been calculated using the constants given in Tables 1 (0.600 M Na(Cl)) and III. The experimental data points show a perfect fit to the calculated model.

The H^+-$H_2VO_4^-$-Adenosine/Uridine-Imidazole systems. Using the H^+-vanadate-nucleoside systems as a basis, the effects upon addition of imidazole was studied. The presence of imidazole(ImH) in solutions containing vanadate and adenosine or uridine was shown to generate isomers of vanadate-nucleoside-imidazole complexes. This type of complex is likely to be very important for the mechanisms with which vanadate interacts in biological systems.

Interactions between vanadate and monodentate nitrogen compounds (like ImH) have been reported only in a few cases (*17,18*). At the moderate (mM) concentrations used in our studies, no interaction of imidazole with vanadate or adenosine could be observed in the ternary subsystem H^+-$H_2VO_4^-$-ImH. In the quaternary H^+-$H_2VO_4^-$-AdH/UrH_2-ImH systems, however, mixed ligand species are formed. These give rise to a broad ^{51}V NMR resonance at -483 ppm in the pH range ~5.5 to ~10.5 with maximum area at pH ~ 8.5. To obtain the same amount of vanadium bound in these mixed ligand species as in the $V_2Nucleoside_2^{n-}$ complexes, a large excess of ImH is needed.

Changing pH, concentrations or concentration ratios influenced neither the shift nor the form of the broad, asymmetric V-AdH/UrH_2-ImH resonances, indicating the presence of two isomers in each system, one major at -483.6 ppm (Ad), -483.2 (Ur) and one minor at -479.6 ppm (Ad), -480.1 (Ur). The chemical shift difference of 4.0 ppm (Ad) and 3.1 (Ur) between the two isomers is similar to that observed between the 2:2 vanadate-nucleoside isomers.

LAKE calculations showed the resonances to originate from -1 charged, mononuclear, mixed ligand (0,1,1,1) species, $VAdIm^-$ and $VUrIm^-$. In the uridine

Downloaded by MONASH UNIV on October 31, 2012 | http://pubs.acs.org
Publication Date: December 10, 1998 | doi: 10.1021/bk-1998-0711.ch002

system, an additional -2 charged $VUrIm^{2-}$ complex is formed, which can be expected as uridine has a deprotonation site. In the vanadate-adenosine system, an additional protonated zero charged VAdIm species could be expected to form but was not found. The reason for the absence of such a species is probably the strong competetive formation of decavanadate complexes. Formation constants are given in Table III.

The diagram shown in Figure 6 is constructed to compare the complexation of vanadate in the AdH and UrH_2 systems when excess of imidazole is present. Since mixed ligand Ad and Ur dimeric vanadate complexes are likely to be formed, it doesn't reflect the full speciation in the five component system but clearly shows the analogy of the two systems and that the the base part of the nucleoside is of minor importance for the formation of species. In the diagram only the sum of homonuclear species are shown for clarity. As mentioned above, -2 charged 2:2 complexes are the predominant species. The additional $V_2Ur_2^{3-}$ species is stronger than the $V_2Ad_2^-$ species, binding almost 20% in contrast to at most 5% of $[V]_{tot}$ for the adenosine species (at $[V]_{tot}$ =5 mM, $[Ad/Ur]_{tot}$ =20 mM). The weaker formation constant for $V_2Ad_2^-$ is probably caused by the formation of strong competitive decavanadate complexes in the pH range where $V_2Ad_2^-$ is formed.

The H^+-Vanadate-Maltol System. The motivation for the H^+-$H_2VO_4^-$-MaH study comprises the known insulin mimetic effects of both V(IV)- and V(V)-maltol(MaH) complexes. The system was studied by potentiometry and by ^{51}V NMR and V(IV) ESR spectroscopy (*5*). In contrast to the vanadate-dipeptide (*1*,*2*) and vanadate-nucleoside (*3*,*4*) studies, the vanadate-maltol system was studied in physiological 0.150 M Na(Cl) medium.

V-MaH complexation occurs within a wide pH range, from around 1 up to 10.5. However, to establish the stoichiometry and formation constants of the complexes formed, the pH range was restricted to $7.4 < pH < 9.9$, due to reduction of V(V) in acid solution and polycondensation of maltol in alkaline solutions As the presence of even a small amount of V(IV) would disturb the speciation study, precautions were taken not to include reduced solutions. Therefore, prior to quantitative NMR measurements each solution was checked for paramagnetism by ESR spectroscopy. The equilibration is fast in the pH range studied

^{51}V NMR spectra show two resonances originating from vanadium-maltol complexes. Both exist in a wide pH range. A main resonance has a shift of -496 ppm and a minor one occurs at -509 ppm. At pH higher than 8.5 the latter resonance is shifting upfield, indicating deprotonation. At acid pH a downfield shifting, and changes in relative amounts of the two resonances occur. However, it was not possible to determine the speciation in the unstable acid solutions.

The results from the LAKE calculations on data at pH 5 to 10 are shown in Table IV. The -496 ppm resonance originates from a VMa_2^- species and the -509 ppm resonance is explained by two monomeric complexes, VMa^- and VMa^{2-}. The VMa^{2-} complex appears as the main species in a pH range from 4.5 to 8.5, whereas both mononuclear monoligand species are minor. For $[V]_{tot}$= 10 mM and a 1:2 ratio, the same as in the main complex formed, more than 90 % of both vanadium and maltol is complexed. This strong complexation between vanadium and maltol at neutral and slightly acidic pH makes it physiologically very important. However, if the concentrations are lowered by a factor of 100 ([V] = 0.1 mM), the calculated amount of vanadium bound in different complexes changes dramatically. At a 1:2 ratio only

Downloaded by MONASH UNIV on October 31, 2012 | http://pubs.acs.org
Publication Date: December 10, 1998 | doi: 10.1021/bk-1998-0711.ch002

Downloaded by MONASH UNIV on October 31, 2012 | http://pubs.acs.org
Publication Date: December 10, 1998 | doi: 10.1021/bk-1998-0711.ch002

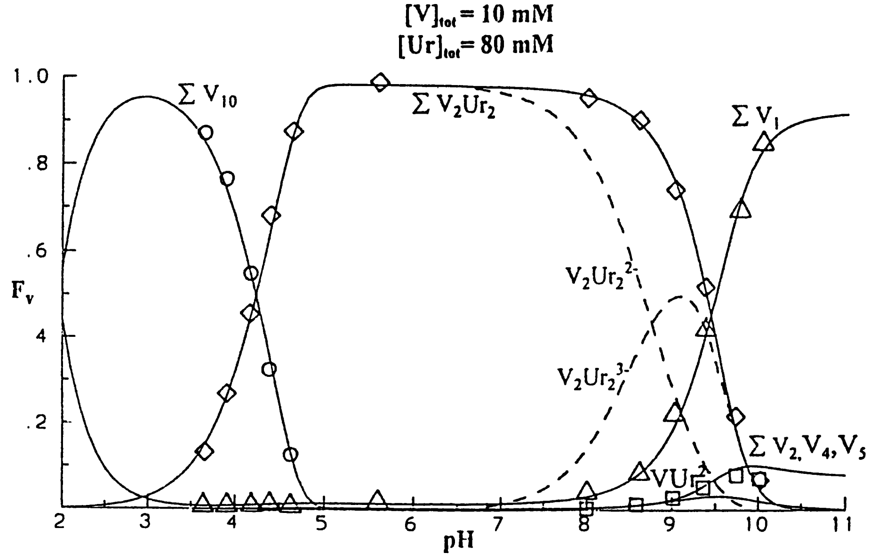

Figure 5. Distribution of vanadium vs pH at $[Ur]_{tot}/[V]_{tot} = 8$. Symbols represent experimental points.

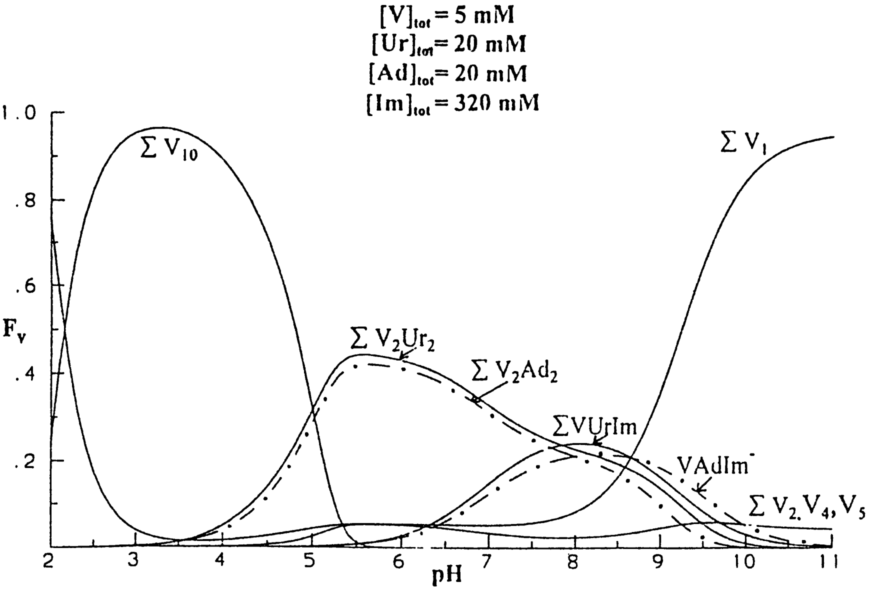

Figure 6. Distribution diagram derived from a model calculation using the formation constants in Table III and Table I (0.600 M Na(Cl)).

18% is bound in the VMa^{2-} complex, but 6% in the VMa^- species (cf. Figure 7). At even lower vanadium concentrations (0.01 mM) and a twofold excess of maltol, equal amounts of vanadium will be bound in each of the VMa^{2-} and VMa^- species. However, at these very low concentrations the total amount of vanadium bound is only 2%. This clearly shows the importance of taking total concentrations and not only ratios into account in extrapolating the results of an equilibrium analysis to physiological conditions.

Table IV. Formation Constants (β) in the Maltol System [0.150 M Na(Cl)]

(p,q,r)	Notation	$\log\beta$ (3σ)	pK_a
0,0,1	MaH	0	8.437
-1,0,1	Ma^-	-8.437 (5)	-
0,1,2	VMa_2^-	7.02 (3)	-
0,1,1	VMa^-	2.66 (5)	10.0
-1,1,1	VMa^{2-}	-7.37 (21)	-

Summary of the Speciation Studies. In the histidine system spontaneous reduction of V(V) prohibited a speciation study.

For all the dipeptide systems studied -1 charged 1:1 species are formed. In the V-AH system a non-charged complex is also formed having a pK_a value of 6.89. This from a biochemical point of view very interesting species could only be detected thanks to the combination of potentiometry and quantitative NMR data.

In the nucleoside systems, both AdH and UrH_2 form strong -2 charged 2:2 complexes. Whereas AdH forms an additional protonated -1 charged species, UrH_2 forms a deprotonated -3 charged species. The only mononuclear 1:1 complex found was a -2 charged uridine species. With ImH, both AdH and UrH_2 form fairly strong -1 charged 1:1:1 complexes and the uridine complex deprotonates to a -2 charged species. The binding of imidazole to vanadium in the presence of nucleosides is very interesting. Numerous imidazole residues are present in biological systems and the question of whether the coordination of such species to vanadium is also enhanced in the presence of nucleosides was studied in some experiments on the vanadate-uridine-histidine system. Histidine is known to bind to vanadate (see above). In addition to the uncomplexed vanadate, vanadate-uridine and vanadate-histidine species, a ^{51}V NMR resonance is present at approximately the same chemical shift (-481 ppm) value as the vanadate-uridine-imidazole complexes (*5*). No further study on this system has yet been performed, but clearly a 1:1:1 vanadate-uridine-histidine complex analogous to the vanadate-uridine-imidazole complex is formed with coordination occurring through the imidazole-N(l) atom, as in the vanadate-nucleoside-imidazole systems.

Downloaded by MONASH UNIV on October 31, 2012 | http://pubs.acs.org
Publication Date: December 10, 1998 | doi: 10.1021/bk-1998-0711.ch002

Downloaded by MONASH UNIV on October 31, 2012 | http://pubs.acs.org
Publication Date: December 10, 1998 | doi: 10.1021/bk-1998-0711.ch002

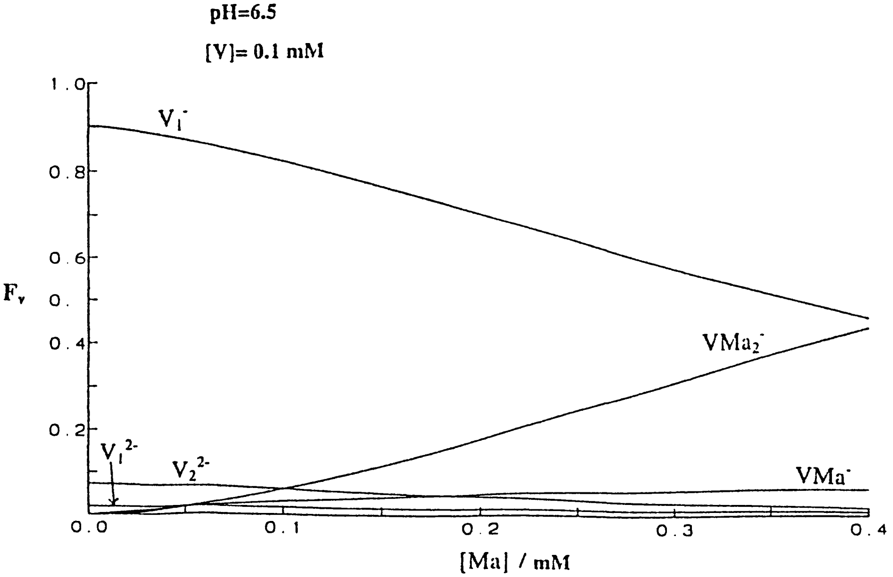

Figure 7. Diagrams showing the distribution of vanadium ($[V]_{tot}$=0.1 mM) vs the total concentration of maltol at pH = 6.5.

In the maltol system a -1 charged 1:2 complex, as well as two minor 1:1 species with charges -1 and -2 are formed. Severe reduction of V(V) in acidic solution restricted the range of equilibrium data to pH > 5.

Speciation at Low Vanadium Concentration. As mentioned previously, the relative amounts of different vanadium-containing species vary considerably between samples of millimolar concentrations and samples of physiological concentrations (0.1-1 μM). To visualise the complexation at $[V]_{tot}$ = 1 μM and large excess of the ligands (20 mM), model calculations were performed. Distribution diagrams are presented in Figure 8. The VAH^{n-} complexes bind almost 90% of total vanadium in a pH range from 4 to 8. The non-charged VAH^0 complex, which has potential to pass through cellular membranes, amounts to 50% of ΣVAH at physiological pH. $VPAH^-$ (not shown) shows a behaviour very similar to VAH^{n-}. The $VAGH^-$ complex binds 50%. In the vanadate-maltol system, all vanadium is bound in the 1:2 complex and the monomeric VMa^- species is very minor and not present at physiological pH. The conditions for the nucleosides are illustrated with the V-AdH-ImH distribution diagram. Since the major complexes at mM concentrations are dimeric, the distribution changes when reducing the vanadium total concentration (cf. Figures 5 and 6). The 2:2 complexes are then only minor species, but $VAdIm^-$ amounts to almost 20% of $[V]_{tot}$ despite the 1:1 ImH/AdH ratio. At mM concentrations of vanadium, a high ratio is needed to obtain appreciable amounts of this mixed ligand species.

Downloaded by MONASH UNIV on October 31, 2012 | http://pubs.acs.org
Publication Date: December 10, 1998 | doi: 10.1021/bk-1998-0711.ch002

Structural Remarks. From ^{13}C, ^{1}H, ^{14}N, and ^{17}O NMR spectroscopy, valuable structural information including co-ordination sites of the ligands have been obtained. In the dipeptide systems AH, PAH and AGH all coordinate to V(V) by building up two five-membered rings each, with vanadium five- or six-coordinated. The nucleosides AdH and UrH_2 bind through the ribose oxygens with vanadium five-coordinated (*4,19*). Maltol acts as a bidentate ligand and vanadium is proposed to be six-coordinated (*20*).

Some information on the coordination to vanadium can also be obtained from the ^{51}V chemical shift values and widths of the resonanses. In Figure 9, the chemical shift values are shown for all of the vanadium-organic ligand complexes studied in this work. The inorganic vanadate species are included for comparison. As can be seen from the position of the inorganic species, there is a tendency that tetrahedrally coordinated vanadium appears at higher field (lower shift), whereas octahedrally coordinated vanadium appears at lower field. The vanadium-organic ligand complexes in the "octahedral coordination area" are expected to be five- or six-coordinated, for example $V_2Ad_2^{n-}$ and $V_2Ur_2^{n-}$ (five) and VMa_2^- (six), whereas complexes in the "tetrahedral coordination area" are four-coordinated (for example V-His at -571 ppm). However, since a chemical shift value is affected by many factors it is impossible to predict the exact coordination number from the chemical shift value alone. An additional factor that can be used is the linewidth of the resonance. As a symmetric environment of a vanadium atom will give rise to a narrow resonance, vanadium in a tetrahedral coordination sphere produces resonances with considerably smaller linewidths than penta- and hexa-coordinated vanadium. Thus, a narrow resonance at a low chemical shift value most likely originates from a tetrahedral complex.

Downloaded by MONASH UNIV on October 31, 2012 | http://pubs.acs.org
Publication Date: December 10, 1998 | doi: 10.1021/bk-1998-0711.ch002

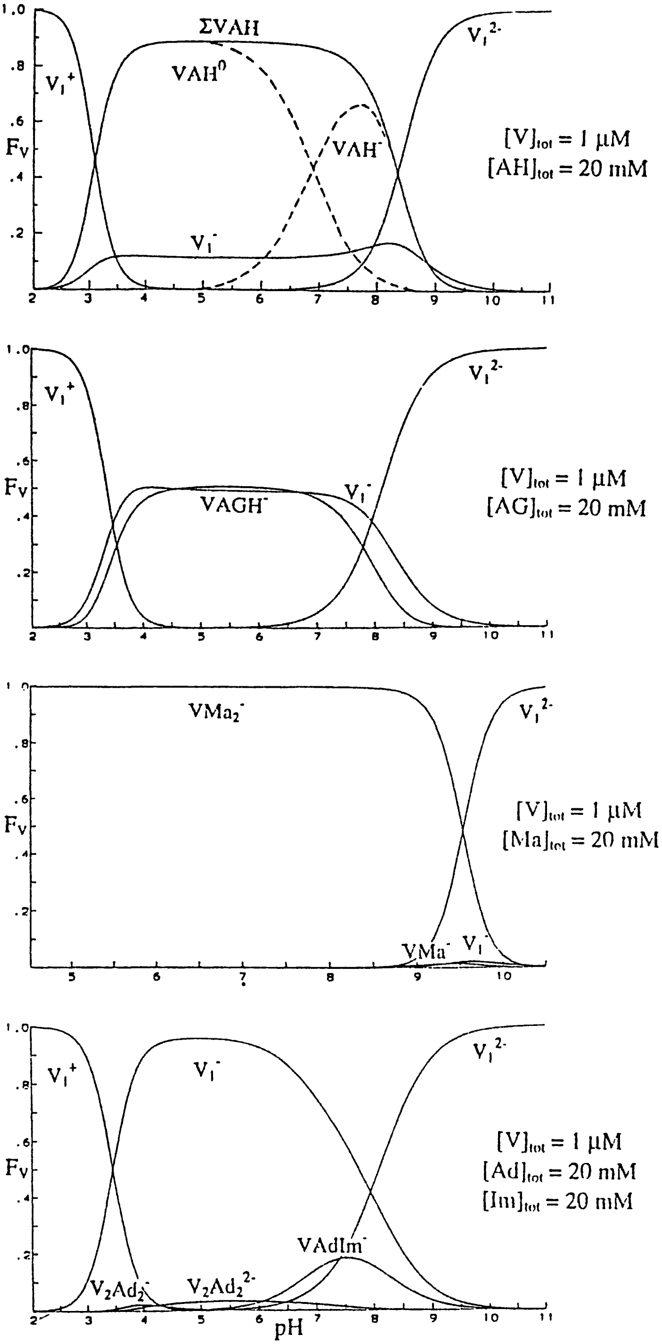

Figure 8. Diagrams showing the distribution of vanadium for selected systems at approximate physiological concentrations.

Downloaded by MONASH UNIV on October 31, 2012 | http://pubs.acs.org
Publication Date: December 10, 1998 | doi: 10.1021/bk-1998-0711.ch002

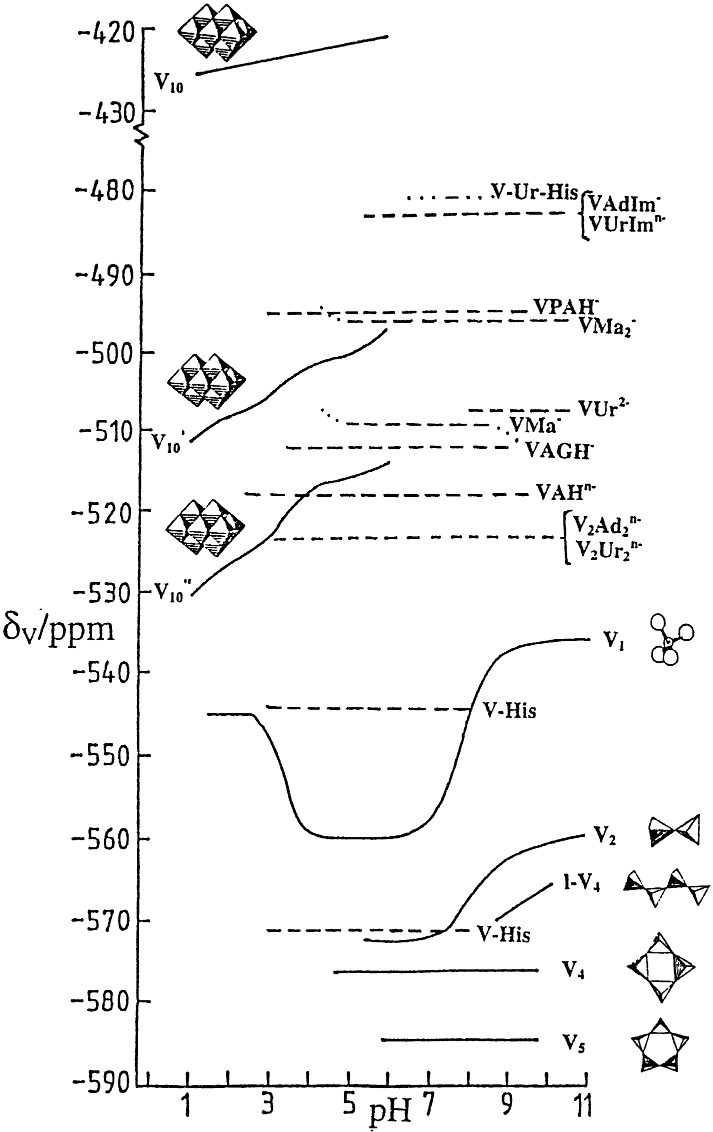

Figure 9. Chemical shift values vs pH for all complexes formed in the vanadate-ligand systems studied. The vanadate hydrolysis species are shown for comparison.

Acknowledgments. We wish to thank Prof. Debbie C. Crans for encouraging us to study vanadium complexes of biochemical interest and for the rewarding collaboration on the nucleoside systems. The dipeptide systems have been studied in close collaboration with Prof. Dieter Rehder and Dr. Martina Fritzsche. Prof. Chris Orvig is acknowledged for suggesting us to study the the vanadium-maltol system in physiological 0.150 M Na(Cl) medium and Dr Ana González Baró for much of the experimental work on this system. We thank Res. Eng. Ingegärd Andersson for preparing some of the figures and Dr. Sarah Angus-Dunne for linguistic revision. Financial support by the Swedish Natural Science Research Council is gratefully acknowledged.

Literature Cited

1. Elvingson, K.; Fritzsche, M.; Rehder, D.; Pettersson, L. *Acta Chem. Scand.* **1994**, *48*, 878-885.
2. Fritzsche, M.; Elvingson, K.; Rehder, D.; Pettersson, L. *Acta Chem. Scand.* **1997**, *51*, 483-491.
3. Elvingson, K.; Crans, D. C.; Pettersson, L. *J. Am. Chem. Soc.* **1997**, *119*, 7005-7012.
4. Elvingson, K.; Keramidas, A. D.; Crans, D. C.; Pettersson, L. *Inorg. Chem.,* submitted.
5. Elvingson, K.; González Baró, A.; Pettersson, L. *Inorg. Chem.* **1996**, *35,* 3388.
6. Elvingson, K. *Ph. D. Thesis*, Umeå University, Sweden, **1997**.
7. Sjöberg, S.; Hägglund, Y.; Nordin, A.; Ingri, N. *Mar. Chem.* **1983**, *13*, 35.
8. Ingri, N.; Andersson, I.; Pettersson, L.; Yagasaki, A.; Andersson, L.; Holmström, K. *Acta Chem. Scand.* **1996**, *50*, 717.
9. Eriksson, G. *Anal. Chim. Acta.* **1979**, *112*, 375.
10. Pettersson, L.; Hedman, B.; Andersson, I.; Ingri, N. *Chem. Scr.* **1983**, *22*, 254.
11. Pettersson, L.; Hedman, B.; Nenner, A.-M.; Andersson, I.; *Acta Chem. Scand.* **1985**, *A39*, 499.
12. Cruywagen, J. J.; Heyns, J. B. B.; Westra, A. N. *Inorg. Chem.* **1996**, *35*, 1556.
13. Tracey, A. S.; Jaswal, J. S.; Angus-Dunne, S. J. *Inorg. Chem.* **1995**, *34*, 5680.
14. Ivakin, A. A.; Kurbatova, L. D.; Kruchinina, M. V. *Zh. Neorg. Khim*, **1986**, *31*,510.
15. Chasteen, N. D. *Struc. Bond.*, **1983**, *53*, 105.
16. Gresser, M. J.; Tracey, A. S.; *J. Am. Chem. Soc.* **1986**, *108*, 1935.
17. Crans, D. C.; Schelble, S. M.; Theisen, L. A. *J. Org. Chem.* **1991**, *56*, 1266.
18. Galeffi, B.; Tracey, A. S. *Inorg. Chem.* **1989**, *28*, 1726.
19. Angus-Dunne, S. J.; Batchelor, R. J.; Tracey, A. S.; Einstein, F. W. B. *J. Am. Chem. Soc.*, **1995**, *117*, 5292.
20. Caravan, P.; Gelmini, L.; Glover, N.; Herring, F. G.; Li, H.; McNeill, J. H.; Rettig, S. J.; Setyawati, I. A.; Shuter, E.; Sun, Y.; Tracey, A. S.; Yuen, V. G.; Orvig, C *J. Am. Chem. Soc.* **1995**, *117*, 12759.

Downloaded by MONASH UNIV on October 31, 2012 | http://pubs.acs.org
Publication Date: December 10, 1998 | doi: 10.1021/bk-1998-0711.ch002

Downloaded by MONASH UNIV on October 31, 2012 | http://pubs.acs.org
Publication Date: December 10, 1998 | doi: 10.1021/bk-1998-0711.ch003

Chapter 3

Vanadium(V) Equilibria: Thermodynamic Quantities for Some Protonation and Condensation Reactions

J. J. Cruywagen, J. B. B. Heyns, and A. N. Westra

Department of Chemistry, University of Stellenbosch, Stellenbosch 7600, South Africa

The protonation and condensation equilibria of vanadium(V) at pH ≥ 8 have been investigated by enthalpimetric titrations at 25°C in 1.0 M $NaClO_4$. Thermodynamic quantities have been determined for the formation, from HVO_4^{2-}, of the following species: VO_4^{3-}, $V_2O_7^{4-}$, $HV_2O_7^{3-}$, $V_3O_{10}^{5-}$, $V_4O_{13}^{6-}$, $V_4O_{12}^{4-}$ and $V_5O_{15}^{5-}$. The energetics of oligomerization is discussed in terms of the enthalpy and entropy changes of the various reactions.

Protonation of the tetrahedral VO_4^{3-} ion leads to the formation of various mono- and polynuclear species which occur in successive overlapping equilibria extending over the entire pH range. The protonated mononuclear species HVO_4^{2-}, $H_2VO_4^-$ and also $VO_2(H_2O)_4^+$ (except at very low pH) are predominant only at very high dilution due to the great tendency of vanadate to oligomerize, forming species of nuclearity 2, 3, 4, 5, 6 and 10 (1-9). Thermodynamic quantities for the mononuclear equilibria have been determined (9-11), but little thermodynamic information, other than equilibrium constants, are available for the condensation reactions. Enthalpy and entropy changes have been determined for the dimerization of HVO_4^{2-} in 1.0 M NaCl medium (10) and very recently thermochemical values for a number of vanadium(V) species have been obtained at low ionic strength from NMR measurements at temperatures 0, 25, and 50°C (12). The interpretation of enthalpimetric data for such a complex system of simultaneous equilibria depends heavily on reliable equilibrium constants which in turn must be based on a well-characterized reaction model. The vanadate(V) system has now been characterized to such an extent that a calorimetric investigation can be attempted (2-4, 7-9).

Thermodynamic quantities are needed to extend the basic knowledge of vanadate(V) equilibria, but are also of interest in view of the structural characteristics of the various condensation products. Vanadium(V) is six-coordinate in the decavanadate ion, $V_{10}O_{28}^{6-}$, and its protonated forms (1,4,7), but four-coordinate in the oligomers of lower nuclearity which have either linear or cyclical structures. The hexameric, pentameric, and tetrameric ions, $V_6O_{18}^{6-}$, $V_5O_{15}^{5-}$ and $V_4O_{12}^{4-}$ are presumably all cyclical in aqueous solution (2-4, 9). The $V_4O_{12}^{4-}$ ion has been shown by X-ray analysis to be cyclical in the solid state (13,14,). The existence of the linear tetra- and tri-vanadate ions, $V_4O_{13}^{6-}$, and $V_3O_{10}^{5-}$, has recently been confirmed (8,9).

In this paper we report the results of an enthalpimetric investigation of the protonation and condensation reactions of vanadate, conducted at pH > 8 so as to include all oligomers except the decavanadates which are involved in slow equilibria.

Experimental

Reagents and Solutions. All reagents were of analytical grade (Merck, p.a.) and solutions were prepared with water obtained from a Millipore Milli-Q system. A sodium vanadate stock solution was prepared from $NaVO_3$ and standardized as described previously (11). Sodium hydroxide was standardized with potassium hydrogenphthalate. Sodium perchlorate solution was prepared from recrystallized $NaClO_4.H_2O$. The solution was standardized by evaporating known volumes to dryness and heating to constant weight at 160°C. Solutions for enthalpimetric titrations were prepared by appropriate dilution of the vanadate stock solution and addition of sodium hydroxide solution to obtain the desired pH_c. Sodium perchlorate was added to all solutions to maintain a constant sodium concentration of 1.0 M.

Stability Constants. Stability constants for the various vanadium(V) species have been determined by potentiometry in 1.0 M $Na(ClO_4)$ at 25°C according to methodology described in previous papers (15). The electrode system was standardized in terms of hydrogen ion concentration by titration of a 1.0 M $NaClO_4$ solution with $HClO_4$. Measurements were conducted on eight different vanadium solutions in the concentration range 0.001 - 0.08 M. The symbol pH_c is used to denote - log $[H^+]$.

Calorimetric Titrations. An isothermal titration calorimeter, Tronac model 1250, was used for the enthalpy measurements. Sodium vanadate solutions (20.0 cm^3) were titrated with sodium hydroxide, either 0.6 or 1.0 M, from a precision microburette (2.50 cm^3). A reverse titration of an alkaline vanadate solution with acid is not feasible. Even at high pH the addition of acid results in the instantaneous formation of the kinetically stable yellow decavanadate ions and it can take 24 hours or longer before equilibrium is established. The initial concentrations of vanadate were 0.03, 0.05, 0.08, 0.10, 0.15 and 0.20

Downloaded by MONASH UNIV on October 31, 2012 | http://pubs.acs.org
Publication Date: December 10, 1998 | doi: 10.1021/bk-1998-0711.ch003

Downloaded by MONASH UNIV on October 31, 2012 | http://pubs.acs.org
Publication Date: December 10, 1998 | doi: 10.1021/bk-1998-0711.ch003

M. Several of the titrations were carried out in duplicate and for some vanadium concentrations different pH ranges were covered. The data were collected automatically by means of a personal computer using software supplied by Tronac. Blank titrations were carried out to correct for the heat of dilution (exothermic) which varied from ~ 0.4 to 0.3 kJ/mol of sodium hydroxide added and amounted to 1 - 3% (depending on the titration conditions) of the total heat measured.

Results and Discussion

The results of two representative enthalpimetric titrations are shown in Figure 1 where the total amount of heat measured, Q, is plotted against the volume of hydroxide added to a vanadate solution containing two protons per vanadium atom. Breaks occur in the curves where the analytical concentrations of vanadate and protons are about the same. For the solution 0.03 M in vanadate, for example, the break occurs at $pH_c \sim 11.3$ where all species have been converted to HVO_4^{2-} and $V_2O_7^{4-}$ (cf. Figure 2). Further addition of sodium hydroxide results in the formation of VO_4^{3-}, a process for which much less heat is generated. This shows that for these reactions the excess heat, which is the balance between deprotonation/dissociation (endothermic) and the neutralization of protons with formation of H_2O (exothermic) is much smaller than for the reactions occurring in the pH_c region 8 to 11.

The computer program SIRKO (16) was used to calculate the ΔH values for the various species from the measured heat, Q, corrected for dilution effects. The calculated ΔH values actually include the heat of reaction for the formation of water. By using the enthalpy change for the formation of water in 1 M $NaClO_4$, namely, $\Delta H_w = -56.1$ kJ/mol (17) the calculated parameters were converted to values applicable to the protonation and oligomerization reactions as expressed in the following general equation:

$$p\,HVO_4^{2-} + q\,H^+ \rightleftharpoons [(HVO_4^{2-})_pH_q^+] \qquad (1)$$

The ΔH°_{pq} values listed in Table I are therefore the molar enthalpy change for the formation of a given species from the above components at 25°C and in 1.0 M $Na(ClO_4)$ medium. The values of the equilibrium constants pertaining to this medium, β_{pq}, used to calculate these molar enthalpy changes (Table I) are consistent with those reported for 0.6 M NaCl and 3.0 M $NaClO_4$ and are based on the same reaction model (3-4). The percentage concentration of the $V_5O_{15}^{5-}$, however, is somewhat higher than that calculated from these literature values which were obtained from a combination of potentiometric and NMR data. A slight overestimation of the value of β_{55} as determined by potentiometry alone is not unlikely because of the stoichiometric relationship and correlation between the concentrations of the $V_4O_{12}^{4-}$ and $V_5O_{15}^{5-}$ ions, but it would not be more than about 0.4 log units. The effect on the calculated

Downloaded by MONASH UNIV on October 31, 2012 | http://pubs.acs.org
Publication Date: December 10, 1998 | doi: 10.1021/bk-1998-0711.ch003

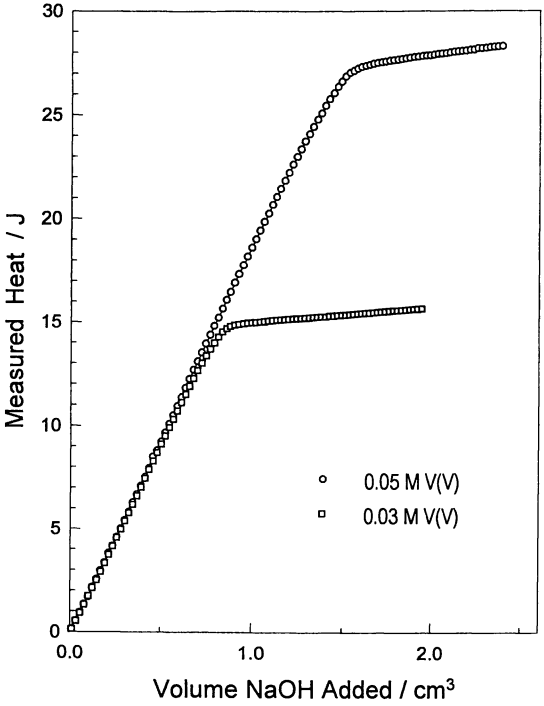

Figure 1. Measured heat as a function of volume of sodium hydroxide (0.60 M) added to vanadate(V) solutions (0.03 and 0.05 M) starting at $pH_c \sim 8.3$.

Downloaded by MONASH UNIV on October 31, 2012 | http://pubs.acs.org
Publication Date: December 10, 1998 | doi: 10.1021/bk-1998-0711.ch003

Table I. Values for the Formation Constants and Other Thermodynamic Quantities (kJ/mol) for Vanadium(V) Species in 1.0 M $Na(ClO_4)$ Medium at 25°C: $p HVO_4^{2-} + q H^+ \rightleftharpoons [(HVO_4^{2-})_p H_q^+]$

(p,q)	Formula	Log β_{pq}	ΔG°	ΔH°	$T\Delta S^\circ$
(1,-1)	VO_4^{3-}	-13.27 ± 0.02	75.7	27	-49
(1,0)	HVO_4^{2-}	0	0	0	0
(1,1)	$H_2VO_4^-$	7.92 ± 0.02	-45.2	-9	36[a]
(1,3)	VO_2^+	14.68 ± 0.04	-83.8	-42	42[a]
(2,0)	$V_2O_7^{4-}$	0.9 ± 0.1	-5.1	-28	-23
(2,1)	$HV_2O_7^{3-}$	10.7 ± 0.1	-61.0	-35	26
(2,2)	$H_2V_2O_7^{2-}$	18.1 ± 0.5	-	-	-
(3,1)	$V_3O_{10}^{5-}$	12.3 ± 0.2	-70	-55	15
(4,2)	$V_4O_{13}^{6-}$	23.6 ± 0.2	-135	-82	53
(4,3)	$HV_4O_{13}^{5-}$	31.7 ± 0.5	-	-	-
(4,4)	$V_4O_{12}^{4-}$	41.9 ± 0.1	-239	-122	117
(5,5)	$V_5O_{15}^{5-}$	52.9 ± 0.1	-310	-156	154
(6,6)	$V_6O_{18}^{6-}$	62.6 ± 0,5	-	-	-

[a] Reference (11)

$\Delta H°$ values of these species would be rather small, estimated to be less than 3%.

Although it is possible in principle to calculate $\Delta H°$ values for all species included in the reaction model, some occur in such low percentage concentrations that the calculation of their $\Delta H°$ values is not justified. Inevitable uncertainties in the values of formation constants and in particular those of very minor species, together with experimental errors in the measured heat (even if very small), usually results in the calculation of meaningless ΔH values. The species, $H_2V_2O_7^{2-}$ and $HV_4O_{13}^{5-}$, of which the percentage concentrations are very small under the experimental conditions (< 3% in terms of monovanadate) were therefore neglected in the calculations. For the mononuclear ion, $H_2VO_4^-$, which also occurs in very low concentrations, the value previously determined by spectrophotometry and pertaining to the same ionic medium (11), was introduced as a fixed parameter.

The hexavanadate ion $V_6O_{18}^{6-}$ is also known to be a minor species in the pH_c region in question (4,9); it might reach a maximum percentage concentration of more than 5 %, possibly up to 10% at $pH_c = 8$ if the uncertainty in the formation constant is taken into account. However, it had to be omitted in the calculations due to the strong correlation of its concentration with those of the $V_5O_{15}^{5-}$ and $V_4O_{12}^{4-}$ ions (cf. Figure 2) causing the system of linear equations to be poorly conditioned which means that a unique set of parameters cannot be calculated. Excluding the hexamer from the reaction model implies that the heat involved in its formation is accommodated in the $\Delta H°$ values of the $V_5O_{15}^{5-}$ and $V_4O_{12}^{4-}$ species, but the effect can be expected to be very small. Solutions that would contain a higher percentage concentration of the hexamer would also contain significant amounts of decavanadates which react slowly. Under these conditions enthalpimetric titrations are not feasible and ΔH values for the species involved must be determined from the variation in the formation constants with temperature. Such experiments at $pH_c < 7.5$ have been carried out in our laboratory and the data are currently being treated.

The $\Delta H°$ values calculated from the combined data of nine enthalpimetric titrations covering different pH_c ranges from 8 to 13 are given in Table I. Considering the approximations mentioned above, the error limits are estimated to be about 5 % of the parameter values. The agreement between the calculated and experimental values for all curves, however, is very good and the error limits calculated by the program (based on the goodness of the fit) were actually less than 1% of the parameter values.

The enthalpy changes obtained for the formation of $V_2O_7^{4-}$ and VO_4^{3-}, $\Delta H°_{2,0} = -28$ kJ/mol and $\Delta H°_{1,-1} = 27$ kJ/mol, can be compared with the values -28 and 24 kJ/mol previously determined in 1.0 M NaCl medium (10). For the formation of $V_4O_{12}^{4-}$, the enthalpy change $\Delta H° = -122$ kJ/mol agrees well with the value reported by Larson (12) namely -128 kJ/mol. When the $\Delta H°$ values for the cyclic oligomers $V_4O_{12}^{4-}$ and $V_5O_{15}^{5-}$ are compared

Downloaded by MONASH UNIV on October 31, 2012 | http://pubs.acs.org
Publication Date: December 10, 1998 | doi: 10.1021/bk-1998-0711.ch003

Downloaded by MONASH UNIV on October 31, 2012 | http://pubs.acs.org
Publication Date: December 10, 1998 | doi: 10.1021/bk-1998-0711.ch003

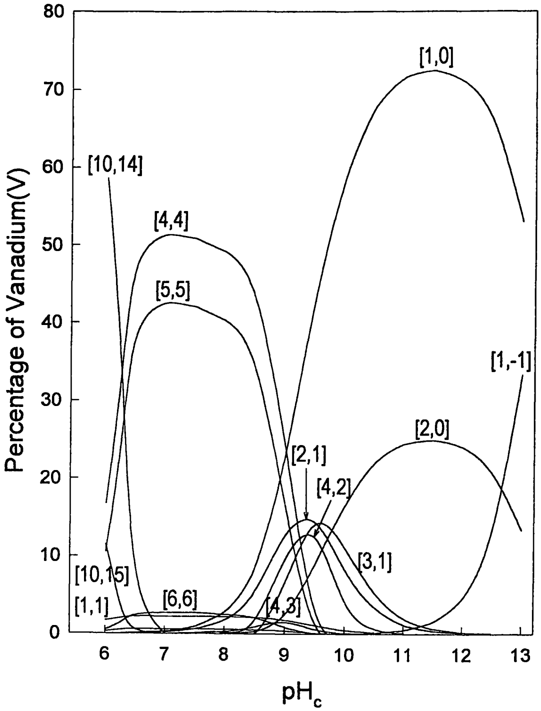

Figure 2. Distribution of vanadium(V) species as a function of pH_c ($-\log[H^+]$). The total vanadium concentration is 0.03 M.

Downloaded by MONASH UNIV on October 31, 2012 | http://pubs.acs.org
Publication Date: December 10, 1998 | doi: 10.1021/bk-1998-0711.ch003

it is seen that the enthalpy change per vanadium atom is about the same, -30 and -31 kJ/mol respectively; the $T\Delta S^{\circ}$ values per vanadium atom are the same, namely 29 kJ/mol.

It is informative to compare the thermodynamic quantities for the formation of the linear trimer and tetramer when formulated as follows:

	ΔH°	$T\Delta S^{\circ}$	
$V_2O_7^{4-} + HVO_4^{2-} + H^+ \rightleftharpoons V_3O_{10}^{5-} + H_2O$	-27	38	(2)
$V_3O_{10}^{5-} + HVO_4^{2-} + H^+ \rightleftharpoons V_4O_{13}^{6-} + H_2O$	-27	38	(3)

The addition of a tetrahedral unit to either the dimer or trimer is accompanied by similar enthalpy and entropy changes. The enthalpy and entropy changes involved when a tetrahedron is linked without an accompanying proton can be seen in the following reaction:

$HV_2O_7^{3-} + HVO_4^{2-} \rightleftharpoons V_3O_{10}^{5-} + H_2O$ -21 -10 (4)

The entropy change is unfavourable and the enthalpy change is actually the driving force for the condensation as in the case of the dimerization of HVO_4^{2-} for which $\Delta H^{\circ}_{2,0} = -28$ kJ/mol and $T\Delta S^{\circ}_{2,0} = -23$ kJ/mol.

The addition of a VO_4 group to the linear trimeric and tetrameric species to form the cyclic tetramer and pentamer respectively can be compared in the following reactions:

$V_3O_{10}^{5-} + HVO_4^{2-} + 3\,H^+ \rightleftharpoons V_4O_{12}^{4-} + 2\,H_2O$ -67 101 (5)

$V_4O_{13}^{6-} + HVO_4^{2-} + 3\,H^+ \rightleftharpoons V_5O_{15}^{5-} + 2\,H_2O$ -74 93 (6)

If a quite reasonable contribution of about 40 kJ/mol per proton to the $T\Delta S^{\circ}$ values in reactions (5) and (6) is assumed, the net entropy changes would be negative as is the case in reaction (4) and which would be consistent with the restrictions placed on the freedom of the species.

Finally for the reaction of the conversion of the linear tetramer to the cyclic tetramer by protonation and condensing out a water molecule the following thermodynamic quantities apply:

$V_4O_{13}^{6-} + 2\,H^+ \rightleftharpoons V_4O_{12}^{4-} + H_2O$ -40 64 (7)

Subtracting about 2 x 40 kJ/mol from the entropy change for the contribution of the two protons would also result in a negative $T\Delta S^{\circ}$ value for this condensation process.

From the above analysis it can be concluded that a self-consistent set of thermodynamic quantities have been obtained for the various reactions. The condensation reactions involve species in which vanadium is four coordinate. For the formation of decavanadate ions, in which vanadium is six coordinate, the enthalpy change per vanadium might be more favourable owing to the increase in the number of vanadium oxygen bonds.

Acknowledgments

Financial support by the Foundation for Research Development and the University of Stellenbosch is gratefully acknowledged.

References

1. Pope, M. T., *Heteropoly and Isopoly Oxometallates.* Springer, Berlin **1983,** 34-40 and refs. cited.
2. Heath, E.; Howarth, O. W., *J. Chem. Soc., Dalton Trans* **1981,** 1105.
3. Pettersson, L.; Hedman, B.; Andersson, I.; Ingri, N., *Chem. Script.* **1983**, *22*, 254 and refs. cited.
4. Pettersson, L.; Andersson, I.; Hedman, B., *Chem. Script.* **1985**, *25*, 309.
5. Ivakin, A. A.; Kurbatova, L. D.; Kruchinina, M. V.; Medvedeva, N. I., *Russ. J. Inorg. Chem. (Eng. Transl.)* **1986**, *31*, 219.
6. Cruywagen, J.J.; Heyns, J.B.B.; Visagie, J.L., *Polyhedron* **1989**, *8*, 1800.
7. Crans, D. C., *Comments Inorg. Chem.* **1994**, *16*, 1-33 and refs. cited.
8. Andersson, I.; Pettersson, L.; Hastings, J.J.; Howarth, O.W., *J. Chem. Soc., Dalton Trans.*, **1996**, 3357.
9. Tracey, A. S.; Jaswal, J. S.; Angus-Dunne, S. J., *Inorg. Chem.* **1995,** *34*, 5680.
10. Cruywagen, J.J.; Heyns, J.B.B., *Polyhedron* **1991**, *10*, 249.
11. Cruywagen, J. J.; Heyns, J. B. B.; Westra, A. N., *Inorg. Chem.* **1996**, *35*, 1556.
12. Larson, J.W., *J. Chem. Eng. Data* **1995**, 40, 1276.
13. Day, V. W.; Klemperer, W. G.; Yagasaki, A., *Chem. Lett.* **1990,** 1267.
14. Fuchs, S. M.; Mahjour, S.; Pickardt, J., *Angew. Chem. Int. Ed. Eng.* **1976,** *15*, 374.
15. Cruywagen, J.J.; Krüger L.; Rohwer, E.A., *J. Chem. Soc., Dalton Trans* **1997**, 1925 and refs. cited.
16. Vetrogon, V.I.; Lukyanenko, N.G.; Schwing-Weill, M.-J.; Arnaud-Neu, F., *Talanta*, **1994**, *41*, 2105.
17. Arnek, R., *Arkiv Kemi* **1970**, *32*, 55.

Downloaded by MONASH UNIV on October 31, 2012 | http://pubs.acs.org
Publication Date: December 10, 1998 | doi: 10.1021/bk-1998-0711.ch003

Downloaded by MONASH UNIV on October 31, 2012 | http://pubs.acs.org
Publication Date: December 10, 1998 | doi: 10.1021/bk-1998-0711.ch004

Chapter 4

Structural and Functional Models for Biogenic Vanadium Compounds

D. Rehder, M. Bashirpoor, S. Jantzen, H. Schmidt, M. Farahbakhsh, and H. Nekola

Chemistry Department, University of Hamburg, D-20146 Hamburg, Germany

Model compounds are described for the following biogenic vanadium systems: (i) Vanadate-ionophore interaction; (ii) vanadate-dependent haloperoxidases; (iii) vanadium-nitrogenase; (iv) vanadium-thiolate redox interaction; (v) alkyne-reductase and isonitrile-reductase/ligase activities of nitrogenases. The complexes model the coordination sphere (or part of it) of the active site in biogenic vanadium systems, and some of them are also functional mimics for biological systems and also catalyze industrially relevant reactions. Thus, penta-coordinate aminoalcohol and Schiff base complexes with NO_4 donor sets mimic peroxidase activity and catalyze the peroxidation of thioethers, and isonitrile complexes model active intermediates of in vivo (by nitrogenases) and in vitro C-C coupling reactions. Dinitrogenvanadium complexes undergo reductive protonation of nitrogen to ammonia.

Although the biological role of vanadium had already been recognized at the beginning of this century, its establishment as a bio-metal is of more recent nature. As an analog of phosphate, vanadate inhibits or stimulates a variety of phosphate metabolizing enzymes and thus possibly attains a general role in the majority if not all of the living organisms. This role includes its insulin-mimetic effect, which may be traced back to the inhibition of a tyrosine kinase or tyrosine phosphatase. In its physiologically relevant forms, vanadium occurs in the oxidation states +V (anionic mainly as dihydrogen vanadate, although some oligovanadates are also active), +IV [mainly as the vanadyl(2+) cation] and +III (as a cationic aqua complex or, at physiological pH, stabilized by ligands). Vanadium(III) is the main form present in those marine organisms that accumulate vanadium from sea water, viz. certain sea squirts and fan worms. A terrestrial organism, the fly agaric toad stool, contains a molecular non-oxo vanadium(IV) complex - called amavadin - of unknown function. In addition, vanadium is the active center of two enzymes: a haloperoxidase, containing V^V (VO^{3+}), and an alternative nitrogenase with medium-valent vanadium.

In Vanadium Compounds; Tracey, A., et al.;
ACS Symposium Series; American Chemical Society: Washington, DC, 1998.

A Decavanadate Sandwiched by Cryptand-2,2,2

Vanadate inhibits or stimulates a variety of phosphorylation enzymes. It also inhibits the inositoltriphosphate-induced Ca^{2+} release. The potentially active forms of vanadate are monovanadate, divanadate, tetra- and decavanadate. The physiological effects of decavanadate are particularly noteworthy, since kinetically rather stable decavanadate should not be present at physiological vanadium concentrations and in the reducing intracellular medium. Once administered or formed, however, e.g. at vanadate accumulating cell sites, it may be stabilized towards hydrolysis and reduction by embodiment into ionophores. We have shown that cryptands, which are commonly considered to model biogenic ionophores, can protect decavanadate by forming sandwich-like contact ion pairs as shown in Figure 1 for the interaction between a centrosymmetric dihydrogendecavanadate and two diprotonated cryptands C222 (*1*). There are no hydrogen bonding interactions between anion and cations. The protons on the decavanadate are bound to the C-site μ_2-oxo ions, the protons in the cryptands are trapped in the cavities formed by the 2 Ns and the 4 Os pointing towards the anion.

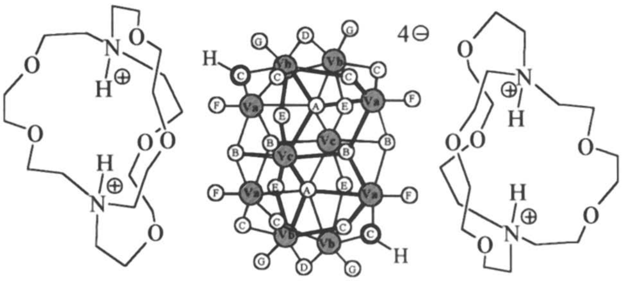

Figure 1. $[C222(H^+)_2]_2[H_2V_{10}O_{28}]$ may be considered to model the stabilization of decavanadate by ionophores under physiological conditions.

Two Enzymes with Vanadium in Their Active Center

To this date, two vanadium-dependent enzymes have been found in nature: Vanadate-dependent haloperoxidases are present in a variety of brown see weeds, but have also been isolated from red algae, a lichen and, more recently, from a primitive fungus. In the active enzyme, vanadium is in the +V state in an environment dominated by oxygen functions. The reduced (V^{IV}) form is inactive. The second enzyme is an alternative nitrogenase, containing vanadium instead of the more common molybdenum. Vanadium-nitrogenases from free-living nitrogen-fixing bacteria such as *Azotobacter* contain vanadium as a constituent of an iron-vanadium-sulfur cluster in an oxidation state between II to IV (XANES evidence). In this contribution, we will address model complexes of the two enzymes, models which mainly mimic the coordination environment but, in several instances, also the function of these enzymes, and which should provide deeper insight into the structure/function synergism of biological catalysts - to the benefit of, inter alia, related *in vitro* processes. In several cases, the relation between in vivo and in vitro processes will we pointed out.

Downloaded by MONASH UNIV on October 31, 2012 | http://pubs.acs.org
Publication Date: December 10, 1998 | doi: 10.1021/bk-1998-0711.ch004

Downloaded by MONASH UNIV on October 31, 2012 | http://pubs.acs.org
Publication Date: December 10, 1998 | doi: 10.1021/bk-1998-0711.ch004

The Peroxidation of Halides and Sulfides. The structure of a chloroperoxidase from the mold *Curvularia inaequalis* has recently been resolved by X-ray structure analysis (*2, 3*). In the native form, vanadium is in a trigonal-bipyramidal array in a O_4N donor set (Figure 2), where the only covalent link is provided by N^{ε} of a histidine residue. The O_4N donor set is retained in the peroxo form, but the geometry changes to tetragonal pyramidal. First results of an X-ray diffraction analysis of bromoperoxidase from the knobbed wrack (*Ascophyllum nodosum*) points into the same direction (*4*), although earlier X-ray absorption studies have suggested a somewhat different coordination environment, including a short V-O single bond typical of an alkoxide bonded to vanadium, possibly provided by serine (*5*). The peroxidases oxidize halide to hypohalide, which in turn generates halogenated hydrocarbons. The overall mechanism (*6*) is represented in Figure 3. The primary product is a peroxovanadium compound, verified by an X-ray structure analysis of the peroxoenzyme (*3*) (Figure 2). Halide is then oxidized and reacts with a hydrocarbon or, if no substrate hydrocarbon is available, produces singlet oxygen.

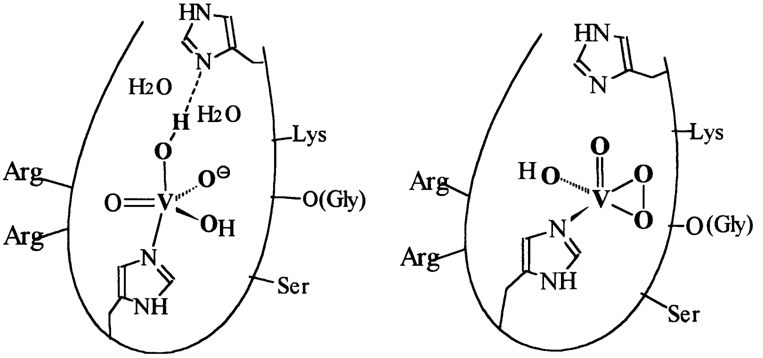

Figure 2. Vanadium site in vanadate-dependent peroxidase, native [left, (*2*)] and peroxo form [right, (*3*)], according to X-ray diffraction.

Selected structural models are shown in Figure 4. The compounds constitute an O_4N or O_5N donor set and contain, in the case of **1**, **3** and **4**, a labile ligand. The selection has been carried out so as to demonstrate the versatility of vanadium complexes with respect to coordination number and coordination geometry, essential requisites for catalytic activity. Thus, **1** is tetragonal-pyramidal, **2** distorted trigonal-bipyramidal, and **3** and **4** octahedral/tetragonal-pyramidal (*7-9*). Compound **2** in Fig. 4, with a coordination geometry in-between tetragonal-pyramidal and trigonal-bipyramidal (*7*), perhaps is closest to the structure of the active center of the vanadate-dependent haloperoxidases (cf. Figure 2). Further, compound **2** is a functional model, as is complex **4**. In either case, the intermediately formed peroxo complex, identified by ^{51}V NMR spectroscopy, catalyzes the bromination of organic substrates (such as acetanilide, phenol red, trimethoxybenzene) under mildly acidic conditions. Ethanolamine complexes of the kind represented by compound **4** in Figure 4 also catalyze the oxidation by peroxide of organic sulfides to sulfoxides (*8*) (Figure 5). Several interme-

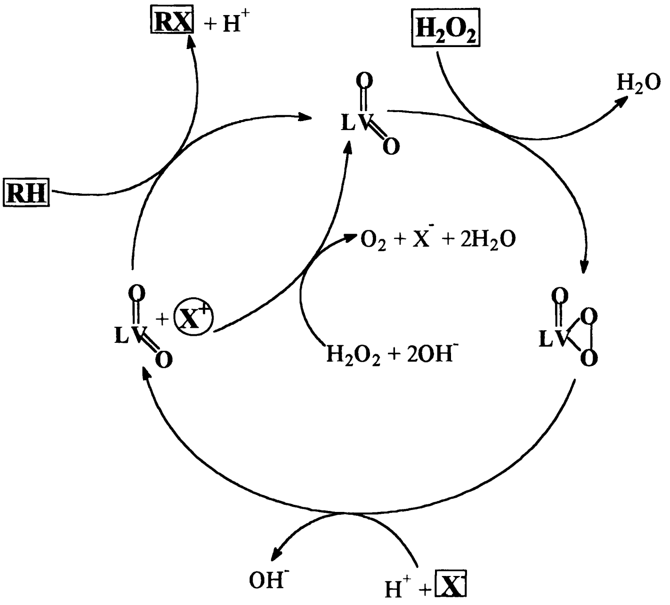

Figure 3. Mechanism of haloperoxidation by peroxovanadium as proposed by Pecoraro et al. (*6*). X^+ (X = halogen) stands for Enz-X^+, VO-X^+, HXO or X_3^+. The peroxo intermediate has recently been structurally characterized (*3*).

diates containing the oxidizing agent (H_2O_2) or the substrate (methyl-phenyl-sulfide or sulfoxide) coordinated to vanadium have been detected (Figure 5). If there is a center of chirality in the catalyst, one of the sulfoxide enantiomers is formed in excess.

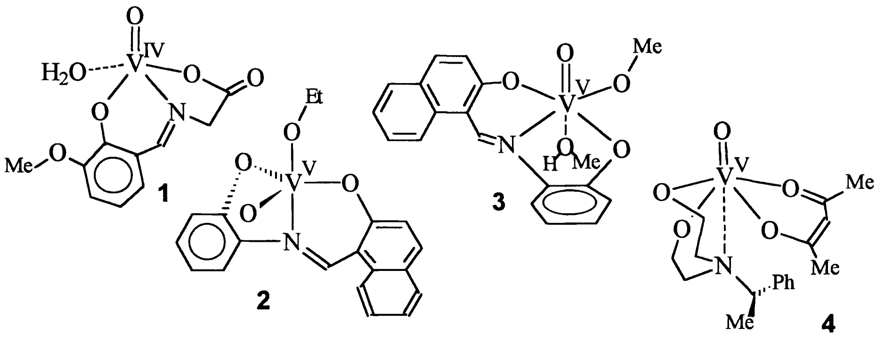

Figure 4. Models for the vanadium site in peroxidases. A dashed line (cf. **1**, **3** and **4**) represents a weak bond. The supporting ligands are Schiff bases (**1**-**3**) or diethanolamine (**4**). **2** and **4** have also been shown to be active in the oxidation (by peroxide) of thioethers.

Downloaded by MONASH UNIV on October 31, 2012 | http://pubs.acs.org
Publication Date: December 10, 1998 | doi: 10.1021/bk-1998-0711.ch004

Downloaded by MONASH UNIV on October 31, 2012 | http://pubs.acs.org
Publication Date: December 10, 1998 | doi: 10.1021/bk-1998-0711.ch004

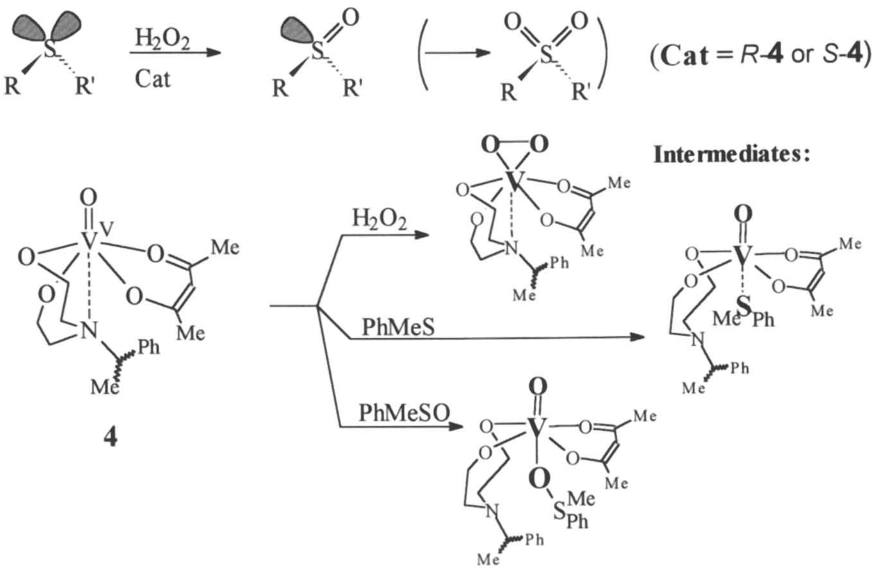

Figure 5. Enantioselective peroxidation of thioethers by **4**, and intermediates.

The vanadyl group itself can act as an oxidation reagent. This is demonstrated by the reaction between $VOCl_2(thf)_2$ and *o*-mercaptoaniline (*9*), Figure 6, part of which is oxidized to the disulfide, and part of which coordinates to the V^{IV} center to form a labile complex **5**. Reaction of **5** with hydroxynaphthaldehyde yields the non-oxo enamine complex **6**, where vanadium is in a highly distorted trigonal prismatic array.

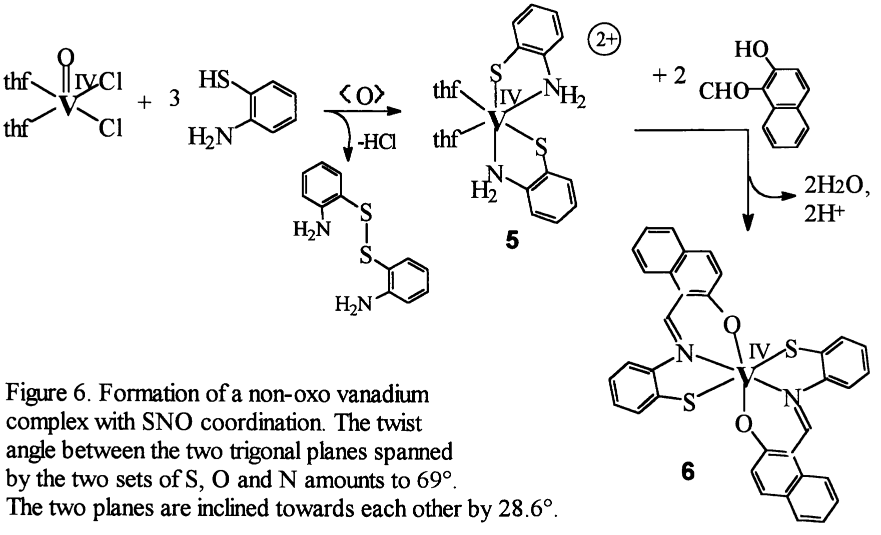

Figure 6. Formation of a non-oxo vanadium complex with SNO coordination. The twist angle between the two trigonal planes spanned by the two sets of S, O and N amounts to 69°. The two planes are inclined towards each other by 28.6°.

The Fixation of Nitrogen, and the Oxidation of Thiolate. Compound **6** in Figure 6 presents a few features which are also relevant for the V site in vanadium nitrogenase, namely the coordination of sulfur, the coordination of an enamine nitrogen, and the absence of an oxo group. So far, no crystal structure has been reported for a vanadium-nitrogenase, but there is much evidence that the active site of the iron-vanadium cofactor is built in essentially the same manner as the active site in the iron-molybdenum cofactor of the structurally characterized Mo nitrogenase (*10*). The immediate environment of vanadium hence contains three sulfides (which link vanadium to three irons in one half of the M-cluster of the iron-vanadium protein, Figure 7), the enamine nitrogen from a histidine, and the vicinal carboxylate and alkoxide of homocitrate. As for the molybdenum analog, vanadium nitrogenase exhibits concomitant hydrogenase activity, and alkyne-, alkene and isonitrile-reductase/ligase activities. The formation of the *Z*-isomer of ethylene if alkyne reduction is carried out in deuterated water, clearly indicates that the substrate alkyne is coordinated to and activated by a metal site - possibly vanadium - prior to reductive protonation.

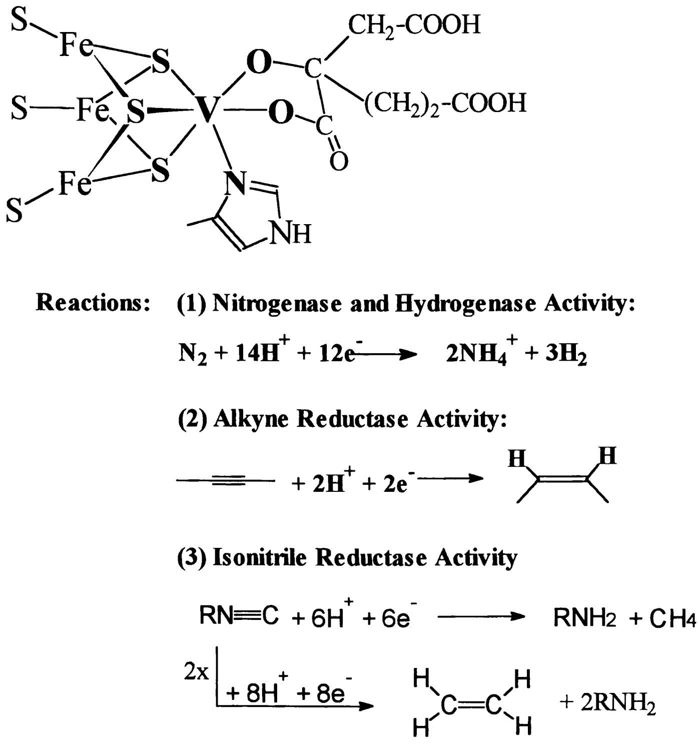
S
Fe
S
S
Fe
S
V
O
C
CH2-COOH
(CH2)2-COOH
O
C
O
S
Fe
S
N
NH
Reactions:
(1) Nitrogenase and Hydrogenase Activity:
N2 + 14H+ + 12e- → 2NH4+ + 3H2
(2) Alkyne Reductase Activity:
+ 2H+ + 2e-
H
H
(3) Isonitrile Reductase Activity
RN≡C + 6H+ + 6e- → RNH2 + CH4
2x
+ 8H+ + 8e-
H
H
C=C
H
H
+ 2RNH2

Figure 7. Plausible structure of the vanadium site in vanadium nitrogenase, and some reactions which are catalyzed by nitrogenases.

In order to model thio-ligation to vanadium, we have synthesized a variety of vanadium(II, III and IV) complexes with thiolates and thioether (sulfide) ligands (*11*-,

Downloaded by MONASH UNIV on October 31, 2012 | http://pubs.acs.org
Publication Date: December 10, 1998 | doi: 10.1021/bk-1998-0711.ch004

Downloaded by MONASH UNIV on October 31, 2012 | http://pubs.acs.org
Publication Date: December 10, 1998 | doi: 10.1021/bk-1998-0711.ch004

13). Compound **6** in Fig.6 is an example for V^{IV}. Selected V^{II} and V^{III} complexes are shown in Figure 8: A mixed thiolato/sulfide coordination to V^{II} is realized by complex 7, which can be oxidized reversibly to the V^{III} analog at –0.37 V (relative to SCE). A second ligand giving rise to a X_2VL_4 arrangement in an octahedral array, providing two reactive cisoid positions for the two X ligands, is the V^{II} complex **8**. The two chlorines can be substituted in salt metathesis reactions. Compound **9** finally, a dinuclear V^{III} complex bridged by thiophenolate, contains one replaceable chlorine at each vanadium center.

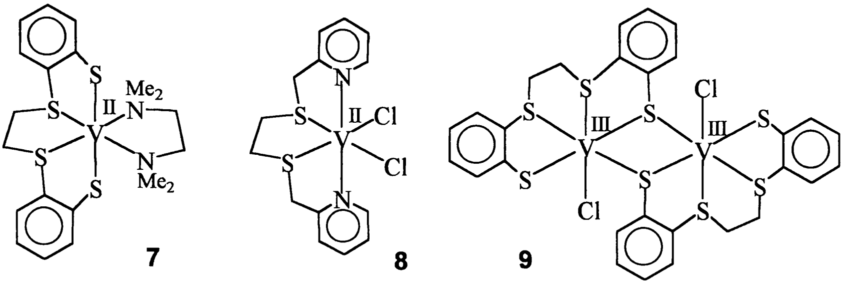

Figure 8. Thiolate and sulfide coordination to vanadium(II and III) centers.

Vanadium nitrogenase is not the only biogenic case for vanadium-sulfur coordination. Vanadate and vanadyl have been shown to interact with the sulfhydryl of cysteinyl residues in proteins, and there is at least one reported case, where the inhibition of an enzyme (viz. glyceraldehyde 3-phosphate dehydrogenase) can be traced back to a redox reaction between cysteine and vanadium (*14*). We have modeled such a reaction by the interaction of vanadyl chloride with the tetradentate dithiolate-diamine ligand shown in Figure 9 (*11, 12*). Three concomitant processes can be observed in this reaction: First, part of the ligand is oxidized to a heterocycloeicosane containing two disulfide groups. Part of the vanadium precursor looses its oxo function in this process. Second, an amide is formed by deprotonation of one of the amine functions. Third, the trianionic ligand thus generated coordinates to vanadium, forming an asymmetrically oxo-bridged, dinuclear vanadium complex, **10**, with formally V^{III} and V^{V}. There are additional interesting features in this complex, such as a hydrogen-bonding interaction between the amine hydrogen in one half of the molecule to the thiolate sulfur in the other half.

Coming back to vanadium-nitrogenase: Apart from the thio coordination, another main point in the coordination environment of vanadium is homocitrate. Its simultaneous coordination via vicinal alkoxide and carboxylate can be modeled by appropriate ligands, benzilate in our case, as shown in Figure 10 (*15*). The starting material is the vanadyl complex **11** with the double Schiff base salen. **11** is converted to the trans-dichloro complex **12**. This type of reaction can quite generally be applied to vanadyl complexes containing ONNO or ONO donor sets. In the latter case, the cis-dichloro complex forms. **12** reacts with dilithiumbenzilate to the non-oxo V^{IV} complex **13**, with benzilate occupying cis positions. **13** can be reversibly oxidized (+0.920 V) and reduced (-0.338 V; vs. SCE).

Downloaded by MONASH UNIV on October 31, 2012 | http://pubs.acs.org
Publication Date: December 10, 1998 | doi: 10.1021/bk-1998-0711.ch004

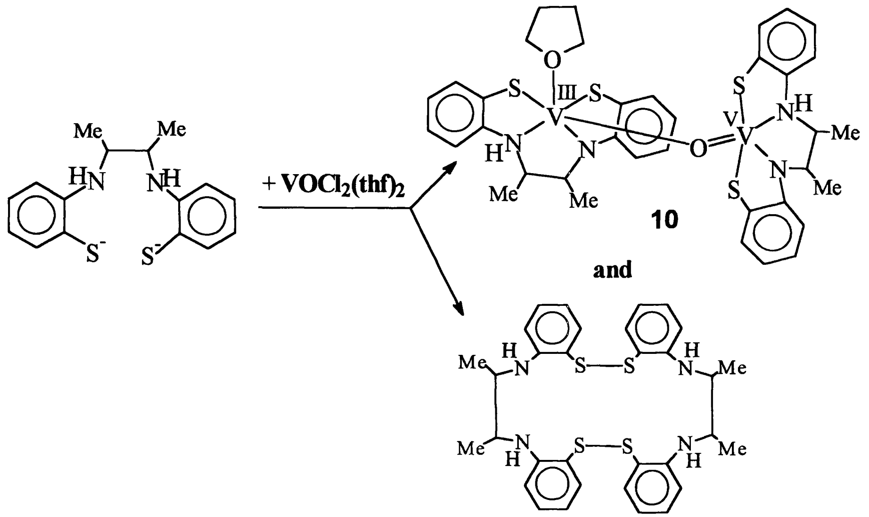
Me
Me
HN
NH
S⁻
S⁻
+ VOCl₂(thf)₂
O
S
III
V
S
HN
N
Me
Me
O
V
NH
Me
N
Me
S
S
10
and
Me
H
N
S
S
H
N
Me
Me
N
H
S
S
N
H
Me

Figure 9. Deprotonation, coordination and oxidation by VO^{2+}.

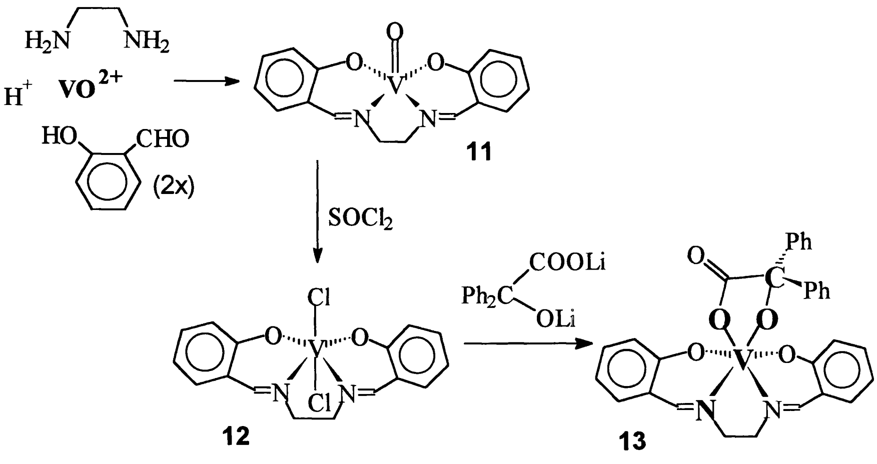
H₂N
NH₂
H⁺ VO²⁺
HO
CHO
(2x)
O
O
V
O
N
N
11
SOCl₂
Cl
O
V
O
N
Cl
N
12
COOLi
Ph₂C
OLi
O
Ph
C
Ph
O
O
O
V
O
N
N
13

Figure 10. Generation of a complex with vicinal carboxylate-alkoxide coordination.

The complexes **6-10** and **13** model part of the structure of the vanadium site in nitrogenase; they are, however, inactive as functional models (as is the isolated cofactor by itself). *Functional* models - dinitrogen complexes of vanadium - can be generated as shown in Figure 11: The starting material is THF-stabilized VCl$_3$ which, in the presence of lithium or sodium and an oligodentate phosphine, is reduced to a chlorophosphinevanadium(II) (**14**) and a mixed valence V$^{I/II}$ complex (**15**). In the presence of dinitrogen and catalytic amounts of naphthalene, the reduction proceeds to the formation of mono- and bis(dinitrogen) complexes of V^{-I}, the latter in the cis and trans

Downloaded by MONASH UNIV on October 31, 2012 | http://pubs.acs.org
Publication Date: December 10, 1998 | doi: 10.1021/bk-1998-0711.ch004

(**16**) conformation. These anionic complexes are stabilized by close contact ion-pair interaction with the alkaline metal ion. Addition of proton-active substances such as HCl converts one of the four nitrogens to ammonia. A small amount of hydrazine is also formed – as by the native enzyme. The electrons for the reduction of nitrogen stem from the vanadium center, which is recovered in the +II or +III state. The structures of the complexes have been verified by ^{51}V NMR spectroscopy of the ^{15}N-enriched compounds in solution, by ^{7}Li NMR spectroscopy and, for p_2 = dppe and Na^+ as the counter ion, by X-ray diffraction analysis (*16*).

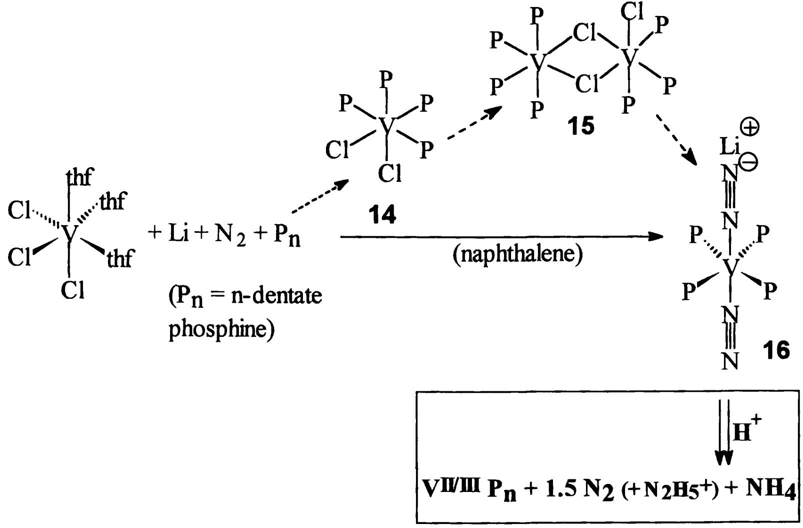
thf
Cl
thf
Cl
V
thf
Cl
+ Li + N₂ + Pₙ
(Pₙ = n-dentate phosphine)
14
15
16
(naphthalene)
H⁺
VII/III Pₙ + 1.5 N₂ (+N₂H₅⁺) + NH₄

Figure 11. Dinitrogenvanadium complexes: Synthesis and protonation. The dashed arrows connect intermediates which can be isolated if no redox catalyst (naphthalene) is added. Li can be replaced by Na. P_n represents an oligodentate phosphine.

Reductive Protonation of Alkynes and Reductive C-C Coupling of Isonitriles. As mentioned previously (cf. Figure 7), the nitrogenases can also reduce other unsaturated substrates. Thus, acetylene is converted to ethylene (and further to ethane by vanadium-nitrogenase), and isonitrile is converted to methane and primary amine. In a side reaction, C-C coupling, accompanied by the formation of ethylene is observed along with the generation of primary amine. The nitrogenases hence attain an alkyne-reductase activity and an isonitrile-reductase plus -ligase activity (*17*). As in N_2 fixation, the activation of the unsaturated substrate is probably connected with its coordination to a metal center. Whether this is iron or the hetero metal – V or Mo – is still under debate. There are good arguments for assuming that the hetero metal plays the decisive role. Hence, to model these additional activities of nitrogenases, we have synthesized several compounds which indicate that (i) alkynes and isonitriles do coordinate to low-valent vanadium, (ii) isonitriles undergo reductive C-C coupling when attached to vanadium, and (iii) coordinated alkynes produce alkenes with H^+/H^- or H_2. Examples of complexes and their reactions are given in Figure 12: The V^I-alkyne complex **17** (*18*), when treated successively with hydride and protons, yields styrene, and the V^I-isonitrile complex **18**

(*19*) reacts in the presence of small amounts of water to form the V^{III} alkyne complex **19** [see ref. (*20*) for the Nb analog]. A similar vanadium complex has been shown to split off a *Z*-olefin when treated with hydrogen under slightly elevated pressure (*21*). These reactions are, of course, also of relevance for the in vitro catalysis of reductive coupling and protonation reactions carried out by certain vanadium-based catalysts (*22*).

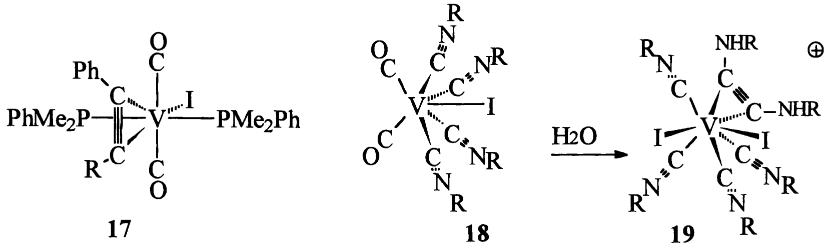

Figure 12. Reactions modeling alkyne-reductase and isonitrile-lyase activities of nitrogenases.

Acknowledgment. This work was supported by the Deutsche Forschungsgemeinschaft and the Fonds der Chemischen Industrie.

Literature Cited

(*1*) Farahbakhsh, M.; Schmidt, H.; Rehder, D. *Chem. Ber./Recueil* **1997**, *130*, 1123.

(*2*) Messerschmidt, A.; Wever, R., *Proc. Natl. Acad. Sci. U.S.A.* **1996**, *93*, 392.

(*3*) Messerschmidt, A.; Prade, L.; Wever, R. *Biol. Chem.* **1997**, *378*, 309.

(*4*) Weyand, M. Ph. D. Thesis, Gesellschaft für Biotechnologische Forschung Braunschweig, **1996**.

(*5*) Arber, J.M.; de Boer, E.; Garner, C.D.; Hasnain, S.S.; Wever, R. *Biochemistry* **1989**, *28*, 7968.

(*6*) Colpas, G.J.; Hamstra, B.J.; Kampf, J.W.; Pecorao, V.L. *J. Am. Chem. Soc.* **1996**, *118*, 3469.

(*7*) Bashirpoor, M.; Schmidt, H.; Schulzke, C.; Rehder, D. *Chem. Ber./Recueil* **1997**, *130*, 651.

(*8*) Schmidt, H.; Bashirpoor, M.; Rehder, D. *J. Chem. Soc., Dalton Trans.* **1996**, 3865.

(*9*) Farahbakhsh, M.; Nekola, H.; Schmidt, H.; Rehder, D. *Chem. Ber./Recueil* **1997**, *130*, 1129.

(*10*) Chan, M.M.; Kim, J.; Rees, D.C. *Science* **1993**, 792.

(*11*) Tsagkalidis, W.; Rehder, D. *J. Bioinorg. Chem.* **1996**, *1*, 507.

(*12*) Tsagkalidis, W.; Rodewald, D.; Rehder, D. *Inorg. Chem.* **1995**, 34, 1943.

(*13*) Tsagkalidis, W.; Rodewald, D.; Rehder, D. *J. Chem. Soc., Chem. Commun.* **1995**, 165.

(*14*) Banabe, J.E.; Echegoyen, L.A.; Pastrona, B.; Martinez-Maldonado, M. *J. Biol. Chem.* **1987**, 262, 9555.

(*15*) Vergopoulos, V.; Jantzen, S.; Rodewald, D.; Rehder, D. *J. Chem. Soc., Chem. Commun.* **1995**, 377.

Downloaded by MONASH UNIV on October 31, 2012 | http://pubs.acs.org
Publication Date: December 10, 1998 | doi: 10.1021/bk-1998-0711.ch004

(16) Gailus, H.; Woitha, C.; Rehder, D., *J. Chem. Soc., Dalton Trans.* **1994**, 3471.

(17) Miller, R.W. In *Biology and Biochemistry of Nitrogen Fixation*; Dilworth, M.J.; Glenn, A.R., Eds; Elsevier: Amsterdam, 1991, pp 9-36.

(18) Gailus, H.; Maelger, H. Rehder, D. *J. Organomet. Chem.* **1994**, *465*, 181.

(19) Böttcher, C.; Rodewald, D.; Rehder, D. *J. Organomet. Chem.* **1995**, *496*, 43.

(20) Collazo, C.; Rodewald, D.; Schmidt, H.; Rehder, D. *Organometallics* **1996**, *15*, 4884.

(21) Protasiewicz, J.D.; Lippard, S.J., *J. Am. Chem. Soc.* **1991**, *113*, 6564.

(22) Rehder, D.; Gailus, H. *Trends Organomet. Chem.* **1994**, *1*, 397.

Downloaded by MONASH UNIV on October 31, 2012 | http://pubs.acs.org
Publication Date: December 10, 1998 | doi: 10.1021/bk-1998-0711.ch004

Downloaded by MONASH UNIV on October 31, 2012 | http://pubs.acs.org
Publication Date: December 10, 1998 | doi: 10.1021/bk-1998-0711.ch005

Chapter 5

Synthesis, Structure and Reactivity of V^v-Thiolate and V^v-η^2-Sulfenate Complexes

Charles R. Cornman, Thad C. Stauffer, and Paul D. Boyle

Department of Chemistry, North Carolina State University,
Raleigh, NC 27695–8204

Oxidation of the oxovanadium(V)-dithiolate complex V^VO(btap) (**1**, H_3btap is 2-(bis-ethane-2-thiol)amino-4-methylphenol) with oxo-atom donors such as *m*-CPBA, peroxides, iodosylbenzene and oxaziridines results in the sequential formation of the mono- and di-sulfenate complexes (**2** and **3**, respectively). Structural analysis of **3** has confirmed that the sulfenate ligands are coordinated to the V^V metal center in a unique η^2 side-on manner. ^1H and ^{51}V NMR are consistent with an analogous structure for **2**. ^{18}O-labeling studies have been used to assign the vibrational modes of the η^2-coordinated sulfenate ligand in **2** (810 cm^{-1}). Complex **2** can be prepared in an optically active form using chiral oxaziridines, and acts as a reversible oxo-transfer agent.

The coordination and reaction chemistry of vanadium is important due to the biological activity of this element, especially with respect to phosphate metabolism and the insulin-mimetic influence (*1,2*). It has been known for some time that vanadium is a potent inhibitor of protein tyrosine phosphatases (PTPs) and that vanadium, presumably in the +5 oxidation state, coordinates to the active-site of these enzymes, forming a covalent bond with the thiolate sulfur of a cysteine side-chain (*3*). Due to this biological activity, we have been interested in the structural parameters and reactivity of vanadium(V)-thiolates. Structurally characterized small molecules containing the vanadium(V)-thiolate unit are limited to a few thiophenol and dithiolene complexes and one example of a vanadium(V)-alkylthiolate (*4*). This paucity of structural data leaves a gap in our understanding of the bonding in this motif. Our understanding of the reactivity of vanadium(V) with thiols is limited to the ability of vanadium(V) to oxidize thiol-containing molecules. The reactivity of the vanadium(V) with *coordinated* thiol, *vis.* V^V-SR, such as occurs in PTPs, has remained unexplored.

Vanadium-adducts of two PTPs have been characterized by protein crystallography and the general structure is depicted in Figure 1A (V-S distance 2.13 and 2.5Å) (*5,6*). The five-coordinate vanadium ion, most likely in the +5 oxidation state, is surrounded by a sulfur donor and four oxygen donors in a trigonal bipyramidal (TBP) geometry. The closest model complex is the TBP oxovanadium(V)-trithiolate, depicted in Figure 1B, that has been prepared by

In Vanadium Compounds; Tracey, A., et al.;
ACS Symposium Series; American Chemical Society: Washington, DC, 1998.

Addison and coworkers (V-S distance = 2.25Å) (*4*). The vanadium-PTP structure is distinct from the model complexes in that the protein adduct has an oxygen-rich coordination sphere while the model has a sulfur-rich coordination sphere. Additionally, the orientation of the thiolate ligand with respect to the coordination polyhedron is different for each molecule. In the vanadium-PTP adduct the thiolate ligand is in an axial coordination site, while in the model complex, the thiolate ligands are in equatorial coordination sites.

The reaction of vanadium(V) with thiol-containing molecules generally results in reduction to vanadium(IV) and concomitant oxidation of the thiol-containing molecule. The reduction of aqueous vanadium(V) (vanadate) to vanadium(IV) (vanadyl) using thiol (RSH) reductants has been demonstrated and the sulfur-containing product is invariably the disulfide (*7*). The vanadium(IV)-catalyzed oxidation of sulfides (RSR') to sulfoxides or sulfones, using hydrogen peroxide as the oxidant, is also well documented (*8,9*). In this reaction, it seems that vanadium(V)-peroxo complexes may be intermediates. Interestingly, the oxidation of the active site cysteine of a PTP by a vanadium(V)-peroxo complex, to form the cysteine-sulfone, has recently been reported (*10*).

In light of this recent oxidation chemistry of the active site cysteine in PTP1B, and the propensity of vanadium to coordinate to the active site cysteine in PTPs, we have investigated the ability of oxo donors to oxidize a thiol that is coordinated to vanadium(V). Herein we present our studies on the preparation and characterization of an oxovanadium(V)-thiol complex containing an O, N, and S coordination environment. The reaction of this complex with oxo-transfer agents has been examined and the resulting oxo-transfer products have been characterized with respect to structure, spectroscopy and chemical reactivity (*11*).

Downloaded by MONASH UNIV on October 31, 2012 | http://pubs.acs.org
Publication Date: December 10, 1998 | doi: 10.1021/bk-1998-0711.ch005

Synthesis and Structure of VO(btap), 1

The ligand H_3btap has been prepared from ethylene sulfide and 2-amino-4-methylphenol. This ligand can provide a tripodal four-donor coordination environment and therefore can be used to form five-coordinate complexes of the V^V=O ion. Reaction of H_3btap with VO(O*i*-Pr)$_3$ in CH_2Cl_2 yields VO(btap), **1**, as a red powder (M^+ = 307 by FAB+ mass spectrometry). This complex can be recrystallized by slow diffusion from CH_2Cl_2/hexanes to yield diffraction quality crystals. The structure of **1**, presented in Figure 2, indicates that the complex has a trigonal bipyramidal geometry and approximately C_s symmetry. Two thiolate ligands and one phenolate oxygen ligand define the equatorial plane, while the oxo ligand and 3° amine ligand fill the axial coordination sites. The structural parameters are very similar to the analogous complex characterized by Addison. (*4*). Importantly, the average V-S distance in **1**, at 2.247Å, is identical to the average V-S distance in the Addison complex. Complex **1** is readily soluble in many organic solvents, but slowly decomposes when exposed to hydroxyl-containing solvents. The ^1H and ^{51}V NMR of **1** (*vide infra)* are entirely consistent with the solid state structure.

Reaction of VO(btap) with Oxo-transfer Agents

The dithiolate complex, **1**, reacts with several oxo-transfer agents including H_2O_2, *t*-BuOOH, K_2SO_5, iodosylbenzene, oxaziridines and *meta*-chloroperoxybenzoic acid (*m*CPBA). In a typical reaction, adding excess 30% H_2O_2 to a CH_2Cl_2 solution of **1** results in the rapid formation of a purple solution. Immediate separation of the aqueous and organic layers and addition of hexane facilitates precipitation of a purple solid, **2** (M^+ = 323 by FAB+ mass spectrometry). If the solution of **1** (or **2**) is allowed to react with excess H_2O_2, a green/brown solid can be isolated.

Electronic spectroscopy. The reaction between **1** and *m*-CPBA in CH_2Cl_2 can conveniently be monitored by electronic absorption spectroscopy and the resulting spectra are shown in Figure 3. The red color of **1** (Figure 3A) is due to a LMCT transition at λ_{max} = 491 nm (presumably S→V). Addition of ≈1.2 equivalents of *m*-CPBA to this red solution results in its quantitative conversion to a purple solution of **2**, characterized by an LMCT transition at λ_{max} = 552 nm. Subsequent addition of ≈2 additional equivalents of *m*-CPBA results in conversion of the purple solution to a pale green/brown solution of **3**, as shown in Figure 3B.

^{1}H and ^{51}V NMR spectroscopy. The formation of **2** and **3** can also be monitored by ^{51}V and ^{1}H nuclear magnetic resonance spectroscopy. As shown in Figure 4A, complex **1** has a ^{51}V NMR resonance at +338 ppm (vs. external $VOCl_3$, * denotes an impurity in the external standard; the small signal at ≈-450ppm is the reflection of the $VOCl_3$ resonance about the carrier frequency). The first addition of *m*-CPBA (1.2 equivalents, Figure 4B) yields a solution of **2** with a ^{51}V NMR signal at -186 ppm, while the second addition of *m*-CPBA yields a solution of **3** with a ^{51}V NMR signal at -666 ppm. In general, it has been demonstrated that the ^{51}V chemical shift correlates with the hardness of the first coordination sphere, with hard donors having more negative chemical shifts (*12*). In line with this, oxometalates of vanadium(V), such as vanadate oligomers, usually have shifts between -400 ppm and -850 ppm. Complexes such as **1**, with soft thiol donors, should resonate significantly downfield of this range and the chemical shift for **1** (+338 ppm) is consistent with shifts observed for other thiol-containing complexes. The upfield shift of 524 ppm observed upon converting **1** to **2** is indicative of a harder first coordination sphere for **2** relative to **1**. The conversion of **2** to **3** yields a similar upfield shift (480 ppm) in the ^{51}V NMR spectrum. These similar upfield shifts suggest that similar chemical transformations occur at each step. Since only one equivalent of oxidant is needed for the first step, it is reasonable that each step is the transfer of a single oxygen atom from the donor (*m*-CPBA in this case) to the acceptors **1** or **2**. Since the vanadium ion is already in its highest oxidation state, the oxidation must be ligand-centered, probably at the coordinated thiolate.

^{1}H NMR spectroscopy should be a sensitive probe of these chemical transformations since the methylene protons are expected to be strongly influenced by the oxidation level of the neighboring sulfur ligands and the symmetry of the resulting complexes. Based on the X-ray structure, complex **1** has C_s symmetry, with the symmetry plane containing the non-sulfur coordinating atoms and bisecting the S-V-S angle (see Figure 2). Thus, for the two symmetry equivalent thioethyl arms of **1**, one expects *at most* four proton magnetic environments. The observed pattern for the methylene region of the ^{1}H NMR spectrum of **1**, shown in Figure 5A, confirms this expectation. The ^{1}H NMR spectrum of **2** (Figure 5B) has six methylene proton magnetic environments indicating the loss of the mirror plane. In the case of **2**, two of the potentially eight magnetic environments for the methylene protons must be accidentally degenerate. Figure 5C, with four methylene proton magnetic environments, strongly suggests that the mirror plane is reestablished for **3**.

Taken together, the ^{51}V and ^{1}H NMR studies are consistent with the oxidations shown in equation 1. In two sequential steps, each of the thiolate ligands is oxidized to the sulfenate (sul*fen*ates are thiol-monooxygenates while sul*fin*ates are thiol-dioxygenates), thereby changing the first coordination sphere to contain harder donor groups (sulfenates are harder than thiolates). This partially explains the upfield shift in the ^{51}V NMR on going from **1** to **2** and **2** to **3**. Additionally, oxygenation of the first sulfur to form **2** breaks the mirror symmetry of **1**, while the second oxygenation to form **3** reestablishes the mirror symmetry as observed in the ^{1}H NMR.

Downloaded by MONASH UNIV on October 31, 2012 | http://pubs.acs.org
Publication Date: December 10, 1998 | doi: 10.1021/bk-1998-0711.ch005

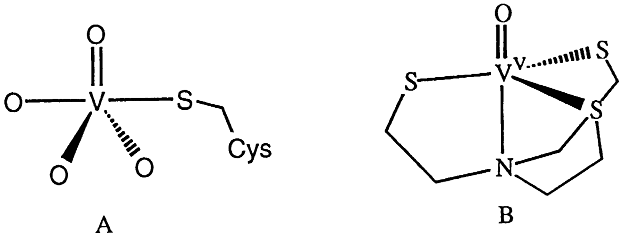

Figure 1. Structures of vanadium adducts of two PTPs (A) and oxovanadium(V)-tristhiolato complex (B).

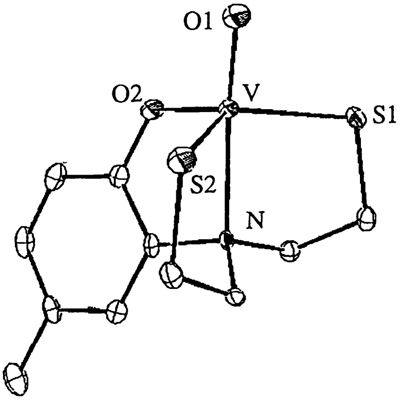

Figure 2. X-ray structure of $V^VO(btap)$, **1**.

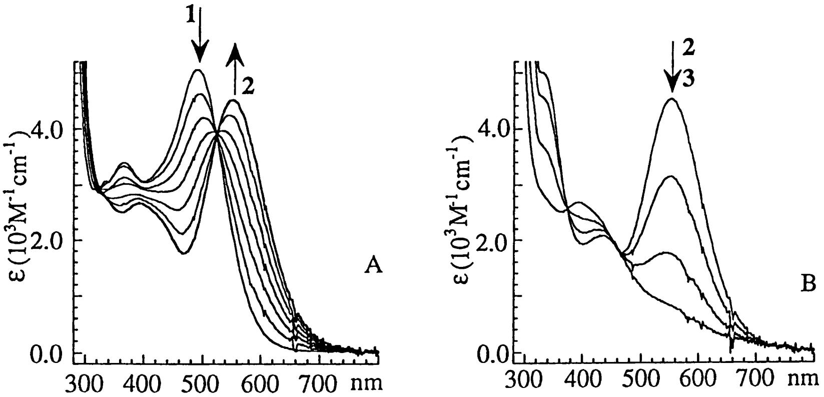

Figure 3. UV-Vis spectra monitoring the oxidation of **1** to **2** (A) and **2** to **3** (B).

Downloaded by MONASH UNIV on October 31, 2012 | http://pubs.acs.org
Publication Date: December 10, 1998 | doi: 10.1021/bk-1998-0711.ch005

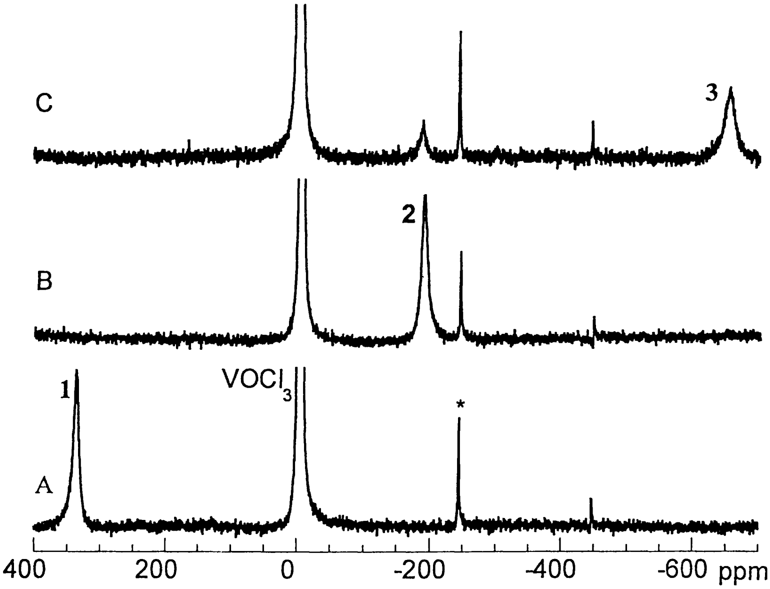

Figure 4. ^{51}V NMR spectra of **1** (A), **2** (B), and **3** (C) in CH_2Cl_2 at -70 °C.

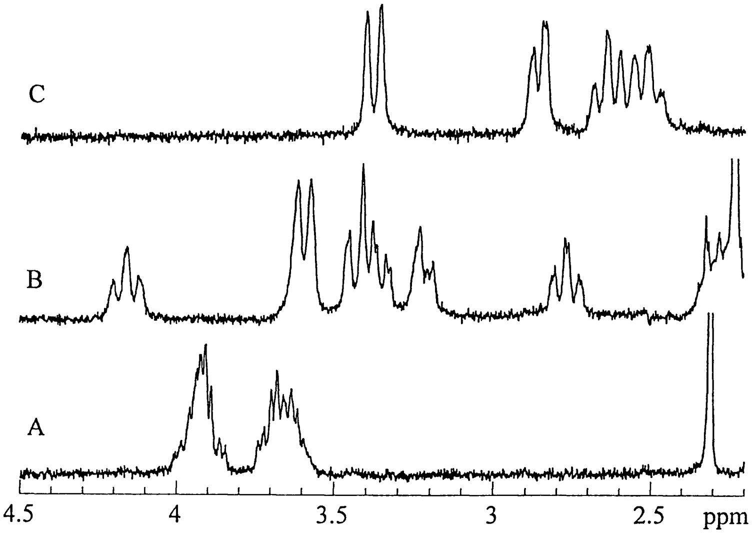

Figure 5. ^{1}H NMR spectra of **1** (A), **2** (B), and **3** (C) in CH_2Cl_2 at -70 °C.

Downloaded by MONASH UNIV on October 31, 2012 | http://pubs.acs.org
Publication Date: December 10, 1998 | doi: 10.1021/bk-1998-0711.ch005

Downloaded by MONASH UNIV on October 31, 2012 | http://pubs.acs.org
Publication Date: December 10, 1998 | doi: 10.1021/bk-1998-0711.ch005

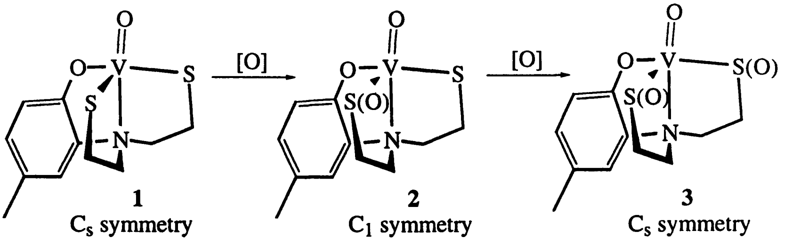

(*1*)

The coordination chemistry of the sulfenate ligand has been studied extensively for nickel(II) and other group 8 metals (*13,14*). Metal-sulfenates usually coordinate in an η^1-fashion through the sulfur atom. However, this is not necessarily the case for hard, early transition elements such as vanadium(V). Clues to the type of bonding exhibited by the V-S(O) unit are provided by the large upfield shifts in the ^{51}V NMR that are observed upon oxygenation. The extreme high field resonance for **3** (-666 ppm) is similar to vanadium(V) complexes with exclusively hard donors (O,N) in the first coordination sphere. This suggests that the oxygen atoms of **3** (and **2**) may directly interact with the vanadium center. Furthermore, studies on vanadium(V)-peroxides, -hydroxylamines (three-membered ring) and -carboxylates (four-membered ring) have shown that additional upfield shifts are observed for molecules in which the vanadium is part of a three- or four-membered metallacycle (*12*). Coordination of the sulfenate ligand in an η^2-fashion would place the oxygen in the first coordination sphere of the vanadium *and* create a three-membered ring, thereby more fully explaining the large ^{51}V resonance shifts observed upon oxygenation of each sulfur.

Structures of the V^V-η^2-sulfenates

X-ray structure of 3. X-ray quality crystals of **3** were obtained by slow evaporation of a CH_2Cl_2/hexanes solution of the double oxygenation product. The molecular structure of **3**, presented in Figure 6, shows that the sulfenate ligands are coordinated in the η^2 manner as suggested by the ^{51}V NMR. The seven-coordinate structure is best described as a pentagonal bipyramid. This structure is becoming a common motif in the coordination chemistry of vanadium complexes containing potentially η^2 ligands such as sulfenates, peroxides (*15*) and hydroxylamines (*16,17*). Complex **3** has approximate C_s symmetry with the mirror plane containing the nitrogen, oxo and phenolate oxygen, and vanadium atoms (analogous to the mirror plane in **1**). The sulfenate oxygens are directed towards each other and away from the coordinated phenolate ligand. The vanadium atom is displaced from the mean equatorial plane by 0.381Å towards the oxo ligand. As expected, the average V-S distances in **3** (2.365Å) is longer than the average V-S distance in the dithiolate **1** (2.249Å) as well as in the corresponding distance for Ni^{II}-sulfenates (2.157Å). The average S-O bond distance in **3** (1.598Å) is 0.053Å longer than the corresponding distance in Ni^{II}-sulfenates (1.545Å). The distance between the sulfenate oxygens is 2.567Å. Complex **3** is not chiral; however, it does contain two chiral centers, the sulfenate sulfur atoms, which have the *R*- and *S*-configuration.

Molecular structure of 2. NMR evidence suggests that **2** is the monosulfenate analog of **3**. Therefore, complex **2** is six coordinate with one η^2-sulfenate ligand as depicted in Figure 7A. By analogy to **3**, we predict that the sulfenate oxygen is directed away from the phenolate oxygen (as shown in Figure 7A).

Coordination of a single sulfenate ligand creates three chiral centers, the sulfenate sulfur atom, the amine nitrogen, and the vanadium. As depicted in Figure

Downloaded by MONASH UNIV on October 31, 2012 | http://pubs.acs.org
Publication Date: December 10, 1998 | doi: 10.1021/bk-1998-0711.ch005

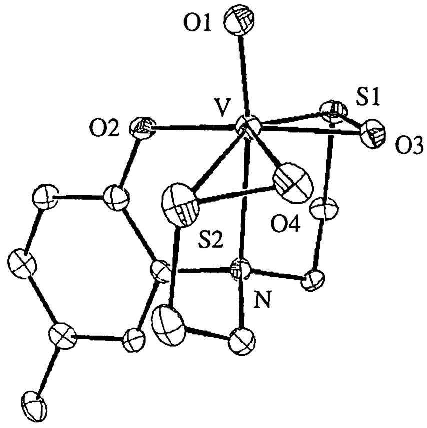

Figure 6. X-ray structure of **3**.

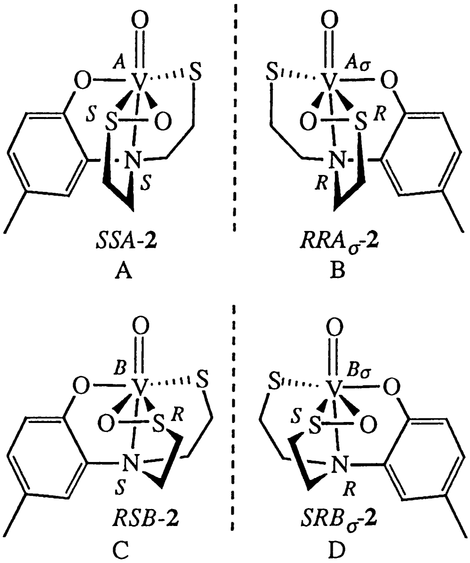

SSA-**2**
A

RRA$_\sigma$-**2**
B

RSB-**2**
C

SRB$_\sigma$-**2**
D

Figure 7. Proposed structure of **2** -- a racemic mixture of the enantiomers shown in A and B-- and other diastereomers with the sulfenate oxygen pointed toward the phenolate ligand (C and D).

7A, the sulfenate sulfur and the amine nitrogen are in the *S* configuration. The mirror image (Figure 7B) has the sulfur and amine in the *R* configuration. For simplicity, if we define the vanadium center in Figure 7A as *A*, then the stereochemistry about the vanadium center in the mirror image is A_σ (where A_σ is the mirror image of *A*). (*8*). We believe that **2**, formed by the reaction of **1** with achiral oxidants, is a racemic mixture of the enantiomeric pair shown in Figures 7A and B, *S*-sulfenate-*S*-amine-*A*-vanadium-**2** (*SSA*-**2**)and *R*-sulfenate-*R*-amine-A_σ-vanadium-**2** (RRA_σ-**2**), respectively. Other diastereomers, shown in Figures 7C and D, have not been observed and are believed to be less stable. The diastereomer in Figure 7C could arise from inversion about the sulfenate sulfur (but not the amine) to give *RSB*-**2** (where the new chirality about the vanadium center has been defined as *B*). The mirror image of *RSB*-**2** is SRB_σ**2** (Figure 7D). The formation of *SSB*-**2** and RRB_σ**2** is precluded by the presence of the ethylene linker between the sulfenate sulfur and the amine. Therefore, the vanadium chirality is coupled to the chirality of the sulfenate sulfur and the amine.

Preparation of 2 with Chiral Oxaziridines

The stereochemistry of **2** can be controlled by using a chiral oxidant as the source of the sulfenate oxygen atom. We have used the optically active isomers of camphorsulphonyloxaziridine to prepare **2** in solution. Circular dichroism spectra, shown in Figure 8, confirm that optically active solutions of **2** are formed. The CD intensity decreases slowly (over hours) primarily due to the decomposition of **2** in the presence of the oxidant (as monitored by UV-Vis spectroscopy). This decomposition has prevented measurements of the rate of racemization. Chiral sulfoxides (RR'SO) have an inversion barrier of $E_a \approx 40$ kcal/mol which corresponds to appreciable rates of inversion occurring only at temperatures near 200 °C (*19*). Racemization of *SSA*-**2** to RRA_σ-2 via an inversion mechanism would be a complex process requiring inversion at the sulfenate sulfur *and* the vanadium center. In a simpler process, complex **2** can racemize *via* an intramolecular oxo-atom transfer (oxo transfer from the sulfenate to the thiolate *via* a C_s-symmetric transition state). We are currently exploring methods to isolate **2** as an optically pure complex, measure the racemization rate, and probe the racemization mechanism.

Reaction of η^2-sulfenates with Oxo-atom Acceptors.

Stereospecific oxo-atom transfer using transition metal complexes has received much attention in recent years. Optically active sulfenates such as **2** provide an interesting alternative to the more familiar transfer of a metal-bound oxo- or peroxide oxygen. In preliminary studies, racemic **2** (prepared and isolated from **1** and aqueous H_2O_2) reacts with rapidly added Ph_3P to give Ph_3PO (confirmed by gc/ms) and **1** (monitored by UV-Vis and ^{51}V NMR). The success of the reaction is quite sensitive to the rate of addition and other parameters that are just now being defined. Under slow addition conditions, the vanadium containing product is ^{51}V NMR silent and gives only a weak EPR signal. Complex **3** also reacts with Ph_3P to give undefined vanadium-containing products. We have not been able to oxidize prochiral olefins such as styrene with **2** or **3**. The full scope of the oxo-atom transfer chemistry of these complexes is under further investigation.

Vibrational Spectroscopy of η^2-sulfenates

The infrared spectra of **1** and **2** (400-1600 cm^{-1}, A and B, respectively) are presented in Figure 9. Interestingly, the spectrum for **2** is less complicated than the spectrum of **1**, despite the more complex structure of **2**. Specifically, vibrations of the coordinated sulfenate moiety are not readily observed. Ni^{II}-η^1-sulfenates have ν(S=O) between 900 and 930 cm^{-1}. To assign the vibrations of the sulfenate unit in **2**, we have

Downloaded by MONASH UNIV on October 31, 2012 | http://pubs.acs.org
Publication Date: December 10, 1998 | doi: 10.1021/bk-1998-0711.ch005

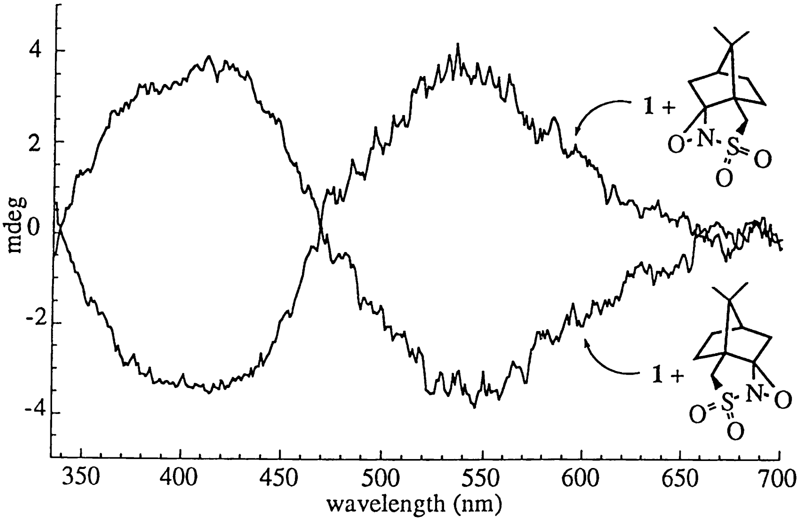

Figure 8. Circular dichroism spectra of **2** prepared with enantiomerically pure oxaziridines.

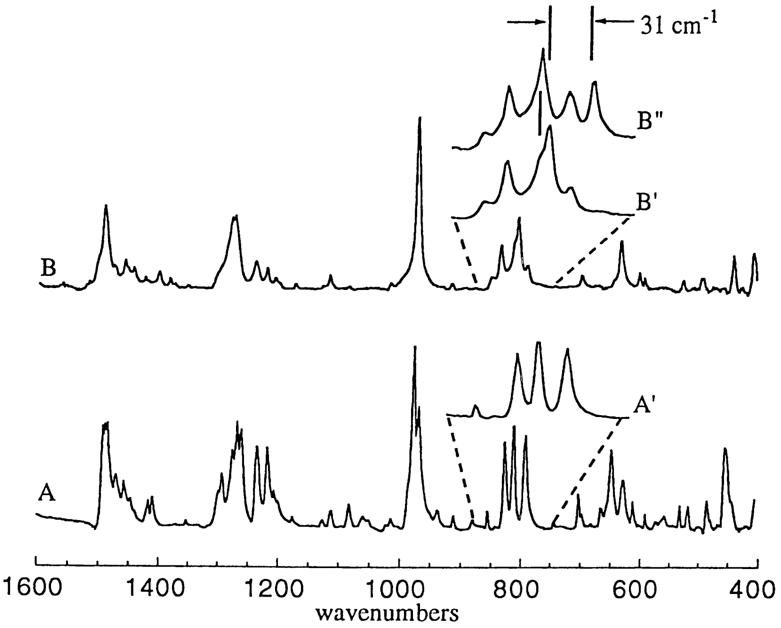

Figure 9. Infra red spectra of **1** (A), **2**, (B and B') and ^{18}O-**2** (B").

Downloaded by MONASH UNIV on October 31, 2012 | http://pubs.acs.org
Publication Date: December 10, 1998 | doi: 10.1021/bk-1998-0711.ch005

prepared the ^{18}O-sulfenate isotopomer of **2** using $H_2{}^{18}O_2$. Expansions of the 800 cm^{-1} region of the spectra for **1**, ^{16}O-**2**, and ^{18}O-**2** are presented in the insets of Figure 9 (spectra A', B' and B", respectively). Upon ^{18}O substitution, the peak at 810 cm^{-1} in spectrum B' is shifted by 31 cm^{-1} to lower energy (779 cm^{-1}, spectrum B"). This transition at 779 cm^{-1} is assigned to a vibrational mode of the V-η^2-sulfenate unit. To a first approximation, the nearly 100 cm^{-1} decrease in energy for this vibration relative to Ni^{II}-η^1-sulfenates suggests a weaker S-O bond in the V-η^2-sulfenates. This is consistent with the slight lengthening of the S-O distance in **3** (and presumably **2**) relative to the Ni^{II}-η^1-sulfenates. However, the bonding in these two complexes is very different, and direct comparisons of "S-O" vibrational energies are probably inappropriate. Preliminary resonance Raman data (excitation at 568 and 514 nm, data not shown) on ^{16}O-**2** and ^{18}O-**2** do not show transitions in this region, indicating that vibrations in the η^2-sulfenate unit are not influenced by the ligand-to-metal charge-transfer (552 nm).

Downloaded by MONASH UNIV on October 31, 2012 | http://pubs.acs.org
Publication Date: December 10, 1998 | doi: 10.1021/bk-1998-0711.ch005

Conclusions

The coordination chemistry of vanadium(V)-thiolate complexes, which are present in the vanadate-inhibited forms of protein tyrosine phosphatases, is just now being elucidated. In the two structurally characterized model complexes, V^V-thiolates prefer a trigonal bypyramidal geometry with the thiolate ligands in the equatorial plane. This is in contrast to the recent protein crystal structures of vanadium adducts of two PTPs in which the thiolate ligand occupies an axial site in the TBP coordination sphere of the metal atom. The vanadium(V)-dithiolate complex studied here (**1**) is an oxo-atom acceptor and can accept one or two oxygen atoms (from a variety of oxo-atom donors) to form vanadium-sulfenate (**2**) or -disulfenate (**3**) complexes. Under specific conditions Ph_3P reacts with **2** to form **1** and Ph_3PO. An unprecedented η^2-coordination mode for the sulfenate ligand has been demonstrated for the disulfenate complex. Chiral complexes of the monosulfenate can be prepared using chiral oxaziridines. The V^V-η^2-sulfenate moiety has a vibrational transition at 810 cm^{-1}. Ongoing studies into the reactivity and physical properties of V-η^2-sulfenates will further define their chemical and biochemical importance. Specifically, we are interested in these complexes as chemical oxo-atom transfer agents, as well as intermediates in (and models for) the oxidation of biochemically important cysteine residues that are present at the active sites of enzymes such as protein tyrosine phosphatases.

References

1. *Vanadium in Biological Systems*; Chasteen, N. D., Ed..; Kluwer Academic Publishers: Dordrecht, 1990.
2. *Vanadium and its role in life*; Sigel, H.; Sigel, A., Eds.; Marcel Decker: 1995; Vol. 31.
3. Gresser, M. J.; Tracey, A. S.; Stankiewicz, P. J. *Adv. Prot. Phosphatases* **1987**, *4*, 35-57.
4. Nanda, K. K.; Sinn, E.; Addison, A. W. *Inorg. Chem.* **1996**, *35*, 1-2.
5. Zhang, M.; Zhou, M.; Van Etten, R. L.; Stauffacher, C. V. *Biochemistry* **1997**, *36*, 15-23.
6. Denu, J. M.; Lohse, D. L.; Vijayalakshmi, J.; Saper, M.; Dixon, J. E. *Proc. Natl. Acad. Sci. USA* **1996**, *93*, 2493-2498.
7. Shaver, A.; Ng, J. B.; Hall, D. A.; Lum, B. S.; Posner, B. I. *Inorg. Chem.* **1993**, *32*, 3109-3113.
8. Bolm, C.; Bienwald, F. *Angew. Chem.* **1995**, *34*, 2640-2642.
9. Schmidt, H.; Bashirpoor, M.; Rehder, D. *J. Chem. Soc. Chem. Commun.* **1996**, 3865-3870.

10. Huyer, G.; Liu, S.; Kelly, J.; Moffat, J.; Payette, P.; Kennedy, B.; Tsaprailis, G.; Gresser, M. J.; Ramachandran, C. *J. Biol. Chem.* **1997**, *272*, 843-.
11. A preliminary account of some of this work has appeared: Cornman, C. R.; Stauffer, T. C.; Boyle, P. D. *J. Am. Chem. Soc.* **1997**, *119*, 5986-5987.
12. Rehder, D.; Weidmann, C.; Duch, A.; Priebsch, W. *Inorg. Chem.* **1988**, *27*, 584-587.
13. Buonomo, R. M.; Font, I.; Maguire, M. J.; Reibenspies, J. H.; Tuntulani, T.; Darensbourg, M. Y. *J. Am. Chem. Soc.* **1995**, *117*, 963-973.
14. Tuntulani, T.; Musie, G.; Reibenspies, J. H.; Darensbourg, M. Y. *Inorg. Chem.* **1995**, *34*, 6279-6286.
15. Butler, A.; Clague, M. J.; Meister, G. E. *Chem. Rev.* **1994**, *94*, 625-638.
16. Paul, P. C.; Angus-Dunne, S. J.; Batchelor, R. J.; Einstein, F. W. B.; Tracey, A. S. *Can. J. Chem.* **1997**, *75*, 183-191.
17. Keramidas, A. D.; Miller, S. M.; Anderson, O. P.; Crans, D. C. *J. Am. Chem. Soc.* **1997**, *119*, 8901-8915.
18. Sloan, T. E. In *Topics in Inorganic and Organometallic Stereochemistry*; G. L. Geoffroy, Ed.; John Wiley & Sons: New York, 1981; Vol. 12; pp 1-36.
19. Raynor, D. R.; Gordon, A. J.; Mislow, K. *J. Am. Chem. Soc.* **1968**, *90*, 4854-4860.

Downloaded by MONASH UNIV on October 31, 2012 | http://pubs.acs.org
Publication Date: December 10, 1998 | doi: 10.1021/bk-1998-0711.ch005

Downloaded by MONASH UNIV on October 31, 2012 | http://pubs.acs.org
Publication Date: December 10, 1998 | doi: 10.1021/bk-1998-0711.ch006

Chapter 6

Peroxo, Hydroxylamido, and Acac Derived Vanadium Complexes: Chemistry, Biochemistry, and Insulin-Mimetic Action of Selected Vanadium Compounds

Debbie C. Crans

Department of Chemistry and Cell and Molecular Biology Program, Colorado State University, Fort Collins, CO 80523–1872

In this chapter, the chemistry of selected vanadium compounds and their ability to inhibit phosphatases and exhibit insulin-mimetic activities will be described. First, chemical properties are presented for three target groups of vanadium compounds inducing insulin-mimetic responses. The simple vanadate salts represent the group of vanadium compounds most studied and exhibit the most complex chemistry. The chemistry of a new peroxovanadium(V) compound is presented and a corresponding, isoelectronic hydroxylamido vanadium(V) complex is characterized. The similarities and differences between peroxovanadium and hydroxylamido compounds are identified. Bis(2,4-pentanedionato-*O,O'*)oxovanadium(IV) (VO(acac)$_2$) derivatives undergo hydrolysis reactions in aqueous solution which must be unraveled in order to appropriately interpret biological studies. Second, the effect of coordination number of vanadium compounds on their potency as a transition state analog inhibitor for a phosphatase is described. The five-coordinate vanadium(V) dipicolinic acid complex is found to be a more potent inhibitor than the six-coordinate vanadium(IV) dipicolinic acid complex and the seven-coordinate peroxooxovanadium(V) dipicolinic acid complex because of the structural analogy with the transition state of phosphate ester hydrolysis. Third, the effects of four types of peroxovanadium(V) compounds in phosphatase, insulin receptor and glucose-uptake assays are determined. The results show that although a series of peroxo compounds have significantly higher activity than vanadate in cell culture assays, such large differences are no longer apparent in the rat epitochlearis muscle.

The insulin-mimetic effects of simple vanadium salts have prompted exploration of the insulin-mimetic properties of new, as well as other known vanadium complexes with organic ligands (2-9). Despite advances, little is known concerning the detailed

In Vanadium Compounds; Tracey, A., et al.;
ACS Symposium Series; American Chemical Society: Washington, DC, 1998.

molecular mechanism by which these vanadium compounds, in general, induce their insulin-mimetic effects. This is, in part, due to the hydration, alkylation and oligomerization reactions and redox chemistry of the simple vanadium salts under physiological conditions and in part due to the intricacies related to studies of insulin action in general. Although the chemistry of more complex vanadium compounds may be more tractable than the simple salts, it is only recently that the insulin-mimetic community is beginning to appreciate the complications related to the vanadium chemistry (10, 11). This point is well documented by the fact that little aqueous chemistry of most vanadium compounds with reported insulin-mimetic effects has been examined under relevant conditions (10-12). This manuscript will focus on recent findings related to vanadium compounds and their insulin action. This chapter will describe both published (9, 13, 14) and unpublished (15-17) results that have been discovered by the Crans group in the last few years. First, details of the solid-state and solution chemistry of three classes of vanadium compounds (peroxo (14, 18), hydroxylamido (14) and acac derived (15-17) vanadium compounds) currently of interest to the insulin-mimetic community will be described, followed by studies exploring the favored coordination number of vanadium compounds that inhibit phosphatases (13). Finally, a comparison will be made on the activity of selected vanadium complexes in four different assays used for prediction of insulin-mimetic effects (9).

Downloaded by MONASH UNIV on October 31, 2012 | http://pubs.acs.org
Publication Date: December 10, 1998 | doi: 10.1021/bk-1998-0711.ch006

Three Classes of Vanadium Compounds with Insulin-Mimetic Properties

Three classes of vanadium complexes that have received major attention from the insulin-mimetic community include: the simple vanadium salts, the peroxovanadium complexes (pV) and the bis(maltolato)oxovanadium(IV) (BMOV) and related bis-(2,4-pentanedionato-*O,O'*)oxovanadium(IV) (bis(acetylacetonate)oxovanadium(IV), $VO(acac)_2$) complexes. All of these compounds have limited stability under physiological conditions, in addition to compromised stability at the acidic pH of the stomach. Until recently (6, 19), the aqueous chemistry of none of these compounds had been examined in detail, and obviously such information would be important in understanding the observations made in *in vitro* and *in vivo* studies. In the following sections, some of the chemistry recently elucidated will be summarized and expanded with new chemical properties discovered in studies of these three groups of vanadium compounds.

Simple Vanadium Salts. As has been described previously, the chemistry of simple vanadium salts (sodium, potassium or ammonium orthovanadate; sodium, potassium or ammonium metavanadate; and vanadyl sulfate) is very complex (12, 20). All these salts undergo hydrolytic and redox reactions depending on the pH, ionic strength and other components in the aqueous medium. These vanadium salts will undergo such reactions upon dissolution in the administration fluid, followed by additional reactions upon ingestion and as the drug travels though the stomach to various sites of action. Given the chemistry associated with these simple forms of vanadium, it is exceedingly difficult to determine the active species generating the insulin-mimetic response. However, model reactions can, and should be carried out. Model stability and speciation studies will become increasingly important when biological studies are able to further identify the cellular location and site of action of these compounds.

Peroxooxovanadium Complexes and Related Hydroxylamido Analogs. The potent activity of diperoxovanadium compounds was first reported in 1987 by Posner

Downloaded by MONASH UNIV on October 31, 2012 | http://pubs.acs.org
Publication Date: December 10, 1998 | doi: 10.1021/bk-1998-0711.ch006

and coworkers (21-23). Since then, a wide range of peroxovanadium complexes has been characterized, and, as described elsewhere in these Symposium Proceedings, the chemistry and biochemistry of such compounds is currently of great interest. Reviews describing primarily the structural aspects and synthetic applications of these complexes have been reported (24-27). To date contributions from the Crans group on the chemistry of these compounds include examination of the dynamic processes (i.e., the lability) of these complexes (unpublished work) and a new imidazole peroxo derivative which was recently characterized both in the solid-state and in solution (see below) (9, 14). Given the symmetry of the peroxo ligand, it is non-trivial to establish the dynamic processes with respect to the O_2-group in the peroxo complex. Here one specific approach, which involves the substitution of the O_2-group with a NH_2O-group, will be described (14). Further development of this type of isoelectronic complex will allow direct comparison between the chemistry of peroxo and hydroxylamido complexes.

A few examples of hydroxylamido complexes have previously been reported, including simple inorganic hydroxylamido complexes, dipicolinic acid derivatives and a few others (28-33). Despite the expected similarity between the peroxo and the hydroxylamido complexes, literature comparing these systems is limited to consideration of the effects of these groups on the ^{51}V NMR chemical shifts (31). In Fig. 1, the structures of the known monoperoxo (34) and monohydroxylamido (30) dipicolinic acid vanadium(V) complexes are shown. The hydroxylamido complex shown in Fig. 1 (left) contains a seven-coordinate vanadium atom in a pentagonal bipyramidal geometry, as is the case for the peroxo complex (right). The hydroxylamido group and dipicolinic acid ligand are both in the equatorial plane and an analogous arrangement is observed for the peroxo complex. In both complexes, an H_2O molecule is coordinated trans to the oxo ligand. Thus, these compounds show identical coordination geometries as anticipated from the substitution of the peroxo group with the isoelectronic NH_2O group.

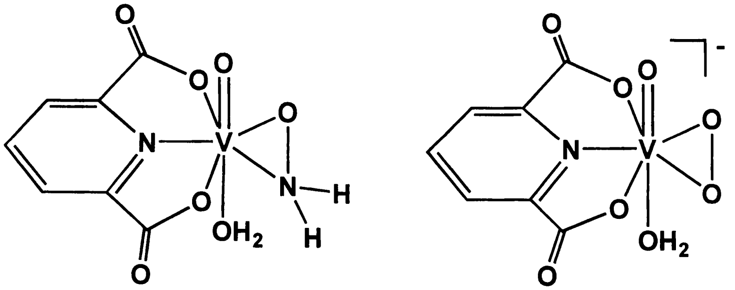

Fig. 1. Structural representation of monohydroxylamidooxovanadium(V) dipicolinic acid (30) (left) for direct comparison with monoperoxooxovanadium(V) dipicolinic acid (mpVdipic) (34) (right).

The bisperoxooxovanadium(V) unit may be critical to some of the insulin-mimetic activities of these complexes, so it would be of interest to generate analogs of diperoxo complexes. Accordingly, we set out to prepare new hydroxylamine complexes (preferably with water solubility) and to ensure that the corresponding peroxo complexes were available for comparison (14). Recognizing that many bisperoxooxovanadium(V) complexes are less labile than corresponding oxovanadium(V) complexes, and that structural characterization of amino acid and

Downloaded by MONASH UNIV on October 31, 2012 | http://pubs.acs.org
Publication Date: December 10, 1998 | doi: 10.1021/bk-1998-0711.ch006

imidazole containing complexes have remained elusive in the absence of stabilizing organic ligands (see for example Ref. 35), we hypothesized that the hydroxylamido group might enable preparation of amino acid derivatives that could be structurally characterized. Indeed, hydroxylamido complexes with glycine, serine and glycylglycine were made successfully (14). While our work was in progress, the Tracey group also had become interested in related peroxo and hydroxylamido complexes, and it now is possible to directly compare the peroxo (36) and hydroxylamido (14,33) vanadium complexes with the ligand glycylglycine (Fig. 2). In contrast to the complexes shown in Fig. 1, the isoelectronic substitution giving rise to the complexes shown in Fig. 2 was not trivial; the peroxo complex has one peroxo unit whereas the hydroxylamido complex has two hydroxylamido units. In the former complex (Fig. 2, right) the dipeptide is a tridentate ligand, whereas in the latter (Fig. 2, left) the dipeptide is a bidentate ligand.

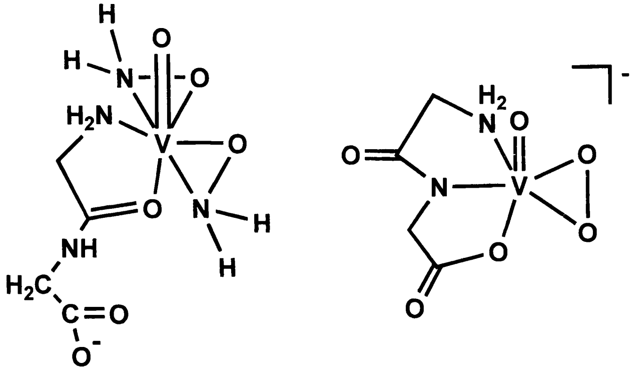

Fig. 2. Structural representation of dihydroxylamidooxovanadium(V) glycylglycine (14,33) (left) and monoperoxooxovanadium(V) glycylglycine (36) (right).

Subtle structural preferences of these complexes, and the geometries of compounds described below, can be rationalized based on other known complexes. The mpVdipic complex also formed the monoperoxo adduct (34), supporting the possibility that a peroxo complex with the tridentate dipeptide would most likely form a monoperoxo complex. However, the mpVdipic also contains one molecule of water trans to the oxo group, which also is observed for a corresponding monoperoxo picolinic acid complex (37) but not for the peroxooxovanadium(V) glycylglycine complex. The latter complex is structurally unusual in the sense that this complex did not crystallize with a water molecule in the apical coordination site. It should be noted here that synthetic conditions can dictate whether the complex contains one or two peroxo groups.

The hydroxylamido complex adduct was found to contain two hydroxylamido functionalities. This complex chelated the dipeptide in a bidentate manner and reserved coordination sites for two NH_2O functionalities. The question remains whether it would be expected for a NH_2O complex to form a complex analogous to the monoperoxo complex or whether the hydroxyamido complexes favor stability of dihydroxylamido adducts more than the corresponding peroxo complexes favor formation of diperoxo adducts. To answer this question, information on additional complexes, including both peroxo and hydroxylamido compounds is desirable. Such complexes preferably would be prepared from ligands like GlyGly that have two or more possibilities for chelation. Since both the diperoxo ($H[VO(O_2)_2(imidazole)_2]$) and dihydroxylamido complex ($[VO(NH_2O)_2(imidazole)_2]Cl$) were characterized by

Downloaded by MONASH UNIV on October 31, 2012 | http://pubs.acs.org
Publication Date: December 10, 1998 | doi: 10.1021/bk-1998-0711.ch006

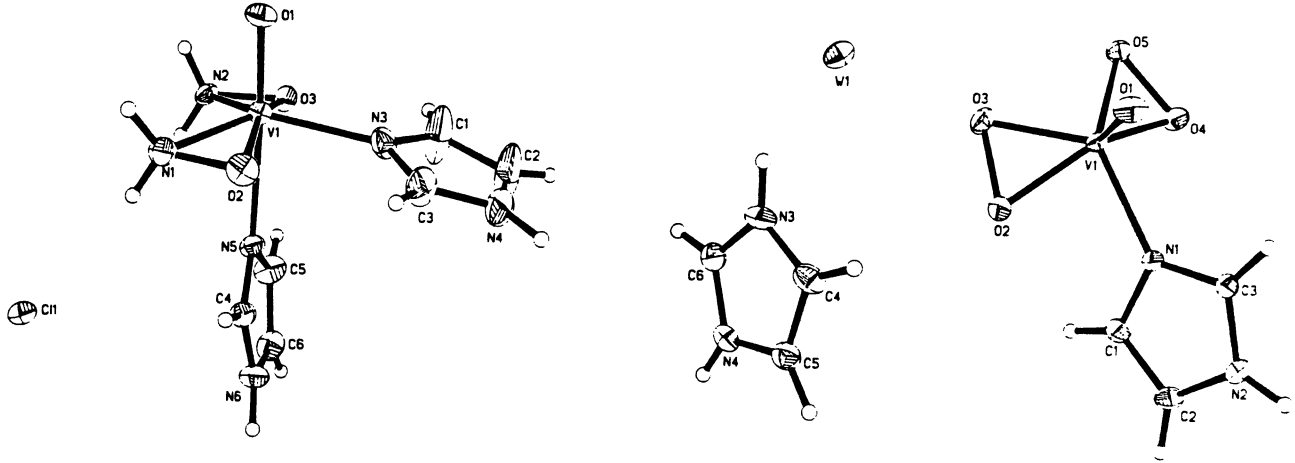
O1
N2
O3
V1
N1
O2
N3
C1
C2
C3
N4
N5
C5
C4
C6
N6
Cl1
W1
N3
C6
C4
N4
C5
O5
O1
O3
O4
V1
O2
N1
C3
C1
N2
C2

Fig. 3 The X-ray structures of [VO(NH_2O)$_2$(imidazole)$_2$]Cl (dhVim, left) and imidazoleH[VO(O_2)$_2$(imidazole)] (dpVim, right). Adapted with permission from Refs. 9 and 14.

X-ray crystallography as well as by their aqueous solution chemistry (Figs. 3-5), discussion will turn to these two compounds (9, 14).

The hydroxylamido complex (dhVim) in Fig. 3 (left) contains a seven-coordinate vanadium atom in a pentagonal bipyramidal geometry (14). The hydroxylamido groups reside in the equatorial plane with the nitrogen atoms of the hydroxylamido group trans to the equatorial nitrogen of the imidazole group. The second imidazole group is coordinated axially trans to the oxo group. The vanadium atom is raised 0.3 Å out of the plane which also is typically observed for seven-coordinate diperoxovanadium complexes. Thus, one would expect that the corresponding bisperoxooxovanadium(V) imidazole complex (dpVim) would have a very similar structure. However, as seen from the structure of dpVim (Fig. 3 (right)), the second imidazole group protonates and accordingly serves as a cation for the bisperoxooxovanadium(V) imidazolate anion (9, 14). The vanadium atom in this complex is, therefore, only six-coordinate and the complex has a pentagonal pyramidal geometry.

In line with the discussion above, we now examine both the hydroxylamido and the peroxo complex to evaluate whether a standard coordination geometry has been obtained. Of all the known diperoxovanadium complexes, there is only precedence for one six-coordinate complex, $(NH_4)[VO(O_2)_2NH_3]$, suggesting that the structure of this compound is unusual (38). However, this conclusion would be premature, because $(NH_4)[VO(O_2)_2NH_3]$, as well as our imidazole complex, has an attractive structural alternative to the seven-coordinate pentagonal bipyramidal geometry; one of the amine ligands protonates and becomes the accompanying cation. Only the peroxovanadium complex, and not the hydroxyamidovanadium complex, chooses to adopt such an alternative geometry. Presumably, this reflects the fact that the overall charge for the bisperoxooxovanadium(V) unit is minus one and the overall charge of the bishydroxylamidooxovanadium(V) group is plus one. Thus, protonation of a potential ligand is electrostatically favorable in the case of the peroxovanadium compound but not in the case of the hydroxylamido compound.

Comparing the two hydroxylamido complexes shown in Fig. 2 and Fig. 3, both complexes formed bishydroxylamidooxovanadium(V) adducts in the solid state. Since the corresponding peroxo complexes take on alternative geometries, it is likely that dihydroxylamido complexes favor this geometry in the solid state. Thus, it is possible that the NH_2O unit stabilizes the dihydroxylamido adduct more than the O_2-unit stabilizes the diperoxo adduct. Close comparison of the two hydroxylamido complexes shown in Figs. 2 and 3 indicates that the NH_2O unit is coordinated differently in the two complexes, documenting the existence of isomers for these types of compounds. Indeed, the solution chemistry described below suggests that not only do such isomers form, but they also undergo various exchange processes.

The solution properties of dpVim have been examined and its stability and lability will be briefly summarized here (14). Dissolving dpVim in aqueous solution generates a solution with only one ^{51}V NMR signal at -744 ppm. The ^{1}H NMR spectrum shows that dissolved dpVim contains one free imidazole. Below pH 6, a signal is observed by ^{51}V NMR which is presumably due to $[H_2VO_2(OO)_2]^-$ (39). Formation of the dissociated bisperoxooxovanadium(V) complex may be indicative of the higher lability of imidazole than the two peroxo groups. This expectation is further substantiated in homonuclear ^{1}H and ^{51}V EXSY NMR experiments (Conte and Crans, unpublished and Ref. 14). The 2D EXSY spectrum of a solution containing 100 mM dpVim at pH 6.5 and 4 °C is shown in Fig. 4 (right) The ^{1}H NMR spectrum contains signals assigned to free imidazole and coordinated imidazole

Downloaded by MONASH UNIV on October 31, 2012 | http://pubs.acs.org
Publication Date: December 10, 1998 | doi: 10.1021/bk-1998-0711.ch006

in a 1:1 ratio, consistent with the solid-state structure. However, the off-diagonal cross signals in the ^{1}H NMR EXSY spectrum are indicative of exchange between the free and coordinated imidazole protons. This spectrum further documents the lability of the coordinated imidazole in dpVim.

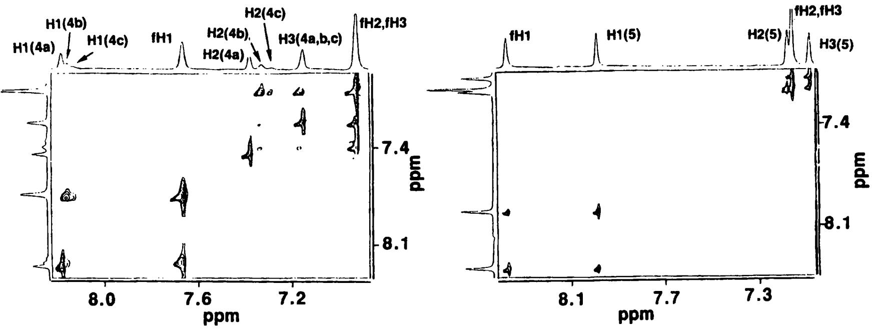

Fig. 4. Partial 2D ^{1}H-EXSY NMR spectra of dhVim, 100 mM pH 7.8 and 4.8 °C in aqueous solution (left) and dpVim, 100 mM pH 6.5 and 4.8 °C in aqueous solution (right). Adapted with permission from Ref. 14.

The solution properties of dhVim have been examined and its stability and lability will be briefly discussed (14). Dissolving analytically-pure and crystalline dhVim in aqueous solution generates a spectrum with three ^{51}V NMR signals at -850 (minor), -856 (minor) and -868 (major) ppm. Solution studies at various concentrations and in the presence of excess imidazole and/or hydroxylamine show that the stoichiometry of these signals is the same. Given the fact that the hydroxylamido complex has the possibility for forming structural isomers, and that we have already provided solid-state structural information on two of these isomers, it is likely that the three signals reflect three different isomers. Recording ^{1}H NMR spectra of solutions of crystalline dhVim confirms the presence of these isomers in that signals for one equivalent of free imidazole are observed additionally. Regardless of the solid-state nature of dhVim, in solution it loses one of the coordinated imidazole residues. Further examination of the spectra for hydroxylamido vanadium complexes provides information regarding the exchange processes that these molecules undergo.

In Figs. 4 (left) and 5, the 2D ^{1}H EXSY NMR spectra of dhVim in D_2O and in CD_3CN/dmso-d_6 (3:4) are shown (14). The intermolecular exchange between free and coordinated imidazole is observed in water (Fig. 4). This spectrum clearly shows that the isomers exchange with different rates than with free imidazole ligand. The difficulties in resolving the signals for isomeric complexes in these spectra are improved by using an organic solvent. There is a greater chemical shift difference between the isomers in this solvent system, but the ratio of the isomers has changed. In addition, the CD_3CN/dmso-d_6 mixture also allows observation of the hydroxylamido protons which provide additional information regarding the exchange of the hydroxylamido group. In Fig. 5, an excerpt of the 2D EXSY spectrum recorded in CD_3CN/dmso-d_6 is depicted focusing on the exchange between free and coordinated imidazole. The structure for the three proposed isomers are referred to as **4a**, **4b** and **4c** (Fig. 6), and the respective signals for the protons in these isomers are referred to as H1(4a), H1(4b) and H1(4c) in the spectra. The differences in the rates of intermolecular exchange between isomers and free imidazole is clearly observed in

Downloaded by MONASH UNIV on October 31, 2012 | http://pubs.acs.org
Publication Date: December 10, 1998 | doi: 10.1021/bk-1998-0711.ch006

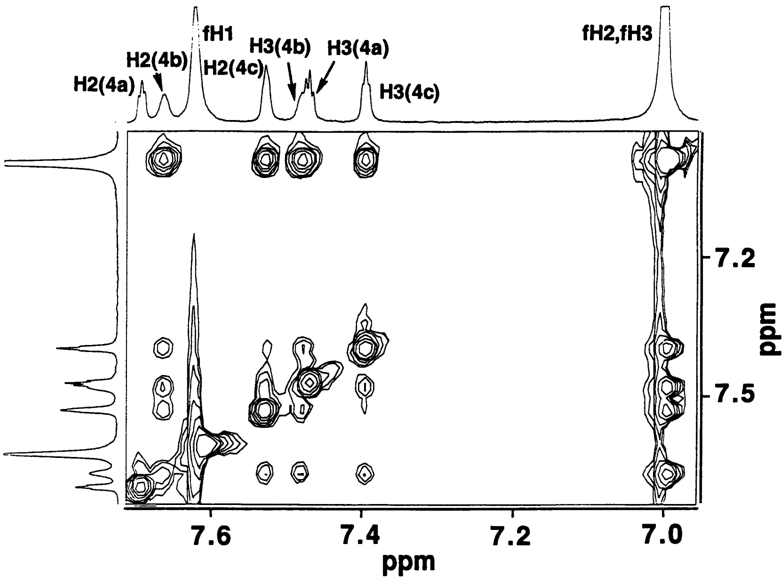

Fig. 5. Partial 2D ^1H-EXSY NMR spectrum of dhVim, 100 mM and 5.8 °C in CD_3CN/dmso-d_6 (3:4). Adapted with permission from Ref. 14.

CD_3CN/dmso-d_6. For example, the exchange between isomer **4a** and free imidazole has been reduced so much, it is barely observable in CD_3CN/dmso-d_6 (it is necessary

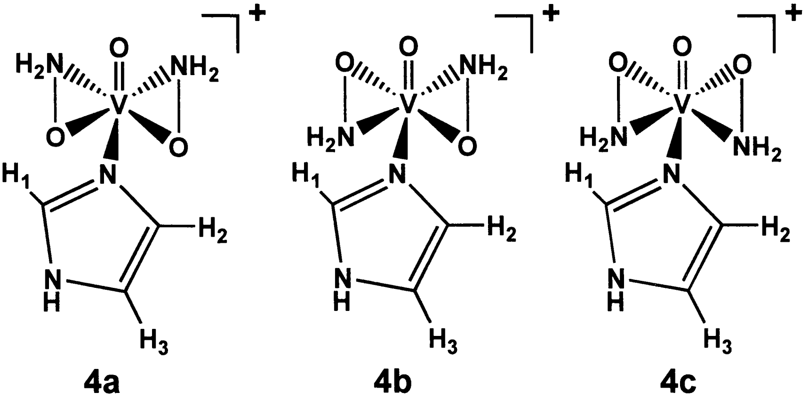

4a **4b** **4c**

Fig. 6. Three structural proposals for the three isomers that form upon dissolution of crystalline dhVim. Structural precedences exist for isomers 4a and 4c, however no structural precedence has been reported for any metal complexes, for isomer 4b. Adapted with permission from Ref. 14.

to examine each row in the 2D EXSY spectrum individually to distinguish signal originating in true exchange reactions from spectral noise).

In addition to the exchange between coordinated imidazole and free imidazole, additional intermolecular processes can be identified in the spectrum in CD_3CN/dmso-d_6. For example, exchange between isomeric proton pairs is readily observed such as in the exchange between H1(4a)/H1(4b) and H1(4b)/H1(4c), and H2(4a)/H2(4b) and H2(4b)/H2(4c), and H3(4a)/H3(4b) and H3(4b)/H3(4c) (Fig. 5).

Downloaded by MONASH UNIV on October 31, 2012 | http://pubs.acs.org
Publication Date: December 10, 1998 | doi: 10.1021/bk-1998-0711.ch006

These processes suggest that exchange between isomers is also occurring rapidly, and this can be explained by the dissociation and reassociation of the imidazole ligand to generate the different isomer. In addition, we were able to observe the exchange of the hydroxylamido protons (data not shown); however, this exchange was only observed under conditions where the imidazole proton exchange was difficult to visualize, in part because of the much faster relaxation times of the hydroxylamido protons. Last, the exchange between H2(4b) and H3(4c) can not simply be explained by simple imidazole and hydroxylamine exchange. This exchange pattern is indicative of a multistep process or a more complex exchange pathway.

The solution properties of the peroxo and hydroxylamido compounds can now be readily compared utilizing the available structural information in the solid-state (9, 14). Both compounds form six-coordinate complexes in solution, even though the dhVim is seven-coordinate in the solid state. The EXSY spectra show that both the hydroxylamido and peroxo complexes are very labile with respect to organic ligand. From qualitative examination of the EXSY spectra of both the peroxo and hydroxylamido complexes, it is difficult to determine with certainty which compound is more labile. Although hydroxylamido complexes react more readily by redox processes we find that the they are significantly more stable in dilute solutions than in concentrated solutions. This observation is in sharp contrast to the peroxovanadium complexes for which radical mechanisms are proposed for the reactivity and/or decomposition (40-42). In the case of diperoxo complexes the decomposition may be dependent on the competition between dissociation of one peroxo group (resulting in disproportionation) and dissociation of the organic ligand. This type of decomposition pathway would explain the instability of peroxo compounds in dilute solutions, and the fact that coordinating ligands can accelerate (37,42) or decrease (43,44) the rate of peroxide consumption. Since the hydroxylamido complex is more stable in dilute solutions and it also undergoes ligand dissociation, it follows that the intact complex, or an oligomeric species, will be key to complex decomposition.

The complex nature of drug interactions with dietary compounds is very difficult to anticipate and compounds explored for their beneficial properties at some early stage of consideration will benefit tremendously from whole animal testing. There is no doubt that an oral agent will travel through the stomach and thus be exposed to an acidic environment as well as all the compounds ingested by diet. Thus, it is important to consider a compounds general stability, as well as its acid stability. These considerations are particularly important because it is not yet known how the organic vanadium compounds act. Do they act when decomposing to vanadate or vanadyl sulfate in a semi-controlled manner, or do they act as intact complexes? Thus, at this time, it is not clear whether conversion to vanadate or vanadyl sulfate in the stomach or elsewhere, is an undesirable or desirable property. In the absence of such information, it seems reasonable to seek vanadium compounds with various properties (i.e. hydrolytic and redox stability) at acid and neutral pH. Use of compounds with known properties in cell and animal studies is desirable and studies with such a series of related peroxooxovanadium(V) compounds are considered below in this chapter.

The observed instability of dpVim at acidic pH is readily reconciled with the fact that free imidazole will be protonated at these pH levels. The concentration of neutral imidazole will be low, such that once the complex is dissociated, the necessary concentration of imidazole will not be present to favor reformation of equivalent concentrations of the complex that hydrolyzed. Thus, the complex will decompose. However, at higher pH and particularly in the physiological pH range, this compound is not only kinetically inert but also remains stable even in the presence of effective

Downloaded by MONASH UNIV on October 31, 2012 | http://pubs.acs.org
Publication Date: December 10, 1998 | doi: 10.1021/bk-1998-0711.ch006

complexing ligands such as EDTA, for reasonable time periods (9). Specifically, the appearance of <5% decomposition products is observable for dpVim in solution with 5 mM EDTA at pH 7.0 after 24 hrs. This observed solution-stability pattern is similar to the stability of other peroxovanadium complexes, regardless of the nature of the coordinating ligand. Since the pK_a value of 7.0 for protonated imidazole is significantly higher than the relevant pK_a values for acids such as picolinic and dipicolinic acids, the solution stability profile for dpVim will be shifted toward higher pH. Thus, peroxovanadium complexes of picolinic acid (dpVpic) will be more stable than dpVim at acid pH.

Although the dhVim complex remained intact in the solid state, upon dissolution, it immediately dissociated into one equivalent of free imidazole and complex. This mixture is less stable at both basic and acidic pH. The acid-instability is observed for the same reasons as described for the corresponding peroxovanadium compound. However, the base instability is clearly related to the chemistry of hydroxylamines, which at alkaline pH undergoes a series of reactions, some of which presumably also occur for the series of compounds described here (45, 46).

Combined, these considerations imply that designing a peroxovanadium(V) compound sufficiently resistant to withstand the acidic pH of the stomach would involve selection of an organic ligand with a low pK_a value; the lower its pK_a value the greater acid-stability such a complex should have.

Bis(maltolato)oxovanadium(IV) and Related Bis(2,4-pentanedionato-*O,O'*) Oxovanadium(IV) Complexes. Bis(maltolato)oxovanadium(IV) (BMOV) is a complex that has generated appreciable interest both in *in vitro* and *in vivo* studies (5, 6). Its chemistry, biochemistry, and pharmacology will be discussed in detail elsewhere in this volume. The close relationship between this complex and $VO(acac)_2$ is generally not recognized, although the acac complex has recently been reported to have insulin-mimetic properties better than those of vanadyl sulfate (8). Our laboratory is currently involved in a collaboration with Sonia M. Brichard and coworkers in testing a few of these compounds *in vivo*. Specifically this study will include a comparison of the effects of equal amounts of vanadium-element in $VOSO_4$, BMOV and $VO(acac)_2$ on glycemia in STZ (streptozotocin) diabetic rats (16, 17). In light of the recent report (8), the insulin-mimetic properties of $VO(acac)_2$ and the interest in BMOV and related systems, it is appropriate to describe the solution chemistry of these compounds here. Both the chemical and pharmacological aspects of this work will be reported soon in full detail (16, 17).

Upon dissolution of $VO(acac)_2$ in water in the presence of nucleophilic ligands, $VO(acac)_2$ forms an adduct. Such an adduct has the incoming ligand coordinated either cis or trans to the oxo group (Fig. 7). Numerous studies of the $VO(acac)_2$-adducts in methanol and other organic solvents have been done using a variety of spectroscopic methods including EPR and ENDOR. These investigations suggest that when the incoming group is methanol, it coordinates trans to the oxo group (47-50). However, as the nucleophilicity of an incoming ligand increases, as in the case of alkyl-substituted pyridines, the geometry of the adduct changes to having the incoming ligand coordinated cis (relative to the oxo group) (51, 52). The bis(maltolato)oxovanadium(IV) complex has been studied carefully in this regard using variable temperature EPR spectroscopy (6, 19). The asymmetric geometry of this ligand requires additional considerations in the study of BMOV because additional isomers are possible in comparison with $VO(acac)_2$. These solution studies led to the conclusion that the major isomer was the cis complex, in part based on the isolation and solid-state characterization of a corresponding vanadium(V) complex.

Downloaded by MONASH UNIV on October 31, 2012 | http://pubs.acs.org
Publication Date: December 10, 1998 | doi: 10.1021/bk-1998-0711.ch006

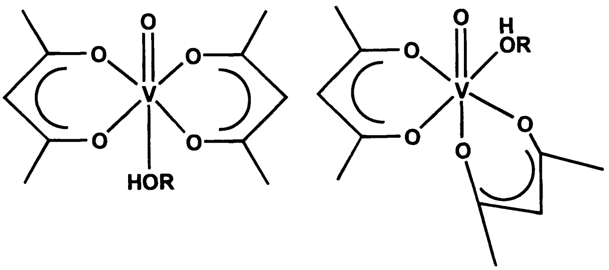

Fig. 7. The structural representation of solution structures for the trans (left) and cis (right) bis(acetylacetonate)oxovanadium(IV)-methanol (VO(acac)$_2$-CH$_3$OH) adduct.

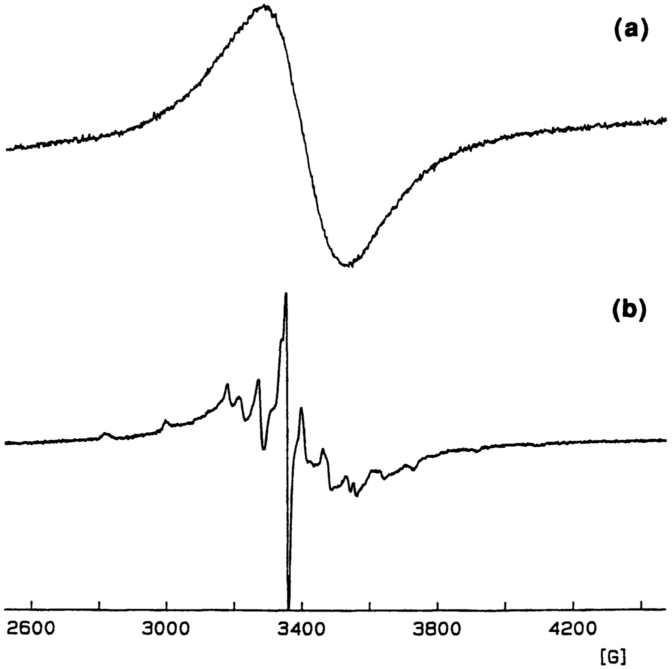

Fig. 8. EPR spectra recorded of 1 mM VO(acac)$_2$ solutions at -133 °C. (a) 1 mM VO(acac)$_2$ recorded in frozen aqueous solution, (b) 1 mM VO(acac)$_2$ recorded in frozen aqueous solution containing 85 mM NaCl.

Unfortunately, very little information is currently available on the corresponding chemistry of VO(acac)$_2$ in water (53). This is due in part to the fact that even low concentrations of VO(acac)$_2$ in water give EPR signals at -133 °C which are broadened by molecular association and the electron delocalization accompanying such interaction (Fig. 8a). As expected, the addition of methanol to VO(acac)$_2$ solutions generates different complexes, so one cannot simply carry out the studies in methanol or any other solvent that would generate a better glass (50). VO(acac)$_2$ and derivatives are administered to animals in their drinking water and these solutions contain NaCl. Sodium cloride addition is necessary to disguise the taste of the water containing the vanadium compounds. In our studies, we discovered that the addition of 85 mM NaCl to a solution of VO(acac)$_2$ at -133 °C disrupted the molecular

Downloaded by MONASH UNIV on October 31, 2012 | http://pubs.acs.org
Publication Date: December 10, 1998 | doi: 10.1021/bk-1998-0711.ch006

association and generated a spectrum which began to show some spectral details (Fig. 8b). By comparison, we have been much more successful in recording spectra at ambient temperatures of aqueous $VO(acac)_2$ solutions (Figs. 9a-9c). The spectra shown in Figs. 9a-9c are of aqueous solutions containing no NaCl, although for $VO(acac)_2$ no observable differences were observed in the presence or absence of salt. As illustrated in the spectrum shown in Fig. 9a, the $VO(acac)_2$ generates a fairly resolvable spectrum immediately upon dissolution. However, when such solutions are left at ambient temperature (6 days, Fig. 9b and 11 days, Fig. 9c), one other major species and one minor species form. We are currently completing these studies, and at this point we present some preliminary information regarding the structure of these species.

Downloaded by MONASH UNIV on October 31, 2012 | http://pubs.acs.org
Publication Date: December 10, 1998 | doi: 10.1021/bk-1998-0711.ch006

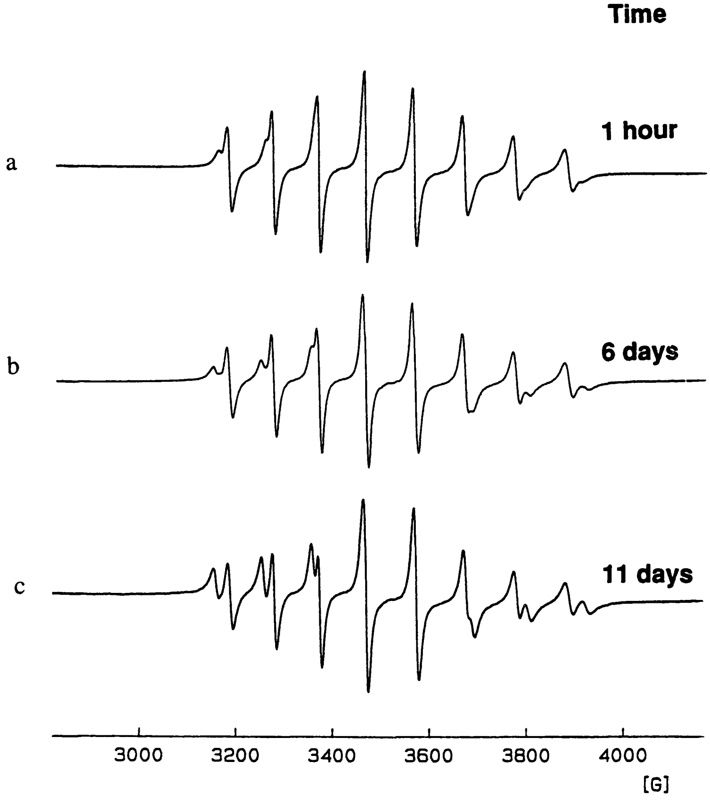

Fig. 9. EPR spectra recorded of 5.0 mM $VO(acac)_2$ solutions at ambient temperature. (a) recorded at ambient temperature immediately after aqueous solution preparation, (b) recorded at ambient temperature after 6 days incubation in aqueous solution and (c) recorded at ambient temperature after 11 days incubation in aqueous solution. The spectra shown were scaled (16).

The effects of NaCl on the low-temperature EPR spectra of $VO(acac)_2$ were also observed for other derivatives of $VO(acac)_2$. Given the greater hydrophobicity of these compounds, the effect of NaCl was also studied on spectra recorded at ambient temperature (16). The nucleophilic chloride anion (Cl^-) could readily form a new adduct by coordinating to the vanadium center and/or disrupting molecular aggregation. Distinguishing these two possibilities is not trivial for other $VO(acac)_2$ derivatives, considering the fact that no hyperfine information can be obtained from the EPR spectrum recorded in the absence of NaCl, thus making a direct comparison difficult. We observe effects in the spectra more consistent with the formation of new complexes rather than with disruption of compound aggregation. Based on spectra recorded of solutions containing excesses of Hacac ligand we conclude, that the major species slowly formed in the spectra shown in Figs. 9a-9c is a complex with a 1:1 stoichiometry. At this time, we believe that the major species observed in solution is an adduct between VO(acac)$_2$ (or derivative) and water with the incoming group trans to the oxo group, and that the minor isomer generated upon prolonged incubation times may be the cis isomer.

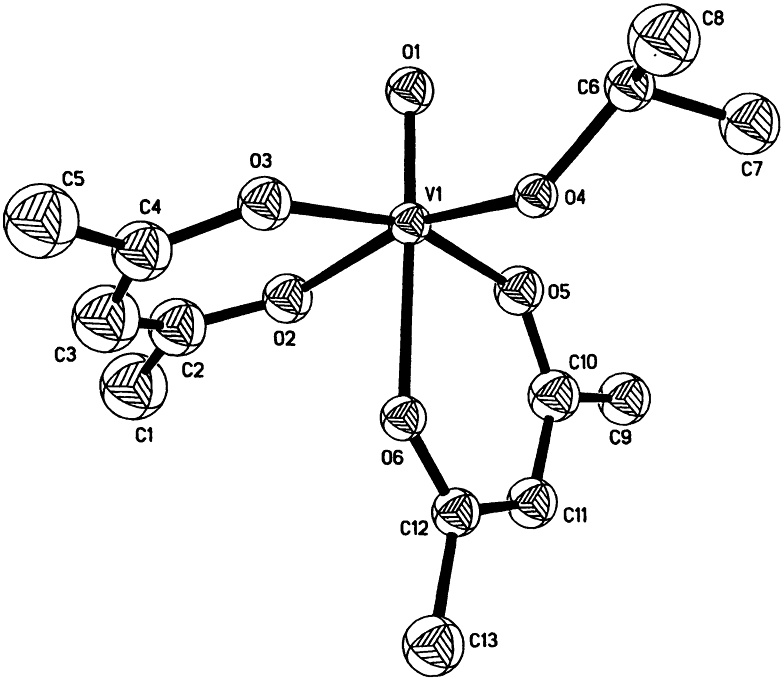

Fig. 10. The X-ray structure for VO(acac)$_2$OiPr (15).

Downloaded by MONASH UNIV on October 31, 2012 | http://pubs.acs.org
Publication Date: December 10, 1998 | doi: 10.1021/bk-1998-0711.ch006

Several VO(acac)$_2$-adducts have been structurally characterized in the solid state (52, 54, 55). These complexes all had the incoming ligand trans to the oxo group, except in a complex where the substituent is a substituted pyridine and the adduct is cis (51). In the BMOV system both the vanadium(IV) and (V) complexes have the incoming nucleophilic cis in the major isomers in solution (6, 19). Since solution studies of VO(acac)$_2$ with methanol support the trans structure, one could expect that a corresponding vanadium(V) complex would have the alkoxide trans. However, in characterization of a series of vanadium(V) alkoxide derivatives stabilized by the acac$^-$ ligand, we have recently been successful in crystallization of the first mononuclear adduct of these types of complexes, VO(acac)$_2$OiPr (Fig. 10), and characterized this material in solution (15, 56). As shown in Fig. 10 (15), the isopropoxide group is cis to the oxo group as also observed in the corresponding maltol compound. VO(acac)$_2$OiPr provides the structural evidence for the building blocks we have used for generation of alkoxide complexes, and provides a firm basis on which to understand formation of various alkoxide clusters with the oxovanadium(V) acac derivative. Interestingly, these compounds will not form with $VO(acac)_2$ as starting material. However, the observed cis geometry in this vanadium(V) complex (in contrast to the spectroscopic observations of trans geometries in the vanadium(IV) complexes) suggests it may be premature to infer a structural analogy in these systems of different oxidation states even though the vanadium(IV) and (V) complexes of the BMOV system showed the same structural preferences (6, 19).

Interaction of Vanadium Compounds with Phosphatases.

Vanadate is a known inhibitor of a wide range of phosphatases (57). It is often hypothesized that the insulin-mimetic properties of vanadate may be linked to inhibition of protein tyrosine phosphatases, resulting in enhanced or sustained insulin receptor autophosphorylation and tyrosine kinase activity (58). The specific mode of action of vanadate, vanadyl sulfate and other vanadium compounds with phosphatases is, in general, of interest. The hypothesis that these compounds act as transition state analogs is commonly accepted in the scientific community. Recent reports of several crystal structures with vanadate in the active site have supported such a hypothesis (59,60); however, solid-state structures are not always capable of representing mechanistic aspects of enzyme catalysis (60). Additionally, the matter is complicated by the fact that most protein tyrosine phosphatases contain a thiol group in the active site, which may very well undergo redox chemistry with vanadium compounds. Indeed, a recent study showed that peroxovanadate interacted with a protein phosphatase in an irreversible manner (61).

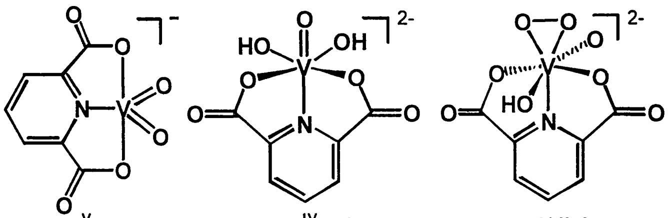

V^Vdipic V^{IV}dipic mpVdipic

Fig. 11. The structures and charges of V^V*dipic (61),* V^V*dipic (62) and mpVdipic (34), at pH 8.0 based on X-ray crystallographic data and* pK_a *determinations. Redrawn (and corrected) illustration reported in Ref. 13.*

Taking a fundamental approach to this problem, we set out to determine if the coordination number of a series of vanadium compounds would effect the inhibitory potency of the vanadium compound against phosphatases (13). These studies were undertaken to first focus on the structural aspects of vanadium compounds, in order to determine if the five-coordinate vanadium compound which best mimics the structural aspects of phosphate ester hydrolysis would be the most potent inhibitor. The model phosphatase chosen to examine this structural question should be innocuous to redox chemistry in the active site (no active site cysteine). Such a choice would ensure that the complexes would inhibit the enzyme through the same mechanism. Accordingly, we chose a phosphatase with a nucleophilic serine in the active site, alkaline phosphatase. Three vanadium compounds were chosen, containing three different coordination numbers; five (V^Vdipic) (62), six (V^{IV}dipic) (63) and seven (mpVdipic) (34), see Fig. 11. (Note, the deprotonated form of the

Downloaded by MONASH UNIV on October 31, 2012 | http://pubs.acs.org
Publication Date: December 10, 1998 | doi: 10.1021/bk-1998-0711.ch006

mpVdipic characterized by X-ray is shown in Fig. 11, since this is the species present at pH 8.0 in the enzyme assay.) Thus, the three compounds under examination contain only one organic ligand and the possibility that the organic ligand effected the observed inhibition is negligible.

Phosphatase activity is commonly assayed in aqueous solution in the physiological pH range (Refs. 9 and 13). A recent report showed that two of the vanadium dipic compounds decomposed at neutral pH (11), thus underscoring the importance of determining the stability of these compounds under the specific assay conditions (13). Determination of the inhibitory effects of ligand, vanadate and other assay components (i.e., hydrolysis and other decomposition products) separately, is necessary before the inhibitory effects of the complex can be measured. In this manner the true inhibition for each compound can be determined. Such extraordinary considerations are necessary given the solution properties of these complexes. We have previously carried out many studies in which enzyme inhibition was determined in solutions with several different species (64). In such solutions, the concentrations of all vanadium complexes were measured so that the total inhibition was obtained by summing the effects of each of the vanadium complexes and free ligand in the assay.

Downloaded by MONASH UNIV on October 31, 2012 | http://pubs.acs.org
Publication Date: December 10, 1998 | doi: 10.1021/bk-1998-0711.ch006

Under the conditions of the phosphatase assay used (5.0-50 mM PNPP, 50 mM HEPES, 1.00 M KCl, 5.0 mM $MgCl_2$ at 25 °C), none of the three dipic complexes were stable. Therefore, it was necessary to measure the stability of V^Vdipic using a combination of ^{51}V NMR and absorption spectroscopy at 860 nm, of V^{IV}dipic using a combination of EPR and absorption spectroscopy at 845 nm and of mpVdipic using a combination of ^{51}V NMR and absorption spectroscopy at 430 nm. With V^{IV}dipic it was necessary to add excess free dipic to the assay solution and conduct the assay at pH 7.0 in order to generate sufficient levels of V^{IV}dipic. The analysis of this system is exceedingly complex and involves identification of the starting complex and its decomposition pathways. Part of this work has already been reported with additional experimental detail and inhibition constants for the other species involved (13), and given the complexity of the experiments and analysis, it is not described further here.

Table 1. The K_i values for Chicken Intestine Alkaline Phosphatase (13).[a]

Compound	pH value of measurements	K_i value (μM)	uncorrected K_i value (μM)[b]
V_i	8.0	2.8±0.4	---
V_i	7.0	5.7±1.0	---
V^Vdipic	8.0	1.9±0.6	4.4±0.8
V^{IV}dipic	7.0	~6	4.9±1.0
mpVdipic	8.0	13±1	4±1
bpV	8.0	23±4	---
dipic	8.0	3200±800	---

[a] *The uncertainties represent 2SDs and were calculated using Excel.*

[b] *These K_i values were calculated assuming 100% of complex remained after they were added to the assay solution and measurement carried out.*

From the results shown in Table 1, it is clear that the V^Vdipic is the most potent inhibitor; although surprisingly the difference is very small. The K_i value for V^{IV}dipic was measured at lower pH, where the K_i value for vanadate is a factor of two higher, but even after adjustment, the K_i value for V^Vdipic was smaller than the other vanadium compounds examined. Importantly, this study does provide evidence that the structural preference for phosphatases is for a five-coordinate transition state. Furthermore, this study underscores the importance of other properties (such as redox properties) of vanadium compounds in interaction with tyrosine phosphatases or other phosphatases. Indeed, it is possible that alternative orders of compound inhibition could be attributed to redox reactions presumably taking place with the active-site cysteine residue (see elsewhere in this Symposium Proceedings).

The fact that five-coordinate vanadium complexes have a geometry more closely resembling the transition state for phosphate ester hydrolysis than other vanadium complexes may affect inhibitory potency. As we have demonstrated, vanadium complexes do not need to be five-coordinate to be reasonable inhibitors for phosphatases. This conclusion is in accord with the early work by van Etten and coworkers which found that other oxometalate anions also were potent inhibitors for acid phosphatases (65). Further support for this conclusion has been obtained in studies in our laboratory (66) and that of Lindquist (67) on comparing the effects of vanadyl cation and vanadate with a series of phosphatases. The report by Shechter and coworkers demonstrating that selected protein tyrosine phosphatases are also inhibited by tungstate and molybdate (68), the study by Cornman and coworkers on the interaction of vanadium(IV) complexes and protein phosphatases and protein phosphatase models (69) and the studies by Gresser and coworkers on the inhibition of protein-tyrosine phosphatase by vanadate and peroxovanadate all document the general inhibitory properties of vanadium compounds for phosphatases (61).

Insulin-Mimetic Properties of Selected Peroxovanadium Compounds.

Our laboratory recently reported on the insulin-mimetic properties of the bisperoxooxovanadium(V) imidazole (dpVim) compound described earlier (9). In this study, the insulin-mimetic effects of a series of peroxovanadium compounds were tested using four types of representative assays (in cell extracts, cell culture or excised organs) customarily employed to detect insulin-mimetic properties. We chose to work with a series of peroxovanadium compounds because of the interest these

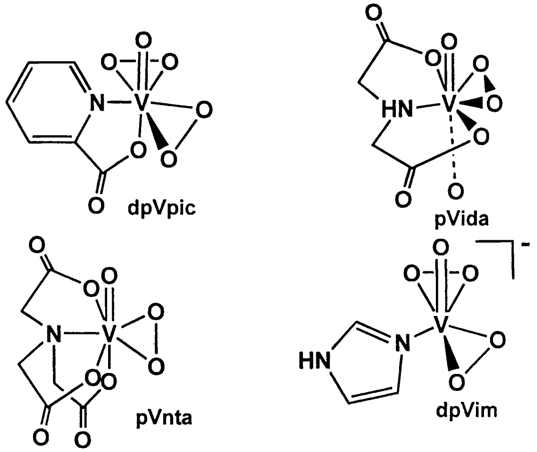

Fig. 12. The structural representation for the compounds examined in four different insulin-mimetic assays: bisperoxooxovanadium(V) picolinic acid (dpVpic), the peroxovanadium iminediacetic acid (pVida), the peroxovanadium(V) nitrilotriacetic acid (pVnta) and the bisperoxooxovanadium(V) imidazole monoanion (dpVim). Adapted with permission from Ref. 9.

Downloaded by MONASH UNIV on October 31, 2012 | http://pubs.acs.org
Publication Date: December 10, 1998 | doi: 10.1021/bk-1998-0711.ch006

compounds have generated in the insulin-mimetic community (40). Specifically, we chose four peroxovanadium compounds with different properties (Fig. 12): bisperoxooxovanadium(V) picolinic acid (dpVpic), peroxooxovanadium(V) iminodiacetic acid (pVida), peroxooxovanadium(V) nitrilotriacetic acid (pVnta) and bisperoxooxovanadium(V) imidazole (dpVim).

The dpVpic is the best characterized complex in the literature (4, 10, 70). This complex is a diperoxovanadium complex which contains a bidentate chelated ligand and thus represents the group of peroxo complexes with bidentate organic ligands. In addition, we chose dpVim (9), which, as described above, is a new complex and distinguishes itself both structurally and with respect to solution properties, from the diperoxovanadium complexes with bidentate ligands. We also chose two monoperoxovanadium complexes, pVnta (71,72) and pVida (73). The former, pVnta, is a compound that has not only been characterized with respect to its solid-state chemistry, but it has been shown to have insulin-mimetic properties in cell culture and it has been found to induce a somewhat different effect than treatment with vanadate alone (18). Finally, pVida is of interest due to its unusual trans dioxo monomeric unit in a polymeric network in the solid state. The unusual trans dioxo unit is not likely to persist in solution and presumably this complex has solution properties somewhat different than most other monoperoxovanadium complexes.

These compounds were tested in a cell-free total phosphatase assay, in an insulin receptor phosphorylation assay, and in glucose uptake experiments in either a rat adipocyte assay, or a rat epitrochlearis muscle assay. Given the variation in properties of these complexes, a range of responses would have been anticipated. The stabilities of the complexes alone vary significantly and should a response require, for example, the intact bisperoxooxovanadium(V) unit of the complex, one would expect that the two diperoxo complexes would show significantly higher activities than the monoperoxo complexes and vanadate alone. The results will briefly be summarized in the following.

The inhibition of total phosphatase activity was measured in cell lysate of H4 rat liver cell extracts from 1 μM to 1 mM concentration of vanadium compound. The effects of V_i, dpVpic, dpVim, and pVida were similar in this concentration range, whereas pVnta was a weaker inhibitor. The effects of dpVpic, dpVim, and pVida on insulin receptor phosphorylation were all higher than the effects of pVnta and V_i. It is interesting that only pVnta showed significant activity at 1 mM concentration, whereas V_i showed only low activity in the entire concentration range. In both the glucose uptake assays, dpVpic and dpVim induced statistically significant greater responses than the monoperoxo complexes (Table 2). In the glucose uptake assay for rat adipocytes, vanadate induced a smaller response, even compared to pVida and pVnta. This pattern was reversed in the glucose uptake assay in rat epitrochlearis muscle. Although the biological importance of the various levels of responses to these assays is not clear, the monoperoxovanadium complex, pVnta, is the peroxovanadium complex that consistently generates the lowest response. The fact that the other monoperoxo complex, pVida, generates a reasonable insulin-mimetic effect may indicate the lack of activity of pVnta is not simply because the complex contains only one peroxo unit. However, combining the observed biological responses with the fact that pVida is likely to be less stable in solution than pVnta, it is possible that a stable and kinetically inert monoperoxovanadium complex may exhibit fewer insulin-mimetic properties in *in vitro* assays. However, in some experiments (data not shown here), the response generated by pVnta is not statistically significant from that generated by V_i, so it is premature to infer that stable

Downloaded by MONASH UNIV on October 31, 2012 | http://pubs.acs.org
Publication Date: December 10, 1998 | doi: 10.1021/bk-1998-0711.ch006

and kinetically inert monoperoxovanadium(V) complexes do not have insulin-mimetic activities *in vivo*.

Table 2. Glucose Uptake in Rat Adipocytes and Rat Epitrochlearis Muscle.[a] Adapted and modified from Ref. 9.

compound	rat adipocytes (%)[b]	rat epitochlearis muscle (%)[b]
dpVim	191(±7)	208(±28)
V_i	82(±41)	173(±33)
dpVpic	211(±27)	182(±13)
pVida	165(±13)	164 (±17)
pVnta	137(±11)	151(±11)

[a] *Results are presented as percent of the submaximal insulin response.*

[b] *Results are shown with SEM, n = 4.*

Downloaded by MONASH UNIV on October 31, 2012 | http://pubs.acs.org
Publication Date: December 10, 1998 | doi: 10.1021/bk-1998-0711.ch006

Associating Compound Characteristics with Insulin-Mimetic Effects. The scientist loses the ability to control speciation when vanadium compounds are added to whole cells, perfused organs or administered to animals. Thus, it becomes difficult to determine which compound actually is responsible for a specific biological response. However, the hydrolytic stability of the peroxovanadium(V) unit in the complexes used in this work is likely to be sufficient to withstand at least a few hours incubation at neutral pH. Furthermore, it is likely that the observed responses in cell-free systems are due to these complexes and/or simple metabolic derivatives thereof. The lower responses of pVida and pVnta show that a monoperoxo complex has a decreased insulin-mimetic response compared to the diperoxo complexes, dpVpic and dpVim. This observation is further substantiated by the fact that the most labile monoperoxo compound, pVida, has a greater effect than the more stable and kinetically inert monoperoxo complex, pVnta. Similar observations have been reported by the Posner and Shaver team (4). The auxiliary ligands have been reported to markedly influence the potency of peroxovanadium compounds as insulin receptor kinase activators and phosphatase inhibitors (4). Such effects have not yet been documented in animal studies. In our study we also observed differences in the insulin receptor assay, but in the glucose uptake experiments in rat adipocytes and epitrochlearis muscle, we only observe subtle differences with the four ligands examined in our studies. Using vanadium compounds with a variety of different properties in biological studies will begin to address and identify some specific and common characteristics of various insulin-mimetic compounds.

Summary.

Three areas of relevance to vanadium complexes as insulin-mimetic agents were described in this chapter. First, the chemistry of three classes of vanadium compounds currently under examination with respect to inducing insulin-mimetic responses was described. Second, studies exploring the effect of coordination number of vanadium compounds on their potency as phosphatase inhibitors were discussed. Third, the insulin-mimetic effects of four different peroxovanadium(V) compounds in four different assay systems commonly used to describe insulin action were presented. We combined our unpublished work with recent work reported in the literature with the objective of summarizing the state-of-the-art in the areas covered.

The simple vanadate salts represent the group of vanadium compounds most studied. This group is also likely to be the last group in which a mechanistic understanding of its mode of action will be obtained, given the complex chemistry that vanadate and vanadyl cation undergo under physiological conditions. The peroxovanadium compounds encompass a group that has been explored with success in cellular assays, and has been shown to have a very potent insulin-mimetic effect. The chemistry of selected compounds of this group has been characterized in some detail, although important questions remain and still need additional study. The most studied representative of the third group, bis(maltolato)oxovanadium(IV), has been found to do particularly well in animal studies. Related derivatives such as bis(acetylacetonate)oxovanadium(IV) also have very promising insulin-mimetic properties. Although the latter parent compound has been used as a synthetic reagent for decades, the detailed chemistry of these complexes and their stability in aqueous solutions have not been examined, in part because of technical difficulties in recording the EPR spectra in aqueous solution.

It is generally accepted that a five-coordinate vanadium compound is an excellent transition state analog for phosphate ester hydrolysis reactions. The structural effect of coordination number on the potency of vanadium dipicolinic acid derivatives as phosphatase inhibitors was demonstrated. The vanadium(V) dipicolinic acid complex is five-coordinate and found to be a more potent inhibitor than the six-coordinate vanadium(IV) dipicolinic acid complex and the seven-coordinate bisperoxooxovanadium(V) dipicolinic acid complex. Surprisingly, this study suggests that all vanadium compounds regardless of coordination number are potent inhibitors for phosphatases suggesting that the structural component, although important, is not the determining factor for phosphatase inhibition.

Studies probing the mechanism by which vanadium compounds induce insulin action must consider the chemistry of these compounds and the possibility that the target compound will not remain intact during the study. This consideration is particularly important in cellular studies because the scientist has no control over the speciation and compartmentalization of the complex. Approaches to counter these difficulties include spectroscopic characterization of the biological system and studies of a series of compounds. Studies of a series of complexes with different properties will assist in the identification of which aspects are important for inducing insulin action. Using the latter strategy, we confirmed for a series of peroxovanadium(V) compounds in phosphatase, insulin receptor and glucose uptake assays that the diperoxovanadium compounds have significantly greater activity than monoperoxovanadium compounds or vanadate. However, the differences in effects for various ligands in insulin receptor kinase and phosphatase assays were not confirmed in glucose uptake assays in epitrochlearis muscle. These studies document the need for *in vivo* animal studies for more compounds in this class.

Downloaded by MONASH UNIV on October 31, 2012 | http://pubs.acs.org
Publication Date: December 10, 1998 | doi: 10.1021/bk-1998-0711.ch006

Acknowledgements.

DCC thanks the Institutes for General Medical Sciences at the National Institutes of Health for funding this work. DCC thanks Drs. Feilong Jiang, Sean S. Amin, Boyan Zhang, Oren P. Anderson and Ms. Susie M. Miller for sharing results before their publication. DCC also thanks Drs. Sean S. Amin and Kirk Cryer for reading this manuscript and Dr. Boyan Zhang for recording the spectra shown in Figs. 8 and 9.

References.

1. Abbreviations: dmso-d_6; hexadeutero-dimethylsulfoxide, dhVim;

$[VO(NH_2O)_2(imidazole)_2]Cl$, dpVim; $H[VO(O_2)_2(imidazole)_2]Cl$, dpVpic, bisperoxooxovanadium(V) picolinic acid; mpVdipic, peroxooxovanadium(V) dipicolinic acid; pVida, peroxovanadium iminediacetic acid; pVnta, peroxovanadium(V) nitrilotriacetic acid; V^Vdipic, oxovanadium(V) dipicolinic acid; V^{IV}dipic, oxovanadium(IV) dipicolinic acid; $VO(acac)_2$, bis(2,4-pentanedionato-*O,O'*)oxovanadium(IV) and bis(acetylacetonate)oxovanadium(IV); $VO(acac)_2$OiPr, bis(acetylacetonate)oxovanadium(V) isopropoxide.

2. Goldfine, A. B.; Simonson, D. C.; Folli, F.; Patti, M.-E.; Kahn, C. R., *J. Clin. Endo. Metab.* **1995**, *80*, 3311-3320.
3. Cohen, N.; Halberstam, M.; Shlimovich, P.; Chang, C. J.; Shamoon, H.; Rossetti, L., *J. Clin. Invest.* **1995**, *95*, 2501-2509.
4. a) Posner, B. I.; Faure, R.; Burgess, J. W.; Bevan, A. P.; Lachance, D.; Zhang-Sun, G.; Fantus, I. G.; Ng, J. B.; Hall, D. A.; Soo Lum, B.; Shaver, A., *J. Biol. Chem.* **1994**, *269*, 4596-4604; b) Yale, J.-F.; Lachance, D.; Bevan, A. P.; Vigeant, C.; Shaver, A.; Posner, B. I., *Diabetes* **1995**, *44*, 1274-1279; c) Bevan, A. P.; Burgess, J. W.; Yale, J.-F.; Drake, P. G.; Lachance, D.; Baquiran, G.; Shaver, A.; Posner, B. I., *Amer. J. Physiol.* **1995**, *268*, E60-E66.
5. McNeill, J. H.; Yuen, V. G.; Hoveyda, H. R.; Orvig, C., *J. Med. Chem.* **1992**, *35*, 1489-1491.
6. Caravan, P.; Gelmini, L.; Glover, N.; Herring, F. G.; Li, H.; McNeill, J. H.; Rettig, S. J.; Setyawati, I. A.; Shuter, E.; Sun, Y.; Tracey, A. S.; Yuen, V. G.; Orvig, C., *J. Am. Chem. Soc.* **1995**, *117*, 12759-12770.
7. Watanabe, H.; Nakai, M.; Komazawa, K.; Sakurai, H., *J. Med. Chem.* **1994**, *37*, 876-877.
8. Li, J.; Elberg, G.; Crans, D. C.; Shechter, Y., *Biochemistry* **1996**, *35*, 8314-8318.
9. Crans, D. C.; Keramidas, A. D.; Hoover-Litty, H.; Anderson, O. P.; Miller, M. M.; Lemoine, L. M.; Pleasic-Williams, S.; Vandenberg, M.; Rossomando, A. J.; Sweet, L. J., *J. Am. Chem. Soc.* **1997**, *119*, 5447-5448.
10. Shaver, A.; Ng, J. B.; Hall, D. A.; Posner, B. I., *Mol. Cell. Biochem.* **1995**, *153*, 5-15.
11. Crans, D. C.; Mahroof-Tahir, M.; Keramidas, A. D., *Mol. Cell. Biochem.* **1995**, *153*, 17-24.
12. Crans, D. C., *Comm. Inorg. Chem.* **1994**, *16*, 1-33.
13. Crans, D. C.; Keramidas, A. D.; Drouza, C., *Phosphorus, Sulfur, and Silicon,* **1996**, *109-110*, 245-248.
14. Keramidas, A. D.; Miller, S. M.; Anderson, O. P.; Crans, D. C., *J. Am. Chem. Soc.* **1997**, *119*, 8901-8915.
15. Jiang, F.; Jiang, F.; Anderson, O. P.; Miller, S. M.; Chen, J.; Mahroof-Tayir, M.; Crans, D. C., submitted.
16. Amin, S. S.; Crans, D. C., in preparation.
17. Brichard, S. M.; Amin, S. S.; Crans, D. C. in preparation.
18. Etcheverry, S. B.; Crans, D. C.; Keramidas, A. D.; Cortizo, A. M., *Arch. Biochem. Biophys.* **1997**, *338*, 7-14.
19. Hanson, G. R.; Sun, Y.; Orvig, C., *Inorg. Chem.* **1996**, *35*, 6507-6512.
20. Chasteen, N. D. In Biological Magnetic Resonance; Berliner, L. and Reuben, J., Eds.; Plenum Press: New York, 1981; Vol. 3, pp. 53-119.
21. Kadota, S.; Fantus, I. G.; Deragon, G.; Guyda, H. J.; Posner, B. I., *J. Biol. Chem.* **1987**, *262*, 8252-8256.
22. Kadota, S.; Fantus, I. G.; Deragon, G.; Guyda, H. J.; Hersh, B.; Posner, B. I., *Biochem. Biophys. Res. Comm.* **1987**, *147*, 259-266.

Downloaded by MONASH UNIV on October 31, 2012 | http://pubs.acs.org
Publication Date: December 10, 1998 | doi: 10.1021/bk-1998-0711.ch006

23. Posner, B. I.; Shaver, A.; Fantus, I. G. In New Antidiabetic Drugs; Bailey, C. J. and Flatt, P. R., Eds.; Smith-Gordon: London, 1990; Chapter 8, pp. 107-118.
24. Butler, A.; Clague, M. J.; Meister, G., *Chem. Rev.* **1994**, *94*, 625-638.
25. Conte, V.; Di Furia, F.; Modena, G. In *Organic Peroxides*; Ando, W., Ed.; John Wiley & Sons, Ltd.: New York, 1992, pp. 559-598.
26. Bonchio, M.; Conte, V.; Coppa, F.; Di Furia, F.; Modena, G. In *Dioxygen Activation and Homogeneous Catalytic Oxidation*; Simándi, L. I., Ed.; Elsevier Science Publishers: Amsterdam, 1991, pp. 497-504.
27. Conte, V.; Di Furia, F.; Moro, S., *J. Phys. Org. Chem.* **1996**, *9*, 329-336.
28. Bengtsson, G., *Acta Chem. Scand.* **1973**, *27*, 2554-2558.
29. Quilitzsch, U.; Wieghardt, K., *Z. Naturforsch.* **1979**, *34b*, 640-641.
30. Nuber, B.; Weiss, J., *Acta Cryst.* **1981**, *B37*, 947-948.
31. Rehder, D.; Wieghardt, K., *Z. Naturforsch.* **1981**, *36b*, 1251-1254.
32. Paul, P. C.; Angus-Dunne, S. J.; Batchelor, R. J.; Einstein, F. W. B.; Tracey, A. S., *Can. J. Chem.* **1997**, *75*, 429-440.
33. Paul, P. C.; Angus-Dunne, S. J.; Batchelor, R. J.; Einstein, F. W. B.; Tracey, A. S., *Can. J. Chem.* **1997**, *75*, 183-191.
34. Drew, R. E.; Einstein, F. W. B., *Inorg. Chem.* **1973**, *12*, 829-835.
35. Bhattacharjee, M.; Chaudhuri, M. K.; Islam, N. S.; Paul, P. C., *Inorg. Chim. Acta* **1990**, *169*, 97-100.
36. Einstein, F. W. B.; Batchelor, R. J.; Angus-Dunne, S. J.; Tracey, A. S., *Inorg. Chem.* **1996**, *35*, 1680-1684.
37. Mimoun, H.; Saussine, L.; Daire, E.; Postel, M.; Fischer, J.; Weiss, R., *J. Am. Chem. Soc.* **1983**, *105*, 3101-3110.
38. Drew, R. E.; Einstein, F. W. B., *Inorg. Chem.* **1972**, *11*, 1079-1083.
39. Harrison, A. T.; Howarth, O. W., *J. Chem. Soc. Dalton Trans.* **1985**, 1173-1177.
40. Arransio, D.; Super, L.; Shul-pin, G. B., *Izv. Akad. Nauk. Ser. Khim.* **1992**, *8*, 1918-1921.
41. Bonchio, M.; Conte, V.; Di Furia, F.; Modena, G.; Moro, S., *Inorg. Chem.* **1994**, *33*, 1631-1637.
42. Bonchio, M.; Conte, V.; Di Furia, F.; Modena, G.; Moro, S., *J. Org. Chem.* **1994**, *59*, 6262-6267.
43. Jaswal, J. S.; Tracey, A. S., *Inorg. Chem.* **1991**, *30*, 3718-3722.
44. Jaswal, J. S.; Tracey, A. S., *J. Am. Chem. Soc.* **1993**, *115*, 5600-5607.
45. Mehrotra, R. C.; Rai, A. K.; Singh, A.; Bohra, R., *Inorg. Chim. Acta* **1975**, *13*, 91-103.
46. Roberts, J. S., *Compr. Org. Chem.* **1979**, *2*, 185-217.
47. Taguchi, H.; Isobe, K.; Nakamura, Y.; Kawaguchi, S., *Chem. Lett.* **1975**, 757-760.
48. Selbin, J.; Manning, H. R.; Cessac, G., *J. Inorg. Nucl. Chem.* **1963**, *25*, 1253-1258.
49. Atherton, N. M.; Gibbon, P. J.; Shohoji, M. C. B., *J. Chem. Soc., Dalton Trans.* **1982**, 2289-2290.
50. Mustafi, D.; Makinen, M. W., *Inorg. Chem.* **1988**, *27*, 3360-3368.
51. Caira, M. R.; Haigh, J. M.; Nassimbeni, L. R., *Inorg. Nucl. Chem. Lett.* **1972**, *8*, 109-112.
52. Frausto da Silva, J. J. R.; Wooton, R., *J. Chem. Soc., Dalton Trans.* **1969**, *8*, 421-422.
53. Boucher, L. J.; Tynan, E. C.; Yen, T. F. in *Electron Spin Resonance of Metal Complexes*; Yen, T. F., Ed.; Plenum Press: New York, 1969, pp 111-130.

Downloaded by MONASH UNIV on October 31, 2012 | http://pubs.acs.org
Publication Date: December 10, 1998 | doi: 10.1021/bk-1998-0711.ch006

54. Dichmann, K.; Hamer, G.; Nyburg, S. C.; Reynolds, W. F., *Chem. Comm.* **1970**, 1295-1296.
55. Reynolds, J. G.; Jones, E. L.; Huffman, J. C.; Christou, G., *Polyhedron* **1993**, *12*, 407-414.
56. Jiang, F.; Crans, D. C., in preparation.
57. Gresser, M. J.; Tracey, A. S.; Stankiewicz, P. J., *Adv. Prot. Phosphatases* **1987**, *4*, 35-57.
58. Wilden, P. A.; Broadway, D., *J. Cell. Biochem.* **1995**, *58*, 279-291.
59. Lindqvist, Y.; Schneider, G.; Vihko, P., *Eur. J. Biochem.* **1994**, *221*, 139-142.
60. Zhang, M.; Zhou, M.; Van Etten, R. L.; Stauffacher, C. V., *Biochemistry* **1997**, *36*, 15-23.
61. Huyer, G.; Liu, S.; Kelly, J.; Moffat, J.; Payette, P.; Kennedy, B.; Tsaprailis, G.; Gresser, M. J.; Ramachandran, C., *J. Biol. Chem.* **1997**, *272*, 843-851.
62. Nuber, B.; Weiss, J.; Wieghardt, K., *Z. Naturforsch.* **1978**, *33b*, 265-267.
63. Bersted, B. H.; Belford, R. L.; Paul, I. C., *Inorg. Chem.* **1968**, *7*, 1557-1562.
64. Crans, D. C., *Comm. Inorg. Chem.* **1994**, *16*, 35-76.
65. Van Etten, R. L.; Waymack, P. P.; Rehkop, D. M., *J. Am. Chem. Soc.* **1974**, *96*, 6782-6785.
66. Simone, C. "Vanadium and protein interactions: Inhibition, redox chemistry, and conversion of cofactor analogs," Ph.D. dissertation, Colorado State University, 1992.
67. Lindquist, R. N.; Lynn, J. L., Jr.; Lienhard, G. E., *J. Am. Chem. Soc.* **1973**, *95*, 8762-8768.
68. Li, J.; Elberg, G.; Gefel, D.; Shechter, Y., *Biochemistry* **1995**, *34*, 6218-6225.
69. Cornman, C. R.; Zovinka, E. P.; Meixner, M. H., *Inorg. Chem.* **1995**, *34*, 5099-5100.
70. Shaver, A.; Hall, D. A.; Ng, J. B.; Lebuis, A.-M.; Hynes, R. C.; Posner, B. I., *Inorg. Chim. Acta* **1995**, *229*, 253-260.
71. Djordjevic, C.; Wilkins, P. L.; Sinn, E.; Butcher, R. J., *Inorg. Chim. Acta* **1995**, *230*, 241-244.
72. Sívak, M.; Joniakova, D.; Schwendt, P.. *Transition Met. Chem.* **1993**, *18*, 304-308.
73. Djordjevic, C.; Craig, S. A.; Sinn, E., *Inorg. Chem.* **1985**, *24*, 1281-1283.

Downloaded by MONASH UNIV on October 31, 2012 | http://pubs.acs.org
Publication Date: December 10, 1998 | doi: 10.1021/bk-1998-0711.ch006

Downloaded by YORK UNIV on October 31, 2012 | http://pubs.acs.org
Publication Date: December 10, 1998 | doi: 10.1021/bk-1998-0711.ch007

Chapter 7

Interaction of the Vanadyl (VO^{2+}) Cation with Guanosine Nucleotides and Elongation Factor Tu

Anindya Banerjee[1], Shan Chen[1], Heike Ruetthard[1,2], Fashun Jiang[1], Victor W. Huang[1], Mathias Sprinzl[2], and Marvin W. Makinen[1]

[1]Department of Biochemistry and Molecular Biology, The University of Chicago, 920 East 58th Street, Chicago, IL 60637
[2]Laboratory of Biochemistry, University of Bayreuth, 95440 Bayreuth, Germany

The vanadyl (VO^{2+}) cation is used as a paramagnetic substitute of Mg^{2+} for electron paramagnetic resonance (EPR) and electron nuclear double resonance (ENDOR) studies to investigate metal-nucleotide and metal-protein interactions in guanosine nucleotide complexes formed with elongation factor Tu (EF-Tu) of *Thermus thermophilus*. Scatchard plot analysis of the affinity of GDP and GTP to the protein in the presence of VO^{2+} together with EPR studies showed formation of ternary EF-Tu : VO^{2+} : guanosine nucleotide complexes of 1:1:1 stoichiometry. While the binding of GDP in the presence of VO^{2+} was less tight by one order of magnitude than in the presence of Mg^{2+}, GTP was bound with comparable affinity. By EPR no secondary binding sites on the protein could be detected. Different classes of hydrogens in the active site in the vicinity of the metal ion corresponding to solvent exchangeable and covalently bound hydrogens could be identified by ENDOR for the protein complexes formed in ^2H_2O or with the recombinant protein purified from *E. coli* grown in deuteriated minimal medium. VO^{2+} was also found to support hydrolysis of GTP catalyzed by EF-Tu. These preliminary results show that VO^{2+} may serve as a sensitive ENDOR probe to investigate active site structure and structural flexibility of residues controlling the conformational change of the protein during GTP hydrolysis.

During protein biosynthesis in bacteria, the elongation factor Tu (EF-Tu) recognizes, transports, and positions the codon-specified aminoacyl-transfer RNA onto the A site of the ribosome (*1*). In its cellular role, the interactions of EF-Tu with other factors important in protein biosynthesis are governed by the binding of GTP and GDP, which act as effector molecules to control the conformation of the protein. Not only is there a marked change in the affinity of binding of these guanosine nucleotides by two orders of magnitude in the presence of Mg^{2+} as a required divalent metal ion cofactor

In Vanadium Compounds; Tracey, A., et al.;
ACS Symposium Series; American Chemical Society: Washington, DC, 1998.

(*2, 3*), but also, as shown for the protein from *Thermus thermophilus*, EF-Tu exhibits a dramatic conformational change in the nucleotide binding region upon GTP hydrolysis (*4-7*). In the triphosphate complex, residues 54-59 (*T. thermophilus* numbering) form a small helix which assume an extended conformation in the diphosphate complex. While Asp-51 is coordinated to the metal ion in both diphosphate and triphosphate complexes, Thr-25 and Thr-62 supply hydroxyl groups to coordinate the divalent metal ion together with the terminal phosphate group of GTP in the trinucleotide complex. Upon nucleotide hydrolysis, however, solvent molecules replace the γ-phosphate group, and the side chain of Thr-62 moves to a new position 16 Å distant from its site in the ternary EF-Tu : Mg^{2+} : GTP complex. The influence of the metal ion and how changes in metal-ligand interactions control the conformation of the protein in the effector binding region are not known. To investigate the influence of metal-ligand interactions on the dynamics of protein structural changes requires a spectroscopic approach. Unfortunately, Mg^{2+}, as the naturally occurring cofactor, is spectroscopically silent.

The vanadyl (VO^{2+}) cation is a versatile paramagnetic substitute for divalent metal ions in macromolecules (*8*), and we have found that it not only substitutes specifically for Mg^{2+}, but it also mimics closely the interactions of Mg^{2+} with nucleotides (*9-12*). By employing VO^{2+} as a paramagnetic probe for electron nuclear double resonance (ENDOR) spectroscopy, we have determined the detailed structure of VO^{2+}-nucleotide complexes in solution showing that they are identical to Mg^{2+} complexes defined by X-ray crystallography. In these studies the precision of structure analysis in the form of spectroscopically determined metal-nucleus distances over a 3-8 Å range was at a level of accuracy exceeded only by that of X-ray diffraction. We have consequently turned our attention to the use of VO^{2+} as a paramagnetic probe of metal coordination geometry and active site structure in EF-Tu. In this report we present preliminary results showing that the binding of VO^{2+} to EF-Tu is specific and competitive with Mg^{2+} and in the presence of GDP and GTP it forms ternary EF-Tu : VO^{2+} : guanosine nucleotide complexes of 1:1:1 stoichiometry.

Experimental Procedures

General. All guanosine nucleotides were obtained as their sodium salts from Sigma (St. Louis, MO 63178); vanadyl sulfate hydrate, deuterium oxide (> 99%), and β-mercaptoethanol from Aldrich (Milwaukee, WI 53233); urea (ultrapure, > 99.9%) from Amresco (Solon, OH 44139); aqueous solutions of [8-^{3}H]GDP and [8-^{3}H]GTP as ammonium salts with a specific activity of 11.5 Ci/mmol and a radioactive concentration of 1.0 mCi/mL were obtained from Amersham Life Sciences (Arlington Heights, IL 60005). [γ-^{32}P]GTP was obtained from Hartmann Analytik (Braunschweig, Germany). Nitrocellulose membranes (HA 0.54 μm) were purchased from Millipore Corporation (Belford, MA 01730). Filter-Count scintillation fluid from Packard Instruments (Meriden, CT 06450) was used to detect radioactivity in a Packard Instruments Minaxβ Tri-Carb 4000 Series Liquid Counter. Chelex resin (100-200 mesh biotechnology grade) was obtained from Bio-Rad Laboratories (Hercules, CA 94547). Bovine serum albumin (BSA) was obtained from Boehringer Mannheim (Indianapolis, IN 46250); DNase I (from bovine pancreas) and lyzozyme (from chicken egg white), Q Sepharose Fast Flow (anion exchanger), and CM

Downloaded by YORK UNIV on October 31, 2012 | http://pubs.acs.org
Publication Date: December 10, 1998 | doi: 10.1021/bk-1998-0711.ch007

Sepharose CL-6B (cation exchanger) were obtained from Sigma. Sephacryl S-200 HR (gel filtration medium) and column systems C 16/20, XK 26/60 and XK 26/100 were obtained from Pharmacia Biotech, Inc. (Piscataway, NJ 08854).

Purification of EF-Tu. Cell paste of *Escherichia coli* (JM109) engineered (*13*) with the *tufl* gene of *Thermus thermophilus* (HB8) was provided by Philip Johnson of the Pilot Plant, Department of Biochemistry, University of Wisconsin (Madison, WI 53705). Thermostable EF-Tu was isolated and purified from cell paste using the procedure of Blank *et al.* (*14*). Variations in the procedure were as follows: Cell lysis was performed by freeze-thaw cycles instead of nitrogen decompression. In each cycle the suspension was frozen in a methanol-dry ice bath (-80° C) and then allowed to thaw to 0° C. This cycle was repeated four times. All subsequent procedures were carried out at 4° C. The homogenate obtained was centrifuged at 8000 x *g* for 90 min to remove cell debris. The supernatant was then centrifuged at 113,000 x *g* for 3 hr, and to the clear supernatant (150 mL) solid $(NH_4)_2SO_4$ was added under gentle stirring to 70 % saturation over a 2-3 hr period. After the addition of $(NH_4)_2SO_4$, the mixture was stirred for another hour and then allowed to stand overnight at 4° C. The protein was dissolved in and dialyzed against the anion exchange-buffer (*14*) and applied to a 2 x 10 cm Q Sepharose Fast-Flow column. The fractions containing the protein were concentrated to a volume of 5 mL by ultrafiltration using a membrane with minimum molecular weight cut-off of 10,000 (Amicon, Inc., Beverly, MA 01915). The protein was stored in 50 % (v/v) glycerol at -20° C for further use.

Nucleotide free EF-Tu was obtained based on procedures described by Limmer *et al.* (*15*). The fractions containing the protein, eluted from the cation exchange column, were pooled and dialyzed against 0.2 M NaCl (5 x 100 mL), buffered to pH 7.5 with 0.025 M PIPES, and concentrated to a final volume of 20 mL using Centriprep-10 Concentrators (Amicon). Protein concentration was determined using the bicinchoninic acid assay (Sigma), based on the method of Smith *et al.* (*16*). Perdeuteriated EF-Tu was obtained by growth of *E. coli* (JM109) cells (*13*) on minimal medium containing ^2H_2O and $[^2H_3]$acetate (6 g/L) in addition to M9 salts and vitamins. Perdeuteriated EF-Tu was then obtained by treatment of cells as grown under natural abundance isotope conditions. The purified EF-Tu was found to be enriched to $\geq$ 98% deuteriation by MALDI-TOF mass spectrometry.

Measurement of Nucleotide Binding Affinity of EF-Tu. The interaction of guanosine nucleotides with EF-Tu was measured by application of the procedure of Arai and coworkers (*2, 3, 17*). The incubation mixture contained 0.05 M KCl buffered to pH 7.5 with 0.05 M HEPES. The concentration of EF-Tu was 8.8×10^{-9} M and the guanosine nucleotide concentration was varied from 12.5 to 500×10^{-9} M in a constant reaction volume of 0.175 mL. After an aliquot of the incubation mixture was applied to the nitrocellulose membrane, the filter was washed with three aliquots of 0.05 M KCl buffered to pH 7.5 with 0.05 M HEPES.

Binding of radioactive GDP or GTP to the membrane independent of added protein was also detected, particularly at high nucleotide concentrations. The observed counts for binding in the presence of EF-Tu were corrected for this background binding activity.

Downloaded by YORK UNIV on October 31, 2012 | http://pubs.acs.org
Publication Date: December 10, 1998 | doi: 10.1021/bk-1998-0711.ch007

To measure the binding affinity of nucleotides to EF-Tu in the presence of Mn^{2+} and VO^{2+} as well as in the absence of added metal ion, the protein and nucleotide were treated first with a suspension of Chelex to ensure removal of all trace divalent metal ions, including low levels of Mg^{2+} (assessed to be $\leq$ 0.01 g-ion % by atomic absorption spectroscopy) that may be protein-bound after nucleotide removal. Chelex resin was then removed by centrifugation. For nucleotide binding in the presence of Mg^{2+} or Mn^{2+}, an aliquot of the metal ion solution was added to the buffer to a final concentration of 0.01 M. For GDP binding in the presence of VO^{2+}, the nucleotide was added to the protein over the range of concentrations stated above, followed by addition of VO^{2+} in 1:1 stoichiometric ratio with EF-Tu. For GTP binding, the protein and nucleotide were individually treated with Chelex resin, and a 1 molar equivalent of VO^{2+} was added first to the GTP solution. The VO^{2+} - GTP mixture was then added to the protein over a 10-500 x 10^{-9} M concentration range. This order of addition of reagents was required for reproducibility of results in the presence of VO^{2+}.

Downloaded by YORK UNIV on October 31, 2012 | http://pubs.acs.org
Publication Date: December 10, 1998 | doi: 10.1021/bk-1998-0711.ch007

Intrisic GTPase Activity of EF-Tu. The intrinsic GTPase activity of EF-Tu was determined by measuring the rate of [^{32}P]phosphate release during hydrolysis of [γ-^{32}P]GTP in the presence of various divalent metal ions under single-turnover conditions. While initial studies were carried out as described below, the results were subsequently confirmed using a phosphorimager technique adapted from that of Peter *et al.* (*18*). Aliquots of the reaction mixture at different times were quenched in formic acid, stored on ice, and chromatographically separated on PEI-Cellulose sheets (Macherey-Nagel, Doeren, Germany). Electronic autoradiography was carried out with an InstantImager 2024 (Packard Instruments, Meriden, CT 06450).

EPR and ENDOR. Electron paramagnetic resonance (EPR) absorption spectra were recorded with a Bruker ESP300E spectrometer equipped with an Oxford Instruments ESR910 liquid helium cryostat and a Bruker digital ENDOR accessory, as previously described (*9,10*). The sample temperature (10 K) was controlled with an Oxford Instruments ITC4 temperature controller. For collection of EPR and ENDOR spectra, solutions of ternary EF-Tu : VO^{2+} : nucleotide complexes were prepared by addition of nucleotide to EF-Tu in 0.2 M NaCl buffered with 0.025 M PIPES to pH 7.5, followed by addition of small aliquots of a stock solution of $VOSO_4$ at pH ~ 4. The solution was allowed to incubate at 0° C for 5-10 min to ensure that no precipitate from the metal hydroxide (*8*) was present and then placed in an Amicon Centriprep-1 Concentrator and centrifuged to a final volume of 0.5 mL. The filtrate and retentate were transferred to separate EPR tubes and frozen in liquid nitrogen. The samples in ^2H_2O were prepared by dialyzing the protein against 0.2 M NaCl buffered to pD 7.5 with 0.025 M PIPES. The samples were then prepared as described above but with the buffer prepared with ^2H_2O. The final concentration of EF-Tu in the EPR sample tube was approximately 1.0 x 10^{-3} M.

Results and Discussion

Dissociation Constants of Guanosine Nucleotide Binding to *T. thermophilus* EF-Tu. The interaction of guanosine nucleotides binding to EF-Tu and its dependence on the presence of a divalent metal ion cofactor was quantitatively measured by a nitrocellulose membrane filter procedure (*2, 3, 17*). As shown in Figure 1, in the presence of either Mg^{2+} or VO^{2+}, the amount of [8-^{3}H]GDP retained on the filter as the protein bound nucleotide increased as a function of GDP concentration. From the Scatchard plots (*19*), it is seen that the graph extrapolates to a stoichiometry of ~ 1.0 for nucleotide binding for both divalent metal ion cofactors. The binding of GDP in the presence of Mg^{2+}, as indicated by the slope, is tighter by one order of magnitude than in the presence of VO^{2+}.

In Table I results of Scatchard plot analyses of GDP and GTP binding to EF-Tu dependent on the presence of a divalent metal ion are summarized for a variety of conditions. In these experiments we found that it was necessary, as described in Experimental Procedures, to treat the protein and the radioactive nucleotide solution with Chelex resin to remove all trace divalent metal ions prior to addition of the metal ion cofactor. Without this treatment the nucleotide binding affinity in the absence of added divalent metal ion was uniformly greater than indicated in Table I. We consequently pretreated the protein and [8-^{3}H]GDP and [8-^{3}H]GTP solutions with Chelex resin prior to introduction of VO^{2+} and Mn^{2+} to ensure that the observed binding affinity was not influenced by low levels of Mg^{2+} or other trace divalent metal ions.

The results for GDP binding when plotted according to Scatchard (*19*) indicated dissociation binding constants of the order of 10^{-9} M with a 'biphasic' distribution suggestive of heterogeneity of protein in binding affinity. It was observed that the biphasic character of the plots disappeared and stoichiometry coefficients of ~ 1.0 for nucleotide binding were consistently observed in the presence of BSA (0.016 mg/mL). Binding of radioactive nucleotides to BSA alone was not detected under these conditions. No difference in the binding curves was observed dependent on addition of BSA first to the incubation mixture followed by EF-Tu, nucleotide, and metal ion, or addition of BSA to the mixture after all other reagents had been mixed together. Therefore, the binding affinity of GDP and GTP was routinely measured with added BSA in the incubation mixture. Since no binding of radioactive nucleotide to BSA alone under these conditions was observed, it is probable that the effect of BSA is due to its neutral protectant role, as commonly observed in biochemical assays, in view of the very dilute concentration of EF-Tu required to measure binding over a wide range of nucleotide concentration.

In these experiments we also observed that biphasic Scatchard plots were obtained unless correction was made for binding of radioactive nucleotide to the nitrocellulose membrane, especially at high nucleotide concentrations. While similar observations have not been reported by Arai and coworkers (*2, 3, 17*), results of Crechet and Parmeggiani (*20*) for the *E. coli* protein show curvature in Scatchard plots suggestive of heterogeneity in binding affinity.

Although binding affinity of EF-Tu for GTP was measured with use of [8-^{3}H]GTP rather than with use of [γ-^{32}P]GTP, there is essentially no contribution to the observed binding due to GTP hydrolysis. Under the conditions of the binding assay, we estimate that less than 5 % of GTP would be hydrolyzed. In addition, the results for GTP binding are in good agreement with estimates based on other procedures (*2, 3, 17*).

Downloaded by YORK UNIV on October 31, 2012 | http://pubs.acs.org
Publication Date: December 10, 1998 | doi: 10.1021/bk-1998-0711.ch007

Downloaded by YORK UNIV on October 31, 2012 | http://pubs.acs.org
Publication Date: December 10, 1998 | doi: 10.1021/bk-1998-0711.ch007

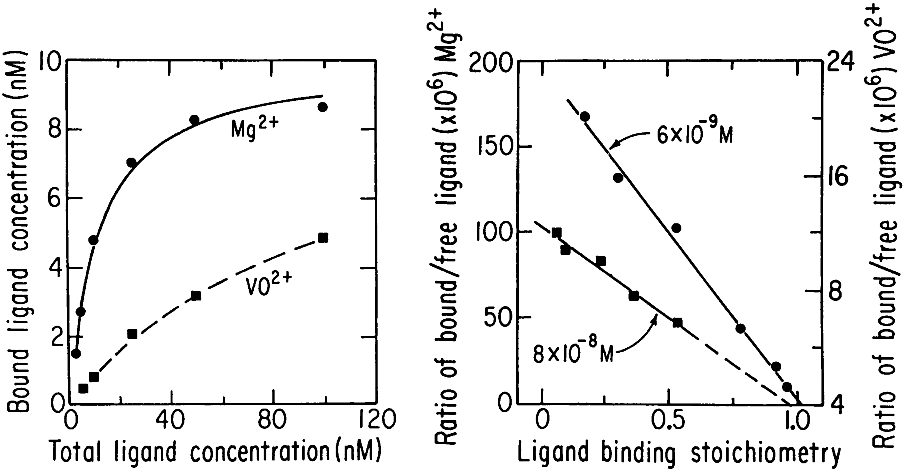

Figure 1. Scatchard plots illustrating the binding of GDP to nucleotide-free EF-Tu as a function of GDP concentration in the presence of Mg^{2+} or VO^{2+}. The binding was measured as described in Experimental Procedures. No change in the binding characteristics was observed dependent on incubation of the mixture at 0° C or 20° C (●, Mg^{2+}; ■, VO^{2+}).

Table I

Comparison of Equilibrium Dissociation Binding Constants of GDP and GTP to *Thermus thermophilus* EF-Tu in the Presence and Absence of Divalent Metal Ions.

Nucleotide	Metal Ion			
	Mg^{2+}	Mn^{2+}	VO^{2+}	no added metal ion
			(M) x 10^9	
GDP	5.9 ± 0.9	4.8 ± 0.5	84 ± 2	100 ± 9
GTP	28 ± 2	–	24 ± 1	110 ± 40

The results in Table I show that the binding constant for GDP in the presence of Mg^{2+} is in agreement with the value of 1.1 x 10^{-9} M reported by Arai and coworkers for *T. thermophilus* EF-Tu (*3,17*). Similarly the binding affinity of GTP in the presence and absence of Mg^{2+} is in good agreement with that of 5.8 x 10^{-8} M estimated by GDP displacement from the *T. thermophilus* protein (*3*). While binding of nucleotides to the *T. thermophilus* protein dependent on other divalent metal ions has not been reported, the binding affinity of GDP in the presence of Mn^{2+} given in Table I is comparable to that observed for the *B. stearothermophilus* protein (*21*). It is seen in Table I that VO^{2+} mimics the action of Mg^{2+} in forming a ternary EF-Tu : Me^{2+} : GDP complex although the binding affinity is reduced by one order of magnitude. On the other hand, the binding of GTP is of comparable affinity in the presence of either Mg^{2+} or VO^{2+}. This difference in the two pairs of binding constants probably reflects the marked specificity that EF-Tu exhibits in binding GDP for which the influence of the metal ion is greater. It is also of interest to note that in the absence of a divalent metal ion cofactor, GDP and GTP bind with equivalent affinity.

We have further investigated the specificity of VO^{2+} binding to EF-Tu by EPR. In Figure 2 we illustrate the first-derivative EPR absorption spectrum of the ternary EF-Tu : VO^{2+} : GDP complex for which the metal ion was added in near 1:1 molar stoichiometry to the protein. Ultrafiltration of the solution allows unbound VO^{2+}-GDP, if present, to be detected in the filtrate since the free, hydrated VO^{2+} ion becomes EPR-silent through formation of a polymeric $VO(OH)_2$ species above pH 5 while protein or nucleotide bound VO^{2+} exhibits EPR absorption (*8-12*). It is seen that there is no unbound VO^{2+}-GDP complex in the filtrate detectable under identical conditions of incident microwave power and receiver gain. Moreover, addition of up to a 4-fold molar excess of VO^{2+} to the ternary EF-Tu : Mg^{2+} : GDP complex showed no evidence of secondary binding sites on the protein. These observations are, thus, consistent with the results in Table I.

GTPase Activity of EF-Tu Dependent on Metal Ion. The intrinsic GTPase activity of EF-Tu in the absence of ribosomes was determined by measuring the rate of [^{32}P]phosphate release during hydrolysis of [γ-^{32}P]GTP catalyzed by the protein in the presence of Mg^{2+}, Mn^{2+}, and VO^{2+}. The activity in the presence of Mn^{2+} was equivalent to that observed in the presence of Mg^{2+}. Figure 3 compares the time dependent release of [^{32}P]phosphate at 23° C for EF-Tu in the presence of Mg^{2+} and VO^{2+} under single turnover conditions. While Mg^{2+} remains soluble in the reaction mixture and could, therefore, be added directly to the buffer, as pointed out above, VO^{2+} forms an insoluble precipitate at neutral pH (*8-11*), requiring its addition as a VO^{2+}-GTP complex. It is seen in Figure 3 that in the presence of VO^{2+}, EF-Tu catalyzes GTP hydrolysis similarly to that in the presence of Mg^{2+} and Mn^{2+}. Since metal ion and nucleotide were added only in equimolar equivalents to the protein, kinetic rate constants cannot be directly calculated from these results to compare the catalytic efficiency of the enzyme dependent on the metal ion because the turnover rate is dependent on the concentrations of protein, nucleotide, and metal ion. Nonetheless, it is evident that VO^{2+} appears to support GTP hydrolysis catalyzed by EF-Tu like other divalent metal ions and does not cause hydrolysis of GTP in solution in the absence of the protein.

Downloaded by YORK UNIV on October 31, 2012 | http://pubs.acs.org
Publication Date: December 10, 1998 | doi: 10.1021/bk-1998-0711.ch007

Downloaded by YORK UNIV on October 31, 2012 | http://pubs.acs.org
Publication Date: December 10, 1998 | doi: 10.1021/bk-1998-0711.ch007

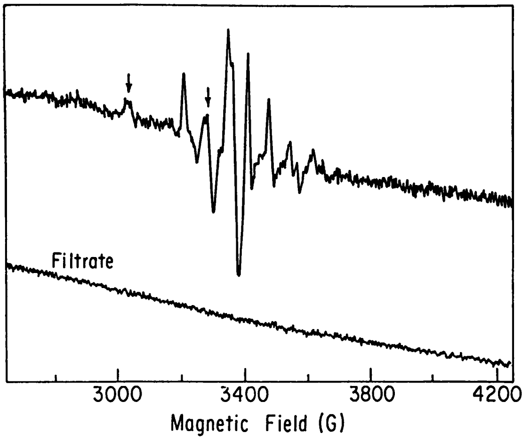

Figure 2. First-derivative EPR absorption spectrum of the ternary EF-Tu : VO^{2+} : GDP complex. The complex was formed in 0.2 M NaCl buffered to pH 7.5 with 0.03 M PIPES as described in Experimental Procedures. The upper spectrum belongs to the complex while the lower spectrum is that of the filtrate collected under identical conditions of temperature (10 K), microwave power, and spectrometer gain. The arrows designate the $-5/2 \parallel$ and $-3/2 \perp$ resonance features near 2900 and 3260 G, respectively, that are saturated with microwave power for collection of ENDOR spectra.

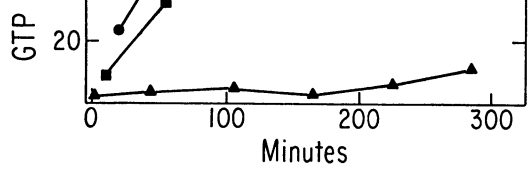

Figure 3. Hydrolysis of GTP determined by release of $[^{32}P]$phosphate from $[\gamma\text{-}^{32}P]$GTP catalyzed by EF-Tu. The protein was added to the reaction mixture (0.15 M NH_4Cl buffered to pH 7.5 with 0.05 M HEPES) to a final concentration of 10 x 10^{-6} M. Premixed nucleotide and metal ion were then added in equimolar equivalents. Aliquots were taken with time. The reaction was quenched by addition of the aliquot to perchloric acid and the $[^{32}P]$phosphate was separated from the reaction mixture by passing the aliquot and acid mixture through an activated charcoal column with 0.1 M HCl. The reactions were monitored with incubation at 23° C (●, Mg^{2+}; ■, VO^{2+}; ▲, VO^{2+}, GTP only).

We have also evaluated the catalytic activity of isotopically enriched EF-Tu with use of a phosphorimager technique under single-turnover conditions following the procedure described by Peter *et al.* (*18*). Under conditions of equimolar Mg^{2+}, native *T. thermophilus* EF-Tu exhibited a turnover rate of ~ 0.035 min^{-1} at 37° C, in good agreement with the results of others (*22*), while perdeuteriated EF-Tu exhibited a turnover rate of ~ 0.027 $min.^{-1}$ Kalbitzer *et al.* have shown that the GDP binding activity of perdeuteriated EF-Tu of *E. coli* is essentially identical to that of native EF-Tu (*23*).

ENDOR of EF-Tu : VO^{2+} : Guanosine Nucleotide Complexes. ENDOR spectroscopy provides the most precise method of measuring the strength of electron-nucleus hyperfine (hf) interactions. On this basis application of ENDOR yields very high resolving power for the study of molecular structure. ENDOR spectroscopy is performed by saturating the electronic transitions of the paramagnetic system under high microwave power and simultaneously irradiating the system with a strong radiofrequency (rf) field. When the rf field is scanned under these conditions and the resonance of a magnetic nucleus is reached, such as that of ^{1}H or ^{19}F interacting with the paramagnetic site, a forbidden transition involving both the unpaired electron and the nearby magnetic nucleus occurs, giving rise to increased EPR signal amplitude. Thus, the ENDOR method is equivalent to detection of nuclear resonance absorption by observing changes in the intensity of EPR absorption.

In this laboratory the VO^{2+} cation has been used as a paramagnetic probe for ENDOR to determine nucleotide structure and conformation (*9-12*) and to investigate the ligand coordination structure of VO^{2+} in solution and in proteins (*24, 25*). As demonstrated through Figures 1 and 2 and Table I, VO^{2+} binds specifically with guanosine nucleotides in the active site of EF-Tu to form a ternary EF-Tu : VO^{2+} : GXP complex of 1:1:1 stoichiometry. Thus, VO^{2+}, as a paramagnetic probe, is ideally positioned for investigation of the immediate coordination environment of the metal ion in complexes formed with both GDP and with GTP. Here we provide a preliminary comparison of the ENDOR spectra of nucleotide di- and tri-phosphate complexes of EF-Tu, identifying through deuteriation different classes of protons of active site residues in the nearby environment of the metal ion.

In Figure 4 we have compared the ENDOR spectra of the ternary complex of EF-Tu formed with GTP to that formed with guanosine-5′-(β,γ-imido)-triphosphate (GMPPNP), as a slowly hydrolyzing analog of GTP. The X-ray structure of the ternary trinucleotide complex was determined with GMPPNP as an analog of GTP to avoid triphosphate hydrolysis during crystallization of the protein complex (*4,5*). It is seen that the ENDOR spectra of both ternary complexes are identical indicating that the active site structure in the vicinity of the metal ion is isomorphous for both types of complexes. While X-ray studies have by necessity characterized the complex formed with GMPPNP, the ENDOR spectra in Figure 4 demonstrate unambiguously that the GMPPNP analog forms a complex structurally identical to that formed with the catalytically active substrate GTP.

For the $-3/2 \perp$ setting of $\mathbf{H}_0$ both complexes exhibit a pair of resonance features at 12.4 and 15.6 MHz, indicated by the stick diagram in Figure 4, that are not observed in the ENDOR spectrum with $\mathbf{H}_0$ set to the $-5/2 \parallel$ feature of the EPR spectrum. The amplitude of these ENDOR features is also diminished for the complex

Downloaded by YORK UNIV on October 31, 2012 | http://pubs.acs.org
Publication Date: December 10, 1998 | doi: 10.1021/bk-1998-0711.ch007

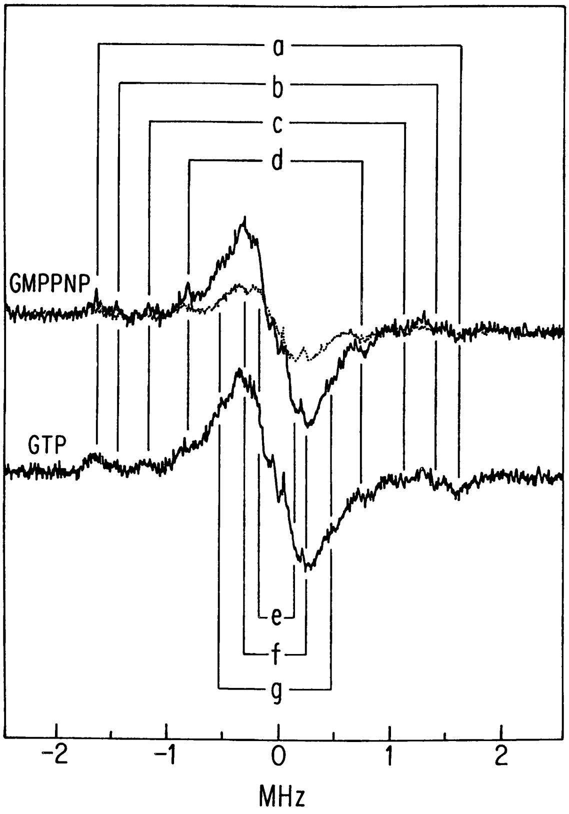

Figure 4. Proton ENDOR spectra of ternary complexes of EF-Tu formed with GTP and GMPPNP in the presence of VO^{2+}. The laboratory magnetic field was set to the $-3/2 \perp$ setting of $\mathbf{H}_0$. The upper spectra are of the EF-Tu : VO^{2+} : GMPPNP complex formed with addition of 1 molar equivalent of VO^{2+} in H_2O (solid line spectrum) and ^2H_2O (dotted line spectrum). The lower spectrum is of the EF-Tu : VO^{2+} : GTP complex formed with addition of 1 molar equivalent of VO^{2+} in H_2O. Pairs of resonance features identified by stick diagrams correspond to clusters of residues with the following averaged radial separations (in Ångstroms) from the vanadium nucleus: **a**, 2.98; **b**, 3.11; **c**, 3.38; **d**, 3.77; **e**, 5.89; **f**, 5.35; and **g**, 4.42. The vanadium-proton separations calculated from the resonance features are assumed to correspond to perpendicular hf couplings. The abscissa indicates the ENDOR shift $\Delta\nu = \nu_\pm - \nu_H$, where $\nu_\pm$ is the observed frequency and the ν_H is the Larmor frequency of the proton (13.88 MHz). Other conditions as in Figure 2.

Downloaded by YORK UNIV on October 31, 2012 | http://pubs.acs.org
Publication Date: December 10, 1998 | doi: 10.1021/bk-1998-0711.ch007

formed in ^2H_2O. These characteristics are specific for an axially coordinated water molecule bound within the inner coordination sphere of the metal ion (*11,24*). As shown by the spectrum of the GMPPNP complex formed in ^2H_2O, there are also other identifiable classes of solvent exchangeable protons near the metal ion.

In Figure 5 we have compared ENDOR spectra of the EF-Tu : VO^{2+} : GDP complex with $\mathbf{H_0}$ set to the central absorption feature to achieve maximum signal-to-noise ratio although loss of selection of molecular orientation occurs. The spectrum of the native protein dissolved in ^2H_2O compared to that formed in buffer of natural abundance isotope composition shows a markedly decreased amplitude of the central resonance feature, illustrating the loss of nearby protons in the active site that are exchangeable with solvent. Finally, the spectrum of the complex formed with perdeuteriated EF-Tu in ^2H_2O shows only one resonance feature centered at the Larmor frequency greatly reduced in amplitude that derives from disordered protons distant from the metal ion. This resonance feature probably represents the small fraction of protiated residues that have not been totally removed by growth of the *E. coli* cells on perdeuteriated medium and the resonances of protons belonging to the nucleotide, which are not resolvable under these conditions of protein concentration and spectrometer gain.

The spectra of these three types of complexes demonstrate different classes of protons in the active site that may be used separately for structure analysis. Again, it is seen that the pair of resonance features near 12.4 and 15.6 MHz disappear upon formation of the complex in ^2H_2O, characteristic of an axially coordinated water molecule, as in the ternary EF-Tu : VO^{2+} : GTP complex. Furthermore, it is seen that classes of resonances can be separated as originating from solvent exchangeable and covalently bound hydrogens. In addition, the loss of broad proton resonance features by perdeuteriation allows further distinctions to be made. For instance, introduction of a protiated or fluorinated amino acid, e.g. *m*-fluoro-tyrosine, in the perdeuteriated growth medium would permit both the ^{19}F and ^1H resonances from Tyr-47 (*4,5*) to be detected with little background interference from the broad, overlapping contributions of distant, disordered protons. *Meta*-fluoro-tyrosine has been incorporated into the *E. coli* protein for nuclear magnetic resonance studies through use of an auxotroph (26).

Through these ENDOR studies an interesting observation has been made, indicative of greatly restricted dynamical flexibility of the EF-Tu : VO^{2+} : GDP complex. While we have demonstrated exchangeable protons in the active site by comparing spectra of complexes formed in H_2O and in ^2H_2O, as shown in Figures 4 and 5, addition of H_2O to the complex of the perdeuteriated protein formed in ^2H_2O showed no evidence for reappearance of the exchangeable proton resonance features. This observation suggests that the active site rigidly contains the metal ion and diphosphate-nucleotide ligand with markedly restricted dynamical motion so that solvent molecules cannot easily find their way into the metal binding site from the exterior of the protein. This observation is no doubt consistent with the 10^{-9} M value of the K_d for GDP binding, as given in Table I. Further ENDOR investigations of the active site region of EF-Tu may be able to identify which residues exhibit differential structural fluctuations dependent on nucleotide and metal binding and thus may bring increased insight into the control of conformational changes by metal ion and nucleotide binding.

Downloaded by YORK UNIV on October 31, 2012 | http://pubs.acs.org
Publication Date: December 10, 1998 | doi: 10.1021/bk-1998-0711.ch007

Downloaded by YORK UNIV on October 31, 2012 | http://pubs.acs.org
Publication Date: December 10, 1998 | doi: 10.1021/bk-1998-0711.ch007

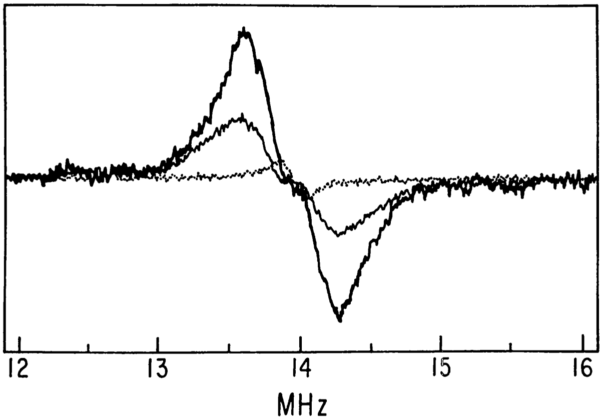

Figure 5. Comparison of proton ENDOR spectra of the ternary EF-Tu : VO^{2+} : GDP complex formed with native and perdeuteriated protein. The laboratory magnetic field $\mathbf{H}_0$ was set to the central EPR feature at about 3360 G (*cf.*, Figure 2). Thick line spectrum, complex of native EF-Tu in H_2O; thin-line spectrum, complex of native EF-Tu formed in ^2H_2O; dotted line spectrum, complex of perdeuteriated EF-Tu formed in ^2H_2O. Other conditions as in Figure 2.

Acknowledgment. This work has been supported by grants of the NSF (MCB-9513538) awarded to M. W. M., NATO (CRG960629) awarded to M. W. M. and M. S., and a grant of the Deutsche Forschungsgemeindschaft (Sp 243/-2) awarded to M. S.

Literature Cited.

1. Miller, D. L. and Weisbach, H. In *Molecular Mechanism of Protein Biosynthesis;* Weissbach, H. and Petka, S., Eds.; Academic Press: New York, 1977, pp. 323-340.
2. Arai, K. I.; Kawakita, M.; Kaziro, Y. *J. Biochem.* **1974**, *76*, 293-306.
3. Arai, K. I.; Arai, N.; Nakamura, S.; Oshima, T.; Kaziro, Y. *Eur. J. Biochem.* **1978**, *92*, 521-531.
4. Berchtold, H; Reshetnikova, L.; Reiser, C. O. A.; Schirmer, N. K.; Sprinzl, M.; Hilgenfeld, R. *Nature* **1993**, *365*, 126-132.
5. Kjeldgaard, M.; Nissen, P.; Thirup, S.; Nyborg, J. *Structure* **1993**, *1*, 35-50.
6. Polekhina, G.; Thirup, S.; Kjeldgaard, M.; Nissen, P.; Lippmann, C.; Nyborg, J. *Structure* **1996**, *4*, 1141-1151.
7. Abel, K.; Yoder, M. D.; Hilgenfeld, R.; Jurnak, F. *Structure* **1996**, *4*, 1153-1159.
8. Chasteen, N. D. *Structure and Bonding (Berlin)* **1983**, *53*, 105-138.
9. Mustafi, D.; Telser, J.; Makinen, M.W. *J. Am. Chem. Soc.* **1992**, *114*, 6219-6226.
10. Jiang, F. S.; Makinen, M. W. *Inorg. Chem.* **1995**, *34*, 1736-1744.
11. Makinen, M.W. and Mustafi, D. In *Metal Ions in Biological Systems;* Sigel, H., Ed.; Vol. 31, Marcel Dekker: New York, 1995, pp. 89-127.
12. Banerjee, A.; Chen, S.; Jiang, F. S.; Ruetthard, H.; Makinen, M. W., manuscript in preparation.
13. Ahmadian, M. R.; Kreutzer, R.; Sprinzl, M. *Biochimie* **1991**, *73*, 1037-1043.
14. Blank, J.; Grillenbeck, N. W.; Kreutzer, R.; Sprinzl, M. *Prot. Exp. Purif.* **1995**, *6*, 637-645.
15. Limmer, S.; Reiser, C. O. A.; Schirmer, N. K.; Grillenbeck, N. W.; Sprinzl, M. *Biochemistry* **1992**, *31*, 2970-2977.
16. Smith, P. K.; Krohn, R. I.; Hermansen, G. I.; Mallia, A. K.; Gartner, F. H.; Provezano, M. D.; Fujitomo, E. K.; Goeke, N. H.; Olsen, B. J.; Klenck, D. C. *Anal. Biochem.* **1955**, *150*, 76-85.
17. Arai, K. I.; Kawakita, M.; Kaziro, Y.; *J. Biol. Chem.* **1972**, *247*, 7029-7037.
18. Peter, M. E.; Schirmer, N. K.; Reiser, C. O. A.; Sprinzl, M. *Biochemistry* **1990**, *29*, 2876-2884.
19. Scatchard, G. *Ann. N.Y. Acad. Sci.* **1949**, *51*, 660-672.
20. Crechet, J. B.; Parmeggiani, A. *Eur. J. Biochem.* **1986**, *161*, 647-653.
21. Antonsson, B.; Kalbitzer, H. R.; Wittinghofer, A. *Hoppe-Seyler's Z. Physiol. Chem.* **1981**, *362*, 735-743.
22. Knudsen, C. R.; Kjaersgard. I.V.; Wiborg, O.; Clark, B. F. *Eur. J. Biochem.* **1995**, *228*, 176-183.
23. Kalbitzer, H. R.; Leberman, R.; Wittinghofer, A. *FEBS Letters* **1985**, *180*, 40-42.
24. Mustafi, D.; Makinen, M.W. *Inorg. Chem.* **1988**, *27*, 3360-3368.
25. Mustafi, D.; Nakagawa, Y. *Proc. Natl. Acad. Sci. U.S.A.* **1994**, *91*, 11323-11327.
26. Eccleston, J.F.; Molloy, D.P.; Hinds, M.G.; King, R.W., Feeney, J. *Eur. J. Biochem.* **1993**, *218*, 1041-1047.

Downloaded by YORK UNIV on October 31, 2012 | http://pubs.acs.org
Publication Date: December 10, 1998 | doi: 10.1021/bk-1998-0711.ch007

Downloaded by MONASH UNIV on October 31, 2012 | http://pubs.acs.org
Publication Date: December 10, 1998 | doi: 10.1021/bk-1998-0711.ch008

Chapter 8

Composition and Structure of Vanadium(V) Peroxo Complexes

P. Schwendt and M. Sivák

Department of Inorganic Chemistry, Faculty of Natural Sciences, Comenius University, SK 842 15 Bratislava, Slovakia

All of more than sixty known crystal structures of vanadium(V) peroxo complexes can be classified into several types closely related to peroxovanadate species formed under various conditions in aqueous solutions. The six- seven dichotomy of the coordination number for vanadium in these complexes is discussed and new data on structure of dinuclear vanadium peroxo complexes with chiral α-hydroxycarboxy-lato heteroligands are presented.

Our contribution is an overview of vanadium(V) peroxo complexes discussing mainly their composition and structure. Why do we consider the summarization of these data to be useful?

1. The found insulin mimetic properties and discovery of vanadium haloperoxidases have considerably increased the interest in these complexes(*1*).
2. The recent review by Butler et al (*2*) was focused mainly on the reactivity. Moreover, since this review has been published in 1994, the number of solved crystal structures of vanadium peroxo complexes was doubled.
3. Some unreproducible and unreliable data have been published on these compounds even in prestigious journals; the duty of careful literature search was often ignored.

For clarity, we shall distinquish, when needed, between the peroxovanadium species which are formed by dissolution of vanadates in a diluted H_2O_2 solution at various pH values and containing only oxo, peroxo, hydroxo and aqua ligands, and heteroligand complexes (the term introduced by Djordjevic(*3*)) in which other ligands (heteroligands) are also bound to vanadium .

In Vanadium Compounds; Tracey, A., et al.;
ACS Symposium Series; American Chemical Society: Washington, DC, 1998.

Downloaded by MONASH UNIV on October 31, 2012 | http://pubs.acs.org
Publication Date: December 10, 1998 | doi: 10.1021/bk-1998-0711.ch008

Diluted hydrogen peroxide solutions of vanadates.

The composition of peroxovanadium species in aqueous solution depends mainly on:

a) H_2O_2 / V ratio in solution
b) pH
c) vanadium concentration
d) ionic strength
e) temperature

Except of the number of coordinated water molecules, which still remains a matter of discussion, it is generally accepted that the principal mononuclear species and their protonation products are: tetraperoxovanadate $[V(O_2)_4]^{3-}$, triperoxovanadates $[VO(O_2)_3]^{3-}$ and $[V(OH)(O_2)_3]^{2-}$, diperoxovanadates $[VO(O_2)_2(OH)_2]^{3-}$(or $[VO_2(O_2)_2]^{3-}$), $[VO(O_2)_2(OH)]^{2-}$, $[VO(O_2)_2(H_2O)]^{-}$ and $[HVO(O_2)_2(H_2O)]$ (with unknown site of protonation), and monoperoxovanadium species $[VO(O_2)(OH)_3(H_2O)_u]^{2-}$ (or$[VO_2(O_2)(OH)(H_2O)_v]^{2-}$) , $[VO(O_2)(OH)_2(H_2O)_x]^{-}$, $[VO(O_2)(OH)(H_2O)_y]$ and $[VO(O_2)\,(H_2O)_z]^{+}$ (*4, 5, 6, 7*).

The condensation of different mononuclear complex ions results in formation of various dinuclear species. The most probable reactions are:

$2\,[VO(O_2)_2(OH)]^{2-} \rightleftharpoons [V_2O_3(O_2)_4]^{4-} + H_2O$ (1)

$[VO(O_2)_2(OH)]^{2-} + [VO(O_2)_2(H_2O)]^{-} \rightleftharpoons [V_2O_2(OH)(O_2)_4]^{3-} + H_2O$ (2)

$2\,[VO(O_2)_2(H_2O)]^{-} \rightleftharpoons [V_2O_2\,(O_2)_4(H_2O)]^{2-} + H_2O$ (3)

$[VO(O_2)(\,H_2O)_z]^{+} + [VO(O_2)_2(H_2O)]^{-} \rightleftharpoons [V_2O_2\,(O_2)_3(H_2O)_z] + H_2O$ (4)

$2\,[VO(O_2)(\,H_2O)_z]^{+} \rightleftharpoons [V_2O_2\,(O_2)_2(H_2O)_{2z-1}]^{2+} + H_2O$ (5)

The formation constans have been determined for the majority of species formed (*2, 4, 8*).

Solid peroxovanadates.

The best example for many inconsistent data concerning the composition of peroxovanadates is the variety of potassium peroxovanadates described in the literature: $K_3[V(O_2)_4]$, K_3VO_6 . 2.5 H_2O, $K_4V_2O_{12}$. 4 H_2O, $K_6H_2V_2O_{16}$. H_2O, $K_4V_2O_{11}$, $K_3HV_2O_{11}$, $K_2H_2V_2O_{11}$, KH_2VO_6 . H_2O, KVO_4, KVO_5 . $0.5H_2O$, $K_2H_2V_2O_{10}$. $0.5H_2O$, KVO_5 . H_2O_2 . nH_2O and others. We consider only the following peroxovanadates to be the products of crystallization from solutions of vanadate in diluted hydrogen peroxide:

a) Blue tetraperoxovanadates $M_3[V(O_2)_4]$. aq which can be obtained from alcaline solutions with large excess of H_2O_2.

b) $(N(CH_3)_4)_2\,[V(O_2)_3OH]$ (with a short structure announcement but no synthesis description in ref.*11*)

c) Three types of dinuclear diperoxo complexes formed by crystallization from solutions with lower H_2O_2 / V ratios: $M_4^{I}[V_2O_3(O_2)_4]$. aq, $M_3^{I}[V_2O_2(OH)(O_2)_4]$. aq and $M_2^{I}[V_2O_2(O_2)_4(H_2O)]$. aq.

In spite of the fact that solid mononuclear monoperoxo- or diperoxovanadates have not been reliably characterized, and they presumably do not exist, the studies devoted to such „unprobable" compouds repeatedly occur up to date (e.g. *9,10*).

A detailed knowledge on the characteristics (IR, X-ray) of solid peroxovanadates is required if we are attempting to synthesize heteroligand complexes, since the peroxovanadates often form admixtures in the product expected. The ignorance of this requirement has led to serious mistakes.

Solid heteroligand vanadium(V) peroxo complexes.

All heteroligand complexes can be derived from the peroxovanadate species found to be present in solution by formal substitution of H_2O or OH groups by one or more heteroligands. The following types of heteroligand complexes can thus be expected:

1. $[VO(O_2)L_n]$ (n = 3,4)
2. $[VO(O_2)_2L_m]$ (m = 1,2)
3. $[V(O_2)_3L]$
4. $[V_2O_2(O_2)_2L_r]$ (r = 4,5; bridging and/or non-bridging L)
5. $[V_2O_2(O_2)_3L_p]$ (p = 3,4; non-bridging, eventually bridging and non-bridging L)
6. $[V_2O_2(O_2)_4L]$ (non-bridging or bridging L)

where L stands for a monodentate ligand. Two L can be substituted by a bidentate ligand, three L by a tridentate or combination of a mono- and bidentate ligands and so on. With the exception of the type 3, in which a capped trigonal prismatic geometry can be expected, all other heteroligand complexes have a pentagonal pyramidal or pentagonal bipyramidal structure. For dinuclear complexes, various bridge configurations are possible; the configurations found so far are presented in Table I. The bridging bonds are usually complemented by weaker interactions of the A-F types. The review of structurally characterized vanadium(V) peroxo complexes is presented in Table II.

There is no trinuclear structure known for vanadium(V) peroxo complexes. The tetranuclear anion in $K_7[V_4O_4(O_2)_8(PO_4)]$. $9H_2O$ (*27*) is built up from two dinuclear $V_2O_2(O_2)_4$ units connected by PO_4 group. The polymeric structure of the $[VO(O_2)ida^-]_n$ ion in $NH_4[VO(O_2)ida^-]$ (*28*) and eventually that of the $[VO(O_2)_2F^-]_n$ ion in $NH_4[VO(O_2)_2F^-]$ (weak interaction O=V········O=V) (*2*) are formed due to special interactions in the solid state. The discussions about the coordination number of vanadium in monoperoxo and diperoxo complexes are focused mainly on the pentagonal pyramidal - pentagonal bipyramidal dichotomy. The $V\text{-}L_{ax}$ bond *trans* to the V=O bond is due to the structural *trans* effect always relatively long (d $(V\text{-}L_{ax})$ = 2.1-2.6 A or more). For a geometry corresponding to $d(V\text{-}L_{ax})$ ~2.5 A, the term pseudopentagonal bipyramidal was suggested (*29*). Some correlations between the stretching mode absorptions and structure of vanadium(V) diperoxo complexes have been found (*26, 30*). Especially, there is a correlation between the position of the characteristic Raman band corresponding to the $V\text{-}O_{peroxo}$ stretching and the $V\text{-}L_{ax}$ bond length. For $d(V\text{-}L_{ax}) > 2.6$ A no effect of the distance on the characteristic band position was observed. With aim to simplify the problem , in structures with $d(V\text{-}L_{ax})$ values smaller than approx. 2.6 A, we propose for vanadium to consider the coordination number seven, while for larger values, the pentagonal pyramidal arrangement. This classification is arbitrary, of course. Nevertheless, there are structures in which any L_{ax} cannot be found at distances considerably exceeding 3 A. In this case a pentagonal pyramidal structure is beyond doubt.

The number of structures with different coordination number of vanadium are

Downloaded by MONASH UNIV on October 31, 2012 | http://pubs.acs.org
Publication Date: December 10, 1998 | doi: 10.1021/bk-1998-0711.ch008

Downloaded by MONASH UNIV on October 31, 2012 | http://pubs.acs.org
Publication Date: December 10, 1998 | doi: 10.1021/bk-1998-0711.ch008

Table I. Bridge configurations found in dinuclear vanadium(V) peroxo complexes.

Type	*Structure*	*Type of bridging*
A	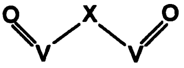	μ-X[a]
B	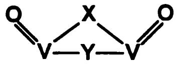	μ-X, μ-Y, nonplanar bridge
C	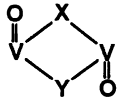	μ-X, μ-Y, planar bridge
D	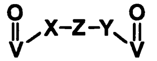	μ-X-Y-Z
E	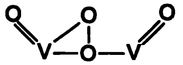	μ-η^1:η^2 O_2
F	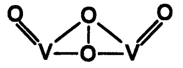	μ-η^2:η^2 O_2

[a] X and Y are donor and Z are other atoms of ligand.

Table II. Structurally characterized vanadium(V) peroxo complexes (including peroxovanadates).

Mononuclear	*CN*	*Ligand(s)*	*Ref.*[a]	*Mononuclear*	*CN*	*Ligands*	*Ref.*
$[VO(O_2)L_n]$	6	glygly[b]	12	$[VO(O_2)_2L_m]$	6	NH_3	2
n = 3,4	7	2 C_2O_4 (2)[c]	2	m = 1,2	6	F (2)	2
	7	dipic, H_2O	2		6-7	F	2
	7	pic, 2 H_2O	2		7	2 F	2
	7	bpy, 2 F	13		7	C_2O_4 (2)	2
	7	2 bpy	2		7	CO_3	2
	7	2 phen	2		7	bpy (2)	2
	7	pic, bpy	2		7	pic	2
	7	2 pic	14		7	picOH	2
	7	pic, phen	14		7	2,4 pdc	20

Downloaded by MONASH UNIV on October 31, 2012 | http://pubs.acs.org
Publication Date: December 10, 1998 | doi: 10.1021/bk-1998-0711.ch008

Table II. - continued

3-acetpic, 3-acetoxypicolinato; 5-nitrophen, 5-nitro-1,10-phenanthroline; dpot, 1,3-diamino-2-propanol-tetraacetato.

[c] In parenthesis is the number of structures with given ligand but different number of crystal water molecules or different cation.

[d] M. Sivák et al - to be published.

[e] P. Schwendt et al - to be published.

7	phen, 2 H_2O	14		7	3-acetpic	20
7	nta (4)	15		7	5-nitrophen	21
7	Hedta (2)	16		6	imidazol	22
7	ada	17	$[VO(O_2)_3L]$	7	OH	11
7	Hheida	18			F (?)	2
7	pan, py	2	$[V(O_2)_4]^{3-}$	8	-	23
7	ceida	[d]				
7	bpg	19				

Dinuclear	*Bridge*	*CN*	*Ligand(s)*	*Ref.*
$[V_2O_2(O_2)_2)\ L_r]$ r = 4, 5	C, -	7	citrato	2
r=4,5	C, -	7	malato	24
	B, A	7	L-tartrato, H_2O	[e]
	B, A	7	D-tartrato, H_2O	[e]
	C, -	6	glycolato	[e]
	C, -	6	DL-lactato	[e]
	C, -	6	DL-mandelato	[e]
	A, D	7	dpot	25
$[V_2O_2(O_2)_3L_p]$ p = 3, 4	A, F	7	3 F	2
$[V_2O_2(O_2)_4L]$	E, -	6	H_2O (3)	2
	A, E	6-7	O	2
	A, E	6-7	OH (2)	2
	D, E	7	PO_4	26

[a] When possible, we use from space reasons the review (*2*) as reference and apologize for it to the authors of original papers.

[b] Abbreviations: glygly, glycylglycinato; dipic, pyridine-2,6-dicarboxylato; pic, picolinato; bpy, 2,2'-bipyridine; phen, 1,10-phenanthroline; nta, nitrilotriacetato; edta, etylenediaminetetraacetato; ada, N-(carbamoylmethyl)iminodiacetato; heida, N-(2-hydroxyethyl)iminodiacetato; pan 1-(2-pyridylazo-)-2-naphtol; py, pyridine; ceida, N-(carbamoylethyl)iminodiacetato; bpg, N,N bis(2-pyridylmethyl)-glycine; picOH, 3-hydroxypyridine-2-carboxylato; 2,4 pdc, 2,4 pyridinedicarboxylato;

given in Table III, which is including also compounds with the same complex anion, but different cations or other components in a unit cell. As follows from this table, besides the common coordination number seven also the coordination number six is quite frequent.

Peroxo complexes of vanadium with chiral ligands.

In spite of generally widespread interest paid to the enantioselective reactions, except for several reactivity studies (*2*), it is surprisingly little known on chiral peroxovanadium complexes. Using stereoisomers of α- hydroxycarboxylic acids (tartaric, lactic, mandelic and others) as ligands we have prepared dinuclear complexes: $M_2[V_2O_2(O_2)_2L_2] . xH_2O$.

We have not determined the crystal structures of all three compounds with possible combinations of ligands (L-L; D-D and D-L) in a dinuclear anion. Nevertheless the differences in the X-ray powder diffraction patterns and vibrational spectra unequivocally indicate that we have succeded in their preparation. The following compounds have been isolated and characterized:

1. $K_2[V_2O_2(O_2)_2(D\text{-tart}H_2)_2 (H_2O)] . 5H_2O$, $K_2[V_2O_2(O_2)_2(L\text{-tart}H_2)_2 (H_2O)] . 5H_2O$, (both with crystal structure determined) and $K_2[V_2O_2(O_2)_2(D\text{-tart}H_2)(L\text{-tart}H_2)] . 6H_2O$ (tart = $C_4O_6H_2^{4-}$).
2. $(N(C_4H_9)_4)_2[V_2O_2(O_2)_2(D\text{-lact})(L\text{-lact})] . 2H_2O$ (crystal structure solved) and $(N(C_4H_9)_4)_2 [V_2O_2(O_2)_2(L\text{-lact})(L\text{-lact})] . 2H_2O$ (lact = $C_3O_3H_4^{2-}$).

In the dinuclear complexes with two bridging anions of the same stereoisomer, the configuration B (Table I) seems to be preferied. Two vanadium atoms, moreover bridged by one water molecule, are in these complexes seven- coordinated (Fig. 1). The L-D combination of heteroligands seems to enforce the C type of the bridge with pentagonal pyramidal surroundings of central atoms (Fig. 2). L-L (or D-D) and D-L complexes exhibit distinct ^{51}V NMR solution spectra. This fact indicates that their mutually different structures are maintained in solution. The seventh position in the coordination polyhedron around vanadium atom is in these complexes vacant or occupied by a weakly bonded ligand (H_2O). This fact, together with their solubilities which can be tuned by a cation, predestine these complexes as candidates for enantioselective oxygen transfer reactions in various media.

Acknowledgements:

Thanks are gratefully extended to the Ministry of Education of the Slovak Republic (Grant 1/2169/95) and Open Society Fund Slovakia for financial support.

Literature cited:

1. Vanadium and its role in life. Sigel, H.; Sigel, A., Eds., Metal ions in biological systems. Vol. 31. Marcel Dekker, New York, Basel, Hong Kong 1995.
2. Butler, A.; Clague, M. J.; Meister, G.E. , Chem. Rev. 1994, 94, 625-638.
3. Djordjevic, C., Chem. Brit. 1992, 554-557.
4. Harrison, A.T.; Howarth, O. W., J. Chem. Soc., Dalton Trans. 1985, 1173-1177.
5. Campbell, N. J.; Dengel, A. C.; Griffith, W. P., Polyhedron 1989, 11, 1379-1386.

Downloaded by MONASH UNIV on October 31, 2012 | http://pubs.acs.org
Publication Date: December 10, 1998 | doi: 10.1021/bk-1998-0711.ch008

Table III. Number of structures of vanadium(V) peroxo complexes classified according to coordination number.

Type	*Total*	*Coordination number*		
		6	*7*	*8*
Mononuclear				
Monoperoxo	22	1	21	-
Diperoxo	16	4	12	-
Triperoxo	2	-	2	-
Tetraperoxo	2	-	-	2
Dinuclear				
Monoperoxo	8	3	5	-
Diperoxo	7	3	4	-
Triperoxodivanadates	1	-	1	-
Tetranuclear				
Diperoxo	1	-	1	-
Polymeric				
Monoperoxo	1	-	1	-
Σ	60	11	47	2

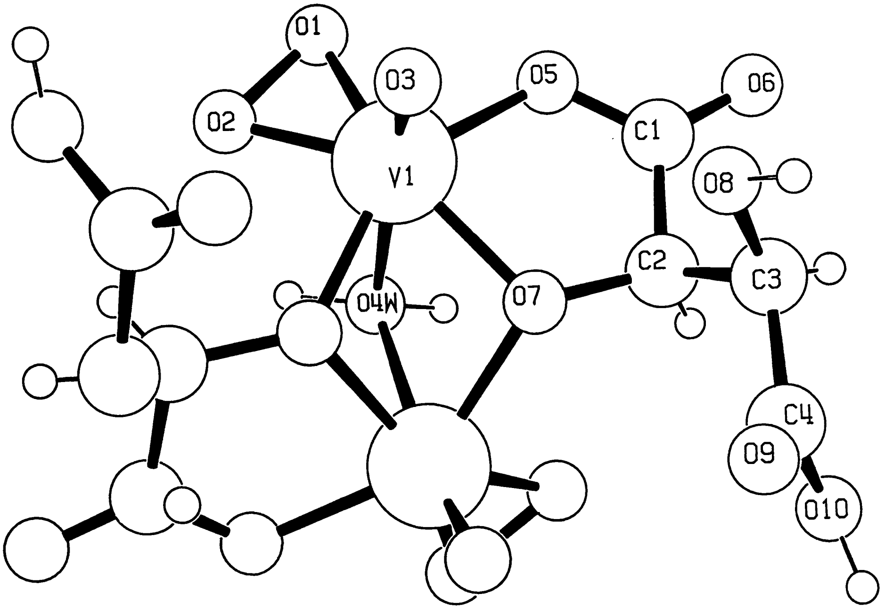

Figure1. Structure of $[V_2O_2(O_2)_2(L\text{-}tartH_2)_2(H_2O)]^{2-}$

Downloaded by MONASH UNIV on October 31, 2012 | http://pubs.acs.org
Publication Date: December 10, 1998 | doi: 10.1021/bk-1998-0711.ch008

Downloaded by MONASH UNIV on October 31, 2012 | http://pubs.acs.org
Publication Date: December 10, 1998 | doi: 10.1021/bk-1998-0711.ch008

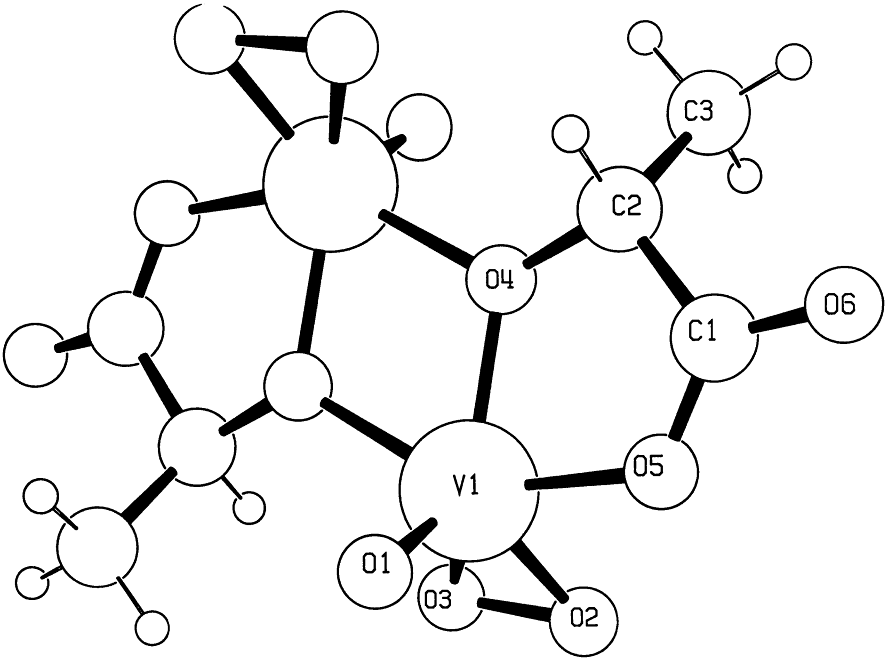

Figure2. Structure of $[V_2O_2(O_2)_2(\text{L-lact})(\text{D-lact})]^{2-}$

6. Jaswal, J. S.; Tracey, A. C., Inorg. Chem. 1991, 30, 3718-3722.

7. Conte, V.; Di Furia, F.; Moro, S., J. Mol. Catal. A 1997, 139-149.

8. Clague, M. J.; Butler, A., J. Am. Chem. Soc. 1995, 117, 3475-3484.

9. Kwong, D. W. J.; Chan, O. Y.;Wong, R. N. S.; Musser, M. S.; Vaca L.; Chan, S. I., Inorg. Chem. 1997, 36, 1276-1277.

10. Rao, V. S. A.; Islam, N. S.; Ramasarma, T., Arch. Biochem. Biophys. 1997, 342, 289-297.

11. Drew, R. E.; Einstein, F. W. B.; Field, J. S.; Begin, D., Acta Crystallogr. 1975, A 31, 135.

12. Einstein, F. W. B.; Batchelor, R. J.; Angus-Dunne, S. J.; Tracey, A. S., Inorg. Chem. 1996, 35, 1680-1684.

13. Sergienko, V.S.; Borzunov, V. K.; Porai-Koshits, M.A., Dokl. Akad. Nauk SSSR 1983, 301, 1141-1144.

14. Sergienko, V.S.; Porai-Koshits, M.A.; Borzunov, V. K.; Ilyukhin, A. B., Koord. Khim. 1993, 19, 767-781.

15. Lapshin, A. E.; Smolin, J. Y.; Shepelev, Y. F.; Sivák, M.; Gyepesová, D., Acta Crystallogr. 1993, C 49, 867-870.

16. Schwendt, P.; Sivák, M.; Lapshin, A. E.; Smolin, J. Y.; Shepelev, Y. F.; Gyepesová, D., Transition Met. Chem. 1994, 19, 34-36.

17. Sivák, M.; Tyršelová, J.; Pavelčík, F.; Marek, J., Polyhedron 1996, 15, 1057-1062.

18. Colpas, G. J.; Hamstra, B. J.; Kampf, J. W.; Pecoraro, V. L., J. Am. Chem. Soc. 1994, 116, 3627-3628.

19. Colpas, G. J.; Hamstra, B. J.; Kampf, J. W.; Pecoraro, V. L., J. Am. Chem. Soc. 1996, 118, 3469-3478.

20. Shaver, A.; Hall, D. A.; Ng, J. B.; Lebnis, A. M.; Hynes, R. C.; Posner, B. I., Inorg. Chim. Acta 1995, 229, 253-.

21. Shaver, A.; Ng ,J. B.; Hynes, R. C.; Posner, B. I., Acta Crystallogr. 1994, C 50, 1044-.

22. Crans, D. C.; Keramidas, A. D.; Hoover-Litty, H.; Anderson, O. P.; Miler, M. M.; Lemoine, L. M.; Pleasic-Williams, S.; Vandenberg, M.; Rossomando, A. J.; Sweet, L. J., J. Am. Chem. Soc. 1997, 119, 5447-5448.

23. Won, T. J.; Barnes, Ch. L.; Schlemper, E. O.; Thompson, R. C., Inorg. Chem. 1995, 34, 4499-.

24. Djordjevic, C.; Lee-Rensloo, M.; Sinn, E., Inorg. Chim. Acta 1995, 233, 97-.

25. Kanamori, K.; Nishida, K.; Toda, A.; Okamoto, K., Abstracts, 31st ICCC, Vancouver, Canada 1996, p.32.

26. Schwendt, P.; Tyršelová, J.; Pavelčík, F., Inorg. Chem. 1995, 34, 1964-1966.

27. Schwendt, P.; Oravcová, A.; Tyršelová, J.; Pavelčík, F.; Marek, J., Polyhedron 1996, 15, 4507-4511,

28. Djordjevic, C.; Craig, S. A.; Sinn, E., Inorg. Chem. 1985, 24, 1281-1283.

29. Campbell, N. J.; Flanagan, J.; Griffith, W. P.; Skapski, A. C., Transition Met. Chem. 1985, 10, 353-.

30. Schwendt, P.;Volka, K.; Suchánek, M., Spectrochim. Acta 1988, 44A, 839-844.

Downloaded by MONASH UNIV on October 31, 2012 | http://pubs.acs.org
Publication Date: December 10, 1998 | doi: 10.1021/bk-1998-0711.ch008

Chapter 9

Bis-Peroxo-Oxovanadium(V) Complexes of Histidine-Containing Peptides as Models for Vanadium Halo-Peroxidases

J. A. Guevara-García[1], N. Barba-Behrens[2], R. Contreras[3], and G. Mendoza-Díaz[4]

[1]Centro de Química-Instituto de Ciencias, Benemérita Universidad Autónoma de Puebla, P.O. Box 1613, Puebla 72000, México
[2]División de Estudios de Posgrado-Facultad de Química, Universidad Nacional Autónoma de México, Ciudad Universitaria, México, D.F. 04510, México
[3]Departamento de Química, Centro de Investigación y Estudios Avanzados del Instituto Politécnico Nacional, P. O. Box 14-740, México, D.F. 07000, México
[4]Facultad de Química, Universidad de Guanajuato, Guanajuato 36050, México

Downloaded by YORK UNIV on October 31, 2012 | http://pubs.acs.org
Publication Date: December 10, 1998 | doi: 10.1021/bk-1998-0711.ch009

Reaction products of V_2O_5/H_2O_2 with histidine-containing-peptides and NH_4OH with formula $NH_4[VO(O_2)_2(P)]$ [where P= gly-L-his (**1**), gly-gly-L-his (**2**) and gly-L-his (**3**)] are isolated and characterized by IR, ^1H, solution ^{13}C and ^{51}V and solid ^{13}C NMR. Solution ^1H and ^{13}C NMR spectra for **2** and **3** show three sets of signals for each peptide product, which agree with the ^{51}V NMR features; an HETCOR experiment enable to propose that compounds **1-3** correspond to the peptide complexes coordinated through the imidazole. Solid ^{13}C NMR spectra is consistent with solution ^{13}C NMR. These complexes may be models for the enzyme vanadium chloroperoxidase, since the vanadium-histidine bond is the only anchor of the prostetic group.

The structural and catalytic role of histidine in the active center of a number of enzymes is well known *(1-3),* as for vanadium haloperoxidases (VHPO) this role has just began to be disclosed *(4,5)*. The first vanadium haloperoxidase isolated was the vanadium bromoperoxidase (VBrPO) *(6)*. EXAFS studies showed that at least one histidine was in the coordination sphere of vanadium(V) *(7)*, while EPR studies suggested that an imidazolic proton from histidine was involved *(8)*. The X-ray structure of the azide complex of the enzyme vanadium chloroperoxidase (VClPO) *(9)* showed that the vanadium(V) ion was coordinated by an axial nitrogen from a histidine with a second histidine hydrogen-bonded to the azide. The position of these histidine residues resembles those found for the proximal and distal histidine residues in hemoperoxidases and catalases. It has been suggested that the proximal histidine regulates the redox chemistry of the metal ion while the distal one plays a role in the acid-base catalysis of the substrate *(2,3)*.

Systems involving peroxo and bis-peroxo vanadates with small peptides in aqueous solution have been extensively studied by ^{51}V NMR *(10-13)*. The formation constants determined for various vanadium/ligand pairs indicate the possibility to obtain stable complexes. The crystal structure for the complex $(NEt_4)[VO(O_2)(glygly)]$ *(14)* and for the compound $[VO(ONH_2)_2(glygly)]$ *(15)*, reported by Tracey *et al*, confirmed this prediction. A bidentade coordination mode is shown for the glycylglycine in the last complex, with the terminal amine bonded to the vanadium ion in the same plane as the two hydroxylamine ligands and the oxygen

In Vanadium Compounds; Tracey, A., et al.;
ACS Symposium Series; American Chemical Society: Washington, DC, 1998.

atom of the amide group coordinated in the apical position. This coordination mode is also observed for other bis-peroxovanadate complexes *(16,17)* with ligands such as oxalic acid *(18,19)*, picolinate*(20)* and phenantroline *(21)* (Figure 1). Polydentade histidine-containing peptides could be better ligands than histidine itself, due to the chelate effect and to the growth of the aminoacids chain which may enhance the stability of the complex through the increase of the hydrogen bonding network.

Herein we report a study of the reaction of three peptides gly-L-his (**1**), gly-gly-L-his (**2**), gly-L-his-gly (**3**), with V_2O_5, H_2O_2 and ammonia in aqueous solution and the spectroscopic characterization of the products by IR, UV, VIS, ^1H, ^{13}C and ^{51}V solution NMR and ^{13}C solid NMR.

Experimental Section

Materials. Absolute EtOH was purchased from J. T. Baker Co. V_2O_5, H_2O_2 (30%) and NH_4VO_3 from Merck Chemical Co.; $VOCl_3$ from Strem Chemical Co.; gly-L-his from Fluka Chemical Co.; gly-gly-L-his and gly-L-his-gly ICN Chemical Co. Water was destilled and deionized.

Physical Measurements. UV-VIS and diffuse reflectance spectra were recorded with a Cary 5E UV-Vis-near infrared spectrophotometer in the range 250-2500 nm. IR spectra were recorded on a Nicolet FT-IR 740 spectrophotometer using nujol mulls in the range 4000-400 cm^{-1} and polyethylene pellets in the range 700-70 cm^{-1}. Elemental analyses for C, H, and N were performed in a Fisons Eager 200. Vanadium analyses by plasma atomic absorption were performed at the Universidad Autónoma de Hidalgo. Magnetic susceptibilities of powder samples were measured at rt with a Johnson Matthey Gouy balance using the Evan's method for solid samples. Conductivity measurements were done in aqueous solution in an Orion 140 conductivity cell.

NMR Studies. Solid CP/MAS ^{13}C NMR spectra were recorded at 75.429 MHz, in a 300 MHz Varian Unity Plus spectrometer using total suppression of lateral bands at *ca.* 3300 spin speed. The following parameters were used: contact times, 1.5 ms; acquisition time, 0.07 s; spectral width, 30030 Hz; number of transients, 512-700; and pulse delay, 4 s. Solution ^{51}V NMR spectra were recorded in the same equipment at 78.850 MHz, chemical shifts were referenced to $VOCl_3$ by using the following parameters: acquisition time, 0.2 s; spectral width, 10^5 Hz; and number of transients, 64-300. The samples were dissolved in a mixture 50/50 of H_2O and D_2O. Solution ^1H and ^{13}C were recorded at rt with a Jeol GSX-300 MHz in D_2O and in DMSO-d_6 using TMS as reference.

Synthesis. The peroxo compounds **1-3** were obtained using the following procedure. The corresponding peptide (2 mmol) was dissolved in H_2O_2 30% (8 ml), V_2O_5 (1 mmol) was added in solid to this solution under constant stirring. After V_2O_5 was dissolved, aqueous ammonia was dropped into the solution up to pH 6. The reaction mixture was stirred until the bubbling stopped. Addition of cold ethanol to the reaction mixture produced a yellow precipitate, the suspension was kept in refrigeration overnight. The suspension was decanted and the solid resuspended with a cold acetone/ethanol mixture (3/1 v/v) and kept in refrigeration, this operation was repeated until the overnatant liquid was clear and colorless. The suspension was decanted and the precipitate dried in a vacuum. The compounds were stable under N_2. Anal. Cald. for **1** $[VO(O_2)_2(\text{gly-L-his})]\cdot 3\frac{1}{2}H_2O$: C, 24.65, H 4.55, N 14.37, V 12.86. Found: C 23.90; H 4.30; N 14.51; V 13.08. Anal. Cald. for **2** $[VO(O_2)_2(\text{glygly-L-his})]\cdot 3H_2O$: C 24.44, H 4.79, N 15.84, V 10.79. Found: C 24.61; H 4.62, N 15.61, V 10.35. Anal.

Downloaded by YORK UNIV on October 31, 2012 | http://pubs.acs.org
Publication Date: December 10, 1998 | doi: 10.1021/bk-1998-0711.ch009

Downloaded by YORK UNIV on October 31, 2012 | http://pubs.acs.org
Publication Date: December 10, 1998 | doi: 10.1021/bk-1998-0711.ch009

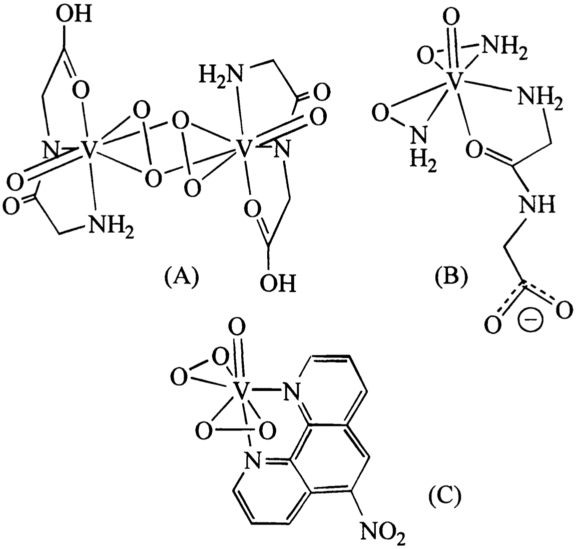

Figure 1. Examples of peroxo-vanadium compounds structures determined by X-ray single crystal studies: Associated pair of anions of $[VO(O_2)(gly\text{-}gly)]^-$ (adapted from ref. 14) (A); Molecular structure of $VO(NH_2O)_2(gly\text{-}gly)$ (adapted from ref. 15) (B); Molecular structure of $[VO(O_2)_2(5\text{-nitro-}1,10\text{-phen})]^-$ (adapted from ref. 21) (C).

Cald. for **3** $NH_4[VO(O_2)_2(gly\text{-}L\text{-}his\text{-}gly)]\cdot H_2O$, C 28.34, H 4.97, N 18.02, V 10.92. Found: C 28.39, H 4.89, N 17.98, V 11.24.

Results and Discussion

The ^{51}V NMR spectra of coordination compounds of imidazole or *N*-methylimidazole bis-peroxovanadate show a signal at -750 ppm attributed to the nitrogen coordination of the vanadium *(12)*. In the histidine coordination compounds two reports indicate that two signals (-750, -740 ppm) appeared for the reaction products. The first one could be attributed to the imidazole coordination whereas the other one could be due to a chelate with the imidazole and carbonyl groups *(12, 22)*. In other report it was established that the coordination with the CO_2^- group from gly-peptides gives a signal at *ca.* -710 ppm *(11)*.

The ^{51}V NMR spectra in D_2O for compound **1** (Table I) showed three signals (Figure 2), one at -752 ppm (90%) attributed to compound **1a**, another one at -742 ppm (10%) attributed to compound **1b** and a third one at -695 ppm corresponds to free bis-peroxovanadate *(10)*. In the ^{13}C NMR spectra only one set of signals was observed attributed to compound **1a**. This compound shows an strong effect on the chemical shift of the imidazole carbon atoms. In the ^{1}H NMR spectrum the signals of the imidazole became broad indicating also the interaction of this ring with the vanadium atom, (Figure 3). An HETCOR experiment was done to assign the resonances. For compounds **2**, the ^{51}V, NMR spectrum has three signals one at -754 assigned to **2a**, another at -737 for **2b** and a third one at -714 for **2c**. ^{13}C and ^{1}H NMR spectra (Table II) showed three sets of signals in the same ratio as for the ^{51}V spectrum. For compound **2a** the spectrum in D_2O solution shows that the coordination of the bis-peroxovanadate is through the imidazole nitrogen of the zwitterionic form of the peptide. For compounds **3**, the ^{51}V NMR spectrum showed the same resonances but in ^{13}C NMR a strong effect on the carbon atoms of the chain is detected, which could indicate that for this molecule an additional interaction through the carbonyl atoms is possible (Table III).

For compound **1a** it was possible to obtain the NMR ^{1}H and ^{13}C spectra in DMSO-d_6 which were compared with those obtained in D_2O solution and for the solid state. A completely different coordination behavior was detected from the spectra in DMSO-d_6 solution. The strong shift to higher frequencies of the signals of the carbon atoms of the aminoacid chain shows coordination of the carbonyl oxygen atoms to the vanadium. We were unable to obtain good NMR spectra in DMSO-d_6 for **2a** and **3a** because of the strong interaction of this solvent with the compounds.

In the ^{13}C solid state NMR spectrum of compound **1a** compared with that obtained in DMSO-d_6 could indicate an interaction through the imidazole ring and histidine carboxylate (Table I). The same effect was observed in the solid state NMR spectrum of **2a** (Table II), whereas comparison of the solid state NMR spectrum for **3a** and its NMR spectra in D_2O solution (Table III) indicates an additional interaction through the carbonyl groups.

The ^{13}C NMR signals for compounds **2b**-**3b** and compounds **2c**-**3c** indicate analogous coordination modes through imidazole.

IR and UV-Vis spectroscopic data for compounds **1** to **3** are displayed in Table IV. The IR spectra of the coordination compounds showed new bands at 950-970 cm^{-1} and 870 cm^{-1} due to $\nu(V{=}O)$ and $\nu(O\text{-}O)$ respectively, characteristic of peroxo-oxovanadium compounds *(23,24)*. Their reflectance spectra contain a band in the region 370-380 nm assigned to the charge transfer band $V(V) \leftarrow O(peroxo)$. In solution, this band is shifted to 330 nm *(25)*, additionally a ligand to metal charge transfer band assigned to $V(V) \leftarrow O(oxo)$ was observed at 210 nm.

Downloaded by YORK UNIV on October 31, 2012 | http://pubs.acs.org
Publication Date: December 10, 1998 | doi: 10.1021/bk-1998-0711.ch009

Downloaded by YORK UNIV on October 31, 2012 | http://pubs.acs.org
Publication Date: December 10, 1998 | doi: 10.1021/bk-1998-0711.ch009

Table I. ^{13}C, ^{1}H and ^{51}V NMR Chemical shifts for compounds 1

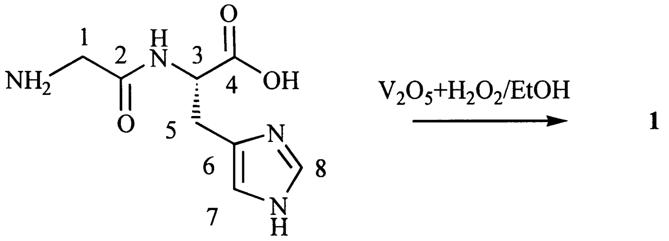

^{13}C	Solvent	C1	C2	C3	C4	C5	C6	C7	C8
gly-L-his	D_2O	35.8	161.9	49.6	171.5	22.5	124.8	112.1	128.7
1a	D_2O	35.8	161.8	49.9	172.2	22.8	123.8	120.3	132.4
gly-L-his	DMSO-d_6	40[a]	165.8	52.5	172.2	28.6	132.4	116.9	134.5
1a	DMSO-d_6	46.7	177.4	56.0	179.8	27.9	129.8	117.2	133.2
(1)	Solid	41.6	167.3	54.8	177.0	28.1	128.8	117.8[b]	137.0

^{1}H		H1	H3	H5	H7	H8
gly-L-his	D_2O	3.63	4.33	2.94, 3.06	7.08	8.40
1a	D_2O	3.62	4.38	2.89, 3.11	7.06	8.00
gly-L-his	DMSO-d_6	3.58	4.50	2.89, 3.00	7.70	8.70
1a	DMSO-d_6	4.79	4.60	3.15, 3.47	7.37	8.68

^{51}V		**1a**	**1b**	$[VO(O_2)_2]^-$
	D_2O	-752 (90%)	-740 (10%)	-695

a- under the signal of DMSO-d_6; b- broad

Downloaded by YORK UNIV on October 31, 2012 | http://pubs.acs.org
Publication Date: December 10, 1998 | doi: 10.1021/bk-1998-0711.ch009

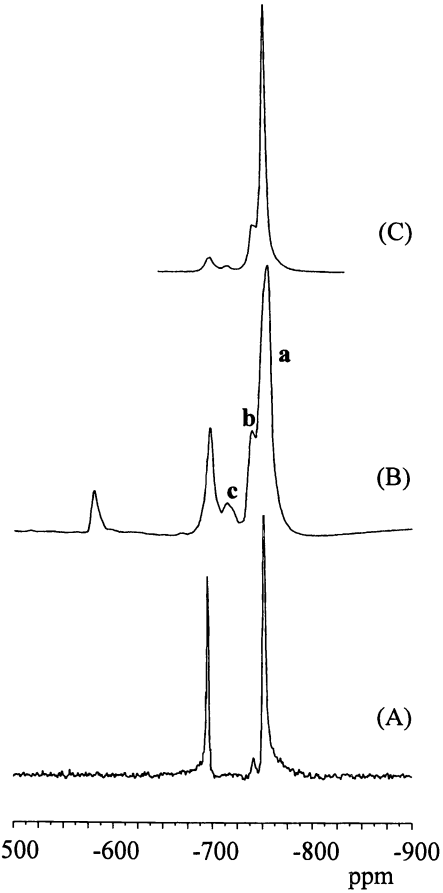

Figure 2. ^{51}V NMR spectra in D_2O of the complexes **1** to **3**, (A) to (C) respectively, showing the signals **a**, **b** and **c**.

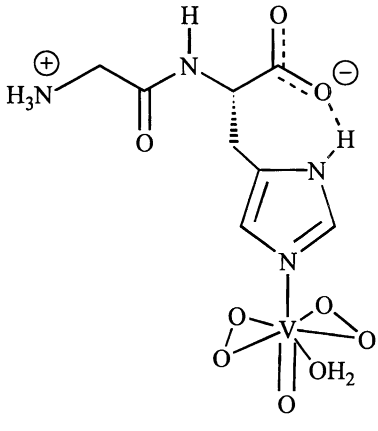

Figure 3. Proposed molecular structure for **1a**.

Downloaded by YORK UNIV on October 31, 2012 | http://pubs.acs.org
Publication Date: December 10, 1998 | doi: 10.1021/bk-1998-0711.ch009

Table II. ^{13}C, ^{1}H and ^{51}V NMR Chemical shifts for compounds 2

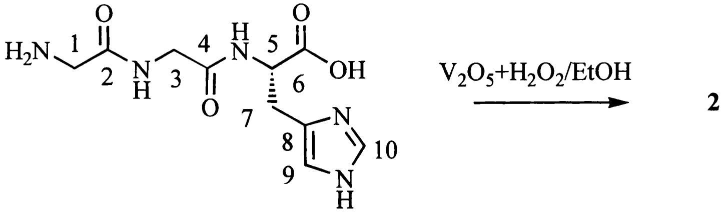

^{13}C	Solvent	C1	C2	C3	C4	C5	C6	C7	C8	C9	C10
glygly-L-his	D_2O	40.7	168.3	42.4	170.4	54.6	176.8	28.0	130.9	117.3	134.3
2a	D_2O	40.8	167.9	42.7	170.5	54.4	176.9	27.5	125.0	116.9	137.1
2b	D_2O	41.0	165.2	45.9	170.6	56.2	a	29.4	128.4	117.3	136.0
2c	D_2O	a	169.2	a	a	a	a	a	130.0	115.0	134.0
glygly-L-his	Solid	41.5	172.1	41.5	168.6	56.8	177.5	25.2	128.0	116.5	134.6
(2a)	Solid	42.6	170.0	42.6	170.0	56.1	177.4	27.7	128.7	120.0[b]	136.6

^{1}H	Solvent	H1	H3	H5	H7	H9	H10
glygly-L-his	D_2O	3.78	3.89	4.40	3.11, 2.97	7.03	8.13
2a	D_2O	3.77	3.86	4.41	3.02, 3.16	7.13	8.10
2b	D_2O	3.82	3.9	a	3.3, 3.4	7.86	8.42

^{51}V	D_2O	**2a**	**2b**	**2c**	$[VO(O_2)_2]^-$	
		-754 (71%)	-737 (24%)	-714 (5%)	-696	-580

a- not observed; b- broad

Downloaded by YORK UNIV on October 31, 2012 | http://pubs.acs.org
Publication Date: December 10, 1998 | doi: 10.1021/bk-1998-0711.ch009

Table III. ^{13}C, ^{1}H and ^{51}V NMR Chemical shifts for compounds 3

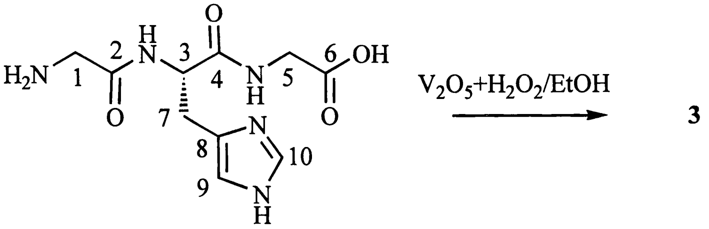

^{13}C	Solvent	C1	C2	C3	C4	C5	C6	C7	C8	C9	C10
gly-L-his-gly	D_2O	36.0	163.1	48.8	167.5	38.7	171.8	23.7	126.5	117.8	131.0
3a	D_2O	40.7	167.2	53.0	171.8	43.5	176.6	27.1	125.6	117.8	137.6
3b	D_2O	40.7	167.2	53.9	172.8	43.5	176.3	29.1	127.2	117.1	137.4
3c	D_2O	a	a	a	171.5	a	a	a	128.8	117.8	134.3
(3)	Solid	42.6	170.9	52.9	170.9	42.6	175.9	27.9	127.4	118.0^b	137.1

^{1}H		H1	H3	H5	H7	H9	H10
gly-L-his-gly	D_2O	3.59	4.53	3.60	2.91, 3.0	7.72	6.88
3a	D_2O	3.68	a	3.74	3.09, 3.2	7.18	8.09
3b	D_2O	a	a	a	3.36, a	7.14	7.87
3c	D_2O	a	a	a	a	a	8.33

^{51}V	D_2O	**3a**	**3b**	**3c**	$[VO(O_2)_2]^-$
		-748 (83%)	-738 (14%)	-713 (3%)	-696

a- not observed; b- broad

Table IV. Spectroscopic data for compounds 1-3

Compound	$\bar{\nu}_{max}$[a]/cm^{-1}		λ_{max}/nm	
	V=O	O-O	d.r.[b]	solution[c] ε/dm^3 mol^{-1}cm^{-1}
$\mathrm{NH_4[VO(O_2)_2(Gly\text{-}L\text{-}His)]\cdot 3\frac{1}{2}H_2O}$ (**1**)	970	870	371	213, 328(741)
$\mathrm{NH_4[VO(O_2)_2(GlyGly\text{-}L\text{-}His)]\cdot 3H_2O}$ (**2**)	968	872	372	205, 328(762)
$\mathrm{NH_4[VO(O_2)_2(Gly\text{-}L\text{-}His\text{-}Gly)]\cdot H_2O}$ (**3**)	972	872	380	208, 330(778)

[a] nujol mull; [b] diffuse reflectance; [c] destilled water

Conclusions

The three peptides behave in similar way with the peroxovanadate as was shown by NMR. All of them form three compounds with analogous structures in the same ratio. The most abundant compounds **a** correspond to the vanadium-imidazole coordination.

Bis-peroxovanadate form monomeric stable compounds with histidine-containing peptides, where bonding through the imidazolic nitrogen is the most important. In the D_2O solution the ligand **1** and **2** seem to form zwitterionic structures with a hydrogen bond between the imidazole and the histidine carboxylate which leaves only one nitrogen atom of the imidazole for coordination. In DMSO or in the solid state a chelate structure might be possible. Compound **3** do not have the histidine carboxylate available for coordination, therefore it is likely that an interaction of the vanadium centre with the aminoacid chain is occurring.

Acknowledgments

This work was supported by DGAPA grant IN222096.

Literature Cited

1. Mukai, M.; Nagano, S.; Tanaka, M.; Ishimori, K.; Morishima, I.; Ogura, T.; Watanabe, Y.; Kitagawa, T. *J. Am. Chem. Soc.* **1997**, *119*, 758.
2. Poulos, T. L. *J. Biol. Inorg. Chem.*, **1996**, *1*, 356
3. Goodin, D. B. *J. Biol. Inorg. Chem*, **1996**, *1*, 360.
4. Hemrika, W.; Renirie, R.; Dekker, H.L.; Barnett, P.; Wever, R. *Proc. Natl. Acad. Sci. USA*. **1997**, *94*, 2145.
5. Wever, R.; Krenn, B. E. in *Vanadium in Biological Systems*; Ed. Chasteen, N. D.; Kluwer Academic Publishers; Dordrecht, 1990; pp. 81-87.
6. Vilter, H. *Bot. Mar.* **1986**, *26*, 451.
7. Arber, J. M.; de Boer, E.; Garner, C. D.; Hasnain, S. S.; Wever, R. *Biochem.* **1989**, *28*, 7968.
8. de Boer, E.; Boon, K.; Wever, R. *Biochem.* **1988**, *27*, 1629.
9. Messerschmidt, A.; Wever, R. *Proc. Natl. Acad. Sci. USA.* **1996**, *93*, 392.
10. Jaswal, J. S.; Tracey, A. S. *Inorg. Chem.* **1991**, *30*, 3718
11. Tracey, A. S.; Jaswal, J. S. *J. Am. Chem. Soc.* **1992**, *114*, 3835
12. Tracey, A. S.; Jaswal, J. S. *Inorg. Chem.* **1993**, *32*, 4235
13. Jaswal, J. S.; Tracey, A. S. *J. Am. Chem. Soc.* **1993**, *115*, 5600
14. Einstein, F. W. B.; Batchelor, R. J.; Angus-Dunne, S. J.; Tracey, A. S. *Inorg. Chem.* **1996**, *35*, 1680.

Downloaded by YORK UNIV on October 31, 2012 | http://pubs.acs.org
Publication Date: December 10, 1998 | doi: 10.1021/bk-1998-0711.ch009

15. Paul, P.C.; Angus-Dunne, S.J.; Batchelor, R.J.; Einstein, F.W.B.; Tracey, A.S. *Can. J. Chem.* **1997**, *75*, 183.
16. Posner, B.I.; Faure, R.; Burgess, J.W.; Bevan, A.P.; Lachance, D.; Zhang-Sun, G; Fantus, I.G.; Ng, J.B.; Hall, D.A.; Shaver, A. *J. Biol. Chem.* **1994**, *269*, 4596.
17. Kwong, D.W.J.; Leung, W.N.; Xu, M.; Zhu, S.Q.; Cheng, C.H.K. *J. Inorg. Biochem.*, **1996**, *64*, 163.
18. Tracey, A.S.; Gresser, M.J.; Parkinson, K.M. *Inorg. Chem.* **1987**, *26*, 629.
19. Ehde, P.M.; Pettersson, L.; Glaser, J. *Acta Chem. Scand.* **1991**, *45*, 998.
20. Galeffi, B.; Tracey, A.S. *Inorg. Chem.* **1989**, *28*, 1726.
21. Shaver, A.; Ng, J.B.; Haynes, R.C.; Posner, B.I. *Acta Cryst. Sect. C.* **1994**, *C50*, 1044.
22. Mukherjee, J.; Ganguly, S.; Bhattacharjee, M. *Indian J. Chem.* **1996**, *35A*, 471.
23. Butler, A.; Walker, J. V. *Chem. Rev.* **1993**, *93*, 1937.
24. Nakamoto, K. *Infrared and Raman Spectra of Inorganic and Coordination Compounds*; 4th edition; John Wiley and Sons: New York, NY, 1986; pp 319.
25. Rehder, D.; Weidemann, C.; Duch, A.; Priebsch, W. *Inorg. Chem.* **1988**, *27*, 584.

Downloaded by YORK UNIV on October 31, 2012 | http://pubs.acs.org
Publication Date: December 10, 1998 | doi: 10.1021/bk-1998-0711.ch009

Downloaded by YORK UNIV on October 31, 2012 | http://pubs.acs.org
Publication Date: December 10, 1998 | doi: 10.1021/bk-1998-0711.ch010

Chapter 10

From the Speciation of Peroxovanadium Complexes in Aqueous Solution to the Chemistry of Haloperoxidases

V. Conte, F. Di Furia, and S. Moro

Centro di Studio sui Meccanismi delle Reazioni Organiche del CNR, Organic Chemistry Department, via Marzolo 1, I-35131 Padova, Italy

Mono- and diperoxo-vanadium complexes, $[VO(O_2)]^+$ or $[VO(O_2)_2]^-$, are formed in aqueous acid solutions, depending on pH and on the excess of H_2O_2. The anionic diperoxo species undergo protonation to form a neutral complex $[HVO(O_2)_2]$. ^{51}V-NMR data and *ab initio* calculations suggest a conceivable structure for such species. A two-phase system, ($H_2O/CHCl_3$ or CH_2Cl_2) where NH_4VO_3, KBr and H_2O_2 are dissolved in the aqueous phase and the organic substrate in the organic, is used to mimic the chemistry of bromoperoxidases enzymes. With selected alkenes, both dibromoderivatives and bromohydrins are formed. Such a products distribution could be ascribed to the formation of a hypobromite-like vanadium complex, which likely is the reactive species in the halofunctionalization of the organic substrate

The chemistry of peroxo complexes formed in aqueous-acid solutions by interaction of vanadates with hydrogen peroxide is receiving continuous attention as demonstrated by numerous studies with different techniques, including heteronuclear NMR*(1-3)* Raman spectroscopy*(4)* and *ab initio* calculations*(5, 6)* recently appeared in the literature. Despite all these studies, however, a fundamental aspect concerning the nature of the first coordination sphere of the peroxovanadium derivatives present in solution, is still uncertain.*(1-3)* In this short general outlook, which by no means intend to be exhaustive, some aspects of the chemistry and biochemistry of peroxovanadium species are presented. For a deeper insight in this field readers may refer to latest books.*(7, 8)*

Structural Studies

Recent ab initio calculations showed that the most likely structure of the oxo-monoperoxo vanadium cation contains three H_2O molecules bound to the metal*(6)*, in

In Vanadium Compounds; Tracey, A., et al.;
ACS Symposium Series; American Chemical Society: Washington, DC, 1998.

Downloaded by YORK UNIV on October 31, 2012 | http://pubs.acs.org
Publication Date: December 10, 1998 | doi: 10.1021/bk-1998-0711.ch010

a distorted octahedral arrangement. This is uneven with solid state structures which indicate a distorted pentagonal bipyramid as the preferred geometry, where, however, the seventh position is looser as compared with the sixth one.*(8, 9)* This last figure can be directly sorted by looking at the bond lengths. Further evidence on the differences between the sixth and the seventh coordination positions, in H_2O/CH_3OH solution, has been obtained with ^{51}V-NMR experiments.*(2)*

We have recently used ^{51}V-NMR spectroscopy to study equilibria involving the peroxospecies formed *in situ* by addition of hydrogen peroxide to NH_4VO_3, as a function of the vanadium-peroxide ratio and of the pH of the solution *(1, 10, 11)*. Our investigation, while confirming the overall picture established by previous studies *(3)* revealed some novel aspects *(1, 2, 10, 11)*. In particular we obtained evidence that, together with the cationic monoperoxospecies **1** and the anionic diperoxovanadium one, **2**, also the neutral diperoxovanadium complex **3** is formed *(11)* (see Scheme 1). **3** exists mainly in the pH region 1.5-3 in less than 5% amount of the total vanadium. Its pK_a value of 0.43 shows that it is a rather strong acid.*(11)*.

Scheme 1[a]

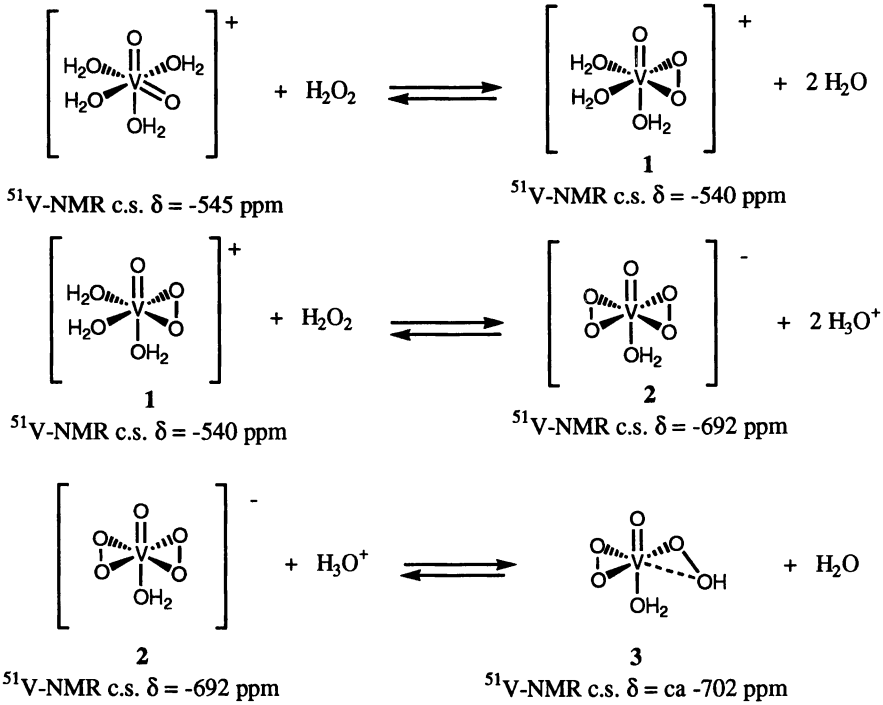
+ H_2O_2
+ $2 H_2O$
1
^{51}V-NMR c.s. δ = -545 ppm
^{51}V-NMR c.s. δ = -540 ppm
+ H_2O_2
+ $2 H_3O^+$
1
2
^{51}V-NMR c.s. δ = -540 ppm
^{51}V-NMR c.s. δ = -692 ppm
+ H_3O^+
+ H_2O
2
3
^{51}V-NMR c.s. δ = -692 ppm
^{51}V-NMR c.s. δ = ca -702 ppm

a. adapted from ref. 11

On the basis of B3LYP/LANL2DZ DFT calculations we have shown that protonation on the peroxo oxygen leads to a hydroperoxo-like structure (complex **3**) which is more stable (ca.1.41 kJ/mol) as compared with the species protonated on the terminal oxo group.*(11)*

Downloaded by YORK UNIV on October 31, 2012 | http://pubs.acs.org
Publication Date: December 10, 1998 | doi: 10.1021/bk-1998-0711.ch010

In a previous study *(1)* we have established a direct correlation between the shielding on the vanadium atom, as measured by its ^{51}V-NMR chemical shift, and the electron density on the metal, which holds for several peroxovanadium complexes *(1)*. This latter property is also related to the oxidizing power of the peroxocomplexes either when they act as electrophiles or as one-electron acceptors. Such relationships holds for structurally similar species in which no other effects than the electron donating ability of the ligands need to be considered *(1,11)*. By applying this line of reasoning to peroxospecies **1** (-540 ppm) and **2** (-692 ppm) the larger shielding effect observed for the latter is in agreement with its anionic nature. The chemical shift observed for **3** is, however, out of trend. In fact, its ^{51}V-NMR chemical shift value of -702 ppm would suggest that the shielding is larger for a neutral species such as **3** than for an anionic one such as **2**. This is taken as an evidence that **3** is structurally different from both **1** and **2** as confirmed by the *ab initio* calculation cited above. For comparison purposes Scheme 2 shows the calculated lengths of O-O bond in the peroxocomplexes discussed above and in H_2O_2.

Scheme 2

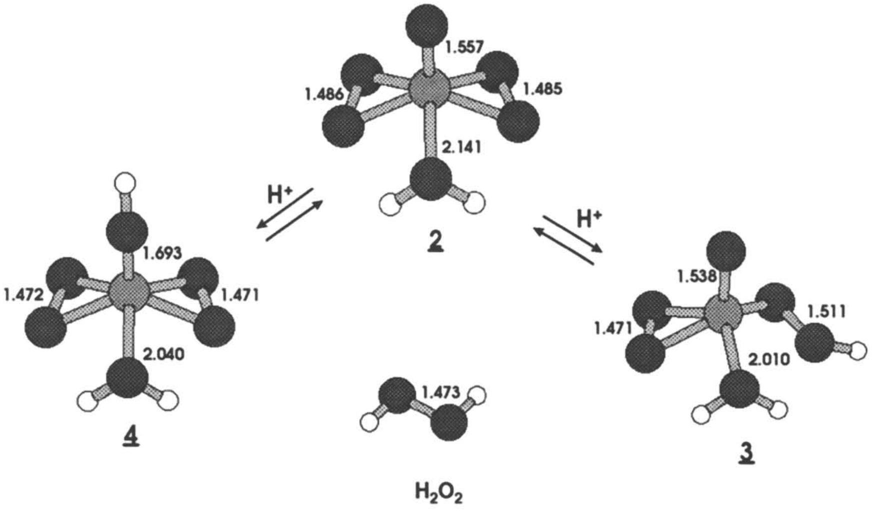

It should be noted that in the hydroperoxo-like structure, **3**, the O-O bond distance is larger than that of H_2O_2 which, on the other hand, is very similar to those found for the hydroxo diperoxo complex, **4**, and for the diperoxo anion, **2**. Differences on the oxidative behavior of **3** in processes involving the cleavage of the peroxidic bond are therefore expected. Reactivity data, recently obtained in our group, by using uracil as model substrate, see Table I, have indeed shown that the protonated diperoxo complex is a stronger oxidant than the diperoxo anionic counterpart **2**.*(11)*

Table I: Uracil (4 x10^{-2} molL^{-1}) oxidation with peroxo vanadium complexes (NH_4VO_3 2 x10^{-3} molL^{-1}, H_2O_2 4.6 x10^{-2} molL^{-1}) in aqueous acid solutions at 37°C.[a] (table adapted from ref. *11*)

Peroxo complex	pH	time (hr.)	Substrate conv.%[b]
1	~ 0[c]	14	> 98
2/3	0.8[d]	6	> 98
2	5.1	n.r.[e]	0

a Uracil cis-diol, uracil trans diol and N-formyl-5-hydroxy-hydantoin are formed, the relative yield have not been measured. b by TLC. c $HClO_4$ 1 molL^{-1}. d pH condition where concentration of [**2**] = [**3**]. e) no disappearance of uracil in several days.

In order to obtain direct experimental information on the structure in solution of the cationic mono-peroxovanadium species, we have also carried out an electrospray ionization mass spectrometry (ESI-MS)*(12,13)* analysis of water-methanol acid solutions of vanadates in the presence of hydrogen peroxide.*(14)* With this technique ionic species are gently transferred from the solution to the gas phase and can be directly observed. Data obtained in such a study showed that cationic complexes, $[(H_2O)_n(CH_3OH)_mVO(O_2)]^+$, containing up to three solvent molecules are the most abundant in solution. Evidence on the formation of tetra coordinated complexes is also obtained, even though their concentration appear to be quite low. A further meaningful outcome of such a study is the evidence that ionic species at higher mass-over-charge values upon isolation of the ion under analysis are detected. This is the case of ion $[VO(O_2)(OH)H]^+$, (m/z 117) which has been isolated within the ion trap analyzer in the presence of relatively small tickling voltages (10-15 mV), for times of about 0.1 msec. Under these conditions no fragmentation products are detected, nevertheless formation of ions at m/z 131, 135, 149, 153 is observed. *(14)* A likely explanation for such a result is the reaction of the selected ion $[VO(O_2)(OH)H]^+$ with neutral solvent molecules present in the ion trap, i.e. exchange between H_2O and CH_3OH, coordination of methanol or coordination of water *(2, 14)*. The plausibility of the exchange process between water and methanol has been supported by *ab initio* calculations*(14)* carried out on addition reactions to the "naked" ion $[VO(O_2)]^+$ of either water or methanol molecule. The data obtained indicate that the binding to the oxo-peroxo "naked" ion of a methanol molecule causes a higher stabilization (ΔE 99.6 kcal/mol for methanol addition against 86.4 kcal/mol for water addition with RHF/3-21G(*) method) as compared with the lowering of the energy obtained with the binding of a water molecule. Such an evidence, supported also by a good agreement of the results obtained with a different level of theory (DFT, B3LYP/LANL2DZ), substantiate the suggestion that exchange between water and methanol molecules in the coordination sphere of oxo-monoperoxo vanadium complexes is a likely process.

We believe that the data so far discussed clearly underline that a better knowledge of the structural details of peroxovanadium species in aqueous solution is of remarkable help in studying biochemical systems where peroxovanadium complexes are involved.

Vanadium Dependent Bromoperoxidases Mimicking Systems

Even though numerous halogenated compounds have been found in the marine environment, their biogenesis has been unknown for long time. Many of those

Downloaded by YORK UNIV on October 31, 2012 | http://pubs.acs.org
Publication Date: December 10, 1998 | doi: 10.1021/bk-1998-0711.ch010

Downloaded by YORK UNIV on October 31, 2012 | http://pubs.acs.org
Publication Date: December 10, 1998 | doi: 10.1021/bk-1998-0711.ch010

compounds display biological activity, which ranges from antibacterial to antiviral and antiinflammatory performance.*(7, 15)* Since the beginning of the century, the involvement of haloperoxidases enzymes in their biogenesysis has been suggested by numerous marine natural chemists.*(7, 15)* Whilst, the presence in the sea water of many transition ions, stimulated the search for metal based enzymes responsible of the halo-functionalization of organic compounds. Marine vanadium dependent haloperoxidases have at length been isolated, purified and in some instances, *i.e.* for a vanadium chloroperoxidase from *Curvularia inaequalis (16)*, their solid state structure has been solved, therefore the mechanism of action of such enzymes is a hot topic of research both from biological and chemical points of view.

Haloperoxidases enzymes catalyze the oxidation of halides by hydrogen peroxide. The presence of vanadium in the oxidation state 5+ in vanadium-dependent bromoperoxidases (V-BrPO) has been firmly established by using a variety of techniques.*(7, 15)* The oxidation state of the metal does not change during the bromination reaction, and the binding of hydrogen peroxide to the metal, to yield a peroxo species as active intermediate, has been proved. Evidence is offered in literature on the formation of HOBr upon oxidation of bromide by peroxovanadium intermediate. The bromination of organic substrates with V-BrPO can be summarized as in Equation 1:

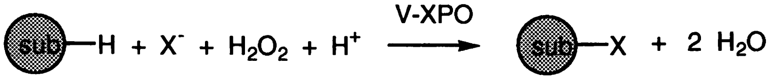

(1)

The stoichiometry corresponds to the oxidation of one equivalent of bromide ion with one equivalent of hydrogen peroxide yielding one equivalent of brominated organic substrate.*(7, 15)* In the absence of an organic halogen acceptor, the oxidized bromine intermediate reacts with a second equivalent of hydrogen peroxide thus producing bromide, water and dioxygen. This latter process formally corresponds to the disproportionation of hydrogen peroxide to dioxygen and water, catalyzed by halides. The dioxygen produced in the bromide-assisted disproportionation of hydrogen peroxide is in the singlet state.*(7, 15)*

The problems experienced in using conventional spectroscopic techniques in the analysis of the active center of V-BrPO enzymes stimulated, *inter alia*, the search for simple systems able to mimic the activity of such enzymes. Indeed, many models have been recently proposed *(7, 15, 17)* based on several metal-catalyzed (mainly vanadium and molybdenum*(18)*) oxidation of bromide by hydrogen peroxide.

In our group some mechanistic information on the chemistry of the peroxospecies involved in the active site of V-BrPO have been obtained by analyzing the chemistry of a set of simple peroxo vanadium complexes whose structure is reported below:

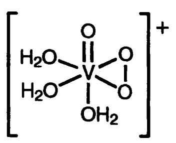

$[VO(O_2)(H_2O)_3]^+$

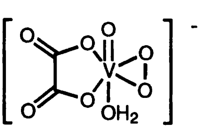

$[VO(O_2)(ox)]^-$

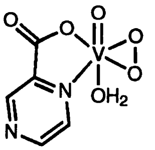

$[VO(O_2)(pyraz)]$

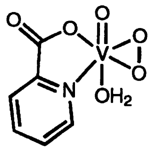

$[VO(O_2)(pic)]$

They are all known to undergo, in acid water, a slow self-decomposition which proceeds through a radical chain mechanism producing dioxygen and V(V) derivatives.*(5, 19)* When bromide ion is added, in otherwise similar experimental conditions, only complex $[VO(O_2)(H_2O)_3]^+$ produces bromine. Such a complex is known to be a better one-electron acceptor as compared with the other monoperoxo derivative.*(1)*

In the reaction of $[VO(O_2)(H_2O)_3]^+$ with bromide, Br_3^- is readily formed at the beginning of the process and then its concentration reaches a constant value (ca. 20% of the initial peroxo complex).*(5)* The lack of Br_3^- formation with $[VO(O_2)(ox)]^-$, $[VO(O_2)(pyraz)]$ and $[VO(O_2)(pic)]$ can be ascribed to a reaction between the bromine radical and the peroxo species. Similar reactions have been already reported with chlorine *(20)* and iodine.*(21)* In agreement with this reactivity, only $[VO(O_2)(H_2O)_3]^+$ mediate the bromination of uracil; the yield of the reaction, however, never exceeded 20% of the initial peroxide employed.*(1)*

On the basis of this evidence and taking also into consideration the involvement of bromine in the decomposition of peroxocomplexes, we suggested that a two-phase system (H_2O/CH_2Cl_2 or $CHCl_3$) could be a better model for V-BrPO activity.*(5, 22, 23)*. In this procedure, Scheme 3, the formation of the monoperoxovanadium complex, out of a V(V) salt and hydrogen peroxide occurs in water, where the oxidation of the Br^- to produce a "bromine equivalent" intermediate also takes place. Such a species is then transferred into the organic phase where the bromination of the substrate occurs.

Scheme 3

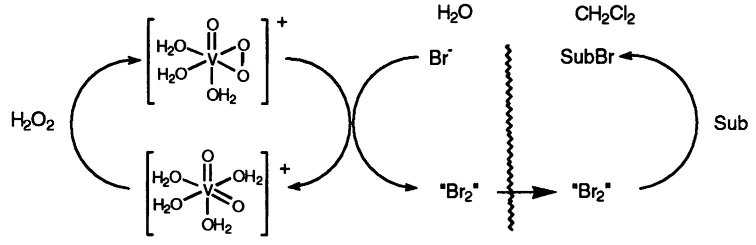

"Br_2" = bromine equivalent intermediate"

The proposal of a two-phase system as model for the V-BrPO activity is based on the assumption that the proteic backbone of the enzyme has two different regions characterized by a largely different lipophilic character.

Bromination of alkenes and aromatic substrates has been carried out and some relevant results are reported in Table II. These experiments show that the bromination reaction in the two-phase system mimics the V-BrPO enzyme activity more effectively as compared with the homogenous counterpart.

The results reported below show that in many instances bromohydrin is the major product. Thus, in order to achieve a better understanding of such a behavior the reactivity of styrene towards other metal-free brominating reagents (*e.g.* $BrO_3^-/Br^-/H^+$; HOBr; Br_2; *N*-Br-succinimide) has been checked and in all cases dibromostyrene is the major product.*(5, 22, 23)*

Further investigations carried out on the two-phase-system showed that the stirring rate (a low stirring rate produces a high yield of dibromoderivative) or the relative volume of the phases (an increase of the volume of the organic phase increases

Downloaded by YORK UNIV on October 31, 2012 | http://pubs.acs.org
Publication Date: December 10, 1998 | doi: 10.1021/bk-1998-0711.ch010

the yield of bromohydrin without affecting the total yield of products) affects the selectivity.*(5, 22, 23)* A mechanistic proposal which accounts for the such experimental results has been already suggested in previous publications *(5, 22, 23)*, where the involvement of different intermediates is invoked in order to explain the formation of the two products.

Table II: Alkenes Bromination with H_2O_2 and KBr, catalyzed by NH_4VO_3 (0.2 mmol) in a two-phase-system (20 mL H_2O/20 mL $CHCl_3$) at 25°C, 1000 rpm.

Substrate	mmol	KBr mmol	H_2O_2 mmol	time hr.	conv.sub. %	bromohydrin / dibromide
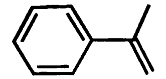	0.2	1.0	0.2	48	79	90:10 plus 8% other products
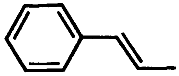	0.2	1.0	0.2	48	76	61:39
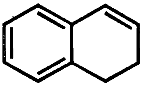	0.2	1.0	0.2	48	78	55.45
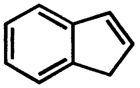	0.2	1.0	0.2	48	71	84:16
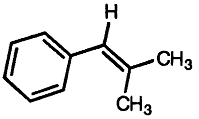	0.2	1.0	0.2	72	72	0:100
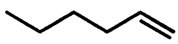	0.4	0.5	0.4	120	61	57:43
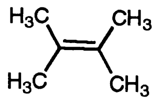	0.4	0.5	0.4	4 72	55 60	75: 25 0 :100*

* bromohydrin is consumed to form *tert*-butyl methyl ketone

Very interesting data were recently obtained with cinnamyl alcohol. With this substrate, see Scheme 4, a total yield of 83% and a 92% bromohydrin selectivity was found. This result has to be compared with the reaction of cinnamyl alcohol with chloroperoxidase from *Caldariomyces fumago* where the almost exclusive formation of the corresponding bromohydrin was observed.*(24)* Hence, it appears that our synthetic model succeeds in mimicking the activity of the natural enzyme.

Scheme 4

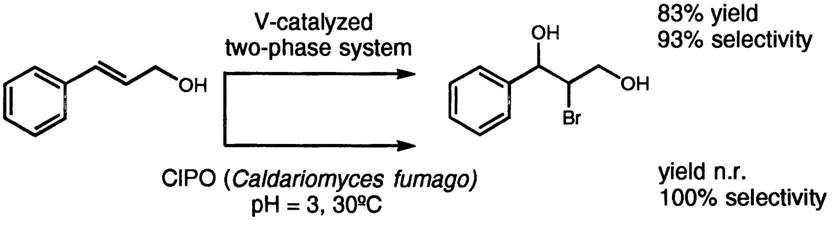

Downloaded by YORK UNIV on October 31, 2012 | http://pubs.acs.org
Publication Date: December 10, 1998 | doi: 10.1021/bk-1998-0711.ch010

All the results collected in our studies have been used in order to offer the mechanistic hypothesis shown in the following Scheme 5.*(5, 23, 24)*

Scheme 5

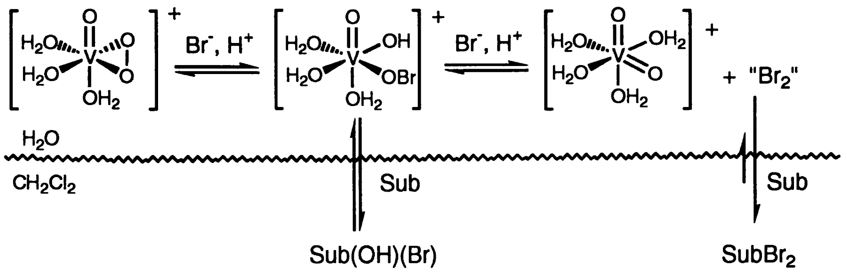

"Br_2" = bromine equivalent intermediate"

Ab initio calculation have been carried out in order to establish the plausibility of the hypobromite-like intermediate, involved in the proposed mechanism. The computation has been performed by optimizing all geometries with no geometry constraints by using RHF/3-21G(*)47 basis set. The suggested hypobromite-like intermediate lies in a hole of potential energy with respect to the reagents, $[VO(O_2)(H_2O)_3]^+$/HBr and $[VO_2(H_2O)]^+$/HOBr.*(5)* Even if this is a very simple approach, it does not disagree with our hypothesis, and it supports, though in an indirect way, the presence of, at least, an intermediate according to our suggestion.

Two-phase Bromination of Adamantylideneadamantane

Adamantylideneadamantane (ADA) has been widely used in the mechanistic study of bromination reaction.*(25, 26)* A peculiar performance of this molecule is that, independently from the brominating reagent used, the reaction stops at bromiranium ion stage. This behavior can be used in order to collect direct evidence on the formation of a bromiranium ion also in the vanadium catalyzed two-phase system.
It is known that when bromine reacts with ADA a yellow precipitate is formed whose empirical formula and properties are consistent with bromiranium-tribromide molecule, shown in Equation 2:*(25-27)*

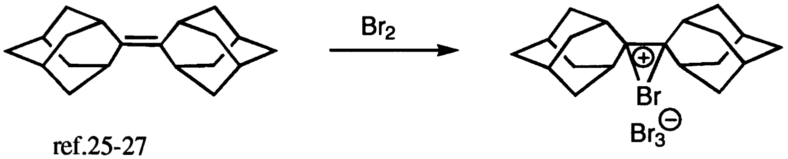

ref.25-27

(2)

We have accomplished different bromination reactions with ADA. First of all, in order to observe the formation of the bromiranium-tribromide ion in a two-phase reaction, ADA (20 mM) was allowed to react in H_2O (2 mL pH ca.1) / $CHCl_3$ (2 mL) mixture with KBr/$KBrO_3$ (40 mM / 8 mM), at 25°C, 1000 rpm. As expected, after the formation of bromine, indicated by the development of the typical yellowish color, the building up of a precipitate in the organic phase was observed. Such a precipitate was

Downloaded by YORK UNIV on October 31, 2012 | http://pubs.acs.org
Publication Date: December 10, 1998 | doi: 10.1021/bk-1998-0711.ch010

separated from the chlorinated solution and its ^{1}H-NMR spectrum was recorded. The spectroscopic data collected were in good agreement with those pertinent to the tribromide salt.*(25-27)* It is, however, necessary to point out that if the NMR sample, in deuterated DCE as solvent, is not kept in the dark at low temperature, a rapid evolution of bromine, indicated by the fading of the yellowish color, is observed. Moreover, we have observed that the NMR spectra of the tribromide salt, recorded at room temperature, show an equilibrium between the substrate and the product, as already reported by Bellucci and coll.*(25)*

When ADA bromination was carried out in the vanadium catalyzed two-phase system (NH_4VO_3 20 mM, H_2O_2 20 mM and KBr 25 mM, H_2O 5 mL, pH ca. 1 / 5 mL $CHCl_3$ containing 20 mM ADA, at 25°C, 1000 rpm.), formation of a yellow precipitate is also observed. At variance with the behavior reported above, however, this latter product dissolved in deuterated DCE appears to be fairly stable and decomposes in several days. Its ^{1}H-NMR spectra (at 200 MHz) is close, yet not completely competent, to that of the classical bromiranium ions. The molecular weight, determined by GC/MS, corresponds to the molecular weight of ADA plus Br, therefore it might be suggested that the stability of this salt can be due to the presence of a different counter-ion X^-, likely derived from the metal catalyst. On the other hand, the occurrence of exchange processes and the complexity of the ^{1}H-NMR spectra requires that low temperature and stronger fields instruments are used in order to obtain clear-cut data on the nature of the isolated intermediate and therefore further support to our mechanistic proposal.

Conclusions

To conclude this short account, concerning some aspects of the chemistry of peroxovanadium derivatives, we would like to emphasize that the knowledge of the real structure in solution of peroxovanadium species, together with the comprehension of the mechanisms of biological relevant oxidations, where peroxovanadium complexes are involved, are necessary prerequisite for a further understanding of the function of vanadium in living organisms.

Acknowledgments. Financial support from Italian National Research Council, CNR and from Italian ministry of the University and Scientific Research is acknowledged. We thanks Dr. C. Chiappe, Universe of Pisa Italy, for a generous gift of adamantylideneadamantane and Prof. O. Bortolini, University of Ferrara, Italy, and Dr. M. Bonchio this CNR center for helpful discussions and suggestions.

References

1. Conte, V.; Di Furia, F.; Moro, S. *J. Mol. Catal.* **1995**, *104*, 159.
2. Conte, V.; Di Furia, F.; Moro, S. *Inorg. Chim. Acta* , **1998**, *00*, 000.
3. a) Howarth, O.W.; Hunt, J.R. *J. Chem. Soc. Dalton Trans.* **1979**, 1388; b) Howarth, O.W.; Harrison, A.T. *J. Chem. Soc. Dalton Trans.* **1985**, 1173; c) Jaswal, J.S.; Tracey, A.S. *Inorg. Chem.* **1991**, *30*, 3718.
4. Campbell, N.S.; Dengel, A.C.; Griffith, W.P. *Polyhedron* **1989**, *8*, 1379.
5. Conte, V.; Di Furia, F.; Moro, S.; Rabbolini, S. *J. Mol. Catal.* **1996**, *113*, 175.

Downloaded by YORK UNIV on October 31, 2012 | http://pubs.acs.org
Publication Date: December 10, 1998 | doi: 10.1021/bk-1998-0711.ch010

6. Bagno, A.; Conte, V.; Di Furia, F.; Moro, S. *J. Phys. Chem. A* **1997**, *101*, 4637.
7. a) N.D. Chasteen, *Vanadium in Biological Systems*; Kluwer Academic Publishers; Dordrecht, 1990. b) *Metal Ions in Biological Systems. Vol. 3. Vanadium and its Role in Life* Sigel, H. Ed.; Marcel Dekker inc. New York NY, 1995.
8. Mimoun, H. *The Chemistry of Peroxides,* Patai, S. Ed.; Wiley: Chichester, U.K., 1983; Ch. 15.
9. Conte, V.; Di Furia, F.; Modena, G. In *Organic Peroxides*; Ando, W., Ed.; Wiley, Chichester, U.K., 1992; Ch. 11.2.
10. Conte, V.; Di Furia, F.; Moro, S. *J. Mol. Catal.* **1994**, *94*, 323.
11. Conte, V.; Di Furia, F.; Moro, S. *J. Mol. Catal.* **1997**, *120*, 93.
12. Whitehouse, C.M.; Dreyer, R.N.; Yamashita, M.; Fenn, J.B. *Anal. Chem.* **1985**, *57*, 675.
13. Fenn, J.B.; Mann, M.; Meng, C.K.; Wong, S.F.; Whitehouse, C.M. *Mass Spectrom. Rev.* **1990**, *10*, 37.
14. Bortolini, O.; Conte, V.; Di Furia, F.; Moro, S. submitted.
15. Butler, A.; Walker, J.V. *Chem. Rev.* **1993**, *93*, 1937.
16. Messerchmidt, A.; Wever, R. *Proc. Natl. Acad. Sc. USA* **1996**, *93*, 392.
17. See as examples a) Meister , G.E.; Butler, A. *Inorg. Chem.* **1994**, *33*, 3269; b) Espenson, J.H.; Pestovsky, O.; Huston, P.; Staudt, S. *J. Am. Chem. Soc.* **1994**, *116*, 2869; c) Colpas, G.J.; Hamstra, B.J.; Kampf, J.W.; Pecoraro, V.L. *J. Am. Chem. Soc.* **1996**, *118*, 3469.

18 See as an example Bhattercharjee, M.; Mukherjee *J. Chem. Res. (S)* **1995**, 238.

19. Conte, V.; Di Furia, F.; Moro, S. *J. Mol. Catal.* **1997**, *117*, 139.
20. Thompson, R.C. *Inorg. Chem.* **1983**, *22*, 584.
21. Secco, F. *Inorg. Chem.* **1980**, *19*, 2722.
22. Conte, V.; Di Furia, F.; Moro, S. *Tetrahedron Lett.* **1994**, *35*, 7429.
23. Andersson, M.; Conte, V.; Di Furia, F.; Moro, S. *Tetrahedron Lett.* **1995**, *36*, 2675.
24. Coughlin, P.; Roberts, S.; Rush, C.; Willetts, A. *Biotech. Lett.* **1993**, *15*, 907.
25. Bellucci, G.; Bianchini, R.; Chiappe, C.; Ambrosetti, R.; Catalano, D.; Bennet. A.J.; Slebocka-Tilk, H.; Aarts, G.H.M.; and Brown, R.S. *J. Org. Chem.* **1993**, *58*, 3401.
26. Slebocka-Tilk, H.; Ball, R.G.; and Brown, R.S. *J. Am. Chem. Soc.* **1985**, *107*, 4504.
27. Strating, J.; Wieringa, J.H.; Wynberg, H. *J. Chem. Soc., Chem. Commun.* **1969**, 907.

Downloaded by YORK UNIV on October 31, 2012 | http://pubs.acs.org
Publication Date: December 10, 1998 | doi: 10.1021/bk-1998-0711.ch010

Chapter 11

Catalytic Oxidations with Biomimetic Vanadium Systems

I. W. C. E. Arends, M. Vos, and R. A. Sheldon

Laboratory for Organic Chemistry and Catalysis, Delft University of Technology, Julianalaan 136, 2628 BL Delft, The Netherlands

Downloaded by YORK UNIV on October 31, 2012 | http://pubs.acs.org
Publication Date: December 10, 1998 | doi: 10.1021/bk-1998-0711.ch011

The active site of vanadium-haloperoxidases was mimicked through incorporation of Schiff's base complexes of vanadium in the supercages of faujasite zeolites with different hydrophilicities. The catalytic activities of these materials were tested in the epoxidation of allylic alcohols with *tert*-butyl hydroperoxide and in the sulfoxidation of thioanisole in a biphasic system with 30% H_2O_2. Bromination reactions, such as the bromination of 1,3,5-trimethoxybenzene in a dichloromethane/water system, were also catalyzed by these materials. It was shown that in pure organic solvents at elevated temperatures, vanadium was released from the lattice with *tert*-butyl hydroperoxide as the oxidant. In the biphasic system with hydrogen peroxide, however, the vanadium zeolites were stable during the course of the reaction.

The widespread occurrence of vanadium-containing enzymes, such as vanadium-chloroperoxidase (V-CPO) from the fungus *Curvularia inaequalis* [*1*] and bromoperoxidase from seaweeds *Ascophyllum nodosum* [*2*], has only in the last decade been fully established [*3*]. The active site of these enzymes contains a vanadate VO_3^- group, which can be exchanged for e.g. phosphate. The X-ray structure for the vanadium-chloroperoxidase has recently been elucidated [*4*]. It was shown that only one histidine is involved in the direct coordination sphere of the vanadium, whereas the negative charge of the vanadate group is compensated by hydrogen bonds to several positively charged protein chains. Vanadium-haloperoxidases are involved in the biogenesis of halogenated marine natural products and e.g. V-CPO has been suggested to be involved in the defense mechanism of fungi, through the production of HOCl [*4*]. Br- or Cl- ions are oxidized in-situ by H_2O_2 to give the halogenating species HOX (or derivatives thereof, depending on the pH) and vanadium remains in the pentavalent state throughout the reaction

In Vanadium Compounds; Tracey, A., et al.;
ACS Symposium Series; American Chemical Society: Washington, DC, 1998.

$$X^- + H_2O_2 + RH + H^+ \xrightarrow{"V"} RX + 2\,H_2O \qquad (1)$$

It is known, that Mo, W, Ti, and V readily form peroxometal species with hydroperoxides, RO_2H (R = H, alkyl), which are very selective oxygen transfer species, e.g. they are able to convert olefins into the corresponding epoxides [*5*]. The mechanism of epoxidation is shown in Figure 1. It involves direct nucleophilic attack of the olefin on the electrophilic oxygen of the alkylperoxometal species. As epoxidation of unfunctionalized alkenes catalyzed by vanadium is rather slow compared to e.g. molybdenum, the ligand environment is critical in allowing the above described heterolytic mechanism to be dominant [*6*]. Epoxidation of allylic alcohols by peroxometal complexes of vanadium is, however, much faster and selective due to the coordination of the allylic alcohol through its alcohol group [*7*].

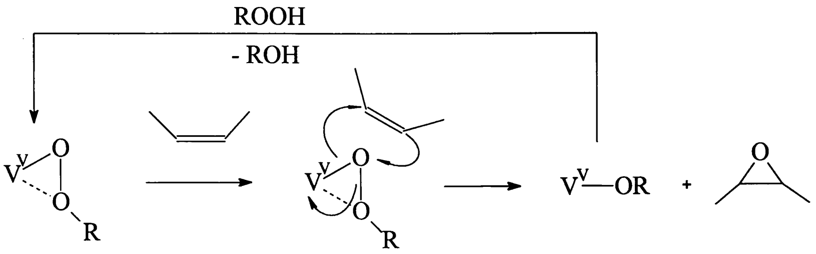

Figure 1. Peroxometal mechanism for vanadium catalyzed epoxidation

In the peroxometal mechanism, vanadium remains in its pentavalent state throughout just as in the vanadium-haloperoxidases, which leads to the obvious conclusion that analogous peroxo species are also involved in the enzymatic process [*8*]. Activation of Cl^- or Br^- in vanadium-haloperoxides is therefore likely to occur via a similar mechanism to that depicted in Figure 1. In the catalytic reaction, the thusly formed RO-vanadyl species must be reactivated and react again with the oxidant to form a new peroxo species. In vitro, it is known that with vanadium this reactivation step is strongly inhibited by the presence of water or alcohols [*9*]. Recently, it was shown that the action of vanadium could be mimicked in the oxidative halogenation of organic substrates with hydrogen peroxide in a biphasic system, under stoichiometric conditions [*10*].

Our goal now is to mimic the optimum activity of the enzyme, through incorporation of a vanadium complex in a zeolite framework and to apply this material in catalytic oxidations. In this way, the zeolite backbone surrounds the vanadium, just as the protein protects the active vanadium site. Recent examples of these so called "zeozymes'[*11*] comprise the encapsulation of iron-phthalocyanines [*12*] and manganese-bipyridines [*13*]. The underlying principle is that owing to space restrictions the complex stays in the zeolite and cannot diffuse out, provided that it is stable. This is essentially different from isomorphously substituted vanadium molecular sieves, such as vanadium-silicalites and V-APOs [*14-15*].

Downloaded by YORK UNIV on October 31, 2012 | http://pubs.acs.org
Publication Date: December 10, 1998 | doi: 10.1021/bk-1998-0711.ch011

Especially, the latter ones have demonstrated problems in leaching. The faujasite zeolite has channels of around 7.3 Å which lead to supercages of 13 Å in diameter.

We reasoned that the stability of the vanadium catalyst could be increased by encapsulation and that aqueous conditions could possibly be applied in vanadium catalyzed (ep)oxidations. Catalytic asymmetric synthesis in intrazeolite space has, in principle, several advantages compared to homogeneous counterparts. Steric constraints, on the one hand, prohibit ligand dissociation and, on the other hand, they limit the number of (bulky) ligands that can coordinate to the metal center, thus leaving vacant coordination sites. For this purpose, trans-(R,R)-1,2-bis(salicylideneamino)-cyclohexane, and a tripodal ligand obtained from *tert*-leucinol and 6-*tert*-butyl-4-methyl-salicylaldehyde were synthesized - in-situ- in the cages of faujasite large pore zeolites, after which vanadium was added to form the corresponding vanadyl-complexes (compounds I and II).

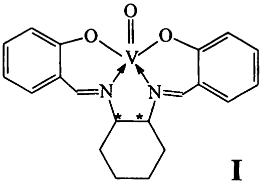

I

VO(sal-R,R-chxn)

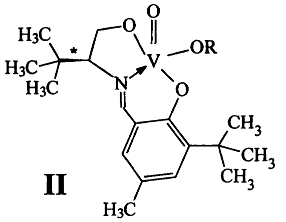

II

VO(sal-aa)

In this way, Wessalith, a low aluminum variant of zeolite Y (Si/Al = 32), with low ion-exchange capability, could be applied as a host for the complex to be studied. This is important, because a hydrophobic framework, is probably necessary, to be able to use aqueous hydrogen peroxide as the oxidant. Complexes of the type II, were shown to catalyze asymmetric oxidation of sulfide with hydrogen peroxide in 85% e.e. [*16*].

Recently we published examples of VO(HPS) (vanadyl-N-(2-hydroxyphenyl)salicylideneimine) and VO(salen) (vanadyl-N,N'(bis)salicylidene-imine) complexes in zeolite Y, which were shown to be active in the epoxidation of cyclohexene, cyclooctene and (-)-carveol at 70°C using *tert*-butylhydroperoxide as the oxidant [*17*]. Selectivities for epoxide formation were similar to those obtained with the analogous homogeneous complexes in solution. And it was shown, through leaching experiments, that the zeolites were not stable and vanadium was released into the solution. Therefore, in this article, special attention will be focused on the stability of vanadium-encapsulated catalysts.

Experimental

Materials. NaY was acquired from AKZO, with a Si/Al ration of 2.44, washed with aq. NaOAc and water, and calcined before use. Wessalith (HY) was obtained from Degussa, with a Si/Al ratio of 32, and washed with water and calcined before use. For material (A), hereafter denoted as VO(sal-RR-chxn)-Y, zeolite Y was exchanged

Downloaded by YORK UNIV on October 31, 2012 | http://pubs.acs.org
Publication Date: December 10, 1998 | doi: 10.1021/bk-1998-0711.ch011

with $(VO)^{2+}$ in 2 mM $VOSO_4$ solution under nitrogen to result in a 0.63 wt% V, zeolite Y. This was dried under nitrogen at 200°C and subsequently mixed under dry conditions in dichloromethane, with the precursors for the ligand, in a stoichiometric ratio with vanadium present, salicylaldehyde, and R,R-diaminocyclohexane resp, and refluxed. This material was extensively soxhletted with DCM, to remove any extraframework complex or residual ligand precursors. Furthermore the material was exchanged with NaAc, to remove the protons formed during complexation.

For materials (B) and (C), Wessalith was mixed in dry THF under nitrogen using Schlenck glassware, with the ligand precursors (1 eq. per unit cell) for compounds I and II according to the method of Ogunwumi and Bein [*18*]. For compound I, salicylaldehyde and (1R,2R)-(-)-1,2-diaminocyclohexane (2:1) and for compound II, 6-*tert*-butyl-4-methyl-salicyladehyde and (S)-*tert*-leucinol (1:1) were added after each other; 1 mmol of ligand precursors / g zeolite was used. Then 1 eq. of $VO(i\text{-}OPr)_3$ was added to the slurry. After removal of the solvent the material was extensively soxhletted with DCM, and dried in vacuo at 80°C before use.

Materials: anhydrous TBHP was applied as a 5 M solution in chlorobenzene. 6-*tert*-butyl-4-methyl-salicylaldehyde was synthesized through formylation of 2-*tert*-butyl-4-methyl-phenol [*19*]. The ligands **sal-R,R-chxn** and **sal-aa** were synthesized through condensation of the precursors in refluxing ethanol (in the presence of $NaSO_4$), followed by recrystallization. The complexes VO(sal-R,R-chxn) (**I**) and VO(sal-aa) (**II**) were prepared through complexation in ethanol of $VO(i\text{-}OPr)_3$ or $VOSO_4$ and the ligand. Other materials were purchased as reagent grade and used as received.

Catalyst characterization. AAS and ICP-OES measurements were carried out with Perkin/Elmer instruments type 1100, 5000 Z and plasma-40. UV/VIS measurements were carried out on a Varian Cary spectrometer. Diffuse reflectance spectra were recorded again a barium-sulphate reference on the Varian Cary-3. IR measurements were recorded from KBr tablets, on a Perkin Elmer spectrum 1000 FT-IR spectrometer. The crystal structure was checked by X-Ray diffraction using a Philips PW 1877 automated powder diffractometer with CuKα radiation.

Catalytic oxidation experiments. Oxidations were anhydrous TBHP were always performed behind safety screens. Quantitative analyses were carried out by GC with a semi-capillary column, CP-Sil-5 CB (50 m x 0.53 mm) or on a CB wax 52 CB (50 m x 0.53 mm) for carveol. Qualitative identification of peaks was made by reference samples and GC/MS analyses. Quantitative analysis was performed by using molar responses with respect to the internal standard. R- and S- sulfoxides were measured using a Chiralcel OD (Baker, 25 x 0.46 cm) HPLC column.

Results

Characterization. ICP analyses indicated the vanadium content to be between 0.4 and 0.9 wt%. One unit cell in the faujasite structure corresponds to 192 (Si+Al) atoms and contains 8 supercages. Thus a ratio of 192 (Si+Al)/V corresponds to 1 vanadium per 8 supercages. In the present case, the occupancy of 1 in every 4 to 8

Downloaded by YORK UNIV on October 31, 2012 | http://pubs.acs.org
Publication Date: December 10, 1998 | doi: 10.1021/bk-1998-0711.ch011

supercages will guarantee reasonable mobility of reactants and reagents through the framework.

Table I. Vanadium content of prepared zeolites

zeolite		*V content before soxhlet*	*V content after soxhlet*	
		V(wt%)	*V(wt%)*	*(Si+Al)/V*
VO(sal-R,R-chxn)-Y	A	0.63	?	
VO(sal-R,R-chxn)-WES	B	0.83	0.39	217
VO(sal-aa)-WES	C	0.83	0.86	90

The diffuse reflectance spectra of zeolite B and C are shown in Figure 2. In general UV-spectra of vanadyl complexes depend on oxidation state, solvent and type of counterions, so that it is difficult to make comparisons. The starting ligands, sal-R,R-chxn and sal-aa, have maxima at resp. 317 and 332 nm. Zeolite B, which shows an absorption maximum around 316 nm, apparently still has some non-complexed ligand present. This is in agreement with the lower vanadium content (Table 1), which corresponded to only half of the amount of ligand precursors that were added to the zeolite. The broad maximum around 500 nm for zeolite B, is also observed for $V^{V}O$(sal-R,R-chxn)Cl dissolved in ethanol. $V^{V}O$(sal-aa)(OEt) dissolved in dichloromethane has absorption maxima at 265 nm and 350 nm (sharp) and a broad maximum around 525 nm, which corresponds with the spectrum for zeolite C.

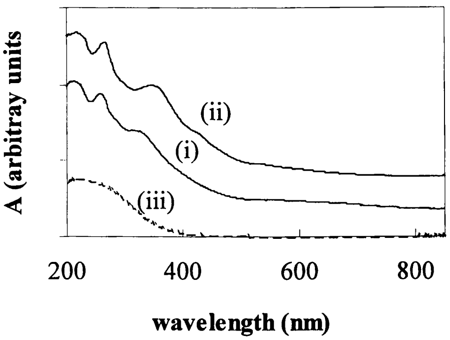

Figure 2. DRA-spectra for vanadium-encapsulated Wessalith zeolites; (i) VO(sal-R,R-chxn)-WES (B); (ii) VO(sal-aa)-WES (C); (iii) Wessalith.

Oxidation experiments with carveol. As a test reaction a mixture of cis- and trans-carveol was oxidized with TBHP. Analogous to what has previously been observed for compounds like geraniol and linalool, epoxidation was fast and selective [7]. Trans-carveol was converted fast and exclusively to the corresponding epoxide, whereas cis-carveol gave a mixture of cis-epoxide and carvone (reactions 2a and 2b). The ratio of the latter two products gives an indication of the selectivity of the vanadium catalyst. Although, the presently prepared vanadium-zeolites gave good

Downloaded by YORK UNIV on October 31, 2012 | http://pubs.acs.org
Publication Date: December 10, 1998 | doi: 10.1021/bk-1998-0711.ch011

activities in the epoxidation of carveol, it is clearly seen from the filter experiment for VO(sal-R,R-chxn)-Y in Table II, that under the conditions applied here (70°C, 1,2-dichloroethane as the solvent) vanadium is released in the solution, because epoxidation continues after the catalyst has been removed.

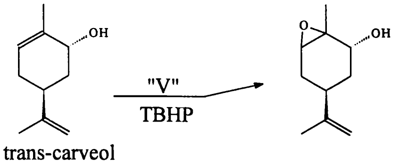

(2a)

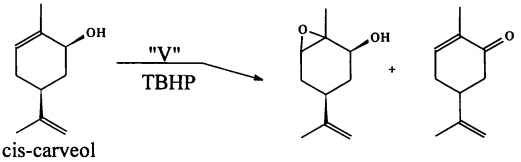

(2b)

Table II. Oxidation of cis-and trans-carveol, catalyzed by vanadium[a].

catalyst	*time*	*yield (%) trans-epoxide[b]*	*yield (%) cis-epoxide[b]*	*ratio cis-epoxide /carvone*
no	5.0 h	0	0	6% carvone[b]
VO(acac)$_2$	1.0 h	100	34	0.89
VO(salen)	5.0 h	100	52	1.4
VO(salen)-Y[c]	24 h	23	-	20% carvone[b]
VO(sal-R,R-chxn)-Y	4.3 h	100	31	1.6
recycle + filter[d]	5.3 h	69	6	0.21
VO(sal-R,R-chxn)-WES	3.2 h	66	5	0.17

[a]Reaction conditions, 70°C, 100 mg zeolite or 0.06 mmol complex; 6 mmol TBHP and 6 mmol (total) carveol in 10 ml 1,2-dichloroethane. Trans:cis carveol = 1.48: 1. [b]Yield based on input cis-epoxide. [c]From ref. *17*; cat. with 0.30 wt% V, prepared via wet V-exchange and direct solid state ligand impregnation. [d]The catalyst was recycled from the previous listed experiment; After 70 min, the catalyst was filtered from the hot solution; at this point 22% trans-epoxide and 1% cis-epoxide was formed; then the reaction was continued with the filtrate.

For the other two vanadium zeolites, coloring of the solution from clear to yellow, indicates that they are also unstable. The species responsible for oxidation in solution after filtration, is different from the vanadium in the zeolite, as shown by the lower cis-epoxide/carvone ratio.

Oxidation experiments of thioanisole. Oxidation of thioanisole to the corresponding sulfoxide and sulfone (reaction 3) with 30% H_2O_2, was studied using different catalysts, see Table III and Figure 3. Consistent to what is known in literature, vanadium catalyzed oxidation of sulfides, leads to both SO and SO_2 [*20*],

Downloaded by YORK UNIV on October 31, 2012 | http://pubs.acs.org
Publication Date: December 10, 1998 | doi: 10.1021/bk-1998-0711.ch011

which is in clear contrast to blank experiments with hydrogen peroxide where sulfoxide is produced exclusively.

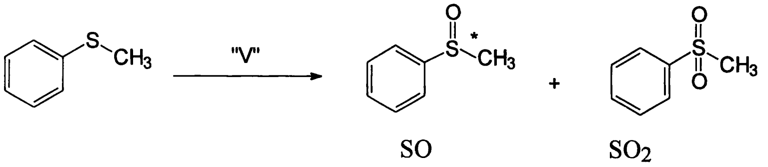

(3)

For the homogeneous catalysts, the reaction is complete in 1 h, with the addition of hydrogen peroxide. Consistent to the results of Bolm [*16*] an enantioselectivity of 58% was observed for the sulfoxide with sal-aa as the ligand, with a preference for the R-isomer. The property of this ligand to exhibit enantioselectivity with hydrogen peroxide is remarkably, because while the **sal-RR-chxn** ligand only demonstrates enantioselectivity with alkyl hydroperoxides (and cumylhydroperoxide in particular) [*21*], **sal-aa**, gives no asymmetric oxidation of thioanisole with *tert*-butylhydroperoxide.

As to the reactions catalyzed by zeolites, reasonable activities are obtained for the hydrophobic zeolites, whereas in the case of VO(sal-R,R-chxn) incorporated in the hydrophilic zeolite Y, no activity was observed. The hydrophobicity index, HI [*22*] for the starting zeolite Y with as Si/Al-ration of 2.44 is much lower (HI = 0.2) than that for Wessalith with a Si/Al ratio of 32 (HI = 14.8). Apparently in case of zeolite Y, water completely blocks the pores and inhibits catalysis. VO(sal-aa)-WES is a better catalyst than VO(sal-R,R-chxn)-WES which is probably due to the higher loading with vanadium (Table I). The fact that in the case of the VO(sal-aa)-WES zeolite no enantioselectivity could be detected is disappointing and the reason for it is not clear yet.

Table III. Sulfoxidation of thioanisole[a]

catalyst	*yield (%) of product in time[b]*				*e.e.*
	1.5 h		*22h*		
	SO	*SO_2*	*SO*	*SO_2*	
no	1.7	-	9	-	
WES	-	-	10	-	
VO(sal-R,R-chxn)			68	29	0%
VO(sal-R,R-chxn)-Y	-	-	1	-	0%
VO(sal-R,R-chxn)-WES	4	-	15	5	0%
VO(sal-aa)	76	13	76	19	58%
VO(sal-aa)-WES	4	1	40	11	0%

[a] 0.55 ml of a 30% H_2O_2 solution was added over one hour (ratio oxidant/substrate = 1.1) to a 10 ml solution dichloromethane, containing 5 mmol thioanisole, internal standard, and catalyst. In the case of zeolite 100 mg was used. For homogeneous catalysis, the complex was generated in-situ from 0.05 mmol $VO(acac)_2$ and 0.075 mmol ligand. [b] Yield is based on input thioanisole: S + SO + SO_2 equals 100%.

When submitting a redox molecular sieve to (oxidative) liquid phase conditions, one always needs to be aware of the possibility of leaching of the metal.

Downloaded by YORK UNIV on October 31, 2012 | http://pubs.acs.org
Publication Date: December 10, 1998 | doi: 10.1021/bk-1998-0711.ch011

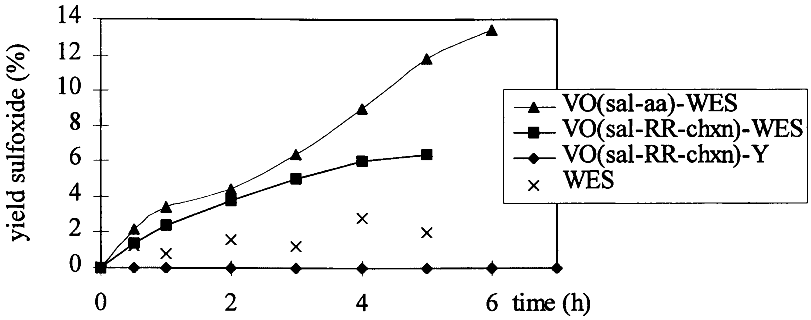

Figure 3. Sulfoxide formation in time for different catalysts.

The stability of catalyst B was tested in a typical reaction with thioanisole: After 2 hrs of reaction in the dichloromethane/water mixture, the zeolite was filtered, washed with some additional dichloromethane and the reaction continued with the filtrate. The sulfoxide formation continued slightly comparable to that anticipated in a blank reaction, while the sulfone production stopped completely. This indicates, that no vanadium was leached into the solution (see Figure 4).

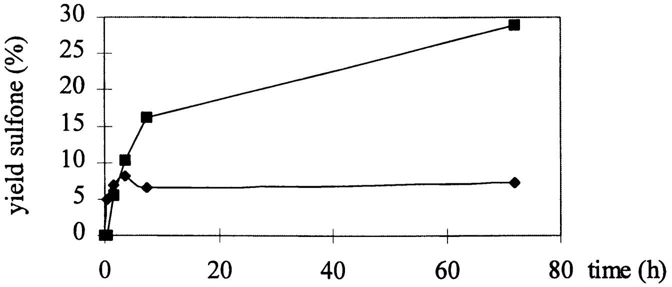

Figure 4. Reaction of 5 mmol thioanisole in 5 ml dichloromethane with 60% H_2O_2 (ratio oxidant: substrate = 1.1), catalyzed by VO(sal-RR-chxn)-WES. Catalyst was present during the whole reaction ■ or filtered after 2h ◆.

A more definite proof of heterogeneity would be to react a bulky sulfide, which cannot enter the zeolite pores (diameter >7.3 Å), under the current conditions and to observe a lack of reactivity [*23*]. Such a substrate is currently being devised.

Examples with manganese complexes incorporated in zeolite Y or EMT [*18,24*], have demonstrated that Mn(salen) type complexes are able to result in enantioselective epoxidation of styrene derivatives, with NaOCl as the oxidant. It must be observed, however, that enantioselectivities in the zeolite case are always equal or lower to those in the analogous homogenous situation.

Bromination experiments. According to reaction 1, vanadium catalyzes the bromination of 1,3,5-trimethoxybenzene (TMB), in the presence of acid. In the

Downloaded by YORK UNIV on October 31, 2012 | http://pubs.acs.org
Publication Date: December 10, 1998 | doi: 10.1021/bk-1998-0711.ch011

present case a small excess of substrate was present, resulting in some overoxidation to the dibromoderivative. In Table IV our preliminary results are shown on the oxidative bromination with hydrogen peroxide in a dichloromethane/water system. For ammonium vanadate, the maximum conversion is reached after 70 min when H_2O_2 is finished. The yield of 56% of monobromo and 5% of dibromo-TMB therefore corresponds with 66% efficiency on hydrogen peroxide consumed. The bromination of 1,3,5-trimethoxybenzene is also catalyzed by VO(sal-RR-chxn)-WES. Although this reaction is bothered by considerable background activity, clearly, the zeolite sieve is capable of catalyzing the reaction.

Table IV. Bromination of 1,3,5-trimethoxybenzene in a 1:1 dichloromethane/water mixture[a]

catalyst	*Yield of bromo-trimethoxybenzene (%)[b]*	
	70 min	5h
no	3.6	11
NH_4VO_3	56[c]	
VO(sal-RR-chxn)-WES	12	42[d]

[a]catalyst + 0.5 mmol $HClO_4$ was added to the reaction vessel, which contained 2.5 ml of 0.5 M KBr aqueous solution, 2.5 ml dichloromethane, 0.5 mmol H_2O_2 and 1 mmol 1,3,5-trimethoxybenzene. Catalyst: 50 mg zeolite or 0.02 mmol NH_4VO_3. [b]Yield relative to input H_2O_2. [c]Together with 10% of dibromo-TMB. [d]Plus 4% of the dibromo-TMB.

Further experiments under one phase conditions, and varying amounts of acid, will have to demonstrate the applicability of this reaction. As to the mechanism, it is assumed that the active brominating species (HOBr or derivatives thereof) is produced in the catalyst/water phase, which must then react with the substrate in the organic phase [*10*]. Although in our case the zeolite channels are large enough, the zeolite does not need to be able to accomodate the substrate itself, just as is the case for the enzyme vanadium-chloroperoxidase

The only other example of redox molecular sieves in oxidative halogenation, is 5-18% titanium(IV) grafted on mesoporous silicalites (MCM-48), which catalyzes the bromination of phenol red in water at pH 6.5 and was published very recently [*25*].

Conclusions

We were able to synthesize zeolite-encapsulated vanadium Schiff's base complexes, which were active in various selective oxidation reactions in the liquid phase. At elevated temperature with TBHP as the oxidant, these materials leach vanadium, which has been observed before for VO(HPS) and VO(Salen) (see introduction). Apparently *tert*-butyl-hydroperoxide or its alcohol, are able to replace the Schiff base as a ligand and in this way remove the vanadium from the interior of the zeolite. Oxidant induced leaching has been observed before for chromium-substituted aluminophosphates [*23,26*]. In general in case metals leach from zeolites, quantities as small as 1% of the metal present in the zeolite, are already able to

Downloaded by YORK UNIV on October 31, 2012 | http://pubs.acs.org
Publication Date: December 10, 1998 | doi: 10.1021/bk-1998-0711.ch011

catalyze oxidation reactions. Therefore recyclability of the zeolite is by no means an indication, of catalysis taking place within the zeolite.

Under biphasic conditions at room temperature with hydrogen peroxide as the oxidant, our materials do seem to be stable. Hydrogen peroxide and water apparently are not able to remove the vanadium from the zeolite. Hydrophobicity of the framework is necessary to guarantee diffusion of substrates and oxidant in and out of the micropores. Further investigations are under way to study the scope of these materials.

References

1. Vilter, H. *Phytochemistry*, **1984**, *23*, 1387-1390.
2. van Schijndel, J.W.P.M.; Krenn, B.E.; Maryani, A.; van Tol, M. *Environ. Sci. Technol.* **1991**, *25*, 446.
3. (a) Wever, R.; Krenn, B.E., In *Vanadium in Biological Systems*; Chasteen, N.D., Ed.; Kluwer, Boston, 1990, pp. 81. (b) Butler, A.; Walker, J.V. Chem. Rev. **1993,** *93,* 1937.
4. (a) Messerschmidt, A.; Wever, R. *Proc. Natl. Acad. Sci.* **1996**, *93*, 392-396. (b) Hemrika, W.; Renirie, R.; Dekker, H.L.; Barnett, P.; Wever, R. *Proc. Natl. Acad. Sci.*, **1997**, *94*, 2145.
5. (a) Sheldon, R.A. *J. Mol. Catal.* **1980**, *7*, 107. (b) Sheldon, R.A.; Kochi, J.K.; *Metal Catalyzed Oxidations of Organic Compounds*, Acad. Press, New York, 1981.
6. Side reactions occur through homolytic decomposition of the peroxide leading to radical pathways.
7. Sharpless, K.B.; Verhoeven, T.R.; *Aldrichimica Acta,* **1979,** *12*, 63.
8. This situation is in contrast, to that for redox metals operating via the so-called oxo-metal mechanism (e.g. Ru, Fe, Co, Mn,etc), in which the active oxidizing species is a M^{n+2}=O species, and for e.g. common peroxidase enzymes containing heme-iron, a typical reaction is accompanied by a change in oxidation state
9. Sheldon, R.A. in *Applied Homogeneous Catalysis by Orhanometallic Compounds*; Cornils, B.; Herrmann, W.A., Eds.; VCH, Weinheim, 1996, Vol. 1, p. 411.
10. (a) Conte, V.; Di Furia, F.; Moro, S.; Rabbolini, S. *J. Mol. Catal. A.: Chemical*, **1996**, *113*, 175. (b) Andersson, M.; Conte, V., Di Furia, F.; Moro, S. *Tet.. Letters* **1995**, *36*, 2675.
11. (a) Parton, R.F.; de Vos, D.E.; Jacobs. P.A. in *Zeolite Microporous Solids: Synthesis, Structure and Reactivity*, Derouane, E.G. et al., Eds, Kluwer, Dordrecht, 1992, pp. 555. (b) Herron, N. *Chemtech*, **1989**, *541.*
12. Herron, N.; Stucky, G.D.; Tolman, C.A. *J. Chem. Soc., Chem. Commun.* **1986**, 1521.
13. Knops-Gerrits, P.P.; de Vos, D.; Thibault-Starzik, F.; Jacobs, P.A. *Nature*, **1994**, *369*, 543.
14. Haanepen, M.J.; Elemans-Mehring, A.M.; van Hooff, J.H.C., *Appl. Catal. A: General* **1997**, *152*, 203.

Downloaded by YORK UNIV on October 31, 2012 | http://pubs.acs.org
Publication Date: December 10, 1998 | doi: 10.1021/bk-1998-0711.ch011

15. Arends, I.W.C.E.; Sheldon, R.A.; Wallau, M. Schuchardt, U. *Angew. Chem. Int Ed. Engl.* **1997**, *36*, 1144 and references cited therein.
16. Bolm, C.; Bienewald, F. *Angew. Chem. Int Ed. Engl.* **1995**, *34*, 2640.
17. Arends, I.W.C.E.; Pellizon Birelli, M.; Sheldon, R.A. *Studies in Surface Science and Catalysis,* **1997,** *110,* 1031.
18. Ogunwumi, S.B.; Bein, T. *Chem. Commun.* **1997**, 901.
19. Casiraghi, G.; Casnati, G.; Puglia, G.; Sartori, G. and Terenghi, G. *J. Chem. Soc. Perkin I* **1980**, 1862.
20. Using thianthrene-5-oxide as a probe: Ballistreri, F.P.; Tomaselli, G.A.; Toscano, R.M.; Conte, V.; Di Furia, F. *J. Am. Chem. Soc.* **1991**, *113*, 6209 and references cited herein.
21. Nakajima, K.; Kojima, K.; Kojima, M.; Fujita, J.; *Bull. Chem. Soc. Jpn.*, **1990**, *63*, 2620.
22 . Weitkamp, J et al. ; *Chem.-Ing. Tech.* **1991**, *63,* 623.
23. Sheldon, R.A.; Wallau, M.; Arends, I.W.C.E.; Schuchardt, U. subm. to *Acc. Chem. Res.*
24. Sabater, M.J.; Corma, A.; Domenech, A.; Fornes, V.; Garcia, H. *Chem. Commun.* **1997**, 1285.
25. Walker, J.V.; Morey, M., Carlsson, H., Davidson, A.; Stucky, G.D.; Butler, A. *J. Am. Chem. Soc.* **1997**, *119*, 6921.
26. Lempers, H.E.B.; Sheldon, R.A. *Stud. Surf. Sci. Catal.* **1997**, *105*, 1061.

Downloaded by YORK UNIV on October 31, 2012 | http://pubs.acs.org
Publication Date: December 10, 1998 | doi: 10.1021/bk-1998-0711.ch011

Downloaded by YORK UNIV on October 31, 2012 | http://pubs.acs.org
Publication Date: December 10, 1998 | doi: 10.1021/bk-1998-0711.ch012

Chapter 12

Synthetic Models for Vanadium Haloperoxidases

Vincent L. Pecoraro, Carla Slebodnick, and Brent Hamstra

Department of Chemistry, The Willard H. Dow Laboratories, The University of Michigan, Ann Arbor, MI 48109–1055

Vanadium halperoxidase (VHPO) model compounds have been extremely useful in helping to illucidate details of the mechanism of activity of the enzymes. This paper summarized mechanistic studies of peroxide binding and halide oxidation by VHPO functional models and how the results of these studies relate to the enzyme. In addition, EPR and ESEEM spectroscopic models for the reduced and inactive V(IV) form of VHPO have been used to predict the vanadium coordinations environment in the enzyme and a mechanism of inactiviation has been proposed.

Vanadium is considered a trace element in biology and has garnered little attention from scientists concerned with its biological roles until the past two decades (*1-3*). The introductory chapter by Kustin and the other articles in this symposium series have presented a testament to the intense studies of scientists and clinicians since the discovery of the vanadium haloperoxidase and the recognition that vanadate and vanadyl complexes exhibit insulin mimetic properties. In this contribution, we present an overview of the synthetic modeling approach that our laboratory has undertaken over the past decade in order to understand the structure, spectroscopy and reactivity of vanadium in biologically relevant oxidation levels. We will focus our attention on studies that provide insight specifically for the vanadium haloperoxidases (VHPOs). These enzymes, found in marine algae, lichens and fungi, are responsible for the oxidation of halides by hydrogen peroxide according to equation 1 (*4-7*).

$$HX + H_2O_2 \dashrightarrow XOH + H_2O \xrightarrow{R\text{-}H} RX + 2\,H_2O \qquad (1)$$

Our first efforts for modeling the reactivity of this enzyme centered on identifying V(V) chelates that might be capable of binding peroxide in a stable and reversible manner (*8,9*). Since the x-ray structure of the vanadium chloroperoxidase had not yet appeared, it seemed reasonable to employ ligands of moderate denticity which utilized functional groups that are biologically relevant. We selected the class of substituted tripodal amines represented by nitrilotriacetic acid (nta^{3-}) and functionalized iminodiacetic acid derivatives (ida) such as hydroxyethyliminodiacetic acid (heida), aminoethyliminodiacetic acid (aeida), pyridylmethyliminodiacetic acid (pmida). These and related ligands are shown in Figure 1. The cis-

Downloaded by YORK UNIV on October 31, 2012 | http://pubs.acs.org
Publication Date: December 10, 1998 | doi: 10.1021/bk-1998-0711.ch012

dioxovanadium(V) complexes of these ligands are easily prepared in aqueous solution and adopt the predicted structure which is shown in Figure 2 for the $[VO_2(ada)]^-$ derivative (Slebodnick, C. Pecoraro, V. L. unpublished data). These molecules are water soluble and stable. In addition, they may be solubilized in non-aqueous solvents such as acetonitrile by the addition of crown ethers which bind the countercations of the salt.

Reaction of $[VO_2(ada)]^-$ or any of the other cis-dioxovanadium(V) derivatives with hydrogen peroxide in aqueous or acetonitrile solutions leads to new complexes which have a side-on coordinated peroxide as illustrated in Figure 3 (*8*). We have recently investigated the details of this binding event and have shown that complexation can occur under neutral or acidic conditions. Under neutral conditions, peroxide binding curves saturate with added peroxide indicating that a reversible intermediate is formed. In contrast, if one equivalent of acid is added to the solution this saturation behavior is eliminated and one observes clean first order kinetics for the binding of peroxide to the dioxo dimer to form the oxo,peroxo derivative $VO(O_2)L$. The reaction sequence shown in Figure 4 illustrates our proposed mechanism for peroxide binding under these two solution conditions (*10*).

We have observed that $VO(O_2)L$ derivatives will not react efficiently to oxidize any halide in water or in acetonitrile. However, dramatic rate enhancements for halide oxidation are obtained in acetonitrile if one equivalent of a strong acid is added to the solution (*8,9*). We have proposed that the $VO(O_2)L$ is activated by protonation of the coordinated peroxide to give $VO(HO_2)L$ which is similar to the highly reactive alkylperoxides that have been reported by Mimoun (*11-13*).

The pK_a for the coordinated peroxide can be deduced from the hydrogen ion concentration dependence of the reaction. Table I provides both the rates for bromide oxidation and the calculated pK_a for the complex. One should notice that the pK_a for hydrogen bromide in acetonitrile is similar to that for $VO(HO_2)L$. Therefore, excess HBr must be added to obtain a maximum rate. We do not see chloride oxidation because the chloride anion is simply too basic. Therefore, rather than attacking $VO(HO_2)L$ as a nucleophile at the protonated peroxo oxygen, the far more rapid and thermodynamically driven proton transfer reaction occurs to generate $VO(O_2)L$ and HCl. Our proposed mechanism for bromide oxidation by a protonated peroxovanadium(V) complex is illustrated in Figure 5 (*8*). At this point, we can not distinguish whether the halide binds to vanadium prior to oxidation, as has been proposed previously for the enzyme (*14*), or if it attacks the peroxide directly. However, we consider halide coordination unlikely because this would reduce the halides nucleophilicity, thus deactivating the system. Halide coordination to vanadium may be possible if the entropic factors resulting from orienting the halide directly next to the peroxide are large enough to compensate for the reduced nucleophilicity of the vanadium-coordinated halide.

Table I. Kinetic Data for Bromide Oxidation by Peroxovanadium Complexes

Complex	k_2, bromide ($M^{-1}s^{-1}$)	pK_a
$[VO(O_2)Hheida]^-$	280 ± 40	6.0 ± 0.3
$[VO(O_2)nta]^{2-}$	170 ± 30	6.0 ± 0.3
$[VO(O_2)ada]^-$	220 ± 30	5.8 ± 0.4
$[VO(O_2)bpg]$	21 ± 3	5.4 ± 0.3
H_2O_2	3.7 ± 0.9	6.0 ± 0.4

It is instructive to contrast the differing roles of protons in the formation versus activation of peroxo vanadium complexes. Protons enhance the rate of binding of peroxide to the cis dioxovanadium complex by protonating the leaving hydroxide in the intermediate complex $VO(OH)(OOH)L$. In the absence of acid, hydroxide can compete with hydroperoxide for binding to vanadium. The more basic

Downloaded by YORK UNIV on October 31, 2012 | http://pubs.acs.org
Publication Date: December 10, 1998 | doi: 10.1021/bk-1998-0711.ch012

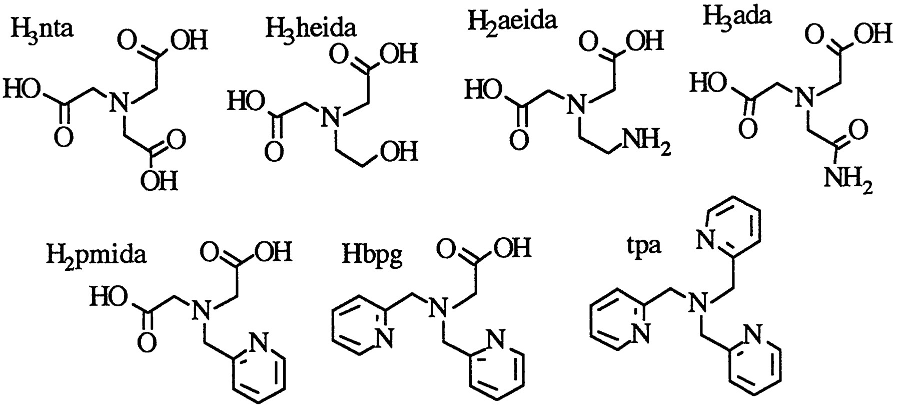
H$_3$nta
H$_3$heida
H$_2$aeida
H$_3$ada
H$_2$pmida
Hbpg
tpa

1. Ligands used in this study.

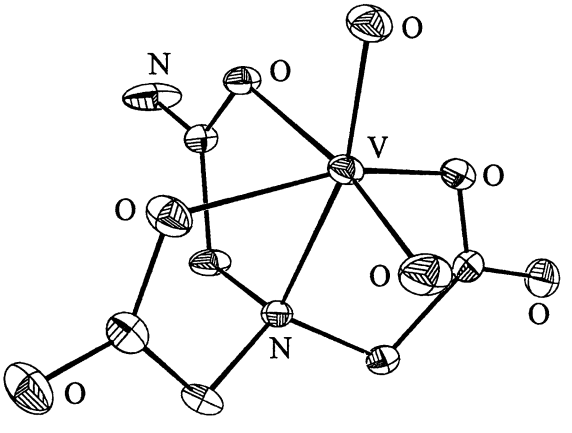
O
N
O
V
O
O
O
N
O
O

2. X-ray structure of [VO$_2$ada]$^-$ (V-O$_{oxo}$ = 1.636 Å and 1.632 Å).

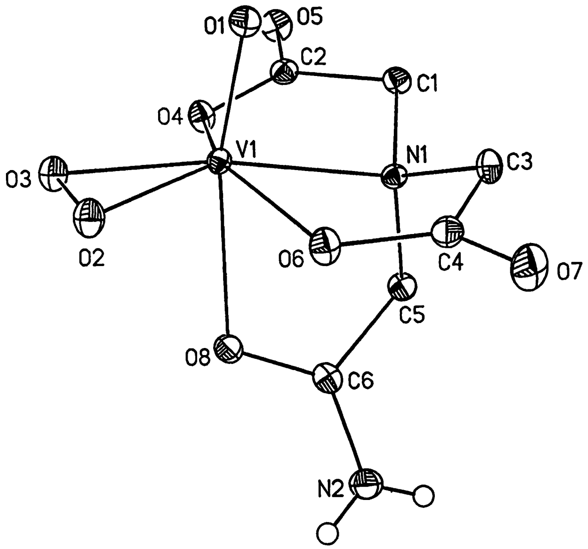
O1
O5
C2
C1
O4
V1
N1
C3
O3
O2
O6
C4
O7
C5
O8
C6
N2

3. X-ray structure of $[VO(O_2)ada]^-$ (V-O_{oxo} = 1.661(1) Å; V-0_{peroxo} = 1.867(1) and 1.872(1) Å) (Adapted from ref. 8).

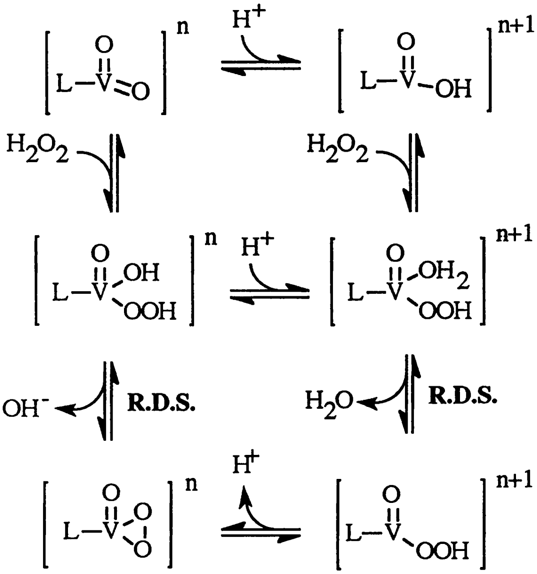
n
H+
n+1
H2O2
H2O2
n
H+
n+1
OH-
R.D.S.
H2O
R.D.S.
H+
n
n+1

4. Proposed mechanism for peroxide displacement of a coordinated terminal oxo from VO_2L (Adapted from ref. 10).

Downloaded by YORK UNIV on October 31, 2012 | http://pubs.acs.org
Publication Date: December 10, 1998 | doi: 10.1021/bk-1998-0711.ch012

hydroxide is protonated under slightly acidic conditions and facilitates the production of $VO(O_2)L$. In contrast, our kinetic studies on model compounds have shown that activation of peroxovanadium complexes requires protonation. Our interpretation of this result is that the proton attacks and activates the vanadium bound peroxide for nucleophilic attack by the halide. Examination of the peroxide structure of VClPO reveals that Lys353 forms a strong hydrogen bond with a side-on bound peroxide (*14*). In our opinion, this interaction is sufficient to activate the peroxide. Alternatively, if the peroxide were to bind in a slightly different position in VClPO, His404 would be a sufficient catalyst. The kinetic studies of VClPO and a number of VBrPOs indicate the presence of an important amino acid residue with a pK_a of 5-6 (*15-20*). This suggests that His may be the more important acid-base catalyst, despite the crystal structure. Nevertheless, it is clear from both the x-ray and kinetic studies that a mechanism consistent with our model chemistry, which requires protonation at the peroxide is feasible (Figure 6).

We have also been interested in the coordination geometry of the one electron reduced V(IV) vanadium haloperoxidase which is not competent to carry out these oxidation reactions. One may prepare the V(IV) analogues of the tripodal amine ligands which all appear to adopt the structure shown for $V(IV)O(OH_2)$(ada) in Figure 7 (*21*). As opposed to the V(V) compounds that orient the tripodal amine nitrogen trans to coordinated peroxide, $V(IV)O(OH_2)L$ complexes invariably form the isomer with the tripodal amine nitrogen trans to the terminal oxo moiety. This illustrates the strong oxophilicity of vanadium(IV) as the poor nitrogen donor is positioned trans to the terminal oxo group. This strong trans influence is observed for all of these compounds.

We have examined the electronic spectra of these V(IV) compounds and have shown that the $b_1 \rightarrow b_2^*$ transition (which corresponds to 10Dq in these materials) tracks as expected based on the ligand field strengths of the various tripodal amine ligands we have studied. This provides us with confidence that the structures for various derivatives that are deduced from x-ray crystallography are retained in solution. EPR spectroscopy can also be an extremely useful handle for establishing the solution structure of V(IV) complexes. In particular, the additivity relationship, which assigns a scalar value for the nuclear hyperfine coupling constant to different ligands bound in the equatorial plane of the vanadium, has often been used to establish ligand type bound to V(IV). We have applied the additivity relationship to these complexes and have obtained excellent fits with the structures predicted from crystallography (in many cases there is a minor component that corresponds to complexes in which water has displaced one of the carboxylate arms) (*21*).

While providing extremely useful information concerning equatorial ligands, the additivity relationship is not generally applied for determining the ligand identity for moieties bound trans to the vanadyl oxygen. This is because there is poor coupling of angular momentum between the single electron in the d_{xy} orbital and the nuclear spin of the trans donor since the σ bonding orbital is perpendicular to the metal's magnetic orbital. In contrast, pulsed EPR techniques such as ESEEM can often extract weak modulation of the EPR spectrum. In collaboration with Professor Wayne Frasch and Dr. Russell LoBrutto at Arizona State University, we have embarked on a systematic study to expand the application of ESEEM spectroscopy to small molecules and proteins (*22*).

The ESEEM spectrum of $[VO(H_2O)(nta)]^-$, given in Figure 8a shows modulations that are in the 1 and 4 MHz range. These values are consistent with a nitrogen bound in the axial site of the V(IV). In contrast, the ESEEM spectrum of $VO(H_2O)$(pmida) (Figure 8b), with nitrogen donors both axial and equatorial, has modulations at both low frequency (1 and 4 MHz) and at much higher frequencies (approximately 5 and 8 MHz). Thus, these studies demonstrate that we can distinguish nitrogenous donors that are found in axial versus equatorial coordination sites (*22*).

At this stage we were prepared to apply both the additivity relationship and our ESEEM parameters to evaluate the coordination geometry for the V(IV) form of

Downloaded by YORK UNIV on October 31, 2012 | http://pubs.acs.org
Publication Date: December 10, 1998 | doi: 10.1021/bk-1998-0711.ch012

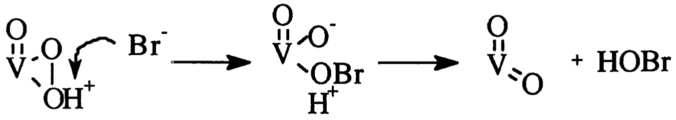
Br⁻
HOBr
OBr
OH⁺
H⁺

5. Proposed mechanism for bromide oxidation by $VO(HO_2)L$.

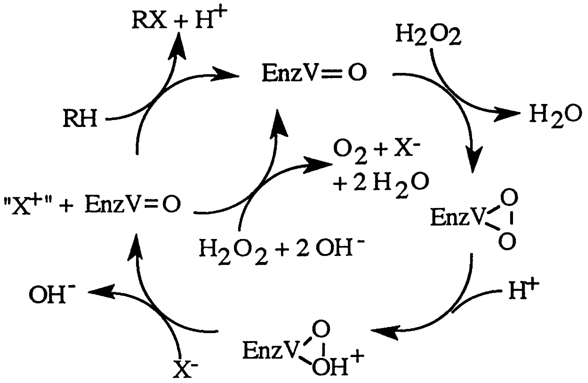
RX + H⁺
RH
EnzV=O
H2O2
H2O
O2 + X⁻
+ 2 H2O
"X⁺" + EnzV=O
H2O2 + 2 OH⁻
OH⁻
X⁻
H⁺

6. Proposed minimal mechanism for halide oxidation by VHPO (Adapted from ref. 3).

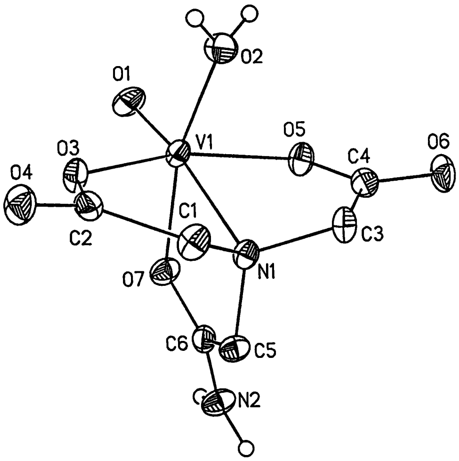
O1
O2
O3
O4
O5
O6
O7
V1
C1
C2
C3
C4
C5
C6
N1
N2

7. X-ray structure of $V^{iv}O(H_2O)(ada)$ (Reproduced from ref. 21).

Downloaded by YORK UNIV on October 31, 2012 | http://pubs.acs.org
Publication Date: December 10, 1998 | doi: 10.1021/bk-1998-0711.ch012

VHPO. Table II illustrates the best fit parameters for the enzyme using $a_\parallel$ values for imidazole reported by Chasteen (*23*) and by Cornman (*24*). We have evaluated both the high and low pH forms of the enzyme. Our analysis is consistent with at least one and possibly two imidazole nitrogens bound in the equatorial plane of the V(IV). In addition, the low pH enzyme form most likely contains coordinated water while the high pH form converts to bound hydroxide. Figure 9 illustrates the ESEEM spectrum for VHPO that was reported by deBoer et al (*25*). One observes high frequency modulations consistent with an equatorially bound nitrogen. In addition, there are low frequency components that are diagnostic of an axially coordinated nitrogen donor.

Table II. Additivity Relationship Analysis of EPR Data for VBrPO

$A_\parallel$	Chasteen's Parameters	Cornman's Parameters
$166.6 \times 10^4\ cm^{-1}$ (low pH)	$2H_2O$, $1RO^-$, 1 His: $A_{\parallel(calc)} = 167.3 \times 10^4 cm^{-1}$	$2H_2O$, 2 His: $A_{\parallel(calc)} = 168.0 \times 10^4 cm^{-1}$
$159.9 \times 10^4\ cm^{-1}$ (high pH)	$1H_2O$, $1OH^-$, $1RO^-$, 1 His: $A_{\parallel(calc)} = 160.4 \times 10^4 cm^{-1}$	$1\ H_2O$, $2\ OH^-$, 2 His: $A_{\parallel(calc)} = 161.0 \times 10^4 cm^{-1}$

Differences in parameters: R-N=R (Chasteen) = 40.7; "aromatic imine" (Cornman) = 38.3

By combining the spectroscopic observations given above with the x-ray structures of the VClPO (*14,26*), we are now in a position to propose a structure for the V(IV) enzyme form. Our model is illustrated in Figure 10. We retain the coordinated imidazole which is bound in the active, V(V) enzyme and assign this nitrogen donor as the species which is responsible for the low frequency ESEEM modulations. The imidazole that has been assigned as an acid base catalyst in the active enzyme form is assigned as the residue which provides the high frequency nitrogenous signals and is implicated in the additivity relationship analysis. It is our view that complexation of the vanadium(IV) by these two imidazoles lowers the reduction potential which stabilizes the V(IV) enzyme and recruits the acid/base catalyst so that it may no longer participate in functional chemistry.

It is interesting to compare the proposed structures of the reduced VHPO, the crystal structures of V(V) forms of VClPO, and our model compounds. In the reduced form we proposed for the enzyme, we find a nitrogen donor trans to the terminal oxo (Figure 10), as is seen in the V(IV) model compounds (Figure 7). In contrast, the peroxide moiety is trans to the amine nitrogen in all of our $V^VO(O_2)L$ model complexes (Figure 3). Similarly, the azide displaces the oxygen trans to the nitrogen of His496 in the azide inhibited VClPO structure (Figure 11a and b) (*26*). Based on this data, we would have expected peroxide to bind trans to His496, as pictured in Figure 11c. This orientation of peroxide would facilitate it's interaction with the imidazole acid-base catalyst (His404), which in turn would enhance catalysis. However, the recent crystal structure of peroxide bound VClPO indicates that hydrogen peroxide binds in a different position than azide and forms a hydrogen bond with Lys353 (Figure 11d) (*14*). This orientation should also be able to activate the peroxide through hydrogen bonding and enhance catalysis. Future studies with 5-coordinate peroxovanadate model systems may help to address the issue of why VHPOs go through a loss of two oxygen donors and a change in coordination geometry upon peroxide binding (Figures 11a and d) while our model compounds system undergo a net displacement of an oxo by peroxide.

In conclusion, we hope that we have shown that model compounds can be used to extract intimate details of enzymatic reactions. Our studies have developed the most active VHPO mimics and, more importantly, they have demonstrated that protonation of coordinated peroxide is essential for catalysis. We have also shown that an acid base catalyst, though not essential, would facilitate the initial binding step

Downloaded by YORK UNIV on October 31, 2012 | http://pubs.acs.org
Publication Date: December 10, 1998 | doi: 10.1021/bk-1998-0711.ch012

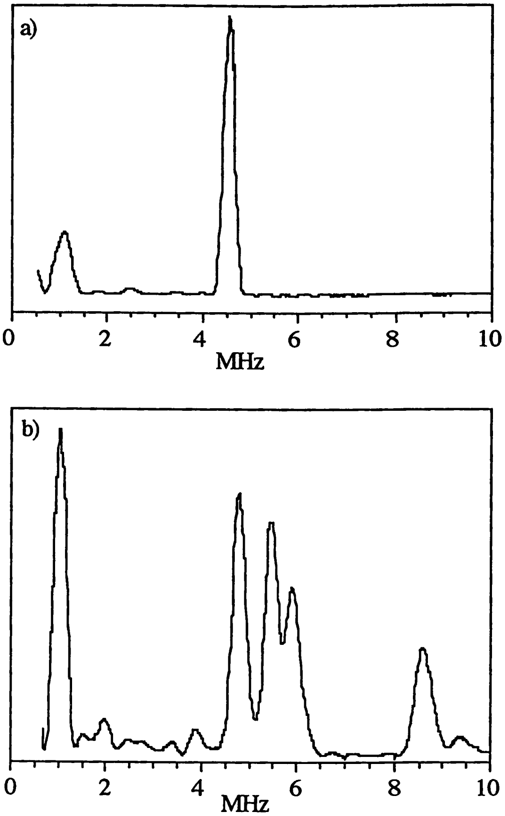

8. ESEEM spectra of A) $[VO(H_2O)(nta)]^-$ and B) $VO(H_2O)(pmida)$. (Reproduced from ref. 22 where reaction conditions are also given).

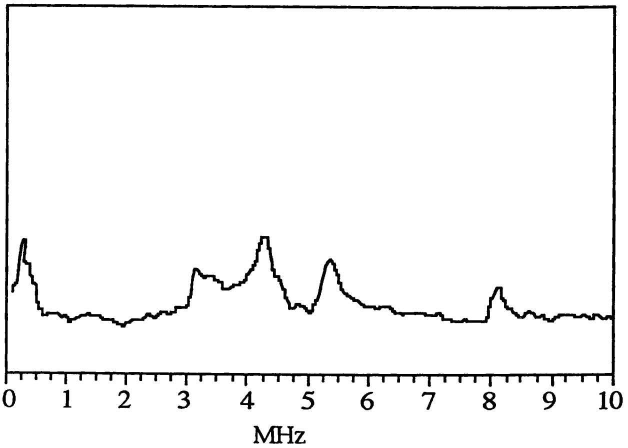

9. ESEEM spectrum of VHPO as reported by deBoer, et al (Reproduced with permission from ref.25. Copyright 1988 Elsevier Science).

Downloaded by YORK UNIV on October 31, 2012 | http://pubs.acs.org
Publication Date: December 10, 1998 | doi: 10.1021/bk-1998-0711.ch012

Downloaded by YORK UNIV on October 31, 2012 | http://pubs.acs.org
Publication Date: December 10, 1998 | doi: 10.1021/bk-1998-0711.ch012

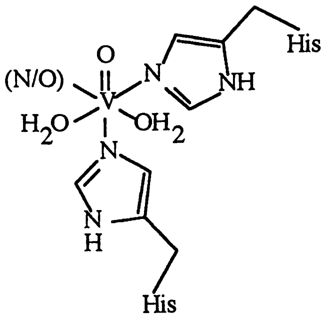

10. Proposed structure of the reduced V(IV) VHPO.

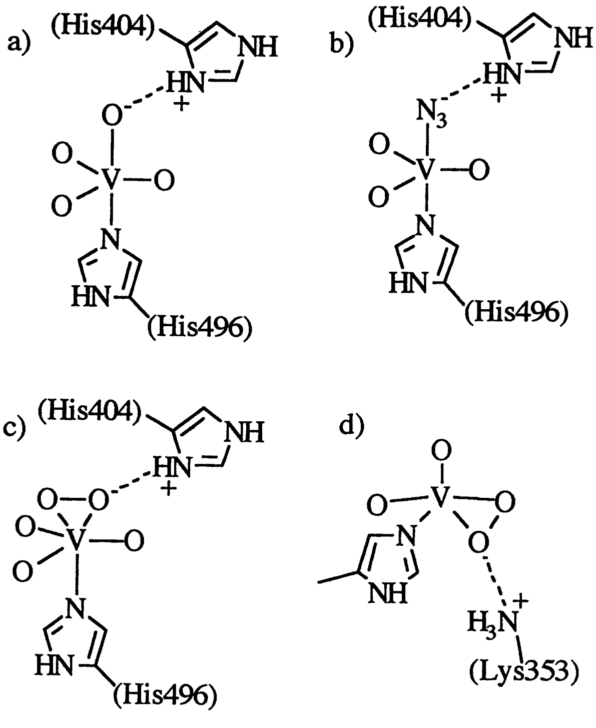

11. Schematics comparisons of VClPO: (a) x-ray structure of native enzyme (V-$O_{equatorial}$ = 1.65 Å; V-O_{axial} = 1.93 Å; V-N = 1.96 Å) (*14*); (b) the azide inhibited x-ray structure (V-$O_{equatorial}$ = 1.65 Å; V-N_{azide} = 1.98 Å, V-N_{His} = 2.25 Å (*26*); (c) the proposed peroxide structure, based on the azide structure and model compounds; and (d) the observed peroxide bound x-ray structure (V-O_{axial} = 1.60 Å;V-$O_{equatorial}$ = 1.93 Å; V-$O_{peroxide}$ = 1.87 Å; V-N = 2.19 Å) (*14*).

of peroxide to the enzyme. Our structural and spectroscopic studies on V(IV) model compounds have allowed us to deduce a reasonable chemical model for the reduced, inactive enzyme and propose a mechanism for enzyme inactivation. While these accomplishments are gratifying, we are still working to achieve the Holy Grail of this field: chloride oxidation. We are happy to report that we now have systems from which we can extract measurable rates of chloride oxidation by vanadium peroxo catalysts and it appears that protonation chemistry is again important in these more demanding reactions (Slebodnick, C.; Colpas, G. J.; Pecoraro, V. L., unpublished data). We hope to present details of this very important new development in small molecule modeling chemistry in the near future.

Acknowledgments

The authors acknowledge Dr. Gerard Colpas for many useful discussions and our collaboration with Professor Wayne Frasch and Dr. Russell LoBruto in our ESEEM studies. This work was supported by the NIH (GM42703 to VLP) and by a postdoctoral fellowship to CS (GM18370).

Downloaded by YORK UNIV on October 31, 2012 | http://pubs.acs.org
Publication Date: December 10, 1998 | doi: 10.1021/bk-1998-0711.ch012

References

1. Chasteen, N. D., Ed. *Vanadium in Biological Systems,* Vol. (Kluwer, Dordrecht, The Netherlands) 1990, pp. 222.
2. Sigel, H.; Sigel, A., Ed. *Vanadium and Its Role in Life,* Metal Ions in Biological Systems, Vol. 31 (Marcel Dekker, Inc., New York) 1995.
3. Slebodnick, C.; Hamstra, B. J.; Pecoraro, V. L. *Structure and Bonding* **1997**, *89*, 51-108.
4. Butler, A.; Baldwin, A. H. *Structure and Bonding* **1997**, *89*, 109-32.
5. Vilter, H. *Metal Ions in Biological Systems* **1995**, *31*, 325-62.
6. Butler, A.; Walker, J. V. *Chem. Rev.* **1993**, *93*, 1937-44.
7. Wever, R.; Krenn, B. E. "Vanadium Haloperoxidases" In *Vanadium in Biological Systems,* Vol. ; N. D. Chasteen, Ed. (Kluwer Academic Publishers, Dordrecht) 1990, pp. 81-97.
8. Colpas, G. J.; Hamstra, B. J.; Kampf, J. W.; Pecoraro, V. L. *J. Am. Chem. Soc.* **1996**, *118*, 3469-78.
9. Colpas, G. J.; Hamstra, B. H.; Kampf, J. W.; Pecoraro, V. L. *J. Am. Chem. Soc.* **1994**, *116*, 3627-8.
10. Hamstra, B. J.; Pecoraro, V. L. *Inorg. Chem.* submitted.
11. Mimoun, H.; Chaumette, P.; Mignard, M.; Saussine, L.; Fischer, J.; Weiss, R. *Nouv. J. Chem.* **1983**, *7*, 467-75.
12. Mimoun, H.; Saussine, L.; Daire, E.; Postel, M.; Fischer, J.; Weiss, R. *J. Am. Chem. Soc.* **1983**, *105*, 3101-10.
13. Mimoun, H.; Mignard, M.; Brechot, P.; Saussine, L. *J. Am. Chem. Soc.* **1986**, *108*, 3711-8.
14. Messerschmidt, A.; Prade, L.; Wever, R. *Biol. Chem.* **1997**, *378*, 309-315.
15. van Schijndel, J. W. P. M.; Barnett, P.; Roelse, J.; Vollenbroek, E. G. M.; Wever, R. *Eur. J. Biochem.* **1994**, *225*, 151-7.
16. Soedjak, H. S.; Butler, A. *Biochim. et Biophys. Acta* **1991**, *1079*, 1-7.
17. Everett, R. R.; Soedjak, H. S.; Butler, A. *J. Biol. Chem.* **1990**, *265*, 15671-9.
18. de Boer, E.; Wever, R. J. *J. Biol. Chem..* **1988**, *263*, 12326-32.
19. Everett, R. R.; Kanofsky, J. R.; Butler, A. *J. Biol. Chem..* **1990**, *265*, 4908-14.
20. de Boer, E.; Boon, K.; Wever, R. *Biochemistry* **1988**, *27*, 1629-35.
21. Hamstra, B. J.; Houseman, A. L. P.; Colpas, G. J.; Kampf, J. W.; LoBrutto, R.; Frasch, W. D.; Pecoraro, V. L. *Inorg. Chem.* **1997**, *36*, 4866-74.
22. LoBrutto, R.; Hamstra, B. J.; Colpas, G. J.; Pecoraro, V. L.; Frasch, W. D. *J. Am. Chem. Soc.* in press.

23. Chasteen, N. D. In *Biological Magnetic Resonance,* Vol. 3; L. J. Berliner and J. Reuben, Ed. (Plenum Press, New York) 1981, pp. 53-119.
24. Cornman, C., R.; Zovinka, E. P.; Boyajian, Y. D.; Geiser-Bush, K. M.; Boyle, P. D.; Singh, P. *Inorg. Chem.* **1995**, *34*, 4213-19.
25. de Boer, E.; Keijzers, C. P.; Klaassen, A. A. K.; Reijerse, E. J.; Collison, D.; Garner, C. D.; Wever, R. *FEBS Letters* **1988**, *235*, 93-97.
26. Messerschmidt, A.; Wever, R. *Proc. Nat. Acad. Sci. U. S. A.* **1996**, *93*, 392-6.

Downloaded by YORK UNIV on October 31, 2012 | http://pubs.acs.org
Publication Date: December 10, 1998 | doi: 10.1021/bk-1998-0711.ch012

Downloaded by NORTH CAROLINA STATE UNIV on October 31, 2012 | http://pubs.acs.org
Publication Date: December 10, 1998 | doi: 10.1021/bk-1998-0711.ch013

Chapter 13

Perspectives on Vanadium Biochemistry

Kenneth Kustin

**Department of Chemistry, Brandeis University, Box 9110,
Waltham, MA 02254–9110**

A background perspective on vanadium biochemistry relevant to the conference is presented. Vanadate is an extremely effective inhibitor of Na,K-ATPase and many other phosphohydrolase enzymes. Vanadate's ability to mimic phosphate in a transition state configuration underlies its potent inhibition. V-containing haloperoxidases utilize vanadate as a prosthetic group in their active sites. These enzymes catalyze hydrogen peroxide oxidation of a halide ion and subsequent addition of the product to an organic substrate, but the oxidation number of vanadium does not change during the catalytic cycle. Vanadate's role is to coordinate peroxide and facilitate halide ion oxidation, probably by O-atom transfer. Recent evidence suggests that the binding site compositions of both types of enzyme are similar. Apart from enzymes, vanadium is spectacularly accumulated in tunicates, but with as yet unknown function. Two models that accomplish this accumulation have been postulated and are discussed. One utilizes a biogenic reductant and metal ion complexing agent such as tunichrome; the other involves direct participation of enzymes.

Biological vanadium, like Sam the piano player in *Casablanca*, was colorful but barely essential, until the late 70s (*1*). At that time, stimulated by attempts to explain the poor reproducibility of ATP hydrolysis kinetics, a dramatic and surprising change in vanadium's status occurred. While working with sodium and potassium ATPase enzyme (Na,K-ATPase), Cantley *et al.* identified *endogenous* vanadium as an inhibitor present in ATP derived from equine muscle, for example, but not present in ATP derived from plant sources (*2*). The kinetics differed, depending on whether the ATP source did or did not contain vanadium. This

In Vanadium Compounds; Tracey, A., et al.;
ACS Symposium Series; American Chemical Society: Washington, DC, 1998.

Downloaded by NORTH CAROLINA STATE UNIV on October 31, 2012 | http://pubs.acs.org
Publication Date: December 10, 1998 | doi: 10.1021/bk-1998-0711.ch013

finding was confirmed by other investigators (*3–5*) in 1978 beginning a new era of vanadium biochemistry.

The discovery that vanadium, as the inorganic vanadate ion ($H_2VO_4^-$, HVO_4^{2-} hereinafter referred to as V_i), inhibits Na,K-ATPase was unexpected and intriguing. It stimulated further experimentation; addition of V_i to enzymes, cells, and organisms followed by observation. In this fashion, it was realized that vanadate polyanions (*6*) are also inhibitory (*7*). While the role of vanadium as biological effector was considerably enhanced, the more well-known occurrences of vanadium in biological systems, particularly vanadium accumulation in tunicates (*8*) and Amanita mushrooms (*9*), vanadium toxicology (*10*), and vanadium essentiality in nutrition (*11*), were also being studied. A function for endogenous vanadium was finally found when it was discovered to be essential for haloenzymes in certain seaweeds (*12*) and for certain nitrogenase enzymes (*13*). Thus, the first phase of the vanadium biochemical era witnessed knowledge of the element's prevalence and applicability enlarged, and true functions found in two of its naturally occurring biological sites.

This symposium heralds the start of a new era in vanadium biochemistry: vanadium therapy. Although a new era may be starting, many themes of vanadium biochemical research continue, of course, such as searching for vanadium function where the element is accumulated in natural sites apart from sea weeds, namely, in tunicates, mushrooms, and fan worms; clarifying the role of vanadium as essential nutrient for humans and other mammals; and using vanadium as a probe of biochemical structure and function. With therapeutic applications as a goal, however, understanding how vanadium achieves its often surprisingly effective biological effects becomes even more important, and chemical modeling of vanadium's biological function is introduced for the first time (*14*).

Therefore, this chapter is aimed at providing the interested reader with sufficient background to place the new advances and directions of biological vanadium research into proper perspective. The topics covered are vanadate inhibition of enzymes, mechanisms of vanadium-containing haloperoxidases, and models of vanadium accumulation in tunicates.

Vanadate As Enzyme Inhibitor

Monomeric V_i's ability to inhibit phosphohydrolase enzymes is a key to understanding much of vanadium's biological activity. V_i inhibits acid and alkaline phosphatases and phosphotyrosyl protein phosphatases, in addition to electrogenic ATPases; V_i polyanions inhibit phosphotransferases such as phosphofructokinase. Morever, V_i is a very effective inhibitor; concentrations capable of lowering an enzyme's activity by one-half can be as low as 4 nM (*15*), although most such concentrations are approximately 1 μM. Decavanadate is likewise effective, a concentration of 0.33 μM having been reported for 50% inhibition of adenylate kinase (*16*).

Phosphate is obviously involved in the reactions catalyzed by these enzymes and V_i's phosphate mimicry clearly contributes to its effectiveness as an inhibitor. But consideration of other inorganic oxoanions indicates that phosphate mimicry is not the full story. Arsenate, for example, is roughly as effective as V_i in inhibiting glyceraldehyde-3-phosphate dehydrogenase, but arsenate is not an effective ion-transport ATPase inhibitor (*17*). Electrogenic ATPases are also not inhibited by chromate, tungstate and molybdate. Tripolyphosphate is virtually identical with the triphosphate moiety of ATP, but this and other polyphosphates do not inhibit phosphotransferases, whereas decavanadate and other oligomeric vanadates do.

Closer examination of the pattern of inhibition of ATPases provides important clues to explaining V_i inhibition (*18*). Bacterial and mitochondrial H^+-translocating ATPases do not form phosphoenzyme intermediates and are not inhibited by V_i; enzymes forming such an intermediate, like Na,K-ATPase, are inhibited by V_i. Shortly after the discovery of V_i inhibition of ion-transporting ATPases, the energy transducing ATPases, referred to as dynein ATPases, were found to be inhibited by V_i (*19*). For this class of enzymes, phosphoenzyme formation is not essential for inhibition. Rather, it is the ability of V_i to form a catalytically inactive ternary complex, enzyme-nucleotide-vanadate, that makes V_i an effective inhibitor.

Reagents that can reduce the oxidation number of vanadium from +5 to +4 or +3 should reverse inhibition without impairing enzyme activity, in essence, by excising the inhibitor from the enzyme's active site. If the oxidized reagent can also function as a chelating agent, the effect should be quite efficient. Such is the case for ascorbic acid and glutathione, which reduce V_i to +4 vanadyl ion. In the absence of chelation, the product vanadyl(IV) ion might also be inhibitory, although the source of this inhibition might be distinct from that of V_i (*20*).

What is the source of V_i's powerful inhibition of phosphohydrolase enzymes? First, it can occupy the phosphate locus in the active site, because V_i is sized and charged similarly to phosphate. Second, at the center of V_i lies a metallic, not a representative, element. Vanadium in V_i is d^0 and forms stable structures in aqueous solution when coordinated to 4, 5, or 6 surrounding atoms, which phosphorus does not do readily. To cleave a phosphorus-oxygen bond by hydrolysis, for example, central phosphorus breaks one type of P-O bond and then makes a second type of P-O bond. In the transition state phosphorus most likely increases its coordination number, weakening the bond to the leaving oxygen and forming a bond to the entering oxygen. It does so while bound to the enzyme; therefore, if a phosphorus-mimicking vanadium compound, with a structure closer

Downloaded by NORTH CAROLINA STATE UNIV on October 31, 2012 | http://pubs.acs.org
Publication Date: December 10, 1998 | doi: 10.1021/bk-1998-0711.ch013

to the transition state than that of the phosphorus compound, is in the vicinity of the active site, chances are very good that it will be bound, *i.e.*, trapped at that spot. By virtue of its "good fit" it does not leave soon enough to effect further progress along the catalytic cycle; it is an inhibitor.

These ideas were first brought out in an insightful study on the inhibition of ribonuclease A by vanadium-uridine complexes (*21*). The enzyme's substrate is single-stranded RNA; it specifically hydrolyzes nucleosides with pyrimidine bases on the 3′ side of the phosphodiester linkage to be split (*22*). In the first step of this double hydrolysis, one nucleoside is released, leaving a 2′, 3′-cyclic monophosphate intermediate. This species then hydrolyzes to a 3′-monophosphate ester. Trigonal bipyramidal transition states are presumably involved in both steps. Both vanadium(IV) and vanadium(V) complexes were shown to be inhibitory, implying that vanadium of either oxidation number easily assumes the transition state structure. Crystals of the vanadium-ligand-enzyme (VLE) complex could be grown, and several X-ray structures have been published. These structures have been reviewed, and additional binding and kinetics studies of VLE complexes were reexamined, primarily by using ^{51}V NMR (*23*).

The transition state analogue can be evaluated from the viewpoint of protein dynamics (enzyme) or coordination energetics (inhibitor). Petsko and coworkers focus attention on the protein (*24*). They note (1) that the V_i-uridine-enzyme complex has a distorted trigonal bipyramidal geometry around the central vanadium atom, and that (2) the amine group of Lys-41 is H-bonded to one of the equatorial trigonal oxygen atoms. They argue that the motion of the protein, rapidly and constantly sampling all of configuration space, effectively keeps Lys-41 away from the active site, so it does not block attachment of the VL complex to the critical locus on the enzyme. Once the VL moiety is docked, the side-chain becomes locked in place, and the enzyme is trapped in this state long enough for substrate turnover to be inhibited.

Leon-Lai, Gresser and Tracey focus attention on the metal-containing inhibitor (*23*). They cite measurements of the rate constants for hydrolysis of ethyl vanadate and ethyl phosphate, and use these values, together with equilibrium binding values, to estimate the different activation energies required by substrate and inhibitor to gain a pentacoordinated transition state structure. Their approach enables them to compare the effectiveness of a VE or VLE structure in attaining the transition state structure for different phosphate-hydrolyzing and -transferring enzymes. For most such enzymes, including ribonuclease, they explain the inhibition as arising from a saving of 22-25 kJ/mol in attaining the transition state when a single phosphate is replaced by a single vanadate in the VE or VLE complex.

For each enzyme susceptible of V_i inhibition, it has been a challenge to determine exactly where in the catalytic mechanism and with what stoichiometry

Downloaded by NORTH CAROLINA STATE UNIV on October 31, 2012 | http://pubs.acs.org
Publication Date: December 10, 1998 | doi: 10.1021/bk-1998-0711.ch013

the inhibition occurs. For example, for the ion-transporting Na,K-ATP enzyme, the overall stoichiometry of the reaction being catalyzed is given by equation 1

$$ATP + H_2O + 3Na_c^+ + 2K_m^+ \overset{E,Mg^{2+}}{\rightleftharpoons} ADP + P_i + 3Na_m^+ + 2K_c^+ \qquad (1)$$

where E is the Na,K-ATPase enzyme, the subscripts c and m represent cytosolic and medium sides of the enzyme-containing membrane, and P_i represents inorganic phosphate ions. Vectorial transport of Na^+ and K^+ ions coupled to ATP hydrolysis arises because the phosphoenzyme exists in two spontaneously interconverting forms, E_1 and E_2, that have different metal ion preferences and transmembrane orientations of the metal ion binding sites (*25*). If one starts the cycle with free enzyme in conformation E_2 bound to $2K^+$ ions on the cytosolic side, the last step in the cycle is dephosphorylation, which yields P_i on the cytosolic side, regenerating E_2. At this point, the enzyme binds V_i, if it is present, becoming trapped in the E_2 conformation.

Two other electrogenic transport enzymes inhibited by V_i are termed the calcium pump and the proton pump. The most frequently studied calcium pump,

$$ATP + H_2O + Ca_c^{2+} \overset{E,Mg^{2+}}{\rightleftharpoons} ADP + P_i + Ca_\ell^{2+} \qquad (2)$$

that of the sarcoplasmic reticulum, catalyzes reaction 2, where E is the Ca-ATPase enzyme, and the subscripts "c" and "ℓ" represent cytosolic and lumenal sides of the sarcoplasmic reticulum vesicle, respectively. The kinetics of this enzyme are subtle, but the mechanism most consistent with all the experimental evidence is similar to that of Na,K-ATPase in general outline (*26*). The proton pump of the gastric mucosa transports protons against an unfavorable concentration gradient by catalyzing the following exchange reaction (3), where E is the H,K-ATPase

$$ATP + H_2O + H_c^+ + K_\ell^+ \overset{E}{\rightleftharpoons} ADP + P_i + H_\ell^+ + K_c^+ \qquad (3)$$

enzyme. The kinetics of this enzyme are complex, but the reaction cycle is similar to the two better-known pumps with one difference: two catalytic sites appear to be involved (*27*).

Prosthetic V_i

An unambiguous function for essential vanadium was not known until the vanadium-containing haloperoxidases were discovered. In this chapter we emphasize the

Downloaded by NORTH CAROLINA STATE UNIV on October 31, 2012 | http://pubs.acs.org
Publication Date: December 10, 1998 | doi: 10.1021/bk-1998-0711.ch013

Downloaded by NORTH CAROLINA STATE UNIV on October 31, 2012 | http://pubs.acs.org
Publication Date: December 10, 1998 | doi: 10.1021/bk-1998-0711.ch013

enzyme's mechanism, and the likely relationship between vanadium-containing haloperoxidases and the phosphohydrolase enzymes.

Haloperoxidase enzymes are normally thought of as catalyzing the addition of a halogen atom to an organic substrate. Producing some such reaction is probably the actual function of a naturally occurring haloperoxidase. But careful investigation, particularly by Butler and coworkers, showed that the vanadium-containing haloperoxidases actually catalyze the halide-assisted disproportionation of hydrogen peroxide to water and *singlet* dioxygen (with Br^-) above pH 10, or the oxidation of a halide ion X^- to the corresponding hypohalous acid HOX as in reaction 4 at lower pH. If organic substrate is present, then nucleophilic HOX

$$H_2O_2 + H^+ + X^- \overset{E}{\rightleftharpoons} H_2O + HOX \qquad (4)$$

halogenates this compound (*28*). Because its purpose is to effect halide ion oxidation, the enzyme is named after the most electronegative halide whose H_2O_2 oxidation it can catalyze; chloroperoxidases oxidize chloride, bromide, and iodide ions, for example.

Experience with iron-containing enzymes suggested that the vanadium-containing haloperoxidases should change oxidation state during catalysis, but such is not the case (*29*). Reducing the enzyme with sodium dithionite, for example, yields an inactive vanadyl(IV) enzyme, from which valuable structural information could, however, be inferred. Structural studies of the native enzyme, including a crystallographic study of a fungus-derived chloroperoxidase (*30*), indicate that the prosthetic vanadium(V) group is bound at the active site as a five- or six-coordinate complex. In the crystal structure, vanadium was directly coordinated to a nitrogen atom of the His-496 residue, while other residues contributed hydrogen bonds to the nonprotein oxygens of the V_i moiety. The vanadium-binding groups formed a distorted trigonal bipyramidal structure. X-ray absorption near-edge structure studies of the enzyme in the presence of high concentrations of H_2O_2 are consistent with vanadium(V)-peroxo adduct formation.

Steady-state and fast reaction studies carried out mainly by Wever and coworkers have established an ordered catalytic mechanism in which hydrogen peroxide binds first followed by halide (*12*). The hydrogen ion-dependence of the vanadium-containing haloenzymes indicates optimal activity in the mid-pH range. The fall-off in activity at low pH is due to disruption of vanadium-peroxo ligand binding. At high pH hydrogen peroxide begins to compete favorably for the oxidized halogen intermediate, and disproportionation begins to occur. Although bromide ion reversibly inhibits the enzyme, the kinetics pattern is pH dependent and complex.

Recently, Pecoraro and coworkers developed a group of chelated oxoperoxovanadium(V) complexes that model all three vanadium-containing haloperoxidase catalytic activities: halide oxidation, halide-assisted hydrogen peroxide disproportionation, and halogenation of organic compounds (*14*). At the heart of these model compounds is a tripodal-amine chelating agent such as nitrilotriacetic acid. Kinetics, equilibrium, and structural studies of these compounds suggest oxygen atom, rather than electron, transfer to halide ion as the molecular mechanism of halide ion oxidation by peroxide. As shown in Figure 1, an organic nucleophilic acceptor, if present, and H_2O_2 compete for the oxidized halogen species. Whether, in the haloperoxidase-catalyzed reaction, this intermediate is enzyme-bound or free; or which one of the equivalent (from an oxidation number viewpoint) species HOX, X_2, or X_3^- it is, is not yet known. Knowledge gained from the reaction pattern exhibited by these model compounds will be helpful in designing insulin-mimetic vanadium-containing therapeutic agents (*31, 32*).

Relationship between Phosphohydrolase and Haloperoxidase Enzymes. The similarity between V_i and P_i that is the basis of V_i's potent inhibition of phosphoryl transfer enzymes can be turned on its head. Active sites of enzymes binding V_i and P_i should be similar; *i.e.*, conserved. A step towards recognition of this relationship was taken first by Crans and coworkers (*33*). They noted that although vanadium derivatives can be effectors for different types of enzymes, even more widespread and effective interactions would be possible if a vanadium compound were designed to mimic as closely as possible the putative phosphoryl transition state structure. To prove their conjecture, they showed that, within a given series of vanadium derivatives, five-coordinate complexes were the most effective with the enzyme chicken intestinal alkaline phosphatase. The implication of this work is that the transition state receptor should be conserved among the enzymes that bind V_i and P_i.

These ideas were confirmed in a very interesting study by Wever and coworkers (*34*). Through database searches of amino acid sequences and crystallographically determined structures they produced amino acid alignments that, with some minor exceptions, showed amino acid residues associated with active sites of V_i-containing haloperoxidases and three families of acid phosphatases are conserved. They point out that this finding is supported by the structural resemblance of vanadate to phosphate, the loss of vanadium-containing haloperoxidase activity in phosphate-containing buffers, and that reconstitution of apo-bromoperoxidase by V_i is inhibited by phosphate (*34*). To clinch their argument that the V_i binding pocket of haloperoxidases and the active sites of phosphatases are similar, these investigators showed that the apo-form of a chloroperoxidase, that is, the V_i-depleted enzyme, could function as a phosphatase, using *p*-nitrophenyl

Downloaded by NORTH CAROLINA STATE UNIV on October 31, 2012 | http://pubs.acs.org
Publication Date: December 10, 1998 | doi: 10.1021/bk-1998-0711.ch013

Downloaded by NORTH CAROLINA STATE UNIV on October 31, 2012 | http://pubs.acs.org
Publication Date: December 10, 1998 | doi: 10.1021/bk-1998-0711.ch013

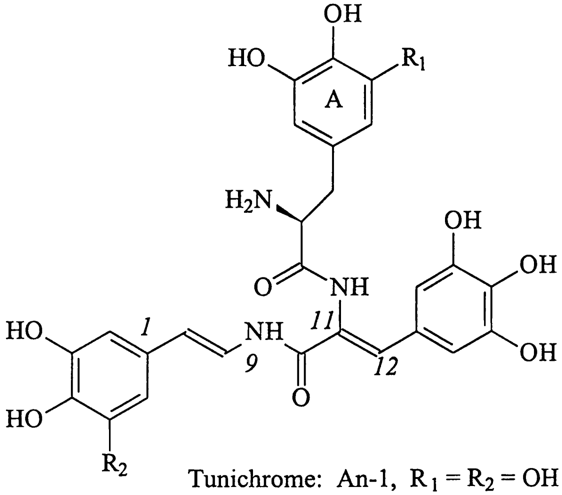

Tunichrome: An-1, $R_1 = R_2 = OH$
An-2, $R_1 = H, R_2 = OH$
An-3, $R_1 = R_2 = H$

Figure 1. Catalytic cycle for vanadium haloperoxidase enzymes. In the mechanism "L" represents a ligand which confers enzyme function to V(V) complexes or apo enzyme. Let X^- be a halide ion, then X^+ is any oxidizing halogen-containing species: HOX, X_2, X_3^- or enzyme-X^+. Note that the mechanism contains acid-base as well as oxidant-reductant steps, both of which would be catalyzed by enzyme. (Adapted from ref. 14.)

phosphate as substrate. These results have important consequences for the design of vanadium compounds with therapeutic applications (*35*).

Mysteries of Vanadium Accumulation in Tunicates

Downloaded by NORTH CAROLINA STATE UNIV on October 31, 2012 | http://pubs.acs.org
Publication Date: December 10, 1998 | doi: 10.1021/bk-1998-0711.ch013

Eighty-six years have elapsed since Henze first reported that certain tunicate blood cells accumulate vanadium prodigiously, and science still does not know how or why they perform this feat (*36*). Tunicates, commonly called sea squirts, are relatively inconspicuous but ubiquitous components of marine fauna. These immobile colonial (size: 1-2 mm) or solitary (size: 10-20 cm) animals are found in all oceans at all depths examined. They are filter-feeders, ingesting suspended microorganisms and organic detritus from which they obtain nutrients and possibly vanadium. However, it has been shown that tunicates can extract vanadium, present in sea water as 35 nM V_i, directly from the aqueous phase (*37*), and concentrate it in specialized blood cells to levels as high as 350 mM (*38*).

Tunicate blood, especially of the order Ascidiacea, is light yellow to yellow-green in color and contains a large number of different blood cell types (*39*). Two of the four spherical (10-12 μ diameter) cells of the vacuolated type, morula (containing 12-14 vacuoles) and signet ring (containing one large vacuole) cells, comprise a majority of blood cells in a given ascidian specimen. For example, blood cell compositions of both *Ascidia nigra* (*40*) and *A. ceratodes* (*41*) are in the range 65-75% morula and signet ring, depending on individual specimen, condition, season, and environmental stress. Some ascidians are vanadium-accumulators but not all tunicates accumulate vanadium, some are iron accumulators, first discovered by Endean in 1953 (*42*). Within the order Ascidiacea there is a correlation between taxonomy and accumulated transition metal and vanadium oxidation number, either +3 or +4 (*38, 43, 44*).

Under an optical microscope, the most noticeable blood cell is the morula. It is mulberry-like in appearance and a bright yellow in color. It was known that solutions of metal ions and metal ion complexes, particularly hemoglobin, are vividly colored. Therefore, in early discussions of tunicate blood cell physiology and vanadium content, a connection between morula cells, their coloration and vanadium content was postulated (*45*). In later studies, this connection unraveled.

After fractionating blood cell lysates of *A. ceratodes* (*43*) and *A. nigra* and *Ciona intestinalis* (*46*), vanadium and the yellow chromogen could be separated from one another. Likewise, a yellow chromogen was separated from iron after fractionating *Molgula manhattensis* blood cell lysates (*46*). There was no connection between morula cells, their coloration, and vanadium content. The yellow color-conferring chromogen, named tunichrome (*47*), was carefully isolated, purified, and its structure determined by Nakanishi and coworkers (*48*). The name actually stands for a family of yellow, polyphenolic tripeptides as shown in Figure 2. Both vanadium and tunichrome can be found in the morula cells of *A. nigra* where it constitutes up to 50% of the cell's dry weight (*40*). Tunichromes have been found in many species collected from Australian (*49*) and North American ocean waters; a European, North Atlantic Ocean ascidian, *Phallusia mamillata*, yielded dihydrotunichromes, *i.e.*, tunichrome An-1 saturated at the C-*11*, -*12* olefin.

To find out which cell types contain vanadium, researchers used primarily three methods: fluorescence-activated cell sorting (flow cytometry) followed by atomic absorption vanadium analysis (*40*), electron microscopy with scanning X-ray dispersion for vanadium analysis (*51*), and density gradient cell sorting followed by neutron-activation vanadium analysis (*38*). It was then discovered that vanadium was distributed among different blood cells, and in most species was more highly concentrated in the signet ring cell than in the morula cell (*51*). Whether the vacuolated, vanadium-containing blood cells are related to one another as they would be if they were stages in an ontogenic sequence, or are unrelated end stages of parallel development is not known at this time (*52*).

Downloaded by NORTH CAROLINA STATE UNIV on October 31, 2012 | http://pubs.acs.org
Publication Date: December 10, 1998 | doi: 10.1021/bk-1998-0711.ch013

Modeling Vanadium Accumulation in Tunicate Blood Cells.

Constructing a realistic model of vanadium accumulation in tunicate blood cells requires knowledge of vanadium uptake dynamics, *in vivo* vanadium distribution, and the nature of the vanadium receptor site. Primarily, three species have been investigated to gather this information: *A. ceratodes* (*53*), *A. nigra* (*54*), and *A. gemmata* (*55*). The results of these studies have been recently reviewed (*56*). Here, we present a synthesis.

One mode of vanadium accumulation is from sea water. It is important to realize that naturally-occurring vanadium in sea water is an anion, which is tolerated much better than a cation by a biological system. Thus, V_i appears to be transported from sea water to blood plasma without benefit of a protein carrier, *e.g.*, a transferrin-like carrier. The concentration of V_i in the plasma is low; transport into the cell is via facilitated diffusion using phosphate channels. Intracellular incorporation is a two-step process. In a rapid first step V(V) is reduced to V(IV). In a slower second step vanadium is incorporated into the accumulation site, this step may involve further reduction to V(III). A second mode of accumulation is transient storage in a tissue other than blood, followed by one or both of two pathways. One pathway is release of the transiently stored vanadium to the blood plasma, from which accumulation proceeds in the same manner as direct uptake from sea water. A second pathway is hematopoiesis (production and proliferation) of vanadium-containing blood cells from the transient storage tissue.

Extensive chemical tests of reactions between a tunichrome from *M. manhattensis* (Mm-1) and vanadium ions in acidic and neutral media indicate that reduction does not proceed appreciably beyond V(IV) (*57*). When catechol was

Downloaded by NORTH CAROLINA STATE UNIV on October 31, 2012 | http://pubs.acs.org
Publication Date: December 10, 1998 | doi: 10.1021/bk-1998-0711.ch013

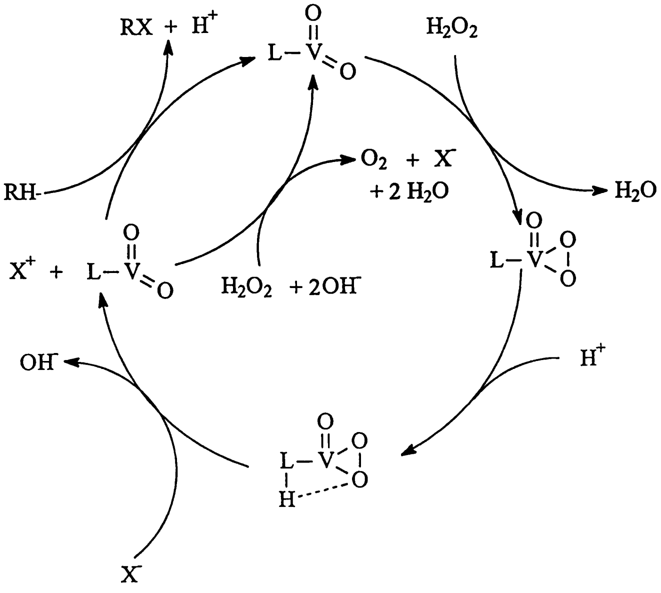
RX + H⁺
O
L—V
O
H₂O₂
RH-
O₂ + X⁻
+ 2 H₂O
H₂O
O
X⁺ + L—V
O
H₂O₂ + 2OH⁻
O
O
L—V
O
OH⁻
H⁺
O
O
L—V
O
H
X⁻

Figure 2. The tunichrome family of A. nigra, a vanadium-accumulator. In the tunichrome family of M. manhattensis, an iron-accumulator, the ring labeled "A" is replaced by glycine. In tunichromes of P. mamillata, a vanadium-accumulator, linkage C-11, -12 is saturated. (Adapted from ref. 36.)

used as a reductant, the V(IV) so generated was complexed by unreacted catechol; Mm-1 was even more effective at complexing and therefore protecting reduced vanadium. In addition to tunichromes, other biogenic reductants were tested for their ability to reduce and complex V(IV) or V(III) and the tunichrome-generated products examined by X-ray absorption spectroscopy (XAS) to characterize the precipitated products (*58*). Although the major products resulting from tunichrome An-1 reduction are V(IV) complexes, at least 9% of the product vanadium was V(III). If tunichrome pays a role in accumulation, its presence in, for example, the signet ring cell would go undetected, because the current assay method cannot detect oxidized tunichrome.

Unprotected V(IV) or V(III) would be unstable in media of neutral or slightly acidic pH. Indeed, while cytosolic pH measurements of unsorted tunicate blood cells appear to lie in this pH range (*59*), the actual, intimate environment of accumulated vanadium appears to be much more acidic (*60*). Electron microscopy suggests that accumulated vanadium may be stored in the form of granular deposits on cell membranes. Therefore, models of vanadium accumulation based on this data do not require direct intervention of proteins, only indirect intervention such as in the facilitated diffusion of vanadium as V_i through anionic channels. The model requires a biogenic reductant and complexing agent such as tunichrome.

A different modeling approach incorporates active participation by proteins following evidence collected along different lines of investigation. It was shown that an inhibitor of vacuolar-type H-ATPases altered the autonomous fluorescence of signet ring cells, but not of morula cells (*61*). In another experiment, monoclonal antibodies against putative vanadium-binding proteins have been raised and applied to sorted tunicate blood cells (*62*). The results indicated that a small fraction of the accumulated vanadium is bound to protein. In this protein participation model, tissue reduction of V_i to V(III) or V(IV) occurs and the reduced vanadium is transported to the cell from the plasma. The reduced vanadium species would then enter the cell and vacuole; perhaps as protons are enzymatically pumped out. Within the vacuole a protein receptor would bind intracellular vanadium. Whether H-pump enzyme activity and protein complexation are involved in vanadium accumulation is currently being investigated (*63*).

Acknowledgment

The author thanks the editors, Debbie Crans and Alan Tracey, for the invitation to contribute to this monograph and for stimulating suggestions about and discussions of vanadium biochemistry.

Downloaded by NORTH CAROLINA STATE UNIV on October 31, 2012 | http://pubs.acs.org
Publication Date: December 10, 1998 | doi: 10.1021/bk-1998-0711.ch013

Literature Cited

1. Faulkner-Hudson, T. G. *Vanadium Toxicology and Biological Significance* Elsevier Publishing Company: Amsterdam, 1964, pp 1-140.
2. Cantley, L. C., Jr.; Josephson, L., Warner, R., Yanagisawa, M., Lechene, G., Guidotti, G., *J. Biol. Chem.* **1977**, *252*, 7421-7423.
3. Beaugé, L.; Glynn, I. M. *Nature*, **1978**, *272*, 551-552.
4. Nechay, B. R.; Saunders, J. P. *J. Environ. Path. and Toxicol.* **1978**, *2*, 247-262.
5. Quist, E. E.; Hokin, L. E. *Biochim. Biophys. Acta* **1978**, *511*, 202-212.
6. *Chemistry, Biochemistry and Therapeutic Application of Vanadium Compounds*; Crans, D. C.; Tracey, A. S., Eds; ACS Symposium Series ; American Chemical Society: Washington, DC, 1998.
7. Choate, G.; Mansour, T. E. *J. Biol. Chem.* **1979**, *254*, 11457-11462.
8. Smith, M. J.; Ryan, D. E., Nakanishi, K.; Frank, P., Hodgson, K. O. In *Vanadium and Its Role in Life*; Sigel, H.; Sigel, A., Eds; Metal Ions in Biological Systems; Marcel Dekker, Inc., New York, NY, 1995, Vol 31; pp 423-490.
9. Koch, E., Kneifel, H., Bayer, E. *Z. Naturforsch.* **1972**, *42C*, 873-
10. Willsky, G. R.; Kostyniak, P. J. In *Chemistry, Biochemistry and Therapeutic Application of Vanadium Compounds*; Crans, D. C.; Tracey, A. S., Eds; ACS Symposium Series ; American Chemical Society: Washington, DC, 1998; pp 278-296.
11. Nielsen, F. H.; In *Chemistry, Biochemistry and Therapeutic Application of Vanadium Compounds*; Crans, D. C.; Tracey, A. S., Eds; ACS Symposium Series ; American Chemical Society: Washington, DC, 1998; pp 297-307.
12. Vilter, H. In *Vanadium and Its Role in Life*; Sigel, H.; Sigel, A., Eds; Metal Ions in Biological Systems; Marcel Dekker, Inc., New York, NY, 1995, Vol 31; pp 325-362.
13. Eady, R. R. In *Vanadium and Its Role in Life*; Sigel, H.; Sigel, A., Eds; Metal Ions in Biological Systems; Marcel Dekker, Inc., New York, NY, 1995, Vol 31; pp 363-406.
14. Colpas, G. J.; Hamstra, B. J.; Kampf, J. W.; Pecoraro, V. L. *J. Am. Chem. Soc.* **1996**, *118*, 3469-3478.
15. Cantley, L. C., Jr.; Cantley, L. G.; Josephson, L. *J. Biol. Chem.* **1978**, *253*, 7361-7368.
16. Boyd, D. W.; Kustin, K.; Niwa, M. *Biochim. Biophys. Acta* **1985**, *827*, 472-475.
17. Stankiewicz, P. J.; Tracey, A. S. In *Vanadium and Its Role in Life*; Sigel, H.; Sigel, A., Eds; Metal Ions in Biological Systems; Marcel Dekker, Inc., New York, NY, 1995, Vol 31; pp 249-286.

Downloaded by NORTH CAROLINA STATE UNIV on October 31, 2012 | http://pubs.acs.org
Publication Date: December 10, 1998 | doi: 10.1021/bk-1998-0711.ch013

18. Stankiewicz, P. J.; Tracey, A. S.; Crans, D. C. In *Vanadium and Its Role in Life*; Sigel, H.; Sigel, A., Eds; Metal Ions in Biological Systems; Marcel Dekker, Inc., New York, NY, 1995, Vol 31; pp 287-324.
19. Gibbons, I. R.; Cosson, M. P.; Evans, J. A.; Gibbons, B. H.; Houck, B.; Martinson, K. H.; Sale, W. S.; Tang, W.-J. *Proc. Natl. Acad. Sci. USA* **1978**, *75*, 2220-2224.
20. North, P.; Post, R. L. *J. Biol. Chem.* **1984**, *259*, 4971-4978.
21. Lindquist, R. N.; Lynn, J. L., Jr.; Lienhard, G. E. *J. Am. Chem. Soc.* **1973**, *96*, 8762-8768.
22. Stryer, L. *Biochemistry, Third Ed.*; W. H. Freeman and Company: New York, NY, 1988, pp 1-1089.
23. Leon-Lai, C. H.; Gresser, J. J.; Tracey, A. S. *Can J. Chem.* **1996** *74*, 38-48.
24. Alber, T.; Gilbert, W. A., Ponzi, D. R.; Petsko, G. A. In *Mobility and Function in Proteins and Nucleic Acids*; Porter, R.; O'Connor, M. Whelan, J., Eds.; Ciba Foundation Symposium 93; Pitman Books Ltd: London, 1983; pp 4-18.
25. Abeles, R. H.; Frey, P.; Jencks, W. P. *Biochemistry*; Jones and Bartlett Publishers: Boston, MA, 1992, pp 1-807.
26. Markus, S.; Priel, Z.; Chipman, D. M. *Biochemistry* **1989**, *28*, 793-799.
27. Faller, L. D.; Rabon, E.; Sachs, G. *Biochemistry* **1983**, *22*, 4676-4685.
28. Butler, A.; Walker, J. V. *Chem. Rev.* **1993**, *93*, 1937-1944.
29. Wever, R.; Kustin, K. *Adv. Inorg. Chem.* **1990**, *35*, 81-115.
30. Messerschmidt, A.; Wever, R. *Proc. Natl. Acad. Sci. USA* **1996**, *93*, 392-396.
31. Slebodnick, C.; Gillis, M. E.; Hamstra, B. J.; Pecoraro, V. L. In *Chemistry, Biochemistry and Therapeutic Application of Vanadium Compounds*; Crans, D. C.; Tracey, A. S., Eds; ACS Symposium Series ; American Chemical Society: Washington, DC, 1998; pp 157-167.
32. Butler, A.; Baldwin, A. Simpson, M. In *Chemistry, Biochemistry and Therapeutic Application of Vanadium Compounds*; Crans, D. C.; Tracey, A. S., Eds; ACS Symposium Series ; American Chemical Society: Washington, DC, 1998; pp 202-215.
33. Crans, D. C.; Keramidas, A. D.; Drouza, C. *Phosphorus, Sulfur, and Silicon* **1996**, *109-110*, 245-248.
34. Hemrika, W.; Renirie, R.; Dekker, H. L.; Barnett, P.; Wever, R. *Proc. Natl. Acad. Sci. USA* **1997**, *94*, 2145-2149.
35. Wever, R.; Hemrika, W.; Renirie, R.; Barnett, P.; Messerschmidt, A.; Dekker, H. In *Chemistry, Biochemistry and Therapeutic Application of Vanadium Compounds*; Crans, D. C.; Tracey, A. S., Eds; ACS Symposium Series ; American Chemical Society: Washington, DC, 1998; pp 216-227.

Downloaded by NORTH CAROLINA STATE UNIV on October 31, 2012 | http://pubs.acs.org
Publication Date: December 10, 1998 | doi: 10.1021/bk-1998-0711.ch013

36. Kustin, K.; Robinson, W. E.; Smith, M. J. *Invert. Repro. Develop.* **1990**, *17*, 129-139.

37. Kustin, K.; Ladd, K. V.; McLeod, G. *J. Gen. Physiol.* **1975**, *65*, 315-328.

38. Michibata, H. *Zool. Sci.* **1996**, *13*, 489-502.

39. Wright, R. K. In *Invertebrate Blood Cells*; Ratcliffe, N. A.; Rowley, A. F., Eds.; Academic Press: London, Vol 2, 1966, pp 565-626.

40. Oltz, E. M.; Pollack, S.; Delohery, T.; Smith, M. J.; Ojika, M.; Lee, S.; Kustin, K.; Nakanishi, K. *Experientia* **1989**, *45*, 186-190.

41. Biggs, W. R.; Swinehart, J. H. *Experientia* **1979**, *35*, 1047-1049.

42. Endean, R. *Nature, London* **1953**, *172*, 123.

43. Swinehart, J. H.; Biggs, W. R.; Halko, D. J.; Schroeder, N. C. *Biol Bull.* **1974**, *146*, 302-312.

44. Hawkins, C. J. Kott, P.; Parry, D. L., Swinehart, J. H. *Comp. Biochem. Physiol.* **1983**, *76B*, 555-558.

45. Goodbody, I. *Adv. Mar. Biol.* **1974**, *12*, 1-149.

46. Macara, I. G.; McLeod, G. C.; Kustin, K. *Comp. Biochem. Physiol.* **1979**, *63B*, 299-302.

47. Macara, I. G.; McLeod, G. C.; Kustin, K. *Biochem. J.* **1979**, 457-465.

48. Oltz, E. M.; Bruening, R. C.; Smith, M. J.; Kustin, K.; Nakanishi, K. *J. Am. Chem. Soc.* **1988**, *110*, 6162-6172.

49. Parry, D. L.; Brand, S. G.; Kustin, K. *Bull. Mar. Sci.* **1992**, *50*, 302-306.

50. Bayer, E.; Schiefer, G.; Waidelich, D.; Scippa, S.; de Vincentiis, M. *Angew. Chem. Int. Ed. Engl.* **1992**, *31*, 52-54.

51. Botte, L. S.; Scippa, S.; de Vincentiis, M. *Experientia* **1979**, *35*, 1228-1230.

52. Ballarin, L.; Cima, F.; Sabbadin, A. *Boll. Zool.* **1993**, *60*, 19-24.

53. Anderson, D. H.; Berg, J. R.; Swinehart, J. H. *Comp. Biochem. Physiol.* **1991**, *99A*, 151-158.

54. Dingley, A. L.; Kustin, K.; Macara, I. G.; McLeod, G. *Biochim. Biophys. Acta* **1981**, *649*, 493-502.

55. Michibata, J.; Seki, Y.; Hirata, J.; Kawamura, M.; Iwai, K.; Iwata, R.; Ido, T. Zool. Sci. **1991**, *8*, 447-452.

56. Kustin, K.; Robinson, W. E. In *Vanadium and Its Role in Life*; Sigel, H.; Sigel, A., Eds; Metal Ions in Biological Systems; Marcel Dekker, Inc., New York, NY, 1995, Vol 31; pp 511-542.

57. Ryan, D. E.; Grant, K. B.; Nakanishi, K. *Biochemistry* **1996**, *35*, 8640-8650.

58. Ryan, D. E.; Grant, K. B.; Nakanishi, K.; Frank, P.; Hodgson, K. O. **1996**, *35*, 8651-8661.

59. Brand, D. G.; Hawkins, C. J.; Parry, D. L. *Inorg. Chem.* **1987**, *26*, 627-629.

Downloaded by NORTH CAROLINA STATE UNIV on October 31, 2012 | http://pubs.acs.org
Publication Date: December 10, 1998 | doi: 10.1021/bk-1998-0711.ch013

60. Frank, P.; Carlson, R. M. K.; Hodgson, K. O. *Inorg. Chem.* **1986**, *25*, 470-478.
61. Uyama, T.; Moriyama, Y.; Futai, M.; Michibata, H. *J. Exp. Zool.* **1994**, *270*, 148-154.
62. Uyama, T.; Nishikata, T.; Satoh, N.; Michibata, H. *J.Exp. Zool.* **1991**, *259*, 196-201.
63. Michibata, H. In *Chemistry, Biochemistry and Therapeutic Application of Vanadium Compounds*; Crans, D. C.; Tracey, A. S., Eds; ACS Symposium Series ; American Chemical Society: Washington, DC, 1998; pp 248-258.

Downloaded by NORTH CAROLINA STATE UNIV on October 31, 2012 | http://pubs.acs.org
Publication Date: December 10, 1998 | doi: 10.1021/bk-1998-0711.ch013

Chapter 14

Chloroperoxidase from *Curvularia inaequalis*: X-ray Structures of Native and Peroxide Form Reveal Vanadium Chemistry in Vanadium Haloperoxidases

Albrecht Messerschmidt[1], Lars Prade[1], and Ron Wever[2]

[1]Max-Planck-Institute für Biochemie, Am Klopferspitz 18 A, D-82152, Martinsried bei München, Germany
[2]E. C. Slater Institute, University of Amsterdam, Plantage Muidergracht 12, 1018 TV Amsterdam, The Netherlands

Downloaded by YORK UNIV on October 31, 2012 | http://pubs.acs.org
Publication Date: December 10, 1998 | doi: 10.1021/bk-1998-0711.ch014

Crystal structures of different forms of the vanadium-containing chloroperoxidase from the fungus *Curvularia inaequalis* have been determined. The 2.03 Å crystal structure (R = 19.7%) of the native enzyme reveals the geometry of the intact catalytic vanadium center. The vanadium is bound as hydrogen vanadate(V). It is coordinated by four nonprotein oxygen atoms and one nitrogen (NE2) atom from histidine 496 in a trigonal bipyramidal fashion. Three oxygens are in the equatorial plane and the fourth oxygen and the nitrogen are at the apexes of the bipyramid. In the 2.10 Å crystal structure (R = 20.0%) of the azide enzyme complex the azide directly coordinates to the vanadium replacing the apical vanadium oxygen ligand. In the 2.24 Å crystal structure (R = 17.7%) of the peroxide derivative the peroxide is bound to the vanadium in an η^2-fashion after the release of the apical oxygen ligand. The vanadium is coordinated also by 4 non-protein oxygen atoms and one nitrogen (NE2) from histidine 496. The coordination geometry around the vanadium is that of a distorted tetragonal pyramid with the two peroxide oxygens, one oxygen and the nitrogen in the basal plane and one oxygen in the apical position. The 2.50 Å crystal structure (R = 17.1%) of apo CPO shows that a water molecule is present at the position of the vanadate cofactor. Tungstate is bound in a similar fashion as the hydrogen vanadate(V) group in the native form as determined from the 2.30 Å crystal structure of tungstate CPO (R = 16.2 %). Amino acid sequence comparisons show that the fold of the C terminal halves of CPO and of vanadium containing haloperoxidases of marine algae and the architecture of their vanadium binding sites are very similar. A mechanism for the catalytic cycle has been proposed based on these X-ray structures and kinetic data.

In Vanadium Compounds; Tracey, A., et al.;
ACS Symposium Series; American Chemical Society: Washington, DC, 1998.

The bioinorganic chemistry of vanadium has been advanced by the recent first x-ray structure determination of a vanadium containing protein, a chloroperoxidase from the fungus *Curvularia inaequalis* (*1*). This chloroperoxidase (CPO) belongs to a group of vanadium containing haloperoxidases that oxidize halides (Cl^-, Br^-, I^-) in the presence of hydrogen peroxide to the corresponding hypohalous acids according to :

$$H_2O_2 + X^- + H^+ \rightarrow H_2O + HOX.$$

The hypohalous acid, HOX, will react to a diversity of halogenated products if a convenient nucleophilic acceptor is present. The vanadium haloperoxidases are isolated primarily from marine algae, although they have been identified and characterized from a terrestrial lichen and fungi (*2-5*). Many of the organohalogens generated by these enzymes are biocidal and thus may provide defense functions. The marine haloperoxidases (for a review see Butler and Walker (*6*)) are widespread in the marine environment and are probably responsible for the formation of huge amounts of organohalogens like bromoform which are released to the atmosphere. The bromoperoxidase (BPO) from the seaweed *Ascophyllum nodosum* has been best characterized. The molecular mass of the monomer is ca. 65000 which is comparable to that of the monomer of the CPO of this study. BPO has been crystallized some times ago (*7*) and the crystal structure analysis is almost finished (Schomburg, D., University of Köln, personal communication, 1997.) but not published yet. Another haloperoxidase from the seaweed *Corallina officinalis* has been crystallized as well (*8*). The vanadium bromoperoxidases have been studied in great detail using a variety of biophysical techniques (*9*) including EXAFS (*10, 11*) and ESEEM (*12, 13*). Vanadium(IV) or (III) states have not been observed by EPR or K-edge x-ray studies in the presence of substrates or during turnover and the reduced enzyme is inactive. Apparently the redox state of the metal does not change during catalytic turnover and a model has been suggested (*13*) in which the vanadium site functions by binding hydrogen peroxide to yield an activated peroxo-intermediate which is able to react with bromide to produce HOBr. Similar models have now been proposed (*14, 15*) for a number of metal-catalyzed oxidations of bromide by hydrogen peroxide.

A detailed kinetic study of the formation of HOCl by the chloroperoxidase (*16*) revealed many similarities with the kinetics of the vanadium bromoperoxidase. Azide was found to be a weak inhibitor for the vanadium-containing marine bromoperoxidase (*17*).

Overall Protein Structure of CPO from *Curvularia inaequalis*

The crystal structure of CPO from *Curvularia inaequalis* in the complex with azide at an resolution of 2.1 Å (*1*) and of the native form at a resolution of 2.03 Å (*18*) have been published and revealed the architecture of the protein part and the coordination of the vanadium metal center. The structure solved by multiple

Downloaded by YORK UNIV on October 31, 2012 | http://pubs.acs.org
Publication Date: December 10, 1998 | doi: 10.1021/bk-1998-0711.ch014

isomorphous replacement (MIR) techniques reveals one molecule per asymmetric unit of the trigonal crystals (space group *R*3 with lattice constants $a = b = 131.69$ Å, $c = 112.97$ Å, $\alpha = \beta = 90^\circ$, $\gamma = 120^\circ$). The molecule has an overall cylindrical shape with a length of about 80 Å and diameter of 55 Å (Fig. 1). The molecules are arranged in the crystals as trimers around the crystallographic threefold axis. The secondary structure, which was analyzed with the program DSSP (*20*), is mainly helical (about 44% of the atomic model) consisting of 20 helices, a small part of β-structures (6 short β-strands, pairwise arranged as three antiparallel β-ladders) and the rest of extended strand and loop regions (Fig. 2). Two four-helix bundles (α-helices B, C, E, F and α-helices K, L, N, O) are the main structural motifs of the tertiary structure and are spatially related by a rotation of about 180° around an axis perpendicular to the sketch plane in Fig. 2. These helices are between 14 and 31 residues long. α-Helices G and S are each packed against one of the four-helix bundles and α-helices I and J are located on top of the four-helix bundles and approximately perpendicular to their helical axes. There are 8 short helices found in connecting segments. Four of them are α-helical (H, M, P, Q in Fig. 2) and the other four are 3_{10}-helices (A, D, R, T in Fig. 2). At a first glance, the compact α-helical structure of CPO resembles those of the R2 subunit of ribonucleotide reductase from *Escherichia coli* (*21*) and the first domain of the α-subunit and the β-subunit of the hydroxylase protein of methane monooxygenase from *Methylococcus capsulatus* (Bath) (*22*), both non-heme di-iron proteins. However, the main motif in both non-heme di-iron proteins is an eight-helix bundle with a special topological sequence and arrangement of the α-helices different from that found here. Recently, the crystal structure of a bacterial bromoperoxidase (*23*) has been determined. This enzyme lacks cofactors and shows the general topology of the α/β hydrolase fold. Apparently, the vanadium chloroperoxidase and the bacterial bromoperoxidase lack any structural similarities and are very different enzymes.

Vanadium Binding Site

The vanadium center is located on top of the second four-helix bundle (Fig. 1) and the residues forming the metal binding site are coming from helices J, L, N and O and from turns 290-294, 355-363, 395-406 and 492-502 (Fig. 3). Thus, all residues building up the metal center are from the C-terminal half of the molecule. The difference electron density map of the native form at the vanadium site (Figure 4) as reported in (*18*) obtained by refining the model of the azide form without the vanadate and azide groups against the observed structure factors of the native form clearly shows the vanadium bound to 4 oxygen atoms forming an orthovanadate group and to the NE2 nitrogen atom of histidine 496. The vanadium coordination geometry is trigonal bipyramidal with 3 nonprotein oxygen atoms in the equatorial plane (bond lengths about 1.65 Å), one nonprotein apical oxygen atom (bond length 1.93 Å) and the other apical nitrogen atom of histidine 496 (bond length 1.96 Å). The

Downloaded by YORK UNIV on October 31, 2012 | http://pubs.acs.org
Publication Date: December 10, 1998 | doi: 10.1021/bk-1998-0711.ch014

Downloaded by YORK UNIV on October 31, 2012 | http://pubs.acs.org
Publication Date: December 10, 1998 | doi: 10.1021/bk-1998-0711.ch014

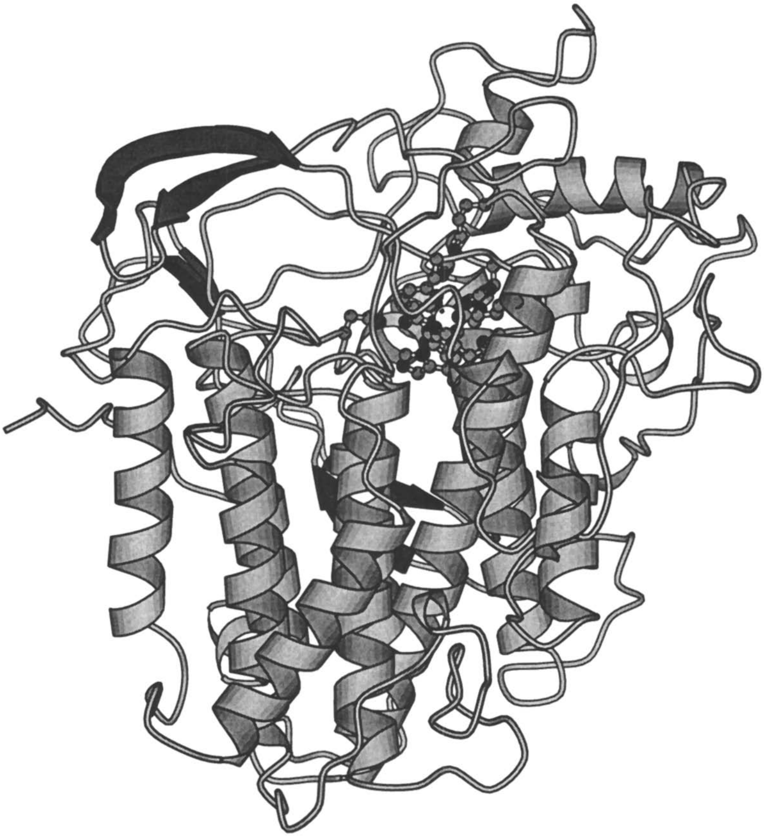

Fig. 1. Ribbon-type representation of the CPO molecule (MOLSCRIPT (*19*)).

Downloaded by YORK UNIV on October 31, 2012 | http://pubs.acs.org
Publication Date: December 10, 1998 | doi: 10.1021/bk-1998-0711.ch014

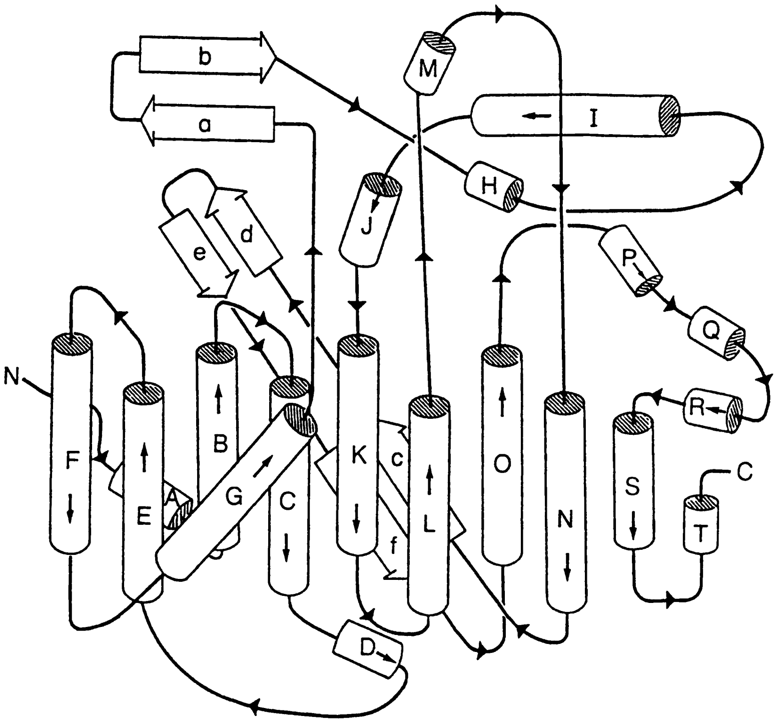

Fig. 2. Schematic drawing of the secondary structure elements of CPO. All helices are drawn as cylinders; β-strands are depicted as arrows. The N and C termini are indicated.

Downloaded by YORK UNIV on October 31, 2012 | http://pubs.acs.org
Publication Date: December 10, 1998 | doi: 10.1021/bk-1998-0711.ch014

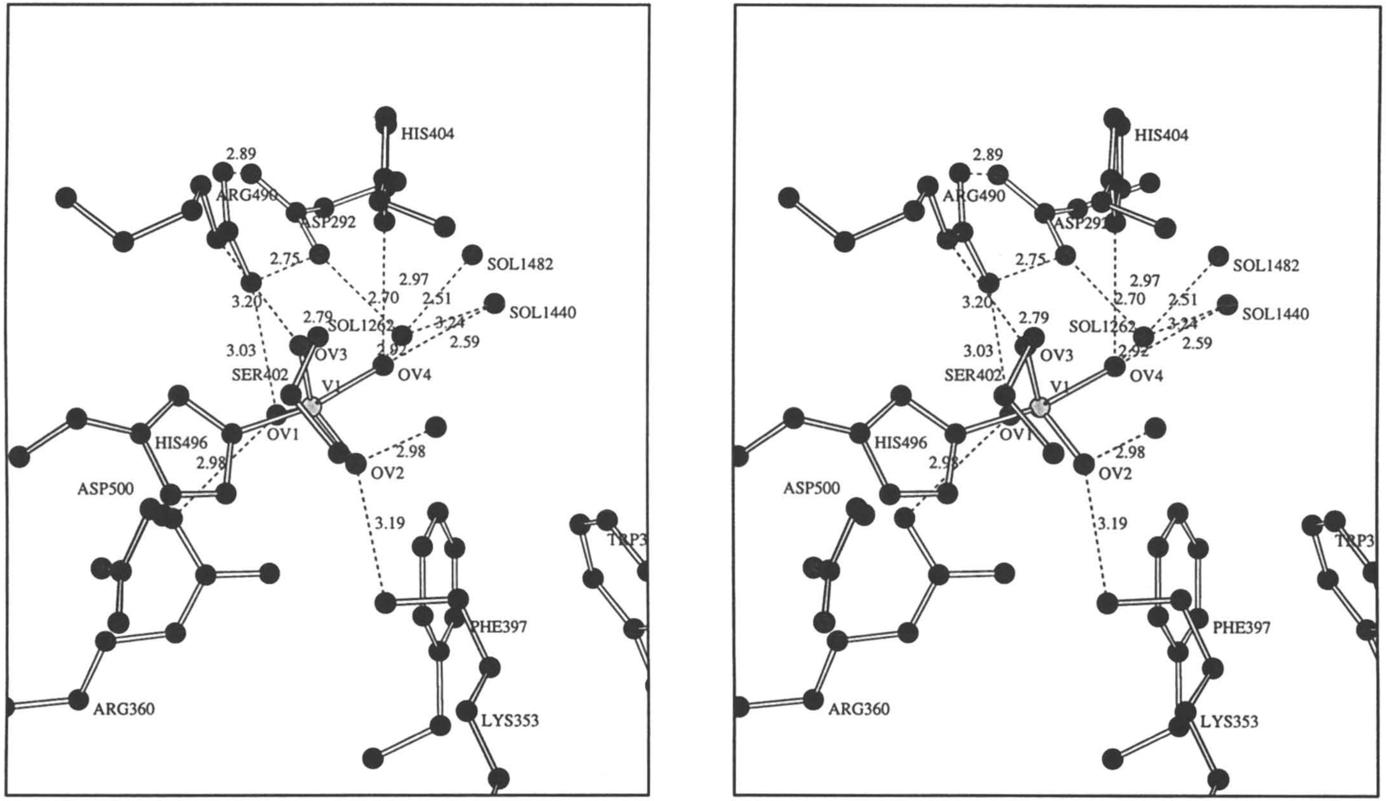
HIS404
2.89
ARG490
ASP292
2.75
2.97
SOL1482
3.20
2.70
2.51
SOL1440
2.79
SOL1262
3.24
2.59
3.03
OV3
2.92
SER402
V1
OV4
HIS496
OV1
2.98
2.98
ASP500
OV2
3.19
TRP3
PHE397
ARG360
LYS353

Fig. 3. Vanadium binding site of the native form of CPO with hydrogen bond pattern (MOLSCRIPT (*19*)).

Downloaded by YORK UNIV on October 31, 2012 | http://pubs.acs.org
Publication Date: December 10, 1998 | doi: 10.1021/bk-1998-0711.ch014

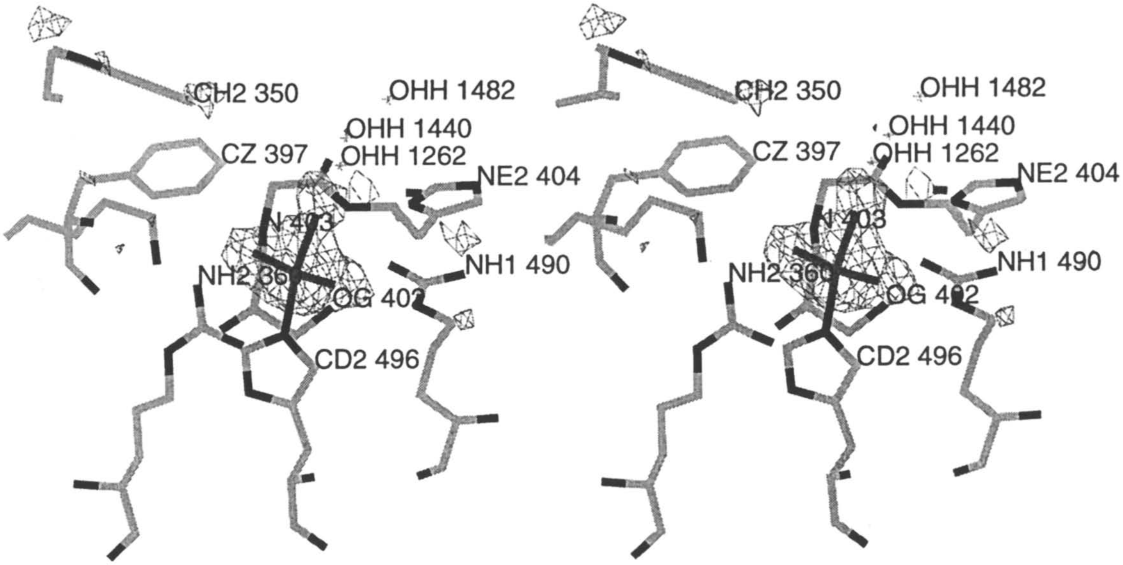
CH2 350
OHH 1482
OHH 1440
CZ 397
OHH 1262
NE2 404
N 403
NH1 490
NH2 360
OG 402
CD2 496
CH2 350
OHH 1482
OHH 1440
CZ 397
OHH 1262
NE2 404
N 403
NH1 490
NH2 360
OG 402
CD2 496

Fig. 4. Difference electron density map of the native form of CPO around the vanadium binding site contoured at 3.0 σ. The difference electron density for the hydrogen orthovanadate(V) is the strongest feature in the whole map.

bond length of the apical oxygen OV4 to the vanadium is with 1.93 Å in the range of an OH ligand, indicating that the VO_4 group is bound as hydrogen vanadate(V). The negative charge of the hydrogen vanadate(V) group is compensated by hydrogen bonds to surrounding positively charged or hydrophilic protein functions. Oxygen OV1 of the VO_4 group makes hydrogen bonds to nitrogens NE1 of Arg360 (2.98 Å) and NE2 of Arg490 (3.03 Å), oxygen OV2 to nitrogen NZ of Lys353 (3.19 Å) and nitrogen N of Gly403 (2.98 Å), oxygen OV3 to oxygen OG of Ser402 (2.79 Å) and nitrogen NE of Arg490 (3.20 Å). The apical oxygen OV4 forms three hydrogen bonds, two to water molecules (SOL 1440, 2.59 Å; SOL 1262, 2.92 Å), one to nitrogen ND1 of histidine 404 (2.97 Å). The latter one seems to be important because histidine 404 has been identified as being necessary for the catalytic activity (see (*1*)). Binding of peroxide is inhibited when histidine 404 is doubly protonated.

In the azide CPO complex (the crystallization buffer contained 2 mM azide for this crystal form), the azide coordinates directly to the vanadium replacing the apical oxygen atom OV4. A water molecule from solvent is hydrogen bonded to the azide nitrogen atom N1 which coordinates to the vanadium.

The binding site for the hydrogen-vanadate(V) is a pocket preformed by the protein which is located at the end of a broad channel filled by solvent molecules. This channel supplies good access and release for the substrates and products of the enzymatic reaction. One contiguous half of its surface is mainly hydrophobic with Pro47, Pro211, Trp350, Phe393, Pro395, Pro396 and Phe397 as contributing side chains. The other half is predominantly polar with several main chain carbonyl oxygens and the ion pair Arg490 - Asp292. It is intriguing that the vanadium(V) is bound directly as hydrogen-vanadate(V) with one immediate protein ligand only.

Downloaded by YORK UNIV on October 31, 2012 | http://pubs.acs.org
Publication Date: December 10, 1998 | doi: 10.1021/bk-1998-0711.ch014

Peroxide Form of CPO

The peroxide complex as reported in (*18*) was produced by soaking the crystals in mother liquor [2.0 M $(NH_4)_2SO_4$ in 0.1 M Tris-H_2SO_4, pH 8.0], containing 20 mM H_2O_2, for two hours. The X-ray measurements were done on a Hendrix/Lentfer X-ray image-plate system (Mar-Research, Hamburg, Germany) mounted on a Rigaku rotating anode generator operated at 5.4 kW ($\lambda = CuK_\alpha = 1.5418$ Å). The peroxide crystals were measured at 100 K. For the cryo-measurement the peroxide soaked crystals were brought into a cryo-buffer (20 mM peroxide, 1.7 M $(NH_4)_2SO_4$ in 0.1 M Tris-H_2SO_4, pH 8.0, 30.1% glycerol), transferred into a cryo-loop, shock frozen and kept in a stream of evaporating liquid nitrogen using a cryo-device (Vectotherm, Karlsruhe) mounted on the image-plate system. The peroxide derivative diffracts to 2.24 Å resolution with satisfying data completeness (83.8 %). The crystal structure was solved by difference Fourier techniques using the phases of the isomorphous native form and refined to a crystallographic R-factor of 17.7% (*18*).

The difference electron density map of the peroxide form at the vanadium site reported in (*18*) is shown in Fig. 5. The phases used for the calculation of this map

Downloaded by YORK UNIV on October 31, 2012 | http://pubs.acs.org
Publication Date: December 10, 1998 | doi: 10.1021/bk-1998-0711.ch014

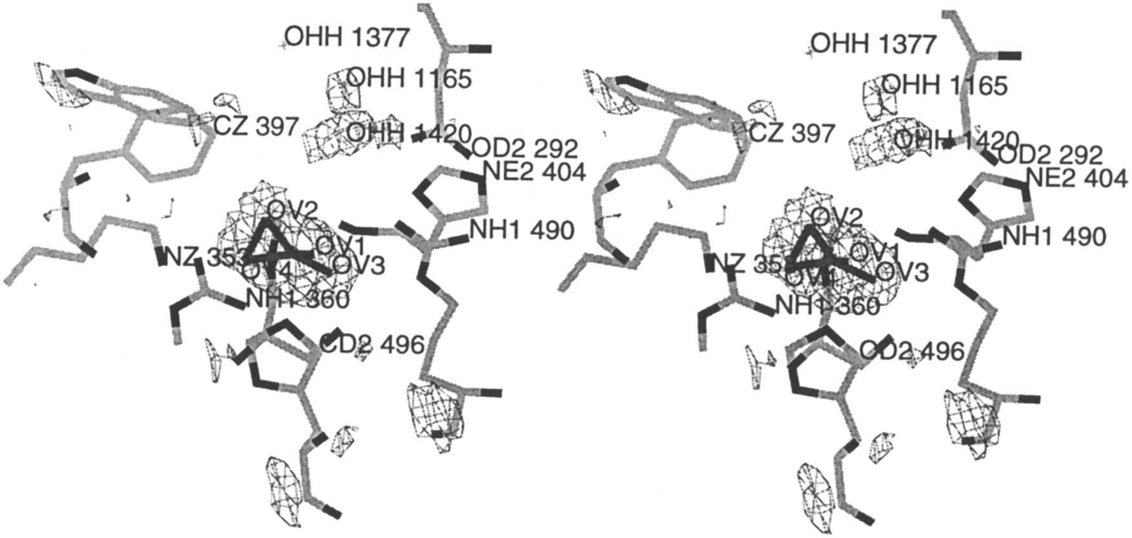
OHH 1377
OHH 1165
CZ 397
OHH 1420
OD2 292
NE2 404
OV2
NH1 490
OV1
NZ 353
OV4
OV3
NH1 360
CD2 496

Fig. 5. Difference electron density map of the peroxide form of CPO around the vanadium binding site contoured at 3.0 σ. The difference electron density for the peroxide metavanadate(V) is the strongest feature in the whole map.

have been obtained from an atomic model which did not contain the vanadate group and the two water molecules 1420 and 1377. The difference electron density map demonstrates that the peroxide has reacted with the vanadate group. The apical oxygen OV4 has been released and the peroxide binds side-on in the equatorial plane to the vanadium. Positive electron density is visible for two additional water molecules in the active site (1165, 1420). The vanadium peroxide complex has 5 direct ligands only. The coordination geometry is that of a distorted tetragonal pyramid. The apical ligand is oxygen OV3 (bond length about 1.60 Å) identifying this as a V=O bond. The two peroxide oxygens OV2 and OV4 (bond lengths: V-OV2 and V-OV4, about 1.87 Å; OV2-OV4, 1.47 Å), oxygen OV3 (bond length 1.93 Å), and nitrogen NE2 from histidine 496 (bond length 2.19 Å) constitute the basal plane. One empty apical coordination site at the vanadium is sterically blocked by the side chain of Arg360. The empty coordination site generated by the release of OV4 seems to be predestinated to accept the chloride ion during continuation of turnover. The bound peroxo species may be addressed as a monoperoxo-metavanadate(V). The hydrogen bonding network around the vanadium site of the peroxide derivative is depicted in Fig. 6. His404 is no longer hydrogen-bonded to any oxygen function of the vanadium group. It forms a hydrogen bond to water molecule 1420. OV4 of the peroxide group is hydrogen-bonded to NZ of Lys353 and to the amide nitrogen of Gly403. OV2 of the peroxide group is linked via a hydrogen-bond to the same amide nitrogen. OV3 makes hydrogen-bonds to OG of Ser402 and NE of Arg490, and OV1 to NH1 of Arg360 and NH2 of Arg490. The empty vanadium coordination site generated by the release of OV4 is directed towards the active site pocket supplying good access for the second substrate from the solvent.

Downloaded by YORK UNIV on October 31, 2012 | http://pubs.acs.org
Publication Date: December 10, 1998 | doi: 10.1021/bk-1998-0711.ch014

Apo and Tungstate Forms of CPO

The x-ray structures of the apo and tungstate form of vanadium chloroperoxidase (CPO) from the fungus *Curvularia inaequalis* have been solved by difference Fourier techniques using the atomic model of native chloroperoxidase (*24*). In the 2.50 Å crystal structure (R = 17.1 %) of apo CPO, a water solvent molecule is found in place of the vanadate cofactor. The 2.30 Å crystal structure of tungstate CPO (R = 16.2 %) reveals the binding of the tungstate to the metal-cofactor binding site. It binds in a similar fashion as the hydrogen vanadate(V) group in the native form. But the tungsten atom is not or only weakly bound to the NE2 nitrogen atom of His496 in contrast to native CPO where the vanadium atom forms a bond to the NE2 nitrogen atom of histidine 496. The overall protein structure and the metal-cofactor binding site of apo and tungstate CPO remain virtually unchanged. This means that the CPO protein matrix provides a rigid preformed metal-cofactor binding site. The binding mode of vanadate or tungstate can be described as rack-induced bonding according to Gray and Malmström (*25*).

Downloaded by YORK UNIV on October 31, 2012 | http://pubs.acs.org
Publication Date: December 10, 1998 | doi: 10.1021/bk-1998-0711.ch014

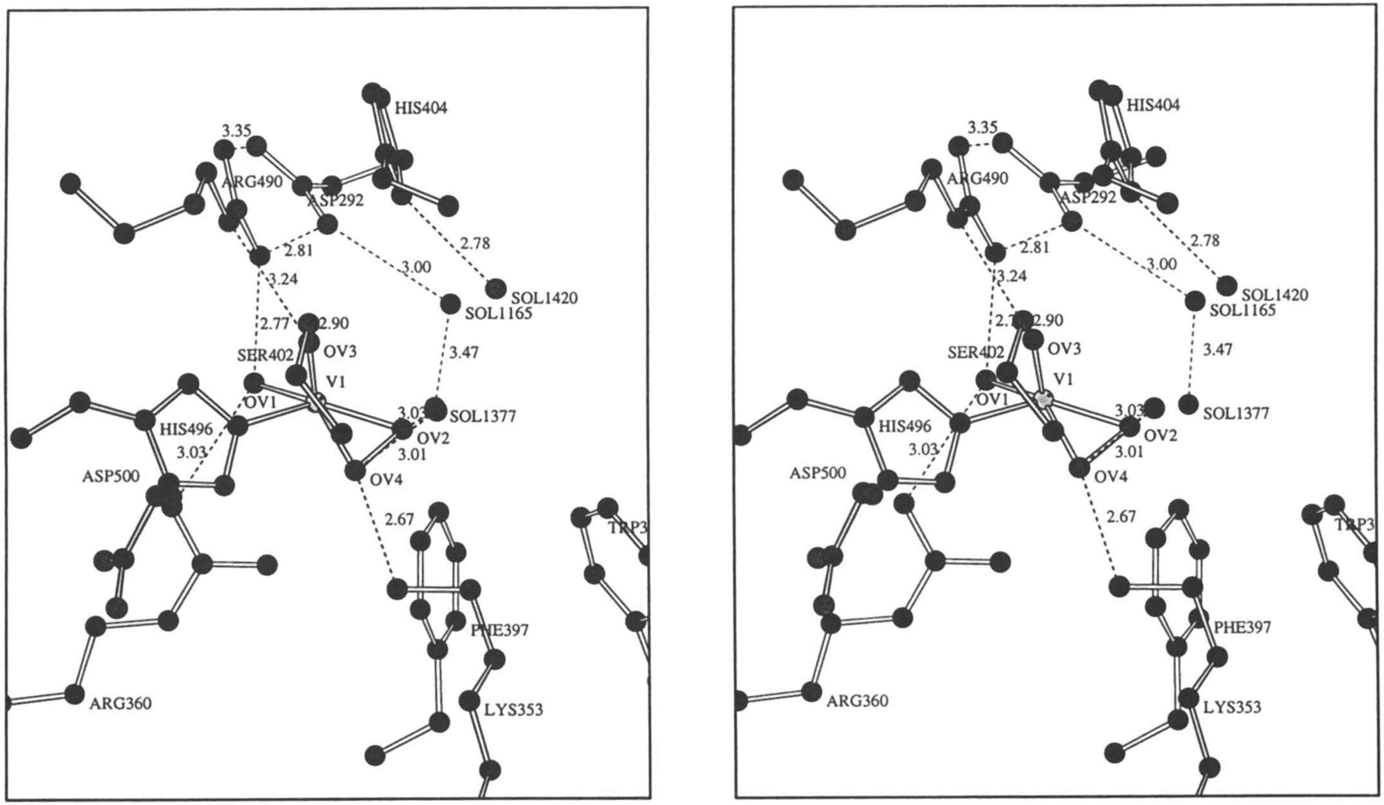
HIS404
3.35
ARG490
ASP292
2.78
2.81
3.00
3.24
SOL1420
SOL1165
2.77
2.90
SER402
OV3
3.47
V1
OV1
SOL1377
3.03
HIS496
OV2
3.03
3.01
ASP500
OV4
2.67
TRP3
PHE397
ARG360
LYS353

Fig. 6. Hydrogen bonding pattern of the peroxide form of CPO around the vanadium binding site (MOLSCRIPT (*19*)).

Downloaded by YORK UNIV on October 31, 2012 | http://pubs.acs.org
Publication Date: December 10, 1998 | doi: 10.1021/bk-1998-0711.ch014

Relatedness of CPO with Other Vanadium Containing Haloperoxidases

Vanadium containing haloperoxidases have been isolated from all classes of marine algae (see (*6*)). An amino acid sequence alignment of the sequence of CPO with the recently determined partial sequence (236 residues) of the vanadium-containing bromoperoxidase from the brown alga *Ascophyllum nodosum* (*26*) has been carried out and the regions of high similarities are shown in Table I. There are three stretches of high similarity in the regions of residues providing the vanadium histidine ligand (His496), the vanadate-interacting residues (Lys353, Arg360, Ser402, Gly403, Arg490) and the catalytic His404. The alignment demonstrates that the metal binding sites in both vanadium-containing haloperoxidases and the overall protein fold in the C terminal half of the proteins will be very similar reflecting the close relationship of both enzymes. This will also be valid for the vanadium containing haloperoxidases from the other marine algae.

Table I. Amino Acid Sequence Alignment of Stretches of High Similarities of CPO (*27*) and Vanadium Containing Bromoperoxidase from *Ascophyllum nodosum* (BRPO) (*26*). The alignment was carried out manually. Residue 24 of the BRPO partial sequence was published to be an Asn (*26*) but turned out to be a Lys after resequencing (Schomburg, D., University of Köln, personal communication, 1997). *, Protein ligand directly bound to vanadium; Δ, residue hydrogen bonded to vanadate oxygen; ♦, catalytic histidine.

CPO	343	TDAGIFSW KEKWE F- EFWRP LS-GV
BRP	14	ELAQRSSWYQKWQVHRFARPEALGG
Consensus		A SW KW F RP G
Function		Δ Δ
CPO	393	FKPPFPAYPSGHATFGGAVFQMVRRY
BRPO	90	GTPTHPSYPSGHATXNGAFATVLKAL
Consensus		P P YPSGHAT GA
Function		ΔΔ♦
CPO	480	WELMFENAIS RI F LGVHWRFDAAA
BRPO	152	KKLAVNVAFGRQMLG IHYRFDGIQ
Consensus		L A R LG H RFD
Function		Δ *

It has recently been shown that the amino acid residues contributing to the active sites of the vanadium containing haloperoxidases are conserved within three families of acid phosphatases suggesting that the active sites of these enzymes are very similar (*28*).

Proposal of a Catalytic Mechanism for CPO

The determination of the native form and the peroxide intermediate by X-ray structure analysis made it possible to propose a catalytic reaction scheme (*18*). Steady-state kinetic studies on CPO (*16*) had shown that in the pH range between 6 and 7 the enzyme mechanism is a ping-pong type. It has also been demonstrated that peroxide binds first. The proposed catalytic mechanism (*18*) is displayed in Fig. 7. We start from the native enzyme (panel 1). The apical oxygen is hydrogen-bonded to His404. This hydrogen-bond makes the apical OH-group more nucleophilic than a normally bound OH. The peroxide molecule approaches this apical OH and gets singly deprotonated. The generated apical water molecule is a weak vanadium ligand only and may leave the vanadium coordination sphere (panel 2). The hydroperoxide coordinates to the vanadium at this empty coordination site (panel 3) and the more nucleophilic oxygen OV2 abstracts the proton from the peroxide. The OH-ligand is displaced by the now more nucleophilic negatively charged peroxide oxygen (panel 4). The peroxide is now bound as in the peroxide complex which is observed in the crystal structure. At this stage the chloride ion binds to the empty vanadium coordination site (panel 5 and 6). In the original paper describing the structure of the azide CPO complex (*1*) a possible chloride binding site close to Trp350 and Phe397 in the active site and near the vanadium binding site has been discussed. Both hydrophobic side chains provide a hydrophobic environment, which seems to be necessary to stabilize the chloride binding. This has been found in chloride binding sites of various amylases where one side chain close to the chloride ion is donated from a hydrophobic residue (*29*). Similarly, in the haloalkane dehalogenase of *Xanthobacter autotrophicus* two tryptophan residues are present in halogen and halide binding (*30*). However, the coordination geometry of the peroxide intermediate in the peroxide CPO crystal structure makes a direct coordination of the chloride to the vanadium very probable. The bound peroxide is an oxidizing species and accepts two electrons from the chloride. The peroxide bond will be broken after the acceptance of the first electron and the O-Cl bond will be formed, and the V-O bond of the upper peroxide oxygen will be broken after uptake of the second electron. The OCl^- molecule will take up a proton from a surrounding water molecule and will leave the active site as HOCl (panel 7). An alternative possibility is that the chloride ion reacts directly with one of the presumably polarized peroxide oxygen atoms. This results in vanadium bound OCl^- which also takes up a proton from a water molecule. The generated OH^- will coordinate to the vanadium site to rebuild the native state (panel 8). The formation of the peroxide intermediate should be impossible when His404 is doubly protonated. In this case the apical OH group could no longer form a hydrogen bond to His404 and would lose its ability to activate the peroxide by its deprotonation.

Downloaded by YORK UNIV on October 31, 2012 | http://pubs.acs.org
Publication Date: December 10, 1998 | doi: 10.1021/bk-1998-0711.ch014

Downloaded by YORK UNIV on October 31, 2012 | http://pubs.acs.org
Publication Date: December 10, 1998 | doi: 10.1021/bk-1998-0711.ch014

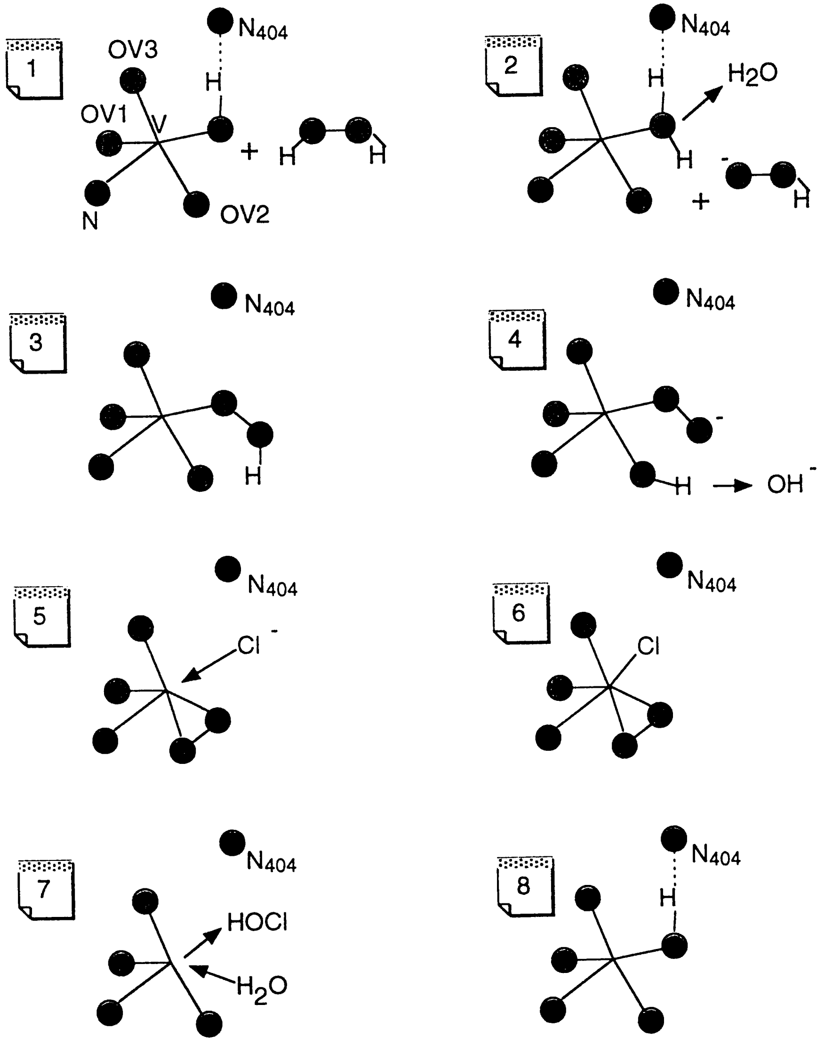
1
OV3
N404
H
OV1
V
+
H
H
N
OV2
2
N404
H
H2O
H
-
+
H
3
N404
H
4
N404
-
H
OH-
5
N404
Cl-
6
N404
Cl
7
N404
HOCl
H2O
8
N404
H

Fig. 7. Proposal for the catalytic mechanism of CPO from *Curvularia inaequalis*.

Acknowledgments.

We thank Prof. R. Huber for supporting this project and for valuable suggestions, Dr. J.W.P.M. van Schijndel for supplying the purified CPO and Ms. E.G.M. Vollenbroek for her help in culturing fungi. A.M. thanks the Deutsche Forschungsgemeinschaft (Schwerpunktthema: Bioanorganische Chemie) for financial support. This work was also supported by grants from the Netherlands Foundation for Chemical Research (SON) and was made possible by financial support from the Netherlands Organization for Scientific Research (NWO) and the Netherlands Technology Foundation (STW).

Downloaded by YORK UNIV on October 31, 2012 | http://pubs.acs.org
Publication Date: December 10, 1998 | doi: 10.1021/bk-1998-0711.ch014

Literature Cited.

1. Messerschmidt, A.; Wever, R. *Proc. Natl. Acad. Sci. USA* **1996,** *93,* 392.
2. Vilter, H. *Phytochemistry* **1984,** *23,* 1387.
3. de Boer, E.: Tromp, M.G.M.; Plat, H.; Krenn, B.E.; Wever, R. *Biochim. Biophys. Acta* **1986,** *872,* 104.
4. Plat, H.; Krenn, B.; Wever, R. *Biochemical J.* **1987,** *248,* 277.
5. Vollenbroek, E.G.M.; Simons, L.H.; van Schijndel, J.W.P.M.; Barnett, P.; Balzar, M.; Dekker, H.; Wever, R. *Biochem. Soc. Trans.* **1995,** *23,* 267.
6. Butler, A.; Walker, J.V. *Chem. Rev.* **1993,** *93,* 1937.
7. Müller-Fahrnow, A.; Hinrichs, W.; Saenger, W.; Vilter, H. *FEBS Lett.* **1988,** *239,* 292.
8. Rush, C.; Willetts, A.; Davies, G.; Dauter, Z.; Watson, H.; Littlechild, J. *FEBS Lett.* **1995,** *359,* 244.
9. Wever, R.; Kustin, K. *Adv. Inorg. Chem.* **1990,** *35,* 81.
10. Arber, J.M.; de Boer, E.; Garner, C.D.; Hasnain, S.S.; Wever, R. *Biochemistry* **1989,** *28*, 7678.
11. Carrano, C.J.; Moham, M.; Holmes, S.M.; de la Rosa, R.; Butler, A.; Charnock, J.M.; Garner, C.D. *Inorg. Chem.* **1994,** *33,* 646.
12. de Boer, E.; Keijzers, C.P.; Klaasen, A.A.K.; Reijerse, E.J.; Collison, D.; Garner, C.D.; Wever, R. *FEBS Lett.* **1988,** *235,* 93.
13. de Boer, E.; Boon, K.; Wever, R. *Biochemistry* **1988,** *27,* 1629.
14. Meister, G.E.; Butler, A. *Inorg. Chem.* **1994,** *33,* 3269.
15. Espenson, J.H.; Pestovsky, O.; Huston, P.; Staudt, S. *J. Amer. Chem. Soc.* **1994,** *116,* 2869.
16. van Schijndel, J.W.P.M.; Barnett, P.; Roelse, J.; Vollenbroek, E.G.M.; Wever, R. *Eur. J. Biochem.* **1994,** *225,* 151.
17. Vilter, H. *Proc. Int. Conf. Coord. Chem. 17th,* **1989,** M62 (abstr.).
18. Messerschmidt, A.; Prade, L.; Wever, R. *Biol. Chem.* **1997,** *378,* 309.
19. Kraulis, P. *J. Appl. Crystallogr.* **1991,** *24*, 946.

20. Kabsch, W.; Sander, C. *Biopolymers* **1983,** *22,* 2577.

21. Nordlund, P.; Sjöberg, B.-M.; Eklund, H. *Nature* **1990,** *345,* 593.

22. Rosenzweig, A.C.; Frederick, C.A.; Lippard, S.J.; Nordlund, P. *Nature* **1993,** *366,* 537.

23. Hecht, H.J.; Sonek, H.; Haag, T.; Pfeifer, O.; van Pée, K.-H. *Nat. Struct. Biol.* **1994,** *1,* 532.

24. Messerschmidt, A.; Wever, R. *Inorg. Chim. Acta* **1998**, in press.

25. Gray, H.B.; Malmström, B.G. *Comments Inorg. Chem.* **1983,** *2,* 203.

26. Vilter, H. In *Metal Ions in Biological Systems;* Sigel, H.; Sigel, A.; Dekker: New York, 1995, Vol. 31; pp 326-362.

27. Simons, B.H.; Barnett, P.; Vollenbroek, E.G.M.; Dekker, H.L.; Muijers, A.O.; Messerschmidt, A.; Wever, R. *Eur. J. Biochem.* **1995,** *229,* 566.

28. Hemrika, W.; Renirie, R.; Dekker, H.L.; Barnett, P.; Wever, R. *Proc. Natl. Acad. Sci. USA* **1997,** *94,* 2145.

29. Machius, M.; Wiegand, G.; Huber, R. *J. Mol. Biol.* **1995**, *246*, 545.

30. Verschueren, K.H.G.; Kingma, J.; Rozeboom, H.J.; Kalk, K.H.; Janssen, D.B.; Dijkstra, B.W. *Biochemistry* **1993**, *32*, 9031.

Downloaded by YORK UNIV on October 31, 2012 | http://pubs.acs.org
Publication Date: December 10, 1998 | doi: 10.1021/bk-1998-0711.ch014

Downloaded by NORTH CAROLINA STATE UNIV on October 31, 2012 | http://pubs.acs.org
Publication Date: December 10, 1998 | doi: 10.1021/bk-1998-0711.ch015

Chapter 15

Reactivity of Vanadium Bromoperoxidase

Alison Butler, Richard A. Tschirret-Guth, and Matthew T. Simpson

Department of Chemistry, University of California, Santa Barbara, CA 93106–9510

Vanadium haloperoxidases catalyze the halogenation of organic substrates (i.e., chloride, bromide or iodide) or the halide-assisted (i.e., chloride, bromide or iodide) disproportionation of hydrogen peroxide forming dioxygen and water. Competitive kinetic studies and fluorescent quenching studies have been used to probe binding of organic substrates to vanadium bromoperoxidase (V-BrPO). Certain organic substrates have been found to bind to V-BrPO such as the indole derivatives presented herein, among other substrates. When organic substrates bind to V-BrPO, a freely diffusible oxidized bromine intermediate is not released from the enzyme active site. The pH dependence and the selectivity of V-BrPO is also examined.

Haloperoxidases catalyze the oxidation of a halide (e.g., chloride, bromide or iodide) by hydrogen peroxide, which can result in halogenation of organic substrates, i.e., R-H in Equation 1,

$$Br^{-1} + H_2O_2 + R\text{-}H \rightarrow Br\text{-}H + 2H_2O \qquad \text{Eqn 1}$$

the production of dioxygen through subsequent oxidation of a second equivalent of hydrogen peroxide, or the production of hypohalous acid (i.e., HOCl), depending on the identity of the haloperoxidase. The three types of haloperoxidases which have been identified to date include the vanadium haloperoxidases (1-4), the FeHeme haloperoxidases (5,6) and the nonmetallo haloperoxidases (7). Vanadium bromoperoxidase, which is the focus of this article, has been isolated primarily from marine algae (for recent reviews see references 8,9). Because of the abundance of halogenated marine

In Vanadium Compounds; Tracey, A., et al.;
ACS Symposium Series; American Chemical Society: Washington, DC, 1998.

natural products, and because V-BrPO can catalyze halogenation reactions, the physiological role of V-BrPO is thought to be in the biosynthesis of the halogenated marine natural products. These natural products range from relatively simple volatile halogenated hydrocarbons (e.g., $CHBr_3$, CH_2Br_2 $CHBr_2Cl$ (10-12)) to more complex compounds, including halogenated indoles and terpenes (13; Figure 1).

Scope

We are interested in the reactivity of V-BrPO towards organic substrates that are likely precursors of the halogenated natural products, including substituted indole derivatives. In this article we will review the results of competitive kinetic studies which address the mechanism of halogenation and then examine new results on the pH dependence of the competitive kinetic studies as well as fluorescent quenching studies which can probe binding of organic substrates to V-BrPO.

Downloaded by NORTH CAROLINA STATE UNIV on October 31, 2012 | http://pubs.acs.org
Publication Date: December 10, 1998 | doi: 10.1021/bk-1998-0711.ch015

The Vanadium Site

Recently, the crystal structure of V-ClPO isolated from *C. inaequalis* as well as the peroxide-bound V-ClPO derivative were reported by Messerschmidt and Wever (14,15 and see related articles in this volume). The x-ray structure of V-BrPO (*A. nodosum*) has not yet been reported (16,17), however, the sequence alignment of V-BrPO (*A. nodosum*) and V-ClPO (*C. inaequalis*) (1,14,15) shows good overlap, particularly in the active site region. Thus the structure of V-BrPO is expected to be very similar to V-ClPO.

The main structural motif of V-ClPO is α-helical. Vanadium is coordinated at the top of one of two four-helix bundles in a broad channel which is lined on one side with predominantly polar residues including an ion-pair between Arg-360 and Asp-292 and several main chain carbonyl oxygens (Figure 2). The other side of the channel is hydrophobic, containing Pro-47, Pro-211, Try-350, Phe-393, Pro-395, Pro-396, and Phe-397.

The vanadium site is remarkably simple, comprised essentially of vanadate coordination to a single amino acid residue, His 496 (V-N 1.96 Å), in a pentagonal bipyramidal geometry (Figure 3A) (14,15). The "vanadate" site (i.e., three equatorial oxygens at a V-O distance of 1.65 Å and one apical V-O at 1.93 Å, interpreted as V-OH) is stabilized by multiple hydrogen bonding between the vanadate oxygen atoms and certain positively charged protein residues (see Figure 3A). His 404 (*C. inaequalis*) is hydrogen bonded to the apical hydroxide ligand; this residue is important for peroxide binding and catalysis (18) and is referred to as the acid-base histidine.

The x-ray structure of the peroxide form of V-ClPO (2.24 Å resolution) reveals a distorted tetragonal pyramid in which vanadium(V) is coordinated by peroxide in an η^2 fashion (1.87 Å V-O bond lengths; 1.47 Å O-O bond length), His 496 (2.19 Å V-N bond length) and an oxygen atom (1.93 Å) in the basal plane and by an oxo ligand (1.60 Å) in the axial position (Figure 3B (15)). His 404 is no longer hydrogen bonded to the vanadium center, however, one of the peroxide oxygen atoms is hydrogen bonded to Lys 353. The shortening of the apical V-O bond length from 1.93 Å to 1.60 Å upon

Downloaded by NORTH CAROLINA STATE UNIV on October 31, 2012 | http://pubs.acs.org
Publication Date: December 10, 1998 | doi: 10.1021/bk-1998-0711.ch015

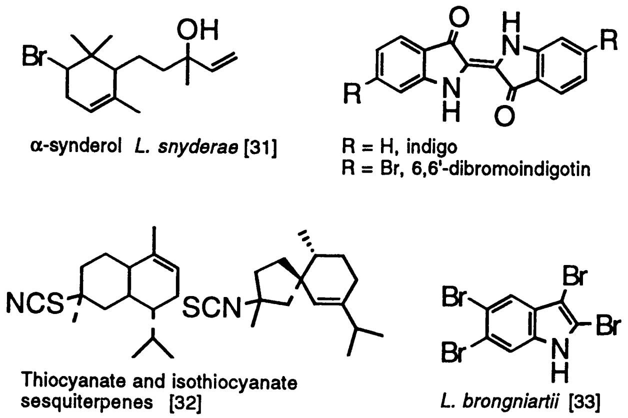
OH
Br
α-synderol *L. snyderae* [31]
O
H
N
R
R
N
H
O
R = H, indigo
R = Br, 6,6'-dibromoindigotin
NCS
SCN
Thiocyanate and isothiocyanate sesquiterpenes [32]
Br
Br
Br
Br
N
H
L. brongniartii [33]

Figure 1. Selected Marine Natural Products
(Reproduced with permission from reference 8. Copyright 1997 Springer-Verlag.)

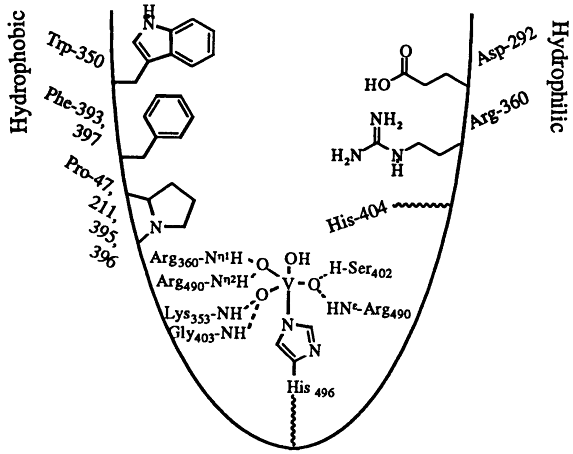
Hydrophobic
Trp-350
Phe-393, 397
Pro-47, 211, 395, 396
Hydrophilic
Asp-292
Arg-360
HO
O
NH2
H2N
N
H
His-404
H
N
N
Arg360-Nη1H
Arg490-Nη2H
Lys353-NH
Gly403-NH
O
OH
V
O
O
H-Ser402
HNε-Arg490
N
N
His 496

Figure 2. The V-ClPO Active Site Channel

coordination of peroxide is cited to support the shift from hydroxide coordination (V-OH) to oxide coordination (V=O) (15).

The Reactivity of Vanadium Bromoperoxidase

V-BrPO catalyzes peroxidative halogenation reactions (e.g., equation 1) (2) and the halide-assisted disproportionation of hydrogen peroxide, producing dioxygen (19-23):

$$X^- + 2H_2O_2 \rightarrow O_2 + 2\ H_2O + X^- \qquad \text{Eqn 2}$$

Direct disproportionation is not observed with V-BrPO. The V-BrPO catalytic mechanism involves first coordination of hydrogen peroxide to the vanadium(V) center (24). Halide oxidation follows (Scheme 1) and because halide saturation kinetics are observed (for both V-ClPO (26) and V-BrPO (*A. nodosum*) (20,25)) halide binding must occur. One possible halide binding site is the vanadium center (15), although other sites are possible (14).

The nature of the oxidized halogen intermediate, such as hypobromous acid (HOBr), bromine (Br_2), tribromide (Br_3^-), or an enzyme-trapped bromonium ion equivalent (e.g., Enz-Br, Venz-OBr, Enz-HOBr, etc), in the case of bromide, has been the subject of much speculation (25,27-29). Under the optimum catalytic conditions for V-BrPO (*A. nodosum*) (i.e., pH 6.5, 2 mM H_2O_2, 0.1 M KBr, 50 μM MCD), an intermediate cannot be observed, because the halogenation of the substrate or the oxidation of a second equivalent of hydrogen peroxide by the oxidized halogen intermediate is very fast (19-21). At pH 5.0, Br_3^- has been detected (25), because at this pH the rate of oxidation of a second equivalent of H_2O_2 is slow; thus Br_3^- builds up in solution. However, at pH $\leq$ 5, V-BrPO is also irreversibly inactivated upon turnover through formation of 2-oxohistidine (30). Even addition of "aqueous bromine" to V-BrPO at pH $\leq$ 5, inactivates V-BrPO and produces 2-oxohistidine (30). Since V-BrPO is not inactivated at higher pH, the oxidized halogen intermediate produced at neutral pH or optimal V-BrPO conditions, cannot be the same as that at pH 5.

The Selectivity of V-BrPO

V-BrPO does selectively halogenate certain organic substrates (28). Many indoles and

Downloaded by NORTH CAROLINA STATE UNIV on October 31, 2012 | http://pubs.acs.org
Publication Date: December 10, 1998 | doi: 10.1021/bk-1998-0711.ch015

Downloaded by NORTH CAROLINA STATE UNIV on October 31, 2012 | http://pubs.acs.org
Publication Date: December 10, 1998 | doi: 10.1021/bk-1998-0711.ch015

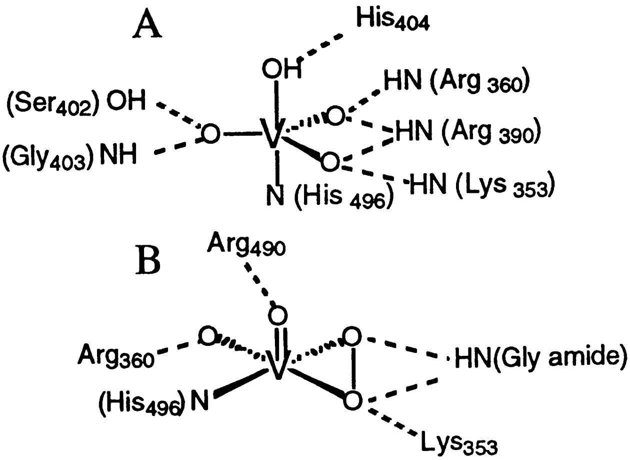
A
His404
OH
(Ser402) OH
(Gly403) NH
O
V
O
O
HN (Arg 360)
HN (Arg 390)
HN (Lys 353)
N (His 496)
B
Arg490
O
Arg360
O
V
O
O
HN(Gly amide)
(His496) N
Lys353

Figure 3. The V-ClPO Vanadium Site: A) Native Enzyme; B) the Peroxo-V-ClPO Derivative.

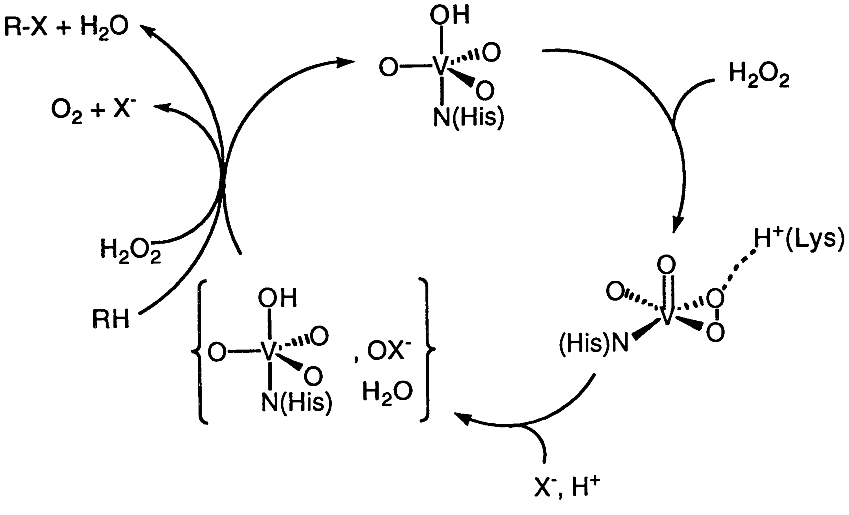
R-X + H2O
O2 + X-
H2O2
RH
OH
O
V
O
O
N(His)
H2O2
H+(Lys)
O
O
V
O
O
(His)N
OH
O
V
O
O
N(His)
, OX-
H2O
X-, H+

Scheme 1. Proposed Catalytic Cycle for V-BrPO

(Reproduced with permission from reference 8. Copyright 1997 Springer-Verlag.)

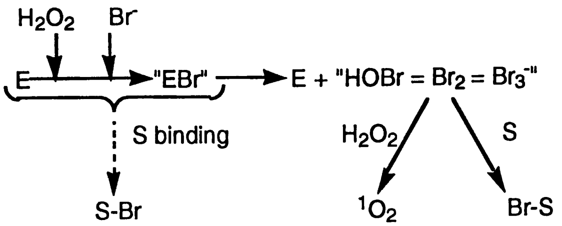

Scheme 2. Reaction Scheme Showing Substrate Binding to V-BrPO

terpenes are preferentially brominated or oxidized over monochlorodimedone (2-chloro-5,5-dimethyl-1,3-dimedone, MCD), the common substrate used to assay haloperoxidase activity in the V-BrPO catalyzed reaction. Of several indoles competed against equimolar MCD, e.g., 2-methylindole (2-MeI), 2-*tert*-butylindole, 2-phenylindole, 5-hydroxyindole, 3-methylindole, V-BrPO displayed its greatest selectivity with 2-MeI (28).

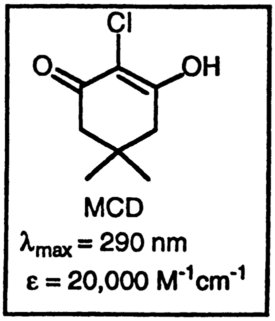

MCD
λ_{max} = 290 nm
ε = 20,000 $M^{-1}cm^{-1}$

Through competitive kinetic studies comparing the reactivity of the V-BrPO/H_2O_2/KBr system with aqueous bromine (i.e., considered to be a mixture of HOBr, Br_2, or Br_3^-), we have shown that the nature of the oxidized halogenating species produced by V-BrPO depends on the nature of the organic substrate (27). Working initially at pH 6.5, we found that V-BrPO preferentially brominated 2-MeI (forming 3-bromo-2-methylindole) over phenol red, PR, (forming tetrabromophenol blue, PB), as shown by a lag phase in the appearance of bromophenol blue (Figure 4b). The lag phase is proportional to the concentration of 2-MeI, although after the lag phase, the rate of bromination of PR was independent of the 2-MeI concentration. By comparison, a lag phase was not observed in the competitive bromination of 2-MeI and PR by HOBr (Figure 5b); under these conditions, bromination of 2-MeI and PR occur concurrently and an increase in the 2-MeI concentration leads to a decrease in the appearance of bromophenol blue. This differential reactivity between V-BrPO and HOBr suggests that released HOBr is not the active brominating species in the V-BrPO-catalyzed reactions of 2-MeI, a situation arising from indole binding to V-BrPO (27; and see below).

The pH dependence of this competition shows that the V-BrPO selectivity is greatest at the lower pH values. At pH 5.5 (Figure 4a) the rate of the V-BrPO catalyzed bromination of PR is the same as at pH 6.5 (Figure 4b), however the lag phase in the presence of 2-MeI increases, possibly reflecting a decreased rate of bromination of 2-MeI at pH 5.5. Above pH 6.5 (Figure 4c-f), the rate of the V-BrPO catalyzed bromination of PR decreased. At the higher pH values, the sharp delineation

Downloaded by NORTH CAROLINA STATE UNIV on October 31, 2012 | http://pubs.acs.org
Publication Date: December 10, 1998 | doi: 10.1021/bk-1998-0711.ch015

between the end of 2-MeI bromination (i.e., the end of the lag phase) and the beginning of PR bromination becomes more curved, although the general trend of a lag phase followed by the appearance of PB is still evident. Indeed, concomitant bromination of

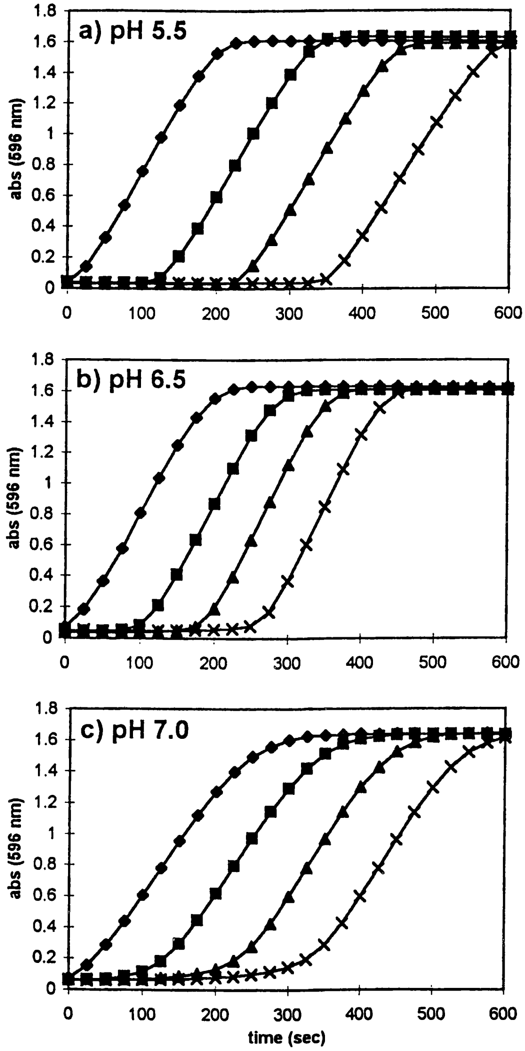

Figure 4. pH Dependence of the Competitive Bromination of Phenol Red and 2-Methylindole by V-BrPO (*Ascophyllum nodosum*). Conditions: 25.3 μM Phenol Red, 40 mM KBr, 0.416 mM H_2O_2, 10 nM V-BrPO in 0.1 phosphate buffer at pH 5.5-7.5 or in 0.1 M Hepes buffer at pH 8.0 and 20% ethanol with varying concentrations of 2-MeI: ◆, 0 M; n, 28.8 μM; s, 57.6 μM; X , 86.4 μM.

Downloaded by NORTH CAROLINA STATE UNIV on October 31, 2012 | http://pubs.acs.org
Publication Date: December 10, 1998 | doi: 10.1021/bk-1998-0711.ch015

Downloaded by NORTH CAROLINA STATE UNIV on October 31, 2012 | http://pubs.acs.org
Publication Date: December 10, 1998 | doi: 10.1021/bk-1998-0711.ch015

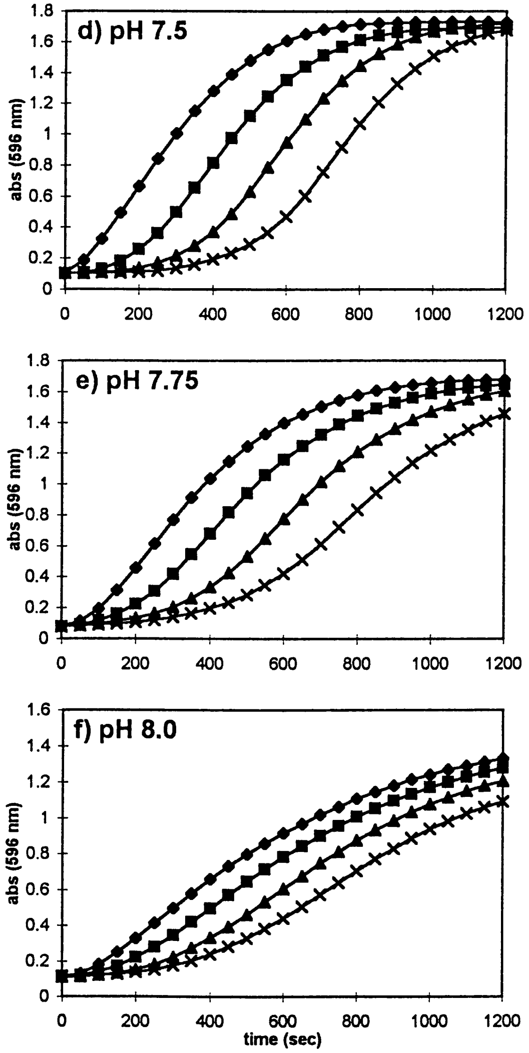

Figure 4. *Continued.*

Downloaded by NORTH CAROLINA STATE UNIV on October 31, 2012 | http://pubs.acs.org
Publication Date: December 10, 1998 | doi: 10.1021/bk-1998-0711.ch015

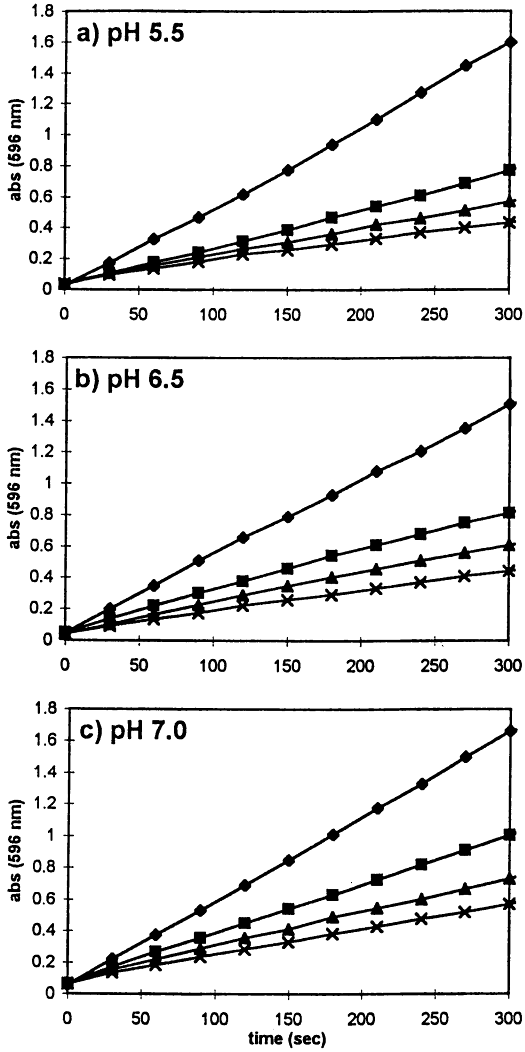

Figure 5. pH Dependence of the Competitive Bromination of Phenol Red and 2-Methylindole by Aqueous Bromine. Conditions: 25.3 μM Phenol Red, 40 mM KBr, in 0.1 phosphate buffer at pH 5.5-8.0 and 20% ethanol with varying concentrations of 2-MeI: ♦, 0 M; n, 28.8 μM; s, 57.6 μM; X , 86.4 μM. Hypobromite solutions were prepared by dilution of bromine vapors into 0.01 N sodium hydroxide. The final concentration of hypobromite in solution was determined spectrophotometrically by the oxidation of iodide to triiodide, λ_{max} 353 nm; ε 26,000 $M^{-1}cm^{-1}$: aliquots of the standard hypobromite solution were diluted into 100 mM potassium iodide in 100 mM acetate buffer, pH 4.5.

Downloaded by NORTH CAROLINA STATE UNIV on October 31, 2012 | http://pubs.acs.org
Publication Date: December 10, 1998 | doi: 10.1021/bk-1998-0711.ch015

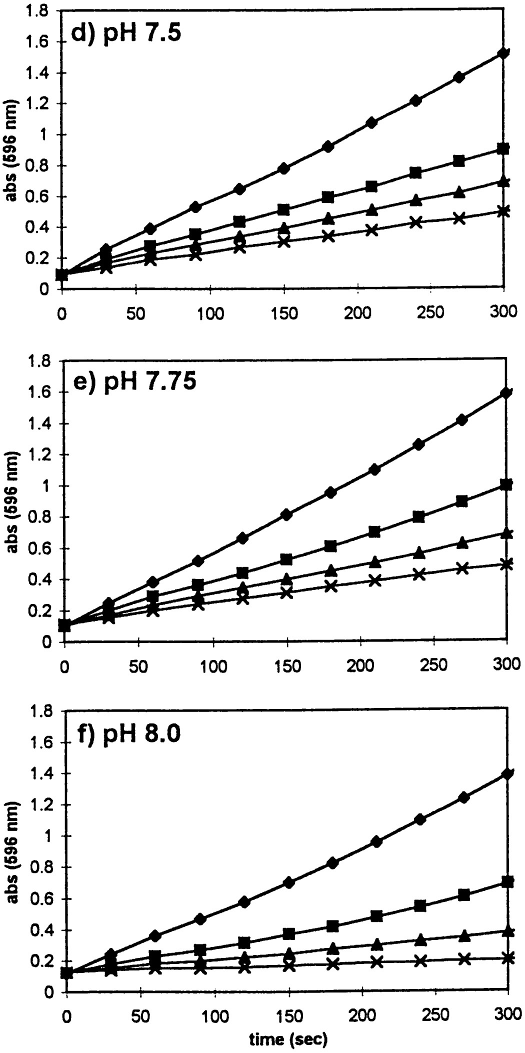

Figure 5. *Continued.*

2-MeI and PR may be occurring in the lag phase. However it is also likely that the dioxygen formation reaction is also occurring at the higher pH values (23). Further work is in progress. In contrast to the V-BrPO catalyzed reaction, there is very little effect of pH on reaction of aqueous bromine with PR and 2-MeI (Figure 5).

Further evidence that the enzyme-catalyzed bromination of indoles is not mediated by enzyme-released HOBr was established from comparison of the rate of V-BrPO-catalyzed bromide-assisted disproportionation of H_2O_2 (forming O_2) in the presence and absence of 2-MeI *versus* the rate of oxidation of H_2O_2 by "aqueous bromine" (forming O_2) in the presence and absence of 2-MeI (27). In the enzyme reaction, indole bromination is favored over H_2O_2 oxidation, whereas in the non enzymatic reaction, H_2O_2 was preferentially oxidized by aqueous bromine, forming O_2 (see Figure 3 in reference 27). The pH dependence of these competitive reactions is in progress.

Fluorescence quenching of 2-phenylindole by V-BrPO established that the indole binds to V-BrPO (see Figure 4 in reference 27). The data fit a modified Stern Volmer equation (Eqn 3) in which the dynamic quenching pathways are negligible:

$$F_o/F = e^{V([V\text{-}BrPO])} \qquad \text{Eqn 3}$$

From a plot of $\log(F_0/F)$ vs [V-BrPO], the static quenching constant, V, was found to be $1.1 \times 10^5\ M^{-1}$ (Figure 6).

The radius of the active volume calculated from V using the "Sphere of Action" model is about 34 Å. This value is within the range of the estimated sum of the molecular radii of quencher, V-BrPO,and fluophore, 2-phenylindole, and is consistent with binding of 2-phenylindole and V-BrPO. A mechanistic scheme involving substrate binding is shown in Scheme 2 (27). V-BrPO binds H_2O_2 and Br^- leading to a putative "enzyme-bound" or "active-site trapped" brominating moiety, "E-Br", which in the absence of an indole may release HOBr (or other bromine species, e.g., Br_2, Br_3^-). When indole is present, it binds to V-BrPO, preventing release of an oxidized bromine species and leading to indole bromination.

Summary

In summary, V-BrPO displays selectivity in its peroxidative halogenation or oxidation reactions with certain organic substrates (e.g., particularly with indole and related substrates). At pH 6.5, the reactivity is not consistent with bromination or oxidation

Downloaded by NORTH CAROLINA STATE UNIV on October 31, 2012 | http://pubs.acs.org
Publication Date: December 10, 1998 | doi: 10.1021/bk-1998-0711.ch015

Downloaded by NORTH CAROLINA STATE UNIV on October 31, 2012 | http://pubs.acs.org
Publication Date: December 10, 1998 | doi: 10.1021/bk-1998-0711.ch015

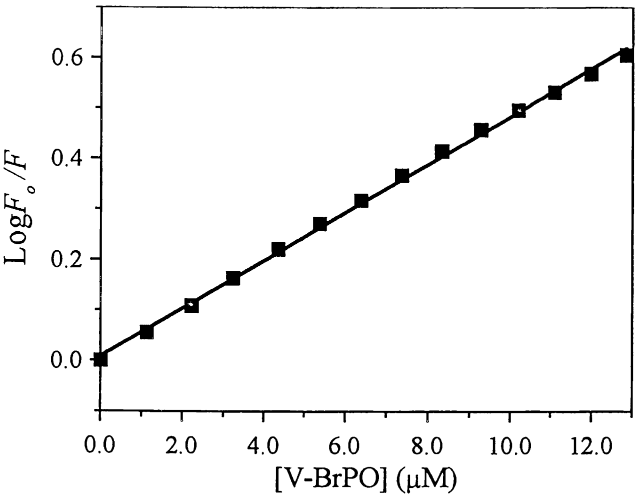

Figure 6. Stern Volmer and Modified Stern-Volmer Plots of the Fluorescent Quenching of 2-Phenylindole by V-BrPO. A) F_0/F vs [V-BrPO]. B) Log(F_0/F) vs [V-BrPO]. Conditions: The experiment was carried out at 21°C by addition of 20 μL aliquots of a 97 μM V-BrPO stock solution to 1.7 mL of 0.57 μM 2-phenylindole in 0.1 M Tris buffer, pH 8.13.

by aqueous bromine species (e.g., HOBr = Br_2 = Br_3^-), but rather from an enzyme-trapped species which results from indole binding to V-BrPO. The state of the oxidized halogen species at higher pH is under investigation. Given the hydrophobic nature of the indole derivatives and the hydrophobic portion of the active site channel, one can better understand the binding of indoles to V-BrPO.

Acknowledgments

AB gratefully acknowledges support from the National Science Foundation (CHE96-29374). A.B. is an Alfred P. Sloan Research Fellow. Partial support for this work is also sponsored by NOAA, U.S. Department of Commerce under grant number NA66RGO447, project number R/MP-76 through the California Sea Grant College System and in part by the California State Resources Agency. The views expressed herein are those of the author and do not necessarily reflect the views of NOAA. The U.S. Government is authorized to reproduce and distribute for governmental purposes. R.T-G was a Sea Grant Trainee.

Downloaded by NORTH CAROLINA STATE UNIV on October 31, 2012 | http://pubs.acs.org
Publication Date: December 10, 1998 | doi: 10.1021/bk-1998-0711.ch015

Literature Cited

1. Vilter, H. *Metal Ions in Biological Systems*, **1995**, *31*, 32.
2. Wever, R.; Plat, H; de Boer, E. *Biochim. Biophys. Acta* , **1985**, *830*, 181-186.
3. Wever, R.; Krenn, B.E., In *Vanadium in Biological Systems: Physiology and Biochemistry*, Ed. N. D. Chasteen; Kluwer Academic Publishers, 1990. pp 81-98.
4. Butler, A.; Walker, J.V. *Chem. Rev.* **1993**, *93*, 1937-1944.
5. Hager, L.P.; Morris, D.R.; Brown, F.S.; Eberwein, H. *J. Biol. Chem.* **1966**, *241*, 1769-1777.
6. Sundaramoorthy, M; Terner, J; Poulos, T. L. *Structure* (London), **1995**, *3*, 1367-1377.
7. Van Pee, K-H. *Annual Review of Microbiology*,**1996**, *50*, 375-399.
8. Butler A; Baldwin A.H. *Structure & Bonding:Metal Sites in Proteins and Models* **1997**, *89*, 109-131.
9. Butler, A. In *Comprehensive Biological Catalysis* Editor, M. Sinnott, British Academic Press, 1997, *4*, 1-12.
10. Gschwend, P.M; MacFarlane, J.K.; Newman, A. *Science*, **1985**, *227*, 1033.
11. Walter, B.; Ballschmiter, K. *Chemosphere*, **1991**, *22*, 557.
12. Manley, S.L.; Goodwin, K.; North, W.J. *Limnology And Oceanography*, **1992**, *37*,1652.

13. Faulkner, D.J. *Natural Product Reports*, **1993**, *10*, 497-539 and references therein.
14. Messerschmidt, A.; Wever, R. *Proc. Natl Acad. Sci., USA,* **1993**, *93*, 392-396.
15. Messerschmidt, A.; Prade, L.; Wever, R. *Biological Chemistry* **1997**, *378,* 309-315.
16. Weyand, M.; Hecht, H.J.; Vilter, H.; Schomburg, D. *Acta Crystallographica Section D-Biological Crystallography*, **1996**, *52*, 864-865.
17. Muller-Fahrnow, A.; Hinrichs, W.; Saenger, W.; Vilter, H. *Febs Lett.* **1988**, *239*, 292.
18. van Schijndel, J.W.P.M.; Barnett, P.; Roelse, J.; Vollenbroek, E.G.M.; Wever, R. *Eur. J. Biochem.*,**1994**, *225*, 151-157.
19. Everett, R.R; Butler, A. *Inorg. Chem.* **1994**, *28*, 393-5.
20. Everett, R.R.; Soedjak, H.S.; Butler, A. *J. Biol. Chem.* **1990**, *265,* 15671-9.
21. Everett, R.R.; Kanofsky, J.R.; Butler, A. *J. Biol. Chem.* **1990**, *265*, 4908-14.
22. Soedjak, H.S.; Butler, A. *Inorg. Chem.*, **1990**, *29*, 5015-5017.
23. Soedjak, H.S.; Walker, J.V.; Butler, A. *Biochemistry*, **1995**, *34*, 12689-12696.
24. Tromp, M.G.M.; Olafsson, G.; Krenn, B.E.; Wever, R. *Biochim. Biophys. Acta* **1990**, *1040*, 192-198.
25. de Boer, E.; Wever, R. *J. Biol. Chem.*, **1988**, *263*, 12326-32.
26. Simons, L.H.; Barnett, P.; Vollenbroek, E.G.M.; Dekker, H.L.; Muijsers, A.O.; Messerschmidt, A.; Wever, R. *Eur. J. Biochem.* **1995**, *229*, 566.
27. Tschirret-Guth, R.A.; Butler, A. *J. Am. Chem. Soc.* **1994**, *116*, 411-412.
28. Butler, A.; Tschirret-Guth, R.A. *Proceedings of the Royal Netherlands Academy of Arts and Sciences*, **1997**
29. Itoh, N.; Izumi, Y.; Yamada, H. *J. Biol. Chem.***1987**, *262*, 11982-11987.
30. Meister Winter, G.E.; Butler, A. *Biochemistry* **1996**, *35*, 11805-11811.
31. Kato, T.; Ichinose, I., Kamoshida, A., Hirata, Y. *Chem Commun.*, **1976**, 518-519
32. He, H-Y., Faulkner, D.J.; Shumsky, J.S.; Hong, K.; Clardy, J. *J. Org. Chem.***1985**, *54,* 2511-2514.
33. Carter, G.T.; Rinehart, K.L.; Li, L.H.; Kuentzel, S.L.; Conner, J.L. *Tetrahedron Lett.* **1978**, *46*, 4479.

Downloaded by NORTH CAROLINA STATE UNIV on October 31, 2012 | http://pubs.acs.org
Publication Date: December 10, 1998 | doi: 10.1021/bk-1998-0711.ch015

Downloaded by YORK UNIV on October 31, 2012 | http://pubs.acs.org
Publication Date: December 10, 1998 | doi: 10.1021/bk-1998-0711.ch016

Chapter 16

Vanadate-Containing Haloperoxidases and Acid Phosphatases: The Conserved Active Site

Wieger Hemrika, Rokus Renirie, Henk Dekker, and Ron Wever

E. C. Slater Institute, University of Amsterdam, Plantage Muidergracht 12, 1018 TV Amsterdam, The Netherlands

We have shown that the amino acid residues contributing to the active site of vanadate-containing chloroperoxidase from the fungus *Curvularia inaequalis*, of which the crystal structure is known, are conserved within a large and diverse group of acid phosphatases, that include amongst others bacterial acid phosphatases, mammalian glucose-6-phosphatases and type 2 phosphatidic acid phosphatases. The suggestion that the active sites of these enzymes are structurally similar is confirmed by activity measurements showing that apochloroperoxidase exhibits phosphatase activity. These observations not only reveal interesting evolutionary relationships between these groups of enzymes but also have important implications for the research on acid phosphatases since structural data are lacking for this group of enzymes. Based on the conservation of the active sites we propose a new membrane topology model for glucose-6-phosphatase.

Vanadate-containing haloperoxidases form a group of enzymes that have been isolated from seaweeds, fungi and a lichen (*1-4*). These enzymes catalyse the oxidation of a halide (X^-) to the corresponding hypohalous acid according to (1).

$$H_2O_2 + H^+ + X^- \rightarrow H_2O + HOX \qquad [1]$$

In the presence of a suitable nucleophilic acceptor a second reaction can occur by which a diversity of halogenated compounds can be formed. Vanadate-containing haloperoxidases are named after the most electronegative halide they are able to oxidise implying that a chloroperoxidase is able to oxidise chloride, bromide and iodide and a bromoperoxidase only bromide and iodide. Hydrogen vanadate (HVO_4^{3-}), the prosthetic group of these enzymes, does not change its redox state during catalysis but remains in its highest (5^+) oxidation state. The metal most probably functions as a Lewis acid thus co-ordinating and activating the substrates in such a way that catalysis occurs. Vanadate-containing haloperoxidases are very chemo- and thermostable enzymes. They are also able to resist high concentrations of their substrate (H_2O_2) and product (HOX) that would readily inactivate members of the other well known group of haloperoxidases; the heme-containing haloperoxidases as exemplified by the chloroperoxidase from the fungus *Caldariomyces fumago* (*5*) or myeloperoxidase which is present in white blood cells (*6*).

In Vanadium Compounds; Tracey, A., et al.;
ACS Symposium Series; American Chemical Society: Washington, DC, 1998.

The above mentioned properties make the vanadate-containing haloperoxidases a very interesting research subject and as a result there has been a large increase in publications on this subject since the first isolation and identification of one such enzyme from seaweed (*7,8*) in the early eighties.

The Vanadate-containing Chloroperoxidase of *Curvularia inaequalis*

For the last years research in our laboratory has mainly focused on the vanadate-containing chloroperoxidase (V-CPO) from the fungus *Curvularia inaequalis* resulting in a description of its kinetic properties (*9*), the recent cloning and sequencing of the gene encoding this enzyme (*10*) and also (see the chapter by Messerschmidt, Prade and Wever in this book), in the determination of the X-ray structure of this enzyme (*11*). Furthermore a proposal for its physiological function has recently been put forward (*12*).

The *V-CPO* gene codes for a protein of 609 amino acids with a calculated molecular mass of 67,488 kDa. The crystal structure of this enzyme at 2.1 Å resolution (*11*) reveals that the protein has an overall cylindrical shape and measures approximately 50x80 Å. The secondary structure is mainly α-helical with two four-helix bundles as main structural motifs of the tertiary structure. The vanadium-binding centre (see Figure 1) is located on top of the second four-helix bundle and the residues binding the prosthetic group span a length of approximately 150 residues in the primary structure. The metal is co-ordinated to the $N^{\varepsilon 2}$ of His^{496} while 5 residues (Lys^{353}, Arg^{360}, Ser^{402}, Gly^{403} and Arg^{490}) donate hydrogen bonds to the non-protein oxygens of vanadate. His^{404} is proposed to be an acid-base group in catalysis (*11*). Alignment of this V-CPO with the partial amino acid sequence of the vanadium-containing bromoperoxidase (V-BPO) of the seaweed *Ascophyllum nodosum* (*7*), an enzyme of which the catalytic mechanism is considered to be analogous to that of the V-CPO (*9*), revealed three stretches of high similarity in the regions providing the metal oxide binding site, whereas the similarity turned out to be very low in the intervening regions. Initial database searches using the entire V-CPO sequence revealed very little sequence similarity to other known proteins (*10*). By using the three stretches of amino acids that provide the metal oxide binding site as templates for database searches we have been able to show that such stretches are also present in at least three families of acid phosphatases that were previously considered unrelated (*13*).

Downloaded by YORK UNIV on October 31, 2012 | http://pubs.acs.org
Publication Date: December 10, 1998 | doi: 10.1021/bk-1998-0711.ch016

Vanadate-containing Haloperoxidases and Acid Phosphatases; A Conserved Active Site

From our initial alignment, as presented in (*13*), it became clear that nearly all residues co-ordinating vanadate in V-CPO were conserved. This allowed the recognition of three separate domains that are highly similar among the aligned proteins. These three domains are connected however, by regions that are highly variable; both in sequence and in length.

We thus suggested (*13*) that the binding pocket for vanadate in the peroxidases is similar to the phosphate-binding site in the aligned acid phosphatases. This is in agreement with the structural resemblance of vanadate and phosphate, with the observation that the vanadium-containing haloperoxidases rapidly loose their activity in phosphate-containing buffers and that reconstitution of the apo-BPO by vanadate is inhibited in the presence of phosphate (*14*). Furthermore, vanadate is recognised as a potent inhibitor of many different phosphatases (*15*).

Since our initial database searches much improvement has been achieved in the available search algorithms and furthermore the linking of the databases, as done by the Entrez Browser provided by the National Centre for Biotechnology Information

(NCBI), enabled us to quickly identify more than 40 (putative) proteins also containing domains 1, 2 and 3 in our more recent database searches (see also (*16,17*)).

The conservation of the active sites among the presented enzymes, both in structure and residues binding the anions, prompted us to determine whether the apo-CPO from *C. inaequalis* could also act as a phosphatase.

Apo-Chloroperoxidase exhibits Acid Phosphatase Activity Since it is difficult to obtain pure apo-enzyme in sufficient amounts from *C. inaequalis* as needed for our experiments we decided to use recombinant enzyme produced from the *C. inaequalis V-CPO* gene in a newly developed *Saccharomyces cerevisiae* expression system (*18*). This enabled us to produce large quantities of pure recombinant enzyme (r-CPO) which was isolated as desrcribed (*18*) with the addition of an extra HPLC MonoQ step. After activation with vanadate the pure r-CPO behaves kinetically very similar to the enzyme as isolated from *C. inaequalis*.

Figure 2 presents the results of an experiment in which the putative phosphatase activity of apo-r-CPO was assayed by measuring the release of *p*-nitrophenol (*p*-NP) from *p*-nitrophenyl phosphate (*p*-NPP), a commonly used phosphatase substrate. This figure shows that *p*-NPP hydrolysis correlates linearly with the amount of enzyme added, demonstrating that the apo-r-CPO has phosphatase activity.

The presented data predict that vanadate and *p*-NPP compete for the same binding site in the apo-enzyme, implying that phosphatase and peroxidase activity are mutually exclusive. We have been able to show that this is indeed the case (*13*). Incubation of fully activated r-CPO with 0.5 mM *p*-NPP at pH 5.0 resulted in a rapid decrease of CPO activity which was not observed in the absence of *p*-NPP. The observed decrease of CPO activity could be prevented by the addition of extra (100 μM) vanadate

We also determined the kinetic parameters of *p*-NPP hydrolysis catalysed by apo-r-CPO as a function of pH (*13*). This revealed that V_{max} was only affected by a factor of 2 in the pH range 3.7-8.0 having an optimum at pH 5.0 (results not shown). The K_M for *p*-NPP remained approximately 50 μM in the pH range 4.5-8.0 but increased strongly in the pH range 3.7-4.5 (K_M 1.9 mM at pH 3.9), indicating that protonation of either a group on the free enzyme or the substrate itself is the cause of the reduced affinity for *p*-NPP.

Vanadate-containing Bromoperoxidases, a Slightly Different Active Site?

Figure 3 shows the alignment of domains 1, 2 and 3 of V-CPO of *C. inaequalis*, V-BPO of *A. nodosum* and 8 (putative) phosphatases or proteins that are representatives of the more recently found homologues (see also Figure 3). The alignment reveals one striking difference between the V-CPOs and the acid phosphatases on one hand and the V-BPO on the other. Since our initial alignment (*13*) it has become clear (see Messerschmidt and Wever in this book) that residue 24 of the partial amino acid sequence of V-BPO is not an asparagine but a lysine. This residue therefore corresponds to Lys^{353} of domain 1 of V-CPO of *C. inaequalis*. This implies that in the V-BPO there are seven residues –and not six as in V-CPO and the acid phosphatases– bridging the Lys^{24} and Arg^{32} residues. The presence of an extra residue in domain 1 of V-BPO may be a factor determining the enzyme's high preference of bromide over chloride as a substrate. This is given weight by the fact Lys^{353} of the *C. inaequalis* enzyme also forms a hydrogen-bond with an oxygen (OV4) of the catalytic peroxo-intermediate (*19*) (see also the chapter by Messerschmidt, Prade and Wever) and thus may play an important role on activating the bound peroxide. The slightly different geometry of the active site which will be the consequence of the additional amino acid in domain 1 of V-BPO might result in a less polarised peroxo-intermediate and therefore in its inability to oxidise the more electronegative chloride ion at physiological concentrations. The presence of a histidine (His^{28}) in domain 1 of the

Downloaded by YORK UNIV on October 31, 2012 | http://pubs.acs.org
Publication Date: December 10, 1998 | doi: 10.1021/bk-1998-0711.ch016

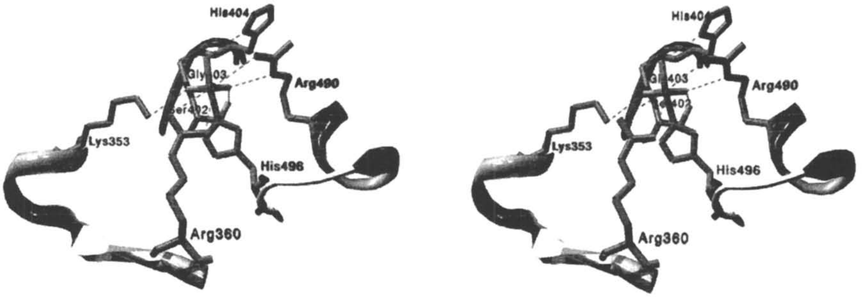
His404
Gly403
Ser402
Arg490
Lys353
His496
Arg360
His404
Gly403
Ser402
Arg490
Lys353
His496
Arg360

Figure 1. Active site of the V-CPO of C. inaequalis showing the conserved amino acid residues donated by Domain 1 (K^{353}, R^{360}), Domain 2 S^{402}, G^{403}, H^{404}) and Domain 3 (R^{490}, H^{496}) and the hydrogen-bonding pattern around the prosthetic group.

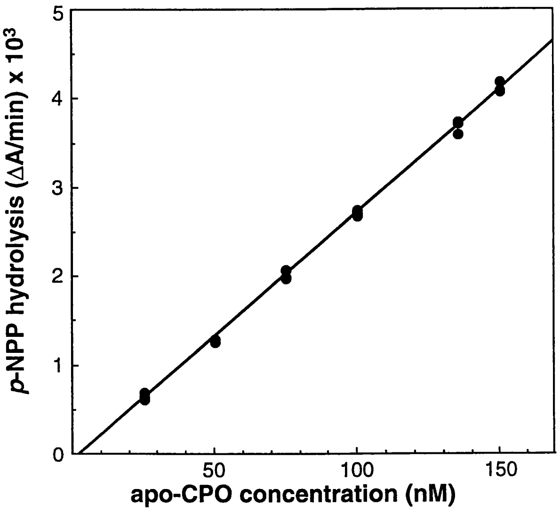

Figure 2. Phosphatase activity as a function of apo-r-CPO concentration. The enzyme was incubated with 1 mM *p*-NPP at 25 ^{0}C in 100 mM citrate (pH 5.0). After 4.5 hours reaction mixtures were quenched with NaOH and production of *p*-NP was measured at 410 nm using $\varepsilon_{410\,nm}$ = 18.3 $mM^{-1}cm^{-1}$ at pH 12. Each measurement was carried out in triplo.

Downloaded by YORK UNIV on October 31, 2012 | http://pubs.acs.org
Publication Date: December 10, 1998 | doi: 10.1021/bk-1998-0711.ch016

Downloaded by YORK UNIV on October 31, 2012 | http://pubs.acs.org
Publication Date: December 10, 1998 | doi: 10.1021/bk-1998-0711.ch016

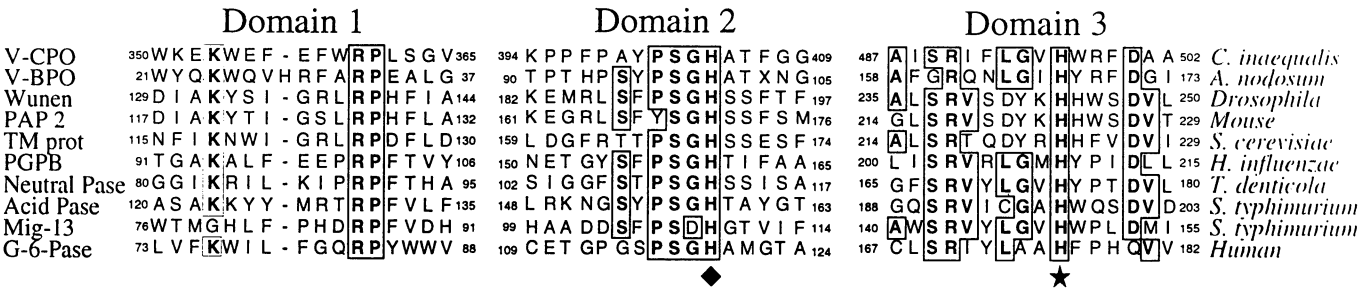
Domain 1
Domain 2
Domain 3
V-CPO 350 WKEKWEF-EFWRPLSGV 365 394 KPPFPAYPSGHATFGG 409 487 AISRIFLGVHWRFDAA 502 C. inaequalis
V-BPO 21 WYQKWQVHRFARPEALG 37 90 TPTHPSYPSGHATXNG 105 158 AFGRQNLGIHYRFDGI 173 A. nodosum
Wunen 129 DIAKYSI-GRLRPHFIA 144 182 KEMRLSFPSGHSSFTF 197 235 ALSRVSDYKHHWSDVL 250 Drosophila
PAP 2 117 DIAKYTI-GSLRPHFLA 132 161 KEGRLSFYSGHSSFSM 176 214 GLSRVSDYKHHWSDVT 229 Mouse
TM prot 115 NFIKNWI-GRLRPDFLD 130 159 LDGFRTTPSGHSSESF 174 214 ALSRTQDYRHHFVDVI 229 S. cerevisiae
PGPB 91 TGAKALF-EEPRPFTVY 106 150 NETGYSFPSGHTIFAA 165 200 LISRVRLGMHYPIDLL 215 H. influenzae
Neutral Pase 80 GGIKRIL-KIPRPFTHA 95 102 SIGGFSTPSGHSSISA 117 165 GFSRVYLGVHYPTDVL 180 T. denticola
Acid Pase 120 ASAKKYY-MRTRPFVLF 135 148 LRKNGSYPSGHTAYGT 163 188 GQSRVICGAHWQSDVD 203 S. typhimurium
Mig-13 76 WTMGHLF-PHDRPFVDH 91 99 HAADDSFPSDHGTVIF 114 140 AWSRVYLGVHWPLDMI 155 S. typhimurium
G-6-Pase 73 LVFKWIL-FGQRPYWWV 88 109 CETGPGSPSGHAMGTA 124 167 CLSRTYLAAHFPHQVV 182 Human
◆
★

Figure 3. Alignment of V-CPO of *C. inaequalis* with representatives of the enzymes proposed to contain a structurally similar active site. Residues identical in 50% or more of the sequences are given in bold face and boxed. The numbers indicate the start and end positions of the domains in the respective proteins. Histidines aligning with the vanadate co-ordinating histidine from V-CPO are indicated by an asterisk, histidines aligning to the proposed acid base histidine of V-CPO are indicated by a diamond.

Downloaded by YORK UNIV on October 31, 2012 | http://pubs.acs.org
Publication Date: December 10, 1998 | doi: 10.1021/bk-1998-0711.ch016

V-BPO may also be an important difference between the bromoperoxidase and the chloroperoxidases/acid phosphatases.

A Conserved Active Site; Consequences for the Acid Phosphatases

The common architecture of the active sites of enzymes carrying domains 1, 2 and 3 may have important consequences for research in the acid phosphatase field since for none of these enzymes structural data are available

Figure 4 shows a dendrogram which is based on the alignment of the complete protein sequences. It should be noted that by using this approach not all domains 1, 2 and 3 are aligned. It does enable us however, to recognise the different protein families that together constitute a newly identified superfamily. Since a histidine is ligating the vanadate in the vanadate-containing haloperoxidases and apparently the phosphate substrate in the phosphatases we propose to call this superfamily the histidine phosphatase/peroxidase superfamily.

Inspection of Figure 4 reveals a bias towards (putative) membrane bound proteins in this superfamily. Until now the only groups (marked by an S in Figure 3) that are shown to consist of soluble proteins are the vanadate-containing haloperoxidases and the non-specific bacterial acid phosphatases (*20*).

A New Membrane Topology for Glucose-6-Phosphatase The knowledge that domains 1, 2 and 3 should be in close contact in order to constitute an active site can be an extra tool in determining the membrane topology of the membrane-bound enzymes contained in the superfamily. We have recently used this knowledge to predict a new membrane topology for the mammalian glucose-6-phosphatase (G-6-Pase) family (*21*). Glucose-6-phosphatase (G-6-Pase) is an enzyme tightly associated with the endoplasmatic reticulum (ER) and nuclear membranes of liver and kidney cells (*22*) and based on its hydropathy profile six membrane-spanning helices were predicted (*23, 24*). G-6-Pase catalyses the last step in both gluconeogenesis and glycogenolysis and as such it is the key enzyme in glucose homeostasis (*22*). G-6-Pase is also known to be efficiently and competitively inhibited by vanadate. This fact may well be a factor contributing to the insulin mimetic effect of vanadate.

Glycogen storage disease type 1 (von Gierke disease) is an autosomal recessive disorder –with an incidence of about 1:100, 000 in humans– that is the consequence of the absence of G-6-Pase activity. This disorder is characterised by severe clinical manifestations such as hypoglycemia, growth retardation, hepatomegaly, kidney enlargement, hyperlipidemia, hyperuriceamia and lactic acidosis (*25, 26*). Without dietary treatment patients suffering from this disease die early, usually in their teens, of liver and kidney complications (*27*). Four missense mutations in the gene encoding human G-6-Pase were recently identified in patients (*23*). A subsequent near-saturation mutagenesis study (*28*) revealed that Arg^{83} was absolutely required for enzyme activity.

In our alignment (see figure 1) Arg^{83} corresponds to Arg^{360} of V-CPO, a residue donating hydrogen-bonds to vanadate. Since it is known that a histidine is the phosphate acceptor during catalysis of G-6-Pase the authors (*28*) also mutated 4 conserved histidines predicted to reside on the same (luminal) side of the ER membrane as Arg^{83}. His^{119} turned out to be the only histidine absolutely required for phosphatase activity. This is in agreement with our alignment since His^{119} of G-6-Pase corresponds to His^{404} of V-CPO, a residue which may function as an acid-base group in catalysis (*11*). His^{176} of G-6-Pase was not mutated but we predict that mutation of this residue will also abolish enzyme activity. His^{176} of G-6-Pase corresponds to His^{496} of V-CPO, the residue covalently linking the metal. It is likely therefore, that in G-6-Pase His^{176}, and not His^{119} as suggested (*28*), is the phosphate acceptor. Consequently, Arg^{83}, His^{119} and His^{176} of G-6-Pase have to reside at the same side of the ER membrane.

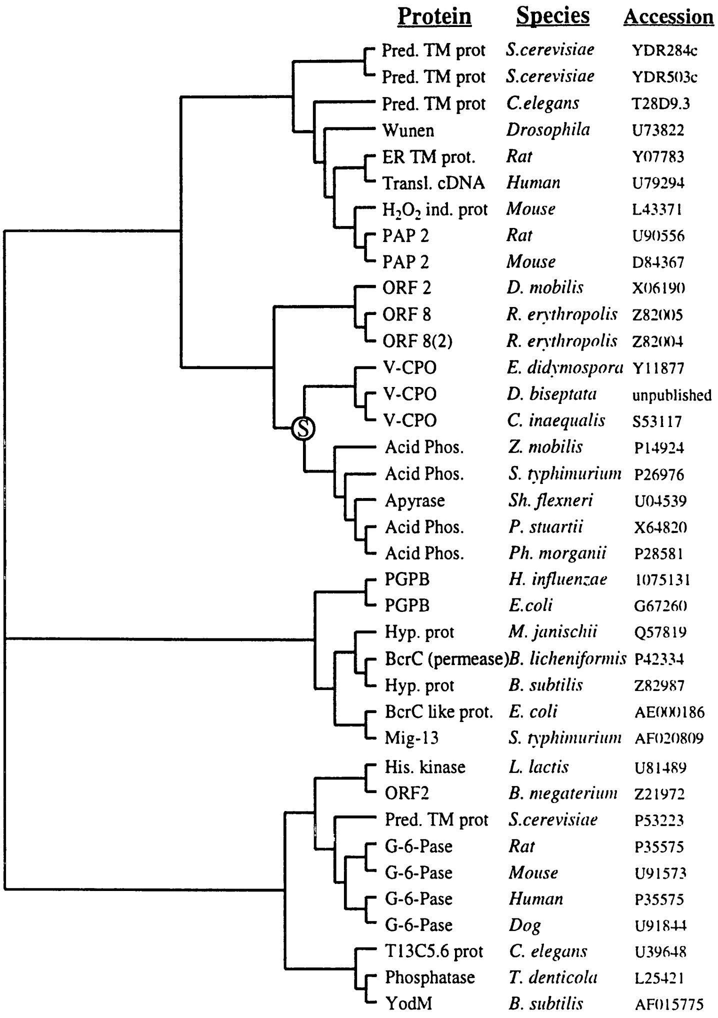
Protein Species Accession
Pred. TM prot S.cerevisiae YDR284c
Pred. TM prot S.cerevisiae YDR503c
Pred. TM prot C.elegans T28D9.3
Wunen Drosophila U73822
ER TM prot. Rat Y07783
Transl. cDNA Human U79294
H2O2 ind. prot Mouse L43371
PAP 2 Rat U90556
PAP 2 Mouse D84367
ORF 2 D. mobilis X06190
ORF 8 R. erythropolis Z82005
ORF 8(2) R. erythropolis Z82004
V-CPO E. didymospora Y11877
V-CPO D. biseptata unpublished
V-CPO C. inaequalis S53117
S
Acid Phos. Z. mobilis P14924
Acid Phos. S. typhimurium P26976
Apyrase Sh. flexneri U04539
Acid Phos. P. stuartii X64820
Acid Phos. Ph. morganii P28581
PGPB H. influenzae 1075131
PGPB E.coli G67260
Hyp. prot M. janischii Q57819
BcrC (permease) B. licheniformis P42334
Hyp. prot B. subtilis Z82987
BcrC like prot. E. coli AE000186
Mig-13 S. typhimurium AF020809
His. kinase L. lactis U81489
ORF2 B. megaterium Z21972
Pred. TM prot S.cerevisiae P53223
G-6-Pase Rat P35575
G-6-Pase Mouse U91573
G-6-Pase Human P35575
G-6-Pase Dog U91844
T13C5.6 prot C. elegans U39648
Phosphatase T. denticola L25421
YodM B. subtilis AF015775

Figure 4. Dendrogram of proteins containing the conserved domains 1, 2 and 3. The dendrogram is based on a Clustal W alignment (default parameters) using the complete protein sequences.

Downloaded by YORK UNIV on October 31, 2012 | http://pubs.acs.org
Publication Date: December 10, 1998 | doi: 10.1021/bk-1998-0711.ch016

Figure 5 shows our new model for the membrane topology of G-6-Pase which is based on the presented evidence concerning the nature of the G-6-Pase active site and the results of two new algorithms for the prediction of membrane-spanning domains (*29-32*). These algorithms independently predict nine transmembrane helices in G-6-Pase as opposed to the previous topology model (*23, 24*). With this newly predicted topology all residues aligning to the active site residues of V-CPO are situated on the same –luminal– side of the ER-membrane. We propose therefore that helices II, III, IV and V are in close contact and provide the glucose-6-phosphate binding and hydrolysis site of G-6-Pase.

In our model His^{176} of G-6-Pase is the nucleophile forming the phosphohistidine enzyme-substrate intermediate. The phosphate moiety is positioned by interaction of the negatively charged oxygens with the positively charged Lys^{76}, Arg^{83} and Arg^{170}, while analogous to V-CPO Ser^{117} and Gly^{118} may also donate hydrogen bonds. His^{119} may provide the proton needed to liberate the glucose moiety.

Drosophila Protein Wunen Another Membrane Bound Phosphatase Another important protein family shown in figure 3 is that of which Wunen (*33*) and plasma membrane bound (type 2) phosphatidic acid phosphatase PAP2 (*34*) are members.

Wunen is a *Drosophila* protein that is responsible for the guiding of germ cells in embryonic development from the lumen of the developing gut towards the mesoderm were they enter the gonads (*33*). Until now nothing is known about the enzymatic activity of Wunen but the occurrence of domains 1, 2 and 3 (see figure 1) and its high similarity to PAP2 –also containing domains 1, 2 and 3– (see figure 1) suggests that Wunen like PAP2 is an acid phosphatase.

Research on PAP has recently received an important impetus with the recognition that its enzymatic activity is not only involved in glycerolipid biosynthesis but that by balancing the levels of the two lipid second messengers diacylglycerol and phosphatidic acid it may also play in important role in signal transduction (see (*35*) and references therein). It should be noted that the predicted membrane topology of Wunen and PAP2 (*33, 34*) is in agreement with a phosphatase active site consisting of the amino acid residues provided by domains 1, 2 and 3.

V-CPO and the High Molecular Weight Acid Phosphatases; A Similar but not Conserved Active Site.

The above presented data indicate that the vanadium-containing haloperoxidases and the phosphatases with a homologous active site have divergently evolved from a common ancestor. Strikingly, the opposite –convergent evolution– also seems to have occurred since the active site of V-CPO resembles that of another class of acid phosphatases –the high molecular weight acid phosphatases (HMWAPs)– both in geometry and in residues contributing to the active site. In this context however, it is important to stress that no sequence similarity is found with this class of enzymes. The resemblance is most evident from the crystal structure of the active site of rat prostatic acid phosphatase complexed with vanadate (*36*) which is bound in the same trigonal bipyramidal geometry as in V-CPO. This co-ordination is analogous to the transition state in the reaction mechanism of several phosphatases (*37*). Furthermore, in rat prostatic acid phosphatase the vanadate is also covalently linked to a histidine (His^{12}) while Arg^{11}, Arg^{15}, Arg^{79} and His^{257} are within hydrogen-bonding distance. The binding of vanadate to His^{12} gives crystallographic evidence for the proposed role of a histidine as a nucleophile in the formation of the phosphoryl adduct (*37*). Our data suggest that such a role can also be fulfilled by His^{496} in apo-CPO and thus most probably also by the corresponding histidines of the phosphatases contained in the alignment.

Downloaded by YORK UNIV on October 31, 2012 | http://pubs.acs.org
Publication Date: December 10, 1998 | doi: 10.1021/bk-1998-0711.ch016

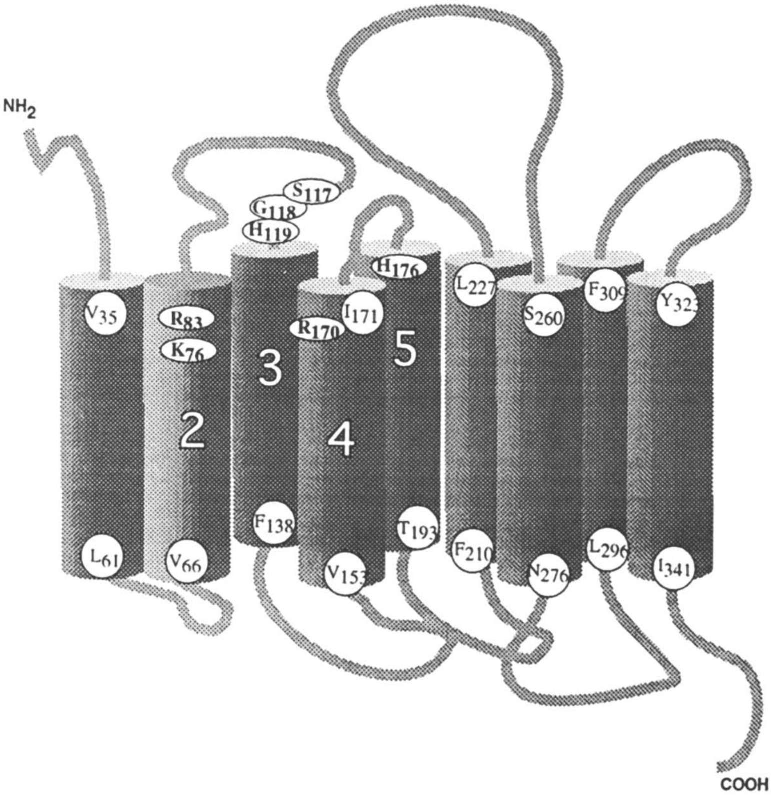
NH2
V35
L61
R83
K76
2
V66
S117
G118
H119
3
F138
R170
I171
4
V153
H176
5
T193
L227
F210
S260
N276
F309
L296
Y323
I341
COOH

Figure 5. Newly proposed nine transmembrane helix topology model for G-6-Pase. Residues predicted to be on the membrane interface are depicted as open ovals. Putative G-6-Pase active site residues are depicted as open circles.

Downloaded by YORK UNIV on October 31, 2012 | http://pubs.acs.org
Publication Date: December 10, 1998 | doi: 10.1021/bk-1998-0711.ch016

A Role of Aspartate in Peroxidase/Acid Phosphatase Catalysis? High molecular weight acid phosphatases also contain an aspartate residue in their active site. Mutational studies on this residue (Asp^{258}) in rat prostatic acid phosphatase and the corresponding Asp^{304} in *E. coli* acid phosphatase indicated that this residue is involved in the protonation of the leaving group in the phosphatase reaction (*38, 39*). Strikingly, an aspartate residue (Asp^{292}) is also found in the active site of V-CPO and both its position and the preliminary results of the analysis of an Asp^{292}-Ala mutation –which is produced using our *S. cerevisiae* expression system– indicate that this residue also has an important role in V-CPO catalysis.

In the alignment however no conserved aspartate is found implying either that such a residue is not important for the catalytic mechanism of the aligned acid phosphatases or that it is contained in a stretch of non conserved residues. Considering the very low degree of sequence conservation outside the conserved domains in the histidine phosphatase/peroxidase family, we consider the latter explanation more likely. In this context it may be important to note that D^{38}-V mutations are identified in French patients suffering from von Gierke disease (*40*). In the six transmembrane helix topology model this residue was situated in the middle of the predicted first transmembrane helix. In the newly proposed topology model this residue is situated in the NH_2-terminal loop at the luminal side of the ER membrane. It is thus very well possible that this loop folds on to the active site and that Asp^{38} of G-6-Pase fulfils a role similar to that of Asp^{292} of V-CPO.

Concluding Remarks.

It is just two years ago when we first realised that the active site histidines of "our" V-CPO were conserved in two regions of the secreted class A bacterial acid phosphatases and thus that the vanadate-containing haloperoxidases were not such an odd group of enzymes as we thought they were. Since then many surprising homologues have been identified in species ranging from *E. coli* to human. Since structural data are absent for these enzymes and off course since many of the proteins have still unidentified functions, recognition of the three domains gives insight into the nature and the structure of the active sites. Furthermore, in the case of membrane proteins –of which there seem to be many in this protein family– positioning of the domains may lead to proposals for the membrane topology model as we showed for G-6-Pase.

Acknowledgments

This work was supported by the Netherlands Foundation for Chemical Research (SON) and was made possible by financial support from the Netherlands Organisation for Scientific Research (NWO) and the Netherlands Technology Foundation (STW) and the Netherlands Association of Biotechnology Centres (ABON).

Literature Cited

(1) Wever, R. In *Biochemistry of Global Change*; Oremland, R. S., Ed.; Chapman and Hall: New York, 1991, p 811-824.

(2) Vilter, H. In *Metal ions in Biological systems*; Sigel, H., Sigel, A., Eds.; Marcel Dekker, Inc: New York, Basel, Hong Kong, 1995; Vol. 31, p 326-362.

(3) Vollenbroek, E. G. M.; Simons, L. H.; Van Schijndel, J. W. P. M.; Barnett, P.; Balzar, M.; Dekker, H. L.; Van der Linden, C.; Wever, R. *Biochem. Soc. Trans.* **1995**, *23*, 267-271.

(4) Plat, H.; Krenn, B. E.; Wever, R. *Biochemical J.* **1987**, *248*, 277-279.

Downloaded by YORK UNIV on October 31, 2012 | http://pubs.acs.org
Publication Date: December 10, 1998 | doi: 10.1021/bk-1998-0711.ch016

(5) Hager, L. P.; Morris, D. R.; Brown, F. S.; Eberwein, H. *J. Biol. Chem.* **1966**, *241*, 1769-1777.
(6) Zeng, J.; Fenna, R. E. *J. Mol. Biol.* **1992**, *226*, 185-207.
(7) Vilter, H. *Phytochemistry* **1984**, *23*, 1387-1390.
(8) De Boer, E.; Van Kooyk, Y.; Tromp, M. G. M.; Plat, H.; Wever, R. *Biochim. Biophys. Acta* **1986**, *869*, 48-53.
(9) van Schijndel, J. W. P. M.; Barnett, P.; Roelse, J.; Vollenbroek, E. G. M.; Wever, R. *Eur. J. Biochem* **1994**, *225*, 151-157.
(10) Simons, L. H.; Barnett, P.; Vollenbroek, E. G. M.; Dekker, H. L.; Muijsers, A. O.; Messerschmidt, A.; Wever, R. *Eur. J. Biochem.* **1995**, *229*, 566-574.
(11) Messerschmidt, A.; Wever, R. *Proc. Natl. Acad. Sci. USA* **1996**, *93*, 392-396.
(12) Barnett, P.; Kruidbosch, D. L.; Hemrika, W.; Dekker, H. L.; Wever, R. *Biochim. Biophys. Acta* **1997**, *1352*, 73-84.
(13) Hemrika, W.; Renirie, R.; Dekker, H. L.; Barnett, P.; Wever, R. *Proc. Natl. Acad. Sci. USA* **1997**, *94*, 2145-2149.
(14) Tromp, M. G. M.; Van, T. T.; Wever, R. *Biochim. Biophys. Acta* **1991**, *1079*, 53-56.
(15) Stankiewicz, P. J.; Tracey, A. S.; Crans, D. C. In *Metal Ions in Biological Systems*; Sigel, H., Sigel, A., Eds.; Marcel Dekker, Inc: New York, Basel, Hong Kong, 1995; Vol. 31, p 660-662.
(16) Stukey, J.; Carman, G. M. *Protein Sci.* **1997**, *6*, 469-472.
(17) Neuwald, A. F. *Protein Sci.* **1997**, *6*, 1764-1767.
(18) Barnett, P.; Hondmann, D. H.; Simons, L. H.; Ter Steeg, P. F.; Wever, R. In *International Patent Application (PCT) WO 95/27046* 1995.
(19) Messerschmidt, A.; Prade, L.; Wever, R. *Biol. Chem.* **1997**, *378*, 309-315.
(20) Thaller, M. C.; Berlutti, F.; Schippa, S.; Lombardi, G.; Rossolini, G. M. *Microbiol.* **1994**, *140*, 1341-1350.
(21) Hemrika, W.; Wever, R. *FEBS Lett.* **1997**, *409*, 317-319.
(22) Nordlie, R. C.; Sukalski, K. A. In *The Enzymes of Biological Membranes*; Martosoni, A. N., Ed.; Plenum Press: New York, 1985; Vol. 2nd Ed., p 349-398.
(23) Lei, K. J.; Shelly, L. L.; Pan, C. J.; Sidbury, J. B.; Yang Chou, J. *Science* **1993**, *262*, 580-583.
(24) Shelly, L. L.; Lei, K. J.; Pan, C. J.; Sakata, S. F.; Ruppert, S.; Schutz, G.; Yang Chan, J. *J. Biol. Chem.* **1993**, *268*, 21482-21485.
(25) Beaudet, A. L. In *Harrison's Principle of Internal Medicine*; Wilson, J. D., Braunwald, E., Isselbacher, K. J., Petersdorf, R. G., Martin, J. B., Fauci, J. S., Root, R. K., Eds.; McGraw-Hill: New York, 1991; Vol. 12th Ed., p 1854-1860.
(26) Hers, H. G.; Van Hoof, F.; Barsy, T. In *The Metabolic Basis of Inherited Diseases*; Scriver, C. R., Beaudet, A. L., Charles, R., Sly, W. S., Valle, D., Eds.; McGraw-Hill, Inc.: New York, 1989, p 425-452.
(27) Lei, K.-J.; Chen, H.; Pan, C., -J.; Ward, J. M.; Mosinger, B.; Lee, E. J.; Westphal, H.; Mansfield, B. C.; Chou, J. Y. *Nature Genetics* **1996**, *13*, 203-209.
(28) Lei, K. J.; Pan, C. J.; Liu, J. L.; Shelly, L. L.; Yang Chou, J. *J. Biol. Chem* **1995**, *270*, 11882-11886.
(29) Hoffman, K.; Stoffel, W. *Biol. Chem. Hoppe Seyler* **1993**, *347*, 166-170.
(30) Rost, B.; Sander, C. *J. Mol. Biol.* **1993**, *232*, 584-599.
(31) Rost, B.; Sander, C. *Proteins* **1994**, *19*, 55-72.
(32) Rost, B.; Sander, C. *Proteins* **1994**, *20*, 216-226.
(33) Zhang, N.; Zhang, J., Purcell, K. J.,; Cheng, Y.; Howard, K. *Nature* **1996**, *385*, 64-67.
(34) Kai, M.; Wada, I.; Imai, S.; Sakane, F.; Kanoh, H. *J. Biol. Chem.* **1996**, *271*, 18931-18938.
(35) Kanoh, H.; Kai, M.; Wada, I. *Biochim. Biophys. Acta* **1997**, *1348*, 56-62.
(36) Lindqvist, Y.; Schneider, G.; Vihko, P. *Eur. J. Biochem.* **1994**, *221*, 139-142.
(37) Van Etten, R. L.; Hickey, M. E. *Arch. Biochem. Biophys.* **1977**, *183*, 250-259.

Downloaded by YORK UNIV on October 31, 2012 | http://pubs.acs.org
Publication Date: December 10, 1998 | doi: 10.1021/bk-1998-0711.ch016

(38) Ostanin, K.; Saeed, A.; Van Etten, R. L. *J. Biol. Chem.* **1994**, *269*, 8971-8978.
(39) Porvari, K. S.; Herrala, A. M.; Kurkela, R.; Taavitsainen, P. A.; Lindqvist, Y.; Schneider, G.; Vihko, P. T. *J. Biol. Chem.* **1994**, *269*, 22642-22646.
(40) Chevalier-Porst, F.; Bozon, D.; Bonardot, A.; Bruni, N.; Mithieux, G.; Mathieu, M.; Maire, I. *J. Med. Genet.* **1996**, *33*, 358-360.

Downloaded by YORK UNIV on October 31, 2012 | http://pubs.acs.org
Publication Date: December 10, 1998 | doi: 10.1021/bk-1998-0711.ch016

Downloaded by UNIV OF GUELPH LIBRARY on October 31, 2012 | http://pubs.acs.org
Publication Date: December 10, 1998 | doi: 10.1021/bk-1998-0711.ch017

Chapter 17

The Vanadium-Containing Nitrogenase System of *Azotobacter vinelandii*

C. Rüttimann-Johnson, R. Chatterjee[1], V. K. Shah, and P. W. Ludden

Department of Biochemistry, Center for the Study of Nitrogen Fixation, College of Agriculture and Life Sciences, University of Wisconsin, Madison, WI 53706

Biological conversion of N_2 into NH_4^+ is catalyzed by the enzyme nitrogenase. *Azotobacter vinelandii,* a member of the family Azotobacteriaceae harbors three genetically distinct nitrogenase systems: a Mo-containing nitrogenase, a V-containing nitrogenase and an Fe-only nitrogenase. All nitrogenases are two-component metalloenzymes, comprised of dinitrogenase and dinitrogenase-reductase. Dinitrogenase contains the active site metal center of the enzyme, while dinitrogenase reductase is the obligate electron donor to dinitrogenase during catalysis. The genes encoding the three nitrogenases are contained in different regulons that carry not only structural genes, but also genes whose products are involved in cofactor biosynthesis and processing of the nitrogenases into mature enzymes. In this article we discuss what is known about the relatively recently discovered V-nitrogenase. The many aspects that are common to V-nitrogenase and the conventional Mo-containing enzyme are reviewed. V-nitrogenase differs from Mo-nitrogenase in its substrate reduction properties and in the subunit composition of the mature enzyme. The δ subunit, present in the catalytically active V-dinitrogenase, is unique to the V- and Fe-only nitrogenases. Its role in the maturation of the enzyme is discussed. Little is known about the synthesis of the active site cofactor of V-dinitrogenase, the iron-vanadium cofactor (FeV-co). Some gene products involved in the synthesis of FeMo-co (the active site cofactor of Mo-dinitrogenase) are known to play a role in FeV-co synthesis too, suggesting that the cofactors share parts of their biosynthetic pathways.

Biological conversion of nitrogen to ammonium, an important process in the cycling of N from the atmosphere to the soil, is catalyzed by the bacterial enzyme nitrogenase. Nitrogenase systems are composed of two separate enzymes: dinitrogenase reductase and dinitrogenase (see (*1*) for a review). The reduction of the substrate, N_2, is catalyzed by dinitrogenase, while dinitrogenase reductase serves as the obligate

---

[1] Current address: Argonne National Laboratories, 9700 South Cass Avenue, Argonne, IL 60439

In Vanadium Compounds; Tracey, A., et al.;
ACS Symposium Series; American Chemical Society: Washington, DC, 1998.

Downloaded by UNIV OF GUELPH LIBRARY on October 31, 2012 | http://pubs.acs.org
Publication Date: December 10, 1998 | doi: 10.1021/bk-1998-0711.ch017

electron donor to dinitrogenase. Dinitrogenase reductase does so by docking with dinitrogenase and transferring electrons, one at a time, in a MgATP-dependent reaction. A schematic representation of the reaction catalyzed by nitrogenase is presented in Figure 1. Both nitrogenase proteins contain metal-sulfur clusters that are involved in the electron transfer reactions. Dinitrogenase reductase is a homodimer that contains a single Fe_4S_4 cluster located in the subunit interface. Dinitrogenase contains two types of unique metal-sulfur clusters: the P-clusters, Fe-S clusters of unusual spectroscopic properties, and an iron-heterometal cofactor, which is the site of substrate reduction.

The most widely studied nitrogenases contain molybdenum as the heterometal in their active site cofactor. In fact, Mo was considered essential for N_2 fixation for many years and all wild-type N_2-fixing organisms studied so far have a Mo-containing nitrogenase system (*nif*-encoded). Research done in recent years, nevertheless, has shown the existence of vanadium-containing nitrogenases (*vnf*-encoded) as well as nitrogenases in which no metal other than Fe has been detected in their active site cofactors (the "Fe-only" nitrogenase, *anf*-encoded). Pioneering work done by Bortels (*2,3*) showed that V could support diazotrophic growth by *Azotobacter vinelandii*, but these findings were ignored and Mo was added routinely to the culture medium of N_2 fixing organisms. Later, in 1976, Burns and colleagues (*4*) reported the purification of a V-containing nitrogenase from *A. vinelandii* grown in the presence of V, but those results were interpreted as the incorporation of V into the molybdenum site of the Mo-dinitrogenase. It was not until strains of *A. vinelandii* with mutations in the structural genes for the *nif*-encoded, Mo-dinitrogenase were shown to be capable of diazotrophic growth in medium lacking Mo that it was suspected that there were nitrogenase systems other than the well studied *nif*-encoded system (*5-7*) . Upon purification, the first of these was found to contain vanadium by Robson and coworkers (*8*), and the genes for this regulon were designated *vnf* (for vanadium-dependent nitrogen fixation). Since then, V-nitrogenases have been purified from *A. vinelandii* (*9-11*) and *Azotobacter chroococcum* (*8,12*). Genes coding for the structural components of V-nitrogenase have been detected by DNA hybridization in a variety of strains of the family Azotobacteriaceae (*13*) and in the cyanobacterium *Anabaena variabilis* (*14*). Another important development in the field of N_2 fixation was the discovery and purification of a third nitrogenase from *A. vinelandii* that lacks both Mo and V by Bishop and coworkers (*15*). This type of nitrogenase has also been shown to be present in other Azotobacteriaceae (*13*) as well as in anaerobes, like *Clostridium pasteurianum* (*16*), and photosynthetic bacteria such as *Rhodobacter capsulatus* (*17*) and *Rhodospirillum rubrum* (*18,19*). Fe is the only metal ion that has been detected in this nitrogenase in stoichiometric amounts (*20*).

The possession of genes coding for V- and Fe-only nitrogenases could be advantageous to an organism for diazotrophy when growing in an environment deficient in Mo and/or V. Moreover, it has been shown that the V-nitrogenase is potentially more efficient at reducing N_2 at temperatures below 30°C than the Mo-nitrogenase (*21*), representing a selective advantage for organisms under conditions of low temperature. Interestingly, the repression of V-nitrogenase expression by Mo (see later) is less effective at 22 °C than at 30°C and does not occur at all at 14°C (*22*). Thus, V-nitrogenase would be expressed at low temperatures regardless of the environmental Mo content.

Structural Components of V-Nitrogenase

The dinitrogenase reductase encoded by *vnfH* is very similar to the enzyme encoded by *nifH* in that it is a homodimer and contains one iron-sulfur cluster. The enzymes show a 95% identity to each other at the amino acid level, with the Cys residues that bind the iron-sulfur cluster conserved (*23*). Given the sequence similarity between VNFH and NIFH, it is not surprising that heterologous complexes between the component proteins

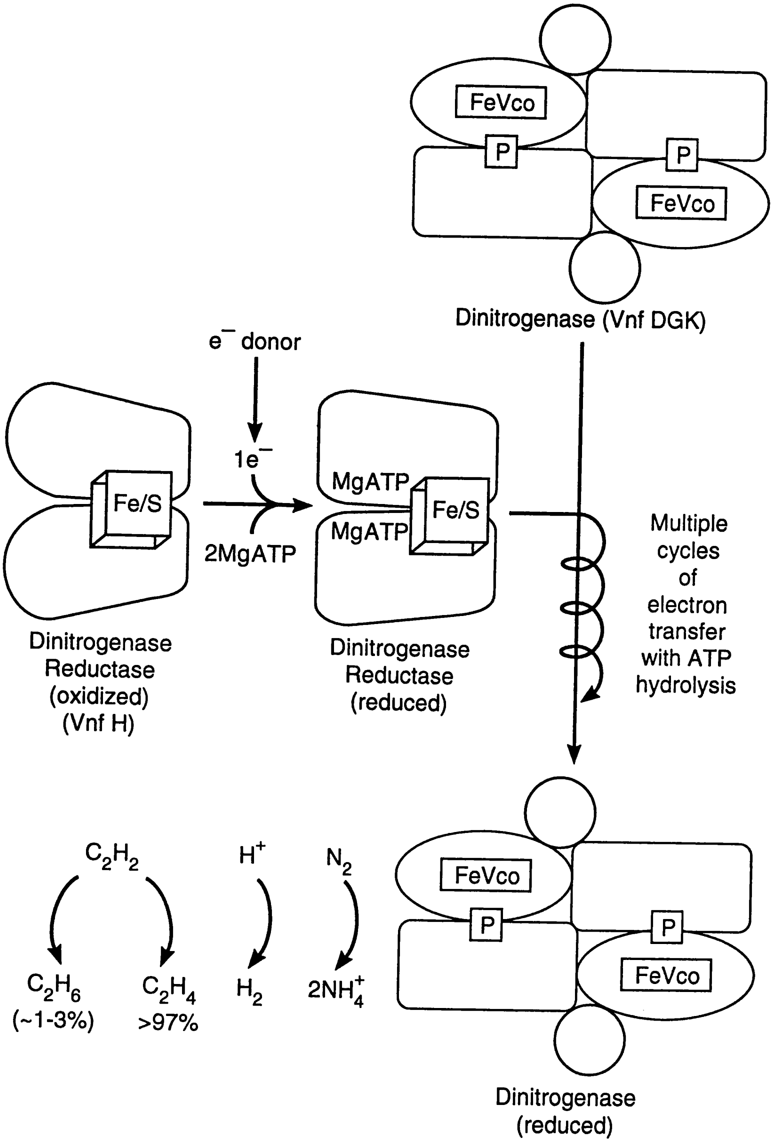
FeVco
P
P
FeVco
Dinitrogenase (Vnf DGK)
e⁻ donor
1e⁻
2MgATP
Fe/S
MgATP
MgATP
Fe/S
Dinitrogenase Reductase (oxidized) (Vnf H)
Dinitrogenase Reductase (reduced)
Multiple cycles of electron transfer with ATP hydrolysis
FeVco
P
P
FeVco
Dinitrogenase (reduced)
C_2H_2
C_2H_6 (~1-3%)
C_2H_4 >97%
H^+
H_2
N_2
$2NH_4^+$

Figure 1. The catalytic cycle of *vnf*-encoded nitrogenase.

Downloaded by UNIV OF GUELPH LIBRARY on October 31, 2012 | http://pubs.acs.org
Publication Date: December 10, 1998 | doi: 10.1021/bk-1998-0711.ch017

of *nif*- and *vnf*-nitrogenases are catalytically competent; that is, VNFH can serve as the electron donor for *nif*-dinitrogenase, and *vice-versa* (*21*). NIFH has several functions in the nitrogenase enzyme system. In addition to reducing dinitrogenase during nitrogenase turnover, it is required for the biosynthesis of FeMo-co (*24,25*) and for the processing of the $\alpha_2\beta_2$ form of apodinitrogenase into the $\alpha_2\beta_2\gamma_2$ form of the enzyme, which is activatable by FeMo-co (*26,27*) . Recent results obtained with enzymes purified from *A. vinelandii* show that VNFH can substitute for NIFH in the last two processes, too (*28*). VNFH was as effective as NIFH in the conversion of $\alpha_2\beta_2$ *nif*-apodinitrogenase into the $\alpha_2\beta_2\gamma_2$ form, which is able to accept FeMo-co. VNFH also required the presence of Mg-ATP for this process, as does NIFH. When tested for its ability to replace NIFH in the synthesis of FeMo-co (using an *in vitro* FeMo-co synthesis assay (*29*)), VNFH exhibited 25-30% of the activity observed with NIFH. These results suggest that the dinitrogenase reductase proteins do not specify the heterometal incorporated into the cofactors of the respective nitrogenase systems.

Downloaded by UNIV OF GUELPH LIBRARY on October 31, 2012 | http://pubs.acs.org
Publication Date: December 10, 1998 | doi: 10.1021/bk-1998-0711.ch017

The α and β subunits of the V-dinitrogenase show similarity to the corresponding subunits of the Mo-dinitrogenase (33% and 31% identity at the amino acid level in *A.vinelandii* (*23*), respectively). In particular, the Cys residues that ligate the P-clusters and the Cys and His residues that bind FeMo-co, which are invariant in all Mo-dinitrogenases, are also conserved in the V-dinitrogenases. The most striking difference between the Mo-dinitrogenases and the V-dinitrogenases is the presence in the latter of the δ subunit. This subunit is unique to alternative nitrogenases. It is coded for by *vnfG*, located between *vnfD* and *K*, the genes coding for the α and β subunits of dinitrogenase. In vivo studies have shown that *A. vinelandii* mutant strains where a stop codon has been introduced at the position of *cys17* in the *vnfG* gene are incapable of V-dependent diazotrophic growth (*30*). The cells, however, were able to reduce acetylene, suggesting that an alternative protein can take the place of δ, to render a dinitrogenase with altered substrate specificity. The δ subunit has been shown to be loosely associated to *vnf*-apodinitrogenase in extracts of a strain incapable of synthesizing FeV-co (*31*). The three subunits comigrated in anoxic native gel electrophoresis, but the δ subunit could be separated from the complex by gel filtration chromatography. The *vnf*-apodinitrogenase (lacking FeV-co, but containing the P-clusters) present in these cell extracts could be activated by addition of partially purified FeV-co. The $\alpha_2\beta_2$ complex lacking δ, however, could only be activated by FeV-co if δ was also added to the reaction mixture. It has also been observed that FeV-co associates specifically with purified δ in vitro (*32*). These observations suggest a role for the δ subunit in the processing of *vnf*-apodinitrogenase into holodinitrogenase. A similar role is performed by the γ protein in the Mo-nitrogenase system. This protein (a non-*nif* protein in *A. vinelandii*) acts as a chaperone-insertase, necessary for the processing of *nif*-apodinitrogenase into the active holodinitrogenase (*27*). Unlike γ, which does not stay attached to the *nif*-holodinitrogenase, δ stays tightly bound to the active *vnf*-dinitrogenase (*32*). Thus, while the subunit composition of the mature *nif*-dinitrogenase is $\alpha_2\beta_2$, that of *vnf*-dinitrogenase is $\alpha_2\beta_2\delta_2$. There is no immunological cross-reactivity between VNFG (δ) and γ. The complete sequence of γ is not known, but available N-terminal sequence of γ does not match the deduced sequence of VNFG (δ). A distinct difference between the systems of cofactor insertion for FeV-co into *vnf*-apodinitrogenase and FeMo-co into *nif*-dinitrogenase is the absence of requirement for VNFH for FeV-co insertion, although MgATP is still required.

The Iron-Vanadium Cofactor

Results from EPR, EXAFS, MCD and Mössbauer spectroscopy have shown that the metal clusters of V-dinitrogenase exhibit similar characteristics as far as number and composition to those of Mo-dinitrogenase (*33-37*). The P-clusters seem to be almost identical in both enzymes (*34,35*). The spectroscopic properties of V-dinitrogenase have been extensively reviewed by Eady (*38*). The V-dinitrogenase contains an iron-vanadium cofactor (FeV-co) analogous to FeMo-co of the molybdenum system (*36*). The cofactor can be extracted from purified V-dinitrogenase by the method employed to obtain FeMo-co, and it is presumed to be structurally very similar to FeMo-co. The isolated cofactor was able to activate *nif*-apodinitrogenase of *K. pneumoniae* (*36*). The hybrid dinitrogenase showed substrate reducing properties of V-dinitrogenase (it reduced acetylene to ethylene and ethane), but was unable to reduce N_2. The last observation suggests that specific interactions between the cofactor and its ligands in the protein are necessary for N_2 reduction to occur. Similarly, a hybrid enzyme obtained by insertion of FeMo-co into highly purified *vnf*-apodinitrogenase was unable to reduce N_2 (*31*), but did reduce acetylene to ethylene, although at a lower rate than *nif*- and *vnf*-dinitrogenases. Interestingly, this hybrid enzyme was also able to reduce acetylene into ethane, a characteristic associated with V-dinitrogenase (see later). Conflicting results by Moore *et al.* (*39*) showed that a similar hybrid dinitrogenase obtained by the insertion of FeMo-co into *vnf*-apodinitrogenase was able to fix N_2 at a rate similar to that of *nif*-dinitrogenase. This discrepancy may result from the fact that the latter authors used a crude extract as a source of the *vnf*-apodinitrogenase.

The ability of FeV-co to activate *nif*-apodinitrogenase suggests that its structure is similar to FeMo-co, fitting in the same pocket in the enzyme. Figure 2 shows the proposed structure for FeV-co, by analogy to the structure that has been determined for FeMo-co (*40*). Other evidence that suggests a similar structure for FeMo-co and FeV-co is the fact that two *nif* genes (*nifB* and *nif V*) that are required for the biosynthesis of FeMo-co are also required for diazotrophic growth in V. The protein encoded by *nifB* synthesizes NifB-co (*41*), a Mo-free precursor of FeMo-co. NifB-co has been shown to bind to NIFEN, and Fe and S from NifB-co are incorporated into FeMo-co (*42*). The fact that mutants deleted in *nifB* are incapable of diazotrophic growth in V-containing medium (*43*) suggests that NifB-co could be serving as the Fe-S donor for FeV-co synthesis. The *nifB* gene is presumed to be expressed in the presence of Mo or V, since there are potential binding sites for both NIFA and VNFA (the transcriptional activators for *nif* and *vnf* genes, respectively, see later) in the region upstream of its transcription start site (*44*). Both NIFA and VNFA have been shown to activate transcription of the *nifB* gene. The *nifV* gene encodes a homocitrate synthetase (*45*), homocitrate being a structural component of FeMo-co (*46*). *A. vinelandii* mutants deleted in *nifV* grew poorly in medium containing vanadate (*47*), strongly suggesting that FeV-co too contains homocitrate as a structural component. Strains with mutations in *nifV* can be cured by addition of homocitrate to the growth medium (*48*).

It has not been possible to reproducibly synthesize FeV-co *in vitro* using methods employed to perform the *in vitro* synthesis of FeMo-co (*29*). This may reflect the chemical species of V present in systems tested to date. Dithionite is present in the in vitro FeMo-co synthesis system both to protect O_2-labile components of the system and to serve as the required reductant for synthesis. Dithionite will reduce vanadate to at least the vanadyl (V(III)) state and it is possible that this oxidation state is not acceptable to the initial step of FeV-co synthesis. It has not been possible to

Downloaded by UNIV OF GUELPH LIBRARY on October 31, 2012 | http://pubs.acs.org
Publication Date: December 10, 1998 | doi: 10.1021/bk-1998-0711.ch017

Downloaded by UNIV OF GUELPH LIBRARY on October 31, 2012 | http://pubs.acs.org
Publication Date: December 10, 1998 | doi: 10.1021/bk-1998-0711.ch017

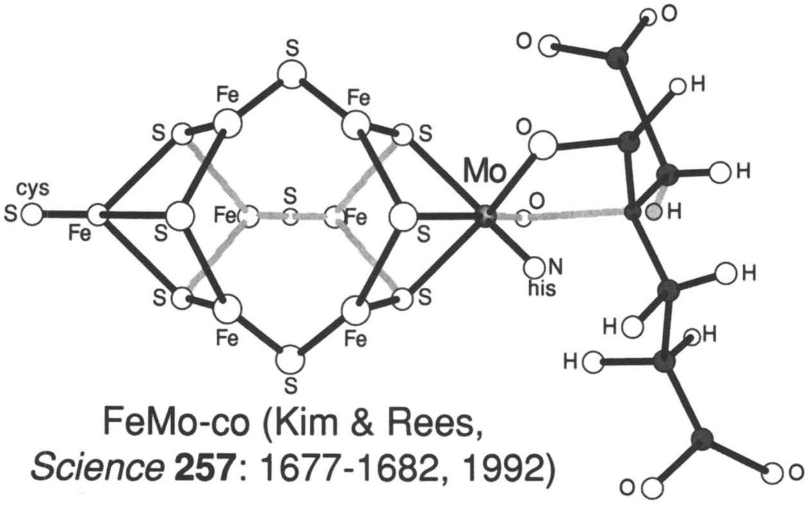
S
Fe
Fe
S
S
Mo
O
O
H
H
cys
S
Fe
S
Fe
S
Fe
S
O
H
N
his
S
S
H
H
H
Fe
Fe
H
S
O
O

FeMo-co (Kim & Rees, *Science* **257**: 1677-1682, 1992)

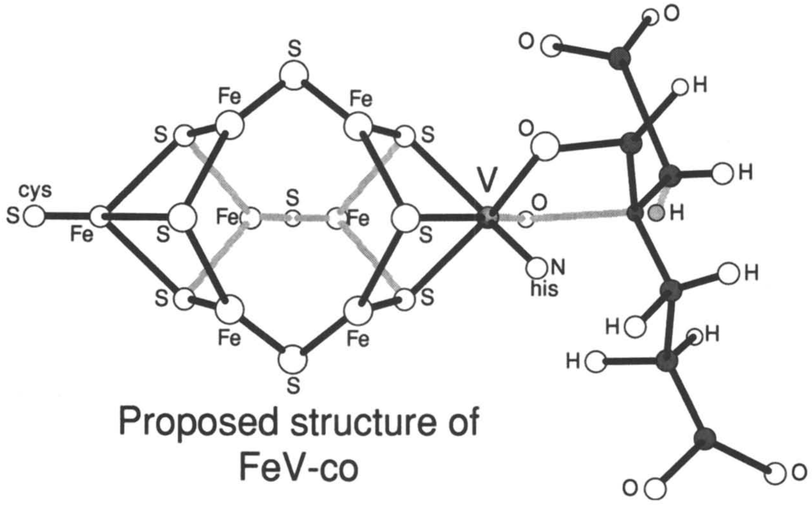
S
Fe
Fe
S
S
V
O
O
H
H
cys
S
Fe
S
Fe
S
Fe
S
O
H
N
his
S
S
H
H
H
Fe
Fe
H
S
O
O

Proposed structure of FeV-co

Figure 2. Proposed structure for FeV-co and structure of FeMo-co, adapted from (*40*).

employ extracts of V-grown cells as a source of V for FeV-co synthesis, suggesting problems even after the initial processing steps might have taken place (Rüttimann-Johnson & Ludden, unpublished results).

Organization of Genes Coding for V-Nitrogenase

The structural components of the three nitrogenase systems are genetically distinct. The organization of the nitrogen fixation genes has been studied in different diazotrophs. The paradigm for the organization of *nif* genes was developed using *Klebsiella pneumoniae* (*49*). In this organism, 19 *nif* genes are clustered in a single 23 Kb region in the genome, which aided much of the early work. Other organisms, like *A. vinelandii*, *A. chroococcum* and *R. capsulatus* were studied later. Comparative studies show that there is a common core of 14 genes, which define a set of genes whose products are necessary for effective nitrogenase biosynthesis (for a review, see (*50*)). Figure 3 shows the gene arrangement for the three nitrogenase systems in *A. vinelandii*. The α and β subunits of Mo-dinitrogenase are coded for by *nifD* and *nifK*, respectively, and the subunits of dinitrogenase reductase are encoded by *nifH*. The *nifA* and *nifL* genes code for transcription activators that regulate the expression of the *nif* operons in response to fixed nitrogen. The rest of the genes are required for synthesis of FeMo-co, synthesis of the iron-sulfur clusters, maturation of dinitrogenase and dinitrogenase reductase, or their role remains unknown. In *K. pneumoniae* the *nifF* and *nifJ* genes encode a flavodoxin and a pyruvate flavodoxin oxidoreductase, respectively, and these serve as the donors of low potential electrons to dinitrogenase reductase.

The genes coding for the structural components of V-dinitrogenase (designated as *vnf* genes) are split in two operons (reviewed in (*51*)). One of them contains the *vnfH* gene, followed by an open reading frame whose predicted product shows sequence similarity with ferredoxins (designated *fdx*). The role of this ferrodoxin-like protein is not exactly known, but it has been suggested to serve as the *in vivo* electron donor to VNFH during enzyme turnover. It has been shown that a strain with a mutation in *vnffdx* is unable to grow diazotrophically in V-containing medium (*52*). The *vnfDGK* operon, located 1 Kbp downstream of the *vnfHFd* operon, encodes the subunits of V-dinitrogenase. The *vnfG* gene codes for a third subunit (δ) of V-dinitrogenase, which does not have a counterpart in Mo-dinitrogenase, but shows significant similarity to *anfG* of the Fe-only nitrogenase system.

Genes Coding for Non-Structural Components of V-Nitrogenase

Non-structural genes identified so far in the *vnf* regulon include *vnfA*, the *vnfENX* operon and two open reading frames located upstream of *vnfA*, whose products and their functions are unknown.

The *vnfA* gene codes for a transcriptional activator, whose counterpart in the Mo-nitrogenase system is *nifA* and in the Fe-only nitrogenase system is *anfA* (*53*). The gene products of *nifA*, *vnfA* and *anfA* are activator proteins that bind to upstream activator sequences (UAS), enabling the RNA polymerase to initiate transcription (for a review, see (*50*)). NIFA, VNFA and ANFA each recognize a different UAS. All three activator proteins are members of the σ^{54}-dependent activator family and have three distinct domains. The central domains of NIFA, VNFA and ANFA are homologous and contain an ATP binding motif. Studies with other activator proteins of this family have shown that they have an ATPase activity, which is strongly stimulated by site-specific DNA binding. The C-terminal domain mediates DNA binding. As expected, this domain differs in NIFA, VNFA and ANFA and provides the specificity of recognition of the UAS. VNFA may also have a role in repression of the *nif* structural

Downloaded by UNIV OF GUELPH LIBRARY on October 31, 2012 | http://pubs.acs.org
Publication Date: December 10, 1998 | doi: 10.1021/bk-1998-0711.ch017

Downloaded by UNIV OF GUELPH LIBRARY on October 31, 2012 | http://pubs.acs.org
Publication Date: December 10, 1998 | doi: 10.1021/bk-1998-0711.ch017

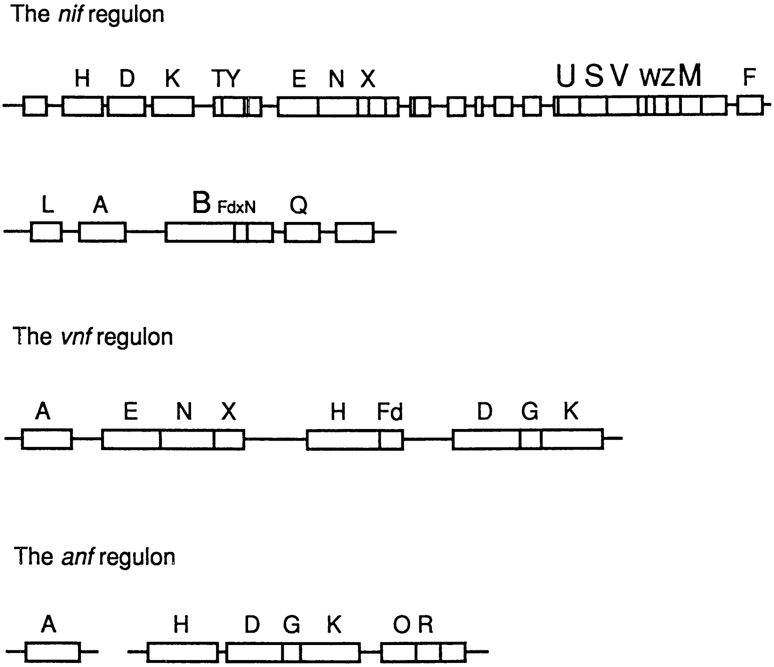
The *nif* regulon
H D K TY E N X
U S V WZM F
L A
B FdxN Q
The *vnf* regulon
A E N X
H Fd
D G K
The *anf* regulon
A
H D G K
O R

Figure 3. Arrangement of genes required for nitrogen fixation in *A. vinelandii.* The genes required for the functionality of the three nitrogenase enzymes are indicated in a larger font size. (Adapted from (*51*) and (*75*)).

genes in the absence of Mo, since a strain with a deletion in *vnfA* was able to synthesize *nif*-dinitrogenase in Mo-deficient medium (*53*).

The two open reading frames designated *vnfEN* show sequence similarity to *nifEN*. The predicted amino acid sequences for *vnfE* and *N* are 66 and 52% identical to the amino acid sequences of *nifE* and *N*, respectively (*54*). The gene products of *nifEN* are required for FeMo-co synthesis and NIFEN has been shown to bind NifB-co, the Fe and S donor for FeMo-co (*42,55*). Based on the amino acid sequence similarity between the *nifDK* and the *nifEN* gene products and on the fact that the *nifDK* gene products are not required for FeMo-co synthesis, it has been proposed that the NIFEN might serve as a scaffold for the synthesis of the cofactor (*56*). Thus, FeMo-co would be partly synthesized on the *nifEN* gene product complex prior to incorporation into apodinitrogenase. A similar role could be performed by the *vnfEN* gene products during FeV-co synthesis. Interestingly, there are four *cys* residues that could serve as metal-binding ligands that are conserved in *nifD*, *nifE* and *vnfE*. Also one *cys* residue conserved between *nifK* and *nifN* is also conserved in *vnfN*. The existence of *nifEN* analogs in the *vnf* regulon might suggest that these gene products are involved in steps unique to the biosynthesis of FeV-co, like the incorporation of V into the cofactor. Nevertheless, it appears that NIFEN can replace VNFEN during FeV-co synthesis *in vivo*, since a strain with a mutation in *vnfE* is still able to grow diazotrophically in V (*54*). A strain with a deletion in *nifEN* and a mutation in *vnfE* is incapable of diazotrophic growth in V. No analog to *nifEN* has been found in the *anf* system. It is important to note that no form of NIFEN has been observed to contain Mo.

The predicted amino acid sequence of the *vnfX* gene shows 33% identity with the NIFX protein (*54*). The exact role of NIFX is not clearly understood, but it is known that it is involved in the synthesis of FeMo-co. Studies using purified proteins to synthesize FeMo-co *in vitro* have shown that addition of purified NIFX stimulates the synthesis reaction by two-fold (*57*). When overexpressed, NIFX also acts as a negative regulator of the *nif* regulon in *K. pneumoniae* (*58*). Whether the gene product of *vnfX* plays any of these roles in the V-nitrogenase system is not known. Curiously, strains of *K. pneumoniae* and *A. vinelandii* with mutations in *nifX* are Nif$^+$ and thus a functional *nifX* gene is not required for production of a functional nitrogenase. It is possible that some other gene product replaces NIFX *in vivo*.

nif Genes Required for V-Dependent Diazotrophic Growth

Other *nif* genes required for full V-nitrogenase activity are *nifU*, *nifS* and *nifM*, as mutants deleted in any of these genes are not able to grow diazotrophically in V-containing medium (*47,59*). The *nifM* gene product is involved in the maturation of the dinitrogenase reductase (*60*). It is not surprising, given the high degree of similarity that exists between *nif*- and *vnf*-dinitrogenase reductases, that the same gene product would be involved in the processing of both enzymes. The products of *nifU* and *nifS* are involved in mobilization of iron and sulfur for cluster biosynthesis and are required for full activity of both dinitrogenase and dinitrogenase reductase (*61*).

Regulation of the Expression of the Different Nitrogenase Systems

The expression of the three different nitrogenase systems is regulated in *A. vinelandii* at the transcriptional level by the metal content of the culture medium (*62*). The presence of Mo appears to be necessary for the full induction of the Mo-containing nitrogenase (*63*). Nanomolar concentrations of molybdate also repress the expression of both *vnf*- and *anf*-encoded nitrogenase systems. Vanadium, in turn, is required for the expression of the V-containing nitrogenase system. This regulation by V does not seem to occur at the transcriptional level, since northern blot analysis has shown that in

Downloaded by UNIV OF GUELPH LIBRARY on October 31, 2012 | http://pubs.acs.org
Publication Date: December 10, 1998 | doi: 10.1021/bk-1998-0711.ch017

the absence of V and Mo *vnfDGK* transcripts are produced by the cell (*62*). V also represses the expression the *anf*-encoded nitrogenase, this regulation being exerted at the transcriptional level (*62*). The expression of the *anf*-encoded nitrogenase, thus, requires the medium to be depleted of both Mo and V.

Substrate Reduction Properties of V-Nitrogenase

All three nitrogenase systems catalyze the reduction of N_2 to NH_4^+, H^+ to H_2 and C_2H_2 to C_2H_4, the latter being used as a routine assay for the enzyme. In addition, the *vnf*-encoded nitrogenase and the *anf*-encoded nitrogenase can also reduce C_2H_2 to C_2H_6 (*64*). This has been used as an indication of the presence of alternative nitrogenases in microorganisms (*13,64*). Alternative nitrogenases are less efficient in reducing N_2 than Mo-nitrogenase. The apparent Km for N_2 is the same for V-nitrogenase and Mo-nitrogenase, but the distribution of electrons to N_2 and H^+ is different. While Mo-nitrogenase transfers a maximum of 75 % of the electrons to N_2 (reaction 1) at most 50% of the electron flux through V-nitrogenase has been observed to be utilized for N_2 reduction (*7*) , the remainder going for reduction of H^+ (reaction 2).

$$N_2 + 8e^- + 10H^+ \rightarrow 2NH_4^+ + H_2 \qquad (1)$$

$$N_2 + 12e^- + 14H^+ \rightarrow 2NH_4^+ + 3H_2 \qquad (2)$$

Early Steps in Mo and V Metabolism in *A. vinelandii*

The early steps of Mo metabolism in the N-fixing organisms *A. vinelandii* and *R. capsulatus* have been the subject of investigation (*65*). Unlike V, Mo has roles in the cell in addition to its role in nitrogen fixation and there must exist mechanisms to apportion the Mo to the various sources. In *A. vinelandii* a periplasmic protein, ModA, binds molybdate and delivers it to an ABC-type transporter. Within the cell, the ModE protein serves as a Mo-responsive transcriptional regulatory protein (*66,67*). Molybdate also binds to the "molbindin" proteins, Mop and ModG. This system is similar to that described for *E. coli* (*68-71*). A non-*nif* molybdenum storage protein has also been purified and described for *A. vinelandii* (*72*). It is unlikely that the molybdenum storage protein described by Pienkos and Brill corresponds to the product of any of the genes for molybdate uptake/binding identified so far. Several catecholate siderophores have been shown to bind molybdate tightly and are proposed to play a role in scavenging molybdate for *A. vinelandii* (*73,74*). Uptake and processing of vandium is far less well understood. The molybdenum storage protein does not appear to accumulate in cells grown in the absence of Mo and the presence of V (Rüttimann-Johnson, unpublished results). Because V in the cell probably exists as the reduced vandyl (VO_3^-) species, it is unlikely that the proteins which handle molybdate play a role in early steps in V metabolism. The inability of vanadate in the medium to inhibit Mo-dependent diazotrophic growth suggests that vanadate does not compete effectively for the uptake of molybdate by the ModABC system.

Future Studies

The study of V metabolism for the production of the FeV-cofactor for nitrogenase is at a very early stage of investigation. Among the questions to be addressed are: How does vanadium enter the cell? in what oxidation state? and by what carrier? Is there a

Downloaded by UNIV OF GUELPH LIBRARY on October 31, 2012 | http://pubs.acs.org
Publication Date: December 10, 1998 | doi: 10.1021/bk-1998-0711.ch017

V-storage protein? Where does V enter the pathway committed to FeV-co synthesis? How many gene products function in FeV-co synthesis? How is V from damaged FeV-co recycled? What gene product specifies the heterometal in FeX-co synthesis? Are the various FeX-cos discriminated by the various nitrogenase proteins in vivo? by the various chaperone/insertases?

These and other questions will occupy our attention for a number of years.

Acknowledgments

We thank Gary Roberts and members of his laboratory for many helpful discussions during the preparation of this review and Priya Rangaraj for critical revision of the manuscript. Work from the authors' laboratory cited herein has been supported by grants from NIH (GM35332) and from USDA NRI (96-35305-3697)

Downloaded by UNIV OF GUELPH LIBRARY on October 31, 2012 | http://pubs.acs.org
Publication Date: December 10, 1998 | doi: 10.1021/bk-1998-0711.ch017

Literature Cited

1. Peters, J. W.; Fisher, K.; Dean, D. R. *Annu. Rev. Microbiol.* **1995,** *49,* 335-366.
2. Bortels, H. *Arch. Mikrobiol.* **1930,** *1,* 333-342.
3. Bortels, H. *Zentralbl. Bakteriol. Parasitenkd. Infektionskr. II. Abt.* **1936,** *95,* 193-218.
4. Burns, R. C.; Stasny, J. T.; Hardy, R. W. F. In *Proc. 1st Symp. Nitrogen Fixation*; Newton, W. E., and Nyman, C. J., Eds.; Washington State University Press: Pullman, WA, 1976, Vol. 1; pp 196-207.
5. Bishop, P. E.; Jarlenski, D. M.; Hetherington, D. R. *Proc. Natl. Acad. Sci. USA* **1980,** *77,* 7342-7346.
6. Bishop, P. E.; Jarlenski, D. M.; Hetherington, D. R. *J. Bacteriol.* **1982,** *150,* 1244-1251.
7. Bishop, P. E.; Hawkins, M. E.; Eady, R. R. *Biochem. J.* **1986,** *238,* 437-442.
8. Robson, R. L.; Eady, R. R.; Richardson, T. H.; Miller, R. W.; Hawkins, M.; Postgate, J. R. *Nature* **1986,** *322,* 388-390.
9. Hales, B. J.; Case, E. E.; Morningstar, J. E.; Dzeda, M. F.; Mauterer, L. A. *Biochemistry* **1986,** *25,* 7251-7255.
10. Hales, B. J.; Langosch, D. J.; Case, E. E. *J. Biol. Chem.* **1986,** *261,* 15301-15306.
11. Blanchard, C. Z.; Hales, B. J. *Biochemistry* **1996,** *35,* 472-478.
12. Eady, R. R.; Robson, R. L.; Richardson, T. H.; Miller, R. W.; Hawkins, M. *Biochem. J.* **1987,** *244,* 197-207.
13. Fallik, E.; Chan, Y. K.; Robson, R. L. *J. Bacteriol.* **1991,** *173,* 365-371.
14. Thiel, T. *J. Bacteriol*. **1993,** *175,* 6276-6286.
15. Chisnell, J. R.; Premakumar, R.; Bishop, P. E. *J. Bacteriol.* **1988,** *170,* 27-33.
16. Zinoni, F. R.; Robson, R. M.; Robson, R. L. *Biochim. Biophys. Acta* **1993,** *174,* 83-86.
17. Schüddekopf, K.; Hennecke, S.; Liese, U.; Kutsche, M.; Klipp, W. *Mol. Microbiol.* **1993,** *8,* 673-684.
18. Lehman, L. J.; Roberts, G. P. *J. Bacteriol.* **1991,** *173,* 5705-5711.
19.Davis, R.; Lehman, L.; Petrovich, R.; Shah, V. K.; Roberts, G. P.; Ludden, P. W. *J. Bacteriol.* **1996,** *178,* 1445-1450.
20. Schneider, K.; Gollan, U.; Dröttboom, M.; Selsemeier-Voigt, S.; Müller, A. *Eur. J. Biochem.* **1997,** *244,* 789-800.
21. Miller, R. W.; Eady, R. R. *Biochem. J.* **1988,** *256,* 429-432.
22. Kennedy, C.; Bali, A.; Blanco, G.; Contreras, A.; Drummond, M.; Merrick,

M.; Walmsley, J.; Woodley, P. In *Nitrogen Fixation: Proceedings of the Fifth International Symposium with Non-Legumes*; Polsinelli, M., Materassi, R., and Vincenzini, M., Eds.; Kluwer Acedemic Publishers: Florence, Italy, 1991, Vol. 48; pp 13-23.

23. Joerger, R. D.; Loveless, T. M.; Pau, R. N.; Mitchenall, L. A.; Simon, B. H.; Bishop, P. E. *J. Bacteriol.* **1990,** *172,* 3400-3408.
24. Robinson, A. C.; Dean, D. R.; Burgess, B. K. *J. Biol. Chem.* **1987,** *262,* 14327-14332.
25. Filler, W. A.; Kemp, R. M.; Ng, J. C.; Hawkes, T. R.; Dixon, R. A.; Smith, B. E. *Eur. J. Biochem.* **1986,** *160,* 371-377.
26. Allen, R. M.; Homer, M. J.; Chatterjee, R.; Ludden, P. W.; Roberts, G. P.; Shah, V. K. *J. Biol. Chem.* **1993,** *268,* 23670-23674.
27. Homer, M. J.; Dean, D. R.; Roberts, G. P. *J. Biol. Chem.* **1995,** *270,* 24745-24752.
28. Chatterjee, R.; Allen, R. M.; Ludden, P. W.; Shah, V. K. *J. Biol. Chem.* **1997,** *272,* 21604-21608.
29. Shah, V. K.; Imperial, J.; Ugalde, R. A.; Ludden, P. W.; Brill, W. J. *Proc. Natl. Acad. Sci. USA* **1986,** *83,* 1636-1640.
30. Waugh, S. I.; Paulsen, D. M.; Mylona, P. V.; Maynard, R. H.; Premakumar, R.; Bishop, P. E. *J. Bacteriol.* **1995,** *177,* 1505-1510.
31. Chatterjee, R.; Allen, R. M.; Ludden, P. W.; Shah, V. K. *J. Biol. Chem.* **1996,** *271,* 6819-6826.
32. Chatterjee, R.; Ludden, P. W.; Shah, V. K. *J. Biol. Chem.* **1997,** *272,* 3758-3765.
33. Arber, J. M.; Dobson, B. R.; Eady, R. R.; Hasnain, S. S.; Garner, C. D.; Matsushita, T.; Nomura, M.; Smith, B. E. *Biochem. J.* **1989,** *258,* 733-737.
34. Morningstar, J. E.; Johnson, M. K.; Case, E. E.; Hales, B. J. *Biochemistry* **1987,** *26,* 1795-800.
35. Ravi, N.; Moore, V.; Lloyd, S. G.; Hales, B. J.; Huynh, B. H. *J. Biol. Chem.* **1994,** *269,* 20920-20924.
36. Smith, B. E.; Eady, R. R.; Lowe, D. J.; Gormal, C. *Biochem. J.* **1988,** *250,* 299-302.
37. Tittsworth, R. C.; Hales, B. J. *Biochemistry* **1996,** *35,* 479-487.
38. Eady, R. R. *Chem. Rev.* **1996,** *96,* 3013-3030.
39. Moore, V. G.; Tittsworth, R. C.; Hales, B. J. *J. Am. Chem. Soc.* **1994,** *116,* 12101-12102.
40. Chan, M. K.; Kim, J.; Rees, D. C. *Science* **1993,** *260,* 792-794.
41. Shah, V. K.; Allen, J. R.; Spangler, N. J.; Ludden, P. W. *J. Biol. Chem.* **1994,** *269,* 1154-1158.
42. Allen, R. M.; Chatterjee, R.; Ludden, P. W.; Shah, V. K. *J. Biol. Chem.* **1995,** *270,* 26890-26896.
43. Joerger, R. D.; Bishop, P. E. *J. Bacteriol.* **1988,** *170,* 1475-1487.
44. Drummond, M.; Walmsley, J.; Kennedy, C. *J. Bacteriol.* **1996,** *178,* 788-792.
45. Zheng, L.; White, R. H.; Dean, D. R. *J. Bacteriol.* **1997,** *179,* 5963-5966.
46. Hoover, T. R.; Imperial, J.; Ludden, P. W.; Shah, V. K. *Biochemistry* **1989,** *28,* 2768-2771.
47. Kennedy, C.; Dean, D. *Mol. Gen. Genet.* **1992,** *231,* 494-498.
48. Madden, M. S.; Paustian, T. D.; Ludden, P. W.; Shah, V. K. *J. Bacteriol.* **1991,** *173,* 5403-5405.
49. Roberts, G. P.; Brill, W. J. *J. Bacteriol.* **1980,** *144,* 210-221.
50. Merrik, M. J. In *New Horizons in Nitrogen Fixation*; Palacios, R., Mora, J., and Newton, W. E., Eds.; Kluwer Academic: Dordrecht, 1993, pp 43-54.
51. Bishop, P. E.; Premakumar, R. In *Biological Nitrogen Fixation*; Stacey, G.,

Downloaded by UNIV OF GUELPH LIBRARY on October 31, 2012 | http://pubs.acs.org
Publication Date: December 10, 1998 | doi: 10.1021/bk-1998-0711.ch017

Burris, R. H., and Evans, H. J., Eds.; Chapman & Hall: New York, 1992, pp 736-762.

52. Raina, R.; Bageshwar, U. K.; Das, H. K. *Mol. Gen. Genet.* **1993,** *236,* 459-462.
53. Joerger, R. D.; Jacobson, M. R.; Bishop, P. E. *J. Bacteriol.* **1989,** *171,* 3258-3267.
54. Wolfinger, E. D.; Bishop, P. E. *J. Bacteriol.* **1991,** *173,* 7565-7572.
55. Roll, J. T.; Shah, V. K.; Dean, D. R.; Roberts, G. P. *J. Biol. Chem.* **1995,** *270,* 4432-4437.
56. Brigle, K. E.; Weiss, M. C.; Newton, W. E.; Dean, D. R. *J. Bacteriol.* **1987,** *169,* 1547-1553.
57. Shah, V. K.; Rangaraj, P.; Chatterjee, R.; Allen, R. M.; Roll, J. T.; Roberts, G. P.; Ludden, P. W. In *25th Steenbock Symposium. Biosynthesis and function of metal clusters for enzymes.*; University of Wisconsin, Madison, 1997, pp 169-174.
58. Gosink, M. M.; Franklin, N. M.; Roberts, G. P. *J. Bacteriol.* **1990,** *172,* 1441-1447.
59. Kennedy, C.; Gamal, R.; Humphrey, R.; Ramos, J.; Brigle, K.; Dean, D. R. *Mol. Gen. Genet.* **1986,** *205,* 318-325.
60. Howard, K. S.; McLean, P. A.; Hansen, F. B.; Lemley, P. V.; Koblan, K. S.; Orme-Johnson, W. H. *J. Biol. Chem.* **1986,** *261,* 772-778.
61. Jacobson, M. R.; Cash, V. L.; Weiss, M. C.; Laird, N. F.; Newton, W. E.; Dean, D. D. *Mol. Gen. Genet.* **1989,** *219,* 49-57.
62. Luque, F.; Pau, R. N. *Mol. Gen. Genet.* **1991,** *227,* 481-487.
63. Jacobson, M. R.; Premakumar, R.; Bishop, P. E. *J. Bacteriol.* **1986,** *167,* 480-486.
64. Dilworth, M. J.; Eady, R. R.; Robson, R. L.; Miller, R. W. *Nature* **1987,** *327,* 167-168.
65. Mouncey, N. J.; Mitchenall, L. A.; Pau, R. N. *J. Bacteriol.* **1995,** *177,* 5294-5302.
66. Anderson, L. A.; Palmer, T.; Price, N. C.; Bornemann, S.; Boxer, D. H.; Pau, R. N. *Eur. J. Biochem.* **1997,** *246,* 119-126.
67. Mouncey, N. J.; Mitchenall, L. A.; Pau, R. N. *Microbiology* **1996,** *142,* 1997-2004.
68. Maupin-Furlow, J. A.; Rosentel, J. K.; Lee, J. H.; Deppenmeier, U.; Gunsalus, R. P.; Shanmugam, K. T. *J. Bacteriol.* **1995,** *177,* 4851-4856.
69. McNicholas, S. A.; Rech, S. A.; Gunsalus, R. P. *Mol. Microbiol.* **1997,** *23,* 515-524.
70. Rech, S.; Deppenmeier, U.; Gunsalus, R. P. *J. Bacteriol.* **1995,** *177,* 1023-1029.
71. Rosentel, J. K.; Healy, F.; Maupin-Furlow, J. A.; Lee, J. H.; Shanmugam, K. T. *J. Bacteriol.* **1995,** *177,* 4857-4864.
72. Pienkos, P. T.; Brill, W. J. *J. Bacteriol.* **1981,** *145,* 743-751.
73. Cornish, A. S.; Page, W. J. *BioMetals* **1995,** *8,* 332-338.
74. Duhme, A.-K.; Hider, R. C.; Khodr, H. *BioMetals* **1996,** *9,* 245-248.
75. Dean, R. D.; Jacobson, M. R. In *Biological Nitrogen Fixation*; Stacey, G., Burris, R. H., and Evans, H. J., Eds.; Chapman & Hall: New York, 1992, pp 763-834.

Downloaded by UNIV OF GUELPH LIBRARY on October 31, 2012 | http://pubs.acs.org
Publication Date: December 10, 1998 | doi: 10.1021/bk-1998-0711.ch017

Downloaded by NORTH CAROLINA STATE UNIV on October 31, 2012 | http://pubs.acs.org
Publication Date: December 10, 1998 | doi: 10.1021/bk-1998-0711.ch018

Chapter 18

A Possible Role for Amavadine in Some *Amanita* Fungi: A Unique Case in Biology

C. M. M. Matoso[1], Armando J. L. Pombeiro[1], J. J. R. Fraústo da Silva[1,3], M. Fátima C. Guedes da Silva[1], J. Armando L. da Silva[1], J. L. Baptista-Ferreira[2], and Fátima Pinho-Almeida[2]

[1]Centro de Química Estrutural, Instituto Superior Técnico, Av. Rovisco Pais, 1, 1096 Lisboa Codex, P-Portugal
[2]Centro de Micologia da Universidade de Lisboa, 1294 Lisboa Codex, P-Portugal

In the present communication we provide preliminary evidence that amavadine, a natural bare V(IV) complex of (S,S)-2,2'-(hydroxyimino)dipropionic acid present in some *Amanita* fungi, besides acting as a peroxidase which catalyses the oxidation of particular thiols to the corresponding disulfide compounds, can also act as catalase, promoting the decomposition of H_2O_2 generated in many biological processes. We suggest, therefore, that amavadine could well be a kind of proto-enzyme, acting both as a peroxidase or as a catalase, depending on the conditions, being in essence a multi-purpose protective/defensive agent against mushroom body damage or external microbial pathogens.

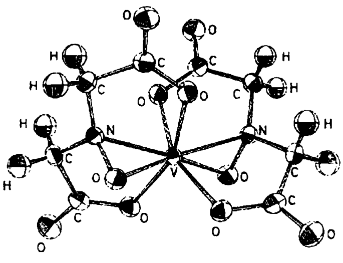

Fig. 1 - The X-ray structure of V(IV)2,2'-(hydroxyiminodiacetate) - V(HIDA)$_2$ (Adapted from ref. *3*).

Amavadine is a unique natural 1:2 vanadium(IV) complex of (S,S)-2,2'-(hydroxyimino)dipropionic acid (H_3.HIDPA^{3-}), present in some *Amanita* fungi such as Amanita *muscaria* (*1*) and closely related species. Initially it was thought to be a oxovanadium(IV) complex, but later an unusual octa-coordinated structure of the bare vanadium(IV) complex was suggested by Bayer *et al.* (*2*) and independently confirmed by some of us on the basis of X-ray determination of the crystal structure of the V(IV) complex of an analogous synthetic ligand - 2,2'-(hydroxyimino)diacetic acid (H_3.HIDA^{3-}) (*3*), see Figure 1. More recently Garner *et al.* synthesized the

In Vanadium Compounds; Tracey, A., et al.;
ACS Symposium Series; American Chemical Society: Washington, DC, 1998.

stereochemical equivalent of the natural ligand and determined the structure of its vanadium(V) complex, which is identical to that of the reduced form but with shorter vanadium-oxygen bond distances (*4*). There was no evidence for the formation of V(IV) peroxo complex. The identity of the reduced form and of natural amavadine was fully established by comparison of optical, CD and ^1H and ^{13}C NMR spectra (*4*).

The biological role of amavadine has not been clarified yet, although there is considerable circumstantial evidence suggesting that it may be involved in some kind of electron transfer process (*5*). Electrochemical studies have been carried out by our group (*6,7*) and by other researchers (*8,9*) and led to the conclusion that this complex can act as a mediator in the oxidation of thiolic compounds with carboxylic or ester groups, some of biological significance such as cysteine and glutathione. We have been able to establish recently a Michaelis-Menten type of mechanism for these electrochemical oxidation reactions mediated by a model of amavadine giving the corresponding disulfides (*7*).

The electrochemical studies in aqueous solutions (*6,8*) established also that the amavadine models $[VL_2]^{2-}$ (L = $HIDPA^{3-}$ or $HIDA^{3-}$), which have a bright blue color, undergo a single-electron reversible oxidation to give the corresponding red vanadium(V) complex. These vanadium(V) complexes are stable in some non-aqueous organic solvents (*10*), but in aqueous solution they are unstable and revert to the air stable vanadium(IV) complexes either by acting as mediators for the oxidations of *e. g.* thiols, if present, see above, or through other still some unknown mechanism, which can only involve the (unlikely in this case) internal oxidation of the ligand itself or the oxidation of the solvent, water.

In this paper we present preliminary evidence showing that the ligands are not affected to any appreciable extent even after a series of oxidation-reduction cycles and that oxidation of water is, therefore, the most likely subsequent event in the absence of other substrates. Although the mechanism of the reaction has not been studied in detail, the results afford further insights as to the possible biological role of amavadine in *Amanita* fungi.

Results and discussion

As stated above, in aqueous solution only the blue $[V(IV)(HIDA)_2]$ and $[V(IV)(HIDPA)_2]$ complexes are stable and can be kept in contact with air without any apparent change. This was expected given the value of the redox potential of the V(V)/V(IV) system ($\approx$ 0.8V at pH 7, *versus* the standard H^+/H_2 electrode) (*6*), too close to that of O_2/H_2O system, and was confirmed by monitoring the visible spectra of the solutions.

Stronger oxidants, such as permanganate, oxidize the V(IV) complexes, but the reactions are difficult to follow.

Since our interest was centered on the biological role of amavadine these aspects were not explored further and we concentrated onto the action of a biological oxidant, H_2O_2. Studies have been carried out initially at pH $\approx$ 2 (in absence of buffer) for which the $[V(IV)L_2]$ complexes are still the major complex species present (the stability constant of the $[V(IV)(HIDPA)_2]$ complex is quite high, $\log\beta_2 = 23.4$ (*11*)). Upon the addition of an equivalent amount of H_2O_2 (0.270ml of a 0.185M solution) to

Downloaded by NORTH CAROLINA STATE UNIV on October 31, 2012 | http://pubs.acs.org
Publication Date: December 10, 1998 | doi: 10.1021/bk-1998-0711.ch018

a solution of the blue [V(IV)(HIDPA)$_2$] complex (5ml of a 0.02M) the solution turned red, but reverted slowly to the blue form and its final visible spectrum was completely superimposable with the original one (after correcting for the effect of dilution). Evolution of small gaseous bubbles was also noticed. This behavior, which can be repeated several times, is observed in Figure 2, which refers to an analogous experiment when only 20% of the equivalent amount of H_2O_2 was added to have all the spectra within an adequate comparable absorbance range. The spectra of the blue and red forms correspond to those of the V(IV) and V(V) complexes of the ligand and an isosbestic point is apparent in Figure 2, showing a simple interconversion of the two forms. Experiments conducted at higher pH values (pH 4.6 and pH 7) produced also initial and final superimposable spectra (of the V(IV) complex), but the addition of the equivalent amount of H_2O_2 gives a violet color, resulting from incomplete oxidation of the V(IV) complex, which reverts more rapidly to the initial blue color again with evolution of small gaseous bubbles. These observations are in accord with a mechanism in which the V(IV) complex is firstly oxidized to the V(V) form, which then oxidizes water and reverts quantitatively to the original V(IV) form. The oxidation of V(IV) complex is favored by low pH values while the oxidation of water by the V(V) complex is favored by higher pH values as expected from the redox behavior of H_2O_2:

$$H_2O_2 + 2H^+ + 2e^- \rightarrow 2H_2O$$

$$2H_2O \rightarrow O_2 + 4H^+ + 4e^-$$

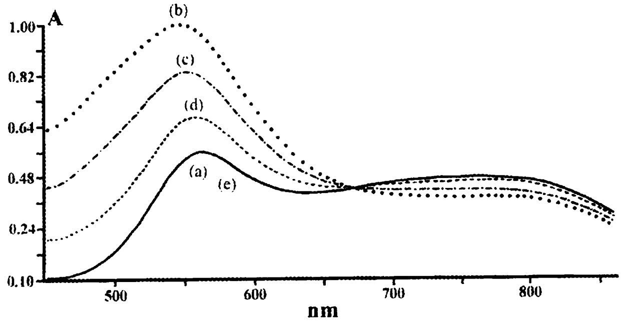

Fig. 2 - Absorbance visible spectra of an unbuffered solution with 3ml of V(HIDPA)$_2$ (0.02M) and 0.014ml of H_2O_2 (0.865M) (pH≈2), 1cm cell: (a) before the addition of H_2O_2; (b) 5min after addition; (c) 1h 15min; (d) 17h; (e) 25h 30min.

The gaseous bubbles which formed in all the experiments were identified as gaseous dioxygen, which must come from the oxidation of water thus adding further support to this hypothesis. Figure 3 shows a typical experiment, when the V(IV) complex of HIDPA was first oxidized to the V(V) form, whereupon it oxidized water releasing oxygen whose concentration in solution was measured with an oxygen meter.

Although most of the observations reported were semi-quantitative and several mechanistic aspects remain to be clarified, *e. g.* the conciliation of 2-electron redox reactions (H_2O_2 and H_2O) with 1-electron redox reactions (V(V)/V(IV)), a clearer picture of the possible role(s) of amavadine in *Amanita* fungi begins to emerge.

In effect, there appears to be the following two possibilities (Scheme 1):

Downloaded by NORTH CAROLINA STATE UNIV on October 31, 2012 | http://pubs.acs.org
Publication Date: December 10, 1998 | doi: 10.1021/bk-1998-0711.ch018

Downloaded by NORTH CAROLINA STATE UNIV on October 31, 2012 | http://pubs.acs.org
Publication Date: December 10, 1998 | doi: 10.1021/bk-1998-0711.ch018

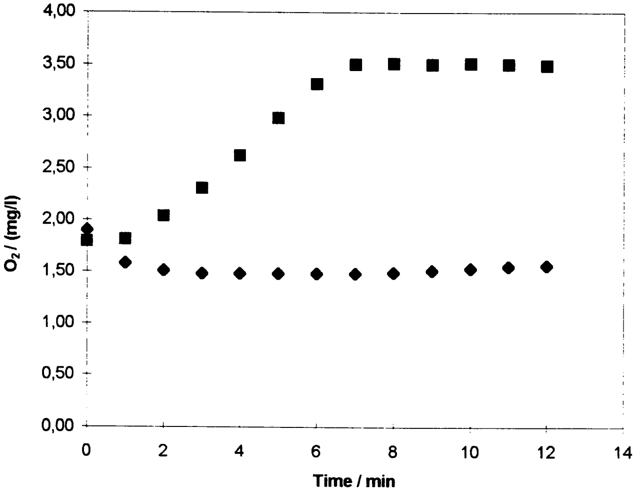

Figure 3- Evolution of O_2 in an unbuffered solution (pH≈2) of 5ml of [V(IV)(HIDPA)$_2$] 0.02M and 0.29ml of H_2O_2 0.187M (■), and in a blank solution (◆).

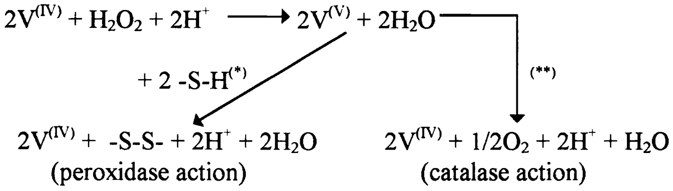
$2V^{(IV)} + H_2O_2 + 2H^+ \longrightarrow 2V^{(V)} + 2H_2O$
$+ 2\ \text{-S-H}^{(*)}$
$(**)$
$2V^{(IV)} + \text{-S-S-} + 2H^+ + 2H_2O$
(peroxidase action)
$2V^{(IV)} + 1/2O_2 + 2H^+ + H_2O$
(catalase action)

(*) In presence of adequate biological thiols
(**) In absence of biological thiols

Scheme 1- The double role of amavadine (the ligand is ommited for the sake of simplicity)

Hence, we suggest (speculatively) that amavadine could be a primitive peroxidase, which uses H_2O_2 produced by the fungus as a defensive agent to cross-link thiol groups in side chains of proteins by analogy with what happens in some higher plants (*12*) where H_2O_2 is produced as a by-product in multiple metabolic functions and is used by peroxidases; this might aid the self-regeneration of severed tissues and protect against external microbial pathogens. These hypotheses are supported by the high concentration of vanadium in the cap of the fungi and the significant amount in the lamellae of the basidiomata, see below (*13-15*). Oxidative damage which may be caused by excess of this oxidant is minimized by other anti-oxidant enzymes, such as catalases which decompose H_2O_2 into O_2 and H_2O. As shown in Scheme 1, amavadine can also catalyse the same reaction.

Of course, the process is not very effective compared with catalase and is not extraordinary since several metal ions (*e. g.* Fe^{3+}) can also promote the decomposition of hydrogen peroxide (*16*), but it must be stressed that amavadine is not an enzyme or a co-factor of an enzyme - it is a simple, although unusual, complex. Clearly, the relatively high amount and even distribution in the fungus suggest a required biological role for this unique vanadium(IV) complex, but it is likely that in more recent species in the evolutionary process it has been replaced by more effective heme based peroxidases and catalases (*17*).

The puzzling question is why does it occur (significantly) in only a few *Amanita* species, namely in *Amanita muscaria* (L.:Fr.) Hook. and the related species *Amanita regalis* (Fr.:Fr.) Mich. (*A. muscaria* var. *umbrina* Fr., after Moser (*18*)), as well as in *Amanita velatipes* Atkinson (illegitimate taxon = *Amanita gemmata* f. *Amici* (Gill.) Gill., very close to *A. pantherina* (DC.:Fr.) Sécr. or to *A. muscaria* (L.:Fr.) Hook., as suggested by Gilbert (*19*)) (*20*). Does the presence of amavadine confer some relative advantage to these compared to other toadstools? Our answer to this question can only be speculative, but it is curious to notice that the species *Amanita muscaria* has an unusual capacity of micorrization with a large spectrum of tree species with a widespread distribution all over the world in acid soils (conifer forests), and that its fruitbodies are of large habitat and have a relatively long standing life compared with other fungal species (*21*). We have already mentioned that in the lamellae of the

Downloaded by NORTH CAROLINA STATE UNIV on October 31, 2012 | http://pubs.acs.org
Publication Date: December 10, 1998 | doi: 10.1021/bk-1998-0711.ch018

basidiomata, where the basidiospores are formed (the entities that guarantee the continuity of the species and the success through genetic variability) the concentration of vanadium appears to be relevant (*15*), as if the presence of amavadine was necessary to confer added protection, probably, as stated above, against external microbial pathogens. Although these may be just coincidences, the present evidence suggests that amavadine could be a kind of proto-enzyme acting both as a peroxidase or catalase, being in essence as a multi-purpose primitive protective/defensive agent against body damage or external microbial pathogens.

Experimental procedure

The HIDPA and HIDA were synthesized as described previously, using a method adapted from Anderegg *et al.* (*11*). Spectra were obtained with a UV/vis spectrometer Lambda 2, of Perkin-Elmer, and the data was acquired in a PC computer with PECSS software package version. The concentration of dioxygen in solution was measured using a ProfiLab Dissolved Oxygen Meter Oxi 597 with a Oxygen sensor CellOx 325 from WTW.

Acknowledgments

Program PRAXIS XXI (P/2/2.1/QUI/14/94) and JNICT (Programa Plurianual) for financial support.

References

(*1*) Bayer, E.; Kneifel, H. *Z. Naturforsch.* **1972**, *27B*, 207.

(*2*) Bayer, E.; Koch, E.; Anderegg, G. *Angew. Chem. Int. Engl.* **1987**, *26*, 545-546.

(*3*) Carrondo, Maria A. A. F. de C. T.; Duarte, M. Teresa Leal S.; Costa Pessoa, J.; Silva, J. Armando L.; Fraústo da Silva, J. J. R.; Vaz, M. Cândida T. A.; Vilas-Boas, L. F. *J. Chem. Soc., Chem. Commun.* **1988**, 1158-1159.

(*4*) Armstrong, E. M.; Beddoes, R. L.; Calviou, L. J.; Charnock, J. M.; Collison, D.; Ertok, N.; Naismith, J. H.; Garner, C. D. *J. Am. Chem. Soc.* **1993**, *115*, 807-808.

(*5*) Fraústo da Silva, J. J. R. *Chem. Speciation Bioavailability* **1989**, *1*, 139-150.

(*6*) Fraústo da Silva, J. J. R.; Guedes da Silva, M. F. C.; Silva, J. A. L.; Pombeiro, A. J. L. in *Molecular Electrochemistry of Inorganic, Bioinorganic and Organometallic Compounds*; Eds. Pombeiro, A. J. L.; McCleverty, J. A.; Kluwer Academic Publishers: The Netherlands, 1993, p.411-415.

(*7*) Guedes da Silva, M. F. C.; Silva, J. A. L.; Fraústo da Silva, J. J. R.; Pombeiro, A. J. L.; Amatore, C.; Verpeaux, J.-N. *J. Am. Chem. Soc.* **1996**, *118*, 7568-7573.

(*8*) Nawi, M. A.; Riechel, T. L. *Inorg. Chim. Acta* **1987**, *136*, 33-39.

(*9*) Thackrey, R. D.; Riechel, T. L. *J. Electroanal. Chem.* **1988**, *245*, 131-143.

(*10*) Silva, J. A. L. Ph. D. Thesis, I.S.T., Lisboa, 1992.

(*11*) Anderegg, G.; Koch, E.; Bayer, E. *Inorg. Chem. Acta* **1987**, *127*, 183-188.

(*12*) Durner, J.; Klessig, D. F. *Proc. Natl. Acad. Sci. USA* **1995**, *92*, 11312-11316.

Downloaded by NORTH CAROLINA STATE UNIV on October 31, 2012 | http://pubs.acs.org
Publication Date: December 10, 1998 | doi: 10.1021/bk-1998-0711.ch018

(*13*) Bertrand, D. *Amer. Museum Nat. Hist. Bull.* **1950**, *94*, 403-456.

(*14*) Watkinson, J. H. *Nature* **1964**, *202*, 1239-1240.

(*15*) Meisch, H.-U.; Schmitt, J. A.; Reinle, W. *Z. Naturforsch.* **1978**, *33C*, 1-6.

(*16*) Cotton, F. A.; Wilkinson, G. *Advanced Inorganic Chemistry - a comprehensive text*; 2nd Ed.; Interscience: 1966.

(*17*) Williams, R. J. P.; Fraústo da Silva, J. J. R. *The Natural Selection of the Chemical Elements*; Oxford University Press: 1996.

(*18*) Moser, M. in *Key to Agarics and Boleti*; Roger Philips: London, 1978; p.226-227.

(*19*) Gilbert, E. J. *Iconographia Mycologica* **1941**, *27*, 260-261.

(*20*) Meisch, H.-U.; Reinle, W.; Schmitt, J. A. *Z. Naturforsch.* **1979**, *66*, 620-621.

(*21*) Molina, R.; Trappe, J. M. *Forest Science* **1982**, *28*, 423.

Downloaded by NORTH CAROLINA STATE UNIV on October 31, 2012 | http://pubs.acs.org
Publication Date: December 10, 1998 | doi: 10.1021/bk-1998-0711.ch018

Downloaded by UNIV OF GUELPH LIBRARY on October 31, 2012 | http://pubs.acs.org
Publication Date: December 10, 1998 | doi: 10.1021/bk-1998-0711.ch019

Chapter 19

The Accumulation Mechanism of Vanadium by Ascidians

An Interdisciplinary Study between Biology and Chemistry on Extraordinary High Levels and Reduced Form of Vanadium in Vanadocytes

H. Michibata[1], T. Uyama[1], and K. Kanamori[2]

[1]Marine Biological Laboratory, Faculty of Science and Laboratory of Marine Molecular Biology, Graduate School of Science, Hiroshima University, Mukaishima-cho, Hiroshima 722, Japan
[2]Department of Chemistry, Faculty of Science, Toyama University, Gofuku, Toyama 930, Japan

The unusual phenomenon whereby some ascidians, known as tunicates, accumulate high levels of vanadium in their blood cells has attracted the interest of many investigators. The highest concentration of vanadium, 350 mM, in vanadocytes corresponds 10^7 times higher than that in sea water and vanadium is stored in the +3 oxidation state. Enzymes in the pentose phosphate pathway in vanadocytes have a possibility to participate the reduction of vanadium. The content of the vacuole of signet ring cells was kept to be highly acidic, pH 1.9 to 4.2, by the function of a vacuolar type H^+-ATPase. A vanadium-associated protein (VAP) was isolated from the blood cells and a monoclonal antibody against VAP was raised. Biochemical characterization of VAP and cloning of the gene encoded VAP are in progress.

Ascidians, known as tunicates or sea squirts, are phylogenically classified into the phylum Chordata between Invertebrata and Vertebrata. A German chemist, Martin Henze discovered high levels of vanadium in the blood cells (coelomic cells) of an ascidian collected from the Bay of Naples (Henze, 1911). His finding attracted not only analytical chemists, but also physiologists, biochemists, and chemists of natural products, in part because of the initial interest in the extraordinary high level of vanadium never before reported in other organisms but also because of the considerable interest in the possible participation of vanadium in oxygen transport as a third candidate in addition to iron and copper. After the first finding of vanadium in ascidian blood cells, many species of ascidians were analyzed for presence of vanadium. The data obtained vary widely in sensitivity and in precision as do data on dry weight, wet weight, ash weight, or amount of protein. Re-determination of the contents of vanadium was, therefore, required.

In Vanadium Compounds; Tracey, A., et al.;
ACS Symposium Series; American Chemical Society: Washington, DC, 1998.

Downloaded by UNIV OF GUELPH LIBRARY on October 31, 2012 | http://pubs.acs.org
Publication Date: December 10, 1998 | doi: 10.1021/bk-1998-0711.ch019

Many species of ascidians belonging to two of three suborders, Phlebobranchia and Stolidobranchia were collected by ourselves mainly from the waters around Japan and the Mediterranean. Samples of blood cells, plasma, tunic, mantle (muscle), branchial basket, stomach, hepatopancreas, and gonad were submitted to neutron-activation analysis in a nuclear reactor, which was an extremely sensitive method for the quantification of vanadium (Michibata, 1984; Michibata *et al.*, 1986). The data obtained are summarized in Table 1. Although vanadium was detectable in samples from almost all species examined, the ascidian species belonging to the suborder Phlebobranchia apparently contained higher levels of vanadium than those belonging to Stolidobranchia. We also confirmed that blood cells contained the highest amounts of vanadium among the tissues examined. Furthermore, the highest concentration of vanadium, 350 mM (mmol/dm^3) was found in the blood cells of *Ascidia gemmata* belonging to the suborder Phlebobranchia (Michibata *et al.*, 1991a); 350 mM corresponds 10^7 times the vanadium concentration in sea water (Cole *et al.*, 1983; Collier, 1984).

Blood cells were confirmed to contain the highest amounts of vanadium among the tissues examined in ascidians. Ascidian blood cells are classified into nine to eleven different types that can be grouped into six categories on the basis of their morphology: hemoblasts, lymphocytes, leucocytes, vacuolated cells, pigment cells and nephrocytes (Wright, 1981). The vacuolated cells can be further divided into at least four different types: morula cells, signet ring cells, compartment cells and small compartment cells. For many years, the morula cells were thought to be the so-called vanadocytes (Webb, 1939; Endean, 1960; Kalk, 1963a, b; Kustin *et al.*, 1976), because their pale-green color resembles that of a vanadium complex dissolved in aqueous solution and the dense granules in morula cells, which can be observed under an electron microscope after fixation with osmium tetroxide, were assumed to be deposits of vanadium.

At the end of the 1970's, with the increasing availability of scanning transmission electron microscopes equipped with an energy disperse X-ray detector, it became possible to address with greater confidence the question of whether morula cells are the true vanadocytes. An Italian group was the first to demonstrate that the characteristic X-ray due to vanadium was not detected from morula cells but from granular amoebocytes, signet ring cells and compartment cells and, moreover, that vanadium was selectively concentrated in the vacuolar membranes of these cells where vanadium granules was present inside the vacuoles (Botte *et al.*, 1979a; Scippa *et al.*, 1982, 1985; Rowley, 1982). Identification of the true vanadocytes became a matter of the highest priority to those concerned with the mechanism of accumulation of vanadium by ascidians.

To end the controversy and identify the true vanadocytes, we used a combination of density gradient centrifugation, for the isolation of specific types of blood cells and neutron-activation analysis, for the quantification of the vanadium contents of the isolated subpopulations of blood cells (Michibata *et al.*, 1987). The subpopulation of blood cells recovered from each layer was submitted to

Downloaded by UNIV OF GUELPH LIBRARY on October 31, 2012 | http://pubs.acs.org
Publication Date: December 10, 1998 | doi: 10.1021/bk-1998-0711.ch019

neutron-activation analysis. The distribution pattern of vanadium coincided with that of signet ring cells but not with that of morula cells or compartment cells. These results proved that the signet ring cells are the true vanadocytes (Fig. 1) (Michibata *et al.*, 1987, 1991a; Hirata and Michibata, 1991).

The establishment of reliable cell markers for the recognition of different types of blood cells is necessary to clarify not only the function but also the lineage of each type of cell. We prepared a monoclonal antibody, which we hoped might serve as a powerful tool for solving these problems, using a homogenate of the subpopulation of signet ring cells from *Ascidia sydneiensis samea* as the antigen (Uyama *et al.*, 1991). The monoclonal antibody obtained, S4D5, was shown to react specifically with the vanadocytes not only from *A. sydneiensis samea* but also from two additional species, *A. gemmata* and *A. ahodori*. Immunoblotting analysis showed that this antibody recognizes a single polypeptide of about 45 kDa from all three species.

Henze (1911) was the first to suggest the existence of vanadium in the +5 oxidation state. Later, many workers reported the +3 oxidation state of vanadium. More recently, studies using noninvasive physical methods, including ESR, XAS, NMR, and SQUID, indicated that the vanadium ions in ascidian blood cells were predominantly in the +3 oxidation state, with a small amount being in the +4 oxidation state (Carlson, 1975; Tullius *et al.*, 1980; Dingley *et al.*, 1981; Frank *et al.*, 1986; Lee *et al.*, 1988; Brand *et al.*, 1989). These results were, however, derived not from the vanadocytes but from the entire population of blood cells. Thus, some questions remained to be answered. In particular, does vanadium exist in two oxidation states in one type of blood cell, or is each state formed in a different cell type? After separation of the various types of blood cells of *A. gemmata*, we made noninvasive ESR measurements of the oxidation state of vanadium in the fractionated blood cells under a reducing atmosphere (Hirata and Michibata, 1991). Consequently, it was revealed that vanadium in vanadocytes is predominantly in the +3 oxidation state, with a small amount being in the +4 oxidation state. The ratio of vanadium(III) to vanadium(IV) was 97.6:2.4 (Table 2).

A considerable amount of sulfate has always been found in association with vanadium in ascidian blood cells (Henze, 1932; Califano *et al.*, 1950; Bielig *et al.*, 1954; Levine, 1961; Botte *et al.*, 1979a, b; Scippa *et al.*, 1982; 1985; 1988; Bell *et al.*, 1982; Pirie *et al.*, 1984; Lane *et al.*, 1988; Frank *et al.*, 1986, 1987, 1994, 1995; Anderson and Swinehart, 1991), suggesting that sulfate might be involved in the biological function and/or the accumulation and reduction of vanadium. Raman spectroscopy can be also used to detect sulfate ion selectively in ascidian blood cells because sulfate ion gives a very intense Raman band at the diagnostic position, 983 cm^{-1}. We observed fairly good Raman spectrum of the blood cell lysate from *Ascidia gemmata*, which has the highest concentration of vanadium(III) among ascidians (Kanamori and Michibata, 1994). Vanadium(III) ions in the blood cells were converted to vanadyl(IV) ions by air-oxidation prior to Raman measurements so as to facilitate detection based on V=O stretching vibration. From analysis of

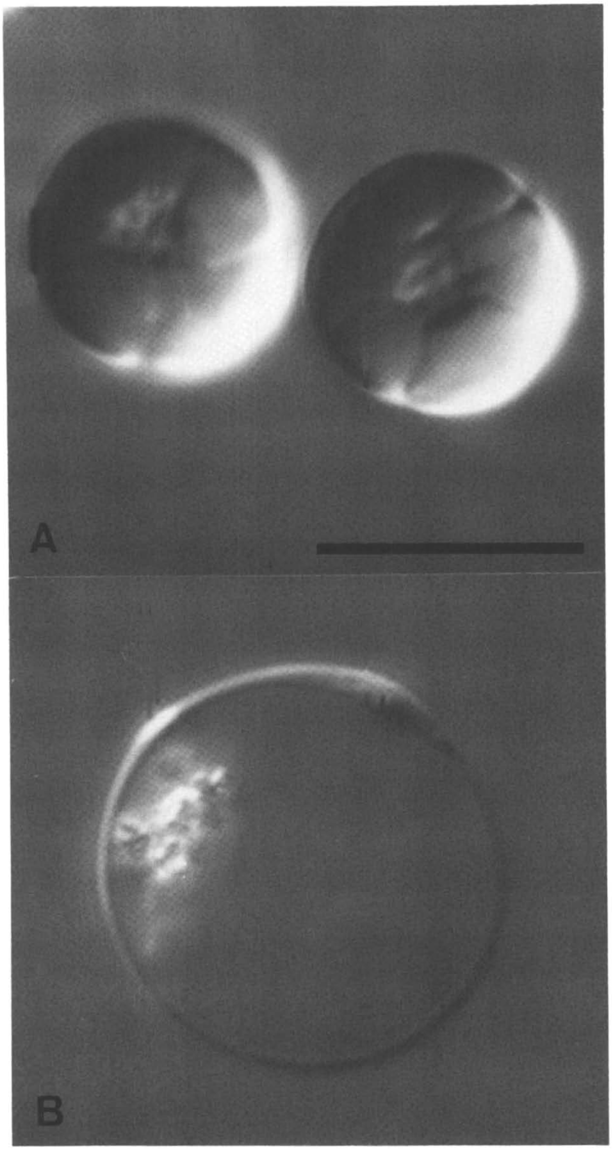

Figure 1. Morula cells (A), misidentified initially as vanadocytes, and signet ring cells (B), identified newly as vanadocytes, in the ascidian, *Ascidia ahodori*. Scale bar indicates 10 μm. (Michibata *et al.*, *J. Exp. Zool.*, 1987, 244: 33-38.)

Downloaded by UNIV OF GUELPH LIBRARY on October 31, 2012 | http://pubs.acs.org
Publication Date: December 10, 1998 | doi: 10.1021/bk-1998-0711.ch019

Table 1. Concentrations of Vanadium in Tissues of Several Ascidians (mM)

	Tunic	Mantle	Branchial basket	Serum	Blood cells
Phlebobranchia					
Ascidia gemmata	N.D.	N.D.	N.D.	N.D.	347.2
A. ahodori	2.4	11.2	12.9	1.0	59.9
A. sydneiensis	0.06	0.7	1.4	0.05	12.8
Phallusia mammillata	0.03	0.9	2.9	N.D.	19.3
Ciona intestinalis	0.003	0.7	0.7	0.008	0.6
Stolidobranchia					
Styela plicata	0.005	0.001	0.001	0.003	0.007
Halocynthia roretzi	0.01	0.001	0.004	0.001	0.007
H. aurantium	0.002	0.002	0.002	N.D.	0.004

N.D.: not determined.

(Michibata *et al.*, *Biol. Bull.*, 1986, 171: 672-681.; Michibata *et al.*, *J. Exp. Zool.*, 1991, 257: 306-313.)

Table 2. Vanadium Spceies and Ratio between Vanadium and Sulfate in Ascidian Blood Cells

$V^{3+} : VO^{2+} = 98 : 2$

$V^{3+} : SO_4{}^{2-} = 1 : 1.5$

(Michibata *et al.*, *J. Exp. Zool.*, 1991, 257: 306-313.; Kanamori, K. and H. Michibata, *J. Mar. Biol. Ass. U.K.*, 1994, 74: 279-286.)

Downloaded by UNIV OF GUELPH LIBRARY on October 31, 2012 | http://pubs.acs.org
Publication Date: December 10, 1998 | doi: 10.1021/bk-1998-0711.ch019

the band intensities due to $V{=}O^{2+}$ and $SO_4{}^{2-}$ ions, we estimated the content ratio of sulfate to vanadium to be approximately 1.5, as would be predicted if sulfate ions were present as the counter ions of vanadium(III) (Table 2). Carlson (1975) reported a similar value of the content ratio for *Ascidia ceratodes*, but lower values were obtained by Bell *et al.* (1982) and Frank *et al.* (1986).

The monoclonal antibody, designated S4D5, specific to vanadocytes was revealed to react with a single polypeptide of about 45 kDa extracted from not only *A. sydneiensis samea* which offered the antigen but also the other vanadium-rich ascidians, *A. ahodori*, *A. gemmata* and *Ciona intestinalis*. The antigen of 45 kDa peptide was further disclosed to be localized in the cytoplasmic region and around the intravacuolar vesicle of the vanadocytes by immunocytological studies. This polypeptide is predominant among many peptides extracted from a subpopulation of vanadocytes in *A. sydneiensis samea*. However, the function of the polypeptide is not known. The recent experiments demonstrate that the antigen of 45 kDa localized in vanadocytes is 6-phosphogluconate dehydrogenase (6-PGDH: EC1.1.1.44) which is an enzyme of the pentose phosphate pathway, based on cDNA isolation of RNA samples from blood cells of the ascidian. Soluble extract of vanadocytes further exhibited a correspondingly high level of 6-PGDH enzymatic activity (Submitted). Almost all vanadium ions are reduced to V(III) via V(IV) in vanadocytes (Hirata and Michibata, 1991), although vanadium ions are dissolved in V(V) in sea water. Some reducing agents must, therefore, participate in the accumulation process. V(V) is reported to stimulate oxidation of NAD(P)H; i.e., V(V) is reduced to V(IV) by the addition of NAD(P)H *in vitro* (Vyskocil *et al.*, 1980; Nour-Eldeen *et al.*, 1985). Taken together, these observations suggest that NADPH produced in the pentose phosphate pathway conjugates reduction of vanadium from V(V) through V(IV) in vanadocytes of ascidians.

Henze (1911, 1912, 1913, 1932) was the first to report that the homogenate of ascidian blood cells is extremely acidic. Almost all subsequent investigations have supported his observation, however, Kustin's group disputed the earlier reports. They reported that the intracellular pH was neutral on the basis of measurements made by a new technique, which involved the transmembrane equilibrium of ^{14}C-labeled methylamine (Dingley *et al.*, 1982; Agudelo *et al.*, 1983). Hawkins *et al.* (1983) and Brand *et al.* (1987) also reported nearly neutral values for the pH of the interior of ascidian blood cells, which they determined noninvasively from the chemical shift of ^{31}P-NMR. However, Frank *et al.* (1986) demonstrated that the interior of the blood cells of *Ascidia ceratodes* has a pH of 1.8, basing their results on the new finding that the ESR line width accurately reflects the intracellular pH. Thus, the reported pH inside ascidian blood cells has excited considerable controversy.

We consider that the main reason for the extreme variations is that the measurements of pH were made with entire populations of blood cells and not with the subpopulation of vanadocytes specifically. Thus, one or two specific types of blood cells might have a highly acidic solution within their vacuoles, in which vanadium would be present in a reduced state. With this possibility in mind, we designed an experiment in which we combined the separation of each type of blood cell, measurement of pH with a microelectrode under anaerobic conditions to avoid air-oxidation, and ESR spectrometry as a noninvasive method for the measurement of pH to confirm the results obtained with the microelectrode (Michibata *et al.*, 1991a). Three species of vanadium-rich ascidians, *Ascidia gemmata, A. ahodori*, and *A. sydneiensis samea*, were used. Blood cells drawn from each species were fractionated by density-gradient centrifugation, as described above. The distribution of each type of blood cell, the concentrations of protons ([H$^+$]), and the levels of vanadium in each layer of cells are compared in Fig. 2. It is clear that the distribution patterns of protons and vanadium were similar. Thus, the signet ring cells contain high levels of both vanadium and proton in all three species.

ESR spectrometry was also used for noninvasive measurements of the intracellular acidity of blood cells (Michibata *et al.*, 1991). The method is based on the ESR line width due to oxo-vanadium [VO(IV)] ions, which increases (Frank *et al.*, 1986) almost linearly from pH 1.4 to pH 2.3. The low pH values obtained with a microelectrode were confirmed not to be artifacts by the fact that the ESR line width also indicated a low pH for the contents of signet ring cells from *A.*

Downloaded by UNIV OF GUELPH LIBRARY on October 31, 2012 | http://pubs.acs.org
Publication Date: December 10, 1998 | doi: 10.1021/bk-1998-0711.ch019

gemmata. To avoid any misunderstandings, we have to note the assumption that the acidic solution was contained in the vacuole of each signet ring cells. However, the greater part of each signet ring cell is, in fact, occupied by the vacuole itself, so the contents of the vacuole are almost equivalent to the contents of the cell.

A comparison of pH values with the levels of vanadium in the signet ring cells of three different species, as shown in Table 3, suggested that there might be a close correlation between a higher level of vanadium and lower pH, namely, a higher concentration of protons. It is well known that H^+-ATPases can generate a proton-motive force by hydrolyzing ATP. Therefore, we examined the presence of H^+-ATPase in the signet ring cells of the ascidian *Ascidia sydneiensis samea* (Uyama *et al.*, 1994). The vacuolar-type H^+-ATPase is composed of several subunits, and subunits of 72 kDa and 57 kDa have been reported to be common to all eukaryotes examined. Antibodies prepared against the 72 kDa and 57 kDa subunits of a vacuolar-type H^+-ATPase from bovine chromaffin granules did indeed react with the vacuolar membranes of signet ring cells. Immunoblotting analysis confirmed that the antibodies reacted with specific antigens in ascidian blood cells. Furthermore, addition of bafilomycin A_1, a specific inhibitor of vacuolar-type H^+-ATPases (Bowman *et al.*, 1988), inhibited the pumping function of the vacuoles of signet ring cells, resulting in neutralization of the contents of the vacuoles. We are trying to obtain direct evidence for such an association.

The route for the accumulation of vanadium ions from seawater in the blood system has not yet been revealed. The uptake of vanadium ions was studied with radioactive vanadium ions (^{48}V). Previous studies were, however, with a few exceptions (Hawkins *et al.*, 1980; Roman *et al.*, 1988) commonly designed with an assumption of the direct uptake of vanadium ions from the surrounding seawater and were, therefore, limited in their determination of how much vanadium was incorporated directly into some tissues (Goldberg *et al.*, 1951; Bielig *et al.*, 1963; Dingley *et al.*, 1981; Michibata *et al.*, 1991b). However, generally, heavy metal ions incorporated into the tissues of living organisms are known to bind to macromolecules such as proteins. Using an anion-exchange column, we first succeeded in isolating a vanadium-associated protein (VAP) composed of 12.5 kDa and 15 kDa peptides with a minor peptide of 16 kDa (Kanda *et al.*, 1997). We raised a monoclonal antibody against VAP, designated F8DH. Immunoblot analysis showed that F8DH recognized 2 related peptides of 15 kDa and 16 kDa of VAP (Wuchiyama *et al.*, 1997). Using F8DH, VAP was shown to be in the cytoplasm of vanadocytes and compartment cells, both of which were reported to contain vanadium. F8DH also stained the vanadocytes distributed in the connective tissues around the alimentary canal, suggesting that vanadocytes in the connective tissue contained VAP. Furthermore, blood cells of 3 different species of ascidian having high levels of vanadium, *A. sydneiensis samea*, *A. ahodori*, and *Ciona intestinalis*, showed reactivity of F8DH but little reactivity was observed in 2 species having less vanadium, *Halocynthia roretzi* and *Pyura michaelseni*, suggesting that VAP recognized by F8DH is a common protein in vanadium-rich ascidians. Biochemical characterization of VAP and cloning of the gene encoded VAP are in progress.

Downloaded by UNIV OF GUELPH LIBRARY on October 31, 2012 | http://pubs.acs.org
Publication Date: December 10, 1998 | doi: 10.1021/bk-1998-0711.ch019

Downloaded by UNIV OF GUELPH LIBRARY on October 31, 2012 | http://pubs.acs.org
Publication Date: December 10, 1998 | doi: 10.1021/bk-1998-0711.ch019

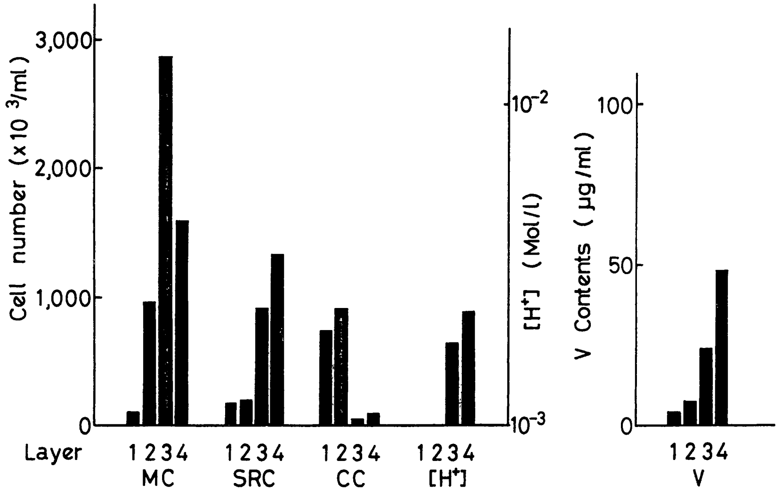

Figure 2. Determination of acidic blood cells of *Ascidia gemmata*. Histograms depict the number of each type of blood cell and the concentrations of H^+ and vanadium in three different layers (layers 1, A and F, cf. Michibata *et al.*, 1991a) of blood cells which were fractionated by density-gradient centrifugation in Percoll. MC, morula cells; SRC, signet ring cells; CC, compartment cells; [H^+], concentration of protons; V, vanadium (Michibata *et al.*, *J. Exp. Zool.*, 1991, **257**: **306-313**.)

Table 3. Correlation between Concentrations of Vanadium and pH Values in Ascidian Blood Cells

Species	Conc. of vanadium	pH
Ascidia gemmata	350mM	1.86
A. ahodori	60mM	2.67
A.sydneiensis samea	13mM	4.20

(Michibata *et al.*, *J. Exp. Zool.*, 1991, 257: 306-313.)

The physiological roles of vanadium remain to be explained. Recently, the polychaeta, *Pseudopotamilla occelata,* was reported to be a new accumulator of high levels of vanadium (Ishii *et al.*, 1993). We have disclosed that *P. occelata* has the same antigens with those in the ascidian *Ascidia sydneiensis samea,* which were recognized by two types of antibodies, a polyclonal antibody against vanadium-associated proteins extracted from blood cells and a monoclonal antibody against vanadocytes in the vanadium-rich ascidian *A. sydneiensis samea.* There is, therefore, a possibility that similar mechanism works on the accumulation of vanadium among the Polychaeta and the Ascidiidae (Uyama *et al.*, 1997). Characterization of these phenomena can be expected to help elucidate the reason for the unusual accumulation of vanadium by one class of marine organisms.

Downloaded by UNIV OF GUELPH LIBRARY on October 31, 2012 | http://pubs.acs.org
Publication Date: December 10, 1998 | doi: 10.1021/bk-1998-0711.ch019

ACKNOWLEDGMENTS

H. M. and T. U. would like to express hearty thanks to their associates for their unstinting assistance. Particular thanks are due to Dr. T. Numakunai and the staff of the Marine Biological Station of Tohoku University, Mr. K. Morita of Ootsuchi Marine Research Center, Ocean Research Institute, University of Tokyo, Prof. M. Yamamoto and his staff of the Marine Biological Station of Okayama University, and Mr. N. Abo of our laboratory for their kind cooperation in collecting the materials for so many years. K. K. also would like to express a sincere thanks to his colleagues, Ms. Y. Ookubo, Ms. H. Maeda, Mr. K. Ino, Ms. M. Fukagawa, and Mr. E. Kameda. Thanks are also due to Prof. K. Okamoto, University of Tsukuba, for the X-ray crystallographic analysis. This work was supported in part by Grant-in-Aids from the Ministry of Education, Science and Culture of Japan, by the Asahi Glass Foundation and by the Salt Science Research Foundation (to H.M.).

Literature Cited

Agudelo, M. I., Kustin, K., and McLeod, G. C. *Comp. Biochem. Physiol.*, 1983, 75A, 211-214.

Anderson, D. H. and Swinehart, J. H. *Comp. Biochem. Physiol.*, 1991, 99A, 585-592

Bell, M. V., Pirie, B. J. S., McPhail, D. B., Goodman, B. A., Falk-Petersen, I. -B., and Sargent, J. R. *J. Mar. Biol. Ass. UK.*, 1982, 62, 709-716.

Bielig, H. -J., Bayer, E., Califano, L., and Wirth, L. *Publ. Staz. Zool. Napoli*, 1954, 25, 26-66.

Bielig, H. -J., Pfleger, K., Rummel, W., and de Vincentiis, M. *Nature*, 1963, 197, 1223-1224.

Botte, L. S., Scippa, S., and de Vincentiis, M. *Experientia*, 1979a, 35, 1228-1230.

Botte, L., Scippa, S., and de Vincentiis, M. *Dev. Growth Differ.*, 1979b, 21, 483-491.

Bowman, E. J., Siebers, A., and Altendorf, K. *Proc. Natl. Acad. Sci. USA*, 1988, 85, 7972-7976.

Brand, S. G., Hawkins, C. J.,and Parry, D. L. *Inorg. Chem.*, 1987, 26, 627-629.

Brand, S. G., Hawkins, C. J., Marshall, A. T., Nette, G. W., and Parry, D. L. *Comp. Biochem. Physiol.*, 1989, 93B, 425-436.

Califano, L. and Boeri, E. *J. Exp. Zool.*, 1950, 27, 253-256.

Carlson, R. M. K. *Proc. Natl. Acad. Sci. USA*, 1975, 72, 2217-2221.

Cole, P. C., Eckert, J. M., and Williams, K. L. *Anal. Chim. Acta*, 1983, 153, 61-67.

Collier, R. W. *Nature*, 1984, 309, 441-444.

Dingley, A. L., Kustin, K., Macara, I. G., and McLeod, G. C. *Biochim. Biophys. Acta*, 1981, 649, 493-502.

Dingley, A. L., Kustin, K., Macara, I. G., McLeod, G. C., and Roberts, M. F. *Biochim. Biophys. Acta*,1982, 720, 384-389.

Endean, R. *Quart. J. Microscop. Sci.*, 1960, 101, 177-197.

Frank, P., Carlson, R. M. K., and Hodgson, K. O. *Inorg. Chem.*, 1986, 25, 470-478.

Frank, P., Hedman, B., Carlson, R. K., Tyson, T. A., Row, A. L., and Hodgson, K. O. *Biochem.*, 1987, 26, 4975-4979.

Frank, P., Hedman, B., Carlson, R. M. K., and Hodgson, K. O. *Inorg. Chem.*, 1994, 33, 3794-3803.

Frank, P., Kustin, K., Robinson, W. E., Linebaugh, L., and Hodgson, K. O. *Inorg. Chem.*,1995, 34, 5942-5949.

Goldberg, E. D., McBlair, W., and Taylor, K. M. *Biol. Bull.*, 1951, 101, 84-94.

Hawkins, C. J., Merefield, P. M., Parry, D. L., Biggs, W. R., and Swinehart, J. H. *Biol. Bull.*, 1980, 159, 656-668.

Hawkins, C. J., Kott, P., Pary, D. L., and Swinehart, J. H. *Comp. Biochem. Physiol.*,1983, 76B, 555-558.

Henze, M. *Hoppe-Seyler's Z. Physiol. Chem.*, 1911, 72, 494-501.

Henze, M. *Hoppe-Seyler's Z. Physiol. Chem.*, 1912, 79, 215-228.

Henze, M. *Hoppe-Seyler's Z. Physiol. Chem.*, 1913, 88, 345-346.

Henze, M. *Hoppe-Seyler's Z. Physiol. Chem.*, 1932, 213, 125-135.

Hirata, J. and Michibata, H. *J. Exp. Zool.*, 1991, 257, 160-165.

Ishii, T., Nakai, I., Numako, C., Okoshi, K., and Otake, T. *Naturwissenschaften*, 1993, 80, 268-270.

Kalk, M. *Quart. J. Microscop. Sci.*, 1963a, 104, 483-493.

Kalk, M. *Nature*, 1963b, 198, 1010-1011.

Kanamori, K. and Michibata, H. *J. Mar. Biol. Ass. U.K.*, 1994, 74: 279-286.

Kanda, K., Nose, Y., Wuchiyama, J., Uyama, T., Moriyama, Y., and Michibata, H. *Zool. Sci.*, 1997,14, 37-42.

Kustin, K., Levine, D. S., McLeod, G. C., and Curby, W. A. *Biol. Bull.*, 1976, 150, 426-441.

Lane, D. J. W. and Wilkes, S. L. *Acta Zool. (Stockholm)*, 1988, 69, 135-145.

Lee, S., Kustin, K., Robinson, W. E., Frankel, R. B., and Spartalian, K. *Inorg. Biochem.*, 1988, 33, 183-192.

Levine, E. P. *Science*, 1961, 133, 1352-1353.

Michibata, H. *Comp. Biochem. Physiol.*, 1984, 78A, 285-288.

Michibata, H., Terada, T., Anada, N., Yamakawa, K., and Numakunai, T. *Biol. Bull.*, 1986, 171, 672-681.

Michibata, H., Hirata, J., Uesaka, M., Numakunai, T., and Sakurai, H. *J. Exp. Zool.*, 1987, 244, 33-38.

Michibata, H., Iwata, Y., and Hirata, J. *J. Exp. Zool.*,1991a, 257: 306-313.

Downloaded by UNIV OF GUELPH LIBRARY on October 31, 2012 | http://pubs.acs.org
Publication Date: December 10, 1998 | doi: 10.1021/bk-1998-0711.ch019

Michibata, H., Seki, Y., Hirata, J., Kawamura, M., Iwai, K., Iwata, R., and Ido, T. *Zool. Sci.*, 1991b, 8, 447-452.

Nour-Eldeen, A. F., Craig, M. M., and Gresser, M. J. *J. Biol. Chem.* 1985, 260, 6836-6842.

Pirie, B. J. S. and Bell, M. V. *J. Exp. Mar. Biol. Ecol.*, 1984, 74, 187-194.

Roman, D. A., Molina, J., and Rivera, L. *Biol. Bull.*, 1988, 175, 154-166.

Rowley, A. F. *J. Mar. Biol. Ass. UK.*,1982, 62, 607-620.

Scippa, S., Botte, L., and de Vincentiis, M. *Acta Zool. (Stockholm)*, 1982, 63, 121-131.

Scippa, S., Botte, L., Zierold, K., and de Vincentiis, M. *Cell Tissue Res.*, 1985, 239, 459-461.

Scippa, S., Zierold, K., and de Vincentiis, M. *J. Submicroscop. Cytol. Pathol.*, 1988, 20, 719-730.

Tullius, T. D., Gillum, W. O., Carlson, R. M. K., and Hodgson, K. O. *J. Am. Chem. Soc.*, 1980, 102, 5670-5676.

Uyama, T., Nishikata, T., Satoh, N., and Michibata, H. *J. Exp. Zool.*,1991, 259, 196-201.

Uyama, T., Moriyama, Y., Futai, M., and Michibata, H. *J. Exp. Zool.*, 1994, 270, 148-154.

Uyama, T., Nose, Y., Wuchiyama, J., Moriyama, Y., and Michibata, H. *Zool. Sci.*, 1997, 14, 43-47.

Vyskocil, F., Teisinger, J., and Dlouha, H. *Nature*, 286, 1980, 516-517.

Webb, D. A. *J. Exp. Biol.*,1939, 16, 499-523.

Wright, R. K. In *Urochordata;* N. A. Ratcliffe and A. F. Rowley, Ed., *Invertebrate Blood Cells*; Academic Press: London, 1981,Vol. 2, pp 565-626.

Wuchiyama, J. , Nose, Y., Uyama, T., and Michibata, H. *Zool. Sci.*, 1997, 14, 409-414.

Appendix: A referee pointed out that vanadocytes are used ambiguously. Therefore, we give a definition of vanadocytes as vanadium-containing blood cells in this paper. As far as using a combination of density-gradient centrifugation for cell separation and neutron-activation analysis and/or flameless atomic absorption spectrometry for determination of vanadium, high levels of vanadium are detected in signet ring cells.

Downloaded by UNIV OF GUELPH LIBRARY on October 31, 2012 | http://pubs.acs.org
Publication Date: December 10, 1998 | doi: 10.1021/bk-1998-0711.ch019

Downloaded by NORTH CAROLINA STATE UNIV on October 31, 2012 | http://pubs.acs.org
Publication Date: December 10, 1998 | doi: 10.1021/bk-1998-0711.ch020

Chapter 20

A New Class of Insulin-Mimetic Compounds. *N,N*-Dimethylhydroxamidovanadates: Aspects of Their Chemistry and Function

Fikile Nxumalo[1], Alan S. Tracey[1], Nancy Detich[2], Michael J. Gresser[2], and Chidambaram Ramachandran[2]

[1]Department of Chemistry and Institute of Molecular Biology and Biochemistry, Simon Fraser University, Burnaby, British Columbia V5A 1S6, Canada
[2]Merck Frosst Centre for Therapeutic Research, Merck Frosst Canada, Incorporated, C.P. 1005, Pointe-Claire—Dorval, Quebec H9R 4P8, Canada

In aqueous solution bis(N,N-dimethylhydroxamido)hydroxooxovanadate (DMHAV) undergoes favorable condensation reactions with a variety of related bidentate sulfhydryl-containing ligands such as dithiothreitol, cysteine and glutathione. The vanadate complex is a micromolar inhibitor of two protein tyrosine phosphatases, GST-LAR-D1 and flag-PTP1B. In cell cultures, DMHAV, promotes an increase in the level of phosphotyrosine on a variety of proteins at a level slightly higher than does vanadate. In the JURKAT line of T-lymphoma cells, DMHAV was found to be highly active whereas vanadate showed little or no activity. The activity of DMHAV in cell cultures is ascribed to its inhibitory influence on phosphatase activity and this in turn derives from the facile reaction of DMHAV with the cysteine and associated functional groups in the active site of the PTPase.

The discovery that vanadium oxoanions had insulin-mimetic properties in animals ushered in an era of interest, speculation and research in the biochemical properties of

In Vanadium Compounds; Tracey, A., et al.;
ACS Symposium Series; American Chemical Society: Washington, DC, 1998.

vanadium oxides and their complexes. Our interest in vanadium proceeded from a different perspective in that our interest was mostly in the aqueous chemistry of vanadium and how this chemistry predicated the role of the vanadium(V) oxide, vanadate, as a phosphate mimic in biochemical systems. The two streams of research recently converged because of our investigations into inhibitors of a special class of phosphate-transferring enzymes, the protein tyrosine phosphatases (PTPases).

The PTPases are crucial to the regulation and expression of many fundamental cellular responses, examples of which include T-cell activation, onset of cell division and autoimmune responses (1-3). Most of these activities are influenced by the presence of vanadium complexes, such as for instance, the activation of T-cells by peroxovanadate (4). The kinase activity of the insulin receptor is regulated by specific PTPases. There is evidence that suggests the PTPase, PTP1B, is specific to the insulin receptor (5,6) while a second PTPase, LAR, also is involved with regulating the activity of the insulin receptor (7,8). Binding of insulin to the insulin receptor alters the conformation of the receptor and leads to autophosphorylation of the receptor on the regulatory tyrosine residues. This increases the kinase activity of the receptor which then phosphorylates "down-stream" substrates and thereby alters their function. The kinase activity of the receptor and the autophosphorylation and autoactivation has been shown to be essential for insulin to elicit most of its biological effects. However, even in the absence of insulin, the insulin receptor will have a basel level of activity that is kept in check by the appropriate PTPase. Inhibition of that phosphatase allows unfettered function of the kinase activty of the insulin receptor. As a consequence, in the absence of insulin, it should be possible to promote the insulin-signaling cascade by having effective inhibitors of the insulin receptor PTPase present in the medium.

Effective promoters of the function of the insulin receptor include vanadate and vanadyl, the complexes of vanadate with hydrogen peroxide, and the complex of vanadyl with the organic ligand, maltol. Of these materials, we have been interested in the function of peroxovanadates. These complexes can form quite stable products with ancilliary ligands which leads to the possibility of building selectivity into the inhibition process. However, there is evidence that suggests the peroxo complexes inhibit via an oxidative inactivation of the PTPase simply by oxidizing the critical active site cysteine (9). This seems to be the case with peroxovanadates themselves and with at least one additional peroxo complex, the glycylglycinato complex with monoperoxovanadate (10).

Hydroxylamine is isoelectronic with hydrogen peroxide and forms complexes of a stability comparable to those formed with hydrogen peroxide (11,12). Figure 1 shows a vanadium NMR spectrum obtained under conditions where a variety of complexes formed with N,N-dimethylhydroxylamine (DMHA) are observable. The bisligand complex can be obtained from aqueous solution quite readily. It crystalizes as a dimer that is maintained in non-aqueous solvents but that readily dissociates to the monomer when dissolved in water (12). The monomer is kinetically quite stable with little hydrolysis occurring even after several days. A particularly interesting facit of the chemistry of these dimethylhydroxamidovanadates (DMHAV) is their reaction with sulfur-containing ligands. Figure 2 shows the result of combining DMHAV with the

Downloaded by NORTH CAROLINA STATE UNIV on October 31, 2012 | http://pubs.acs.org
Publication Date: December 10, 1998 | doi: 10.1021/bk-1998-0711.ch020

Downloaded by NORTH CAROLINA STATE UNIV on October 31, 2012 | http://pubs.acs.org
Publication Date: December 10, 1998 | doi: 10.1021/bk-1998-0711.ch020

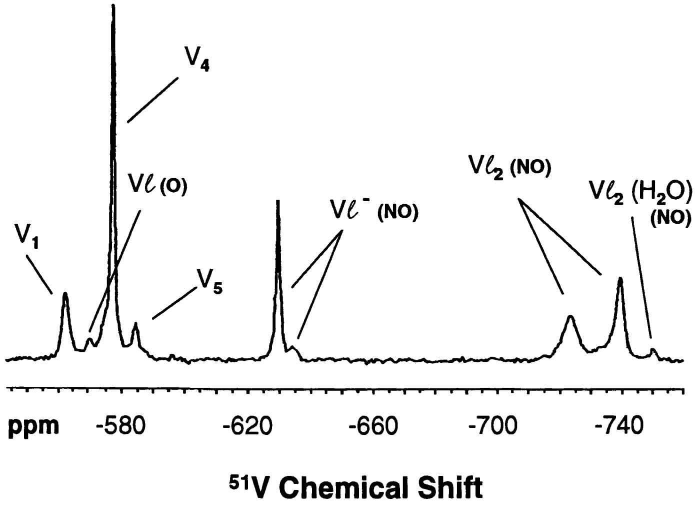

Figure 1. *^{51}V NMR spectrum showing various vanadium signals deriving from vanadate, its oligomers, and the products of its reaction with N,N-dimethylhydroxylamine. The spectrum was obtained under conditions of 3.0 mM total vanadate, 3.0 mM total N,N-dimethylhydroxylamine, 20 mM HEPES buffer, pH 7.2 and 1.0 M KCl.*

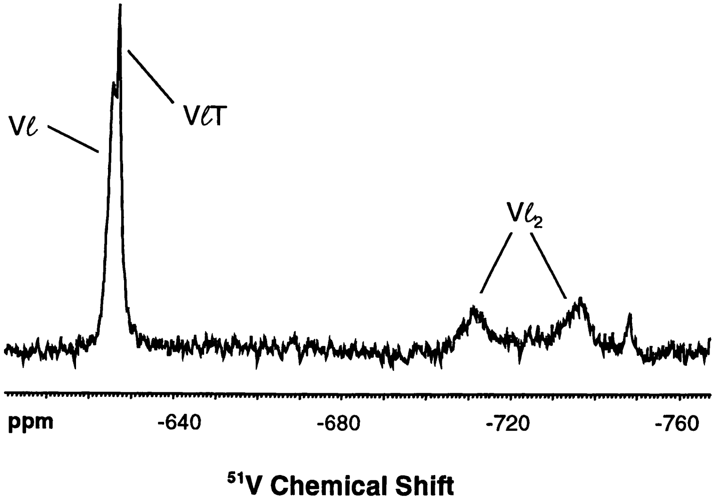

Figure 2. *^{51}V NMR spectrum showing the additional product signal ($V\ell T$) obtained when dithiothreitol (T) was included in the vanadate solution. The spectrum was obtained under conditions of 0.30 mM vanadate, 15 mM N,N-dimethylhydroxylamine, 30 mM dithiothreitol, 2.5 mM HEPES buffer and pH 7.3.*

redox buffer, dithiothreitol (DTT). Under similar conditions, DTT would be very rapidly oxidized by the corresponding peroxovanadium complex (13). Other sulfur-containing ligands such as cysteine and glutathione also form easily characterizable complexes with DMHAV. However, products have only been observed in cases where the ligand is bidentate, containing a sulfur and a second liganding group such as oxygen or nitrogen. At higher concentrations, less favoured products may well be observable. A list of some of the ligands studied (10) and their reactivity is indicated in Table 1.

Table I. Selected examples of the reactivity of N,N-dimethylhydroxamidovanadate towards various hydroxyl and sulfhydryl-containing ligands.

Ligand	*Structural Formula*	*Complex Formation*
ethanol	CH_3CH_2OH	no
propylene glycol	$CH_3CHOHCH_2OH$	no
tert-butylmercaptan	$(CH_3)_3CSH$	no
thioacetic acid	CH_2SHCO_2H	yes
dithiothreitol (DTT)	$CH_2SHCHOHCHOHCH_2SH$	yes
L-serine (Ser)	$NH_3CH(CH_2OH)CO_2$	no
L-cysteine (Cys)	$NH_3CH(CH_2SH)CO_2$	yes
glutathione	GluCysGly	yes

The stoichiometry of the product formed from reaction with DTT has been obtained by solution equilibrium studies and found to be 1:1:1, DTT:V:DMHA. The same stoichiometry was found for the reaction with cysteine. Product formation with the other reactive ligands of Table 1 has not yet been studied in detail but the evidence available suggests the reaction chemistry is similar, except perhaps for the reaction with thioacetic acid. The reaction between DMHAV and ancilliary sulfur-containing ligands occurs rapidly, certainly within a minute or so. This compares with a timescale of many days for the dissociation of the DMHAV to vanadate and free ligand.

There is quite strong evidence available that indicates that DMHAV in aqueous solution consists predominently of two six-coordinate compounds (Fig 3 a,b) while a minor component has been assigned to a seven-coordinate bisligand product (Fig 3c) (11,12). Certainly, the crystalline product is six-coordinate (12). This compares with the nominally analogous bisperoxovanadates that are most likely seven-coordinate (14), perhaps in a geometry similar to that of 3c in Figure 3. There is some dispute about this type of coordination for the peroxovanadates (15,16). Evidently, however, the bis(N,N-dimethylhydroxamido)vanadates (Fig 3a,b) are coordinatively unsaturated. The condition is then appropriate for an associative reaction followed by displacement of one of the dimethylhydroxylamido ligands to form the product 1:1:1 complex that is observed. Such a process would account for the rapid reaction of DMHAV with sulfur-containing ligands to form mixed ligand products as compared to the much slower dissociation reaction to give vanadate and the free DMHA. An associative mechanism

Downloaded by NORTH CAROLINA STATE UNIV on October 31, 2012 | http://pubs.acs.org
Publication Date: December 10, 1998 | doi: 10.1021/bk-1998-0711.ch020

for product formation suggests that these complexes might be good inhibitors of PTPases. A sulfur (cysteine), together with other functionalized groups such as carboxylate (aspartate) and hydroxyl (serine) occur within the active site and are available for associative type reactions in a bidentate-like reaction.

Inhibition studies with both GST-LAR and flag-PTP1B confirmed the inhibitory properties of DMHAV. Using flourescein-3,6-bisphosphate (FDP) as a substate, a K_m of 26 ± 6 μM (error, ± 3σ) was obtained for GST-LAR-D1 (the glutathione-S-transferase (GST) fusion protein of domain 1 of LAR) while the corresponding K_m for flag-PTP1B (AspTyrLysAspAspAspAspLys fusion of PTP1B) was 24 ± 8 μM (± 3σ). The inhibition was competitive with K_i values of 2.2 ± 0.3 μM (±3σ) and 3.4 ± 0.6 μM (± 3σ), respectively, for LAR and PTP1B. The reversible nature of the inhibition was easily established by a dilution experiment. The problem with the above experiments is that they are only partially correct.

For studies of PTPases, a redox buffer is frequently utilized in order to keep the active site cysteine in its active, reduced form. For the kinetics studies, DTT was utilized as the redox buffer. Because of the reactivity of DMHAV with DTT, both DMHAV and DTTDMHAV are present in solution and either, or both complexes, are potential inhibitors. Through an appropriate combination of relative concentrations of DMHA and DTT the ratio of DMHAV to DTTDMHAV can be varied from about 10:1 to close to 1:10 without engendering adverse affects on the function of the PTPases. The appropriate equations can then be written for inhibition by two inhibitors and the inhibition results analyzed. The results provided the constants K_i = 1.0 ± 0.3 μM (± 3σ) for DMHAV and K_i = 2.3 ± 0.8 μM (± 3σ) for DTTDMHAV for GST-LAR-D1. The factor of 2 difference in inhibition constants may simply represent a statistical factor. It is likely that DTTDMHAV can only go into the active site in one orientation while molecular symmetry makes two orientations available to DMHAV. The inhibition constant of 1 μM is only about a factor of 10 poorer than that of vanadate. Considering the structure of the DMHAV inhibitor, this seems quite remarkable.

If the factor of 2 between the inhibition constants of DMHAV and DTTDMHAV is correctly interpreted as being a statistical one, then it is evident that the DTT ligand is having a minimal influence on the activity of the complex and this opens up a host of possibilities for potentially new inhibitors. Such possibilities include modification of the methyls of one of the dimethylhydroxylamine ligand so that it can reach out to possible recognition groups so as to generate additional stabilizing interactions. Alternatively, modifications could be made to the DTT, or similar ligands, to reach to potential sources of binding interactions. Building ligands with such complementary properties has the potential of generating very powerful PTPase inhibitors, but equally, if not more importantly, allows for the possibility of building in inhibitor selectivity.

Figure 4 shows DMHAV docked into the active site. This docking procedure has not taken into account any possible partially developed covalent bonds that might be expected if the reaction is an associative one. It simply reveals that there is adequate space within the active site for the complex. Also, the influence of rotating the inhibitor within the binding pocket on the calculated binding energies suggested that

Downloaded by NORTH CAROLINA STATE UNIV on October 31, 2012 | http://pubs.acs.org
Publication Date: December 10, 1998 | doi: 10.1021/bk-1998-0711.ch020

Downloaded by NORTH CAROLINA STATE UNIV on October 31, 2012 | http://pubs.acs.org
Publication Date: December 10, 1998 | doi: 10.1021/bk-1998-0711.ch020

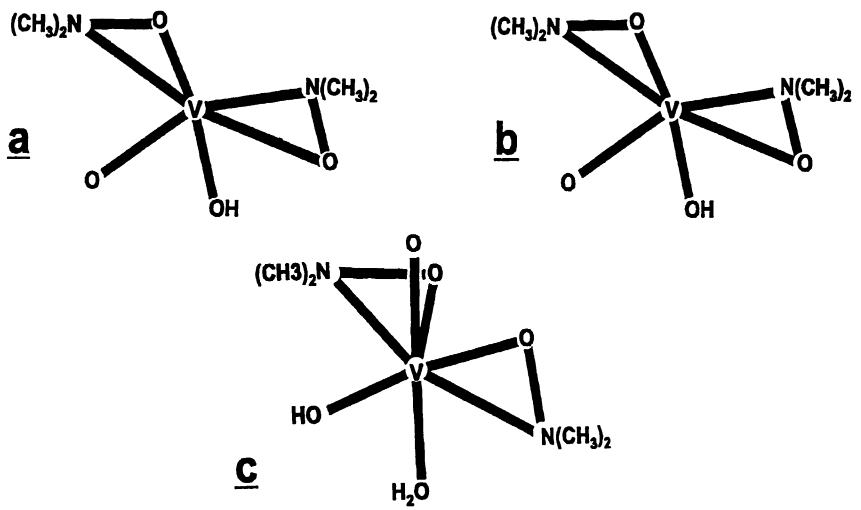
a
(CH3)2N
O
V
N(CH3)2
O
O
OH
b
(CH3)2N
O
V
N(CH3)2
O
O
OH
c
O
(CH3)2N
O
V
O
HO
N(CH3)2
H2O

Figure 3. The coordination geometries (a, b) thought to correspond to the two major bisligand products of the reaction of N,N-dimethylhydroxylamine with vanadate and the coordination (c) assigned to the minor bisligand product.

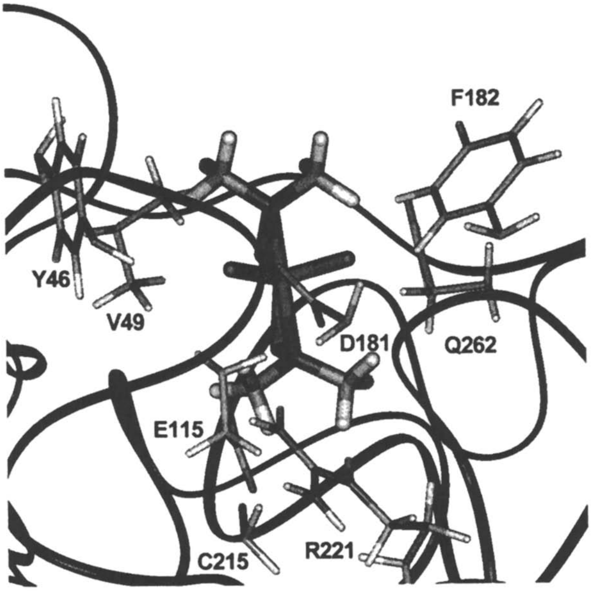
F182
Y46
V49
D181
Q262
E115
C215
R221

Figure 4. A representation of bis(N,N-dimethylhydroxamido)hydroxooxovanadate docked in the active site of the protein tyrosine phosphatase, PTP1B. Only the region of the enzyme surrounding the active site pocket is displayed.

Downloaded by NORTH CAROLINA STATE UNIV on October 31, 2012 | http://pubs.acs.org
Publication Date: December 10, 1998 | doi: 10.1021/bk-1998-0711.ch020

there is a preferred orientation (that depicted in Fig 4) that might be adopted in the initial stages of the binding interaction. In the orientation depicted, the cysteine sulfur is about 5 Å from the vanadium center. In the absence of a major structural change, this suggests that the active site cysteine might not be important in the binding of this inhibitor. However, without further evidence it is not possible to whether a coordination change has occurred. In fact, though, other residues seem ideally situated for both the development of strong hydrogen bonds (Asp181) and strong hydrophobic stabilization interactions (Phe182 and Tyr46, for example).

Because DMHAV reversibly inhibits both GST-LAR-D1 and flag-PTP1B there is a reasonable possibility that it has biological activity. To test this hypothesis, the influence of DMHAV on phosphotyrosine levels was studied in a selection of cell cultures and the influences compared to those of vanadate. In all cases DMHAV was either equal to or more effective than vanadate in increasing phosphotyrosine levels. This activity is demonstrated in Figure 5 for cell cultures of Chinese hamster ovary cells that overexpress the human insulin receptor (17). The efficacy of insulin and peroxovanadate is also shown for comparison. A concentration profile that clearly indicates that the activities of vanadate and dimethylhydroxamidovanadate are similar is shown in Figure 6. The slightly higher activity of DMHAV over vanadate was mirrored in similar studies with 3T3L1, a mouse fibroblast cell line.

The most remarkable behavior exhibited was found for Jurkat cells. Jurkat cells are a strain of human leukaemic T-cells. Vanadate gives little or no response in these cells while peroxovanadium is known to activate them (4). In contrast to the minimal influence of vanadate, it is evident from Figure 7 that DMHAV gives rise to a response that is comparable in magnitude to the reponse engendered in Chinese hamster ovary and mouse fibroblast cell lines.

The chemistry of DMHAV, as briefly discussed above, makes it highly unlikely that the biological influences of this complex arise from free vanadate that is released because of dissociation of the complex to vanadate and ligand. The function of DMHAV in Jurkat cells when compared to that of vanadate also strongly suggests that DMHAV is the active material. The stability of DMHAV against dissociation and its ability to react with ancilliary ligands such as DTT, cysteine and glutathione, also without dissociation, combined with the fact that DMHAV is a potent inhibitor of flag-PTP1B and GST-LAR-D1 lend strong support to the proposal given here that DMHAV is the active component that is responsible for the increased phosphotyrosine levels. Whether some of this activity involves the product of the reaction of DMHAV with the cellular glutathione cannot be judged. However, considering the activity of DTTDMHAV in flag-PTP1B and GST-LAR-D1, it seems quite possible that such a glutathione complex also is active in cell cultures.

Literature Cited

1. Jia, Z. *Biochem. Cell Biolog.* **1997**, *75*, 17-26.
2. Fauman, E. B.; Saper, M. A. *TIBS* **1996**, *21*, 413-417.
3. Zhang, Z. -Y.; Dixon, J. E. *Adv. Enzymol.* **1994**, *68*, 1-36.

Downloaded by NORTH CAROLINA STATE UNIV on October 31, 2012 | http://pubs.acs.org
Publication Date: December 10, 1998 | doi: 10.1021/bk-1998-0711.ch020

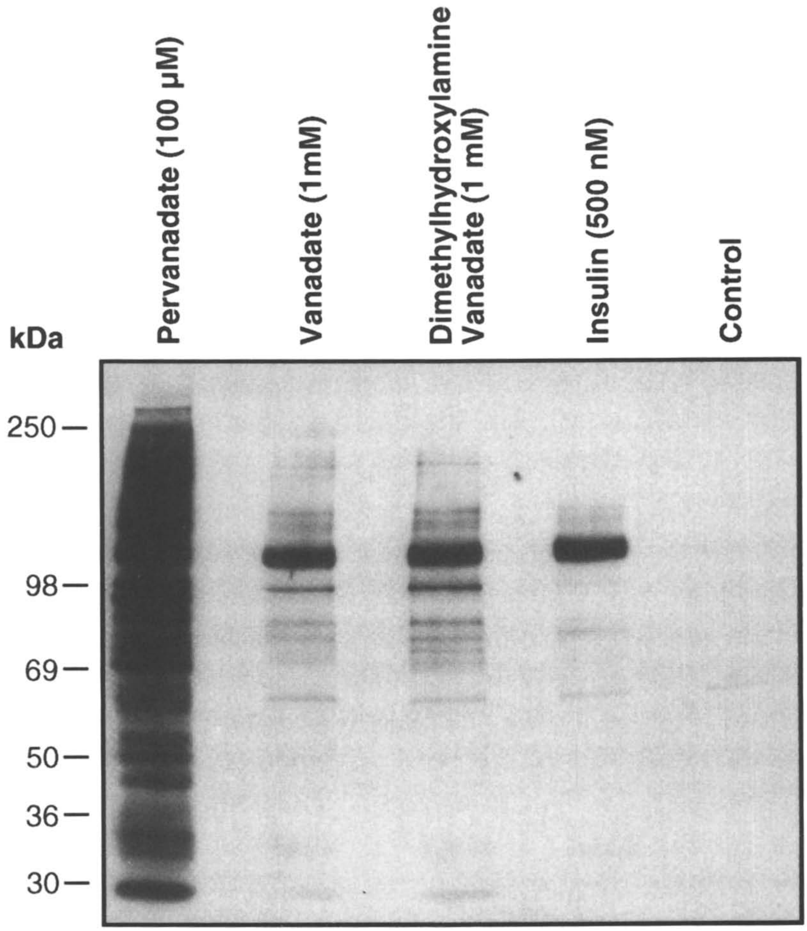
kDa
Pervanadate (100 μM)
Vanadate (1mM)
Dimethylhydroxylamine
Vanadate (1 mM)
Insulin (500 nM)
Control
250—
98—
69—
50—
36—
30—

Figure 5. *Comparative influences of vanadate, peroxovanadate, bis(N,N-dimethylhydroxamido)hydroxooxovanadate and insulin on protein phosphotyrosine levels in cell cultures of Chinese hamster ovary cells that have been modified to overexpress the human insulin receptor. Experimental conditions: whole cell lysate antiphosphotyrosine Western blot; incubation times; vanadate and bis(N,N-dimethylhydroxamido)hydroxooxovanadate, 45 min; peroxovanadate, 10 min; insulin, 5 min.*

Downloaded by NORTH CAROLINA STATE UNIV on October 31, 2012 | http://pubs.acs.org
Publication Date: December 10, 1998 | doi: 10.1021/bk-1998-0711.ch020

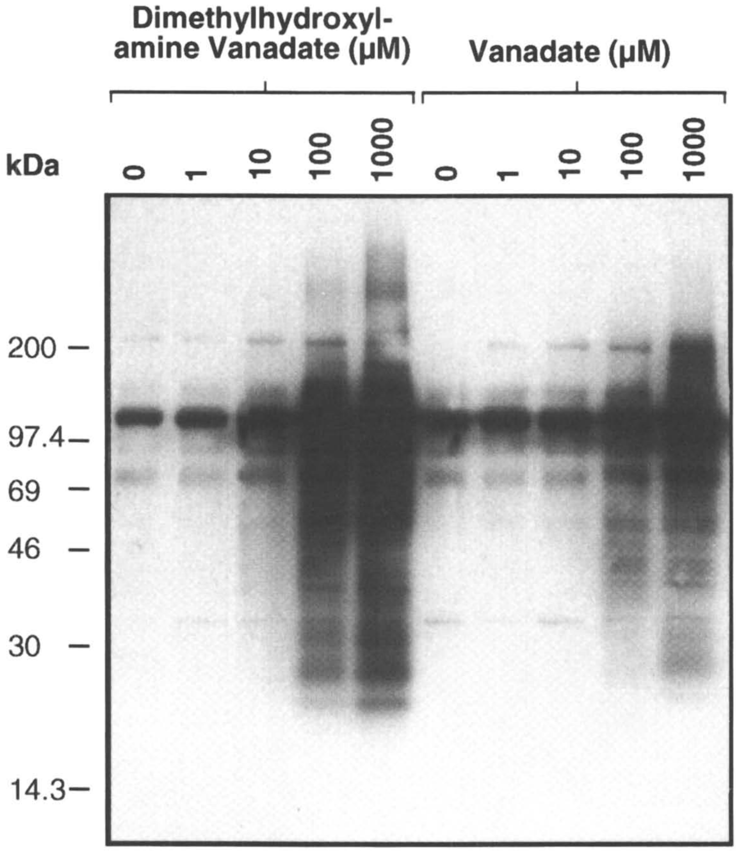
Dimethylhydroxyl-amine Vanadate (μM)
Vanadate (μM)
kDa
0
1
10
100
1000
0
1
10
100
1000
200
97.4
69
46
30
14.3

Figure 6. Comparative concentration profiles showing the relative influences of vanadate and bis(N,N-dimethylhydroxamido)hydroxooxovanadate on protein phosphotyrosine levels in Chinese hamster ovary cells that have been modified to overexpress the human insulin receptor. Experimental conditions: whole cell lysate antiphosphotyrosine Western blot; incubation times; vanadate and bis(N,N-dimethylhydroxamido)-hydroxooxovanadate, 45 min

Downloaded by NORTH CAROLINA STATE UNIV on October 31, 2012 | http://pubs.acs.org
Publication Date: December 10, 1998 | doi: 10.1021/bk-1998-0711.ch020

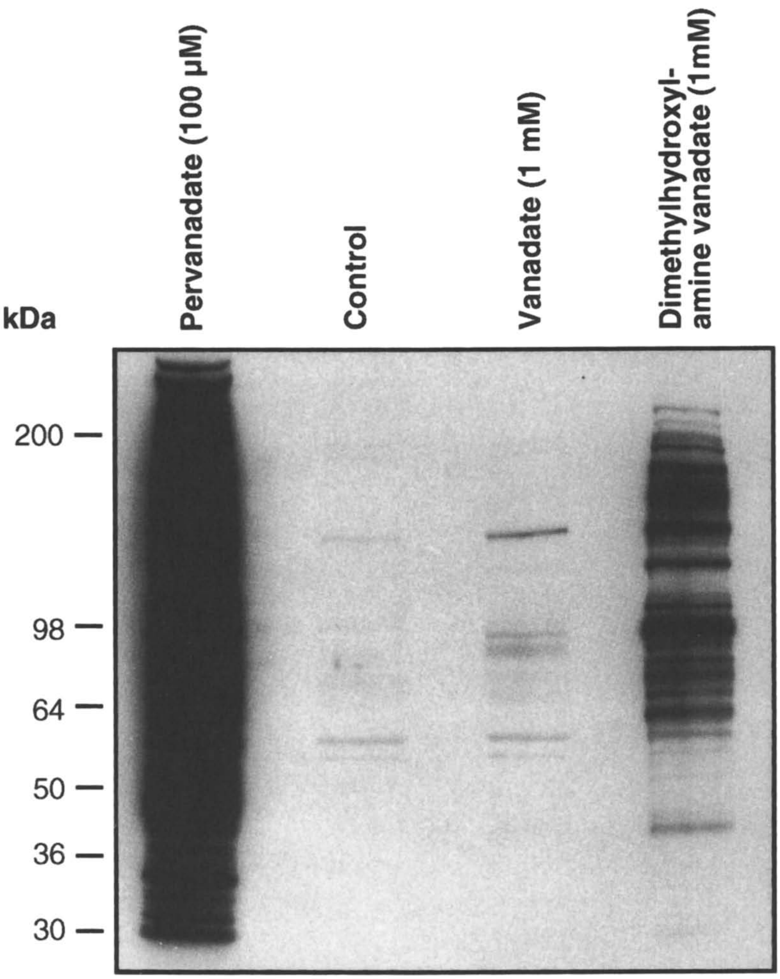
kDa
Pervanadate (100 µM)
Control
Vanadate (1 mM)
Dimethylhydroxyl-
amine vanadate (1mM)
200
98
64
50
36
30

Figure 7. *The relative influences of peroxovanadate, vanadate and bis(N,N-dimethylhydroxamido)hydroxooxovanadate on protein tyrosine phosphate levels in leukaemic T-cells (Jurkat cells). Experimental conditions: whole cell lysate antiphosphotyrosine Western blot; incubation times; vanadate and bis(N,N-dimethylhydroxamido)hydroxooxovanadate, 45 min; peroxovanadate, 10 min.*

4. Imbert, V.; Peyron, J. -F.; Farahi Far, D.; Mari, B.; Auberger, P.; Rossi, B. *Biochem. J.* **1994**, *297*, 163-173.
5. Seely, B. L.; Staubs, P. A.; Reichardt, D. R.; Berhanu, P.; Milarski, K. L.; Saltiel, A. R.; Kusari, J.; Olefskey, J. M. *Diabetes* **1996**, *45*, 1379-1385.
6. Bandyopadhyay, D.; Kusari, A.; Kenner, K. A.; Liu, F.; Chernoff, J.; Gustafson, T. A.; Kusari, J. *J. Biol. Chem.* **1997**, *272*, 1639-1645.
7. Kulas, D. T.; Goldstein, B. J.; Mooney, R. A. *J. Biol. Chem.* **1996**, *271*, 748-754.
8. Li, P-M.; Zhang, W-R.; Goldstein, B. J. *Cell. Signal.* **1996**, *8*, 467-473.
9. Huyer, G.; Liu, S.; Kelly, J.; Moffat, J.; Payette, P.; Kennedy, B.; Tsaprailis, G.; Gresser, M. J.; Ramachandran, C. *J. Biol. Chem.* **1997**, *272*, 843-851.
10. Nxumalo, F. *Influence of Vanadium(V) Complexes on the Catalytic Activity of Protein Tyrosine Phosphatases*; M. Sc. Thesis, Simon Fraser University: Burnaby, 1997.
11. Angus-Dunne, S. J.; Paul, P. C.; Tracey, A. S. *Can. J. Chem.* **1997**, *75*, 1002-1010.
12. Paul, P. C.; Angus-Dunne, S. J.; Batchelor, R. J.; Einstein, F. W. B.; Tracey, A. S. *Can. J. Chem.* **1997**, *75*, 429-440.
13. Paul, P. C.; Tracey, A. S. *J. Biol. Inorg. Chem.* **1997**, *2*, 644-651.
14. Campbell, N. J.; Dengel, A. C.; Griffith, W. P. *Polyhedron* **1989**, *8*, 1379-1386.
15. Harrison, A. T.; Howarth, O. W. *J. Chem. Soc., Dalton Trans.* **1985**, 1173-1177.
16. Schwendt, P. *13th Conf. Coord. Chem. Proceed.* **1991**, 243-246.
17. Yoshimasa, Y.; Paul, J. I.; Whittaker, J.; Steiner, D. F. *J. Biol. Chem.* **1990**, *265*, 17230-17237.

Downloaded by NORTH CAROLINA STATE UNIV on October 31, 2012 | http://pubs.acs.org
Publication Date: December 10, 1998 | doi: 10.1021/bk-1998-0711.ch020

Downloaded by CORNELL UNIV on October 31, 2012 | http://pubs.acs.org
Publication Date: December 10, 1998 | doi: 10.1021/bk-1998-0711.ch021

Chapter 21

Vanadium Bioactivity on Cells in Culture

S. B. Etcheverry[1,2] and A. M. Cortizo[1]

[1]Cátedra de Bioquímica Patológica, [2]CEQUINOR, Facultad de Ciencias Exactas, Universidad Nacional de La Plata, 47 y 115, 1900 La Plata, Argentina

Vanadium compounds show insulin-mimetic and growth factor-like properties in different biological systems. This issue has renewed the scientific interest in the synthesis and characterization of new vanadium derivatives with potential therapeutic applications. Vanadium (V) compunds like vanadate, V-oxal, V-cit, BMV (a maltol complex), as well as pervanadate and V-NTA (a peroxovanadium derivative) induce metabolic and proliferative events on two osteoblast-cell lines (UMR106 and MC3T3E1) in culture. Vanadium (IV) compounds like vanadyl, V-tar and BMOV behave similarly. The potency of the biological effect depends on the oxidation state of vanadium, the coordination sphere and the stability of the vanadium compounds under physiological conditions. Vanadium derivatives at higher tested doses caused morphological transformation in the MC3T3E1 cells with a variable potency. The transforming effect seems to correlate with the level of cellular tyrosine phosphorylation induced by the vanadium derivatives under culture conditions.

It has been known for several years, that vanadium and related compounds exert insulin-like effects on different cellular types. Comprehensive studies have been carried out on tissues and cells which are typical targets of insulin action. Among the observed actions, vanadium compounds show antilipolytic effects on adipocytes, and stimulate glucose uptake and glucose oxidation in skeletal muscle and adipocytes. Besides glycogen synthesis in the liver is stimulated by vanadium derivatives. Vanadate also increases calcium influx, inhibits Ca,Mg-ATPase in plasmatic membranes and enhances potassium uptake in intact cells (*1-3*).

Vanadium compounds, like growth factors, act on cellular proliferation and differentiation, and they also induce protooncogene expression (*2,4*). However, other studies have shown that vanadium inhibits cell growth and causes cytotoxicity (*5,6*). This effect seems to depend on the proliferative rate of the cells in culture (*7*). Thus, it has been shown that in cultures of high cellular density, with low level of

In Vanadium Compounds; Tracey, A., et al.;
ACS Symposium Series; American Chemical Society: Washington, DC, 1998.

proliferation, vanadium does not affect the mitogenicity. On the contrary, cells grown at low cellular density and with high proliferative rate are inhibited by micromolar concentrations of vanadium. For instance, the rapidly proliferative chondrocytes (*8*) and Syrian hamster's embryonic cells (*9*) are highly sensitive to vanadium cytotoxic effects. In addition, it has been reported that vanadium compounds induced morphological transformations in different cell types (*10*). In the presence of vanadium derivatives, cells become shrinkage and show a condensed chromatin, with few connections among them. It has been suggested that morphological changes are associated with an increase of tyrosine phosphorylation of numerous intracellular proteins (*2*).

The mechanism through which vanadium compounds produce growth factor-like effects are not completely known. Most of the growth factors regulate the cellular levels of phosphotyrosine proteins *via* specific cellular receptors. This effect depends on the balance between the activities of proteintyrosine kinases (PTKs) and phosphotyrosine phosphatases (PTPases). It has been demonstrated that vanadium compounds inhibit PTPases (*11*).

Concerning animals and human beings, vanadium compounds enter the organism primarily through the respiratory tract. Vanadium is rapidly distributed on tissues and finally is mainly retained on bones (*12*). On the other hand, it has been previously reported that vanadium deficiency causes growth inhibition and skeletal deformations (*13*). Numerous studies have shown that vanadium produces significant biological effects on skeletal tissues (*14-17*).Thus, the effects of vanadium derivatives in bone-related cells are of great interest.

Downloaded by CORNELL UNIV on October 31, 2012 | http://pubs.acs.org
Publication Date: December 10, 1998 | doi: 10.1021/bk-1998-0711.ch021

Glucose consumption induced by vanadium compounds on bone-related cells

One of the first studied insulin-like effects of vanadium on different cells in culture was the enhancement of glucose uptake and metabolism (*1*). In NIH3T3 mouse fibroblasts, vanadate induced an increase in GLUT-1 (glucose transporter) mRNA, in its protein expression and in the 2-deoxiglucose uptake. This effect was dose-dependent and required the presence of serum in the culture (*18*).

In our laboratory, we have observed that different vanadium compounds (vanadate, complexes with oxalate, citrate and tartrate, and V-NTA, a peroxovanadium complex) increased the glucose consumption in the osteoblast-like cells UMR106 and MC3T3E1 after a 24-hour of incubation (*19*). V-NTA (25 μM) was the strongest tested inductor of glucose consumption in UMR106 osteoblast-like cells (250 % over basal). This observation was in agreement with previous results obtained in adipocytes (*16,20,21*), showing that the peroxovanadium derivatives are more potent enhancers of glucose metabolism than vanadate.

The insulin-induced glucose consumption in UMR106 cells is a dose-dependent function. After 24-hour incubation, the maximum effect was 160 % over basal. Thus, like insulin, vanadium compounds stimulate glucose metabolism in osteoblasts-like cells.

Mitogenic effects of vanadium compounds on bone-related cells

Vanadium in the cells regulates several early events like protein phosphorylation, glucose transport, ATPases inhibition, glucose and lipid metabolism. In addition, vanadium also acts over the proliferation and differentiation of different cells in culture (*10*). The induction of cell growth by vanadium is similar to that produced by growth factors. The observation of this mitogenic effect requires 24-48 hs and it takes place in a narrow range of concentrations. This latter feature contrasts with the action of growth factors which occurs in a wide range of concentrations (10^{-10} - 10^{-7} M) and in a dose-response manner.

In particular, using different models of bone-related cells in culture, it has been previously demonstrated the direct effect of vanadate on DNA synthesis and cell replication (*14-17*). We have also addressed the issue on behalf of the fate of vanadium mitogenicity by using several vanadium compounds in fibroblasts and osteoblast-like cells in culture (*19,22-24*). We have chosen a series of vanadium compounds for previous biological studies characterized with physicochemical properties. In our models, the proliferative effects of the vanadium derivatives were biphasic, with a maximum between 10-25 μM, while high doses caused cytotoxic effects. We have tested different vanadium (V) and vanadium (IV) derivatives. Among the first ones there are: vanadate, vanadium (V) complexes with citrate, oxalate and maltol (bis(maltolato dioxo vanadate(V)) (BMV)). We have also tested two peroxovanadium (V) compounds. In addition to oxovanadium (IV) cation (vanadyl), complexes of vanadium (IV) with tartrate and maltol (bis(maltolato) oxovanadium (IV)) (BMOV)) were also studied. The potency of these vanadium compounds was similar for vanadium (V) and vanadium (IV) derivatives with the exception of peroxovanadium compounds that were less effective and more cytotoxic for all the cellular types studied.

The sensitivity of the cells towards the vanadium derivatives seems to depend on the stage of cellular development and also on the cellular density in the cultures. Thus, comparing 70% confluent cultures of Swiss 3T3 fibroblasts, MC3T3E1 osteoblast-like cells in the proliferative phase and the more differentiated osteoblast line UMR106, the latter showed less sensitivity to the cytotoxic effect of vanadate and vanadyl.

On the other hand, it has also been suggested that the cytotoxicity depends on the proliferative rate of the cell type. The cytotoxic effects of vanadium complexes seem to be dependent on several factors: the vanadium concentration in the culture media, the oxidation state of the vanadium atom, the coordination sphere, and likely on their ability to inhibit protein tyrosine phosphatases (PTP-ases).

In short, the cytotoxicity is a complex phenomenon under the influence of factors inherent to the cells and physicochemical properties of the vanadium compounds.

Morphological transformations.

The mitogenic and cytotoxic effects produced by vanadium compounds were accompanied by morphological changes (*19,22,24*). Swiss 3T3 fibroblasts and

Downloaded by CORNELL UNIV on October 31, 2012 | http://pubs.acs.org
Publication Date: December 10, 1998 | doi: 10.1021/bk-1998-0711.ch021

MC3T3E1 osteoblast-like cells in the proliferative stages showed a shape change from polygonal to fusiform, a retraction with citoplasm condensation and a loss of lamellar processes. The magnitude of the morphological transformations correlates with the potency of vanadium compounds to induce cytotoxic effects.

The vanadium compounds under study in our laboratory can be divided in three groups according with their decreasing potency as morphological transformer agents. The peroxovanadium compounds, pervanadate and V-NTA, formed the more potent group because they induce the most striking and fastest cellular changes. Vanadate, V-cit, V-oxal and BMOV are in the second group which causes intermediate morphological transformations and, finally, the third group is constituted by vanadyl cation, V-tar (a vanadium (IV) complex) and BMV. From our morphological studies, it can be suggested that in general, peroxovanadium compounds are more potent than vanadium (V) derivatives and these are more potent than vanadium (IV) compounds, with the exception of the maltol derivatives which behave contrarily taking into account the oxidation state of vanadium.

Downloaded by CORNELL UNIV on October 31, 2012 | http://pubs.acs.org
Publication Date: December 10, 1998 | doi: 10.1021/bk-1998-0711.ch021

Vanadium derivatives inhibit osteoblast-like cell differentiation

Studies on vanadium bioactivity have lead to address another growth factor mimetic property of these compounds, that is the ability to regulate cellular differentiation.

Previous reports have demonstrated that low vanadate doses induce the synthesis of collagen and extracellular matrix proteins (*14-16*).

On the other hand, the action of vanadate on the alkaline phosphatase activity of calvaria cells in culture have shown ambiguous results (*14,16*).

In recent studies we have shown that vanadium compounds regulate phenotype characteristics of UMR106 osteoblast-like cells as assessed by the levels of alkaline phosphatase activity (*19,23,24*).

Vanadate and vanadium (V) derivatives (vanadium complexes with oxalate and citrate, VNTA (a peroxo vanadium compound), and also the BMOV were inhibitors of ALP activity at proliferative doses (5-25 μM). On the contrary, vanadium (IV) derivatives (vanadyl sulfate and V-tar) as well as BMV, have shown no significant effect on the cellular ALP activity or they behave as weak inhibitors in these systems.

Our results are in agreement with the early Canalis' paper (*14*) who showed the inhibition of ALP activity in calvaria rat cells by 10 μM vanadate after a 96-hour incubation.

These studies suggest that the coordination of vanadium, its oxidation state and the stability of vanadium compounds under physiological conditions play a role in the cell differentiation process.

Direct effect of vanadium compounds on osteoblast-derived alkaline phosphatase

Not only us, but also other investigators have previously demonstrated the vanadium-inhibition of acid, neutral and alkaline phosphatases using cell-free *in vitro* assays (*2,23,25-27*). In general, all vanadium compounds tested inhibit phosphatases activity with ED_{50} in the order of micromolar concentrations. Specifically, alkaline phosphatase activity associated with particulate- and soluble-UMR106 cells are inhibited at 20 % and 40 % respectively, by 100 µM vanadate or vanadyl (*26*).

Since we evaluate the osteoblast differentiation by measuring the ALP activity, we have also investigated the possibility of a direct inhibition of vanadium compounds on cell associated-ALP. For these studies, we determined the ALP by histochemistry after an overnight incubation with or without 100 µM vanadium compounds in serum-free medium. Cells were washed with PBS, fixed and stained with naphtyl phosphate and fast blue for 15 min at room temperature (*24*). Preincubation of UMR106 cells with or without vanadate or vanadyl did not affect the ALP staining associated with the osteoblast-like cells. However, when the same concentration of vanadate or vanadyl was added to the ALP histochemical assay, the staining almost disappeared. These results suggest that vanadium compounds exert a direct effect on the ALP activity but this inhibition is blunted by washing the cell monolayer. These experiments also suggest that the previously described studies on inhibition of cell differentiation by vanadium compounds are not due to the direct effect of vanadium but rather on the ALP expression on UMR106 cells.

Downloaded by CORNELL UNIV on October 31, 2012 | http://pubs.acs.org
Publication Date: December 10, 1998 | doi: 10.1021/bk-1998-0711.ch021

Biological mechanism of vanadium compounds

The precise mechanisms by which vanadium compounds produced their metabolic, mitogenic and transforming effects still remain unestablished. It is well known that insulin and growth factors promote cell growth by the interaction with specific cellular surface receptors. This interaction leads to the autophosphorylation of the receptors and consequently to the phosphorylation cascade of several intracellular proteins specifically on tyrosine residues (*28*). Most of the evidence suggests that vanadium compounds can act on some steps of these pathways (*29*). Thus, different intracellular proteins become phosphorylated upon vanadium stimulation. It is assumed that vanadium-induced protein tyrosine phosphorylation is mediated mainly by the inhibition of different protein tyrosine phosphatases.

In the MC3T3E1 osteoblast-like cells in culture, we have investigated the effects of different vanadium compounds on the protein tyrosine phosphorylation levels in order to understand the possible mechanism of vanadium action (*30*). We have also attempted to correlate these patterns with the vanadium-induced growth and cell transformation. Vanadate, vanadyl and BMOV appear to be more potent than BMV in stimulating protein phosphorylation in thyrosine residues. This effect was more prominent at low doses than at high doses. At low doses (10 µM), BMV showed a phosphorylation pattern similar to that of insulin, while V , VO and BMOV induced a strong phosphorylation of cell proteins. In our osteoblast system, a 90-95 kDa band presumibly corresponding to the insulin-receptor β-subunit was not observed. The present findings suggest that the vanadium-induced growth regulation and transformation in MC3T3E1 osteoblast-like cells are strongly associated with the ability of these agents to increase the phorphotyrosine protein levels.

Conclusions

Studies concerning the biological effects of vanadium compounds on bone related cells lead to the conclusion that they play a role on hard tissues growth and development. Our results show that vanadium compounds with weaker effect on the inhibition of osteoblast differentiation, as evaluated by alkaline phosphatase activity, are also the weakest transformer agents. These effects correlate with the lesser extension of tyrosine protein phosphorylation induced by these compounds. The model system used in these studies let us evaluate the mechanism by which vanadium compounds could be accumulated and metabolized in the bone.

Aknowledgments

SBE and AMC are indebted to VC Sálice, DA Barrio, MD Braziunas and CM Vescina, all of them members of their research team. The authors wish to thank Mrs. MC Bernal for the language revision. SBE is a member of the Carrera del Investigador Científico (CONICET, Argentina). AMC is a member of the Carrera del Investigador Científico (CICPBA, Argentina). The laboratory work reported herein has been supported by the Facultad de Ciencias Exactas (UNLP), the Universidad Nacional de La Plata (UNLP) (Argentina), and the Third World Academy of Sciences (Italy).

Literature Cited

1. Shechter, Y.; Shisheva, A. *Endeavour* **1993**, *17*, 27-31.
2. Stern, A.; Yin, X.; Tsang, S-S.; Davison, A.; Moon, *J. Biochem. Cell Biol.* **1993**, *71*, 103-112.
3. Sekar, N.; Li, J.; Shecheter, Y. *Crit. Rev. Biochem. Mol. Biol.* **1996**, *31*, 339-359.
4. Wang, H.; Scott, R.E. *Mol. Cell. Biochem.* **1995**, *153*, 59-67.
5. Sabbioni, E.; Pozzi, G.; Pintar, A.; Casella, L.; Garattini, S. *Carcinogenesis* **1991**, *12*, 47-52.
6. Sabbioni, E.; Pozzi, G.; Devos, S.; Pintar, A.; Casella, L.; Fishbach, M. *Carcinogenesis* **1993**, *14*, 2565-2568.
7. Cruz, T.F.; Morgan, A.; Min, W. *Mol. Cell. Biochem.* **1995**, *153*, 161-166.
8. Conquer, J.A..; Grima, D.T.; Cruz, T.F. *Ann. New York Acad. Sci.* **1994**, *732*, 447-450.
9. Afshari, C.A.; Kodama, S.; Bivins, H.M.; Willard, T.B.; Fujiki, H.; Barrett, J.C. *Cancer Res.* **1993**, *53*, 1777-1782.
10. Etcheverry, S.B.; Cortizo, A.M. In *Vanadium in the enviroment, Part I: Chemistry and biochemistry*; Nriagu.J.O., Ed.; John Wiley & Sons, Inc., New York, 1998,Vol 1, pp 359-394.
11. Gresser, M.J.; Tracey, A.S.; Stankiewicz, P.J. *Adv. Prot. Phosphatases* **1987**, *4*, 35-57.
12. Nielsen, F.H. In *Vanadium and its role in life*; Siegel, H., Siegel A. Eds. Marcell Dekker, New York, 1995, vol 31, pp 543-573.

Downloaded by CORNELL UNIV on October 31, 2012 | http://pubs.acs.org
Publication Date: December 10, 1998 | doi: 10.1021/bk-1998-0711.ch021

13. Anke, M.; Groppel, B.; Gruhn, K.; Langer, M.; Arnhold, W. In *6th International Trace Element Symposium, Molybdenum, Vanadium* Anke, M., Baumann, W., Bräunlich, H., Brücker, C., Groppel, B., Grün, M. Eds., Karl-Marx, Universität, Leipzig, 1989, Vol 1, pp 17-27.
14. Canalis, E. *Endocrinology* **1985**, *116*, 855-862.
15. Kato, Y.; Iwamoto, M.; Koile, T.; Suzuki, F. *J. Cell Biol.* **1987**, *104*, 311-319.
16. Lau, K.H.W.; Tanimoto, H.; Baylink, D.J. *Endocrinology* **1988**, *123*, 2858-2867.
17. Davidai, G.; Lee, A.; Schuartz, Y.; Hazum, E. *Am. J. Physiol.* **1992**, *263*, E205-E209.
18. Mountjoy, K.G.; Flier, J.S. *Endocrinology* **1990**, *127*, 2025-2034.
19. Etcheverry, S.B.; Crans, D.C.; Keramidas, A.D.; Cortizo, A.M. *Arch Biochem. Biophys.* **1997**, *338*, 7-14.
20. Fantus, I.G.; Kadota, S.; Deragon, G.; Foster, B.; Posner, B.I. *Biochemistry* **1989**, *28*, 8864-8871.
21. Shisheva, A.; Shechter, Y. *Endocrinology* **1993**, *133*, 1562-1568.
22. Cortizo, A.M.; Sálice V.C.; Vescina, C.M.; Etcheverry, S.B. *Biometals* **1997**, *10*, 127-133.
23. Cortizo, A.M.; Etcheverry, S.B. *Mol. Cell Biochem.* **1995**, *145*, 97-102.
24. Barrio, D.A.; Braziunas, M.D.; Etcheverry, S.B.; Cortizo, A.M. *J. Trace Elements Med. Biol.* **1997**, *11*, 110-115.
25. Crans, D.C.; Bunch, R.L.; Theisen, L.A. *J. Am. Chem. Soc.* **1989**, *111*, 7597-7607.
26. Cortizo, A.M., Sálice, V.C., Etcheverry, S.B. *Biol. Trace Elemen. Res.* **1994**, *41*, 331-339.
27. Vescina, C.M.; Sálice, V.C.; Cortizo, A.M.; Etcheverry, S.B. *Biol. Trace Elemen. Res.* **1996**, *53*, 185-191.
28. Cheatham, B.; Kahn, C.R. *Endocrine Rev.* **1995**, *16*, 117-142.
29. Goldfine, A.B.; Simonson, D.C.; Folli, F.; Patto, M.-E.; Kahn, C.R. *Mol. Cell. Biochem.* **1995**, *153*, 217-231.
30. Sálice, V.C., Cortizo, A.M., Gómez Dumm, C.L., Etcheverry, S.B. *Submitted.*

Downloaded by CORNELL UNIV on October 31, 2012 | http://pubs.acs.org
Publication Date: December 10, 1998 | doi: 10.1021/bk-1998-0711.ch021

Chapter 22

Pharmacology and Toxicology of Oxovanadium Species: Oxovanadium Pharmacology

Downloaded by NORTH CAROLINA STATE UNIV on October 31, 2012 | http://pubs.acs.org
Publication Date: December 10, 1998 | doi: 10.1021/bk-1998-0711.ch022

G. R. Willsky[1], A. B. Goldfine[2], and P. J. Kostyniak[1]

[1]Toxicology Research Center, State University of New York at Buffalo, School of Medicine and Biomedical Sciences, Buffalo, NY 14214
[2]Joslin Diabetes Center, Research Division, Boston, MA 02215

This review covers physiological considerations in the pharmacological use of oxovanadium species as insulin-mimetic and antitumorogenic agents and provides data on the pharmacokinetics of NIDDM patients during oral dosing with vanadyl sulfate. Topics covered are the administration of vanadium to mammals, the determination of vanadium amount and form in cells and tissues, potential physiological effects of decavanadate, pharmacology and toxicology of oxovanadium compounds. Pharmacological factors considered are the interactions of oxovanadium species with cellular oxidation reactions, phosphate metabolism, and metabolic state. Vanadium was determined with graphite furnace atomic absorption spectrophotometer in serum and urine from patients receiving 25 and 50 mg elemental V/day. Using 50 mg V per day the $t_{1/2}$ serum washout was 9.1 ± 3.8 days, with peak serum V values ranging from 49.8 to 125.5 ng/ml with a mean of 82.4 ± 43.2 ng/ml. Clinical details of this study are described by Goldfine, Willsky and Kahn in this volume.

The role of vanadium in biology and chemistry has been the subject of two recent books (1, 2). In addition, papers from a July, 1994, Symposium on Vanadium Compounds has been published as a special volume of Molecular and Cellular Biochemistry (3). This review will try not to repeat information covered in other reviews, but will focus on general points about cellular metabolism of vanadium compounds and the pharmacology and toxicology of vanadium in mammals.

Administration of Oxovanadium Compounds to Mammals

There are various methods to administer oxovanadium compounds to mammals: intravenously, subcutaneously, by mouth or through peritoneal injection. Oxovanadium species of Vanadium (IV) and Vanadium (V) are the most widely used vanadium species in pharmacological experiments. The multiple equilibria governing the distribution of these compounds, their ability to bind to many physiological components, the differing pH of the various physiological fluids and intracellular compartments, the chemical lability of these compounds, and the reduction of

In Vanadium Compounds; Tracey, A., et al.;
ACS Symposium Series; American Chemical Society: Washington, DC, 1998.

vanadium (V) compounds to vanadium (IV) components by cellular components such as glutathione make it difficult to determine what is the active vanadium species in a given experiment. The details of how oxovanadium species are administered using the different methods in mammals has been previously described (4) and is presented by Forrest Nielsen in this volume.

The variability of response of each animal is another problem which must be considered. The study of biological systems introduces much more variety than a simple chemical system. Chemical stability and absorption are major problems (5). If administered by mouth a question to be considered is whether the compound will survive the trip through the gastrointestinal tract, with pH levels dropping to 2 or less. Another factor is the poor absorption of oxovanadium compounds through the gastrointestinal tract. Absorption levels of 1-3% are common in mammals (4). Intravenous, subcutaneous, and peritoneal administration involves placing the oxovanadium compounds in aqueous solutions of approximately pH 7.0. However, there is still be a problem with absorption into cells. In addition, the vanadium compounds in physiological fluids are now in the presence of small metabolites and proteins which bind and metabolize them (4, 6).

The amount of elemental vanadium in the pharmacologically administered vanadium compound must be considered in comparing dosing regimens. When organic chemistry compounds are administered as drugs the pharmacological dose is equivalent to the amount of administered compound. Since the fate of administered oxovanadium species is not know with precision, one should compare the amount of elemental vanadium being administered with different compounds in addition to the amount of total drug. For example, for the simple oxovanadium compounds: vanadyl sulfate ($VOSO_4$) is 31% vanadium, sodium orthovanadate (Na_3VO_4) is 27% vanadium and sodium metavanadate ($NaVO_3$) is 42% vanadium by atomic weight. The slightly more complex insulin-mimetic bis(maltolato)oxovanadium, is only 16% vanadium by weight. Therefore, the actual amount of elemental vanadium administered in a research or clinical study should be used to compare experimental results.

Determination of Vanadium in Cells and Tissues

The pharmacological use of oxovanadium species has lent import to the determination of vanadium in cells and tissues. The amount of vanadium in biological fluids is usually determined using atomic absorption spectrometry (either flame or graphite furnace), neutron activation analysis or inductively coupled plasma atomic emission spectrometry. Care must be taken in sample collection and sample preparation to avoid vanadium contamination. Also, the problems introduced by the biological matrix of the tissue or fluid being studied must be considered. The details of the analytical procedures for the determination of the amount of vanadium in biological materials has been very well described in 1995 by Hans Seiler (7).

In order to understand the mechanism of physiological affects of vanadium it is necessary to also know the oxidation state of vanadium and the oligomeric form of vanadium inside the cell. Although difficult to do in mammalian systems, magnetic resonance spectrometry (^{51}V-NMR or EPR) can be used in isolated cells such as erythrocytes (8) and the eucaryotic microbes *S.cerevisiae* (9). Using EPR vanadium (IV) has been shown to be associated with these cells (8, 9) after exposure to vanadate V(V) in the buffer or growth medium. These techniques can also be used to monitor the binding of oxovanadium species to proteins or small molecules.

Mammalian cells are composed of multiple compartments. In addition to the nucleus and mitochondria major organelles include the endoplasmic reticulum, the golgi and lysosomal vesicle system. Many of these organelles are composed of small vesicular structures which move from one organelle to another. The pH in the cytoplasm of cells is usually about 7.0, while the pH in cellular vesicles can be quite acidic with pH values near 5.0.

Downloaded by NORTH CAROLINA STATE UNIV on October 31, 2012 | http://pubs.acs.org
Publication Date: December 10, 1998 | doi: 10.1021/bk-1998-0711.ch022

Once in serum or other physiological fluids one must consider the fact that oxovanadium compounds will bind to small metabolites such as citrate or succinate. The ability of these bound forms of vanadium to interact with physiological systems is a function of the binding constants for the vanadium and target enzyme and the stability of the oxovanadium-metabolite complex. This can be illustrated by an example involving the eucaryotic microbe *S.cerevisiae*. Yeast are normally sensitive to vanadate in the growth medium (9). Vanadate in the growth medium will bind to EDTA or citrate as seen by ^{51}V-NMR studies. However, only the binding of vanadate with citrate will protect the yeast cell from growth inhibition by vanadate (Willsky, unpublished observations). It appears that the affinity of the vanadate species for the yeast cell surface component is stronger than that of the vanadate for EDTA, but weaker than that of the vanadate for citrate under these conditions.

Vanadium is also known to bind to many proteins in the V(IV) and V(V) state in mammalian systems. In blood V(IV) binds to serum albumin and transferrin, while in tissues it has been shown to bind to ferritin. Vanadium (V) will also bind to ferritin. Vanadium-protein complexes are also formed with many enzymes and calmodulin in mammalian systems. Interactions of vanadium with these and other vanadium-protein interactions has been recently described by N.D. Chasteen (6). The binding of vanadium to proteins will also moderate its pharmacological affect depending on the relative affinity of the oxovanadium species for the protein and it's pharmacological affector.

Potential Physiological Effects of Decavanadate

Decavanadate is a potent inhibitor of the control step in glycolysis, phosphofructokinase 1 (10, 11) and also a noncompetitive inhibitor of the bisphosphatase activity of the 6-phosphofructo-2-kinase/fructose-2.6-bisphosphatase (12) involved in the regulation of glycolysis and gluconeogensis. In addition, decavandate stimulates a 5′ nucleosidase from rat kidney and binds to the G-protein GDP complex mimicking the GTP-bound form of the G protein, allowing signal transduction to occur (13).

In recent years, decavanadate has been shown to interact with more cellular enzymes *in vitro* and to interact with physiological processes in whole cell systems. Decavanadate is a very strong activator of the membrane vanadate-dependent NADH/NADPH oxidation activity (14, and Willsky, unpublished observations). Decavanadate inhibits the binding of inositol (1,4,5)triphosphate to its receptor (15, 16), binds to microtubule-associated proteins which inhibits the assembly of microtubule proteins (17), and is a potent inhibitor of ATP-induced K+ transport pathway (18). Decavanadate is a competitive inhibitor of the substrate kemptide of the cAMP dependent protein kinase (19). Since it is not likely that the negatively charged decavandate binds to the negatively charged active site, it was suggested that the decavandate binds to the kemptide substrate itself. The noradrenaline-mimetic action of decavanadate has been suggested to be due to the similarity of the 2 pairs of unshared O atoms separated by 3.2A that is similar in structure to a form of noradrenaline (20). This hypothesis would explain why V4 and V5 oligomers to not have noradrenylin-mimetic activity.

Using the model system *S.cerevisiae* decavanadate is associated with cells exposed to tetrameric vanadate in the growth medium, but not those exposed to decavanadate in the growth medium (Figure 1). ^{51}V-NMR was used to monitor the type of vanadium present in the original vanadate containing growth medium at pH 4.0 and pH 6.5, the cells after exposure to vanadate for 15 hours, and the growth medium after the cells had been harvested. Decavanadate is present in the original pH 4.0 growth medium and not the pH 6.5 growth medium (Figure 1). However, decavanadate is seen in the cells and growth medium after growth in pH 6.5, and only in the used growth medium at pH 4.0. If vanadate were distributed uniformly across the cell cytoplasm at pH near 7.0, no decavanadate should be seen. The presence of

Downloaded by NORTH CAROLINA STATE UNIV on October 31, 2012 | http://pubs.acs.org
Publication Date: December 10, 1998 | doi: 10.1021/bk-1998-0711.ch022

Downloaded by NORTH CAROLINA STATE UNIV on October 31, 2012 | http://pubs.acs.org
Publication Date: December 10, 1998 | doi: 10.1021/bk-1998-0711.ch022

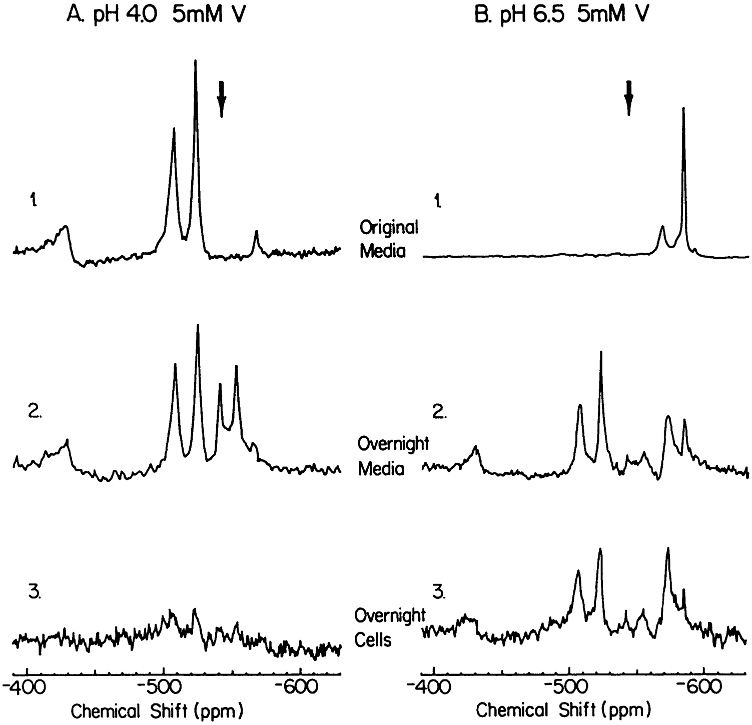

Figure 1. Demonstration of Cell-Associated Decavanadate in *S.cerevisiae* Exposed to Tetrameric Vanadate in the Growth Medium. *S. cerevisiae* strain LL20 was grown in Yeast Nitrogen Base Minimal Medium in the presence of added 5 mM sodium orthovanadate. After 15 hours of incubation, the cells were separated from the medium by centrifugation. Cell and medium samples were analyzed by ^{51}V-NMR as previously described (9). A. Cells grown at pH 4.0. B. Cell grown at pH 6.5. Spectra 1 are from the original media, Spectra 2 are from the overnight media, and Spectra 3 are from the overnight cells. The arrow indicates position of orthovanadate resonance (-541 ppm).

decavanadate in the pH 6.5 growth medium after cell growth is not due to the lowering of the pH of the medium, but appears to be related to the extrusion of decavanadate from the cells. The lack of decavanadate in the cells exposed to pH 4.0 growth medium could be explained by the inability of decavanadate to enter the cells. In EPR studies a vanadyl signal can be seen in both cell samples and is more pronounced in the overnight media from the cells grown at pH 4.0 (data not shown). These results could be explained by the accumulation of vanadate in acidic vesicles as decavanadate.

The concentration of vanadate in cells and vesicles has previously been documented. The concentration of vanadium by marine animals, in particular ascidians is reviewed in this volume by K. Kustin. Tunicates have been shown to concentrate vanadate up to a 1000 fold from sea water. Direct electron-microscopic evidence that vanadium can be found in intracellular vesicles also exits. Experiments with lung macrophages exposed to vanadium compounds and analyzed using Electron Energy Loss Spectroscopy (EELS) or Electron Spectroscopic Imaging (ESI) showed vanadium to be localized in vesicles (21, and personal communication from J. Godleski). However, this technique cannot identify the form of vanadium present in the vesicles. With the growing number of physiological processes known to be affected by decavanadate and the demonstration that decavanadate can be found associated with *S. cerevisiae* cells exposed to tetrameric vanadate (Figure1), the involvement of decavandate in the pharmacological affects of oxovanadium compounds needs to be considered.

Pharmacology of Oxovanadium Species

The overall pharmacology of oxovanadium species has been reviewed in 1996 (22). Oxovanadium compounds are believed to have pharmacological effects due to their interactions with signal transduction phosphorylation and/or their participation in cellular oxidation/reduction reactions including the generation of potential toxic oxygen radicals. The signal transduction pathway is most often invoked in explaining the insulin-mimetic affect, while the oxidation/reduction interaction is used most often in explaining the antitumorogenic properties of vanadium. Various oxovanadium species (vanadate, vanadyl and peroxovanadate) have been used to explore both the insulin-mimetic and anti-carcinogenic properties of vanadium. As previously described, it is not clear what is actual form of oxovanadium that reaches the cells or tissues. Complicating the picture is the fact that how an organism responds to vanadium will be determined by its metabolic state as described below in the insulin-mimetic action of vanadium section. Many of the vanadium compounds being evaluated for pharmacological effects are both insulin-mimetic and antitumorogenic (Table1).

Oxovanadium Interactions with Oxidation/Reduction Reactions. Oxovanadium compounds are known to interact with oxidation/reduction reactions in the cell, which may cause the formation of oxygen radicals. One of the earliest such reaction to be characterized is the plasma membrane vanadate dependent NADH oxidation activity found in both microbial and mammalian plasma membranes which has been studied since the mid 1970's (33). This enzymatic activity is studied over the background non enzymatic vanadate dependent NADH oxidation, can involve the generation of reactive oxygen species and hydrogen peroxide and has been shown to be stimulated by vanadium (V) species of phosphovanadate compounds (34) and decavanadate (14). The superoxide radicals produced in isolated perfused heart by xanthine/xanthineoxidase were quenched by vanadate (35). It is believed that most of the intracellular vanadium is present as V(IV) and vanadium species may be involved as scavengers of oxyradicals (22). The physiological implications of the role of oxovanadium compounds in oxidation/reduction reactions remains to be elucidated.

Downloaded by NORTH CAROLINA STATE UNIV on October 31, 2012 | http://pubs.acs.org
Publication Date: December 10, 1998 | doi: 10.1021/bk-1998-0711.ch022

Downloaded by NORTH CAROLINA STATE UNIV on October 31, 2012 | http://pubs.acs.org
Publication Date: December 10, 1998 | doi: 10.1021/bk-1998-0711.ch022

Table I. Sample Oxovanadium Compounds with Pharmacological Effect

Compound	*Insulin-Mimetic ( ) Reference*	*Anti-Tumorogenic ( ) Reference*
Vanadium (IV)		
vanadyl	+ (23)	+ (24)
vanadocene dichloride	?[c]	+ (25)
bis(maltolato)oxovanadium	+ (26)	+ (27)
bis(cysteine methyl ester)oxovanadium	+ (26)	?
Vanadium (V)		
vanadate	+ (29, 30)	+ (28)
monoperoxovanadate	+ (26, 31)	?
diperoxovanadate[a]	+ (26, 31)	+ (28)
$(NH)_2[OVO(O_2)_2]$[b]	?	+ (25)

[a] Prepared from vanadate and H_2O_2 as described (32).

[b] Prepared as crystalline material as described (25).

[c] Questionmarks (?) represents compounds not yet tested.

Antitumorogenic Effect. The interactions of vanadium V(IV)/V(V) redox potentials with those of iron and hydrogen peroxide has been suggested to be related to the anti tumor activity of oxovandium compounds (25). Vanadyl sulfate was one of the first compounds to be reported to have anti tumor activity (24). Currently, biscyclopentadienyldichloro-V(IV) or vanadocene dichloride is one of the best studied antitumorogenic agents. Recently peroxovanadium compounds, vanadate (28) and BMOV (27) have been shown to have antitumorogenic properties (25). Table 1 shows that all of the antitumorigenic vanadium compounds that have been tested as insulin-mimetics have that property. Peroxocompounds with antitumorigenic properties seem to all have the seven-coordinated V(V) in a distorted pentagonal bipyramid, with the location of the peroxogroup in the pentagonal plane cis to the V=O group (25). The mechanism of these compounds is believed to be different from that of vanadocene dichloride. Clearly more work is needed on the antitumorigenic properties of vanadium compounds.

Insulin Mimetic Action. The insulin-mimetic action of vanadium compounds has been reviewed recently (36, 26, 22). Recent data in the literature has been concerned with the effects of lower levels of feeding on the insulin-mimetic activity. It appears that although reduced feeding could be responsible for some of the insulin-mimetic activity it cannot explain the whole phenomena. Yuen, et al. (37) have shown using STZ diabetic and normal rats in carefully controlled pair feeding and food restriction studies that BMOV exerts insulin-like effects readily discernable from the effects of food restriction. This topic and other animal models for insulin-mimetic action of vanadium is well described in Britchard and Henquin (36). In addition, vanadium treatment has been successfully employed in the insulin resistant db/db mouse model, the genetically obese and somewhat glucose-intolerant fa/fa rats (38), the insulin-deficient streptozotocin-induced diabetes in rat, and the genetic BB rat model. Oxovanadium compounds normalize blood glucose and other physiological parameters altered in the STZ-induced diabetic rat model, but cannot completely alleviate the requirement for insulin in the genetic BB rat model (39). An intriguing effect of oxovanadium treatment of STZ-diabetic rats which has been best studied with vanadyl sulfate is that there is a long term anti diabetic activity after vanadium treatment withdrawal, which has been correlated with increased insulin capacity (40).

Oxovanadium Interactions with Phosphate Metabolism. In considering the pharmacological role of oxovanadium compounds the interaction of vanadium and phosphate chemistry must be considered (41). Cells are usually about 10 mM inorganic phosphate. Since phosphate exists in great excess in cells over vanadium both naturally and after pharmacological administration of vanadium, the potential interactions of the two chemistries are important. Tracy and Gresser have explored the affect of mixed phosphate vanadate compounds on various enzymatic activities (42) and this work has been extended to examine the similarities of the geometries of the effective oxovanadium compounds (13). The plasma membrane vanadate-dependent NADH oxidation activity of yeast plasma membranes has been shown to be stimulated by phosphovanadate complex rather than an oligomeric form of vanadate(34). NADV has been shown to be a cofactor for an alcohol dehydrogenase (43) which could exist in cells given the relative amounts of vanadium and phosphate. Clearly the action of vanadium compounds or phosphovanadium compounds as direct modifiers of metabolic reactions needs to continue to be evaluated.

The effects of oxovanadium compounds on cytosolic signal transduction processes involving protein phosphorylation/and dephosphorylation has been a major area of study concerning the insulin-mimetic action of oxovanadium species. Most of the evidence presented focuses on the action of oxovanadium compounds as inhibitors of tyrosine protein phosphatases (44, 45, 22). The role of protein phosphatases in signal transduction pathways has been recently reviewed by Dixon (46), Denu et al. (47) and Tonks and Neel (48). Protein phosphatases can be complex multi-subunit structures and the protein containing the catalytic domain is usually the first to be isolated. Regulatory protein subunits of some well characterized protein phosphatases may remain to be discovered and could be important in the interaction of vanadium species with these protein complexes. The substrate trapping method of Flint et al. (49) will be very helpful in identifying physiological substrates of protein tyrosine phosphatases and could be extended to other protein phosphatases. Potential protein phosphatases whose inhibition by vanadium compounds may elicit the insulin-mimetic activity have been discussed by Goldfine et al. (50) and Fantus et al. (51) in 1995 and Sekar et al. in 1996 (22). These include the protein whose substrate is the phosphorylated form of the insulin receptor, protein phosphatases involved in the regulation of IRS-1, the cytosolic MAP Kinase system(52), and the dual specificity protein phosphatases such as cdc25 which is involved in cell cycle progression (53).

Crystallographic studies of protein phosphatases (46) have provided evidence concerning the mechanism of action of the tyrosine, serine/threonine, and dual specificity protein phosphatase. The high molecular weight tyrosine protein phosphatases share a universal sequence CXXXXR(S/T) at the active site. The low molecular weight tyrosine protein phosphatases do not share that motif. It is proposed that at pH 7.5 the nucleophilic cysteine (Cys^{12}) forms a covalent bond with vanadate. Recently crystal structures have been obtained of some of these protein phosphatases in the presence of vanadium salts (54) by soaking in the vanadium salt.

Downloaded by NORTH CAROLINA STATE UNIV on October 31, 2012 | http://pubs.acs.org
Publication Date: December 10, 1998 | doi: 10.1021/bk-1998-0711.ch022

However, in order to see the full effect of the oxovanadium salt on the protein phosphatases co-crystallization of the protein and vanadium salt should be carried out. Phosphatase activity may be more widespread in vanadium/protein interactions than originally thought as the active site of the vanadate containing haloperoxidases is conserved in three families of acid phosphatases (55).

Other affects of oxovanadium species on signal transduction pathways and phosphate metabolism need to be examined. If oxovanadium species behaved as a general cytosolic protein phosphatase inhibitors they would not mimic the action of insulin. Nuclear hormone receptors, such as the peroxisome proliferator-activated receptors, are also stimulated by insulin and controlled by phosphorylation (56). Treatment of lymphocyte cell lines with oxovanadium species has also been shown to activate the transcription factor NF-κB (57). Oxovanadium compounds could also affect the function of these or other nuclear proteins. Studies of vanadium stimulation of protein kinase activities in purified systems also adds to our knowledge of how oxovanadium species function in physiological processes. Experiments using partially purified protein kinases are difficult to interpret because these extracts can easily have a very active protein phosphatase present in the same mixture. Oxovanadium compounds could also act as allosteric inhibitors. Recent crystallography studies have led to the proposal that dimerization and active site blockages could be physiologically important in inhibition of protein-tyrosine phosphatases (58). It is possible that the binding of oxovanadium species at sites other than the active site could cause dimerization of protein phosphatases or other proteins of physiological significance. Vanadate treatment of fibroblasts has been show to promote the accumulation of intracellular receptors (59). Oxovanadium compounds could also affect physiological processes by interfering with protein and organelle movement inside cells.

Downloaded by NORTH CAROLINA STATE UNIV on October 31, 2012 | http://pubs.acs.org
Publication Date: December 10, 1998 | doi: 10.1021/bk-1998-0711.ch022

Influence of Metabolic State on the Effect of Oxovanadium Compounds.

In determining the pharmacological effect of oxovandium species it is necessary to consider that the effect of these compounds is altered by the metabolic state of the animal. Oxovanadium compounds clearly affect the diabetic and non-diabetic rat obtained with STZ treatment differently. In experiments with streptozotocin induced diabetic rats treated with oxovanadium species, the data is usually analyzed by a one way ANOVA with multiple means testing and frequently the oxovanadium species is not given to a normal group of animals. Table II shows the affect of various oxovanadium species on streptozotocin-induced diabetes in rats in which data is available for treatment of normal and diabetic animals. The data in this table serves as a survey and is not meant to include all examples. Clearly the pharmacological affects of oxovanadium species are dependent upon the metabolic state of the animal. There are numerous examples in which oxovandium species do not affect the normal animal, but do affect the diabetic animal. If the parameter studied is significantly altered in diabetics compared to normal animals, oxovanadium treatment frequently causes the altered parameter to return towards its normal level. To quantitate this affect the experiments could be analyzed with a two way analysis of variance using both vanadium treatment and diabetes as separate variables. In parameters affected as described above there will be a very significant interaction component found. These results indicate that at least in this animal model there is a different effect of oxovanadium compounds on normal and diabetic animals.

Downloaded by NORTH CAROLINA STATE UNIV on October 31, 2012 | http://pubs.acs.org
Publication Date: December 10, 1998 | doi: 10.1021/bk-1998-0711.ch022

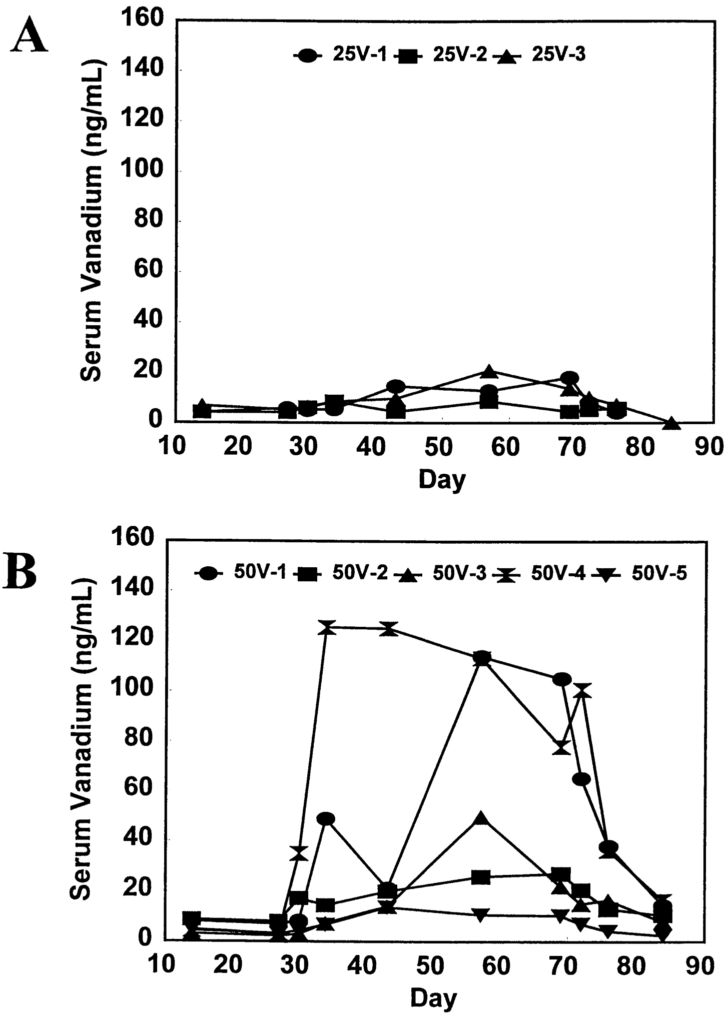

Figure 2. Serum Vanadium Levels in NIDDM Patients After Oral Dosing with Vanadyl Sulfate. A. 25 mg/day elemental vanadium taken as 75 mg of $VOSO_4$ by three patients. B. 50 mg/day elemental vanadium taken as 150 mg $VOSO_4$ by 5 patients. Clinical aspects of the study described by Goldfine et al., this volume.

Downloaded by NORTH CAROLINA STATE UNIV on October 31, 2012 | http://pubs.acs.org
Publication Date: December 10, 1998 | doi: 10.1021/bk-1998-0711.ch022

Table II. Effects of Oxovanadium Compounds on Normal and Diabetic Rats[a]

Oxovanadium Species	*Parameter*	*Effect on Normal (Y/N)*[b]	*Value in Diabetic Compared to Normal*	*Effect on Diabetic (Y/N)*	*Ref.*
Vanadate	Cardiac LVDP	N	↓	Y ↑	30
V(V)	Plasma Glucose	N	↑	Y ↓	60, 61
	Liver Hexose Uptake	Y	↑	Y ↑	29
	Muscle Hexose Uptake	Y	↑	Y ↑	29
	Kidney Sorbitol	N	↑	Y ↓	60
	Liver Albumin	N	↓	Y ↑	61
	Liver Glycogen	N	↓	Y ↑	62
	Liver Phosphorylase Kinase	N	↓	Y ↑	62
	Liver Phosphorylase Phosphatase	N	↑	Y ↑	62
	Liver Protein Kinase	N	↓	Y ↑	62
	RBC Cholesterol	N	↑	Y ↓	63
	RBC Catalase	N	↑	Y ↓	63
	RBC SOD	N	↓	Y ↑	63
Vanadyl	Plasma Glucose	N	↑	Y ↓	23
V(IV)	Plasma Triglyceride	N	↑	Y ↓	23
	Plasma Cholesterol	N	↑	Y ↓	23
	Plasma Creatinine	N	↑	Y ↓	23
	LVDP	N	↓	Y ↑	64, 65
BMOV[b]	Plasma Triglyceride	N	↑	Y ↓	64
	Plasma Cholesterol	N	↑	Y ↓	64
	Plasma Glucose	N	↑	Y ↓	64, 65

[a] Y means yes it has an effect, while N means no it does not have an effect, ↑ indicates increase, while ↓ indicates decrease.

[b] BMOV is bis(maltoalto)oxovanadium(IV), RBC is erythrocyte (red blood cell).

Human Studies. In trying to ascertain the effect of oxovanadium studies in humans it will be helpful to establish whether or not humans react differently to vanadate depending on their metabolic state. Athletes are currently taking oral vanadyl sulfate in the hopes of improving their performance (66). Oral vanadyl sulfate has been shown to be inconclusive in changing body composition in weight-training athletes (39). Recent human studies of vanadate effects on IDDM and NIDDM patients have been reported (67) and vanadyl sulfate has been used in NIDDM and obese subjects (68, 69, 70). Human studies on the insulin-mimetic action of vanadate and vanadyl compound in IDDM and NIDDM patients has been reviewed (36, 22) and are discussed in detail in the chapter by Goldfine et al. in this volume.

Pharmacokinetics of Vanadium in Mammals. Much of the early work with vanadium had dealt with the inhalation route of exposure. Soluble vanadium compounds are generally rapidly cleared from the lung after inhalation exposure in experimental animals (71). Vanadium administered orally as either vanadyl or vanadate is poorly absorbed (4). Upon continuous oral exposure, tissue vanadium levels reached a pleateau at 21 days in the rat (72). Kidney and bone tend to have the highest levels of vanadium after continuous exposure (72, 73). There are indications that the kinetics of vanadium clearance may follow a biphasic exponential decline in experimental animals, with the kidney and skeleton serving as deep compartments (73, 74). Vanadium in the blood can exist in an unbound form initially, and in time is found as a transferrin complex (75, 76, 77). This together with deep tissue compartments may account for the biphasic clearance of vanadium from the blood observed in the rat (77).

The majority of absorbed vanadium is excreted in the urine, although the feces can account for up to10% of the excretion of vanadium administered either IV or IP (77-81). Biliary transport of vanadium is observed after parenteral dosing, and is likely responsible for the fecal elimination (82, 83).

The rate of removal of vanadium from the serum is more rapid than from other tissues following subcutaneous administration of ammonium metavanadate in the mouse (84). Tissue vanadium elimination kinetics appear to be biphasic for blood, kidney, lung and brain, but linear for spleen and thymus. Considerable variability in vanadium measurements occur as the levels approach background for all tissue matrices (84). In another study of both vanadyl and vanadate, first order kinetics of elimination were observed with a kidney half life of 11.7 days in the rat (85). No studies are available indicating whether the kinetic picture is dose dependent.

Serum and urine vanadium concentrations have been used as biomarkers of exposure to vanadium by the inhalation route in the workplace (86, 81). Studies in workers exposed to vanadium report background serum vanadium levels in unexposed workers of approximately 2 ng/ml, the stated detection limit for vanadium, while exposed workers had serum levels up to 37 ng/ml (87). Another study involved the direct exposure of two workers to vanadium pentoxide who had worked with this compound for over 6 months in one case and 4 years in the other. Air concentrations which workers were exposed to ranged from 0.3 to 126 ug/m^3. Urine concentrations of vanadium ranged from the limit of detection of 7 ng/ml to 124 ng/ml (88).

In a study of patients with NIDDM, background levels of vanadium in serum ranged from 10 to 20 ng/mL of serum. Administration of 100 mg vandyl sulfate by mouth as a single acute dose resulted in an increase in serum vanadium which peaked at 8 hours at about 150 ng/ml, followed by a decline to one half of the peak value over 16 hours. The mean data from 3 patients was fit to a single exponential function which had a half-time of 18 hours (70). Serum levels were not followed for longer than 24 hours, and it is not known whether a longer term component of the vanadium decay function in serum would have become apparent. In another study administration of 100 mg/day vanadyl sulfate for 3 weeks to NIDDM patients resulted in plasma vanadium concentrations of 73.3 ± 22.4 ng/ml (68). In one study, 5 IDDM and 5 NIDDM patients were given 125 mg/day sodium metavanadate for 2 weeks. The serum vanadium levels at the end of two weeks were 187.2 ± 28.3 ng/ml for the IDDM and 142.0 ± 40.6 ng/ml for the NIDDM patients. Comparing the results of experiments using vanadate and vanadyl it appears that vanadium is more readily taken up in serum when administered as vanadate.

Pharmacokinetics of Oral Dosing of NIDDM patients with Vanadate Sulfate. The current study was done in collaboration with Drs. Goldfine and Kahn at the Joslin Diabetes Center in Boston, MA. The clinical aspects of this study are discussed in a separate chapter in this volume by Goldfine et al. Seven patients were given an oral placebo for three weeks after one week of observation. This was followed by vanadyl sulfate administered orally at either 25 or 50 mg vanadium per day for six weeks. A two week observation period followed the termination of vanadyl sulfate dosing. Patient blood and urine samples were obtained for vanadium analysis over the 7 week time course at days 14, 26, 30, 32, 42, 56, 68, 72, 75, and 84. Serum and urine vanadium concentrations were determined using graphite furnace atomic absorption spectrophotometry. Figure 2 contains the time courses for serum vanadium concentrations for all patients in this study.

A detailed analysis of the serum vanadium kinetic profile for one patient given the 50 mg/day dose shown in Figure 2A, patient 50V-1 is discussed here. The

Downloaded by NORTH CAROLINA STATE UNIV on October 31, 2012 | http://pubs.acs.org
Publication Date: December 10, 1998 | doi: 10.1021/bk-1998-0711.ch022

Downloaded by NORTH CAROLINA STATE UNIV on October 31, 2012 | http://pubs.acs.org
Publication Date: December 10, 1998 | doi: 10.1021/bk-1998-0711.ch022

background serum vanadium level in the patient prior to vanadyl sulfate administration was 8 ng/ml. The serum vanadium concentration reached a plateau of 114 to 105 ng/ml in approximately 30 days after the start of vanadium administration. The data was analyzed using a first order kinetic model of the type $C = C_0 e^{-kt}$, where C is the serum concentration at any time (t), C_0 is the initial concentration and k is the first order rate constant for elimination of the drug. The model would predict that the approach to steady state with continuous dosing is first order, or $(C_{ss} - C) = C_{ss} e^{-kt}$, such that the achievement of a steady state serum concentration (C_{ss}) would be reached within 5 half-times (89). Thus, the accumulation phase of the serum curve which reaches steady state in 30 days predicts a serum half-time for vanadium of 6 days.

Table III. Summary Vanadium Accumulation in Serum and Urine for NIDDM Patients Given Vanadyl Sulfate

Subject	*Dose (mg V)*	*Weight (kg)*	*Peak Serum V ng/ml*	*Clearance for Serum Vanadium $t_{1/2}$ (days)*	*[V] Urine[a] / [V] Serum*
25V-1	25	76.5	18.2	15.8	4.23
25V-2	25	144.1	8.7	4.2	1.66
25V-3	25	105.0	21.1	8.2	2.7
Mean ± SD		108.53 ± 27.7	16 ± 5.30	9.4 ± 4.81	2.86 ± 1.06
50V-1	50	127.7	113.9	6.14	1.68
50V-2	50	63.1	109.1	14.68	0.243
50V-3	50	79.1	49.8	12.7	0.431
50V-4	50	118.2	125.5	4.85	2.33
50V-5	50	90.9	13.9	7.27	1.67
Mean ± SD		95.8 ± 24.1	82.4 ± 43.2	9.1 ± 3.85	1.3 ± 0.80

[a] The concentration of Vanadium [V] in a 24 hour urine sample obtained after last dose of vanadyl sulfate is compared to the [V] in serum.

Upon termination of vanadyl sulfate dosing, there was an exponential decline in serum vanadium concentration. The half-time calculated from the slope of the decay function was calculated and is shown in Table III. The mean half-time for patients given the 25 mg/day dose was 9.4 days, and that for the patients receiving 50 mg/day was 9.1 days. The range of observed half-times was considerable ranging from 4 to 16 days, which indicates a four-fold inter-individual variation in the decline of serum vanadium.

Peak levels of vanadium in serum and urine were determined. Patients given the 25 mg/day dose of vanadium had a peak serum vanadium concentration ranging from 8.7 to 21 ng/ml. Patients given the higher dose of 50 mg/day had a peak serum vanadium concentration ranging from 14 to 126 ng/ml. Peak urinary vanadium daily excretion in the low and high dose groups were 53 to 162 mcg/day and 77 to 619 mcg/day, respectively. Assuming the patients receiving 50 mg/day are at steady state levels, these data imply that they are absorping 0.15 to 1% of the ingested vanadium.

In comparing these data with other work similar absorption values were found in young men given soluble vanadate salts (90). Peak serum vanadium concentrations in patients receiving 25 mgV per day are similar to serum levels reported in process workers exposed to vanadium pentoxide (91).

The ratio of vanadium concentration in urine to the vanadium concentration in serum for the population receiving the 50 mg/day dose of vanadyl sulfate ranged from 0.43 to 2.33 as indicated in Table III. The half time for serum vanadium in these patients varied inversely with the urine/serum vanadium concentration ratio (R^2=0.97) and also with body weight (R^2 =0.90), see Goldfine et al., in this volume for more information on this study. Data for the fecal elimination of vanadium in these patients was not collected, and would be of interest in future studies.

Toxicology of Vanadium

As an ultratrace element, vanadium appears to have some beneficial effects, with reported deficiency effects including increased thyroid weight with consequent altered response to iodide, decreased erythrocyte glucose-6-phosphate dehydrogenase and cecal carbonic anhydrase (4). Vanadium administered in the vanadyl form is generally considered less toxic than vanadate, possibly owing to a more rapid clearance of injected vanadyl, and its propensity to form a relatively stable transferrin complex (92).

The acute oral LD50 for $NaVO_3$ is 41mg V/kg in the rat, and 31mg V/kg in the mouse. Vanadyl sulfate is generally less acutely toxic having oral LD50s of 90 and 94 mg V/kg in the rat and mouse, respectively. The major signs of toxicity in acutely poisoned animals included irregular respiration, diarrhea, ataxia, and paralysis of the hind limbs. Surviving animals indicated that the signs of intoxication were reversible within 48 hours (93). Subcutaneous administration of 5 to 80 mg/Kg ammonium metavanadate in the mouse produced effects on the nervous system including convulsions, ataxia, and paralysis of the hind limbs. The threshold dose for mortality was approximately 20 mg V/kg (94). An acutely lethal dose of ammonium metavanadate in the sheep was found to be 40 mg V/kg, with deaths occurring within 3 to 4 days. At doses of 9.6 to 12 mg V/kg per day there was a decrease in feed consumption. Pathological findings in animals exposed at the higher doses included intestinal hemorrhages, renal sub-capsular hemorrhages, and fatty degeneration of the liver (95).

Animal studies of varying duration have shown multiple organ system involvement including renal, hepatic, gastrointestinal, hematological, and cardiovascular effects (96, 97). In the streptozotocin induced diabetic rat, vanadyl sulphate ($VOSO_4$) dosing for 39 days resulted in accumulation of vanadium primarily in the bone, kidney, spleen and liver, and while it prevented the manifestation of diabetes-induced renal lesions, it did not prevent impaired growth in diabetic animals (98). Both vanadyl and vanadate administration for 28 days in the drinking water in the streptozotocin induced diabetic rat can reduce food and water intake and lead to serious toxic effects including decreased weight gain, increased biomarkers of renal damage, and death. The drinking water concentrations of the vanadium compounds in this study were in the range of 0.15 to 0.31 mg/ml for sodium metavanadate and vanadyl sulphate pentahydrate, respectively (99). Rats with vanadium exposure in the drinking water for from 2 to 8 weeks at a dose of 23 to 29 mg/kg in the form of ammonium metavanadate showed reduced food and water intake, and exhibited diarrhea, reduced body weight, and effects on erythropoesis and maturation of red cells, as evidenced by reduced erythrocyte count and hemoglobin level, and increased reticulocytes in peripheral blood (100). The intragastric administration of 0.03 mmol Na_3VO_4/kg per day for 14 days decreased myocardial contractile force in the rat myocardium, with an increase in calcium content when compared to controls (101).

Vanadate is acutely toxic in the rat isolated perfused liver model causing release of liver enzymes, depletion of hepatic glutathione, and release of indicators of oxidative damage (102). Exposures in the rat to drinking water containing 40 to 60 ppm vanadium as sodium metavanadate caused a depletion in total lung collagen, and a dose dependent increase of insoluble or cross-linked collagen (103). The mechanism by which vanadium causes oxidative damage is a fruitful area for future investigations.

Downloaded by NORTH CAROLINA STATE UNIV on October 31, 2012 | http://pubs.acs.org
Publication Date: December 10, 1998 | doi: 10.1021/bk-1998-0711.ch022

A variety of vanadium compounds have been tested for genotoxicity in a number of bacterial systems, as well as mouse and human cell lines. Vanadium pentoxide, vanadyl sulfate and sodium metavanadate are all positive in several genotoxic assays, and they do not require metabolic activation (96, 104). Vanadium may be classified as a weak mutagen, which has marked mitogenic activity, with no definitive data as to cacinogenicity (105). Reproductive toxicity has been assessed in male rats dosed 64 days prior to mating with sodium metavanadate in drinking water. Sperm counts were decreased with no effects on sperm motility at 0.2 to 0.4 mg/ml of drinking water, but no reduction in fertility was observed (106). Studies in the rat show vanadium transport across the placenta, and exposure to the neonate can occur via the milk (107). Vanadium pentoxide administered to pregnant mice alters fetal growth and increases the incidence of fetal malformations (108).

Controlled human exposures have resulted in gastrointestinal complaints of cramps and diarrhea. A distinctive green coloration of the tongue has been reported in a number of subjects when vanadium was administered chronically over 5 months at doses in the 13.5 to 22.5 mg/day range (109, 110). Lesser doses given to humans 4.5 to 9 mg V/day for up to 16 months and 13.5 mg V/day for up to 6 weeks were well tolerated without reported adverse effects (4).

Vanadium is used as a dietary supplement and has gained favor among body builders. It is readily available over the counter. When used by athletes as a dietary supplement, oral vanadyl sulfate had no favorable anabolic effects, and was reported by some individuals to enhance tiredness both during and after intensive training (111).

Inhalation exposures to vanadium pentoxide fume has been reported in boilermakers performing welding and cutting tasks in confined spaces with poor ventilation. A vanadium induced bronchitis has developed in scores of exposed workers. Symptoms consist of severe respiratory tract irritation, productive cough, sore throat, dyspnea on exertion, and chest pain and discomfort. This syndrome is common to oil fired boiler work, owing to the presence of up to 40% vanadium in oil fly ash (112, 113). Pulmonary function tests indicate changes in respiratory function can occur rapidly during exposure to fly ash containing up to 15% vanadium, but these effects were reversible within five days (114).

In human studies of NIDDM, vanadyl sulfate (100 mg/day for 3 weeks) treated patients experienced mild gastrointestinal symptoms including nausea, diarrhea, abdominal cramps, and dark discoloration of the stool (68). Sodium metavanadate at a dose of 125 mg/day for 2 weeks caused gastrointestinal effects including vomiting, mild diarrhea, and increased salivation (67).

As with other metals, adverse effects may be minimized through the administration of the metal as a chelate. This approach has been studied in the rat where positive effects on vanadium accumulation and excretion have been reported (97, 115). The value of this approach in treating NIDDM is another fruitful area of investigation for future research.

Perspectives

Oxovanadium species show promise alleviating the symptoms of Diabetes and as anti-tumorogenic agents. In order to ascertain the mechanism of action of these compounds, all known interactions of oxovanadium species with physiological processes should be explored. Oxovanadium species are usually considered interacting with phosphorylation/dephosphorylation signal transduction processes as inhibitors of tyrosine protein phosphatases. Other sites of action of vanadium compounds may also be involved. Interactions of oxovanadium species with enzymes of specific pathways such as glycolysis need to be considered, as well as the effect of metabolic state on the pharmacology of the administered oxovanadium species. Consideration must also be given to what form of vanadium arrives in the cell. Evidence is accumulating that dimer, tetramer and decavanadate species can be found cell-associated after treatment with tetrameric vanadate. Vanadium

Downloaded by NORTH CAROLINA STATE UNIV on October 31, 2012 | http://pubs.acs.org
Publication Date: December 10, 1998 | doi: 10.1021/bk-1998-0711.ch022

oligomerization reactions in cells may also be involved in the specificity of the administered compounds. Chemical considerations, physiological absorption, and binding to components in physiological fluids can all effect the efficacy of the administered oxovanadium species. In addition, toxicological considerations of the administered form of oxovanadium must be carefully monitored. The pharmacological effect of oxovanadium species will probably be found to be the result of multiple mechanisms of action.

Acknowledgments

The authors wish to thank M. Pazik, A. Salloum, E. Johns, and M. Most for experimental technical assistance, and A. Grys for technical assistance in preparing this manuscript. Support for this work came from a Multidisciplinary Grant from SUNY at Buffalo, Buffalo NY, an NIH grant, the Joslin Diabetes Center and the Brigham and Women's Hospital in Boston, MA.

Downloaded by NORTH CAROLINA STATE UNIV on October 31, 2012 | http://pubs.acs.org
Publication Date: December 10, 1998 | doi: 10.1021/bk-1998-0711.ch022

References

1. *Vanadium in Biological Systems;* Chasteen, N.D., Ed.; Kluwar Academic Publishers: Boston, 1990.
2. *Vanadium and its Role in Life;* Sigel, H. and Sigel, A. Eds.; Metal Ions in Biological Systems; Marcel Dekker: New York, NY, 1995; Vol. 31.
3. Vanadium Compounds: Biochemical and Therapeutic Applications, Srivastava, A.K and Chiasson, J.-L., Eds. Kluwer Academic Publishers, Dordrecht, The Netherlands, Volume 153, 1995.
4. Nielson, F.H. In *Vanadium and Its Role in Life;* Sigel, H. and Sigel, A., Eds.; Metal Ions in Biological Systems; Marcel Dekker: New York, NY, 1995; Vol. 31, pp. 543-573.
5. Kustin, K.; Robinson, W.E.; In *Vanadium and Its Role in Life;* Sigel, H. and Sigel, A., Eds.; Metal Ions in Biological Systems; Marcel Dekker: New York, NY, 1995; Vol. 31, pp. 511-542.
6. Chasteen, N.D.; In *Vanadium and Its Role in Life;* Sigel, H. and Sigel, A., Eds.; Metal Ions in Biological Systems; Marcel Dekker: New York, NY, 1995; Vol. 31; pp. 231-247.
7. Seiler, H.G.; In *Vanadium and Its Role in Life;* Sigel, H. and Sigel, A., Eds.; Metal Ions in Biological Systems; Marcel Dekker: New York, NY, 1995; Vol. 31, pp. 671-688.
8. Degani, H.; Gochin, M.; Karlish, S.J.D.; Shechter, Y. *Biochemistry* **1981,** *20,* pp. 5795-5799.
9. Willsky, G.W; White, D.A.; McCabe, B.C. *J. Biolog. Chem.* **1985,** *259,* pp. 13273-13281.
10. Willsky, G.R.; In *Vanadium in Biological Systems*; Chasteen, N.D., Ed.; Kluwar Academic Publishers: Boston, 1990, pp. 1-21.
11. Chaote, G.; and Mansour, T.E. *J. Biolog. Chem.* **1979,** *254,* pp. 11457-11462.
12. Kountz, P.D; McCain, R.W.; El-Maghrabi, M.R.; and Pilkis, S.J. *Archiv. of Biochem. Biophys.* **1986,** *251,* pp. 104-113.
13. Stankiewizc and Tracey; In *Vanadium and Its Role in Life;* Sigel, H. and Sigel, A., Eds.; Metal Ions in Biological Systems; Marcel Dekker: New York, NY, 1995; Vol. 31; pp. 287-324.
14. Kalyani, P.; Ramasarma, T. *Molec. Cell. Biochem.* **1993,** *121,* pp. 21-29.
15. Mochizuki-Oda, N.; Nakajima, Y.; Nakasanishi, S.; Ito, S. *J. Biolog. Chem.* **1994,** *269,* pp. 9651-9658.
16. Coquil, J.F.; Mauger, J.P.; Claret, M. *J. Biolog. Chem.* **1996,** *271,* pp. 3568-3574.
17. Lobert, S.; Isern, N.; Hennington, B.S.; Correia, J.J. *Biochemistry* **1994,** *33,* pp. 6244-6252.
18. Manon, S.; and Guerin, M. *Biochim. Biophys. Acta* **1997,** *1318,* pp. 317-21.

19. Pluskey, S.; Mahroof-Tahir, M.; Crans, D.C.; Lawrence, D.S. *Biochem J.* **1997,** *321,* pp. 333-339.
20. Ramasarma, T. *Molec. Cel. Biochem.* **1997,** *169,* pp. 27-36.
21. Hatch, H.; Stearns, R.C.; Katler, M.; and Godleski, J.J.; In *Proc. 51rst Annual Meeting of the Microscopy Society of America;* Bailey G.W. and Rieder, C.L., Eds.; San Francisco Press, Inc.: San Francisco, CA, 1993, pp. 286-287.
22. Sekar, N.; Li, J.; Shechter, Y. *Crit. Rev. in Biochem and Molec. Biol.* **1996,** *31,* pp. 339-359.
23. Ramanadham, S.; Mongold, J.J.; Brownsey, R.W.; Cros, G.H.; and McNeill, J.H. *Am. J. Physiol.* **1989,** *257 Heart Circ. Physiol.* **1989,** *26,* pp. H904-H911.
24. Thompson, H.J; Chasteen, N.D.; and Meeker, L.D. *Carcinogenesis* **1984,** *6,* pp. 849-851.
25. Djordjevic, C. In *Vanadium and Its Role in Life;* Sigel, H. and Sigel, A., Eds.; Metal Ions in Biological Systems; Marcel Dekker: New York, NY, 1995, Vol. 31, pp. 595-616.
26. Orvig, C.; Thompson, K.H.; Battell,M; and McNeill, J.H.; In *Vanadium and Its Role in Life;* Sigel, H. and Sigel, A. Eds.; Metal Ions in Biological Systems; Marcel Dekker: New York, NY, 1995; Vol. 31, pp. 576-593.
27. Jackson, J.K.; Min,W.; Cruz, T.F.; Cindric, S.; Arsenault, L; Von Hoff, D.D.; Degan, D.; Hunter, W.L.; and Burt, H.M. *Br. J. of Cancer* **1997,** *75(7),* pp. 1014-1020.
28. Cruz,T.F.; Morgan, A.; Min, W. *Mol. Cell. .Biochem.* **1995,** *153,* pp. 161-166.
29. Meyerovitch, J.; Farfel, Z.; Sack, J.; and Shechter, Y. *J. Biolog. Chem.* **1987,** *262,* pp. 6658-6662.
30. Heyliger, C.E.; Tahiliani, A.G.; and McNeill, J.H. *Science* **1985,** *227,* pp. 1474-1478.
31. Shaver, A.; Ng, J.B.; Hall, D.A.; and Posner, P.I. *Mol. Cell. Biochem.* **1995,** *153,* pp. 5-15.
32. Kadota, S.; Fantus, I.G.; Deragon, G.; Guyda, H.J.; Hersh, B.; and Posner, B.I. *Biochem. Biophys. Res. Commun.* **1987,** *147,* pp. 259-266.
33. Liochev, I.S.; Fridovich, I. *Arch. Biochem. Biophys.* **1990,** *279,* pp. 1-7.
34. Minasi, L.-A.; Willsky, G.R. *J. Bacteriol.* **1991,** *173,* pp. 834-841.
35. Matubara, T.; Marcu, S.M.; Misr, P.H.; Dhalla, N.S. *Mol. Cell. Biochem.* **1995,** *153,* pp. 79-85.
36. Brichard, S.M.; Henquin, J.-C. *Trends in Pharacol. Science* **1995,** *16,* pp. 265-270.
37. Yuen, V.G.; Orvig, C.; McNeill, J.H. *Am. J. Physiol. (Endocrinol. Metab.)* **1997,** *35,* pp. E30-E35.
38. Yuen, V.G.; Pederson, R.A.; Dai, S.; Orvig,C.; McNeill, J.H. *Can. J. Physio. Pharmacol.* **1996,** *74,* pp. 1001-1009.
39. Battell, M.L; Yuen, V.G.; and McNeill, J.H. *Pharmacol. Commun.* **1992,** *1,* pp. 291-301.
40. Cros, G.H.; Cam, M.C.; Serrano, J.-J.; Ribes, G.; McNeill, J.H. *Mol. Cell. Biochem.* **1995,** *153,* pp. 191-195.
41. Crans, D.C.; In *Vanadium and Its Role in Life;* Sigel, H. and Sigel, A., Eds.; Metal Ions in Biological Systems; Marcel Dekker: New York, NY, 1995; Vol. 31, pp. 147-209.
42. Gresser, M.J.; Tracey, A.S.; Parkinson, K.M. *J.Am. Chem. Soc.* **1986,** *108,* pp. 6229-6234.
43. Crans, D.C; Marshman, R.W.; Nielsen, R.; Felty, I. *J. of Org. Chem.* **1993,** *58,* pp. 2244-2252.
44. Gresser, M.J.; Tracey, A.S.; and Stankiewicz, P.J. *Adv. Prot Phosphatases.* **1987,** *4,* pp, 35-57.

Downloaded by NORTH CAROLINA STATE UNIV on October 31, 2012 | http://pubs.acs.org
Publication Date: December 10, 1998 | doi: 10.1021/bk-1998-0711.ch022

45. Huyer, G.; Liu, S.; Kelleu, J.; Moffat, J.; Payette, P., Kennedy, B.; Tsaprailis, G.; Gresser, M.J.; and Ramachandran, C.; *J. Biolog. Chem.* **1997.** *272,* pp 843-851.
46. Dixon, J.E. *Rec. Prog. in Horm. Res.* **1996,** *51,* pp. 405-415.
47. Denu, J.M.; Stuckey, J.A.; Saper, M.A.; and Dixon, J. *Cell* **1996,** *87,* pp. 361-364.
48. Tonks, N.K.; Neel, B.G. *Cell, **1996,** 87,* pp. 365-368.
49. Flint, A.J.; Tiganis, T.; Barford, D.; Tonks, N.K. *Proc. Natl. Acad. Sci.USA* **1997,** *94,* pp. 1680-1685.
50. Goldfine,A.B.; Simonson, D.C.; Folli F.; Patti, M.-E.; Kahn, C.R. *Mol. Cell. Biochem.* **1995,** *153,* pp. 217-231.
51. Fantus, I.G.; Deragon, G.; Lai, R.; Tang, S. *Mol. Cell. Biochem.* **1995,** *153,* pp. 103-112.
52. Pandey, S.K.; Chiasson, J.-L.; and Srivastava, A.K. *Mol. Cell. Biochem.* **1995,** *153,* pp. 69-78.
53. Draetta, G.; Eckstein, J. *Biochim. Biophysica Acta* **1997,** *1332(2),* pp. M53-63.
54. Zhang, M.; Zhou, M.; Van Etten, R.L.; Staufgfacher, C.V. *Biochemistry* **1997,** *36,* pp. 15-23.
55. Hemrika, W.; Renirie, R.; Dekker, H.L.; Barnett, P.; Wever, R. *Proc. Natl. Acad. Sci. USA* **1997,** *94,* pp. 2145-2149.
56. Shalev, A.; Siegrist-Kaiser, C.A.; Yen, P.M.; Wahli, W.; Burger, A.G.; Chin, W.W.; and Meier, C.A. *Endocrinology,* **1996,***137* , pp. 4499-4502.
57. Krejsa, C.M.; Nadler, S.G.; Esselstyn, J.M.; Kavanagh, T.J.; Ledbetter, J.A.; and Schieven, G.L. *J. Biolog. Chem.* **1997,** *272,* pp. 11541-11549.
58. Bilwes, A.M.; den Hertog, J.; Hunter, T.; and Noel, J.P.; *Nature,* **1996,** *382,* pp 555-559.
59. Fantus, G.I.; George, R.; Tang, S.; Chong, P.; and Poznansky, M.J. *Diabetes, 1996, 45,* pp 1084-1093.
60. Lohr, J.W.; Bennett, M.I; Pochal, M.A.; McReynolds, J.; Acara, M.; and Willsky, G.R. *Res. Comm. in Chem. Path. and Pharm.* **1991,** *71,* pp. 191-202.
61. Barrera-Hernandez, G.; Wanke, I.E.; and Wong, N.C.W. *Diabetes* **1996**, *45,* pp. 1217-1222.
62. Pugazhenthi, S.; Khandelwal, R.L. *Diabetes* **1990,** *39,* pp. 821-827.
63. Sekar, N.; Kanthasamy, A.; William, S.; Balasubramaniuan, N.; and Govindasamy, S. *Acta Diabetol. Lat.* **1990,** *27,* pp. 285-293.
64. Yuen, V.G.; OLrvig, C.; Thompson, K.H.; and NcNeill, J.H. *Can.J. Physiol. Pharmacol.* **1993**, *71,* pp. 263-269.
65. Yuen, V.G.; OLrvig, C.; Thompson, K.H.; and NcNeill, J.H. *Can.J. Physiol. Pharmacol.* **1993**, *71,* pp. 270-276.
66. Fawcett, J.P.; Farquahr, S.J.; Walker, R.J.; Thou, T.; Lowe, G.; Goulding A. *Inter. J. of Sport Nutr.* **1996,** *6,* pp. 382-390.
67. Goldfine, A.B.; Simonson, D.C.; Folli, F.; Patti, M.-E.; and Kahn, C.R. *J. Clin. Endocrinol. Metab.* **1995,** *80,* pp. 3311-3320.
68. Cohen, N.; Halberstam, M.; Shlimovich, P.; Chang, C.J.; Shamoon, H.; Rosetti, L. *J. Clin. Invest.* **1995,** *95,* pp. 2501-2509.
69. Halberstam, M.; Cohen, N.; Shlimovich, P.; Rossetti, L.; and Shamoon, H. *Diabetes* **1996,** *45,* pp. 659-666.
70. Boden, G.; Chen, S.; Ruiz, J.; van Rossum, G.D.V.; and Turco, S. *Metabolism (*P18) **1996,** *45,* pp. 1130-1135.
71. Orris, P.; Cone, J.; McQuilkin, S. Health Hazard Evaluation Report HETA 80-096-1359; Eureka Company: Bloomington, IL. Washington, D.C.: U.S. Department of Health and Human Services, National Institute of Occupational Safety and Health, 1983; NTIS-PB85-163574.
72. Conklin, A.W.; Skinner,.C.S.; Felten, T.L., et. al. *Toxicol. Lett.* **1982,** *11,* pp. 199-203.

Downloaded by NORTH CAROLINA STATE UNIV on October 31, 2012 | http://pubs.acs.org
Publication Date: December 10, 1998 | doi: 10.1021/bk-1998-0711.ch022

73. Roshchin, A.V.; Ordzhonikidze, E.K.; Shalganova, I.V. *J. Hyg. Epidemiol. Microbiol. Immunol.* **1980,** *24,* pp. 377-383.
74. Edel, J.; Pietra, R.; Sabbioni, E., et al. *Chemosphere* **1984,** *13,* pp. 87-93.
75. Bruech, M.; Quintanilla, M.E.; Legrum, W., et al. *Toxicology* **1984,** *31,* pp. 283-295.
76. Harris, W.R.; Friedman, S.B.; Silberman, D. *J. Inorg. Biochem.* **1984,** *20,* pp. 157-169.
77. Sabbioni, E.; Marafante, E. *Bioinorg. Chem.* **1978,** *9,* pp. 389-408.
78. Kent, N.L.; and McCance, R.A. *Biochem. J.* **1941,** *35,* pp. 387.
79. Hopkins, Jr., L.L.; Tilton, B.E. *Am. J. Physiol.* **1966,** *211,* pp. 169.
80. Hansard, II, S.L.; Ammerman, C.B.; Henry, P.R.; and Patterson, B.W. *J. Anim. Sci.* **1986,** *62,* pp. 804.
81. Wiegmann, T.B.; Day, H.D.; and Patak, R.V. *J. Toxicol. Environ. Health.* **1982,** *10,* pp. 233.
82. Marafante, E.; Pietra, R.; Rade-Edel, J.; and Sabbioni, E. *CEP Consult Ltd.* **1981,** pp. 498ff.
83. Byrne, A.R. and Kosta, L. *Sci. Tot. Environ.* **1978,** *10,* pp. 17.
84. Al-Bayati, M.A.; Culbertson, M.R.; Schreider, J.P.; Rosenblatt, L.S.; Raabe, O.G. *J. Envir. Path. Tox. Oncol.* **1992,** *11(2),* pp. 83-91.
85. Ramanadham, S.; Heyliger, C.; Gresser, M.; Tracey, A.; McNeill, J. *Biol. Trace Element Res.* **1991,** *30,* pp. 119-124.
86. Parker, R.D.; Sharma, R.P. *J. Environ. Pathol. Toxicol.* **1978,** *2,* pp. 235-245.
87. Missenard, C.; Hansen, G.; Kutter, D.; and Kremer, A. *British J. Indust. Medicine* **1989,** *46,* pp. 744-747.
88. Kawai, T.; Seiji, K.; Watanabe, T.; Nakatsuka, H.; Ikeda, M. *Int. Arch. Occup. Environ. Health.* **1989,** *61,* pp. 283-287.
89. Kostyniak, P.J. In Pharmacokinetics, Textbook of Pharmacology; Smith, C.M., Reynard, A.M., Eds.; W.B. Saunders Co.: Philadelphia, PA, 1992, pp. 59-71.
90. Cuman, G.L. et al. *J. Clin. Invest.* **1959,** *38,* pp. 1251-61.
91. Kiviluoto, M.; Pyy, L.; Pakarinen, A. *Int. Arch. Occup. Environ. Health.* **1981b,** *48,* pp. 251-256.
92. Harris, W.R.; Friedman, S.B.; and Silberman, D. *J. Inorg. Biochem.* **1984,** *20,* pp. 157-169.
93. Llobet, J.M.; and Domingo, J.L. *Toxicol. Lett.* **1984,** *23,* pp. 227-231.
94. Wei, C.; Bayati, M.A.; Culbertson, M.R.; Rosenblatt, L.S.; and Hansen, L.D. *J. Toxicol. Environ. Health* **1982,** *10,* pp. 673-687.
95. Hansard, S.L.; Ammerman, C.B.; Henry, P.R.; and Simpson, C.F. *J. Animal Science* **1982,** *55,* pp. 344-349.
96. ATSDR Toxicological Profile for Vanadium, U.S. Public Health Service **1992,** pp. 1-106.
97. Domingo, J.L., et al. *Mol. Cell. Biochem.* **1995,** *153,* pp. 233-240.
98. Mongold, J.J.; Cros, G.H.; Vian, L.; Tep, A. et al. *Pharmacol. & Toxicol.* **1990,** *67,* pp. 192-198.
99. Domingo, J.L.; Gomez, M.; Llobet, J.M.; Corbella, J.; and Keen, C.L. *Pharm. and Toxicology* **1991,** *68,* pp. 249-253.
100. Zaporowska, H.; and Wasilewski, W. *Comp. Biochem. Physio.* **1989,** *93,* pp. 175-180.
101. Pytkowski, B.; and Jagodzinska-Hamann, L. *Toxicol. Lett.* **1996,** *84,* pp. 167-173.
102. Younes, M.; and Strubelt, O. *Toxicology* **1991,** *66,* pp. 63-74.
103. Kowalska, M. *Toxicol. Lett.* **1989,** *47,* pp. 185-190.
104. Owusu-Yaw, J. *Toxicol. Lett.* **1990,** *50,* pp. 327-336.
105. Leonard, A; and Gerber, G.B. *Mutation Reserarch* **1994,** *317,* pp. 81-88.
106. Llobet, J.M.; Colomina, M.T.; Sirvent, J.J.; Domingo, J.L.; and Corbella, J. *Toxicology* **1993,** *80,* pp. 199-206.
107. Edel, J.; and Sabbioni, E. *Biol. Trace Element Res.* **1989,** *22,* pp. 265-275.

Downloaded by NORTH CAROLINA STATE UNIV on October 31, 2012 | http://pubs.acs.org
Publication Date: December 10, 1998 | doi: 10.1021/bk-1998-0711.ch022

108. Altimirano, M.A.; Roldan, E.; and Alvarez, L. *Biol. Reprod.* **1991,** *44,* pp. 133-140.
109. Dimond, E.G.; Caravaca, J.; and Benchimol, A. *J. Clin. Nutr.* **1963,** *12,* pp. 49-53.
110. Uthus, E.O.; and Seaborn, C.D. *J. Nutr.* **1996,** *126,* 2452s-2459s.
111. Fawcett, J.P., et al. *International J. Sport Nutr.* **1996,** *6,* pp. 382-390.
112. Levy, B.S.; Hoffman, L.; and Gottsegen, S. *J. Occupational Med.* **1984,** *26,* pp. 567-570.
113. Sjoberg, S.G. *Arch. Ind. Health* **1955,** *11,* pp. 505-512.
114. Lees, R.E.M. *Brit. J. Indust. Med.* **1980,** *37,* pp. 253-256.
115. Gomez, M., et al. *J. Applied Toxicol.* **1991,** *11,* pp. 195-198.

Downloaded by NORTH CAROLINA STATE UNIV on October 31, 2012 | http://pubs.acs.org
Publication Date: December 10, 1998 | doi: 10.1021/bk-1998-0711.ch022

Downloaded by CORNELL UNIV on October 31, 2012 | http://pubs.acs.org
Publication Date: December 10, 1998 | doi: 10.1021/bk-1998-0711.ch023

Chapter 23

The Nutritional Essentiality and Physiological Metabolism of Vanadium in Higher Animals

Forrest H. Nielsen

Grand Forks Human Nutrition Research Center, Agricultural Research Service, U.S. Department of Agriculture, Grand Forks, ND 58202

In vitro, pharmacological, and lower life form findings have stimulated speculations about the nutritional importance of vanadium. Between 1971 and 1985 several research groups described possible signs of vanadium deficiency for some animals. However, it was difficult to determine whether the changes caused by vanadium deprivation in these early experiments, which used questionable diets, were true deficiency signs, or manifestations of a pharmacological action of vanadium. Since 1985, studies with goats and rats apparently have found true responses to low intakes of vanadium. Responses of goats fed a vanadium-deficient diet included skeletal deformations and death within 90 days of birth. In rats, vanadium deprivation affected changes in thyroid weight and plasma thyroxine and triiodothyronine concentrations caused by feeding deficient or luxuriant iodine. Vanadium deprivation also depressed the activity of pancreatic amylase, and affected serum lactate dehydrogenase in an opposite manner when dietary iodine was deficient than when it was luxuriant. These findings indicate physiological amounts of vanadium affect thyroid hormone and carbohydrate metabolism, and when combined with the knowledge that homeostatic mechanisms exist for vanadium, and that vanadium has functional roles in lower forms of life, provide circumstantial evidence that vanadium is an essential element for higher forms of life. A daily dietary intake of 10 μg of vanadium probably will meet any postulated vanadium requirements of humans.

Since the turn of the nineteenth century, when some French physicians suggested vanadium was a panacea for human disorders (*1,2*), vanadium has been proposed numerous times to be of pharmacological or nutritional importance. Through the years, enthusiasm has risen and fallen for the possible use of vanadium as a pharmaceutical for such things as treating syphilis (*3*), reducing serum cholesterol (*4,5*), and preventing caries (*6*). Currently, attempts are being made to create a pharmaceutical that can safely take advantage of its insulin mimetic properties (*7*). However, the thought that vanadium salts might be useful as antidiabetic agents is not

In Vanadium Compounds; Tracey, A., et al.;
ACS Symposium Series; American Chemical Society: Washington, DC, 1998.

new; this thought existed 100 years ago (*1*). The hypothesis that vanadium has a physiological or essential role in higher animals including humans has gone through periods where it has received much credence then followed by much skepticism. In 1931 it was found that vanadium was superior to copper as a dietary supplement with an incompletely effective dose of iron in alleviating anemia caused by feeding a milk diet to rats; vanadium also improved growth of the rats (*8,9*). Apparently because other elements in addition to vanadium had similar effects, these findings neither stimulated further research nor resulted in the acceptance of vanadium as an essential element. In 1949, Rygh (*10*) suggested that vanadium may be nutritionally important because it stimulated the mineralization of bones and teeth in rats and guinea pigs. However, almost 20 years later, Schroeder and coworkers (*11*) stated that, although vanadium behaves like an essential trace metal, final proof of essentiality for mammals was still lacking. Findings reported between 1971 and 1974 by four different research groups led many to conclude that vanadium is an essential nutrient. In a 1974 review of those findings, Hopkins and Mohr (*12*) stated "we are secure in the concept that vanadium is an essential nutrient." However, in a review 11 years later (*13*) a convincing argument was presented for the judgement that the evidence for the nutritional essentiality of vanadium was still inconclusive. The argument was that the findings accepted as evidence for vanadium essentiality were mostly manifestations of high vanadium supplements that had pharmacological actions in animals fed nutritionally unbalanced diets. Because vanadium can not fulfill all current criteria for essentiality, its nutritional importance for higher animals is being questioned even though some recent convincing circumstantial evidence for essentiality has appeared. In 1963, Schroeder and coworkers (*11*) stated "no other trace metal has so long had so many supposed biological activities without having been proved to be essential;" that statement still could be made today.

Downloaded by CORNELL UNIV on October 31, 2012 | http://pubs.acs.org
Publication Date: December 10, 1998 | doi: 10.1021/bk-1998-0711.ch023

Criteria Used to Establish Essentiality

In the 1960s and 1970s, criteria (*14-18*) were developed to establish essentiality of mineral elements that could not be fed low enough to cause death or to interrupt the life cycle; they usually included the following: 1) The element must react with biological material or form chelates. 2) The element must be ubiquitous in sea water and earth's crust. In other words, it had to be present during the evolution of organisms so it could be incorporated when essential functions developed which required the element. 3) The element must be present in significant quantity in animals. 4) The element should be toxic to animals only at relatively high intakes in comparison to nutritional intakes. 5) Homeostatic mechanisms must exist for the element so that it is maintained in the body in a rather consistent amount during short term variations in intake. 6) Finally, and most importantly, a dietary deficiency must consistently and adversely change a biological function from optimal, and this change is preventable or reversible by physiological amounts of the element.

In the 1980s and 1990s, establishing essentiality on the basis of these criteria was questioned when a large number of elements was suggested to be essential because of some small change in a physiological or biochemical variable. It seemed possible that many of these changes were not necessarily the result of a suboptimal function, but perhaps a consequence of a toxicological or pharmacological action. In this context, pharmacological was defined as the ability of a dietary intake of a substance to alleviate a condition other than the nutritional deficiency of that substance, or to alter a biochemical function or biological structure in a therapeutic manner (*19*).

Today, if dietary deprivation of an element can not be shown to cause death or interrupt the life cycle, a defined biochemical function generally is required before an element is unequivocally accepted as essential.

Status of Vanadium Essentiality

Early Animal Deficiency Experiments. In the 1970s, it was widely believed that vanadium had fulfilled all the necessary criteria and thus should be considered nutritionally essential. However, in the vanadium deprivation studies of the 1970s, "controls" or supplemented animals were fed 0.5 to 3.0 μg V/g diet (*13*). Although these amounts are near those in natural diets which apparently contain about 1.0 μg V/g (*20*), those doses of vanadium in the form of highly available salts apparently are 10 to 50 times those normally found in purified or semipurified diets (*20*). Because vanadium is a relatively toxic and pharmacologically active element, it was difficult to determine whether the "deficiency signs" in early experiments obtained with diets, whose adequacy or balance in other nutrients could be questioned, were true deficiency signs or manifestations of a pharmacological action of vanadium.

For example, in 1971, Strasia (*21*) reported that rats fed less than 100 ng V/g diet exhibited slower growth, higher plasma and bone iron and higher hematocrits than controls fed 500 ng V/g diet. Williams (*22*), using a diet lower in casein and higher in iron and ascorbic acid, was not able to subsequently produce those deficiency signs in the same laboratory in which Strasia had worked. These contrasting findings suggest that, because vanadium can positively affect iron metabolism in rats fed inadequate iron under certain conditions (*23*), the plenteous vanadium supplement in the experiments of Strasia was pharmacologically beneficial for iron metabolism.

In 1971, Schwarz and Milne (*24*) reported that a vanadium supplement of 0.25 to 0.50 μg/g diet gave a positive growth response in suboptimally growing rats fed an amino acid based diet apparently deficient in riboflavin (*25*) and with an unknown vanadium content. On the other hand, Hopkins and Mohr (*26*) reported in 1971 that the only effect vanadium deprivation had in rats was impaired reproductive performance (decreased fertility and increased perinatal mortality) that became apparent only in the fourth generation; the diet they used contained luxuriant amounts of methionine and arginine and was probably deficient in cysteine. The inconsistency in findings and dietary concerns easily allows for the suggestion that vanadium possibly acted in a pharmacological manner in these studies.

Recent Animal Deficiency Experiments. The uncertainty about vanadium deficiency signs stimulated new efforts to produce deficiency signs in animals fed diets apparently containing adequate and balanced amount of all known nutrients. In nine experiments, Anke and coworkers (*27-30*) found that, when compared to controls fed in the first experiments 2 μg V/g diet and in the latest experiments 0.5 μg V/ g diet, goats fed less than 10 ng V/g diet had more difficulty in conceiving, exhibited a higher rate of spontaneous abortion, increased ratio of female to male kids born, and those animals that delivered offspring produced less milk. Between days 7 and 91 of life, 42% of kids from vanadium-deprived goats died with some deaths preceded by

Downloaded by CORNELL UNIV on October 31, 2012 | http://pubs.acs.org
Publication Date: December 10, 1998 | doi: 10.1021/bk-1998-0711.ch023

convulsions; only 8% of kids from vanadium-supplemented goats died during this time. Vanadium-deficient goats had only 50% the life span of control goats. Also, deficient goats exhibited pain in the extremities, swollen forefoot tarsal joints, and skeletal deformations in the forelegs. Biochemical changes exhibited by the vanadium-deficient goats included decreased serum ß-lipoproteins, creatinine, isocitrate dehydrogenase, and lactate dehydrogenase, and increased serum glucose.

Studies with Wistar-Kyoto rats indicated that vanadium affects thyroid metabolism, and thus glucose and lipid metabolism (*32*). Vanadium deficiency increased thyroid weight and thyroid weight/body weight ratio in rats. Moreover, as dietary iodine was increased from 0.05 to 0.33 to 25 μg/g, thyroid peroxidase activity decreased with the decrease more marked in vanadium-supplemented (1 μg V/g diet) than in vanadium-deprived (2 ng V/g diet) rats. The greatest difference between the vanadium-deprived and -supplemented rats occurred when dietary iodine was the lowest. Also as dietary iodine increased, plasma glucose increased in the vanadium-deprived rats but decreased in the vanadium-supplemented rats. As a result, plasma glucose differences between vanadium-deprived and -supplemented rats were most apparent when dietary iodine was low or high; there was essentially no difference when iodine was normal. That vanadium nutriture affects thyroid, glucose and lipid metabolism was confirmed by a three-way 2x2x2 factorially arranged experiment in my laboratory (*32*). In this experiment the variables were deficient and adequate dietary vanadium, or about 2 ng and 500 ng/g diet; low and luxuriant dietary iodine, or about 50 ng and 25 μg/g diet; and type of rat, either the diabetes-prone or diabetes-resistant BB/Wor rat. Each treatment group contained 8 rats that were fed their appropriate casein-ground corn-corn oil based diet for 90 days.

Surprisingly, only five of the diabetes-prone rats developed diabetes which was expected to occur in most all by the end of the experiment. Although these five rats were given implants to supply insulin, with most variables examined, their values were far removed from the values of the rats that did not develop diabetes; thus, the diabetic rats were not included in the comparisons shown in Tables I and II. As found in the earlier experiment with Wistar-Kyoto rats, dietary vanadium markedly affected the response of BB/Wor rats to changing dietary iodine. As shown in Table I, increasing dietary iodine decreased thyroid weight, but the decrease was affected by dietary vanadium. Thyroid weight was slightly higher in the vanadium-deprived than -supplemented rats when dietary iodine was low, but when dietary iodine was high, vanadium-deficient thyroids were 20 to 30% smaller than those from the vanadium-supplemented rats.

The concentration of thyroid hormones found in plasma was also affected by an interaction between vanadium and iodine. When rats were fed a low iodine diet, thyroxine concentrations were much less in vanadium-supplemented than -deprived rats. Increasing dietary iodine markedly increased the thyroxine concentrations in the vanadium-supplemented rats but had very little effect on the concentrations in the vanadium-deprived rats. As a result, the response to a change in dietary vanadium was greatest when dietary iodine was low. The findings with triiodothyronine concentrations were quite different than those of the thyroxine findings. When dietary iodine was low, the plasma triiodothyronine was higher in vanadium-supplemented than -deprived rats. Iodine supplementation decreased the triiodothyronine concentration in vanadium-supplemented rats, but increased it in the vanadium-deprived rats; this effect was most marked in the diabetes-resistant rats. Once again,

Downloaded by CORNELL UNIV on October 31, 2012 | http://pubs.acs.org
Publication Date: December 10, 1998 | doi: 10.1021/bk-1998-0711.ch023

Downloaded by CORNELL UNIV on October 31, 2012 | http://pubs.acs.org
Publication Date: December 10, 1998 | doi: 10.1021/bk-1998-0711.ch023

Table I. Effect of Dietary Vanadium and Iodine on Thyroid Weight, Plasma Thyroxine and Plasma Triiodothyronine in Diabetes-Prone and -Resistant BB/Wor Rats

Dietary[a]		Rat	Thyroid	Plasma	Plasma
V, μg/g	I, μg/g	Type[b]	Weight, mg	Thyroxine, μg/100 ml	Triiodothyronine, ng/100 ml
0.0	0	P	29.6 ± 3.3[c]	5.06 ± 0.98	27.4 ± 7.4
0.5	0	P	26.3 ± 3.7	2.81 ± 0.23	35.1 ± 2.9
0.0	0	R	44.9 ± 6.4	4.78 ± 0.45	31.3 ± 7.9
0.5	0	R	40.3 ± 3.9	2.93 ± 0.43	41.5 ± 6.9
0.0	25	P	10.3 ± 5.9	5.05 ± 0.49	33.1 ± 8.7
0.5	25	P	15.0 ± 6.8	5.65 ± 0.55	32.4 ± 7.7
0.0	25	R	14.6 ± 5.9	5.61 ± 0.40	36.5 ± 6.7
0.5	25	R	17.6 ± 4.7	5.79 ± 0.36	34.4 ± 7.1

Significant effects, Thyroid weight: Iodine, $P<0.0001$; Vanadium x Iodine, $P<0.006$; Diabetes-type, $P<0.0001$; Iodine x Diabetes-type, $P<0.0001$.

Significant effects, Thyroxine: Vanadium, $P<0.0001$; Iodine, $P<0.0001$; Vanadium x Iodine, $P<0.0001$.

Significant effects, Triiodothyronine: Vanadium x Iodine, $P<0.008$; Diabetes-type, $P<0.04$.

[a] Amount of vanadium and iodine supplemented to the diet.

[b] P = diabetes-prone; R = diabetes-resistant.

[c] Mean ± SD

Downloaded by CORNELL UNIV on October 31, 2012 | http://pubs.acs.org
Publication Date: December 10, 1998 | doi: 10.1021/bk-1998-0711.ch023

Table II. Effect of Dietary Vanadium and Iodine on Pancreatic Amylase and Serum Lactate Dehydrogenase Activity in Diabetes-Prone and -Resistant BB/Wor Rats

Dietary[a]		Rat	Pancreatic	Serum Lactate
V, μg/g	I, μg/g	Type[b]	Amylase, U/mg Protein	Dehydrogenase, U/L
0.0	0	P	114 ± 14[c]	964 ± 100
0.5	0	P	102 ± 12	910 ± 101
0.0	0	R	119 ± 12	1060 ± 92
0.5	0	R	74 ± 7	902 ± 174
0.0	25	P	114 ± 15	924 ± 119
0.5	25	P	81 ± 12	977 ± 110
0.0	25	R	105 ± 8	927 ± 154
0.5	25	R	78 ± 11	1106 ± 169

Significant effects, pancreatic amylase: Vanadium, $P<0.0001$; Iodine, $P<0.02$; Diabetes-type, $P<0.008$; Vanadium x Diabetes-type, $P<0.04$; Vanadium x Iodine x Diabetes-type, $P<0.004$.

Significant effects, lactate dehydrogenase: Vanadium x Iodine, $P<0.004$.

[a] Amount of vanadium and iodine supplemented to the diet.

[b] P = diabetes-prone; R = diabetes-resistant.

[c] Mean ± SD

the greatest response to dietary vanadium occurred when dietary iodine was low.

Evidence that dietary vanadium can affect glucose or carbohydrate metabolism is presented in Table II. The activity of pancreatic amylase, which catalyzes the first step in the digestion of dietary starch to glucose, was lower in vanadium-supplemented than -deprived rats. This difference was much greater in the diabetes-resistant than diabetes-prone rat when dietary iodine was low; when dietary iodine was high, this difference was not as apparent between the types of rats. An interaction between iodine and vanadium also affected the activity of serum lactate dehydrogenase, the last enzyme in the glycolytic pathway. When dietary iodine was increased, lactate dehydrogenase activity decreased in the vanadium-deficient rats, while it increased the vanadium-supplemented rats. As a result, when dietary iodine was low, lactate dehydrogenase activity was lower in vanadium-supplemented than -deficient rats, but when dietary iodine was luxuriant, just the opposite occurred.

The use of deficient and excessive amounts of iodine in this experiment might be questioned. This was done because it was thought that the need for vanadium would be very low under normal conditions if its key role in animals involved thyroid metabolism. Thus it would be difficult to obtain a response in experimental animals because current technology results in diets that probably should be considered marginally low in vanadium. It was felt that the response to the marginally low diets would be increased if the need for vanadium was increased, for example, high iodine in the diet; or if there was some interference with the utilization of vanadium, for example, low iodine. The basis for this practice is the formula:

Pathological effects = stress x organic vulnerability (*33*).

Pathological effects are not likely to be seen if the vanadium deficiency or organic vulnerability is not multiplied by some significant stressor. Similarly, an organism probably can handle a specific stressor easily if there is no organic vulnerability or in this case, adequate vanadium. However, the multiplication of a subnormal intake of vanadium times the presence of a stressor affected by vanadium most likely would lead to pathological consequences. This approach apparently was successful because in the Wistar-Kyoto and BB/Wor rat experiments, vanadium responsive variables generally were more markedly affected by vanadium deficiency when dietary iodine was deficient or excessive; there was not much difference when the animals were fed a normal amount of iodine.

The finding that vanadium status affects thyroid metabolism which involves the halide iodine is intriguing. The functional role defined for vanadium in some algae, lichens, and fungi is that of an integral part of some haloperoxidases (*34*), or involved in halide metabolism. Thus, it seems possible that vanadium has an essential function in the metabolism or oxidation of halides in higher animals.

In summary, although vanadium at present is not unequivocally accepted as essential, accumulating circumstantial evidence strongly suggests that it is. This evidence includes the finding of dietary responses to vanadium in higher animals that are difficult to attribute to pharmacological action only, and the finding of biochemical roles for vanadium in lower forms of life.

Physiological metabolism of vanadium

As indicated earlier, one criterion often used to support essentiality for an element is the presence of homeostatic mechanisms to regulate its content in the body. There is

Downloaded by CORNELL UNIV on October 31, 2012 | http://pubs.acs.org
Publication Date: December 10, 1998 | doi: 10.1021/bk-1998-0711.ch023

evidence that tissue concentrations of vanadium are homeostatically controlled through absorptive, excretory and storage mechanisms. Recent reviews (*35,36*) of vanadium metabolism found that most vanadium ingested as a component of food is unabsorbed and is excreted in the feces. Based on the very small concentrations of vanadium normally found in urine compared with the estimated daily intake and fecal content of vanadium, less than 5% of ingested vanadium is absorbed. Animal studies generally support the concept that vanadium is not readily absorbed from the diet. However, two studies with rats fed vanadium as the salt sodium vanadate indicate that vanadium absorption can exceed 10% with some forms of vanadium or under certain dietary conditions (*37,38*); this suggests caution in assuming that a low percentage of ingested vanadium always is absorbed from the gastrointestinal tract.

Vanadium absorption. Most vanadium that is absorbed is probably transformed in the stomach to the vanadyl ion and remains in this form as it passes into the duodenum (*39*). The mechanisms involved in the absorption of vanadium in the cationic or vanadyl form are unknown. In vitro studies suggest that vanadium in the anionic or vanadate form can enter cells through phosphate- or other anion-transport systems (*40*). Vanadate is absorbed 3 to 5 times more effectively than vanadyl (*41*). Apparently the different absorbability rates for vanadate and vanadyl, the effect of other dietary components on the binding and forms of vanadium in the stomach, and the rate at which vanadate is transformed into vanadyl markedly affect the percentage of ingested vanadium absorbed.

Vanadium transport. When vanadate appears in the blood, it is quickly converted into the vanadyl cation (*42-46*). However, as a result of oxygen tension, vanadate still exists in blood. Vanadyl, the most prevalent form of vanadium in blood, is bound and transported by transferrin and albumin (*47*). Vanadate is transported by transferrin only (*47*). Vanadyl also complexes with ferritin in plasma and body fluids (*48,49*). It remains to be determined whether vanadyl-transferrin can transfer vanadium into cells through the transferrin receptor or whether ferritin is a storage vehicle for vanadium. Vanadium is rapidly removed from plasma and is generally retained in tissues under normal conditions at concentrations less than 10 ng/g fresh weight (*35*). Bone apparently is a major sink for excessive retained vanadium.

Vanadium excretion. Excretion patterns after parenteral administration (*50-53*) indicate that urine is the major excretory route for absorbed vanadium. However, a significant portion of absorbed vanadium may be excreted through the bile. This is supported by findings that human bile contains measurable vanadium (about 1.0 ng/g) (*54*), and about 10% of an injected dose of an isotopic tracer of vanadium was found in the feces of humans (*50*) and rats (*52*).

Nutritional requirement for vanadium

If vanadium is essential for humans, its requirement most likely is small. The diets used in animal deprivation studies described above contained only 2 to 25 ng/g; these amounts usually did not have severe consequences; this indicates that the vanadium

Downloaded by CORNELL UNIV on October 31, 2012 | http://pubs.acs.org
Publication Date: December 10, 1998 | doi: 10.1021/bk-1998-0711.ch023

deprivation with these intakes may have been marginal. Most diets supply humans with less than 30 μg daily; many diets supply near 15 μg daily (*35*). Vanadium deficiency signs have not been found in humans with these intakes. These observations suggest that a dietary intake of 10 μg daily probably meets any postulated vanadium requirement. Suggesting an upper safe nutritional intake for vanadium is difficult because humans apparently are more tolerant to high vanadium intakes than experimental animals such as rats, and there are only limited human toxicological data on which to base such a suggestion. As reviewed elsewhere (*35*), there are findings suggesting an intake of over 10 mg daily can result in toxicity signs. However, much lower amounts of vanadium were found to have pharmacological actions in humans which suggests that they may have toxic manifestations under certain conditions. Most mineral elements at intakes 100 times their nutritional requirement are toxic. This suggests that a safe daily intake for vanadium is under 1.0 mg per day and might be 100 μg or less.

As indicated above, the daily intake of vanadium is relatively low in comparison with known essential trace elements. Foods rich in vanadium (greater than 40 ng/g) include shellfish, mushrooms, parsley, dill seed, black pepper and some prepared foods (*55,56*). Cereals, liver and fish tend to have intermediate amounts of vanadium (5 to 40 ng/g) (*54, 56-58*). Beverages, fats and oils, fresh fruits, and fresh vegetables generally contain less than 5.0 ng V/g, and often less than 1.0 ng/g (*54, 56-58*).

Because of its uncertain nutritional essentiality status, the practical nutritional importance of vanadium remains to be determined. The identification of an essential biochemical function for vanadium in higher animals is needed to disentangle pharmacological from nutritional or physiological observations with this element. Determination of a defined function also will facilitate the determination of status assessment indicators as well as data- supported safe and adequate intakes for vanadium. Until a defined function is described, it is unlikely that vanadium will be unequivocally accepted as an essential nutrient for higher animals including humans.

Downloaded by CORNELL UNIV on October 31, 2012 | http://pubs.acs.org
Publication Date: December 10, 1998 | doi: 10.1021/bk-1998-0711.ch023

Literature Cited

1. Lyonett, M.; *Press Medicale,* **1899**, 1, 191-192.
2. Jackson, D.E.; *J. Pharmacol.,* **1912**, 3, 477-514.
3. Proescher, F., Seil, H.A., Stillians, A.W.; *Am. J., Syph.,* **1917**, 1, 347-405.
4. Lewis, C.E.; *AMA Arch. Ind. Health,* **1959**, 19, 419-425.
5. Curran, G.L., Burch, R.E.; *Trace Sub. Environ. Health,* **1968**, 1, 96-104.
6. Tank, G., Storvick, C.A.; *J. Dent. Res.*, **1960**, 39, 473-480.
7. Orvig, C., Thompson, K.H., Battell, M. McNeill, J.H.; In *Vanadium and Its Role in Life;* Sigel, H. and Sigel A. Eds, *Metal Ions in Biological Systems*, Marcel Dekker, Inc, New York, 1995, Vol 31, pp. 575-594.
8. Myers, V.C, Beard, H.H.; *J. Biol. Chem.*, **1931**, 94, 89-110.
9. Beard, H.H., Baker, R.W., Myers, V.C,; *J. Biol. Chem.*, **1931**, 94, 123-134.
10. Rygh, O.; *Bull. Soc. Chim. Biol.*, **1949**, 31, 1052, 1403, 1408.
11. Schroeder, H.A., Balassa, J.J., Tipton, I.H.; *J. Chron. Dis.,* **1963**, 16, 1047-1071.
12. Hopkins, L.L., Jr., Mohr, H.E.; *Fed. Proc.*, **1994**, 33, 1773-1775.

13. Nielsen, F.H.; *J. Nutr.*, **1985**, 115, 1239-1247.
14. Schroeder, H.A., Balassa, J.J., Tipton, I.H.; *J. Chron. Dis.*, **1961**, 15, 51-65.
15. Cotzias, G.C.; *Trace Sub. Environ. Health*, **1967**, 1, 5-19.
16. Underwood, E.J.; In *Trace Elements in Human and Animal Nutrition,* 3rd Edition, Underwood, E.J., Ed; Academic Press, New York, NY 1971; pp. 1-13.
17. Mertz, W.; *Fed. Proc.*, **1970**, 29, 1482-1488.
18. Nielsen, F.H., In *Trace Element Metabolism in Animals - 2;* Hoekstra, W.G., Suttie, J.W., Ganther, H.E., Mertz, W. Eds, University Park Press, Baltimore, MD, 1974, pp. 381-395.
19. Nielsen, F.H., Uthus, E.O; In *Vanadium in Biological Systems, Physiology and Biochemistry,* Chasteen, N.D., Ed; Kluwer, Dordrecht, Netherlands, 1990, pp 51-62.
20. Reeves, P.G., Nielsen, F.H., Fahey, G.C., Jr.; *J. Nutr,* **1993**, 123, 1939-1951.
21. Strasia, C.A.; *Vanadium Essentiality and Toxicity in the Laboratory Rat*; Ph.D. Dissertation, Purdue University, LaFayette, IN, 1971.
22. Williams, D.L.; *Biological Value of Vanadium for Rats, Chickens, and Sheep;* Ph.D. Dissertation, Purdue University, LaFayette, IN, 1973.
23. Nielsen, F.H.; *Nutr. Res. (Supp I)* **1985**, pp. 527-530.
24. Schwarz, K., Milne, D.B.; *Science*, **1971**, 174, 426-428.
25. Moran, J.K., Schwarz, K.; *Fed. Proc.,* **1978**, 37, 671 (abs. 2410).
26. Hopkins, L.L. Jr., Mohr, H.E.; In *Newer Trace Elements in Nutrition;* Mertz, W., Cornatzer, W.E., Eds; Marcel Dekker, New York, NY, 1971, pp. 195-213.
27. Anke, M., Groppel, B, Gruhn, K, Kośla, T., and Szilágyi, M; In *5. Spurenelement-Symposium New Trace Elements;* Anke, M., Baumann, W., Bräunlich, H., Brückner, C., and Groppel, B., Eds; Friedrich-Schiller-Universität, Jena, 1986, pp 1266-1275.
28. Anke, M., Groppel, B., Gruhn, K, Langer, M., and Arnhold, W.; In *6th International Trace Element Symposium, Vol. 1, Molybdenum, Vanadium;* Anke, M., Baumann, W., Bräunlich, H., Brückner, C., Groppel, B., and Grün, M., Eds; Karl-Marx-Universität, Leipzig, 1989, pp. 17-27.
29. Anke, M., Groppel, B., and Krause, U.; In *Trace Elements in Man and Animals,* Momcilovic, B., Ed., IMI, Zagreb, 1991, Vol 7, 11.9-11.10.
30. Anke, M., Groppel, B., Arnhold, W., Langer, M. and Krause, U.; In *Trace Elements in Clinical Medicine,* Tomita, H. Ed., Springer-Verlag, Tokyo, 1990, pp, 361-376.
31. Uthus, E.O., Nielsen, F.H.; *Magnesium Trace Elem.* **1990**, 9, 219-226.
32. Nielsen, F.H, Poellot, R.A., Uthus E.O.; *FASEB J.*, **1997**, 11, A148 (abs 862).
33. Tapp, W.N., Natelson, B.H.; *FASEB J.*, **1988**, 2, 2268-2271.
34. Vilter, H; In *Vanadium and Its Role in Life;* Sigel, H., Sigel A., Eds; *Metal Ions in Biological Systems*, Marcel Dekker, New York, NY, 1995, Vol 31, pp. 325-362.
35. Nielsen, F.H.; In In *Vanadium and Its Role in Life;* Sigel, H., Sigel A., Eds; *Metal Ions in Biological Systems,* Marcel Dekker, New York, NY, 1995, Vol 31, pp. 543-573.
36. Nielsen, F.H.; In *Metal-Ligand Interactions in Biological Fluids, Bioinorganic Medicine;* Berthon, G., Ed; Marcel Dekker, New York, NY, 1995, Vol 1, pp. 425-427.
37. Bogden, J.D., Higashino, H., Lavenhar, M.A., Bauman, J.W., Jr., Kemp, F.W., Aviv, A.; *J. Nutr.* 1982, 112, 2279-2285.

Downloaded by CORNELL UNIV on October 31, 2012 | http://pubs.acs.org
Publication Date: December 10, 1998 | doi: 10.1021/bk-1998-0711.ch023

38. Wiegmann, T.B., Day, H.D., Patak, R.V.; *J. Toxicol. Environ. Health*, 1982, 10, 233-245.
39. Chasteen, N.D., Lord, E.M., Thompson, H.J.; In *Frontiers in Bioinorganic Chemistry;* Xavier, A.V., Ed; VCH Verlagsgesellschaft, Weinheim, FRG, 1986, pp. 133-141.
40. Cantley, L.C., Jr., Resh, M.D., Guidotti, G.; *Nature*, **1978**, 272, 552-554.
41. Parker, R.D.R., Sharma, R.P.; *J. Environ. Pathol. Toxicol.*, **1978**, 2, 235-245.
42. Macara, I.G., Kustin, K., Cantley, L.C., Jr.; *Biochem. Biophys. Acta*, 1980, 629, 95-106.
43. Hansen, T.V., Aaseth, J., Alexander, J.; *Arch. Toxicol.*, **1982**, 50, 195-202.
44. Kustin, K., Toppen, D.L.; *Inorg. Chem.*, **1973**, 12, 1404-1407.
45. Cantley, L.C., Jr., Ferguson, J.H., Kustin, K.; *J. Am. Chem. Soc.*, **1978**, 100, 5210-5212.
46. Sakurai, H., Shimomura, S., Ishizu, K.; *Inorg. Chim. Acta.*, **1981**, 55, 67L-69L.
47. Chasteen, N.D., Grady, J.K., Holloway, C.E.; *Inorg. Chem.*, **1986**, 25, 2754-2760.
48. Chasteen, N.D., Lord, E.M., Thompson, H.J., Grady J.K.; *Biochim. Biophys. Acta.,* **1986**, 884, 84-92.
49. Sabbioni, E., Marafante, E.; In *Trace Element Metabolism in Man and Animals (TEMA-4);* Howell, J. McC., Gawthorne, J.M., White, C.L., Eds; Australian Academy of Science, Canberra, 1981, pp. 629-631.
50. Kent, N.L., McCance, R.A.; *Biochem. J.,* 1941, 35, 837-844.
51. Hansard, S.L. II, Ammerman, C.B., Henry, P.R., Patterson, B.W.; *J. Anim. Sci.,* **1986**, 804-812.
52. Hopkins, L.L. Jr., Tilton, B.E.; *Am. J. Physiol.,* **1966**, 211, 169-172.
53. Sabbioni, E., Marafante, E.; *Bioinorg. Chem.,* **1978**, 9, 389-407.
54. Byrne, A.R., Kosta, L.; *Sci. Tot. Environ.*, **1978**, 10, 17-30.
55. Ikebe, K., Tanaka, R.; *Bull. Environ. Contam. Toxicol.,* **1979**, 21, 526-532.
56. Myron, D.R., Givand, S.H., Nielsen, F.H.; *Agric. Food Chem.*, **1977**, 25, 297-300.
57. Evans, W.H., Read, J.I., Caughlin, D.; *Analyst*, **1985**, 110, 873-877.
58. Pennington, J.A.T., Jones, J.W.; *J. Am. Diet. Assoc.*, **1987**, 87, 1644-1650.

Downloaded by CORNELL UNIV on October 31, 2012 | http://pubs.acs.org
Publication Date: December 10, 1998 | doi: 10.1021/bk-1998-0711.ch023

Downloaded by UNIV OF GUELPH LIBRARY on October 31, 2012 | http://pubs.acs.org
Publication Date: December 10, 1998 | doi: 10.1021/bk-1998-0711.ch024

Chapter 24

Insulin-like Effects of Vanadium; Reviewing In Vivo and In Vitro Studies and Mechanisms of Action

Yoram Shechter[1], Gerald Eldberg, Assia Shisheva, Dov Gefel, Natesampillai Sekar[1], Sun Qian[1], Rafi Bruck, Eythan Gershonov[2], Debbie C. Crans[3], Y. Goldwasser[2], Mati Fridkin[2], and Jinping Li[1]

[1]Departments of Biological Chemistry, and [2]Organic Chemistry, The Weizmann Institute of Science, Rehovot 76100, Israel
[3]Department of Chemistry and Cell and Molecular Biology, Colorado State University, Fort Collins, CO 80523–1872

Vanadium is a nutritional element present in mammalian tissues. Low quantities of dietary vanadium may be required for normal metabolism in higher animals. Vanadium exhibits a complex chemistry, fluctuating between several different oxidation states and hydrolytic forms, depending on the prevailing conditions. Intracellular forms of vanadium fluctuate between the anionic vanadate (vanadium(+5); $H_2VO_4^-$) and the cationic vanadyl (vanadium(+4); hydrated VO^{2+}). Although much research has been performed on vanadium compounds during the last two decades, its physiological function is still obscured (*1, 2*). A remarkable finding was the induction of normoglycemia in diabetic rodents following oral vanadium therapy (*4-7*). *In vitro* studies revealed that vanadium salts virtually mimic most of the effects of insulin (*8-10*). A number of reviews have been recently published on the potential usage of vanadium as a therapeutic antidiabetic agent (*11-14*). This review focuses on the mechanisms by which vanadate facilitates its insulin-like effects at the molecular level.

Insulin-like effects of vanadate

A major role of insulin in mammals is the regulation of glucose homeostasis by modulating glucose production in the liver and glucose utilization in muscle and fat. Reduced potency of insulin to arrest hepatic glucose output or to enhance glucose utilization in peripheral tissues leads to *insulin resistance*. This phenomenon is accompanied with a compensatory over-secretion of insulin by the pancreas (hyperinsulinemia). A failure of the pancreas to secrete insulin in sufficient quantities leads to hyperglycemia (*3*).

The insulin-like effects of vanadium were originally found in intact cells. Subsequently, vanadium was administrated orally to diabetic animals. In vanadate-treated STZ-rats, hyperglycemia was reduced to normal glucose levels within 2-5 days. Sodium metavanadate in drinking water was found to be optimal at a concentration of 0.2 mg/ml, and in some instances normoglycemia persisted after termination of vanadium therapy (*4-6*). The effect of vanadate was also determined in animal models representing insulin-resistance phenotypes. In ob/ob and in db/db mice and in fa/fa rats, administration of vanadate lowered plasma insulin concentrations and lead to a better tolerance to glucose absorption (*15-19*). In *in vitro* experimental systems vanadate mimiced virtually all the rapid metabolic effects of insulin. Vanadate activates glucose transport in myocytes and adipocytes, and glucose metabolism and glycogen synthesis in myocytes, adipocytes and hepatocytes (*8-10, 20-23*). Vanadate also inhibits lipolysis, an insulin-like effect which differs mechanistically from the hormonal effect in facilitating glucose metabolism. In diabetic animals, vanadate therapy corrected the expression of genes encoding key enzymes of glucose metabolism such as glucokinase, 6-phosphofructokinase, acetyl CoA carboxylase, fatty acid synthetase, phosphoenol carboxykinase, and pyruvate kinase (*19, 23-25*).

Downloaded by UNIV OF GUELPH LIBRARY on October 31, 2012 | http://pubs.acs.org
Publication Date: December 10, 1998 | doi: 10.1021/bk-1998-0711.ch024

Insulin receptor and insulin receptor substrate 1 (IRS 1)

The first step in mediating the insulin-dependent cascades consists of insulin binding to its cell surface receptor. The insulin receptor is a transmembrane protein, composed of two α subunits and two β subunits. Binding of insulin to the extracellularly located α subunits activates the intrinsic tyrosine kinase, located intracellularly at the β subunits. This initial event leads to tyrosine phosphorylation of the receptor itself, as well as the phosphorylation of intracellular substrates such as insulin receptor substrate 1 (IRS-1). This cytosolic substrate is a docking protein that follows tyrosine phosphorylation at several sites and associates with several proteins. This association may activate, deactivate or orient these proteins toward their receptive sites. Documented signaling molecules known so far to associate with IRS-1 are phosphatydylinositol-3-kinase (PI3-kinase), the adaptor proteins Grb2, Nck, and the PTPase SHPTP2 (Reviewed in *3, 26, 27*).

Vanadate by itself induced negligible phosphorylation (and receptor activation) in various cells and tissues (*28-31*). Accordingly, IRS-1 was negligibly phosphorylated as well. Additional evidence that the insRTK is not involved in mediating the rapid metabolic effects of insulin by vanadate has been provided by cell-permeable inhibitors of the insulin receptor. In intact adipocytes, inhibition of the phosphotransferase activity of the insulin receptor blocked the biological effects of insulin on glucose transport and glucose metabolism but did not block the same bioeffects when triggered by vanadate (*33*). We conclude that the insulin receptor tyrosine kinase activity and the subsequent phosphorylation of IRS-1 are not required for mediating the rapid effects of insulin by vanadate.

Phosphatidyl inositol-3-kinase (PI3-kinase)

Insulin activates PI3-kinase (*34, 35*). This enzyme phosphorylates the D3 position of the inositol ring phosphatidyl inositol (PI) leading to phospholipid products. PI3-kinase is composed of binding and catalytic subunits of 85 kDa and 110 kDa, respectively (*36*). Association of PI3-kinase with proteins having two PYMPM (or related) motifs activates PI3-kinase. In addition to IRS-1, PI3-kinase can associate with several tyrosine phosphorylated protein tyrosine kinases of receptor and nonreceptor origin such as Src, a cytosolic protein tyrosine kinase (*36*). Binding of PI3-kinase through the p85 kDa subunit activates the catalytic activity located within the p110 subunit. Activation of PI3-kinase is followed by the activation of several ser/thr protein kinases such as pp70 S6 kinase, Akt and c-Jun N-terminal kinase (*37, 38*). Wortmannin, a potent inhibitor of PI3 kinase (*37, 38*), blocked all the rapid metabolic effects of insulin. These included the activation of glucose uptake and glucose metabolism in rat adipocytes, and the activation of glycogen synthase in skeletal muscle cells. The antilipolytic effect of insulin was also reversed by wortmannin (*35*). As with insulin, vanadate also activates PI3-kinase in rat adipocytes. Wortmannin blocks the effects of vanadate in stimulating glucose transport and glucose metabolism. Unlike insulin, however, the antilipolytic effect of vanadate is not quenched by wortmannin (*39*).

Role of nonreceptor protein tyrosine kinases in mediating the insulin-like effects of vanadate

As mentioned earlier the insulin-receptor tyrosine kinase in vanadate treated adipocytes is barely activated. Tyrosine phosphorylation of a 53 kDa protein however is significantly more pronounced in vanadate-treated adipocytes (*28*). With the notion that endogeneous tyrosine phosphorylation is an early prerequiste for manifesting the metabolic effects of insulin, we have searched for a non-receptor protein tyrosine kinase (PTK) which is activated by vanadate. A cytosolic protein tyrosine kinase (CytPTK) with apparent molecular weight of 53 kDa on gel filtration chromatography has been identified. CytPTK activity is elevated 3-5 fold upon treatment of rat adipocytes with vanadate. CytPTK differs from the InsRTK in its molecular weight, in exhibiting greater activity with Co^{2+} than with Mn^{2+} as the divalent metal ion cofactor, and in showing differential sensitivities to protein tyrosine kinase inhibitors such as quercetin and staurosporine. Unlike the InsRTK, cytPTK is resistant to inactivation by N-ethymaleimide (*40-42*). The role of cytPTK in mediating the insulin-like effects of vanadate at the intact cell level has been demonstrated by using staurosporine, a potent inhibitor of cytPTK and a weak inhibitor of the InsRTK (K_i~2nM and ~2μM, respectively, ref.*40*). Staurosporine can be utilized as a general marker for cytosolic protein tyrosine kinases, inhibiting the latter at nanomolar concentration whereas membranal PTKs, including the InsRTK, are inhibited at μM concentration of stuarosporine (*43*). While staurosporine was found to inhibit the effect of vanadate on lipogenesis and glucose oxidation at low concentration, corrsponding insulin-induced stimulations were not affected. Also, other insulinomimetic effects of vanadate such as the activation of glucose transport and inhibition of lipolysis were not inhibited by low staurosporine concentrations (*40-41*). These results suggest that the biological effects stimulated by vanadate, such as lipogenesis and glucose oxidation, are mediated by cytPTK in an InsRTK-independent fashion. However, additional mechanisms are lacking to explain vanadium effects in inhibiting lipolysis and in activating hexose uptake. Recently, we have identified an additional vanadate-activatable nonreceptor-PTK, exclusively located at the plasma membranes (*44*). This membranal PTK seems to be involved in those vanadate effects not mediated by cytPTK and to activate PI3-kinase as well. In summary, two nonreceptor PTKs, one of cytosolic origin, the other of membranal origin, appear to be involved in manifesting the rapid metabolic effects of vanadate.

Inhibition of protein phosphotyrosine phosphatases and the insulin like effects of vanadate; Mechanism of inhibition of PTPases

Vanadate is a well known inhibitor of protein phosphotyrosine phosphatases (PTPases, *45-47*). All members of this PTPase family contain a signature motif in their active site [I/V]HCXAGXXR[S/T]G (*46, 47*). The dephosphorylation reaction occurs through an initial attack by the active site nucleophylic cysteinyl moiety on the substrate tyrosyl phosphate to form a covalent enzyme-phosphate intermediate. Several residues including the motif's histidyl moiety create the hydrophobic 'pocket' interacting with phosphotyrosine. Because of the structural and electronic similarity of vanadate to phosphate, and the ability of vanadate to form stable five-coordinate species resembling the respective transition states, the inhibition by vanadate and other vanadium compounds of phosphatases is well documented (*48, 49*). However, in the presence of externally added nucleophiles, such as hydroxylamine, vanadate fails to inhibit PTPases (*12, 46*) which may be due to the hydrolysis of a covalent enzyme intermediate (*46*) or formation of new innocuious vanadium complexes that may no longer inhibit this enzyme (*50*). In any event, vanadate appears to act by formation of a five-coordinate enzyme complex which may or may not involve the formation a covalent linkage between inhibitor and enzyme (*46, 47, 49*).

Downloaded by UNIV OF GUELPH LIBRARY on October 31, 2012 | http://pubs.acs.org
Publication Date: December 10, 1998 | doi: 10.1021/bk-1998-0711.ch024

The general linkage between inhibition of PTPases and activation of nonreceptor PTKs on one hand, and manifesting insulin effects through receptor-independent pathways on the other hand was further supported by additional inhibitors of PTPases. Those include, molybdate, tungstate and several vanadium(+4) compounds, which exhibit important differences from vanadate in inhibiting PTPases (*51*). For example, tungstate and molybdate are competitive inhibitors of PTPases but are less likely to form covalent intermediates during catalysis (*12, 49*). Vanadyl(+4) cation differs from vanadate(+5) in its oxidation state and in being cationic and a Mg^{2+} analog (13), however, some vanadium(+4) complexes are also potent inhibitors of PTPases (manuscript in preparation). The capacity of all these PTPase inhibitors to evoke insulin-like effects in *in vitro* systems has been systematically analyzed (subsequent paragraphs).

As discussed above, vanadate by itself manifests its insulin-like metabolic effects through the activation of nonreceptor PTKs, in an InsRTK independent manner. Our cell-free experiments show that in intact cells vanadate activates the nonreceptor PTKs (by autophosphorylation on tyrosine moieties) concomitantly with the inhibition of cellular PTPases. Only negligible levels of the InsRTK is autophosphorylated or activated in vanadate-treated adipocytes (*29, 30, 33, 51*). Our previous attempts to tackle these experimental findings were based on the assumption that the adipose tissue contains several members of PTPases out of which the key InsRTK-PTPase is insensitive to vanadate inhibition (*12*). We are currently exploring an alternative interpretation: the possibility that the InsRTK-PTPase is sensitive to vanadate. Perhaps the physical limitations around the active-site receptors' tyrosine moieties will maintain the residue inaccessible and prevent autophosphorylation, even though the specific receptor-PTPase activity is arrested (under study).

If this mechanism will be supported by additional experiments, it is possible that the combined therapies of insulin and vanadium might be very beneficial in human diabetes. The initial activation of the insulin receptor will remain activated because the the presence of vanadate once insulin is removed and/or when its activating potency is decreased as in certain pathophysiological states. In genetically obese fa/fa rats, oral vanadate therapy showed marked antidiabetic effects by increasing the low sensitivity of peripheral tissues (particularly muscle) to insulin (*15, 18*).

Action of other PTPase inhibitors Tungstate and molybdate

Tungstate and molybdate mimic the biological effects of insulin in rat adipocytes. Also administration of tungstate and molybdate to streptozotocin-treated rats reduced blood glucose levels toward normal values. These compounds activate glucose transport and glucose oxidation, stimulate lipogenesis and inhibit lipolysis. However, these effects are obtained at higher concentration as compared to vanadate (*51*). Similarly, higher concentration of tungstate and molybdate were required to activate cytPTK (*42*). These quantitative differences may be attributed to reduced capacity of tungstate and molybdate to inhibit cellular PTPases compared to vanadate. Indeed, significant differences have been observed in complexes of vanadate and molydate with PTPases (*49*). It may result from a different mechanism of inhibition which seems to be less efficient.

Vanadyl(+4) cations

Both exogenously added vanadate(+5) and vanadyl(+4) ions mimic the biological effects of insulin. Qualitatively they resemble each other in activating intracellular protein tyrosine phosphorylation, mimicing the biological actions of insulin, and in being antidiabetic agents in experimental animals (*7, 53, 54*). Early studies suggested that internalized vanadate is reduced intracellularly to vanadyl (*20, 55, 56*). To examine whether vanadyl or vanadate was the active species, we have established a cell-free experimental system that enabled us to determine the

Downloaded by UNIV OF GUELPH LIBRARY on October 31, 2012 | http://pubs.acs.org
Publication Date: December 10, 1998 | doi: 10.1021/bk-1998-0711.ch024

activation of cytPTK by vanadium, under conditions where conversion between redox states of vanadium compounds is slow (*43, 57*). The overall observations from our cell-free studies are as follows: (a) when the cell-free system is constituted solely of the cytosolic fraction, (40,000xg supernatant fraction) vanadate(+5), but not vanadyl(+4) significantly activates cytPTK; (b) similarly, vanadate is the most active species when the cell-free system is constituted of both the cytosolic fraction and broken plasma membrane fragments; (c) dissolution of the broken plasma membrane fragments with Triton X-100 (1%) enables vanadyl(+4) to activate cytPTK. Based on these studies we have concluded that rat adipocytes possess two distinct pathways, one that is activated by vanadate and one activated by vanadyl. The latter is dependent on membranal PTPases. It should be determined, however, whether in this case the cell-free experimental system truely represents the responses at the intact cell level. Note that Triton extractable PTPases (and not 'intact' broken plasma-membrane fragments) supported the activation of cytPTK by vanadyl(+4). In summary, it appears at present that both vanadium(+5) and vanadyl(+4) are insulinomimetic, although additional proofs are required with respect to the latter.

Downloaded by UNIV OF GUELPH LIBRARY on October 31, 2012 | http://pubs.acs.org
Publication Date: December 10, 1998 | doi: 10.1021/bk-1998-0711.ch024

Phenylarsine oxide; paradoxal inhibition pattern of PTPase in rat adipocytes.

In general, inhibition of PTPases correlates with the manifestation of insulin-like effects in rat adipocytes (previous sections). We therefore put special efforts in studying a notable exception. As with vanadate, phenylarsine oxide (PAO) is a documented inhibitor of PTPases. It is a trivalent arsenic compound that can form a covalent adduct with two closely-spaced protein cysteinyl residues. Low concentrations of PAO blocked both the stimulating effects of both insulin and vanadate on hexose uptake and glucose metabolism. However, PAO caused no changes in the antilipolytic effects of insulin and vanadate (*58-60*). The emergence of several phosphotyrosine containing proteins in PAO-treated adipocytes suggested to us that, indeed, PAO does inhibit certain PTPase(s) in this cell type. This in turn, led to a working hypothesis in which both 'stimulatory' and 'inhibitory' PTPases exists; inhibiting the latter arrests the activating effects of both insulin and vanadate on hexose uptake and glucose metabolism. Attempts to identify the PAO-sensitive, 'inhibitory' PTPase, in cell-free experiments were unsuccessful. Based on results from indirect experimental approaches, we concluded that the 'inhibitory' PTPase comprises a miniscule fraction of the total adipocytic PTPase activity, which is exclusively associated with the membrane fraction. Several phosphotyrosine containing proteins emerge in PAO-treated (but not in vanadate-treated) adipocytes. These include a 33 kDa protein, whose phosphorylation on tyrosine residues may produce a negative feedback mechanism and prohibit the activation of glucose uptake and its metabolism by either insulin or vanadate (in preparation).

Peroxovanadium compounds (pV); Differences between vanadium salts and peroxovanadium as insulinomimetic agents

Although both peroxovanadium(+5) (pV, often referred to as pervanadate) and vanadium salts mimic the actions of insulin, our long-term studies in rat adipocytes revealed that they operate through two distinct mechanisms. Vanadate interacts with H_2O_2 to form peroxovanadium complexes, where the peroxide ion (O_2^{2-}) enters the coordination sphere of vanadium to form covalent bonds. One vanadium compound under physiological conditions will contain up to two of such peroxo ligands. Peroxovanadium is about 100-fold more potent (ED_{50}=0.8-1 μM) than vanadate in facilitating the rapid metabolic effects of insulin (*61-64*). Unlike with vanadate, in the pV treated adipocytes, the insulin-receptor undergoes rapid autophosphorylation and activation followed by the phosphorylation of receptor substrates such as the IRS-1 (*62, 63*). These and another study (*33*) further confirmed that pV (but not vanadate) facilitates its insulin-like effects exclusively through receptor-activation and IRS-1 phosphorylating pathways.

What are the unique properties of pV that can explain the above observations? Perhaps most importantly pV differs from vanadate in being a potent oxidizing agent relative to glutathione. It oxidizes a stoichiometric amount of GSH to GSSG (*61*). In cell free experiments, pV is only slightly a more potent inhibitor of adipose PTPases relative to vanadate, but, at the intact cell level, pV is highly potent in this respect and substantially inhibits (or possibly inactivates) adipose PTPases (*64*). Membranal (rather than cytosolic) PTPases are more affected. About 75-85% of the total membranal PTPases are irreversibly inhibited prior to the phosphorylation and activation of the insulin receptor (submitted manuscript). Huer et al. have recently demonstrated that prolonged incubation of PTP1B with pV inactivates the enzyme by irreversibly oxidizing the catalytic cysteine moiety to cysteic acid (*65*). Such inactivation appears to be more efficient at the intact cell level.

Downloaded by UNIV OF GUELPH LIBRARY on October 31, 2012 | http://pubs.acs.org
Publication Date: December 10, 1998 | doi: 10.1021/bk-1998-0711.ch024

Putative role for the intracellular vanadium pool in higher animals

Although we have focused our studies on 'enforcing' insulin-like effects by enriching adipocytes with exogeneously added vanadium, the data accumulated may also bring a feasible putative physiological role for those miniscule quantities of intracellularly located vanadium. Vanadium is a dietary trace element suggested to be essential for higher animals (*1, 2*). Its intracellular concentration is approximately 20 nM. The bulk of the intracellular vanadium is probably in the vanadium +4 oxidation state. The presence of large amount of CytPTK activity in the mammalian cytosolic compartment makes one wonder whether it constitutes a reservoir for adjusting physiological needs not directly controlled by external stimuli. Our cell-free studies which represent exclusively the adipose-cytosolic compartment showed that vanadyl(+4) does not activate cytPTK but vanadate does (*42*). It is generally believed that vanadyl would not be oxidized to vanadate at the reducing intracellular atmosphere maintained by millimolar GSH concentrations, although vanadium(+5) protein complexes have been isolated from blood (*66*). Recently, we demonstrated that at physiological pH and temperatures GSH only slowly reduces vanadate(+5) to vanadyl(+4). Furthermore, aqueous vanadyl(+4) undergoes spontaneous oxidation to vanadate *in vitro* at physiological pH and temperature and in the presence of GSH (*57*). These studies raise questions concerning the validity of the above dogma under conditions of physiological relevance.

Vanadyl(+4) is readily oxidized to vanadate by one equivalent of hydrogen peroxide at neutral pH values. The affinity of vanadium(+4) for H_2O_2 may imply that vanadyl(+4) efficiently competes with GSH for endogenously formed H_2O_2 under physiological conditions (manuscript in preparation). Although dogma accepts and recognizes the reduction of vanadate to vanadyl(+4) (*57*), the reverse is likely to also be true. Activated NADPH oxidase leads to the formation of H_2O_2 which in turn can oxidize a fraction of the endogenous vanadyl pool to vanadate. Increased concentrations of vanadium in soluble and free forms (such as vanadate) will inhibit vanadate-sensitive PTPases, which leads to a higher concentration of steady-states phosphoryled protein and greater activation of cytPTK. Most of the protein tyrosine kinases known to date seem to be activated as a result of autophosphorylation on tyrosine moieties located near or at the active sites of PTKs. That vanadyl(+4) can be converted to vanadate via an NADPH-oxidative pathway has been previously demonstrated (*67*) and a link between vanadate, NADPH, and activation of tyrosine phosphorylation in cells was frequently observed (*68-70*).

Literature Cited

1. Simons, T. J. B. *Nature* **1979** *281*, 337.
2. Macara, I.G. *Trends Biochem. Sci.* **1980** *5*, 92.
3. Kahn, C. R. *Diabetes* **1994** *43*, 1066.
4. Heyliger, C. E.; Tahiliani, A. G.; McNeill, J. H. *Science* **1985** *227*, 1474.
5. Meyerovitch, J.; Farfel, Z.; Sack, J.; Shechter, Y. *J. Biol. Chem.***1987** *262*, 6658.
6. Brichard, S. M.; Okitolonda, W.; Henquin, J. C. *Endocrinology* **1988** *123*, 2048.
7. Venkatesan, N.; Avidan, A.; Davidson M. B. *Diabetes* **1991** *40*, 492.
8. Tolman, E. L.; Barris, E.; Burns, M.; Pansini, A.; Partridge, R. *Life Sci.* **1979** *25*, 1159.
9. Dubyak G. R.; Kleinzeller, A. *J. Biol. Chem.* **1980** *255*, 5306.
10. Shechter, Y.;Karlish, S. J. D. *Nature (Lond.)* **1980** *284*, 556.
11. Shechter, Y.; Shisheva, A. *Endeavour* **1993** *117*, 27.
12. Shechter Y.; Li, J.; Meyerovitch, J.; Gefel, D.; Bruck, R.; Elberg, G.; Miller, D. S.; Shisheva, A. *Mol. Cell. Biochem.* **1995** *153*, 39.
13. Brichard, S. M.; Henquin, J. C. *Trends Pharmacol. Sci.* **1995** *16*, 265.
14. Orvig C.; Thompson, K. H.; Battel, M.; McNeill, J. H. *Biol. Systems* **1995** *31*, 575.
15. Brichard, S. M.; Poltier, A. M.; Henquin ,J. C. *Endocrinology* **1989** *125*, 2510
16. Brichard, S. M.; Bailey, C. J.; Henquin, J. C. *Diabetes* **1990** *39*, 1326.
17. Brichard S. M.; Ongemba, L. N.; Henquin, J. C. *Diabetologia* **1992** *35*, 522.
18. Brichard, S. M.; Assimacopoulos-Jeannet, F.; Jeanrenaud, B. *Endocrinology* **1992** *131*, 311.
19. Ferber, S.; Meyerovitch, J.; Kriauciunas, K.M.; Khan, C.R. *Metab. Clin. Exp.* **1994** *43*, 1346.
20. Degani, H.; Gochin, M.; Karlish, S.J.D.; Shechter, Y. *Biochemistry* **1981** *20*, 5795.
21. Tamura S.; Brown, T. A.; Whipple, J. H.; Yamaguchi, Y. F.; Dubler, R. E.; Cheng, K.; Larner, J. *J. Biol. Chem.* **1984** *259*, 6650.
22. Shechter, Y.; Ron, A. *J. Biol. Chem.* **1986** *261*, 14945.
23. Milrapeix, M.; Decaux, J. F.; Kahn, A.; Bartrons, R. *Diabetes* **1991** *40*, 462.
24. Saxena, A. K.; Srivastava, P.; Baquer, N. Z. *Eur. J. Pharmacol.* **1992** *216*, 123.
25. Brichard, S. M.; Ongemba, L. N.; Girard, J.; Henquin, J. C. *Diabetologia* **1994** *37*, 1065.
26. Czech, M. P. *Annu. Rev. Physiol.* **1985** *47*, 357.
27. Waters, S. B.; Pessin, J. E. *Trends Cell Biol.* **1996** *6*, 1.
28. Mooney , R. A.; Bordwell, K. L.; Luhowskyj, S.; Casnellie, J. E. *Endocrinology* **1989** *124*, 422.
29. Strout, H.V.; Vicario, P.P.; Superstein, R.; Slater, E. E. *Endocrinology* **1989** *124*, 1918.
30. Fantus, I. G.; Ahmad, F.; Deragon, G. *Diabetes* **1994** *43*, 375.
31. D'Onofrio, F.; Le, M. Q.; Chiasson, J. L.; Srivastava, A. K. *FEBS Let.* **1994** *340*, 269.
32. Wilden, P. A.; Broadway, D. *J. Cell. Biochem.* **1995** *58*, 279.
33. Shisheva, A.; Shechter, Y. *Biochemistry* **1992** *31*, 8059.
34. Folli, F.; Saad, M. J. A.; Backer, J. M.; Khan, C.R. *J. Biol. Chem.* **1992** *267*, 22171.
35. Okada, T.; Kawano, Y.; Sakakibara, T.; Hazeki, O.; Ui, M. *J. Biol. Chem.* **1994** *269*, 3568.
36. Klippel, A.; Reinhard, C.; Kavanaugh, W. M.; Appell, G.; Escobedo, M. A.; Williams, L. T. *Mol. Cell. Biol.* **1996** *16*, 4117.
37. Ui, M.; Okada, T.; Hazeki, K.; Aseki, O. *Trends Biochem. Sci.* **1995** *20*, 303.
38. Cross, D. A. E.; Alessi, D. R.; Vandenheede, J. R.; McDowell, H. E.; Hundal, H. S.; Cohen, P. *Biochem. J.* **1994** *303*, 21.

Downloaded by UNIV OF GUELPH LIBRARY on October 31, 2012 | http://pubs.acs.org
Publication Date: December 10, 1998 | doi: 10.1021/bk-1998-0711.ch024

39. Li, J.; Elberg, G.; Sekar, N.; He, Z.; Shechter, Y. *Endocrinology* **1997** *138*, 2274.
40. Shisheva, A.; Shechter, Y. *FEBS Lett.* **1991** *300*, 93.
41. Shisheva, A.; Shechter, Y. *J.Biol. Chem.* **1993** *268*, 6463.
42. Elberg, G.; Li, J.; Shechter, Y. *J. Biol. Chem.* **1994** *269*, 9521.
43. Elberg, G.; Li, J.; Leibovitch, A.; Shechter, Y. *Biochim. Biophys. Acta* **1995** *1269*, 299.
44. Elberg, G.; He, Z.; Sekar, N.; Shechter, Y. *Diabetes*, **1997** *16*, 1684.
45. Swarup, G.; Cohen, S.; Garbers, D.L. *Biochem. Biophys. Res. Com.* **1982** *107*, 1104.
46. Denu J. M.; Stuckey, J. A.; Saper, M. A.; Dixon, J. E. *Cell* **1996** *87*, 361.
47. Tonks, N. K.; Neel, B. G. *Cell* **1996** *87*, 365.
48. Crans, D. C.; Keramidas, A. D.; Drouza, C. *Phosphorus, Sulfur, and Silicon*, **1997** *109-110*, 245.
49. Zhang, M.; Zhou, M.; Van Etten, R. L.; Stauffacher, C. V. *Biochemistry*, **1997** *36*, 215.
50. Paul, P. C.; Angus-Dunne, S. J.; Batchelor, R.J.; Einstein, F. W. B.; Tracey, A. S. *Can. J. Chem.* **1997** *75*, 183.
51. Li, J.; Elberg, G.; Libman, J.; Shanzer, A.; Gefel, D.; Shechter, Y. *Endocrine* **1995** *3*, 631.
52. Bradford, D.; Flint, A. J.; Tonks, N. K. *Science* **1994** *263*, 1397.
53. Sakurai, H.; Tsuchiya, M.; Nukatsuka, M.; Sofue, M.; Kawada, J. *J. Endocrinol.* **1990** *126*, 451.
54. Becker, D. J.; Ongemba, L. N.; Henquin, J. C. *Europ. J. Pharmacol.* **1994** *260*, 169.
55. Cantley, L. C.; Aisen, P. *J. Biol. Chem.* **1979** *254*, 1781.
56. Willsky, G. R.; White, D. A.; McCabe, B. C. *J. Biol. Chem.* **1984** *259*, 13273.
57. Li, J.; Elberg, G.; Crans, D. C.; Shechter, Y. *Biochemistry* **1996** *35*, 8314.
58. Liao, K.; Hoffman, R. D.; Lane, M. D. *J. Biol. Chem.* **1991** *266*, 6544.
59. Shekels, L. L.; Smith, A. J.; Van Etten, R. L.; Bernlohr, D. A. *Protein Sci.* **1992** *1*, 710.
60. Li, J.; Elberg, G.; Shechter, Y. *Biochim. Biophys. Acta* **1996** *1312*, 223.
61. Li, J.; Elberg, G.; Gefel, D.; Shechter Y. *Biochemistry* **1995** *34*, 6218.
62. Fantus, G. I.; Kadota, S.; Deragon, G.; Foster, B.; Posner, B. I. *Biochemistry* **1989** *28*, 8864.
63. Shisheva, A.; Shechter, Y. *Endocrinology* **1993** *133*, 1562.
64. Posner, B. I.; Faure, R.; Burgess, J. W.; Bevan, A. P.; Lachance, D.; Zhang-Sun, G.; Fantus, I. G.; Ng, J. B.; Hall, D. A.; Lum, B. S.; Shaver, A. *J. Biol. Chem.* **1994** *269*, 4596.
65. Huyer, G.; Liu, S.; Kelley, J.; Moffat, J.; Payette, P.; Kennedy, B.; Tsaprailis, G.; Gresser, M. J.; Ramachandran, C. *J. Biol. Chem.* **1997** *272*, 843.
66. Chasteen, D. N.; Grady, J. K.; Holloway, C. E. *Inorg. Chem.* **1986** *25*, 2754.
67. Liochev, S.; Fridovich, I. *Arch. Biochem. Biophys.* **1987** *255*, 274.
68. Trudel, S.; Downey, G. P.; Grinstein, S.; Paquet, R. M. *Biochem. J.* **1990** *269*, 127.
69. Trudel, S.; Paquet, M.; Grinstein, S. *Biochem. J.* **1991** *276*, 611.
70. Grinstein, S.; Furuya, W.; Lu, D. J.; Mills, G. B. *J. Biol. Chem.* **1990** *265*, 318.

Downloaded by UNIV OF GUELPH LIBRARY on October 31, 2012 | http://pubs.acs.org
Publication Date: December 10, 1998 | doi: 10.1021/bk-1998-0711.ch024

Downloaded by CORNELL UNIV on October 31, 2012 | http://pubs.acs.org
Publication Date: December 10, 1998 | doi: 10.1021/bk-1998-0711.ch025

Chapter 25

Mechanism of Insulin Mimetic Action of Peroxovanadium Compounds

B. I. Posner, C. R. Yang, and A. Shaver

Departments of Medicine and Chemistry, McGill University, Montreal, Quebec H3A 2B2, Canada

The peroxovanadium compounds (pVs) have been shown to be insulin mimetic. They achieve this by potently activating the insulin receptor kinase (IRK) in the complete absence of insulin. This mechanism of insulin mimesis differs from that of vanadate (V) whose site(s) of action appear(s) to be distal to the IRK. Evidence to date indicates that pVs activate the IRK by inhibiting an intimately associated phosphotyrosine phosphatase (PTP) which normally prevents IRK autophosphorylation. When this enzyme is inhibited the IRK is able to autoactivate in the absence of any restraint to autophosphorylation. Both V and pVs are potent inhibitors of PTPs. However V, unlike pVs, is readily chelated and hence in biological systems is less available for effecting PTP inhibition. The inhibition of PTP by pVs appears to involve the irreversible oxidation of a key cysteine residue in the catalytic site of the enzyme. In biological systems pV appears to inhibit, relatively selectively, the PTP associated with IRKs which are intracellular (ie. within the endosomal system of the cell). This observation has supported the view that important aspects of IRK transmembrane signaling occur within the cell. The efficacy of pVs to lower blood glucose levels in both normal and diabetic animals indicates that a key molecular target for the development of insulin mimetic drugs is the IRK-associated PTP.

Insulin action begins with the binding of insulin to its receptor; a heterotetrameric protein made up of two α subunits, and two transmembrane β subunits whose cytosolic domains contain tyrosine kinase activity. Following insulin binding to the α subunit of the receptor the β subunit undergoes autophosphorylation on tyrosine residues leading to activation of the insulin receptor kinase (IRK) towards exogenous substrates. Numerous studies have shown that this activation process is the key to insulin signaling (*1*). Indeed mutated IRK molecules, unable to undergo

In Vanadium Compounds; Tracey, A., et al.;
ACS Symposium Series; American Chemical Society: Washington, DC, 1998.

Downloaded by CORNELL UNIV on October 31, 2012 | http://pubs.acs.org
Publication Date: December 10, 1998 | doi: 10.1021/bk-1998-0711.ch025

autophosphorylation and autoactivation, cannot entrain the insulin signaling sequence (*2*). Following the binding of insulin to the IRK there is rapid internalization of the insulin-IRK complex into a tubulovesicular organelle within the cell, known as the endosomal system or endosomes (ENs) (*3*). Substantial evidence now exists establishing this step as part of the mechanism involved in the insulin signaling sequence (*4*).

The Discovery Of pV Complexes. Studies in the early to mid 1980s established vanadate as an insulin mimetic agent in vitro and in vivo. We subsequently showed that the combination of vanadate and H_2O_2 activated the IRK and promoted insulin signaling in a synergistic manner (*5*), and that this was due to peroxovanadium (pV) complexes which formed on combining vanadate and H_2O_2 (*6*). Different pVs, synthesized by incorporating different ancillary ligands into the complex, could be readily differentiated from one another using ^{51}V NMR. The pV complexes were crystallizable from solution, stable at neutral pH in the absence of light and far more potent as insulin mimetics than vanadate (*7*). Subsequent to our discovery of the insulin like activity of pVs these compounds were shown to mimic a wide range of insulin effects (*8-9*).

pVs Inhibit IRK-Associated PTP(s). In subsequent studies we evaluated the mechanism by which pVs activate the IRK in the complete absence of insulin (*7*). Initial studies showed that incubating partially purified IRKs with pVs did not activate the IRK in contrast to what is seen on incubation with insulin (*6*). When ENs, isolated from rats previously treated with insulin, were incubated with ATP we could demonstrate increasing tyrosine phosphorylation of the IRK which spontaneously diminished in parallel with the depletion of ATP in the incubation mixture. Coincubation with pV augmented the level of IRK tyrosine phosphorylation and completely abrogated the diminution of phosphorylation as ATP levels diminished during the incubation (*10*). Thus pVs inhibit a dephosphorylation process affecting the IRK, and we inferred that this was due to the inhibition of an IRK-associated phosphotyrosine phosphatase (PTP) (*10*). It has subsequently been shown that pVs constitute the most potent class of PTP inhibitors described to date (*7*).

The Mechanism of PTP Inhibition Effected by pVs.

To study the mechanism by which pVs inhibit PTPs we evaluated their action on PTP1C (SHPTP1). To do this we prepared highly purified enzyme for our analyses. The coding region of this enzyme was cloned into the plasmid pET-3C which was used to transform E.Coli BL-21 (DE3) which carries the T7 polymerase gene under the control of the lacUV5 promoter. The expression of PTP1C was induced by adding 20 uM isopropylthiogalactoside (IPTG) to the bacterial culture medium, and the cells were subsequently harvested by centrifugation and broken by sonication in the presence of high salt buffer containing mild detergent. Enzyme activity at each step in the purification was evaluated. To assure stability the enzyme was kept in the presence of 1 mM EDTA and 2mM dithiothreitol

(DTT). PTP1C was purified to homogeneity in a 3-step procedure, involving precipitation by ammonium sulphate (30-50%) followed by chromatography on DEAE-Sephadex A-50 (elution with 0-0.4 NaCl gradient at pH 7.5) and then SP-Sephadex C-50 (elution with 0-0.5 M NaCl gradient at pH7.0). This last step yielded a peak of activity, which migrated as a single protein band on gel electrophoresis indicating that attainment of a high level of purity. This was confirmed by establishing that the amino acid composition of the protein band conformed precisely to the predicted composition based on previous studies (*11*).

Figure 1 illustrates the inhibitory effect of bpV (pic), bpV (phen), and vanadate on PTP1C activity. As can be seen 50% inhibition (I_{50}) of PTP1C activity was produced at a concentration of 2.5×10^{-8} M bpV (pic), 2×10^{-7} M bpV (phen), and 6×10^{-7} M vanadate in the absence of EDTA. Whereas 1 mM EDTA had no effect on the inhibitory potency of the pV compounds it reduced the I_{50} of vanadate to 3×10^{-3} M. We have routinely observed that vanadate has an inhibitory potency 0.001% that of pVs on IRK-associated PTP activity in ENs. Thus in complex mixtures the chelation of vanadate is probably responsible for a substantial part of its reduced potency compared to pVs as an inhibitor of PTPs. Further studies of 18 different pVs showed an I_{50} ranging from 2×10^{-7} to 2×10^{-8} M. The I_{50} of the tungstate complex bpW(pic) was 3×10^{-8} M and that of the molybdate complex bpMo (pic) was 7×10^{-7} M.

Table I illustrates that the inhibitory effect of vanadate but not that of pV can be reversed by a strong chelating agent. Thus premixing desferrioxamine B with either vanadate or pV prevented only the inhibitory activity of the former and not the latter. This confirms the above data indicating that vanadate is readily chelated and thereby inactivated but pV is not. When vanadate or pV were first added to the enzyme so as to effect complete inhibition and desferrioxamine was subsequently added only inhibition by vanadate was reversed indicating that it forms a reversible association with the enzyme. The failure to reverse the inhibitory effect of pV may reflect irreversibility of inhibition but can be explained by the failure of desferrioxamine to chelate this compound.

To evaluate the possibility that pV promotes irreversible inhibition of PTP1C we incubated the enzyme with vanadate or bpV (phen) and at various times thereafter added DTT and EDTA to block their interaction with PTP1C (Fig. 2). DTT acts to convert pV compounds to vanadate; whereas EDTA, as shown above and elsewhere (*12*) chelates free vanadate and renders it unavailable to interact with the enzyme. As can be seen the inhibition effected by vanadate is virtually completely reversible. In contrast that effected by bpV (phen) became irreversible in a time and temperature dependent manner. The rate of inactivation evoked by bpV (phen) was considerably accelerated by incubating the mixture at 22° C at which temperature it was essentially complete by 10 mins of incubation.

Previous work has shown that PTP activity involves a critical cysteine residue at the active site of the molecule. It has been shown that pV compounds oxidize this residue in the enzyme PTP1B (*13*). This correlated with the inactivation of PTP1B and hence represents the likely reason for that inactivation. So too in our system we observed that cysteine residues were oxidized by exposure to bpV (phen) under conditions which led to the irreversible inactivation of the enzyme (Table II). We

Downloaded by CORNELL UNIV on October 31, 2012 | http://pubs.acs.org
Publication Date: December 10, 1998 | doi: 10.1021/bk-1998-0711.ch025

Downloaded by CORNELL UNIV on October 31, 2012 | http://pubs.acs.org
Publication Date: December 10, 1998 | doi: 10.1021/bk-1998-0711.ch025

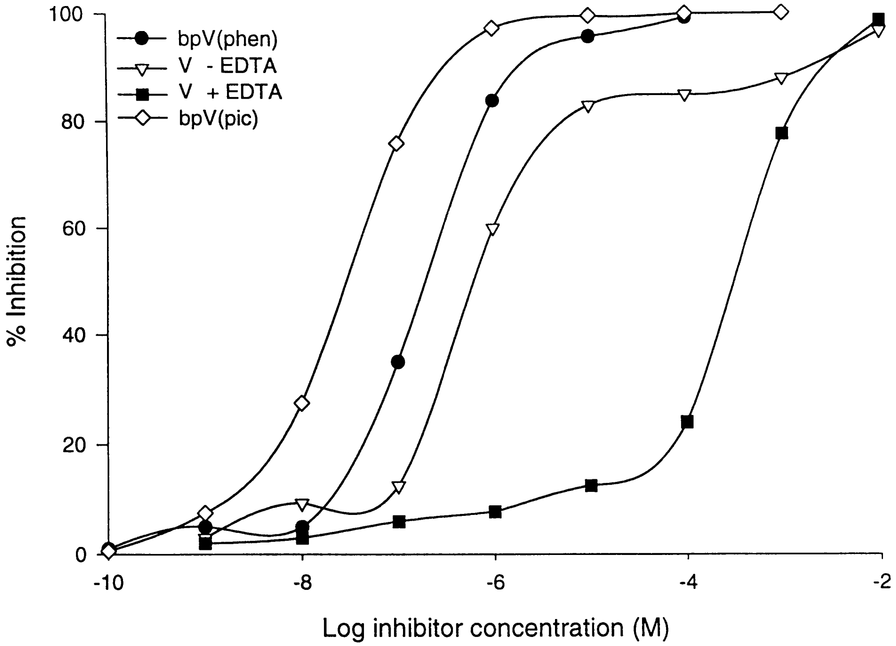

Figure 1: Inhibition of PTP-1C By Vanadate (V) and Peroxovanadium Compounds. PTP-1C (7 ng), purified as briefly described in the text, was incubated with vanadate (V) in the presence (■) or absence (▽) of 1 mM EDTA, bpV(pic) (◊) or bpV(phen) (●) in 25 mM phosphate buffer, pH 7.4 containing 0.01% of Bovine Serum Albumin at 4^{o} C for 10 min. PTP enzyme activity was subsequently measured by adding ^{32}P-labelled poly (Glu-Tyr) (10 μM) to the mixture and evaluting its dephosphorylation. ^{32}P – poly (Glu-Tyr) was prepared by incubating unlabeled material with the activated IRK and ^{32}P-ATP for 1 hr. at 37°C. The percentage inhibition was calculated based on PTP-1C activity in the absence of inhibitors.

Downloaded by CORNELL UNIV on October 31, 2012 | http://pubs.acs.org
Publication Date: December 10, 1998 | doi: 10.1021/bk-1998-0711.ch025

Table I. Reversal by Desferrioxamine B of the Inhibition of PTP-1C by Vanadate but not pV.

Inhibitor	Plus Desferrioxamine B		Enzyme Activity
	Pre	Post	(% Control)
None	-	-	100
Na_3VO_4	-	-	1.5
	+	-	98
	-	+	90
bpV(phen)	-	-	0.5
	+	-	1.5
	-	+	1.5

PTP-1C was incubated with either 1 mM Vanadate or 10 μM bpV(phen) in 25 mM phosphate buffer (pH 7.4) – 0.01% Bovine Serum Albumin for 20 mins at 4°C. Desferrioxamine (final concentration 10 mM) was added to vanadate or bpV(phen) in some experiments (Pre) or incubated with the inhibited enzyme for 20 mins at 4°C (Post) prior to proceeding with enzyme assays as described in the legend of Figure 1.

Downloaded by CORNELL UNIV on October 31, 2012 | http://pubs.acs.org
Publication Date: December 10, 1998 | doi: 10.1021/bk-1998-0711.ch025

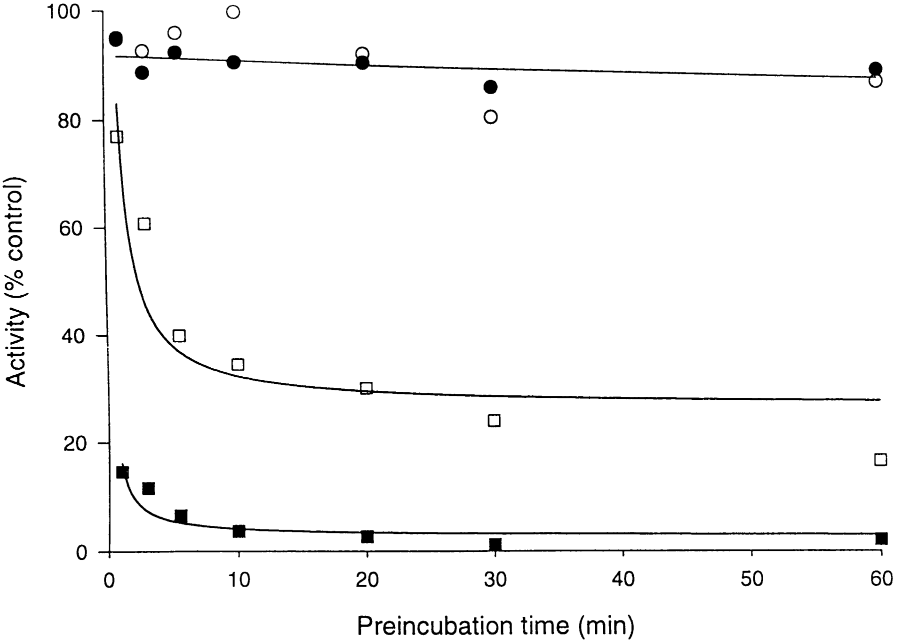

Figure 2: Time and Temperature-Dependent Reversal of Inhibition of PTP-1C Following Preincubation with Vanadate (V) or bpV[phen]. PTP-1C was preincubated with either 1 mM vanadate (o, ●) or 10 μM bpV[phen] (□,■) for different durations at 4° C (o, □) or 22° C (●,■). Following this, 50 mM DTT and 5 mM EDTA (final concentrations) were added to the mixture and PTP activity was assessed by a further incubation for 30 min at 4° C with ^{32}P-poly(Glu-Tyr). The measured PTP activities are depicted as a percentage of the full activity of enzyme in the absence of inhibitor.

Table II. Ratio of Recovery of Amino Acids from PTP-1C incubated with bpV(phen) or buffer (Control) followed by alkylation.

Amino acids		Ratio of Recoveries from Control and bpV(phen)-Treated PTP-1C
Asx		0.99
Val		1.05
Ile		1.05
Tyr		0.97
Phe		0.97
Lys		0.99
Gly		1.00
Met		1.00
CmCys	#1	0.74
	#2	0.72

Purified PTP-1C (200 μg) was incubated with 1 mM bpV(phen) in 20 mM imidazole buffer (pH 7.4) for 5 mins at 22 °C and then for an additional 60 mins at 4 °C. The enzyme was then denatured with 6 M guanidine-HCl and further treated with 0.15 M DTT at 37 °C for 2 hrs. Alkylation of the enzyme was performed by adding iodoacetic acid to a final concentration of 0.3 M for 30 mins in the dark at room temperature. The reaction was terminated by adding 1 % 2-mercaptoethanol. The solution was desalted by chromatography on a SEP-pak column and the protein was hydrolyzed in 6 N HCl by standard procedures. Amino acids were determined on a Beckman 6300 series autoanalyzer. In order to quantitate carboxymethyl cysteine (CmCys) with precision the amounts of loaded sample were larger than in routine assays and hence only some of the amino acid were readily assayable. As is evident the recovery for all assayed amino acids was the same for enzyme pretreated with bpV(phen) and for untreated enzyme except for CmCys. In this latter case the recovery was 30% less in enzyme pretreated with bpV(phen). Since PTP-1C contains 7 cysteine residues we conclude that 2 of the 7 residues were oxidized and hence unavailable for alkylation by iodoacetic acid.

Downloaded by CORNELL UNIV on October 31, 2012 | http://pubs.acs.org
Publication Date: December 10, 1998 | doi: 10.1021/bk-1998-0711.ch025

thus agree with the conclusion of Huyer et al (*13*) that the likely mechanism by which pV compounds inactivate PTPs is by oxidizing the active site cysteine. This implies that the recovery from the inhibition induced by pVs requires the production of new enzyme.

Role of IRK-Associated PTP(s) in IRK Activation.

The observation that pV compounds activate the IRK and correspondingly inhibit the dephosphorylation of IRK argues for a causal relationship between these two processes. In support of this notion is our observation of a close correlation between the level of IRK activation observed and the level of inhibition of the IRK-associated PTP (Figure 3)(*7*).

It is also of interest that under circumstances where bpV (phen) fully inhibited the IRK-associated PTP(s) in ENs little or no inhibition of IRK dephosphorylation was seen in plasma membranes (PM) (*14*). The selectivity of pV action on the endosomal system was further supported by a detailed kinetic analysis of the time course of IRK activation in ENs and PM following bpV (phen) administration to rats (Figure 4). In this study it can be seen that the endosomal IRK was activated earlier and to a greater extent than that of PM. Furthermore it was shown that the presence of activated IRK in PM was secondary to recycling of activated IRK from ENs (*15*). In addition it was shown that a dose of bpV (phen) which fully inhibited the IRK-associated PTP(s) inhibited the activity of other PTPs in ENs by only 20%. Thus the data suggest that the IRK-associated PTP(s) in hepatic ENs are relatively sensitive to inhibition by bpV (phen).

Downloaded by CORNELL UNIV on October 31, 2012 | http://pubs.acs.org
Publication Date: December 10, 1998 | doi: 10.1021/bk-1998-0711.ch025

Mechanism of pV-induced IRK Tyrosine-Phosphorylation

How does the inhibition of IRK-associated PTP activity lead to IRK activation in the absence of insulin? Our model postulates that the IRK is prevented from undergoing tyrosine phosphorylation and hence activation in the absence of insulin by virtue of its associated PTP(s). This arrangement would assure that insulin signaling, entrained by IRK activation, does not occur inappropriately (ie. in the absence of the agonist, insulin). The administration of pVs, by inhibiting IRK-associated PTP(s), would permit tyrosine phosphorylation by either the intrinsic tyrosine kinase activity of the IRK or that of exogenous tyrosine kinase whose impact would now be uncovered in the absence of corresponding PTP function.

To distinguish between these two possibilities we compared the impact of bpV (phen) on the tyrosine phosphorylation of normal and kinase negative mutant IRKs. The latter, in view of their lack of kinase function could not be responsible for any IRK tyrosine phosphorylation seen following exposure to bpV (phen). Conversely, if a significant level of tyrosine phosphorylation was effected by an exogenous tyrosine kinase we would see substantial phosphorylation of the mutant IRK in the presence of pVs.

Figure 5 indicates that when HTC hepatoma cells, bearing normal IRKs, were exposed to bpV (phen) there was IRK tyrosine phosphorylation. In contrast when cells, bearing a mutant IRK devoid of tyrosine kinase activity, were exposed to bpV

Downloaded by CORNELL UNIV on October 31, 2012 | http://pubs.acs.org
Publication Date: December 10, 1998 | doi: 10.1021/bk-1998-0711.ch025

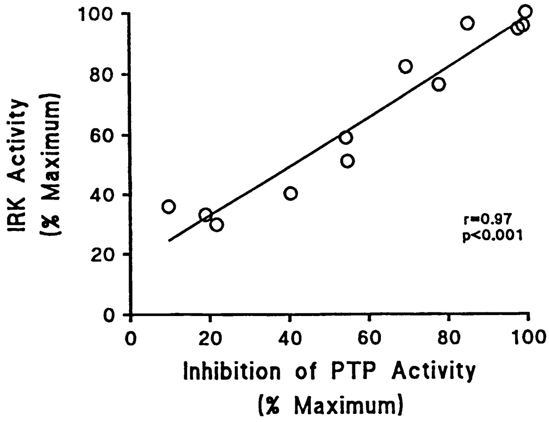

Figure 3: Correlation Between Inhibition of PTP Activity and IRK Activation in ENs after Treatment with bpV(phen) and Insulin. Rats were fasted overnight, and injected with bpV(phen). Insulin was injected at different times thereafter and ENs were isolated and assayed for both IRK activation and inhibition of IRK dephosphorylation as described in detail in ref.15. The level of IRK activation was plotted against the corresponding level of PTP inhibition. As is evident there was a striking correspondence between the 2 supporting a role for IRK-associated PTP inhibition as the basis for IRK activation seen following pVs. These data are adapted from Figure 2 in ref.15.

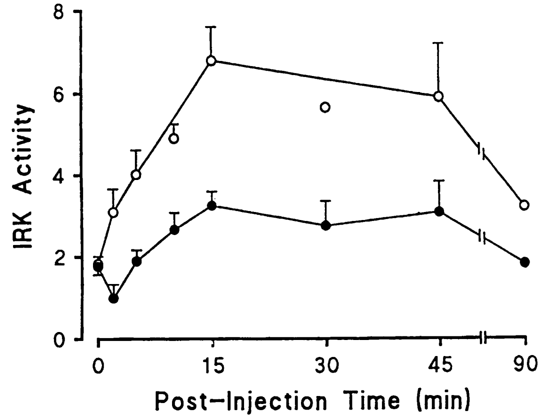

Figure 4: Time Course of IRK Activation in PM and ENs Following Injection of bpV(Phen) into Rats. Fasted rats were injected with bpV(phen) (0.6 uM/100 g bwt) and sacrificed at the noted times after which hepatic ENs and plasma membrane (PM) fractions were isolated. The activity of the IRK in ENs (o) and PM (●) was determined as described in detail in Figure 3 of ref.15 from which this figure is adapted.

Downloaded by CORNELL UNIV on October 31, 2012 | http://pubs.acs.org
Publication Date: December 10, 1998 | doi: 10.1021/bk-1998-0711.ch025

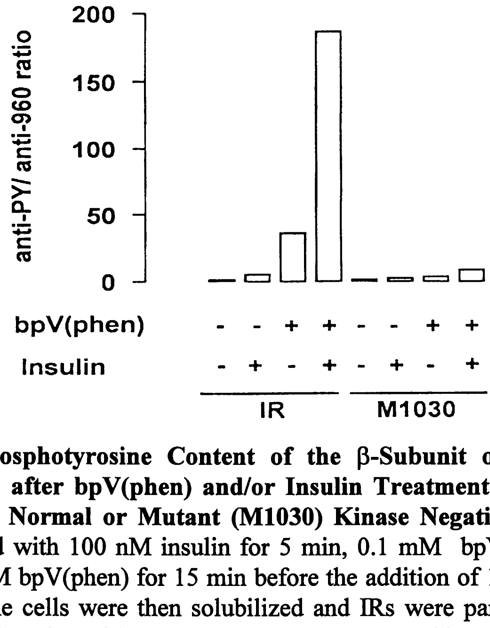

Figure 5: Phosphotyrosine Content of the β-Subunit of the Insulin Receptor (IR) after bpV(phen) and/or Insulin Treatment of Hepatoma Cells Bearing Normal or Mutant (M1030) Kinase Negative IRs. Cells were incubated with 100 nM insulin for 5 min, 0.1 mM bpV(phen) for 20 min, or 0.1 mM bpV(phen) for 15 min before the addition of 100 nM insulin for 5 min. The cells were then solubilized and IRs were partially purified, immunoprecipitated with anti-IR antibodies, subjected to SDS-polyacrylamide gel electrophoresis and immunoblotted with antiphosphotyrosine and anti-IR antibodies as described in detail by Band et al (Molec.Endocrinol., in press) from which this figure was adapted. As can be seen the kinase negative IR (M1030) cannot promote β-subunit tyrosine phosphorylation as can the normal IR in the presence of bpV(phen) ± insulin.

Downloaded by CORNELL UNIV on October 31, 2012 | http://pubs.acs.org
Publication Date: December 10, 1998 | doi: 10.1021/bk-1998-0711.ch025

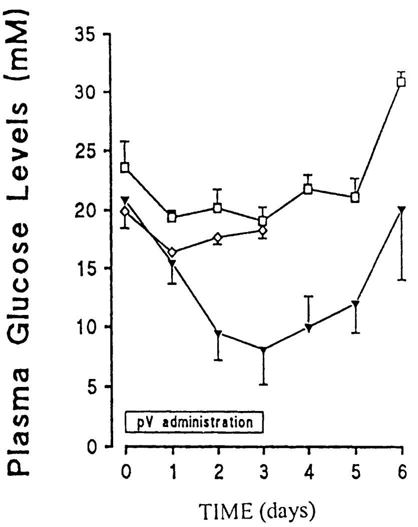

Figure 6: Effect of Subcutaneous Injections of bpV(phen) and vanadate on Fasting Plasma Glucose Levels in Insulin-Deprived Diabetic Rats. Diabetic rats were deprived of insulin for 16 hours so that their blood glucose levels rose to 20 to 25 mM (normal levels = 5-7 mM). They were then injected subcutaneously with bpV(phen), 36 μmol/kg body wt. b.i.d. (▼, n = 6); vanadate, 36 μmol/kg body wt. b.i.d. (◊, n = 6); or phosphate-buffered saline, b.i.d. (□ , n = 6) for 3 days. All injections were withheld from days 4 to 6. Blood glucose determinations and other experimental details are described in detail in Figure 4 of ref.16 from which this figure is adapted. Whereas bpV(phen) injections lowered blood glucose to near-normal levels, an equimolar dose of vanadate was without effect.

(phen) no IRK tyrosine phosphorylation was seen. Thus the source of IRK tyrosine phosphorylation following exposure to pVs is the IRK itself. Presumably the low level of intrinsic kinase activity is sufficient to effect autophosphorylation so that the IRK is "bootstrapped" into a state of augmented activation. The slower time course of activation seen following pV, compared to that seen following insulin (*7*), is consistent with a slow autocatalytic process in which the receptor's active state is augmented as its level of tyrosine phosphorylation increases.

The IRK-Associated PTP(s) as a Therapeutic Target

The above studies have shown that pVs act by inhibiting the function of IRK-associated PTP(s) leading to IRK autophosphorylation and activation with the entrainment of downstream insulin signaling. Thus pVs and other agents able to inhibit the IRK-associated PTP(s) should evoke insulin mimesis and hence be potentially applicable as agents for the treatment of Diabetes Mellitus. In recent studies Jean-Francois Yale et al showed that administering pV compounds to rats lowered blood sugar in both normal and diabetic animals. This was recently well illustrated in a study on diabetic BB Wistar rats whose condition resembles that of Type I Diabetes Mellitus (Insulin Dependent Diabetes Mellitus, IDDM) (*16*). When insulin is withdrawn from these diabetic animals they become hyperglycemic and decline into ketoacidosis and death. As illustrated in Figure 6 giving bpV (phen) by daily intraperitoneal injection to diabetic BB Wistar rats, withdrawn from insulin 24 hours before, resulted in normalization of blood glucose levels. Thus agents directed at the IRK-associated PTP(s) should eventually be able to replace insulin. It is also likely that some of the devised agents will be orally administrable thus precluding the need for treatment by injection as is required when administering insulin.

Summary

Studies to date have clearly established that pVs act to mimic insulin by activating the IRK and hence entraining the insulin signaling cascade. This activation follows on the inhibition by pVs of IRK-associated PTP(s) which enables the IRK to effect autophosphorylation and hence autoactivation. This sequence appears to differ from that involved in the insulin mimetic effects of vanadate which seems to act primarily at postreceptor site(s) to yield insulin signaling. Study of the mechanism of pV action has uncovered an important mechanism for regulating IRK function (ie. the IRK-associated PTP(s)). It is anticipated that agents targeted against the IRK-associated PTP(s) will eventually be developed to effect insulin signaling in the complete absence of insulin.

Literature Cited

1. Kahn, C. R. *Diabetes* **1994**, *43*, 1066-1084.
2. Chou, C. K.; Dull, T. J.; Russell, D. S.; Gherzi, R.; Lebwohl, D.; Ullrich, A.; Rosen, O. M. *J. Biol. Chem.* **1987** *262,* 1842-1847.

Downloaded by CORNELL UNIV on October 31, 2012 | http://pubs.acs.org
Publication Date: December 10, 1998 | doi: 10.1021/bk-1998-0711.ch025

3. Khan, M. N.; Baquiran, G.; Brule, C.; Burgess, J.; Foster, B.; Bergeron, J. J. M.; Posner, B.I. *J. Biol. Chem.* **1989**, *264,* 12931-12940.
4. Bevan, A.P.; Drake, P.; Bergeron, J.J.M.; Posner, B.I. *Trends Endocrinol.Metab.* **1996**, *7*, 13-21.
5. Kadota, S.; Fantus, I. G.; Deragon, G.; Guyda, H. J.; Posner, B. I. *J. Biol. Chem.* **1987** *262,* 8252-8256.
6. Kadota, S.; Fantus, I. G.; Deragon, G.; Guyda, H. J.; Hersh, B.; Posner B. I. *Biochem. Biophys. Res. Commun.* **1987**, *147,* 259-266.
7. Posner, B. I.; Faure, R.; Burgess, J. W.; Bevan, A. P.; Lachance, D.; Zhang-Sun, G.; Fantus, I. G.; Ng, J. B.; Hall, D. A.; Lum, B. S.; Shaver, A. *J. Biol. Chem.* **1994,** *269,* 4596-4604.
8. Fantus, I. G.; Kadota, S.; Deragon, G.; Foster, B.; Posner, B. I. *Biochem.* **1989**, *28,* 8864-8871.
9. Bevan, A. P.; Burgess, J. W.; Yale, J.-F.; Drake, P. G.; Lachance, D.; Baquiran, G.; Shaver, A.; Posner, B. I. *Am. J. Physiol.* **1995**. *268,* E60-E66.
10. Faure, R.; Baquiran, G.; Bergeron, J. J. M.; Posner, B. I. *J. Biol. Chem.* **1992**, *267,* 11215-11221.
11. Shen, S.-H.; Bastien, L.; Posner, B. I.; Chrétien, P. *Nature* **1991,** *352*, 736-739.
12. Crans, D. C.; Mahroof-Tahif, M.; Keramidas, A. D. *Mol. Cell. Biochem.* **1995**, *153,* 17-24.
13. Huyer, G.; Liu, S.; Kelly, J.; Moffat, J.; Payette, P.; Kennedy, B.; Tsaprailis, G.; Gresser, J. J.; Ramachandran, C. *J. Biol. Chem.* **1997**, *272*, 843-851.
14. Drake, P. G.; Bevan,A. P.; Burgess, J. W.; Bergeron, J. J. M.; Posner, B. I.; *Endocrinol.* **1996**, *137*, 4960-4968.
15. Bevan, A. P.; Burgess, J. W.; Drake, P. G.; Shaver, A.; Bergeron, J. J. M.; Posner, B. I. *J. Biol. Chem.* **1995**, *270,* 10784-10791.
16. Yale, J.-F.; Lachance, D.; Bevan, A. P.; Vigeant, C.; Shaver, A.; Posner, B. I. *Diabetes* **1995**, *44,* 1274-1279.

Downloaded by CORNELL UNIV on October 31, 2012 | http://pubs.acs.org
Publication Date: December 10, 1998 | doi: 10.1021/bk-1998-0711.ch025

Downloaded by UNIV OF GUELPH LIBRARY on October 31, 2012 | http://pubs.acs.org
Publication Date: December 10, 1998 | doi: 10.1021/bk-1998-0711.ch026

Chapter 26

Chemical and Pharmacological Studies of a New Class of Antidiabetic Vanadium Complexes

K. H. Thompson[1], V. G. Yuen[2], J. H. McNeill[2], and C. Orvig[1]

[1]Chemistry Department, The University of British Columbia, Vancouver, British Columbia V6T 1Z1, Canada
[2]Faculty of Pharmaceutical Sciences, The University of British Columbia, Vancouver, British Columbia V6T 1Z3, Canada

Bis(maltolato)oxovanadium(IV) (BMOV, $VO(ma)_2$) is a compound recently developed for oral treatment of diabetes mellitus. Therapeutic benefit will derive from optimization of ligand design to improve bioavailability and consistency of biological response. Advantages of BMOV over inorganic vanadium compounds include its increased tissue uptake and absorption characteristics, low toxicity, hydrolytic and thermodynamic stability, and neutral charge. Stability constants for the binding of 1 and 2 maltolato ligands to vanadyl are $\log K_1 = 8.80$, and $\log K_2 = 7.51$, for the bis(ligand) complex, $\log \beta_2 = 16.31$. The geometry around the vanadium in $VO(ma)_2$ is square pyramidal. Two pathways, aquo and hydroxo, give a cis-dioxoanion, $[VO_2(ma)_2]^-$, for oxidation of BMOV with O_2 in water. *In vivo*, BMOV is more orally effective, compared both to inorganic vanadium salts and to close analogues of BMOV, such as bis(kojato)oxovanadium(IV).

Vanadium compounds have a long history as insulin mimetic agents. Sodium vanadate was reported to have an oral insulin-like effect in human diabetics in 1899 (1). The *in vitro* insulin mimetic effects of vanadium salts were first reported almost 20 years ago (2). However, it is only in the last decade or so that vanadium's pharmacological potential has been systematically explored, starting with Heyliger *et al.* in 1985 (3). Other metal salts have been tried [see (4) and references cited therein], both *in vivo* and *in vitro*, but none have rivalled vanadium salts as effective insulin substitutes. Even though the Canadian discovery of exogenous insulin as a viable therapy for insulin-dependent diabetes mellitus (5) revolutionized diabetes care, none of the available insulins (porcine, bovine, and most recently, genetically engineered human) is orally effective. There is thus a great need for an effective oral remedy.

In Vanadium Compounds; Tracey, A., et al.;
ACS Symposium Series; American Chemical Society: Washington, DC, 1998.

Downloaded by UNIV OF GUELPH LIBRARY on October 31, 2012 | http://pubs.acs.org
Publication Date: December 10, 1998 | doi: 10.1021/bk-1998-0711.ch026

Concomitant with renewed pharmacological interest has been an accelerated interest in elucidating the chemistry of vanadium complexes (6-8). Significant progress has been made since the initial studies in understanding the mechanism and the *in vivo* course of vanadium's glucose- and lipid-lowering effects (9, 10) both in experimental animals and, more recently, in human studies (11, 12).

Yet, the very low apparent bioavailability of oral vanadium (13) variability of response (14, 15), and questions about toxicity (16) have limited clinical usefulness so far. A pressing need for better absorbed, more efficacious, vanadium compounds has prompted intensive searches for biologically relevant vanadium complexes.

Classes of Vanadium Compounds Known to be Insulin Mimetics

Three classes of vanadium compounds have been studied for their insulin mimetic effects: 1) inorganic vanadium salts, both anionic (vanadates, $[VO_4]^{3-}$) and cationic (vanadyl, VO^{2+}), 2) combinations of vanadate and hydrogen peroxide, peroxovanadates, and 3) chelated vanadyl complexes. In these three categories a variety of different compounds have been tried. In the pioneering study, sodium metavanadate was shown to have oral insulin-like effects by lowering blood glucose in streptozotocin (STZ)-diabetic rats without raising blood insulin levels (3). Posner *et al.* and Crans *et al.* have recently examined combinations of sodium vanadate and hydrogen peroxide, and have shown that these also have a number of very potent insulin mimetic effects (17, 18). Yale *et al.* have prepared a number of discrete vanadium(V)peroxo compounds with one or two peroxides bound and one organic ligand, usually with a -1 or -2 charge (19). The third category, the chelated vanadyl complexes, offers a wide scope for deliberate design improvements (20). Cam *et al.* have reported a compound, naglivan, which has a cysteine backbone with an octyl group attached (21). In addition, a variety of bis(ligand)vanadyl complexes have been reported by Sakurai and co-workers (22). Dihydroxamate vanadyl complexes have been developed by Shechter *et al.* (23) and bis(hydroxypyrone) vanadyl complexes are being investigated on an ongoing basis in our group (7, 24-26).

Strategic Design of Biologically Active Vanadium Complexes

Biologically (particularly medically) relevant metal complexes have several requirements in terms of their synthetic design. First, a biologically active metal complex should have a sufficiently high thermodynamic stability to deliver the metal to the active site, where it should then possibly fall apart. (A compound should have an even higher thermodynamic stability if the metal complex itself has activity). The metal ligand binding should be hydrolytically stable. Many metals used for synthesis of biologically active complexes (e.g., indium, gallium, aluminum, lanthanides, technetium and rhenium) undergo hydrolysis, particularly in a biological system, if the metal ligand binding constants are not high enough (27). The ligation kinetics are important; if a chelating agent is developed to remove a metal or to deliver a metal to an active site, then the kinetics with which the metal ion undergoes ligation or deligation chemistry are of great importance. The molecular weight of the metal complex is critical because metal complexes may enter cells by passive diffusion. This process requires metal complexes of a relatively low molecular weight and of a neutral charge and water solubility. The complex design needs to incorporate a balance between the lipophilic nature of the complex and its hydrophilicity, in order to maintain neutral charge. Compounds of low molecular weight with neutral charge and some water solubility are soluble in almost any medium, and may slip through biological membranes by passive diffusion. Lastly, functionality of the ligand should be considered; a biologically directing portion of the molecule may be used to functionalize the ligand in order to increase specificity. In the case of insulin mimetic complexes, a key feature is oral bioavailability as this is what distinguishes vanadium insulin-mimetics from the presently available treatment modality; insulin; being a protein, is not orally bioavailable and must be taken by injection.

Bis(maltolato)oxovanadium(IV)

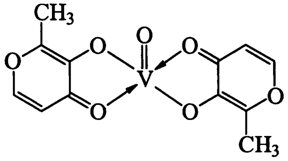

BMOV, $VO(ma)_2$

An insulin mimetic complex which has been extensively tested and characterized recently serves to illustrate many of these principles of strategic design. Bis(maltolato)oxovanadium(IV) (BMOV) is composed of 2 bidentate monoprotic maltolato ligands chelating an oxovanadium(IV) group. It is thermodynamically and hydrolytically stable, of neutral charge, and of low molecular weight. Although functionality of the ligand was not a key element in its design, maltol has proved to be a fortuitous choice, in that it is an approved food additive and has been shown to have antioxidant properties (28), which are desirable for therapy of diabetes (4).

Solubility, Molecular Weight, IR, Crystal Structure. BMOV can be prepared on a large scale (up to 0.5 kg) simply by combining vanadyl sulphate with maltol at roughly neutral pH, to give a 95% yield (26). It has a molecular weight of 317, and is soluble (mM scale) in a number of organic solvents and water (26). BMOV has one unpaired electron, characteristic of the vanadyl unit, and a V=O stretching frequency in the infrared spectrum (995 cm^{-1}), suggesting that there is no ligand (or a weakly bound solvent) in the sixth position. The crystal structure of the compound (Figure 1) shows that the two ligands are oriented trans to one another in the base of a square pyramid (26). The vanadium is out of the plane of the four chelating oxygens by 0.70 Å and the V=O bond is 1.61 Å (26).

Downloaded by UNIV OF GUELPH LIBRARY on October 31, 2012 | http://pubs.acs.org
Publication Date: December 10, 1998 | doi: 10.1021/bk-1998-0711.ch026

Stability Constants, Speciation Data, Reduction Potential, Oxidation Kinetics. The stability constants for the binding of 1 and 2 maltolato ligands to vanadyl are relatively high; the step-wise constants, log K_1 = 8.80, and log K_2 = 7.51, to make the bis(ligand) complex, give an overall log β_2 of 16.31. (Below pH 2, the mono(ligand) complex is already partially formed - hence the necessity for spectrophotometric determination of the first stability constant (26).) At pH 7.4, (the pH in blood plasma) the complex is completely formed; however, at pH 2-3, most of the vanadium is in the form of a mono(ligand) complex and very little (~20%) is in the form of a bis-ligand complex. The stomach has a pH of 2-3, depending on its contents (29) which may preclude passage of the complex through the acidic environment of the stomach without some dissociation (*vide infra*).

A fundamental tenet of vanadium chemistry is that in aqueous solution, lower pH favors vanadyl (vanadium(IV)oxo, as in BMOV), whereas higher pH favors vanadate, vanadium(V) (30). Clearly redox chemistry between the vanadium(IV) and vanadium(V) oxidation states is of fundamental importance in elucidating the mechanism of action of BMOV. The standard reduction potential of vanadium(V) to vanadium(IV) falls dramatically as pH increases (30). Similarly, when a methanol/chloroform solution of BMOV is exposed to ambient oxygen, the 8 line pattern (I=7/2, ^{51}V) falls off dramatically over a period of several days, with a rate constant in methanol of 0.31 M^{-1} sec^{-1} at 25°C (31). In methanol, or in any alcoholic solvent, BMOV oxidizes to form a vanadium(V) alkoxobis(maltolato)oxo complex, $VO(OR)(ma)_2$ (Scheme 1) (31), the oxidation kinetics being second order, a function of the concentrations of both complex and molecular oxygen (31). It is a straightforward reaction between BMOV and molecular oxygen in a 4:1 ratio to give the vanadium(V) species, consistent with the fact that BMOV undergoes a 1-electron oxidation and O_2 is a 4-electron oxidant. The observed rate constant is directly proportional to the molecular oxygen concentration, consistent with this stoichiometry and the overall rate at 25 °C. The crystal structure (Figure 2) of the oxomethoxobis(maltolato) complex shows a six-coordinate vanadium(V) center with two maltolato ligands oriented in a cis fashion and V=O and VOMe in a cis fashion as well. It has a distorted octahedral geometry around the vanadium.

Oxidation of BMOV in Water: Formation of a Cis-dioxoanion, $[VO_2(ma)_2]^-$

In water, an oxidation (similar to that seen in methanol) is observed, except the oxidation of BMOV is now to a cis-dioxoanion $[VO_2(ma)_2]^-$ and the observed rate constant for the oxidation has the characteristic S-shape one expects to see for a pH dependent oxidation. This is due to the fact that molecular oxygen interacts with a vanadium(IV) bis(ligand)aquo species and a vanadium(IV) bis(ligand)hydroxo species (31). The pKa for this bound water is about 7.2. This provides two pathways: an aquo pathway and a hydroxo pathway, both giving the cis-dioxoanion. The aquo pathway is considerably slower (0.08 $M^{-1}s^{-1}$) than the hydroxo pathway (0.39 $M^{-1}s^{-1}$ at 25°C) and both were relatively slow, appropriate to the situation in which experimental animals are drinking continually in a chronic (long-time) experiment. Since the solutions are changed every 48 hours there must

Downloaded by UNIV OF GUELPH LIBRARY on October 31, 2012 | http://pubs.acs.org
Publication Date: December 10, 1998 | doi: 10.1021/bk-1998-0711.ch026

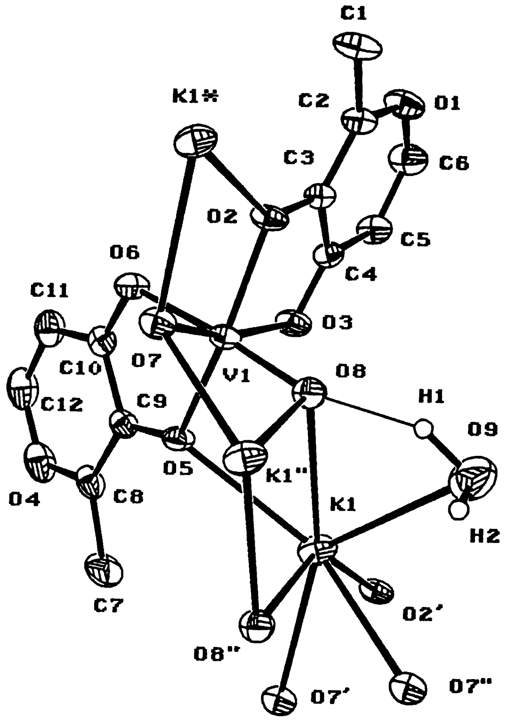
C1
K1*
C2
O1
C3
C6
O2
C5
O6
C4
C11
O3
C10
O7
V1
O8
C12
C9
H1
O9
O5
K1"
O4
C8
K1
H2
C7
O2'
O8"
O7'
O7"

Figure 1. The bis(maltolato)oxovanadium(IV) complex. showing the two maltolato ligands oriented trans in the base of a square pyramid.

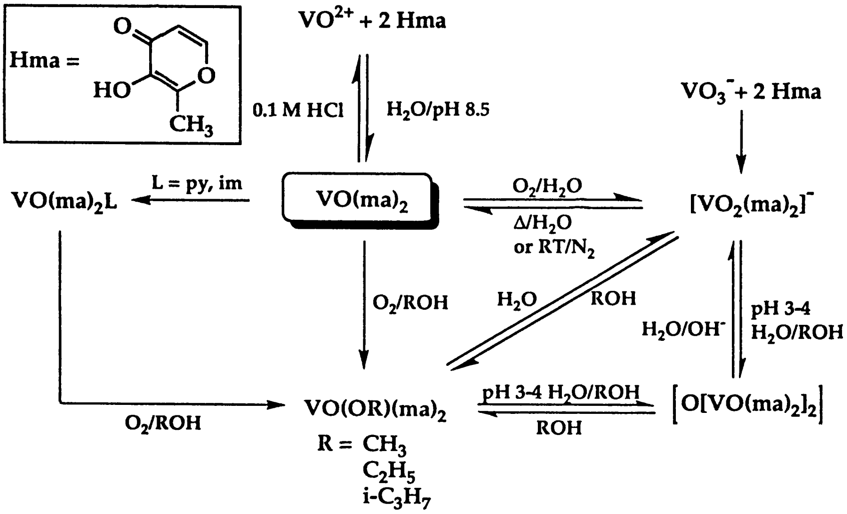
Hma =
O
HO
O
CH3
VO2+ + 2 Hma
0.1 M HCl
H2O/pH 8.5
VO3- + 2 Hma
VO(ma)2L
L = py, im
VO(ma)2
O2/H2O
[VO2(ma)2]-
Δ/H2O
or RT/N2
O2/ROH
H2O
ROH
H2O/OH-
pH 3-4
H2O/ROH
VO(OR)(ma)2
pH 3-4 H2O/ROH
ROH
[O[VO(ma)2]2]
O2/ROH
R = CH3
C2H5
i-C3H7

Scheme 1

Downloaded by UNIV OF GUELPH LIBRARY on October 31, 2012 | http://pubs.acs.org
Publication Date: December 10, 1998 | doi: 10.1021/bk-1998-0711.ch026

Downloaded by UNIV OF GUELPH LIBRARY on October 31, 2012 | http://pubs.acs.org
Publication Date: December 10, 1998 | doi: 10.1021/bk-1998-0711.ch026

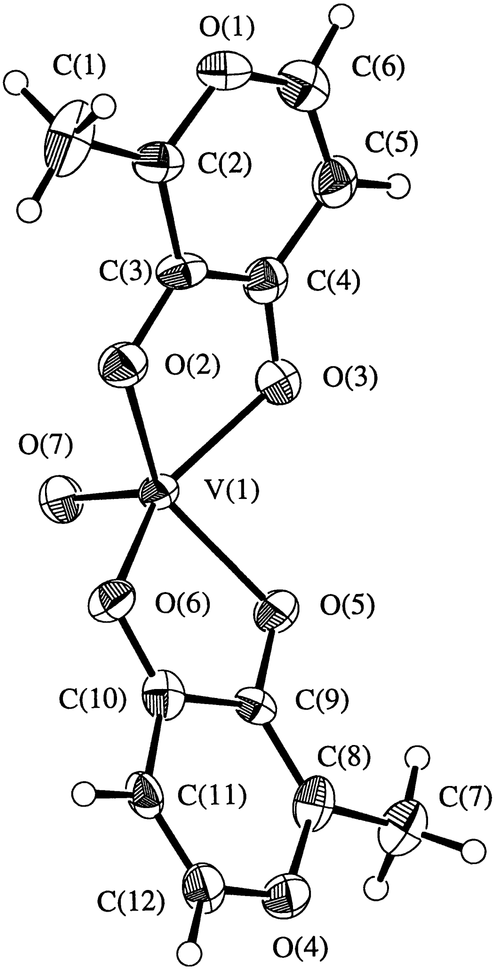
O(1)
C(1)
C(6)
C(5)
C(2)
C(3)
C(4)
O(2)
O(3)
O(7)
V(1)
O(6)
O(5)
C(10)
C(9)
C(8)
C(11)
C(7)
C(12)
O(4)

Figure 2. The bis(maltolato)methoxooxovanadium(V) complex showing the two maltolato ligands oriented cis in a distorted octahedron.

be still a fair amount of vanadium(IV) complex available despite this slow oxidation.

Substitution reactions of BMOV showed that O_2 must bind for the oxidation to $[VO_2(ma)_2]^-$ to take place. With pyridine or imidazole in the sixth position on BMOV, the six-coordinate vanadium(IV) species undergoes oxidation in alcohols much more slowly than does BMOV itself (Scheme 1). In addition to the methoxo species, ethoxo and isopropoxo vanadium(V) complexes can also be prepared (Scheme 1), and all these alkoxo species undergo trans esterification reactions - dissolving the methoxo complex in ethanol results in quantitative formation of the ethoxo complex. Varying the pH conditions (very critically) yields a dimeric vanadium(V)monooxo-bridged analogue $[\mu\text{-}O[VO(ma)_2]_2]$ in which there are two vanadium(V) centers bridged by one oxygen (Scheme 1); however, this is only isolable in the pH range 3 - 4 and only in a mixture of alcohols with water. An interesting observation is that $[VO_2(ma)_2]^-$ undergoes esterification to one of the vanadium(V) esters, $[VO(OR)(ma)_2]$, by dissolution in the appropriate alcohol (ROH), and these esters revert to the cis-dioxoanion when dissolved in water. This chemistry (Scheme 1) is analogous to that of carbon, with a carboxylate, esters and an acid anhydride observed (32).

$[VO_2(ma)_2]^-$ was prepared directly from a genuine vanadium(V) starting material (ammonium metavanadate) and maltol, resulting in the formation of the ammonium salt of the dioxoanion, $NH_4[VO_2(ma)_2]$ (26). This maltol reaction can also be used to make the potassium or sodium salt, both in fairly high yield. The crystal structure of the vanadium(V) complex, $K[VO_2(ma)_2]\cdot H_2O$, is a little more complicated than the other vanadium(V) and vanadium(IV) species (Figure 3) simply because the stoichiometry is one potassium cation to one vanadate anion to one water, and these form an infinite chain. The vanadium center is in the middle of a distorted octahedron and there are two maltolato ligands cis to one another; the two V=O units are cis to one another and are bonded to potassium atoms, which in turn hydrogen bond with water.

Electrochemistry. Variable pH electrochemistry, comparing both BMOV, the vanadium(IV) material, and the cis dioxoanion $[VO_2(ma)_2]^-$, shows a genuine conversion between these two species, reversible only around pH 3 (0.55 volts vs. Ag/AgCl) (26).

Biological Efficacy of BMOV

For most chronic studies, an experimental model of diabetes in the rat was used - the STZ-diabetic rat. In this model, rats are given an injection of streptozotocin (STZ), an antibiotic that specifically attacks the insulin secreting β-cells in the pancreas in a dose responsive fashion (33). This results in greatly reduced insulin secretory capacity of the rat pancreas and hence the development of diabetic characteristics (reduced insulin levels, elevated levels of glucose in blood and urine). A 2 x 2 factorial design was used, with the 2 factors being STZ-induced diabetes and vanadium supplementation. The four treatment groups were therefore: i) controls; ii) BMOV only (control treated); iii) diabetic only, and iv) both diabetic and BMOV-treated (diabetic treated). The vanadium complex was

Downloaded by UNIV OF GUELPH LIBRARY on October 31, 2012 | http://pubs.acs.org
Publication Date: December 10, 1998 | doi: 10.1021/bk-1998-0711.ch026

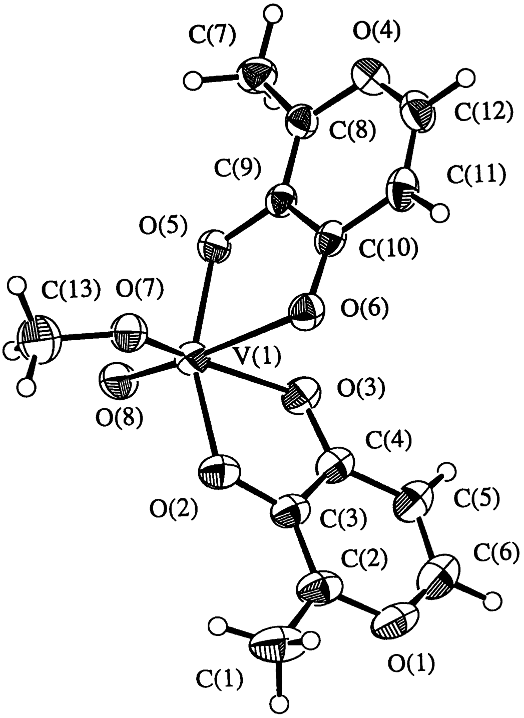
C(7)
O(4)
C(12)
C(8)
C(9)
C(11)
O(5)
C(10)
C(13)
O(7)
O(6)
V(1)
O(3)
O(8)
C(4)
O(2)
C(5)
C(3)
C(2)
C(6)
C(1)
O(1)

Figure 3. The potassium cis-bis(maltolato)oxovanadate(V) complex, an example of a cis dioxoanion salt formed in water. The vanadium center is in the middle of a distorted octahedron.

Downloaded by UNIV OF GUELPH LIBRARY on October 31, 2012 | http://pubs.acs.org
Publication Date: December 10, 1998 | doi: 10.1021/bk-1998-0711.ch026

administered in the drinking water of the rats, and was thus somewhat variable in dose, depending on the *ad libitum* fluid intake of the rats. The key end-point of interest was blood glucose-lowering, which is known to be closely correlated with plasma lipid-lowering in diabetic animals.

Plasma glucose levels of about 5-7 mM for both the control animals and the control treated animals (~5-7 millimolar is average for a rat and also for a human) were significantly lower than those for the diabetic rats, whose plasma glucose levels were 2-3 times higher (34). (Some variation is inherent in this model, because the more diabetic an animal becomes, the less it weighs, and the more it drinks). Within one week following BMOV administration, the diabetic treated animals showed a dramatic drop in plasma glucose levels. The plasma glucose levels for the treated diabetic animals were higher than for the control rats, on average, but BMOV had a stark glucose-lowering effect. Data taken from the same animals over the same time period (~1/2 year study) showed that plasma insulin levels of the control animals were about 40 µU/ml while both the diabetic and the diabetic treated animals had plasma insulin levels that were much lower (35). The fact that the diabetic, as well as the diabetic treated, animals both had low levels demonstrated that, in the diabetic treated animals, production of insulin was not stimulated by the vanadium complex. Glucose must be handled by some mechanism other than insulin production. Surprisingly, the control treated animals had plasma insulin levels significantly lower than the control untreated animals. These were not diabetic animals but they were taking the vanadium complex in their drinking water. Since insulin is secreted in response to a glucose challenge, the vanadium complex was clearly acting as an insulin mimic and stimulating a non-insulin dependent glucose utilization mechanism.

Acute Oral, ip and iv Administration. In both interperitoneal (i.p.) and oral studies (36, 37), a titration of plasma glucose in STZ-diabetic rats vs. the dose of BMOV or vanadyl sulphate showed that plasma glucose levels were lowered to <9 mM by a dose of BMOV that was 2-3 times less than the dose required of vanadyl sulphate, suggesting that BMOV is 2-3 times more potent as an insulin mimic than is vanadyl sulphate.

At pH 2-3 the bis-ligand complex does not predominate; therefore, is it necessary to administer the intact complex to see glucose lowering? To answer this question, an experiment was undertaken in STZ-diabetic rats using gavage administration of a single oral dose, followed by monitoring the plasma glucose as a function of time after administration. This is a simple screen that can be used to avoid the great expense involved in long term, chronic screens for different complexes. Eight different combinations of vanadyl, maltol, BMOV or control (no complex) were tried (26). Only three combinations showed plasma glucose lowering after administration of the one gavage dose to the animals. All three involved intact BMOV being administered. Of these three, one was BMOV only, another was BMOV followed by maltol, the third was maltol followed by BMOV. Administration of vanadyl followed by maltol, maltol followed by vanadyl, vanadyl alone, maltol alone, no vanadyl or maltol all led to no significant glucose lowering. It was only when the intact complex was administered that glucose

Downloaded by UNIV OF GUELPH LIBRARY on October 31, 2012 | http://pubs.acs.org
Publication Date: December 10, 1998 | doi: 10.1021/bk-1998-0711.ch026

lowering was seen, indicating that even at pH 3, there was enough of the intact complex to achieve the desired biological activity (26).

Uptake, Distribution and Excretion of Vanadium Compounds

Where does the vanadium localize in the rat? Our laboratories (15, 25, 38) and others (39) have shown that the plasma vanadium level required for the insulin mimetic effect in rats is between 10-15 μM [2-3 μM in humans, (11, 12)], the biological 'sink' for vanadium is the bone, while both kidney and liver accumulate vanadium in the short term and many be considered biological targets (40, 41). The highest levels for vanadium in any experiments so far were in bone of animals treated with BMOV (25, 35). Vanadium accumulation in the entire bone structure of the rat, based on a concentration of 26.4 μg/g wet weight of tissue (35), was approximately 2 mg. Accumulation in kidney seems unavoidable since absorbed vanadium is excreted in the urine, via the kidneys (42). Elevated levels in the liver most likely reflect endogenous excretion of absorbed vanadium via the bile (24).

To gain a more accurate picture of vanadium's tissue distribution and curve of disappearance following an acute administration, a new preparation of ^{48}V (as $^{48}VOSO_4$) was developed (43). ^{48}V with a 16 day half-life, is a high energy gamma emitter with about 50% high energy gamma and 50% positron emission. This is a very difficult isotope with which to work because of its emission profile; however, we could successfully achieve the desired preparation by bombardment of titanium with protons, for a radiochemical yield of about 1 Ci mg^{-1} (43). This new synthesis was required since all the syntheses in the literature pertained to vanadyl chloride ($VOCl_2$), but we needed vanadyl sulphate in order to compare vanadyl sulphate with BMOV, both administered orally. Experiments undertaken to investigate bio-localization of vanadium (24) involved oral or intraperitoneal (i.p.) administration of ^{48}V in a carrier-added form. From these studies, the absorption of vanadium from an oral dose of ^{48}V-BMOV was determined to be about twice as high as from ^{48}V-vanadyl sulphate; and bio-localization between the two compounds differed. Compartmental analysis of the results showed that the proportion of vanadium taken up by liver following BMOV treatment was almost 4 times higher than with $VOSO_4$ treatment, whereas that taken up by kidney was less than 50% higher, and that by bone (at 24 hours) was almost 3 times higher. The ratio of vanadium predicted by the model in bone:kidney:liver was 8:3:2 for BMOV and 6:4:1 for $VOSO_4$. The average increase in uptake into liver, kidney and bone was 2.7 times higher in BMOV compared to $VOSO_4$. Taking into account total tissue weight, the principal uptake of ^{48}V from an oral dose of BMOV vs. $VOSO_4$ was into bone (8.62% vs. 2.99% administered dose, AD), blood (3.55% vs. 2.73% AD), muscle (1.14% vs. 0.67% AD), liver (0.82% vs. 0.21% AD), and kidney (0.23% vs. 0.17% AD), based on model-predicted compartmental masses at 24 hours following gavage (24).

Overall, after 24 hours, giving the same dose of vanadium as BMOV resulted in about 2-3 times the amount of vanadium in the tissues as did vanadyl sulphate. This correlates well with previous evidence (34) that BMOV was 2-3 times as effective as VS in lowering blood glucose *in vivo* (*vide supra*). These two results suggest strongly that BMOV's greater effectiveness (vs. $VOSO_4$) is due to

Downloaded by UNIV OF GUELPH LIBRARY on October 31, 2012 | http://pubs.acs.org
Publication Date: December 10, 1998 | doi: 10.1021/bk-1998-0711.ch026

improved intestinal absorption and tissue uptake. Another kinetic parameter of interest, turnover times, also showed that BMOV differs substantially from $VOSO_4$. Turnover times for vanadium were shortest in blood, and longest in bone, with intermediate times for liver, kidney and testes. Residence times in blood were 7 minutes for BMOV and 5 minutes for $VOSO_4$. In bone, residence times of 31 days for BMOV and 11 days for $VOSO_4$ were calculated from model simulations.

Other Insulin Mimetics Incorporating Vanadium

Kojic Acid. We have investigated a number of other compounds, some of which are close analogues of BMOV. Kojic acid is commercially available, as is maltol. Instead of having a methyl group at the 2 position on the pyrone ring, kojic acid has a hydroxymethyl at the 5 position.

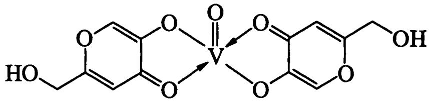

$VO(ka)_2$

We have prepared $VO(ka)_2$ (which is slightly less water soluble than BMOV) and have compared its biological activity with BMOV. BMOV, when administered orally or intraperitoneally, produced a better, sustained decline in plasma glucose vs. $VO(ka)_2$ (44) (Figure 4). (Vanadyl sulphate and $[VO_2(ma)_2]^-$, as its $[NH4]^+$ salt, were equally ineffective). In a chronic oral study (six weeks in duration), comparing BMOV and $VO(ka)_2$, BMOV lowered blood glucose into the normal (5-7mM) range within a couple of weeks of commencement, whereas $VO(ka)_2$ was considerably less effective (44) (Figure 5).

Implications for *in vivo* Mechanism of Action

What are the logical next steps in the research? Of major importance is to learn more about the mechanism of action of this vanadium complex and, indeed, of vanadium in general, regardless of chemical speciation. The insulin receptor is a trans membrane protein (45) and the first step of insulin stimulated lipogenesis or glucose oxidation is insulin binding to the insulin receptor which changes its structure on the inside and initiates autophosphorylation (46). Vanadium interferes with autophosphorylation reactions because vanadate is a very good phosphate analogue. Vanadate interacts with protein phosphorylation and dephosphorylation anywhere inside and outside the cell, and also inhibits or stimulates a variety of intracellular signals (47). Unfortunately, in trying to deduce the mechanism of action, there are a whole variety of sites at which vanadium could interact (10). The intracellular environment is quite reducing and the consensus is that intracellularly vanadium exists as vanadium(IV) and extracellularly it is vanadium(V). Recent evidence suggests that vanadyl may be acting to stimulate a cytosolic protein tyrosine kinase, distinct from the usual insulin receptor

Downloaded by UNIV OF GUELPH LIBRARY on October 31, 2012 | http://pubs.acs.org
Publication Date: December 10, 1998 | doi: 10.1021/bk-1998-0711.ch026

Downloaded by UNIV OF GUELPH LIBRARY on October 31, 2012 | http://pubs.acs.org
Publication Date: December 10, 1998 | doi: 10.1021/bk-1998-0711.ch026

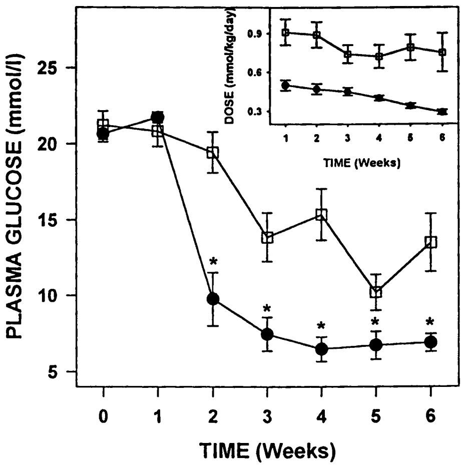

Figure 4. Plasma glucose levels in streptozotocin-diabetic rats following oral gavage. Comparison of four vanadium complexes, 0.55 mmol kg^{-1} each. O VOSO$_4$, n=7; ● VO(ma)$_2$, n=8; ■ [VO$_2$(ma)$_2$]$^-$, n=7; □ VO(ka)$_2$, n=8. (Reproduced from Ref. 44, Copyright 1997, Elsevier Science, Inc.)

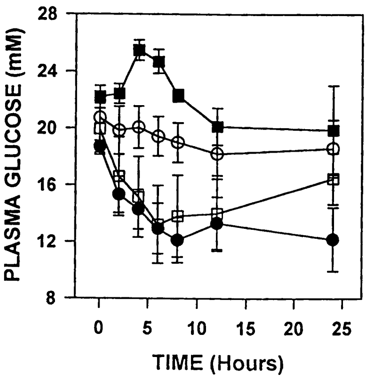

Figure 5. Plasma glucose levels in streptozotocin-diabetic rats following chronic oral administration ; comparison of BMOV (VO(ma)$_2$) and VO(ka)$_2$, 0.5 -1.25 g/L in the drinking water. ● VO(ma)$_2$, n=12; □ VO(ka)$_2$, n=10 (Reproduced from Ref. 44, Copyright 1997, Elsevier Science, Inc.)

mechanism, and also unlike vanadate's mechanism of action (48). Much work remains in order to elucidate clearly the mechanism - one major problem with diabetes is the great difficulty in picking relevant *in vitro* systems which actually relate to the *in vivo* results, such as those reported here.

Summary and Conclusions

Biologically relevant vanadium complexes can be prepared from vanadyl or vanadate to give vanadium(IV) or vanadium(V) compounds which are hydrolytically and thermodynamically stable. BMOV, in particular, has been extensively tested and characterized. Vanadium(IV) BMOV undergoes an O_2-dependent oxidation to vanadium(V) $[VO_2(ma)_2]^-$. It also may partly decomplex at pH levels below 2. However, sufficient biologically active BMOV remains intact *in vivo* to yield distinct advantages over inorganic vanadium compounds in terms of its orally active insulin mimetic properties, ease of administration, low toxicity, enhanced tissue uptake and favorable tissue localization.

Acknowledgement

The authors gratefully acknowledge support from the Medical Research Council of Canada (operating grants), from the Natural Sciences and Engineering Research Council (fellowships), from Nycomed Salutar (contract) and from Angiotech Pharmaceuticals (K.H.T., salary support). We acknowledge with considerable gratitude the contributions to this work of Drs. Lucio Gelmini, Graeme R. Hanson, F. Geoffrey Herring, Steven J. Rettig, Yan Sun and Alan Tracey, as well as Peter Caravan, Ika Setyawati, and Ed Shuter.

Downloaded by UNIV OF GUELPH LIBRARY on October 31, 2012 | http://pubs.acs.org
Publication Date: December 10, 1998 | doi: 10.1021/bk-1998-0711.ch026

Literature Cited

1. Lyonnet, B. M.; Martz Martin, E. *La Presse Medicale* **1899**, *7*: 191-192.
2. Tolman, E. L.; Barris, E.; Burns, M.; Pansisni, A.; Partridge, R. *Life Sci.* **1979**, *25*, 1159-1164.
3. Heyliger, C. E.; Tahiliani, A. G.; McNeill, J. H. *Science* **1985**, *227*, 1474-1477.
4. Thompson, K. H.; Godin, D.V. *Nutrition Res.* **1995**, *15*, 1377-1410.
5. Banting, F. G.; Best, C.H.; Collip, J.B.; Campbell, W.R.; Fletcher, A.A. *Can. Med. Assoc. J.* **1922**, *12*, 141-146.
6. Crans, D. C.; Mahroof-Tahir, M.; Keramidas, A.D. *Mol. Cell. Biochem.* **1995**, *153*, 17-24.
7. Orvig, C.; Thompson, K. H.; Battell, M.; McNeill, J. H. *Metal Ions Biol. Syst.* **1995**, 31, 575-594.
8. Rehder, D. *BioMetals* **1992**, 5, 3-12.
9. Orvig, C.; Thompson, K.H.; Cam, M.C.; McNeill, J.H. In *Inorganic Chemistry in Medicine*; Farell, N., Ed., in press.
10. Tsiani, E.; Fantus, I.G. *Trends Endocrin. Metab.* **1997**, *8*, 51-58.
11. Cohen, N.; Halberstam, M.; Shlimovich, P.; Chang, C. J.; Shamoon, H.; Rossetti, L. *J. Clin. Invest.* **1995**, *95*, 2501-2509.

12. Goldfine, A. B.; Simonson, D. C.; Folli, F.; Patti, M.-E.; Kahn, C. R. *J. Clin. Endocrin. Metab.* **1995**, *80*, 3311-3320.

13. Nielsen, F. H. In *Vanadium and Its Role in Life*; Sigel, H.; Sigel, A., Eds. Marcel Dekker, Inc.: New York/Basel/Hong Kong, **1995**, Vol. 31, pp. 543-574.

14. Bendayan, M.; Gingras, D. *Diabetologia* **1989**, *32*, 561-567.

15. Thompson, K. H.; Leichter, J.; McNeill, J. H. *Biochem. Biophys. Res. Comm.* **1993**, *197*, 1549-1555.

16. Venugopal, B.; Luckey, T.D. *Chemical Toxicity of Metals and Metalloids.*, Plenum Press; New York, NY, **1978**, Vol. 2.

17. Posner, B. I.; Faure, R.; Burgess, J. W.; Bevan, A. P.; Lachance, D.; Zhang-Sun, G.; Fantus, I. G.; Ng, J. B.; Hall, D. A.; Soo Lum, B.; Shaver, A. *J. Biol. Chem.* **1994**, *269*, 4596-4460.

18. Crans, D. C.; Keramida, A.D.; Hoover-Litty, H.; Anderson, O.P.; Miller, M.M.; Lemoine, L.M.; Pleasic-Williams, S.; Vandenberg, M.; Rossomoando, A.J.; Sweet, L.J. *J. Am. Chem. Soc.* **1997**, *119*, 5447-5448.

19. Yale, J.-F.; Lachance, D.; Bevan, A. P.; Vigeant, C.; Shaver, A.; Posner, B. I. *Diabetes* **1995**, *44*, 1274-1279.

20. McNeill, J. H.; Yuen, V. G.; Dai, S.; Orvig, C. *Mol. Cell. Biochem.* **1995**, *153*, 175-180.

21. Cam, M. C.; Cros, G. H.; Serrano, J.-J.; Lazaro, R.; McNeill, J. H. *Diabetes Res. Clin. Practice.* **1993**, *20*, 111-121.

22. Sakurai, H.; Tsuchiya, K.; Nukatsuka, M.; Kawada, J.; Ishikawa, S.; Yoshida, H.; Komatsu, M. *J. Clin. Biochem. Nutrit.* **1990**, *8*, 193-200.

23. Shechter, Y.; Shisheva, A.; Lazar, R.; Libman, J.; Shanzer, A. *Biochemistry* **1992**, *31*, 2063-2068.

24. Setyawati, I. A.; Thompson, K.H.; Sun, Y.; Lyster, D.M.; Vo., C.; Yuen, V.G.; Battell, M.; McNeill, J.H.; Ruth, T.J.; Zeisler, S.; Orvig, C. *J. Appl. Physiol.*, in press.

25. Thompson, K. H.; Battell, M.; McNeill, J.H. In *Vanadium in the Environment*, Nriagu, J.O., Ed., John Wiley & Sons, Inc., Ann Arbor, MI, in press.

26. Caravan, P.; Gelmini, L.; Glover, N.; Herring, F. G.; Li, H.; McNeill, J. H.; Rettig, S. J.; Setyawati, I. A.; Shuter, E.; Sun, Y.; Tracey, A. S.; Yuen, V. G.; Orvig, C. *J. Am. Chem. Soc.* **1995**, *117*, 12759-12770.

27. Nelson, W. O.; Karpishin, T. B.; Rettig, S. J.; Orvig, C. *Inorg. Chem.* **1988**, *27*, 1045-1051.

28. Singh, R. K.; Barrand, M.A. *J. Pharm. Pharmacol.* **1990**, *42*, 276-279.

29. Waldron-Edward, D. In *Intestinal Absorption of Metal Ions, Trace Elements and Radionuclides*, Skoryna, S.C.; Waldron-Edward, D., Eds., Pergamon Press, Toronto, ON, **1971**, pp. 373-382.

30. Butler, A. In *Vanadium in Biological Systems*, Sigel, H.; Sigel, A., Eds., Kluwer Academic, Dordrecht, The Netherlands, **1990**, pp. 25-50.

31. Sun, Y.; James, B. R.; Rettig, S. J.; Orvig, C. *Inorg. Chem.* **1996**, *35*, 1667-1673.

32. Giacomelli, A.; Floriani, C.; Duarte, A. O. d. S.; Chiesi-Villa, A.; Guastini, C. *Inorg. Chem.* **1982**, *21*, 3310-3316.

33. Rakieten, N. *Cancer Chemotherapeutic Reports* **1963**, *29*, 91-98.

Downloaded by UNIV OF GUELPH LIBRARY on October 31, 2012 | http://pubs.acs.org
Publication Date: December 10, 1998 | doi: 10.1021/bk-1998-0711.ch026

34. Yuen, V. G.; Orvig, C.; McNeill, J. H. *Can. J. Physiol. Pharmacol.* **1993,** *71*, 263-269.

35. Yuen, V. G.; Orvig, C.; Thompson, K. H.; McNeill, J. H. *Can. J. Physiol. Pharmacol.* **1993**, *71*, 270-276.

36. Yuen, V. G.; Orvig, C.; McNeill, J.H. *Can. J. Physiol. Pharmacol.* **1995,** *73*, 55-64.

37. Yuen, V. G.; Pederson, R.A.; Dai, S.; Orvig, C.; McNeill, J.H. *Can. J. Physiol. Pharmacol.* **1996**, *74*, 1001-1009.

38. Dai, S.; Thompson, K. H.; McNeill, J. H. *Pharmacol. Toxicol.* **1994**, *74*, 101-109.

39. Shechter, Y. *Diabetes* **1990**, *39*, 1-5.

40. Sabbioni, E.; Marafante, E. *Bioinorg. Chem.* **1978**, *9*, 389-407.

41. Thompson, K. H.; McNeill, J. H. *Res. Comm. Chem. Pathol. Pharmacol.* **1993**, *80*, 187-200.

42. Thompson, K. H.; McNeill, J.H. In *Trace Elements in Man and Animals - 9: Proceedings of the Ninth International Symposium on Trace Elements in Man and Animals* , Fisher, P.W.F.; L'Abbe, M.R.; Cockell, K.A.; Gibson, R.S., Eds. NRC Research Press, Ottawa, ON, **1997**, pp. 349-350.

43. Zeisler, S. K.; Ruth, T. J. *J. Radioanal. Nucl. Chem.. Letts.* **1995**, *200*, 283-290.

44. Yuen, V. G.; Caravan, P.; Gelmini, L.; Glover, N.; McNeill, J.H.; Setyawati, I.A.; Shuter, E.; Zhou, Y.; Orvig, C. *J. Inorg. Biochem.*, in press.

45. Lienhard, G. E.; Slot, J. W.; James, D. E.; Mueckler, M. M. *Sci. Amer.* **1992**, *267*, 86-91.

46. Czech, M. P. *Ann. Rev. Physiol.* **1985**, *47*, 357-381.

47. Shechter, Y.; Li, J.; Meyerovitch, J.; Gefel, D.; Bruck, R.; Elberg, G.; Miller, D.S.; Shisheva, A. *Mol. Cell. Biochem.* **1995,** *153*, 39-47.

48. Li, J.; Elberg, G.; Crans, D.C.; Shechter, Y. *Biochemistry* **1996,** *35*, 8314-8318.

Downloaded by UNIV OF GUELPH LIBRARY on October 31, 2012 | http://pubs.acs.org
Publication Date: December 10, 1998 | doi: 10.1021/bk-1998-0711.ch026

Chapter 27

Structure-Activity Relationship of Insulin-Mimetic Vanadyl Complexes with $VO(N_2O_2)$ Coordination Mode

H. Sakurai, K. Fujii, S. Fujimoto, Y. Fujisawa, K. Takechi, and H. Yasui

Department of Analytical and Bioinorganic Chemistry, Kyoto Pharmaceutical University, Nakauchi-cho 5, Misasagi, Yamashina-ku, Kyoto 607, Japan

Downloaded by CORNELL UNIV on October 31, 2012 | http://pubs.acs.org
Publication Date: December 10, 1998 | doi: 10.1021/bk-1998-0711.ch027

Insulin-dependent diabetes mellitus (IDDM), characterized by hyperglycemia due to an absolute deficiency of insulin, has been demonstrated to be improved by administration of vanadium complexes in place of insulin injections. Recently, we have found that vanadyl ion as well as vanadyl complexes are relevant to both onset and treatment of IDDM. Therefore, we synthesized vanadyl complexes with different coordination modes such as $VO(O_4)$, $VO(N_4)$, $VO(S_4)$, $VO(N_2O_2)$, $VO(S_2O_2)$ and $VO(S_2O_2)$ and evaluated their insulin-mimetic activities in vitro and in vivo. From the recent investigations on the relationship between structure and insulin-mimetic activity for vanadyl complexes of nitrogenous ligands, vanadyl-picolinate and vanadyl-methylpicolonate complexes with moderate partition coefficient and inhibitory effect of free fatty acid-release from rat adipocytes have been proposed to be long-acting insulin-replacements when they are given orally to streptozotocin-induced IDDM rats. The vanadium distribution and metallokinetic analysis in rats administered the vanadyl complexes were also examined to discuss the action of the complexes.

Diabetes mellitus is one of the most widespread diseases of the world. The number of the patients suffering from the diabetes are increasing day by day. According to the definition of WHO (1), diabetes mellitus (DM) is mainly classified into insulin-dependent DM (IDDM) and non-insulin-dependent DM (NIDDM). To treat NIDDM, several therapeutics have already been developed and clinically used involving sulfonylureas, sulfonamides, biguanides and triglydazone (Noscal). However, IDDM can be yet controlled only by daily subcutaneous injections of insulin.

In Vanadium Compounds; Tracey, A., et al.;
ACS Symposium Series; American Chemical Society: Washington, DC, 1998.

Downloaded by CORNELL UNIV on October 31, 2012 | http://pubs.acs.org
Publication Date: December 10, 1998 | doi: 10.1021/bk-1998-0711.ch027

Vanadium, which was found by Seftrom in 1831 and named by him after the goddes, Vanadis, of Scandinavian legend has been proposed to improve the hepatic and peripheral insulin sensitivities in patients with both IDDM and NIDDM by giving simple vanadium compounds such as $VOSO_4$ and $NaVO_3$ around 100 years ago in France (2) and in recent years 1995-1996 in the USA (3-7). These results indicate the need for investigations to establish the safest and long-term effectiveness of vanadyl compounds to treat diabetes mellitus (8, 9).

For the purpose, several synthetic vanadyl coordination complexes, that are active on oral administration in place of insulin as well as simple compounds such as $VOSO_4$ and $NaVO_3$, have been investigated on the basis of the results of experimental animals.

We found first dose-dependent hypogycemic effects of bis(methycysteinato)-oxovanadium(IV) (VO-CYSM) and bis(malonato)- oxovanadium(IV)(VO-MAL) complexes with $VO(S_2N_2)$ and $VO(O_4)$ coordination mode, respectively, that were given by oral administration (10) (Table I, 1 and 9).

Against the principle of Pearson's HSAB (11), which proposed the direction for the formation of stable complexes due to the combination such as hard acid-hard base or soft acid-soft base, the VO-CYSM complex has been found to forms a strong coordination bond between VO_2^+ and the thiolate of the CYSM ligand (12). Encouraged with the results, we have proposed that bis(pyrrolidine-N-carbodithiolato)-oxovanadium(IV) complex (VO(P)) (Table I (12)) is the most insulin-mimetic active compound among 6 prepared complexes with $VO(S_4)$ coordination mode when they are administered orally (13).

On the other hand, we have prepared complexes with $VO(N_2O_2)$ coordination mode to know the structure-activity relationship of antidiabetic vanadyl complexes, in which bis(picolinato)oxovanadium(IV) complex (VO(PA)) (Table I (5)) has been demonstrated to have orally active and long-term acting insulin-like properties (14).

Structure-Activity Relationship of Antidiabetic Vanadyl Complexes with VO(N2O2) Coordination Mode

The orally active insulin-mimetic vanadyl complexes proposed so far are summarized in Table I. However, establishment of a clear correlation between structure of the complex and insulin-mimetic activity is yet very difficult due to absolute lack of available data, in which many important factors such as physico-chemical properties and electronic charges of the complex under physiological conditions, hydrophilicity or lipophilicity, availability for gastrointestinal absorption, organ and subcellular distributions of vanadium and its complex, and toxicity and safety of the complex are involved.

Preparation of Vanadyl Complexes. Since we have found that the VO(PA) complex with the $VO(N_2O_2)$ coordination mode is effective for normalizing the serum glucose levels of streptozotocin (STZ)-induced diabetic rats (STZ-rats) when given intraperitoneally (i.p.) or orally, we have examined the structure-insulin mimetic activity relationship of the vanadyl complexes with a $VO(N_2O_2)$ coordination mode by using VO(PA) as a leading complex as well as other 5 complexes such as (dipicolinato)-,

Downloaded by CORNELL UNIV on October 31, 2012 | http://pubs.acs.org
Publication Date: December 10, 1998 | doi: 10.1021/bk-1998-0711.ch027

Table I. Insulin-mimetic Vanadyl Complexes with Different Coordination Modes

mode	complex				
N_2S_2	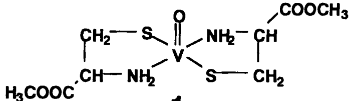 1	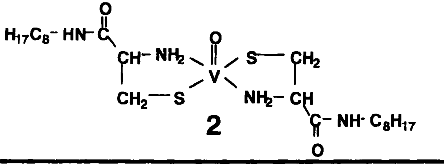 2			
N_2O_2	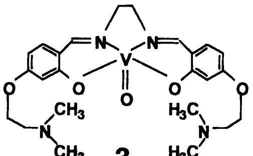 3	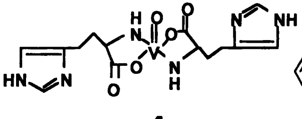 4	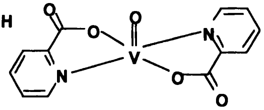 5	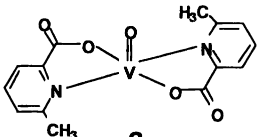 6	
O_4	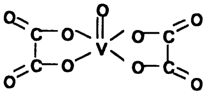 7	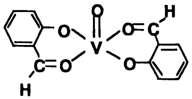 8	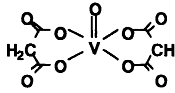 9	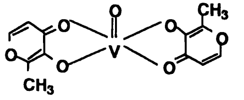 10	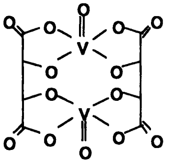 11
S_4	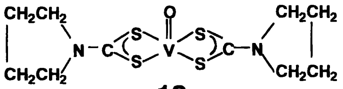 12	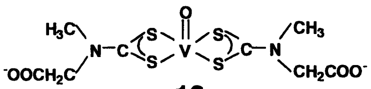 13			

1 Sakurai et al. 1990 (10), 2 EP patent 305246, 3 Junod et al. 1969, 4~6 Sakurai et al. 1994 (14, 16),
7~9 Sakurai et al. 1990 (10), 10 McNeil et al. 1992 (8), 11 Sakurai et al. 1990 (10), 12 Watanabe et al. 1994 (13)
13 Sakurai et al. 1995

bis(picolinamidato)-, bis(6-methylpicolinato)-, bis(quinaldinato)- and bis(histidinato)-oxovanadium(IV), abbreviated as VO(DPA), VO(PAM), VO(MPA), VO(QA) and VO(HIS), respectively (Figure 1). Structures of the complexes were characterized by elemental analysis, visible and infrared absorption spectra as well as ESR spectra measured at room (22) and liquid nitrogen (77 K) temperatures, magnetic susceptibility and partition coefficient.

***In Vitro* Study**. In *in vitro* estimation of insulin-mimetic activity of the complex, we evaluate it by incorporation of radio-labeled glucose into the isolated rat adipocytes as well as by inhibition of release of free fatty acids (FAA) from the adipocytes treated with epinephrin (EP). The latter method has been proved to be simple, sensitive and convenient without use of radioactive glucose compounds (15).

In brief, male Wistar rats, weighing 200g, were sacrificed by dacapitation under anesthesia with ether, and the adipocytes were isolated from the epididymal fat pads. The isolated rat adipocytes ($2.7\text{x}10^6$ cells/mL) were preincubated at 37 C for 0.5 hr with various concentrations of a vanadyl complex in 1 mL KRB buffer (120mM NaCl, 1.27mM $CaCl_2$, 1.2mM $MgSO_4$, 4.75mM KCl, 1.2mM KH_2PO_4 and 24 mM $NaHCO_3$; pH 7.4) containing 20mg bovine serum albumin. A 10 mM EP was added to the reaction mixture and the resulting solution was incubated at 37 C for 3 hr. The reaction was stopped by soaking in ice water and the mixture was centrifuged at 1,200 rpm for 10 min. For the outer solution of the cells, FFA levels were determined with an FFA kit Wako (Osaka, Japan).

The effects of the tested 6 vanadyl complexes on the inhibition of EP-stimulated FFA release from isolated rat adipocytes in the absence of glucose, together with vanadyl sulfate (VS) as a positive control, have been found to be dose-dependent in the concentration range of $5\text{x}10^{-5}$ to 10^{-3}-3 M. From the dose-response curve for each complex, the IC_{50} value, which expresses the 50% inhibition concentration of the complex for FFA-release from the adipocytes by stimulation of EP, was determined. The IC_{50} values, together with the partition coefficients determined so far, are summarized in Table II (16). The IC_{50} values of 6 complexes were found to be lower than that of VS, which is proposed to be a good reagent for treating IDDM of humans (3, 6, 7) as well as STZ-rats (17-21).

Since the partition coefficient of the complex is thought to be essential for predicting in vivo insulin-mimetic action of the complex, those of 6 complexes were measured. However, for VO(PAM), VO(DPA), VO(QA) and VO(HIS), their partition coefficients were not determined due to their low solubility for both buffer and n-octanol solutions as well as due to their instabilities during 6 hr mixing. Nevertheless, the values for VS, VO(PA) and VO(MPA) were obtainable, those for VO(MPA) being found to be higher than those for VS and VO(PA)

In Vivo Study. Among the insulin-mimetic activities of the vanadyl complexes in terms of IC_{50} value, VO(QA) and VO(DPA) exhibited higher values than those for others. Thus VO(QA) was given by daily i.p injections to STZ-rats. Although VO(QA) gave a high effectiveness by i.p. injection, this complex showed no serum glucose normalizing effect on oral administration.

Downloaded by CORNELL UNIV on October 31, 2012 | http://pubs.acs.org
Publication Date: December 10, 1998 | doi: 10.1021/bk-1998-0711.ch027

Downloaded by CORNELL UNIV on October 31, 2012 | http://pubs.acs.org
Publication Date: December 10, 1998 | doi: 10.1021/bk-1998-0711.ch027

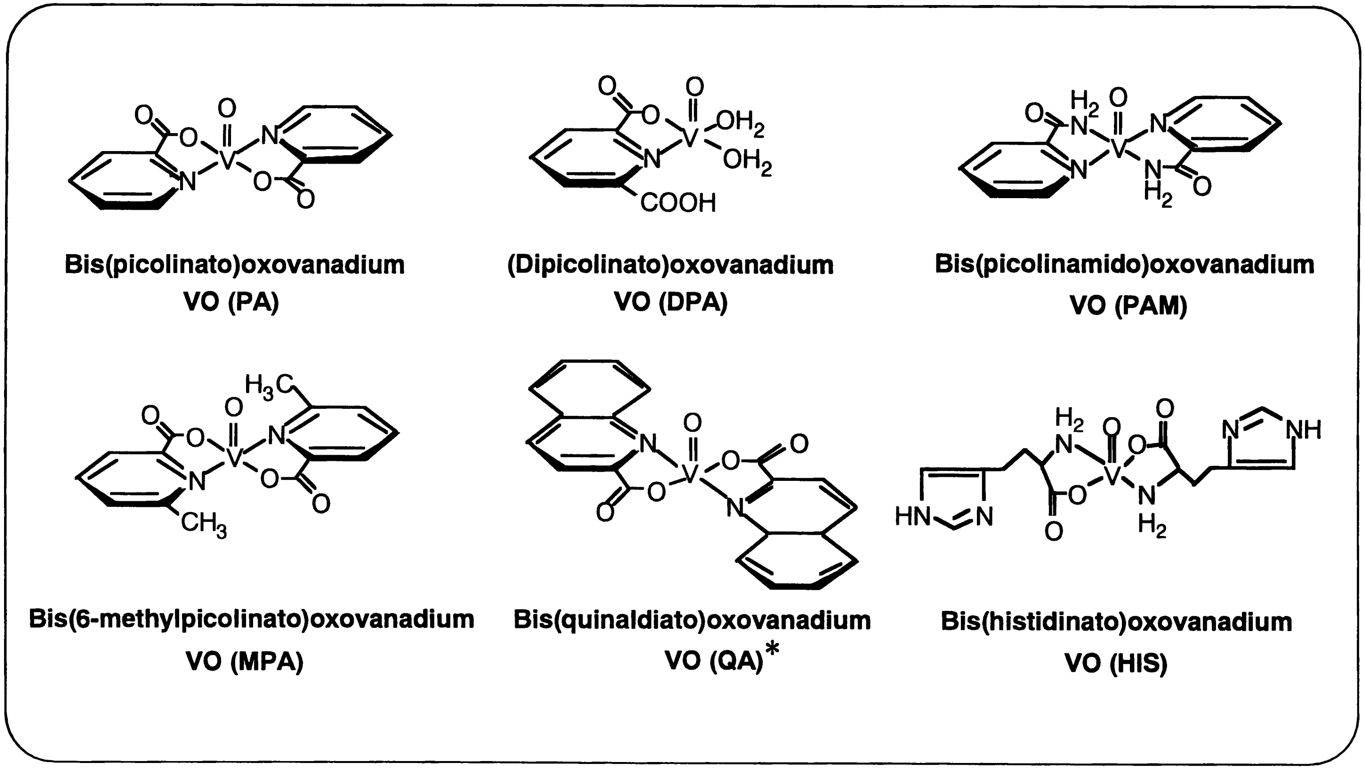
Bis(picolinato)oxovanadium
VO (PA)
(Dipicolinato)oxovanadium
VO (DPA)
Bis(picolinamido)oxovanadium
VO (PAM)
Bis(6-methylpicolinato)oxovanadium
VO (MPA)
Bis(quinaldiato)oxovanadium
VO (QA)*
Bis(histidinato)oxovanadium
VO (HIS)

Figure 1. Structures of vanadyl complexes examined in the present study.
** 3-Dimensional structure was determined by X-ray analysis.*

Downloaded by CORNELL UNIV on October 31, 2012 | http://pubs.acs.org
Publication Date: December 10, 1998 | doi: 10.1021/bk-1998-0711.ch027

Table II. Vanadyl Complexes with VO(N_2O_2) Coordination Mode and Their Insulin-mimetic Activities

complex [a]	coordination number around V(IV)	coordination mode	partition coefficient	insulin-mimetic action		
				IC$_{50}$, mM	*in vitro*	*in vivo*
$VOSO_4$	5	VO(O_4)	0.03	6.0	+	+ + (*i.p.*)
VO(PA)	5	VO(N_2O_2)	0.33	0.46	+ +	+ + (*i.p.* & *p.o.*)
VO(MPA)	5	VO(N_2O_2)	0.60	0.45	+ +	+ + (*i.p.* & *p.o.*)
VO(PAM)	5	VO(N_2O_2)	-	0.30	+ +	
VO(DPA)	5	VO(N_2O_2)	-	0.29	+ +	
VO(QA) [c]	5	VO(N_2O_2)	-	0.28	+ +	+ + (*i.p.*) [b]
VO(HIS)	5	VO(N_2O_2)	-	2.00	+	+ + (*i.p.*)

[a] PA=picolinic acid
MPA=6-methlpicolinic acid
PAM=picolinamide
DPA=dipicolinic acid
QA=quinaldinic acid
HIS=histidine

[b] essentially no effect by p.o. administration

[c] 3 dimensional structure was analysed.

VO(MPA) complex, which has been found to have a similar IC_{50} value to that of VO(PA) and moderate partition coefficient, was then administered to STZ-rats by daily i.p. injections at the doses of 3mg/kg body weight for 2 days, then 2mg/kg for 2 days and finally 1mg/kg for 10 days or daily oral administrations at the doses of 10mg/kg body weight for 10 days and then 5mg/kg for 10 days. This complex has been revealed to have a good insulin-mimetic activity similarly to that of VO(PA) complex not ony by i.p. injection but by oral adiminstration without body weight loss of STZ-rats (22). It is interesting to note that the serum glucose normalizing effect of the VO(MPA) complex continued for at least 80 days after withdrawing the complex administration and the insulin-mimetic effect by the complex was observed at lower doses than those for VO(PA) administration (Sakurai, H. et al., manuscript in preparation)

From the results, the vanadyl complexes with moderate partition coefficient and relatively good IC_{50} value around 0.4mM is expected to be a potent insulin-mimetic compound for experimental animals with IDDM. In addition, we observed preliminary that VO(MPA) is also effective for normalizing the serum glucose levels of rats with NIDDM.

Downloaded by CORNELL UNIV on October 31, 2012 | http://pubs.acs.org
Publication Date: December 10, 1998 | doi: 10.1021/bk-1998-0711.ch027

Organ Distribution of Vanadium, in vivo Coordination Structure around Vanadyl, and ESR-Metallokinetic Analysis of Vanadyl State in Rats Administered Vanadyl-Picolinate Complex

Vanadium Distribution. Previously, we observed that no significant differences in vanadium uptake between normal- and STZ-rats as estimated by neutron activation analysis method for total vanadium as well as by ESR method for vanadyl state (19).

When VS was given to rats, total vanadium in terms of mg V/g wet weight of organ was found to be incorporated into the organs in the following order: kidney>bone>liver>pancreas>spleen as well as in the supernatant of the kidney and mitochondria of the liver. While, in rats given VO(PA) by oral administration the following order for vanadium accumulation was observed: bone>kidney>spleen>liver >pancreas. Vanadium has thus been assumed to act in part on the islet of the pancreas, mineralization of bone, electron transport or induction of metallothionein in the kidney and liver (Sakurai, H. et al. unpublished data).

***In Vivo* Coordination Structure**. Following to our conventional X-band ESR analysis on *in vivo* coordination structure of vanadyl state in the organs of rats given vanadyl complexes (19), ESEEM (electron spin echo envelope modulation) spectroscopy at 77 K has been applied to examine a more detailed *in vivo* coordination structure of vanadyl state in rats treated with VS. ESEEM analysis revealed the occurrence of nitrogen-vanadyl bonds suggesting the presence of *in vivo* coordination of Lys ε-amine or N-terminal α-amine of proteins to vanadyl ion (23). Recently, ESEEM analysis at 4 K on the organs of rats given VO(PA) complex has demonstrated that the complex is partially incorporated in the liver as a ternary complex such as (PA)-VO_2^+-N(amino acid residues of proteins) (Fukui, K. et al., manuscript in preparation).

Metallokinetic Analysis. To develop a therapeutic compound, pharmacokinetic analysis of the compound in blood is essential. We have recently proposed a new pharmacokinetic analysis method combined with ESR spectrometer and named as BCM (blood circulation monitoring)-ESR method, in which the behaviours of several stable spin probes in the blood of rats were successfuly analysed (24). By using the BCM-ESR method, we performed the metallokinetic analysis of VS and VO(PA) complex in rats (25).

VS or VO(PA) complex was given by single i.v. injection to rats under anesthesia with pentobarbital and ESR spectra were collected at room temperature every 30 second. The real-time ESR analysis of vanadyl state revealed that clearance rate of vanadyl from the blood of rats given VS was found to be higher than that given VO(PA) complex in terms of half-life ($t_{1/2}$), being 10 min in VS-treated rats and 16 min in VO(PA)-treated rats. The slow clearance rate of vanady state in rats given VO(PA) complex suggests the high accumulation of vanadium in organs of rats. The metallokinetic analysis by the BCM-ESR method is now under way in more detail.

Downloaded by CORNELL UNIV on October 31, 2012 | http://pubs.acs.org
Publication Date: December 10, 1998 | doi: 10.1021/bk-1998-0711.ch027

Conclusion. The relationship between structure and insulin mimetic activity for vanadyl complexes of nitrogenous ligands was examined. *In vitro* results such as IC_{50} value for the inhibition of FFA release from the isolated rat adipocytes stimulated with EP and partition coefficient suggested the importance for predicting *in vivo* blood glucose normalizing effect of the complex in STZ-induced IDDM rats. Among 6 vanadyl complexes examined, both VO(PA) and VO(MPA) complexes with around 0.45 mM of IC_{50} value and higher partition coefficient than that of VS have been proposed to be potent reagents to treat STZ-rats with IDDM.

Acknowledgments

This research was in part supported by grants from the Ministry of Education, Science and Culture of Japan. HS thanks Drs. J. Takada and R. Matsushita of Research Reactor Institute of Kyoto University, and Drs. K. Fukui, H. Ohya-Nishiguchi and H. Kamada of the Institute for Life Support Technology of Yamagata Technopolis Foundation for their investigations and helpful discussions in the research project.

References

1. WHO; Diabetes mellitus; Reports of a WHO study group. WHO Technical Report Series **1985**, *727*, 876-877.
2. Lyonnet, B.; Martz, X.; Martin, E. *Presse Med.* **1889**, *1*, 191-192.
3. Cohen, N; Halberstam, M.; Shilimovich, P.; Chang, C. J.; Shamoon, H. ; Rosseti, L. *J. Clin. Invest.* **1995**, *95*, 2501-2509.
4. Goldfine, A. B.; Simonson, D. C.; Folli, F.; Patti, M. E.; Kahn, C. R. *J. Clin. Endocrinol. Metab.* **1995**, 80, 3311-3320.
5. Goldfine, A. B.; Simonson, D. C.; Folli, F.; Patti, M. E.; Kahn, C. R. *Mol. Cell. Biochem.* **1995**, *153*, 217- 231.

6. Halberstam, M.; Cohen, N.; Shilimovich, P.; Rosseti, L.; Shamoon, H. *Diabetes* **1996**, *45*, 659-666.
7. Boden, G.; Chen, X.; Ruiz, J.; van Rossum, G. D. V.: Salvatore, T. *Metabolism* **1996**, *45*, 1130-1135.
8. Orvig, C.; Thompson, K. H.; Battell, H.; McNeil, J. H. In *Metal Ions in Biological Systems,* Editors, Siegel, H.; Sigel, A.;*Vanadium and Its Roles in Life,* Marcel Dekker, New York, **1995**,*Vol. 31,* pp. 575-594.
9. Sakurai, H. *Chemistry Today* **1996**, No.304 (7), 14-20. (in Japanese)
10. Sakurai, H.; Tsuchya, K.; Nukatsuka, M.; Kawada, J.; Ishikawa, S.; Komatsu, M.*J. Clin. Biochem. Nutr.* **1990**, *8,* 193-200.
11. Pearson, R.G. *J. Am. Chem. Soc.* **1963**, *85*, 3533-3539. *Inorg. Chim. Acta.* **1980**, *46*, L119-L120.
13. Watanabe, H.; Nakai, M.; Komazawa, K.; Sakurai, H. *J. Med. Chem.* **1994**, *37*, 876-877.
14. Sakurai, H.; Fujii, K.; Watanabe, H.; Tamura, H. *Biochem. Biophys. Res. Commun.* **1995**, *214*, 1095-1101.
15. Nakai, M.; Watanabe, H.; Fujiwara, C.; Kakegawa, H.; Satoh. T.; Takada, J.; Matsushita, R.; Sakurai, H. *Biol. Pharm. Bull.* **1995**, *18*, 719-725.
16. Fujisawa, Y.; Fujimoto, S.; Sakurai, H. *J. Inorg. Biochem.* **1997**, *67*, 396.
17. Pederson, R.A.; Ramanadham, S.; Bucher, A. M. J.; McNeil, J. H. *Diabetes* **1989**, *38*, 1390-1395.
18. Ramanadham, S.; Mongold, J. J.; Brownsey, R.W.; Cros, G. H.; McNeil, J. H. *Am. J. Physiol.* **1989**, *257*, H904-H911.
19. Sakurai, H.; Tsuchiya, K.; Nukatsuka, M.; Sofue, M.; Kawada, J. *J. Endocrinol.* **1990**, *126*, 451-459.
20. Cam, M. C.; Pederson, R. A.; Brownsey, R. W.; McNeil, J. H. *Diabetologia* **1993**, *36*, 218-224.
21. Thompson, K. H.; Leichter, J.; McNeil, J. H. *Biochem. Biophys. Res. Commun.*, **1993**, *197*, 1549-1555.
22. Fujimoto, S.; Tamura, H.; Sakurai, H. *31th Intern. Conf. Coord. Chem.*; Vancouver, Canada, **1996**, Abs. p.21.
23 Fukui, K.; Ohya-Nishiguchi, H.; Nakai, M.; Sakurai, H.; Kamada, H. *FEBS Lett.* **1995**, *368*, 31-35.
24. Takechi, K., Tamura, H.; Yamaoka, K.; Sakurai, H. *Free Rad. Res.* **1997**, *26*, 483-496.
25. Takechi, K.; Sakurai, H. *2nd Intern. Conf. Bioradicals*; Yamagata, Japan, **1997**, Abs. 355.

Downloaded by CORNELL UNIV on October 31, 2012 | http://pubs.acs.org
Publication Date: December 10, 1998 | doi: 10.1021/bk-1998-0711.ch027

Downloaded by UNIV OF GUELPH LIBRARY on October 31, 2012 | http://pubs.acs.org
Publication Date: December 10, 1998 | doi: 10.1021/bk-1998-0711.ch028

Chapter 28

Vanadium Salts in the Treatment of Human Diabetes Mellitus

A. B. Goldfine[1], G. Willsky[2], and C. R. Kahn[1]

[1]Research Division, Joslin Diabetes Center, Department of Medicine, Brigham and Women's Hospital and Harvard Medical School, Boston, MA 02215
[2]State University of New York, Buffalo, NY 14214

Oral insulinmimetic properties and safety of sodium metavanadate ($NaVO_3$) in human IDDM and NIDDM, and vanadyl sulfate ($VOSO_4$) in NIDDM are reviewed and new studies are presented. In a single blind placebo lead in trial with $VOSO_4$, glucose metabolism in a two-step euglycemic insulin clamp did not increase in any of three subjects (age 57.7±0.9 yrs; M/F ½; BMI 39±10 kg/m^2; HbA1 10.7±1.3%) after 6 weeks vanadyl therapy dosed at 25 mg V daily. However, insulin sensitivity improved in 3 of 5 subjects (age 56.2±6.0 yrs; M/F 5/0; BMI 31.9±5.4 kg/m^2; HbA1 10.7±2.1%) when dosed at 50 mg V daily, from 30-83% and 9-230% at 0.5 and 1.0 mU/kg insulin, respectively; and insulin sensitivity improved in 3 of 5 subjects (age 52.0±8.6 yrs; M/F 3/2; BMI 39.0±7.8 kg/m^2; HbA1 6.9±1.0%) when dosed at 100 mg V daily, from 47-775% and 16-75% at 0.5 and 1.0 mU/kg insulin, respectively. Basal hepatic glucose production (HGP) and suppression of HGP by insulin were unchanged at both doses. There was no change in fasting blood glucose, glycohemoglobin, or mean systolic, diastolic, mean arterial blood pressures or in mean heart rates on 24 hr ambulatory monitors. Peak serum V levels for the 25 and 50 mg V dose were 15.7±3.7 and 79.1±24.0 ng/ml, respectively. 50 and 100 mg V doses caused some gastrointestinal intolerance, without biochemical evidence of toxicity. V is well tolerated for six weeks, but at these doses do not dramatically improve insulin sensitivity or glycemic control in all individuals.

In the late 1800's vanadium was proposed to have medicinal value and to be of benefit in nutrition, diabetes, atherosclerosis, anemia, metabolism of lipids, prevention of dental caries, and treatment of infection, especially tuberculosis and syphilis [1,2]. Since 1980,

In Vanadium Compounds; Tracey, A., et al.;
ACS Symposium Series; American Chemical Society: Washington, DC, 1998.

Downloaded by UNIV OF GUELPH LIBRARY on October 31, 2012 | http://pubs.acs.org
Publication Date: December 10, 1998 | doi: 10.1021/bk-1998-0711.ch028

considerable evidence has accumulated to show that vanadium salts, specifically tetravalent vanadyl, usually found as the divalent cation VO^{2+}, and pentavalent vanadate, VO_3^-, will mimic insulin action in a number of isolated cell systems and produce dramatic glucose lowering effects when given orally to animal models of both Types I and II diabetes mellitus [1,3]. In the STZ-diabetic rodent, glucose lowering effects are dramatic and occur within the first 2-4 days after oral administration. In 1995, human clinical trials evaluating the safety and efficacy of vanadium salts in the treatment of diabetes mellitus were first reported [4,5]. These studies administered the vanadium over a 2-3 week interval of time, about 4-7 times the duration required to see an effect in the STZ-diabetic rodent model.

Noninsulin Dependent Diabetes Mellitus

In an open label study of four weeks including a one week baseline period, two weeks of treatment with sodium metavanadate, and a one week post-treatment period, 5 subjects with NIDDM (age 52 ± 3 yrs, BMI 28.7 ± 1.7 kg/m^2, HbA1c 10.9 ± 2.0%) were studied before and after oral sodium metavanadate ($NaVO_3$) 125 mg/day (~50 mg elemental V) [4]. As a primary end-point of short term therapy, insulin sensitivity was measured using two-step euglycemic, hyperinsulinemic clamps at 0.5 mU insulin/kg/min and 1.0 mU insulin/kg/min , and improved in all NIDDM subjects with therapy; glucose disposal increased by 29% at the 0.5 mU insulin dose (1.7 ± 0.4 *vs* 2.2 ± 0.3 mg/kg/min) and by 39% at the 1.0 mU insulin dose (4.1 ± 1.0 *vs* 5.7 ± 1.3 mg/kg/min) (combined p=0.03) (Figure 1). In this study, patients were studied after blood glucose was normalized by administration of a low-dose insulin infusion overnight prior to the clamp. In contrast to the effect on peripheral glucose utilization, vanadate had no effect on basal or insulin suppression of hepatic glucose production (HGP). These data suggest that the improvement in glucose utilization was due to enhanced insulin sensitivity in peripheral tissues (*i.e.* muscle) without a change in hepatic insulin sensitivity. The clamp studies were performed with continuous indirect calorimetry to assess oxidative versus non-oxidative glucose disposal [6,7] at baseline and during the last 60 min of each step of the clamp. Basal oxidative and non-oxidative glucose disposal were similar before and after treatment. The improved insulin sensitivity during vanadate therapy appeared to be accounted for by increased non-oxidative glucose disposal (1.6 ± 1.0 *vs* 2.9 ± 0.8 mg/kg/min, at the higher insulin dose; $p < 0.03$), with no change in oxidative glucose utilization. There was no apparent correlation between the serum vanadium level achieved and the change in insulin sensitivity.

To assess the effects of vanadate on insulin secretion in subjects with NIDDM not requiring insulin, hyperglycemic clamps [8] were performed before and at the end of treatment. There was no change in basal, first or second phase insulin or c-peptide secretion.

Despite improved insulin sensitivity by euglycemic clamp studies, no clinical evidence for improvement in glycemia could be measured. There was no change in the dose of the oral hypoglycemic agent in any NIDDM subject. Fructosamine decreased slightly during the baseline week, but no further drop was seen after two weeks on

Downloaded by UNIV OF GUELPH LIBRARY on October 31, 2012 | http://pubs.acs.org
Publication Date: December 10, 1998 | doi: 10.1021/bk-1998-0711.ch028

vanadate. No significant changes in average blood glucose or weight were demonstrated. In view of the short duration of the study, it was not surprising that there was no significant change in glycohemoglobin (10.9 ± 2.0 *vs* 10.2 ± 1.1%). Serum cholesterol decreased (267.6 ± 29.0 *vs* 204.2 ± 17.9, $p < 0.05$), without significant change in apolipoprotein A-1 and apolipoprotein B levels.

These results are comparable to those seen by Cohen *et. al.* [5], who evaluated six NIDDM subjects (age 50 ± 4 yrs, BMI 27.3 ± 2.2 kg/m^2, HbA1c 9.6 ± 0.6%) on either diet or sulfonylurea therapy at end of three treatment periods [2 weeks placebo; 3 weeks VS (50 mg orally bid) (~33 mg elemental V); 2 weeks placebo] and demonstrated increased glucose infusion rates to maintain euglycemia during hyperinsulinemic clamps, (by ~88%, 1.80 to 3.38 mg/kg/min, $p<0.0001$), and improved insulin stimulated glucose uptake mediated primarily through increased glycogen synthesis consistent with the improved nonoxidative glucose disposal described above, however increased inhibition of hepatic glucose production was seen. In this study subjects did not receive insulin infusions overnight prior to the clamps, which could account for differences seen in basal hepatic glucose production. Improved insulin sensitivity was sustained two weeks after discontinuing the vanadyl. Glycolysis, was not changed during treatment, but increased at the end of the washout, perhaps demonstrating a waning of drug effect. Plasma vanadium concentrations were 73.3 ± 22.4 ng/ml at the end of treatment, and remained detectable at ~13% (9.5 ± 2.3 ng/ml) two weeks after discontinuation.

Improved glycemia could take longer than the time required to improve insulin sensitivity, and the time course of action of vanadium to lower glucose levels in the ob/ob mouse model of NIDDM is longer than in the STZ-diabetic rat. Thus, to determine if the improved insulin sensitivity measured on the clamp could result in improvement in clinical parameters of glycemic control, duration of administration of vanadyl sulfate was lengthened.

Subjects with NIDDM were evaluated in a single blind-placebo lead in trial, with vanadyl sulfate at 25, 50 and 100 mg orally three times a day with meals, for six weeks. A placebo lead in design was selected due to the evidence in animal and human studies of a prolonged effect after drug discontinuation, the duration of which can be over 12 weeks in rodents. Individuals served as their own controls with evaluations at the end of the placebo and drug treatment periods. Patient characteristics are described in Table I. Overall, glucose control was moderate to poor at entry to the study with the exception of the subjects receiving the highest vanadyl dose.

To assess insulin sensitivity pre- and post-treatment, two step euglycemic, hyperinsulinemic clamp studies were performed at 0.5 and 1.0 mU insulin/kg/min. Patients were studied after an overnight fast with blood glucose normalized by administration of a low-dose insulin infusion. No change in insulin sensitivity was demonstrated in the 3 subjects receiving 25 mg elemental V daily, whereas 3 of 5 subjects demonstrated improvements in glucose uptake at each the 50 and 100 mg V doses, ranging from 16 to 700%, with most responses between 30-75% (Figure 2). These changes were comparable in magnitude to those seen by Cohen *et al.* [5] as well as to those seen with the new insulin sensitizers metformin [9,10] and troglitazone [11] now approved for clinical use in the United States. The percent of individuals responding

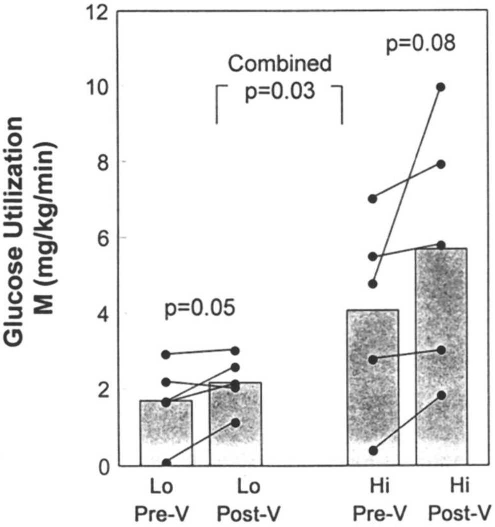

Figure 1: *Effect of two weeks of sodium metavanadate 125 mg daily, divided, on insulin sensitivity in euglycemic hyper-insulinemic clamp studies performed with 0.5 and 1.0 mU insulin/kg/min before and after vanadate in 5 subjects with NIDDM. Mean data is shown in the bars and individual data with the lines.*

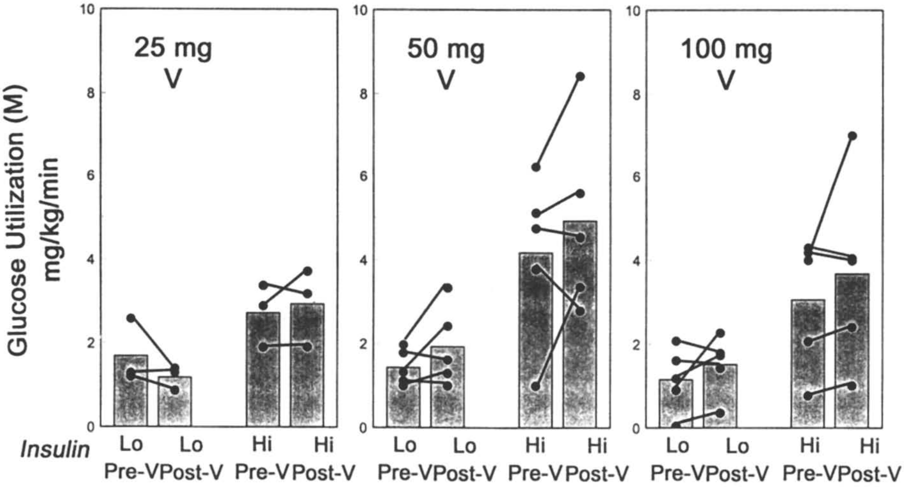

Figure 2: *Effect of vanadyl sulfate, 25, 50 and 100 mg daily, divided, on insulin sensitivity in euglycemic hyperinsulinemic clamp studies performed with 0.5 and 1.0 mU insulin/kg/min after placebo and after six weeks of vanadyl in subjects with NIDDM. Mean data is shown in the bars and individual data with the lines.*

Downloaded by UNIV OF GUELPH LIBRARY on October 31, 2012 | http://pubs.acs.org
Publication Date: December 10, 1998 | doi: 10.1021/bk-1998-0711.ch028

Downloaded by UNIV OF GUELPH LIBRARY on October 31, 2012 | http://pubs.acs.org
Publication Date: December 10, 1998 | doi: 10.1021/bk-1998-0711.ch028

Table I: Patient characteristics

	Age (years)	Age at DX	Sex (M/F)	BMI (kg/m2)	HbA1c (%total Hb)	Fasting Glucose (mg/dl)
25mg V	57.7±0.9	53.7±2.4	1/2	38.9±10.6	10.7±1.3	169.0±27.5
(range)	(57-59)	(52-57)		(26.0-52.0)	(9.1-12.2)	(136.7-204.0)
50mg V	56.2±6.09	46.6±8.5	5/0	31.9±5.4	10.7±2.0	150.3±35.8
	(48-65)	(35-61)		(27.4-39.3)	(8.5-14.2)	(111.8-210.0)
100mg V	52.0±8.6	48.8±8.8	3/2	34.9±7.8	6.9±1.0	121.0±34.5
	(38-65)	(37-52)		(27.1-48.7)	(5.4-8.3)	(82.3-185.0)

Downloaded by UNIV OF GUELPH LIBRARY on October 31, 2012 | http://pubs.acs.org
Publication Date: December 10, 1998 | doi: 10.1021/bk-1998-0711.ch028

to vanadyl (of about 60% on the 50 and 100 mg doses) are also comparable to that seen with metformin [12]. Again no change in basal or insulin suppression of hepatic glucose production was seen at any of the vanadyl doses (Figure 3). With so few patients the effect of vanadyl on glucose utilization as a group was modest, however nonoxidative glucose metabolism appears to be affected more than oxidative metabolism (Data not shown). In relation to clinical measurements of glycemia 100 mg/day V did not dramatically improve either glycohemoglobin, cholesterol, mean daily, fasting or preprandial glucose levels. There was no change in weight, or caloric intake assessed by food logs 3 days per week at the highest dose. However, as pointed out in the initial patient characteristics, the subjects treated with the highest dose of vanadyl started the study with better glycemic control as indicated by more normal glucose levels and glycohemoglobin. There was no hypoglycemia in any subject, including those who started the protocol with normal glycohemoglobins. Furthermore, current studies suggest that improvements in fasting glucose levels can be demonstrated in patients starting with more elevated glucose levels (Figure 4).

Boden *et al.* [13] administered VS 50 mg bid for 4 weeks to 8 NIDDM subjects, 6 subjects continued in the study and received placebo for an additional 4 weeks. Euglycemic hyperinsulinemic clamps were performed before and after VS and placebo. Gastrointestinal side effects were noted in first week in 6 of the 8 subjects, although it was well tolerated after first week. Improved fasting glucose (169±32 vs 135±25 mmol/L, $p<0.5$); decreased hepatic glucose output during hyperinsulinemia (5.0±1.0 vs 3.1±0.9 mcmol/kg/min, $p<0.02$); and no change in rate of total body glucose uptake; glycogen synthesis glycolysis; carbohydrate oxidation, or lipolysis, was demonstrated. Significantly decreased fasting glucose levels were also demonstrated by Cohen *et al.* [5], 210±19 *vs* 181±14 mg/dl, as well as Cusi *et al.* [14], from 191±15 to 155±11 mg/dl in 12 NIDDM subjects given 6 weeks of vanadyl sulfate 150 mg/day. However, in a study comparing diabetic and nondiabetic obese subjects, three weeks of vanadyl sulfate (50 mg bid) found improvements in glucose uptake, glycogen synthesis, and suppression of glucose output only in the NIDDM subjects and not in the insulin resistant obese nondiabetic controls [15].

Vanadium salts may inhibit cholesterol synthesis by interference with formation and utilization of mevalonic acid [16], and inhibit coenzyme A and thus interfere with the conversion of HMG to β-methyl crotonate [17]. Deposition of cholesterol is reduced and mobilization of predeposited cholesterol is increased in rabbits fed vanadium [18,19], and in healthy human subjects administered oxytartratovanadate small reductions in total and free cholesterol levels could be seen [20]. In the diabetic subjects given sodium metavanadate for two weeks total cholesterol levels dropped (267.6 ± 29.0 *vs* 204.2 ± 17.9, $p < 0.05$), without change in apolipoprotein A-1 or apolipoprotein B levels [4]. Although in our studies at the doses of vanadyl sulfate 100 mg tid, cholesterol drops were modest (192±30.7 *vs* 176±20.6 mg/dl, p=ns), significant drops were demonstrated by Cusi *et al.* (total cholesterol 223±14 *vs* 202±16, $p<0.01$; and LDL 141±14 *vs* 129±14 mg/dl, $p<0.05$) [14].

Animal models of insulin resistance, hyperinsulinemia and hypertension include the spontaneously hypertensive rat (SHR) [21], a genetically transmitted model of

Downloaded by UNIV OF GUELPH LIBRARY on October 31, 2012 | http://pubs.acs.org
Publication Date: December 10, 1998 | doi: 10.1021/bk-1998-0711.ch028

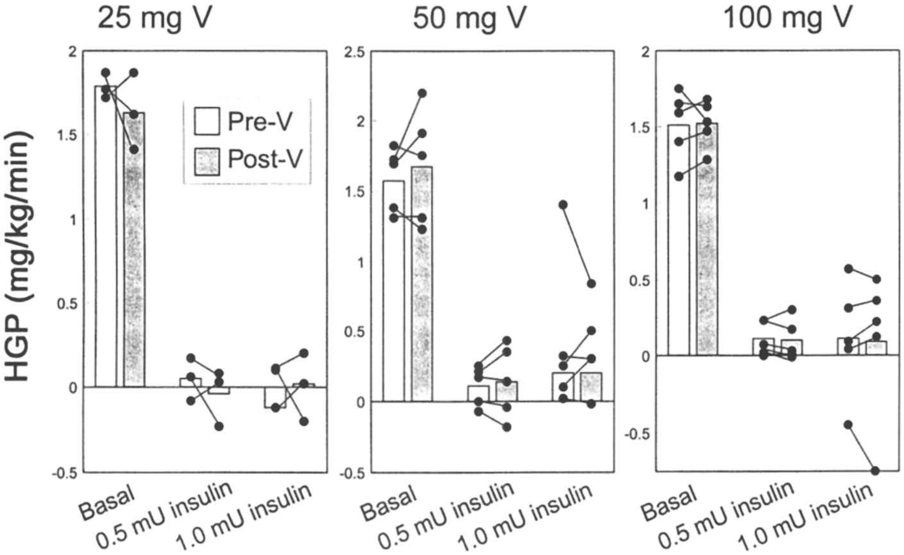

Figure 3: *Basal and insulin suppression of hepatic glucose production was unchanged after placebo and after six weeks of vanadyl sulfate, 25, 50 and 100 mg daily, divided, measured during euglycemic hyperinsulinemic clamp studies performed with 0.5 and 1.0 mU insulin/kg/min, and deuterated glucose, in subjects with NIDDM.*

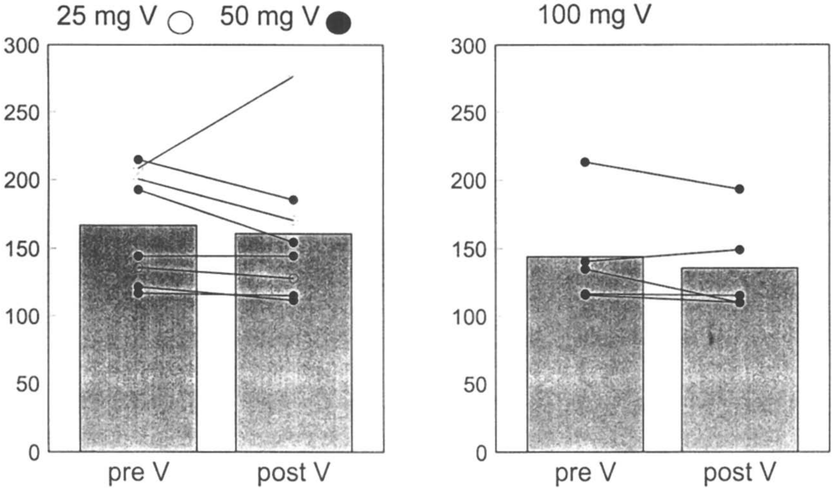

Figure 4: *Fasting glucose levels, performed by subjects with home glucose monitoring, at the end of placebo and after six weeks of vanadyl sulfate, 25, 50 and 100 mg daily, divided. One subject whose fasting glucose increased did not achieve serum vanadium levels above placebo. Patients starting with higher fasting glucose levels appear to have greater improvements.*

hypertension, and the fructose-fed rat [22], an acquired, diet-induced form of systolic hypertension. Vanadyl sulfate has been shown to lower plasma insulin and systolic blood pressure without affecting plasma glucose in the SH rat [23]. When insulin was administered subcutaneously to restore plasma insulin levels to pretreatment levels the effects of vanadyl to lower blood pressure were reversed. Similar effects were seen in the fructose-fed rat, in which chronic oral vanadyl prevents the rise in plasma insulin and blood pressure usually induced by the high fructose diet, as well as improves insulin sensitivity in euglycemic clamps. As with the SHR rats, the effects on blood pressure in the fructose fed rat are reversed when plasma insulin levels were restored to normal with subcutaneously administered insulin [24]. However, current studies reveal no change in either the 50 or 100 mg V (Figure 5) in mean systolic, diastolic, mean arterial pressure, or heart rate during 24 hr ambulatory blood pressure monitoring at the end of placebo and vanadium treatment. No change was seen in the subgroup of individuals whose insulin sensitivity responded by clamp measurements.

Vanadyl sulfate was well tolerated at the 25 and 50 mg V dose. At 50 mg V/daily two of five subjects experienced diarrhea that resolved spontaneously after the first week. At the 100 mg V dose all subjects experienced diarrhea at some point during treatment, however, no one withdrew from the study or required a dose reduction. Several individuals required small doses of Kaopectate or Immodium for symptomatic relief. The biochemical profiles showed no evidence of liver, renal or thyroid toxicity (Table II). Small drops in hematocrit have also been described in other investigations but may be attributed to phlebotomy during the clamp studies.

Lipid peroxidation of cellular structures is thought to play a role in late complications of diabetes mellitus and by-products of lipid peroxidation, such as conjugated dienes and thiobarbituric acid reactive substances (TBARS) are increased in diabetic patients [25]. Although the role of oxidant stress in the development of diabetic complications remains to be clarified, rodent studies suggest that vanadium salts may increase tissue oxidant stress as measured in the TBARS assay, without measurable changes in the antioxidant defense systems [26,27]. To estimate potential susceptibility to peroxidative changes, serum levels TBARS were determined [28,29] and were unchanged even at the highest dose administered dose of vanadium (Figure 6).

Vanadium salts are poorly absorbed after oral administration. Pharmacokinetic information is discussed in detail in Willsky *et al*, this volume. Peak serum vanadium levels were 18.2 ± 5.3 ng/ml, mean, with a range from 8.7-21.1 ng/ml at 25 mg V daily, and 82.4 ±43.2 ng/ml, mean, with a range from 13.9-125.5 ng/ml, at the 50 mg V dose, measured by graphite furnace atomic absorption spectroscopy (see Table III, Willsky chapter). The time from initiation of the study drug for each patient to reach peak serum levels varied greatly among individuals (see Figure 2, Willsky chapter). At the 25 mg V dose, a dose that is comparable or slightly larger than then most over-the counter preparations, one patient did not achieve levels above background. Compliance was assessed by pill count every other week and was considered to be excellent, and could not account for the variability. Peak serum levels did not correlate directly to response as measured by euglycemic hyperinsulinemic clamp, but the percent of subjects responding to vanadium salts does increase with increasing levels. Although

Downloaded by UNIV OF GUELPH LIBRARY on October 31, 2012 | http://pubs.acs.org
Publication Date: December 10, 1998 | doi: 10.1021/bk-1998-0711.ch028

Downloaded by UNIV OF GUELPH LIBRARY on October 31, 2012 | http://pubs.acs.org
Publication Date: December 10, 1998 | doi: 10.1021/bk-1998-0711.ch028

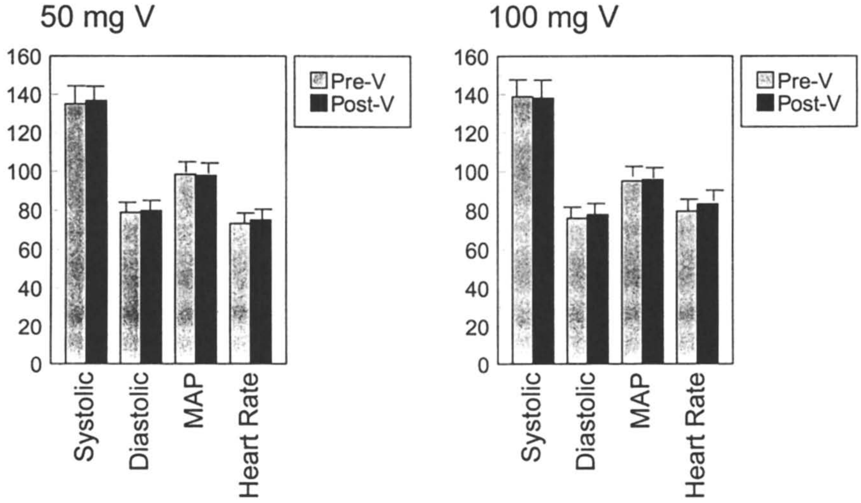

Figure 5: *No change in mean systolic, diastolic, mean arterial pressure or heart rate could be seen by 24 hr ambulatory blood pressure monitoring at the end of placebo or 6 weeks of vanadyl sulfate 50 or 100 mg daily, divided.*

Table II: Effect of V (100 mg) on Biochemical Profiles of Diabetic Subjects

	Pre-V	**Post-V**
Hematocrit (%)	45.8±2.5	43.0±2.4
Aminotransferase-AST (U/L)	17.8±4.8	16.6±5.0
Lactate dehydrogenase (U/L)	172.0±21.5	162.2±26.9
Alkaline Phosphatase (U/L)	65.5±33.3	62.4±32.9
Creatine (mg/dl)	0.9±0.2	0.9±0.2
Thyroxine (μg/dl)	7.1±4.4	9.2±3.5
Thyroid Stimulating Hormone (μU/ml)	2.1±2.3	2.6±3.0

the peak level does not reflect either intracellular levels or intracellular oxidative state, peak levels achieved in the human studies remain below those of the therapeutic rodent levels, *in vivo* (Figure 7). Furthermore, the range of serum values in humans remain below the extracellular vanadium concentrations required to inhibit the cellular and particulate phosphotyrosine phosphatases in hepatoma cells *in vitro* (Figure 8).

The serum $T_{1/2}$ appears to be correlated with the weight of the subject with the heavier subject clearing the vanadium at a faster rate (Figure 9). Although vanadium does not accumulate greatly in fat of control rodents fed vanadium, diabetic adipose tissue may accumulate more vanadium than non-diabetic tissue after similar $VOSO_4$ intake by about 47% [30]. Urinary vanadium excretion was about 1-2 mg/day or slightly less than 1% of the administered dose.

Downloaded by UNIV OF GUELPH LIBRARY on October 31, 2012 | http://pubs.acs.org
Publication Date: December 10, 1998 | doi: 10.1021/bk-1998-0711.ch028

Insulin Dependent Diabetes Mellitus

Vanadium administration has been studied extensively in two rodent models of IDDM, the insulin deficient STZ-diabetic rat and the autoimmune BB rat. It is important to note that there is residual insulin production in the STZ-diabetic animal who can be maintained euglycemic for extended time on vanadium supplementation alone, whereas the completely insulin deficient BB rat has decreased, but not absent insulin requirements in the presence of vanadium salts. Two studies have been performed in human subjects with IDDM [4,13]. 5 subjects with IDDM (age 45 ± 6 yrs, BMI 24.0 ± 0.8 kg/m^2, HbA1c 11.1 ± 1.0%) were studied before and after oral sodium metavanadate ($NaVO_3$) 125 mg/day, divided doses, (~50 mg elemental V). Subjects were studied for four weeks including a one week baseline period, two weeks of treatment with vanadate, and a one week post-treatment period. At the end of the baseline study week and the end of two weeks of vanadate, two step euglycemic, hyperinsulinemic clamp studies were performed to quantitate insulin sensitivity. Although two of the five subjects with IDDM showed an improved rate of glucose utilization after treatment with sodium metavanadate, on average there was no change in the rate of glucose utilization with either the low (3.6 ± 0.6 *vs* 3.2 ± 0.5 mg/kg/min) or high (8.0 ± 0.8 *vs* 9.0 ± 1.1 mg/kg/min) insulin dose. Basal oxidative and non-oxidative glucose disposal were similar before and after treatment and there was no significant change in the proportion of oxidative and non-oxidative glucose disposal at either insulin dose. After two weeks on vanadate individuals with IDDM showed a small (14%), but significant, decrease in mean daily insulin requirements (39.1 ± 6.6 to 33.8 ± 4.7 units insulin/day, $p < 0.05$), but no change in mean blood glucose (157 ± 15 *vs* 152 ± 8 mg/dl) or glycohemoglobin (11.1 ± 1.0 *vs* 10.2 ± 0.8, p=ns). The decrease in insulin requirements did not correlate with the improvement in insulin sensitivity or with any change in caloric intake. Few subjects experienced mild nausea when vanadate therapy was initiated which rapidly dissipated and only one subject could not tolerate the full dose of sodium metavanadate due to nausea and vomiting, requiring a dose reduction. Serum vanadium levels, measured by electrothermal atomization atomic absorption spectroscopy varied from 114 to 283 ng/ml, mean 187 ± 28 ng/ml (~3 mM).

Downloaded by UNIV OF GUELPH LIBRARY on October 31, 2012 | http://pubs.acs.org
Publication Date: December 10, 1998 | doi: 10.1021/bk-1998-0711.ch028

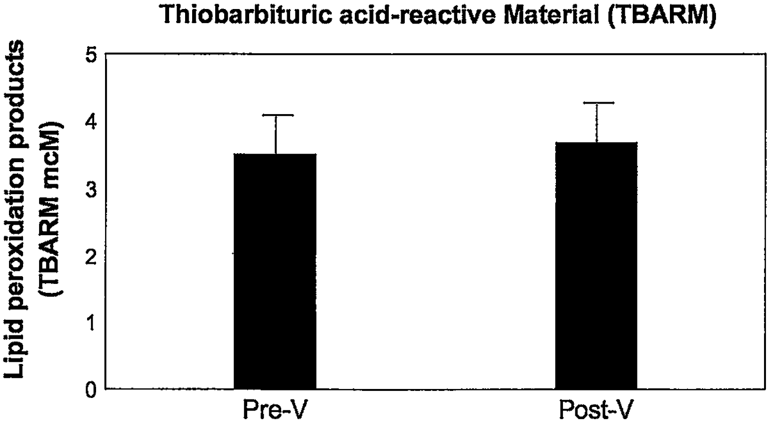

Figure 6: *No change in lipid peroxidation products by Fox assay could be detected after 6 weeks of vanadyl sulfate 100 mg daily, divided.*

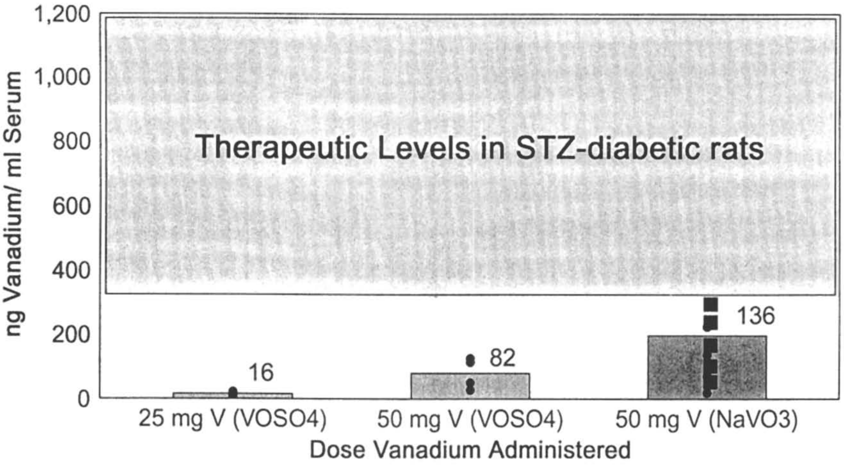

Figure 7: *Serum vanadium levels achieved with 50 mg daily of vanadyl sulfate are lower than those achieved when the vanadium is administered as sodium metavanadate. Serum levels in humans remain below those that are therapeutic in STZ-diabetic rats. The serum levels for sodium metavanadate are from previously reported studies* [4].

Downloaded by UNIV OF GUELPH LIBRARY on October 31, 2012 | http://pubs.acs.org
Publication Date: December 10, 1998 | doi: 10.1021/bk-1998-0711.ch028

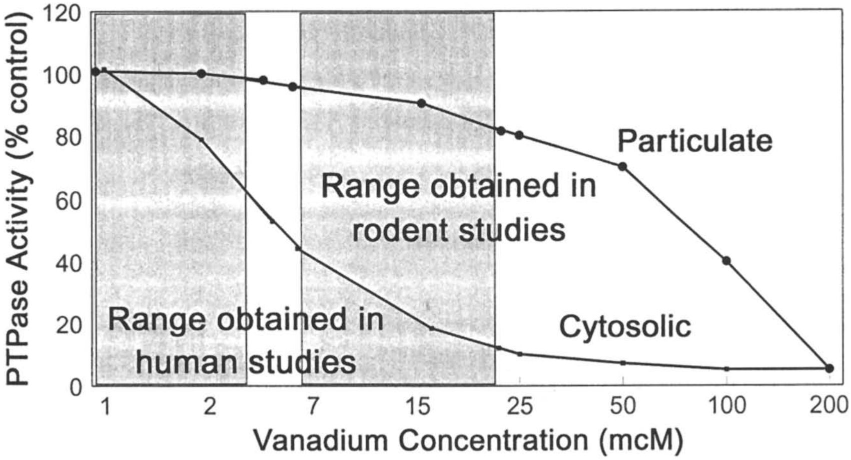

Figure 8: *Serum levels of vanadium in human studies remain below those used to inhibit cytosolic and particulate phosphotyrosine phosphatases in vitro in Hepatoma cells. Hepatic phosphotyrosine phosphatase activity has been previously reported* [41].

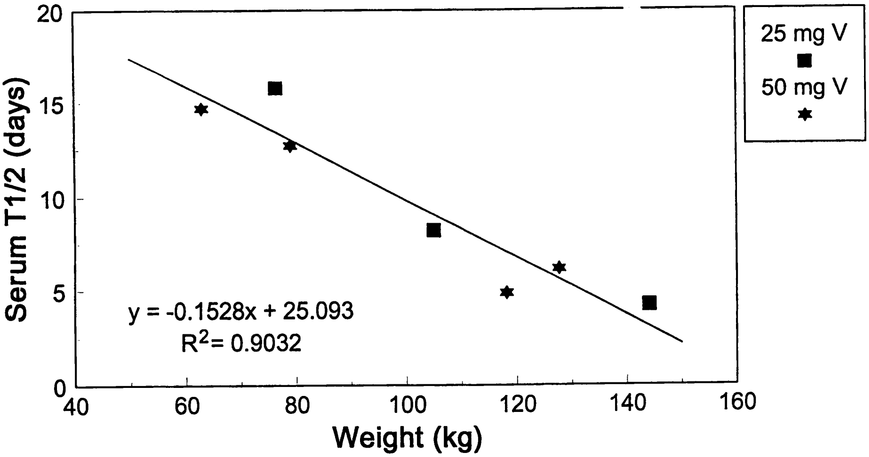

Figure 9: *Serum half life for vanadyl sulfate correlates with subject weight.*

In a single-blind, placebo controlled trial with 5 IDDM subjects (age 31 ± 2 yrs, BMI 24 ± 1.6 kg/m^2, HbA1c 8.1 ± 0.4%) administered vanadyl sulfate 100 mg/day (~30 mg elemental V) for 3 weeks, following 3 weeks of placebo, no change was seen in insulin dose, glucose disposal rates during euglycemic hyperinsulinemic clamp studies, glucose or lipid oxidation rates, or basal or insulin suppression of hepatic glucose production. No change was seen in glucose levels although there was a small drop in HbA1c to 7.6 ± 0.3%, $p<0.05$. No subjects experienced gastrointestinal effects. After 3 weeks of treatment plasma vanadium concentrations were 83 ± 29 ng/ml, slightly lower than levels achieved in the study with vanadate.

Implications and future directions

Considerable evidence exists that vanadium salts can mimic insulin action in many isolated cell systems and produce glucose lowering effects in rodent models of IDDM and NIDDM. Clinical studies in humans demonstrate vanadium salts at doses up to 100 mg elemental V daily, divided, for up to six weeks, appear to be safe and relatively well tolerated in humans. No changes in serum biochemical profiles or in measurements of tissue oxidative stress (TBARM) are demonstrated. However, gastrointestinal side effects are likely to limit higher doses. In some patients or in some studies improvements can be seen in measurements of insulin sensitivity, nonoxidative glucose metabolism, glycogen synthesis, and insulin suppression of hepatic glucose production. However, these changes are not seen in all studies. Clinically relevant improvements in clinical measurements of glycemia are harder to demonstrate, although some patients demonstrate lowered fasting glucose levels. No change is seen in systolic, diastolic, mean arterial pressure or heart rate.

The discrepancies in response in the several studies could relate to bias in subject selection, dose of vanadium administered or to variations in study protocols. It may be that only some patients will respond to treatment with these agents. In nondiabetic rats, there is some suppression of insulin levels, but no hypoglycemia, as seen in well controlled diabetic patients or obese, insulin resistant nondiabetic [15] or healthy controls [20]. It is possible that the disease state could alter the vanadium in the tissue as suggested in one study [30], the oxidative form of vanadium in the tissue, or the quantity or activity of relevant insulin signaling proteins in the tissue where the vanadium is active.

There is compelling evidence that vanadium actions in insulin signaling are mediated to a large degree via inhibition of cellular protein tyrosine phosphatases. Insulin action at the cellular level is complex (reviewed in refs [31,32]). Insulin initiates its actions by binding to its tetrameric membrane receptor. This receptor is a member of the family of receptor tyrosine kinases and following insulin binding undergoes autophosphorylation on multiple tyrosine residues which in turn activates the receptor kinase toward other substrates. In most cells, the major substrates are high molecular weight cytosolic proteins termed IRS-1 and IRS-2 (insulin receptor substrates-1 and -2) [33,34]. IRS proteins in turn may be phosphorylated on tyrosine residues, then serve as "docking proteins" for other intracellular proteins, including enzymes like phosphatidyl-

Downloaded by UNIV OF GUELPH LIBRARY on October 31, 2012 | http://pubs.acs.org
Publication Date: December 10, 1998 | doi: 10.1021/bk-1998-0711.ch028

inositol 3-kinase (PI 3-kinase), and adaptor proteins such as Grb2 [35], linking the signal to a series of serine/threonine kinases and phosphatases such as the MAP kinases, S6 kinases and protein phosphatase-1A via the ras-GTPase system. These serine kinases act on enzymes like glycogen synthase, transcription factors, and other proteins to produce many of the final biological effects of the hormone insulin. In adipose tissue and muscle, insulin stimulation also increases glucose uptake by promoting translocation of an intracellular pool of glucose transporters to the plasma membrane [36]. In the absence of continued insulin secretion, the cellular actions of the hormone are "turned off" in two ways: first insulin either dissociates from its receptor or is internalized and degraded [37], and secondly the activated receptor kinase and IRS molecules are dephosphorylated by the action on a group of enzymes called phosphotyrosine phosphatases (PTPase) [38].

These PTPases are inhibited *in vitro* and *in vivo* by vanadium compounds [39-41]. Thus, one could imagine that vanadium salts would enhance insulin receptor and/or substrate phosphorylation indirectly by inhibiting the dephosphorylation of these proteins. In fact, several acid phosphatases have homologous amino acid residues at the vanadium ligand interaction sites of the haloperoxide enzymes [42]. Skeletal muscle PTPase expression and activity are altered in obese and diabetic humans [43] such that they are increased in obesity and decreased in diabetes. It is possible that the tissue levels achieved in current human trials are not adequate to inhibit the increased levels of PTPases in obesity but are adequate for the decreased amounts in diabetes.

Finally, peak serum vanadium levels and kinetics vary widely among individuals, and serum vanadium levels in humans trials remain below those used in rodent and *in vitro* studies. Further work is necessary to determine if more potent, well tolerated analogues of vanadium salts or delivery systems can be developed, and in which patients these agents may have a clinically useful role in the treatment of diabetes mellitus.

Acknowledgments

This work was supported by NIH grant 5RO1 DK 47462-04 (CRK) and also by the Brigham and Women's Hospital General Clinical Research Center grant GCRC-CAP 3M01RR02635-13. The authors wish to thank Reanne LeBlanc, RN and all other nurses that participated in accumulating this data.

Literature Cited.

(1) Nechay, B.R.; Nanninga, L.B.; Nechay, P.S.E.; Post, R.L.; Grantham, J.J.; Macara, I.G.; Kubena, L.F.; Phillips, T.D.; Nielsen, F.H. *Fed. Proc.* **1986**, *45*, 123-132.

(2) Lyonnet, S.; Martz, A. *La Presse Medicale* **1899**, 191-192.

(3) Nadel, J.A. *J. Clin. Invest.* **1996**, *97*, 2689-2690.

(4) Goldfine, A.B.; Simonson, D.C.; Folli, F.; Patti, M.E.; Kahn, C.R. *J. Clin. Endocrinol. Metab.* **1995**, *80*, 3311-3320.

Downloaded by UNIV OF GUELPH LIBRARY on October 31, 2012 | http://pubs.acs.org
Publication Date: December 10, 1998 | doi: 10.1021/bk-1998-0711.ch028

(5) Cohen, N.; Halberstam, M.; Shlimovich, P.; Chang, C.J.; Shamoon, H.; Rossetti, L. *J. Clin. Invest.* **1995**, *95*, 2501-2509.

(6) Ferrannini, E. *Metabolism* **1988**, *37*, 287-301.

(7) Chu, Y.; Solski, P.A.; Khosravi-Far, R.; Der, C.J.; Kelly, K. *J. Biol. Chem.* **1996**, *271*, 6497-6501.

(8) DeFronzo, R.A.; Robin, J.D.; Andres, R. *Am. J. Physiol.* **1979**, *237*, E214-E223.

(9) Johnson, A.B.; Webster, J.M.; Sum, C.F.; Heseltine, M.; Argyraki, M.; Cooper, B.G.; Taylor, R. *Metabolism* **1993**, *42*, 1217-1222.

(10) Defronzo, R.; Barzilai, N.; Simonson, D.C. *J. Clin. Endocrinol. Metab.* **1997**, *73*, 1294-1301.

(11) Suter, S.L.; Nolan, J.J.; Wallace, P.; Gumbiner, B.; Olefsky, J.M. *Diabetes Care* **1992**, *15*, 193-203.

(12) Hermann, L.S.; Schersten, B.; Melander, A. *Diabet. Med.* **1994**, *11*, 953-960.

(13) Boden, G.; Chen, Z.; Ruiz, J.; Van Rossum, G.D.V.; Turco, S. *Metabolism* **1996**, *45*, 1130-1135.

(14) Cusi, K.; Cukeir, S.; Defronzo, R.; Torres, M. *Diabetes* **1997**, *46*, 34A.

(15) Halberstam, M.; Cohen, A.; Shlimovich, P.; Rossetti, L.; Shamoon, H. *Diabetes* **1996**, *45*, 659-666.

(16) Azarnoff, D.L. *J. Amer. Chem. Soc.* **1957**, *79*, 2968.

(17) Hudson, T.G.F. *The effects of vanadium on metabolism (continued).* In: *Vanadium: Toxicology and Biological significance*; Anonymous Elselvier Publishing Co.: New York, 1964; pp 30-43.

(18) Mountain, J.T.; Stockell, F.R.; Stokinger, H.E. *Proc. Soc. Exp. Biol. Med.* **1956**, *92*, 582.

(19) Curran, G.L.; Costello, R.L. *J. Exp. Med.* **1956**, *103*, 49.

(20) Curran, G.L.; Azarnoff, D.L.; Bolinger, R.E. *J. Clin. Invest.* **1959**, 1251-1261.

(21) Modon, C.E.; Reaven, G.M. *Metabolism* **1988**, *37*, 303-305.

(22) Hwang, I.S.; Ho, H.; Hoffman, B.B.; Reaven, G.M. *Hypertension* **1988**, *12*, 129-132.

(23) Bhanot, S.; McNeill, J.H. *Hypertension* **1994**, *24*, 625-632.

(24) Bhanot, S.; McNeill, J.H.; Bryer-Ash, M. *Hypertension* **1994**, *23*, 308-312.

(25) Griesmacher, A.; Kindhauser, M.; Andert, S.E.; Schreiner, W.; Toma, C.; Knoebl, P.; Pietschmann, P.; Prager, R.; Schnack, C.; Schernthaner, G.; Mueller, M. *Am. J. Med.* **1995**, *98*, 469-475.

(26) Oster, M.H.; Llobet, J.M.; Domingo, J.L.; German, J.B.; Keen, C.L. *Toxicology* **1993**, *83*, 115-130.

(27) Thompson, K.H.; McNeill, J.H. *Res. Commun. Chem. Pathol. Pharmacol.* **1993**, *80*, 187-200.

(28) Jiang, Z.Y.; Woollard, A.C.S.; Wolff, S.P. *Lipids* **1991**, *26*, 853-856.

(29) Jiang, Z.Y.; Hunt, J.V.; Wolff, S.P. *Anal. Biochem.* **1992**, *202*, 384-389.

(30) Olson, E.; Cacini, W. *Diabetes* **1997**, *46*, 221A.

(31) Flier, J.S. *Diabetes* **1992**, *41*, 1207-1219.

(32) Kahn, C.R. *Nature* **1995**, *373*, 384-385.

Downloaded by UNIV OF GUELPH LIBRARY on October 31, 2012 | http://pubs.acs.org
Publication Date: December 10, 1998 | doi: 10.1021/bk-1998-0711.ch028

(33) Rothenberg, P.L.; Lane, W.S.; Karasik, A.; Backer, J.M.; White, M.; Kahn, C.R. *J. Biol. Chem.* **1991**, *266*, 8302-8311.

(34) Sun, X.J.; Rothenberg, P.L.; Kahn, C.R.; Backer, J.M.; Araki, E.; Wilden, P.A.; Cahill, D.A.; Goldstein, B.J.; White, M.F. *Nature* **1991**, *352*, 73-77.

(35) Koch, C.A.; Anderson, D.J.; Moran, M.F.; Ellis, C.A.; Pawson, T. *Science* **1991**, *252*, 668-674.

(36) Gould, G.W.; Derechin, V.; James, D.E.; Tordjman, K.M.; Ahern, S.; Gibbs, E.M.; Lienhard, G.E.; Mueckler, M. *J. Biol. Chem.* **1989**, *264*, 2180-2184.

(37) Berman, M.; McGuire, E.A.; Roth, J.; Zeleznik, A.J. *Diabetes* **1980**, *29*, 50-59.

(38) Fischer, E.H.; Charbonneau, H.; Tonks, N.K. *Science* **1991**, *253*, 401-406.

(39) Swarup, G.; Cohen, S.; Garbers, D.L. *Biochem. Biophys. Res. Commun.* **1982**, *107*, 1104-1109.

(40) Goldstein, B.J. *J. Cell Biochem.* **1992**, *48*, 33-42.

(41) Meyerovitch, J.; Backer, J.M.; Kahn, C.R. *J. Clin. Invest.* **1989**, *84*, 976-983.

(42) Hemrika, W.; Renirie, R.; Dekker, H.L.; Barnett, P.; Wever, R. *Proc. Natl. Acad. Sci. U.S.A.* **1997**, *94*, 2145-2149.

(43) Ahmad, F.; Azevedo, J.; Cortright, R.; Dohm, G.L.; Goldstein, B.J. *J. Clin. Invest.* **1997**, *100*, 449-458.

Downloaded by UNIV OF GUELPH LIBRARY on October 31, 2012 | http://pubs.acs.org
Publication Date: December 10, 1998 | doi: 10.1021/bk-1998-0711.ch028

Author Index

Arends, I. W. C. E., 146
Banerjee, Anindya, 104
Baptista-Ferreira, J. L., 241
Barba-Behrens, N., 126
Bashirpoor, M., 60
Boyle, Paul D., 71
Bruck, Rafi, 308
Butler, Alison, 202
Chatterjee, R., 228
Chen, Shan, 104
Conte, V., 136
Contreras, R., 126
Cornman, Charles R., 71
Cortizo, A. M., 270
Crans, Debbie C., 2, 82, 308
Cruywagen, J. J., 51
da Silva, J. Armando L., 241
Dekker, Henk, 216
Detich, Nancy, 259
Eldberg, Gerald, 308
Elvingson, Katarina, 30
Etcheverry, S. B., 270
Farahbakhsh, M., 60
Fraústo da Silva, J. J. R. , 241
Fridkin, Mati, 308
Fujii, K., 344
Fujimoto, S., 344
Fujisawa, Y., 344
Furia, F. Di, 136
Gefel, Dov, 308
Gershonov, Eythan, 308
Goldfine, A. B., 278, 353
Goldwasser, Y., 308
Gresser, Michael J., 259
Guedes da Silva, M. Fátima C., 241
Guevara-García, J. A., 126
Hamstra, Brent, 157
Hemrika, Wieger, 216
Heyns, J. B. B., 51
Jantzen, S., 60
Jiang, Fashun, 104
Huang, Victor W., 104
Kahn, C. R., 353
Kanamori, K., 248
Kostyniak, P. J., 278
Kustin, Kenneth, 170
Li, Jinping, 308
Ludden, P. W., 228
Makinen, Marvin W., 104
Matoso, C. M. M., 241
McNeill, J. H., 329
Mendoza-Díaz, G., 126
Messerschmidt, A., 186
Michibata, H., 248
Moro, S., 136
Nekola, H., 60
Nielsen, Forrest H., 297
Nxumalo, Fikile, 259
Orvig, C., 329
Pecoraro, Vincent L., 157
Pettersson, Lage, 30
Pinho-Almeida, Fátima, 241
Pombeiro, Armando J. L., 241
Posner, B. I., 316
Prade, L., 186
Qian, Sun, 308
Ramachandran, Chidambaram, 259
Rehder, D., 60
Renirie, Rokus, 216
Ruetthard, Heike, 104
Rüttimann-Johnson, C., 228
Sakurai, H., 344
Schmidt, H., 60
Schwendt, P., 117
Sekar, Natesampillai, 308
Shah, V. K., 228
Shaver, A., 316
Shechter, Yoram, 308
Sheldon, R. A., 146
Shisheva, Assia, 308
Simpson, Matthew T., 202
Siväk, M., 117
Slebodnick, Carla, 157
Sprinzl, Mathias, 104
Stauffer, Thad C., 71
Takechi, K., 344
Thompson, K. H., 329
Tracey, Alan S., 2, 259
Tschirret-Guth, Richard A., 202
Uyama, T., 248
Vos, M., 146
Westra, A. N., 51
Wever, Ron, 186, 216
Willsky, G. R., 278, 353
Yang, C. R., 316
Yasui, H., 344
Yuen, V. G., 329

In Vanadium Compounds; Tracey, A., et al.;
ACS Symposium Series; American Chemical Society: Washington, DC, 1998.

Downloaded by 89.163.35.42 on October 31, 2012 | http://pubs.acs.org
Publication Date: December 10, 1998 | doi: 10.1021/bk-1998-0711.ix001

Subject Index

A

Accumulation mechanism, vanadium by ascidians, 248–258
Acetylacetonate-derived vanadium complexes, 82–103
Acid and alkaline phosphatases, vanadate as enzyme inhibitor, 171–173
Acid phosphatases, high molecular weight, 223, 225
Acidity, blood cells in Ascidians, 253–255
Adamantylideneadamantane, two-phase bromination, 143-144
Adenosine, molecular structure, 41
Adenosine-uridine-H_2VO_4 systems, 40–47
Adenosine-uridine-imidazole-H_2VO_4 systems, 42–43, 45, 47
Adenosine-vanadate nucleoside system 39–42, 45, 47
Alanylhistidine-vanadate system, 35–39, 45, 47
Alkynes, reductive protonation by nitrogenases, 68–69
Amanita fungi, amavadine role, 241–247
Amanita muscaria, amavadine occurrence, 241, 245–246
Amanita pantherina, amavadine occurrence, 245
Amanita regalis, amavadine occurrence, 241
Amanita velatipes, amavadine occurrence, 245
Amavadine
  occurrence in *Amanita* species, 241–247
  primitive peroxidase, 245
  protective/defensive agent, 245–246
  reaction with hydrogen peroxide, 243–244
  redox reactions, 242
  X-ray structure, 241
  See also species names
Amino acid sequence, comparison of chloroperoxidase to vanadium containing bromoperoxidase, 197
Anabaena variabilis, vanadium nitrogenase, structural components, 229
Ananylglycine-vanadate system, 35–39, 45–47
Animal deficiency experiments, vanadium, 299–303
Antidiabetic vanadium complexes, chemical studies, 329–340
Apo-r-chloroperoxidase
  catalysis, *p*-nitrophenyl phosphate, 218
  preparation, 218
  putative phosphatase activity, 218–219
Aqueous equilibrium analysis, biologically important vanadium(V)-organic ligand systems, 32–33
Aqueous interactions
  vanadium(IV) 9–10
  vanadium(V) 7–10
Aqueous solution
  speciation, peroxovanadium complexes, 136–145
  vanadates and hydrogen peroxide, 118
  vanadium chemistry, 2–29
Aqueous structures, deprotonated major oxovanadium(V) ions, 8
Ascidians
  classification
    biological, 248–249
    blood cell, 249–251
  vanadium
    accumulation mechanism, 248–258
    determination, 249
  See also species names
Ascidia ahodri
  intracellular acidity of blood cells, 253–255
  reactivity of F8DH, 254
  vanadium in, 252
  See also Ascidians
Ascidia ceratodes
  blood cell composition, 178–179
  intracellular acidity of blood cells, 253–254
  See also Ascidians
Ascidia gemmata
  intracellular acidity of blood cells, 253–255
  vanadium(III) in, 250, 252
  See also Ascidians
Ascidia nigra
  blood cell composition, 178–179
  See also Ascidians
Ascidia sydneiensis samea
  acidity of blood cells, 253–255
  reactivity of F8DH, 254
  vanadium in, 252
  See also Ascidians
Ascophyllum nodosum, 61, 197, 218
Ascophyllum nodosum, bromoperoxidase from, 146, 187, 197
Aspartate, role in peroxidase/acid phosphatase catalysis, 225
Azide complex with chloroperoxidase, 198

Downloaded by 89.163.35.42 on October 31, 2012 | http://pubs.acs.org
Publication Date: December 10, 1998 | doi: 10.1021/bk-1998-0711.ix002

Downloaded by 89.163.35.42 on October 31, 2012 | http://pubs.acs.org
Publication Date: December 10, 1998 | doi: 10.1021/bk-1998-0711.ix002

Azobacter chroococcum
  organization of gene coding for vanadium-nitrogenase, 234-235
  vanadium nitrogenases from, 229
  See also Azobacter
Azotobacter
  nitrogen-fixing bacteria, 61
  vanadium in iron-vanadium-sulfur cluster, 61
  vanadium nitrogenases from, 61
  See also species names
Azotobacter vinelandii
  molybdenum metabolism, 237
  organization of gene coding for vanadium-nitrogenase, 234–235
  regulation by the metal content of medium, 236–237
  vanadium metabolism, 237
  vanadium nitrogenase system, 228–240
  See also Azobacter

B

Binding pocket for vanadate in peroxidases, 217
Binding site
  hydrogen-vanadate(V), 193
  vanadium, 188–193
Biochemistry, vanadium, 170–185
Biogenesis of halogenated marine natural products, 146
Biogenic vanadium compounds, structural and functional models, 60–70
Biological effects stimulated by vanadate, mediation by cytPTK, 310
Biologically active vanadium complexes, strategic design
  ligand functionality, 331
  ligation kinetics, 330–331
  metal complex molecular weight, 331
  metal ligand binding, hydrolytically stable, 330
  thermodynamic stability, 330
Biomarkers of exposure, serum and urine vanadium concentration used as, 288
Biometic vanadium systems, catalytic oxidation, 146–156
Bis(histidinato)oxovanadium VO(HIS)
  in vitro study 347
  insulin-mimetic activities, 349*t*
  structure, 348*f*
Bis(maltolato)oxovanadium(IV) BMOV
  biological efficacy, 335, 337
  crystal structure, 333*f*
  electrochemistry, 335
  formation of a *cis*-dioxoanion, 332, 335–336*f*
  preparation, 331
  redox chemistry, 332–334*f*
  similarity to bis(2,4-pentanedionato-O,O′)oxovanadium(IV) complexes, 91
  stability constants, 332
Bis(6-methylpicolinao)oxovanadium VO(MPA)
  in vitro study 347
  in vivo study, 350
  insulin-mimetic activities, 349*t*
  structure, 348*f*
Bis(2,4-pentanedionato-O,O′)oxovanadium(IV) complexes, 91–95
Bis-peroxo-oxovanadium(V) complexes, with histidine-containing peptides, 126–135
Bis(picolinamido)oxovanadium VO(PAM)
  in vitro study 347
  insulin-mimetic activities, 349*t*
  structure, 348*f*
Bis(picolinato)oxovanadium VO(PA)
  in vitro study 347
  insulin-mimetic activities, 349*t*
  structure, 348*f*
Bis(quinaldiato)oxovanadium VO(QA)
  in vitro study 347
  in vivo study, 347
  insulin-mimetic activities, 349*t*
  structure, 348*f*
Bridge configurations, dinuclear vanadium(V) peroxo complexes, 120*t*
Bromide oxidation by peroxovanadium complexes, kinetic data, 158*t*
Bromoperoxidase
  amino acid sequence compared to chloroperoxidase, 197
  characterization, 187
  from *Ascophyllum nodosum*, 187
  structure, 61
Bromination
  adamantylideneadamantane, 143-144
  alkenes and aromatic substrates, catalyzed by NH_4VO_3, 141–142
  2-methylindole, pH dependence, 208–211
  organic substrates, 62–63, 140
  Phenol Red, pH dependence, 208–211
Brown sea weeds, 61

C

Caldariomyces fumago, chloroperoxidase from, 142, 216
Carbohydrate vanadium complexes, structural characterization, 20
Carveol, oxidation with *tert*-butyl-hydroperoxide, 150-151
Catalysis
  aspartate in peroxidase/acid phosphatase, 225
  by apo-r-chloroperoxidase, *p*-nitrophenyl phosphate, 218

Downloaded by 89.163.35.42 on October 31, 2012 | http://pubs.acs.org
Publication Date: December 10, 1998 | doi: 10.1021/bk-1998-0711.ix002

  by NH_4VO_3, bromination of alkenes and aromatic substrates, 141–142
  by nitrogenase, N_2 reduction, 228–230
  by vanadium bromoperoxidase, peroxidative halogenation reactions, 205–214
Catalytic asymmetric synthesis in intrazeolite space, 148–149
Catalytic cycle for vanadium bromoperoxidase, 205–206
Catalytic mechanism, chloroperoxidase, 198–199
Catalytic oxidations, biometic vanadium systems, 146–156
Catalytic properties, vanadium peroxo complex, bromination of organic substrates, 62–63*f*
Catalysts, metal ions
  encapsulation of vanadium, 148–149
  in organic synthesis, vanadium and other metal ions, 21
Cationic mono-peroxovanadium species, structure in solution, 139
Characterization of vanadium-zeolite catalyst, 149–150
Chemical studies, antidiabetic vanadium compounds, 329–343
Chiral oxaziridines, source of sulfenate oxygen atom in synthesis, 78–79*f*
Ciona intertinalis, blood cell composition, 178
Cleavage of DNA, effects of vanadium compounds, 16
Cloning, vanadium chloroperoxidase, 217, 219
Condensation reactions, vanadium(V), 8, 118
Coordination environments
  vanadium(IV), ligands with oxygen and nitrogen donor functionality, 10
  vanadium(V), ligands with oxygen and nitrogen donor functionality, 14
Coordination number, vanadium(V) peroxo complexes, 123*t*
Chloroperoxidase
  apo form, 195
  azide complex, 198
  catalytic mechanism, 198–199
  compared to vanadium containing bromoperoxidase, amino acid sequence, 197*t*
  from *Curvularia inaequalis*, 186–201
  peroxide form
    structure, 193–195
    synthesis, 193
  structure, 62*f*, 175, 187–188
  tungstate form, 195
  vanadium binding site, 188, 191*f*–192*f*
Ciona intestinalis
  reactivity of F8DH, 254
  vanadium in, 252
Clostridium pasteurianum, nitrogenase from, 229
Composition, vanadium(V) peroxo complexes
  diluted hydrogen peroxide solutions of vanadates, 118
  solid heteroligand vanadium(V) peroxo complexes, 119–121*t*
  solid peroxovanadates, 118
  with chiral ligands, 122
Condensation reactions
  thermodynamic quantities, 51–59
  See also Enthalpy, Entropy
Conserved active site
  consequences for acid phosphatases, 221–222
  vanadate-chloroperoxidase, 217–218
  vanadate-containing haloperoxidases and acid phosphatases, 216–227
Corallina officinalis, haloperoxidase from, 187
Crystalline products, solutions of vanadate in hydrogen peroxide, 118–119
Curvularia inaequalis
  apo-chloroperoxidase, 218
  vanadium chloroperoxidase, 140, 146, 186–201, 217
Cystosolic signal transduction processes in protein phosphorylation/dephosphorylation, effects of oxovanadium compounds, 284–285

D

Decavanadate
  enzyme inhibitor, 280
  physiological effects, 280–282
  sandwich-like contact ion pairs, 61*f*
Design, biologically active vanadium complexes
  ligand functionality, 331
  ligation kinetics, 330–331
  metal complex molecular weight, 331
  metal ligand binding, hydrolytically stable, 330
  thermodynamic stability, 330
Diabetes Mellitus
  insulin dependent, human treatment with sodium metavanadate, 362–365
  noninsulin dependent, human treatment with sodium metavanadate, 354–361
    effect on blood pressure, 361*f*
    effect on fasting glucose levels, 359*f*
    effect on lipid peroxidation products, 363*f*
    effect on serum vanadium levels, 363*f*
    insulin sensitivity, pre- and post-treatment, 355–356*f*
  See also human diabetes
Diazotrophic growth, *nif* genes required, 236
N,*N*-dimethylhydroxamidovanadates
  as inhibitors, 263–265

Downloaded by 89.163.35.42 on October 31, 2012 | http://pubs.acs.org
Publication Date: December 10, 1998 | doi: 10.1021/bk-1998-0711.ix002

complexes, 261
preparation, 260
reactivity, 262
Dinuclear diperoxo complexes, 118–121*t*
cis-Dioxovanadium(V) complexes, model studies
  aminoethyliminodiacetic acid (aeida), 157–165
  hydroxyethyliminodiactic acid (heida), 157–165
  nitrilotriacetic acid (nta3), 157–160
  pyridylmethyliminodiacetic acid (pmida), 157–165
Dipeptide-vanadate systems, 35–39
Dipicolinato-oxovanadium VO(DPA)
  in vivo study, 347
  in vitro study 347
  insulin-mimetic activities, 349*t*
  structure, 348*f*
Dropsophila protein wunen, 223

E

Electrogenic ATPases, 171, 174
Elongation factor tu (EF-Tu)
  binding dependent of metal ion, 110–112
  from cell paste of *Escherichia coli* engineered with tuf1 gene of Thermus thermophilus, 106
  guanosine nucleotide binding, 107–110
  interaction with vanadyl cation, 104–116
  intrinsic GTPase activity, 107
  measurement of nucleotide binding affinity, 106–107
Enantioselective peroxidation, thioethers, 64*f*
Encapsulation, vanadium catalyst, 148–149
Enthalpy
  calculation, HVO_4^{-2} condensation, 53, 56–58
  experimental determination, HVO_4^{-2} condensation, 51–53
  See also Thermodynamic quantities
Entropy
  calculation, HVO_4^{-2} condensation, 53, 56–58
  experimental determination, HVO_4^{-2} condensation, 51–53
  See also Thermodynamic quantities
Enzymes, model studies, 19–21
Equilibria, vanadate and ligands, 33
Essential mineral elements, criteria, 298–299

F

FeHeme haloperoxidases, *see* Iron hemoglobin haloperoxidases
Fluorescence quenching, 2-phenylindole by vanadium bromoperoxidase, 212–213
Food chain, vanadium, 4
Formation constants
  vanadate and ligands, 30–34
  vanadium(V) species, 55
Functional models, biogenic vanadium compounds, 60–70

G

Gene coding
  non-structural components, vanadium-nitrogenase, 234, 236
  structural components, vanadium-nitrogenase, 234–235
Glucose homeostatis, regulation, 308
Glucose-6-phosphatase, mammalian, membrane topology, 221, 223–224
Glycogen storage disease, 221
Goat, vanadium deficiency experiments, 299–300
Guanosine nucleotides, interaction with elongation factor tu, 104–116

H

Halide-assisted hydrogen peroxide disproportionation, oxoperoxovanadium(V) chelate models, 176–177
Halide oxidation, oxoperoxovanadium(V) chelate models, 176–177
Halogenation by vanadium bromoperoxidase, 207–214
Haloperoxidase enzymes
  catalyze oxidation of halides by hydrogen peroxide, 140–141, 175, 202
  from *Corallina officinalis*, 187
  in biogenesis, 140
  relationship to phosphohydrolase enzymes, 176, 178
Heteroligand vanadium(V) solid peroxo complexes, 119–120*t*
High molecular weight acid phosphatases, 223, 225
Higher animals
  essentiality of vanadium, 297–307
  intracellular concentration, vanadium, 313
  nutritional requirements, 304–305
  putative role of intracellular vanadium pool, 313
  vanadium absorption, 304
  vanadium excretion, 304
  vanadium transport, 304
  See also Goat, Human, Mammal, Rat
Histidine-containing peptides, with bis-peroxo-oxovanadium(V) complexes, 126–135

Histidine-vanadate system, 35–39, 45, 47
Histidine, with vanadium haloperoxidases, 126
Human diabetes
  vanadium, oral insulin-like effect, 329
  vanadium salts in treatment, 353–366
  See also Diabetes Mellitus
Human exposure to vanadium,
  dietary supplement, 291
  occupational exposure by inhalation, 291
  studies of NIDDM patients, 291
Human metabolism, vanadium accumulation in serum and urine of patients with NIDDM, 288-289*t*
Human toxicity, vanadium, 291
Hydrated structure
  vanadium (III), 5
  vanadium (IV), 6
Hydrogen peroxide
  dilute aqueous solutions with vanadates, 118
  halide oxidation, 157–167
  with amavadine, 243–244
Hydrolysis, vanadium (V), 34–35
(*S,S*)-2,2′-(hydroxyimino)dipropionic acid, 1:2 vanadium(IV) complex, *see* Amavadine
Hydroxylamido vanadium complexes, 82–103

I

Inhibitors, model studies, 19–21
Insulin action, 316–317
Insulin activation, phosphatidyl inositol-3-kinase (PI3-kinase), 309
Insulin-like effects
  vanadium, 308–313
  See also Insulin-mimetic properties
Insulin mimetic action, mechanism,
  in vivo, 339, 341
  peroxovanadium compounds, 316–327
  vanadium compounds, 283
Insulin mimetic, Kojic acid, 339
Insulin-mimetic properties, classes of vanadium compounds
  hydroxylamido analogs, 84–90
  peroxovanadium complexes, 83–84
  simple vanadium salts, 83
  See also Insulin-like effects
Insulin-mimetic vanadyl complexes
  orally active, 345–346*t*
  structure–activity relationship, 344–351
Insulin receptor kinase
  (IRK)-associated PTP inhibition, therapeutic target, 327
  role of phosphotyrosine phosphatase in activation, 323–324*f*
Insulin receptor, vanadate and vanadyl as promoters, 260
Insulin resistance, 308
Intracellular concentration, vanadium in higher animals, 313
Iron hemoglobin haloperoxidases, 202
Iron-molybdenum-cofactor, molybdenum dinitrogenase, 232
Iron only containing nitrogenases, 229
Iron-vanadium-cofactor, vanadium dinitrogenase, 232–234
Isonitriles, reductive C–C coupling, 68–69

K

Klebsiella pneumoniae, organization *nif* genes, 234
Kojic acid, insulin mimetic, 339

L

Ligand equilibria, 33–34
Ligands
  aqueous interactions, vanadium, 9–10
  biological interest with vanadium, 11–12, 16–19
  inorganic, with vanadium, 10–13
  organic
    coordination environment, 10, 14
    monodentate with vanadium, 13–14
    oxygen and nitrogen donors with vanadium, 14
    vanadate systems, 30–40

M

Magnetic resonance spectrometry, use in determination of oxidation state, 279
Mammal
  administration of oxovanadium compounds, 278–279
  pharmacokinetics of vanadium in, 287–289
  See also Goat, Higher animals, Human, Rat
Mammalian cells, determination of vanadium in, 279–280
Mammalian glucose-6-phosphatase, membrane topology, 221, 223-224
Mammalian tissues, determination of vanadium in, 279–280
Marine algae
  vanadium bromoperoxidase, 202–203
  vanadium containing haloperoxidases isolation from, 197

Downloaded by 89.163.35.42 on October 31, 2012 | http://pubs.acs.org
Publication Date: December 10, 1998 | doi: 10.1021/bk-1998-0711.ix002

Marine haloperoxidases, organohalogens formation, 187
Marine vanadium-dependent haloperoxidases, 140
Mass balance, vanadate and ligands, 33–34
Mechanism, insulin mimetic action, peroxovanadium compounds, 316–327
Membrane bound phosphatase, *Drosophila* protein wunen, 223
Membrane topology, mammalian glucose-6-phosphatase, 221, 223–224
Metal-based enzymes, halo-functionalization of organic compounds, 140
Metal sulfenates, coordination chemistry, 76
Metallokinetic analysis, 351
Mixed-valence vanadium(IV,V) complexes, 21
Model studies
  aminoethyliminodiacetic acid (aeida), 157–165
  enzymes, substrates, inhibitors, and natural products, 19–21
  hydroxyethyliminodiactic acid (heida), 157–165
  nitrilotriacetic acid (nta3), 157–160
  pyridylmethyliminodiacetic acid (pmida), 157–165
Models, structural and functional, biogenic vanadium compounds, 60–70
Models, vanadium halo-peroxidases, 126–135, 157–167
Molecular sieves, vanadium, 147–148
Molgula manhattensis, blood cell composition, 178–179
Molybdate, PTPas inhibitor, 311
Molybdenum containing nitrogenases, 229
Molybdenum-dinitrogenase structure, similarity to vanadium nitrogenase, 231
Molybdenum metabolism in *Azotobacter vinelandii*, 237

N

Natural occurrence, vanadium
  Amanita mushrooms, 171
  earth's crust, 3–4
  fan worms, 171
  tunicates, 171, 178–181
Naturally occurring enzymes, vanadium-dependent
  chloroperoxidase, in *Curvularia inaequalis*, 146
  haloperoxidases, in brown sea weeds, red algae, lichen, fungus, 61, 146, 187, 216
  nitrogenases, in nitrogen-fixing bacteria, 61
Natural products
  biogenesis of halogenated marine, 146
  model studies, 21
Nitrogen fixation models, 65–68
Nitrogen-fixing bacteria. *See Azotobacter*
Nitrogen reduction catalyzed by nitrogenase, 228–230
Nitrogenase system, vanadium-containing
  from *Azotobacter vinelandii*, 228–240
  substrate reduction properties, 237
p-Nitrophenyl phosphate, catalyzed by apo-r-chloroperoxidase, 218
NMR spectroscopy studies, vanadate-organic ligand systems, 30–50
Non-aqueous solution, vanadium 19
Non-insulin dependent Diabetes Mellitus (NIDDM)
  human treatment with sodium metavanadate, 354–361
  vanadium accumulation in patients' serum and urine, 288–289*t*
Nonmetallo haloperoxidases, 202
Nonreceptor protein tyrosine kinases, mediation insulin-like effects, 310-311
Nucleoside-imidazole-vanadate systems, 42, 45–47

O

Oligomers, vanadium(V), 8–9
Orally active insulin-minetic vanadyl complexes, 345–346*t*
Organic compounds, halogenation with oxoperoxovanadium(V) chelate models, 176–177
Organic ligand-vanadate systems, 30–50
Oxidation reduction reactions, oxovanadium interactions
  antitumorogenic effect, 283
  formation oxygen radicals, 282
  pharmacology, 282
Oxidation state, aqueous vanadium
  pH dependent, 4–7
  reduction potential dependent, 4–7
Oxomonoperoxo vanadium cation, structure, 136–137
Oxoperoxovanadium(V) complexes, models
  halide-assisted hydrogen peroxide disproportionation, 176–177
  halide oxidation, 176–177
  halogenation of organic compounds, 176–177
Oxovanadium(V) ions, aqueous structures, 8
Oxovanadium species
  administration to mammals, 278–279
  insulin mimetic action, 283–284
  pharmacology and toxicology, 278–296
  phosphate metabolism, 284–285

Downloaded by 89.163.35.42 on October 31, 2012 | http://pubs.acs.org
Publication Date: December 10, 1998 | doi: 10.1021/bk-1998-0711.ix002

Downloaded by 89.163.35.42 on October 31, 2012 | http://pubs.acs.org
Publication Date: December 10, 1998 | doi: 10.1021/bk-1998-0711.ix002

Oxovanadium(V)-thiol complex, preparation and chemistry, 72–76

P

Pathological effects formula, 303
Peptides with V_2O_5, H_2O_2, and ammonia
  aqueous solution, 127–134
  characterization
    NMR, 127, 129–134
    UV-VIS and diffuse reflectance spectra, 127
  synthesis, 127, 129
Peroxidative halogenation reactions, catalysis by vanadium bromoperoxidase, 205–214
Peroxometal species, formation, 147
Peroxovanadates
  solid, 118
  with small peptides in aqueous solution, 126
Peroxovanadium compounds
  discovery, 317
  inhibition insulin receptor kinase (IRK)-associated PTP, 317
  insulin mimetic action, mechanism, 316–327
  mechanism PTP inhibition, 317–322
Peroxovanadium complexes
  aqueous solution, speciation, 136–145
  as insulinomimetic agents, 312–313
  bromide oxidation kinetic data, 158
  comparison with hydroxylamido vanadium complex adducts, 85–91
  composition and structure, 117–125
  histadine-containing peptides, as models, 126–135
  insulin mimetic action, 82–103
  oxidizing power, 138
  species formed by adding H_2O_2 to NH_4VO_3, 137
  species with hydrogen peroxide, 118
  with chiral ligands, 122
Peroxovanadium ligand complexes
  biological interest, 16–19
  inhibition of protein tyrosine phosphatases, 17
  reactions with sulfur groups, 17
Pharmacokinetics, vanadium in mammals, 287–289
Pharmacological studies, antidiabetic vanadium complexes, 329–340
Pharmacology, oxovanadium species, 278–296
Phenylarsine oxide, as PTPase inhibitor, 312
Phosphatases, interaction with vanadium compounds, 95–97
Phosphate and vanadate esters, structural analogy, 20
Phosphate metabolism, oxovanadium interactions, 284–285
Phosphatidyl inositol-3-kinase (PI3-kinase), insulin activation, 309
Phosphohydrolase enzymes, relationship to haloperoxidase enzymes 176, 178
Phosphotyrosyl protein phosphatases, vanadate as enzyme inhibitor 171–173
Potassium peroxovanadates, 118
Potentiometric studies, vanadate-organic ligand systems, 30–50
Preparation and characterization, oxovanadium(V)-thiol complex, 72–76
Protein phosphotyrosine phosphatases, mechanism of inhibition
  molybdate, 311
  phenylarsine oxide, 312
  tungstate, 311
  vanadium, 310–312
Protein sequencing
  vanadium bromoperoxidase, 218–220
  vanadium chloroperoxidase, 217–219
Protein tyrosine kinases, nonreceptor, mediation of insulin-like effects of vanadate, 310
Protein tyrosine phosphatase (PTP)
  inhibition by peroxovanadium compounds, 317–322
  role in IRK activation, 323–324*f*
  role in pV-induced IRK tyrosine-phosphorylation, 323–325*f*
  vanadium adducts, structure, 71–72, 74
Protein tyrosine phosphatase (PTP) activity
  influenced by insulin, 266
  influenced by vanadium complexes, 260, 266
Protonation reactions, thermodynamic quantities, 51–59
Pyura michaelseni, vanadium in, 256
Pseudopotamilla occelata, as vanadium accumulator, 256

R

Rat
  acute oral LD_{50}, 290
  dietary vanadium affecting glucose of carbohydrate metabolism, 302*t*–303
  iodine effects, 300–301*t*
  organ distribution of vanadium, 350
  oxovanadium compounds effects on normal and diabetic, 287*t*
  reproductive toxicity, 291
  signs of toxicity, 290
  vanadium deficiency experiments, 299–303
  vanadyl in vivo coordination structure, 350

See also Rat, diabetic BB Wistar, Rat, streptozotocin induced diabetic, Rat, Wistar
Rat, diabetic BB Wistar, bpV (phen) treatment, 326*f*–327
See also Rat, Rat, streptozotocin induced diabetic, Rat, Wistar
Rat, streptozotocin induced diabetic (STZ)
  bis(maltolato)oxovanadium(IV) treated, glucose levels, 335, 337–338
  in vivo study
    bis(quinaldiato)oxovanadium, 347
    bis(6-dipicolinato)oxovanadium, 350
  vanadium compounds
    distribution, 338–339
    excretion, 338–339
    uptake, 338-339
  vanadium toxicity, 290
  vanadate treated, 308–309
Rat prostatic acid phosphatase, vanadium , crystal structure, 223
Rat, Wistar, in vitro study
  bis(histidinato)oxovanadium, 347–349
  bis(6-methylpicolinato)oxovanadium, 347–349
  bis(picolinamido)oxovanadium, 347–349
  bis(picolinato)oxovanadium, 347–349
  (dipicolinato)oxovanadium, 347–349
  bis(quinaldiato)oxovanadium, 347–349
  See also Rat, Rat, streptozotocin induced diabetic
Reactivity, vanadium bromoperoxidase, 202–215
Reductive protonation, alkynes, 68–69
Reductive C–C coupling, isonitriles, 68–69
Red algae, 61
Rhodobacter capsulatus
  iron in nitrogenase, 229
  organization of genes coding for vanadium-nitrogenase, 234–235
Rhodospirillum rubrum, iron in nitrogenase, 229

S

Saccharomyces cerevisiae expression system, 218, 225
Sea water, source of vanadium accumulation in tunicates, 179–181
Sea squirts, *see* Tunicates, Ascidians, individual species names
Sodium and potassium ATPase enzyme (Na,K-ATPbase), vanadium in, 170–171
Speciation, peroxovanadium complexes in aqueous solution, 136–145
Stability constants, *See* Formation constants
Stereospecific oxo-atom transfer, transition metal complexes, 78
Structural models for biogenic vanadium compounds, 60–70
Structure–activity relationship
  insulin-mimetic vanadyl complexes, 344–351
  $VO(N_2O_2)$ coordination model, 345
Styela plicata, vanadium in, 252
Substrate reduction properties, V-nitrogenase, 237
Substrates, model studies, 20
Synthetic models, vanadium haloperoxidases, 157–167

T

Therapeutic target, insulin receptor kinase (IRK)-associated PTP inhibition, 327
Thermodynamic quantities
  vanadium(V) equilibria, 51–59
  vanadium(V) species, 55
  See also Enthalpy, Entropy
Thioethers, enantioselective peroxidation, 64*f*
Thiolate oxidation models, 65–67
Toxicity
  vanadium, 4
  See also Human toxicity, Human exposure, Rat
Toxicology, oxovanadium species, 278–296
Transition metal complexes, stereospecific oxo-atom transfer, 78
Tungstate, as PTPase inhibitor, 311
Tunicates, vanadium accumulation in, 178–181, 282
Tunicates, *see also* Ascidians

U

Uridine, molecular structure, 41
Uridine-vanadate nucleoside system 39–42

V

Vanadate
  acid phosphatases, conserved active site, 216–227
  haloperoxidases, conserved active site, 216–227
Vanadate-maltol system, 43, 45
Vanadate (monomeric) enzyme inhibitor, 171–172
Vanadate organic ligand systems, 30–50
Vanadate (polyanions) enzyme inhibitor, phosphotransferases, 171–172
Vanadium
  aqueous solution, 2–29, 34–35

Downloaded by 89.163.35.42 on October 31, 2012 | http://pubs.acs.org
Publication Date: December 10, 1998 | doi: 10.1021/bk-1998-0711.ix002

Downloaded by 89.163.35.42 on October 31, 2012 | http://pubs.acs.org
Publication Date: December 10, 1998 | doi: 10.1021/bk-1998-0711.ix002

- coordination number, 95–97, 123
- condensation reactions, 8, 118
- determination in mammalian cells and tissues 279-280
- insulin-like effects, 308–313
- non-aqueous chemistry, 19
- oxidation state, 4
- serum and urine concentration used as biomarkers of exposure, 288

Vanadium accumulation
- in Amanita mushrooms, 171
- in mammals, 287–288
- in tunicates, 171

Vanadium atom shielding, 138
Vanadium binding to proteins, 280
Vanadium biochemistry, 170–185
Vanadium bromoperoxidase
- catalysis of peroxidative halogenation reactions, 205–214
- protein sequencing, 218–220
- reactivity, 202–215
- selective halogenation, 207–214

Vanadium chloroperoxidase
- cloning and gene sequencing, 217–219
- peroxide form, structure, 203, 206
- structure, 146, 203

Vanadium complex in a zeolite framework
- bromination of 1,3,5-trimethoxybenzene, 153–154
- Carveol, oxidation with *tert*-butyl-hydroperoxide, 150–151
- characterization, 149–150
- oxidation experiments of thioanisole, 151–153
- synthesis, 147–149

Vanadium compounds as insulin mimetics, 330
Vanadium containing bromoperoxidase compared to chloroperoxidase, amino acid sequence, 197
Vanadium dependent bromoperoxidases mimicking systems, 139–143
Vanadium dependent enzymes, found in nature
- haloperoxidases, 61
- nitrogenases, 61

Vanadium(V) 1,2-diol complexes, 20
Vanadium equilibria, thermodynamic quantities, 51–59
Vanadium essentiality for higher animals, 299–305
Vanadium haloperoxidases
- catalytic role, 126, 202–203
- from *Curvularia inaequalis*, 186–201
- models, 126–135, 157–165

Vanadium in sodium and potassium ATPase enzyme (Na,K-ATPbase), 170–171
Vanadium metabolism in *Azotobacter vinelandii*, 237
Vanadium molecular sieves, leaching in, 147–148
Vanadium-nitrogenase
- gene coding, 234–236
- similarity to molybdenum-dinitrogenase structure, 231
- structure, 229, 231–232
- system, 228–238

Vanadium oligomers, 8–9
Vanadium peroxo complexes, 117–125
Vanadium salts, treatment of human diabetes, 353–366
Vanadium sulfenate complexes, 71–81
Vanadium thiolate complexes, 71–81
Vanadium, toxicity 278–296
Vanadyl cation
- substitute for divalent metal ions, 105
- interaction with guanosine nucleotides and EF-Tu, 104–116

Vanadyl complexes
- insulin-minetic, orally active, 345–346*t*
- structure–activity relationship, insulin-mimetic, 344–351

Von Gierke disease, *see* glycogen storage disease
Vanadocytes, reduced from vanadium, 249–250

W

Wortmannin, inhibitor of PI3 kinase, 309

X

Xanthobacter autotrophicus, haloalkane dehalogenase from, 198

Z

Zeolite framework, vanadium complex,
- bromination of 1,3,5-trimethoxybenzene, 153–154
- Carveol, oxidation with *tert*-butyl-hydroperoxide, 150–151
- characterization, 149–150
- oxidation experiments, thioanisole, 151–153
- synthesis, 147–149

Zeozymes
- iron-phthalocyanine, 147
- manganese-bipyridine, 147